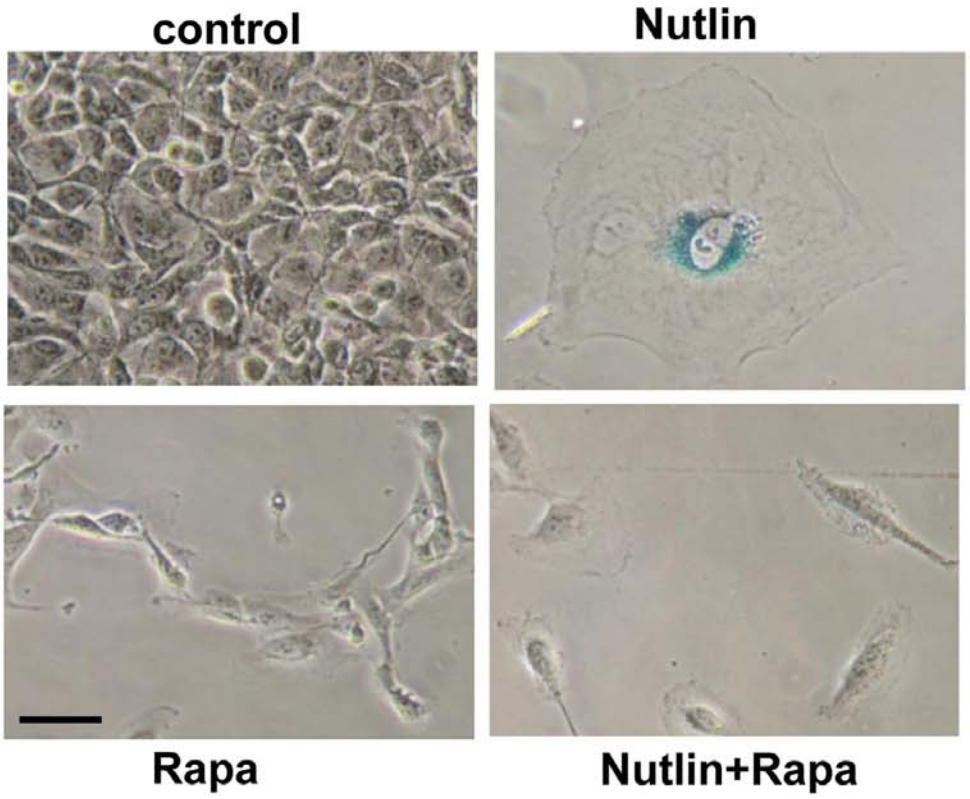

Special Collection on
Cell Senescence and Rapamycin

Effect of rapamycin on nutlin-induced senescence in melanoma cells, see Korotchkina et al. - “The choice between p53-induced senescence and quiescence is determined in part by the mTOR pathway.”

Cell Senescence and Rapamycin

AGING

Editorial and Publishing Office Aging (Albany NY)
6666 E. Quaker Str., Suite 1B
Orchard Park, NY 14127
Phone: 1-800-922-0957, option 1
Fax: 1-716-508-8254
e-Fax: 1-716-608-1380

Submission
Please submit your manuscript on-line at http://aging.msubmit.net

Editorial
For editorial inquiries, please call us or email editors@impactaging.com

Production
For questions related to preparation of your article for publication, please call us or email krasnova@impactaging.com

Indexing
If you have questions about the indexing status of your paper, please email kurenova@impactaging.com

Printing
Each issue or paper can be printed on demand. To make a printing request, please call us or email krasnova@impactaging.com.

Billing/Payments
If you have questions about billing/invoicing or would like to make a payment, please call us or email payment@impactaging.com

Publisher's Office
Aging is published by Impact Journals, LLC
To contact the Publisher's Office, please email: publisher@impactjournals.com, visit www.impactjournals.com, or call 1-800-922-0957, option 5

AGING

EDITORIAL BOARD

Table of Contents

Research Paper

Gerosuppression by pan-mTOR inhibitors

Olga V. Leontieva[1] and Mikhail V. Blagosklonny[1]

[1]Department of Cell Stress Biology, Roswell Park Cancer Institute, Buffalo, NY 14263, USA

Correspondence to: Mikhail V. Blagosklonny; **email:** Mikhail.blagosklonny@roswellpark.org
Keywords: dual mTORC1/C2 inhibitors, rapalogs, sirolimus, aging, cancer, senescence doi:10.18632/aging.101155
Received: August 12, 2016 **Accepted:** November 15, 2016 **Published:** December 30, 2016

ABSTRACT

Rapamycin slows organismal aging and delays age-related diseases, extending lifespan in numerous species. In cells, rapamycin and other rapalogs such as everolimus suppress geroconversion from quiescence to senescence. Rapamycin inhibits some, but not all, activities of mTOR. Recently we and others demonstrated that pan-mTOR inhibitors, known also as dual mTORC1/C2 inhibitors, suppress senescent phenotype. As a continuation of these studies, here we investigated in detail a panel of pan-mTOR inhibitors, to determine their optimal gerosuppressive concentrations. During geroconversion, cells become hypertrophic and flat, accumulate lysosomes (SA-beta-Gal staining) and lipids (Oil Red staining) and lose their re-proliferative potential (RPP). We determined optimal gerosuppressive concentrations: Torin1 (30 nM), Torin 2 (30 nM), AZD8055 (100 nM), PP242 (300 nM), both KU-006379 and GSK1059615 (1000 nM). These agents decreased senescence-associated hypertrophy with IC50s: 20, 18, 15, 200 and 400 nM, respectively. Preservation of RPP by pan-mTOR inhibitors was associated with inhibition of the pS6K/pS6 axis. Inhibition of rapamycin-insensitive functions of mTOR further contributed to anti-hypertrophic and cytostatic effects. Torin 1 and PP242 were more "rapamycin-like" than Torin 2 and AZD8055. Pan-mTOR inhibitors were superior to rapamycin in suppressing hypertrophy, senescent morphology, Oil Red O staining and in increasing so-called "chronological life span (CLS)". We suggest that, at doses lower than anti-cancer concentrations, pan-mTOR inhibitors can be developed as anti-aging drugs.

INTRODUCTION

Rapamycin slows down aging in yeast [1, 2], Drosophila [3-7], worm [8] and mice [9-30]. It also delays age-related diseases in a variety of species including humans [31-46]. Numerous studies have demonstrated life extension by rapamycin in rodent models of human diseases [9-48]. The maximal lifespan extension is dose-dependent [26, 42, 49]. One explanation is trivial: the higher the doses, the stronger inhibition of mTOR. There is another explanation: mTOR complex 1 (mTORC1) has different affinity for its substrates. For example, inhibition of phosphorylation of S6K is achieved at low concentrations of rapamycin, whereas phosphorylation of 4EBP1 at T37/46 sites is insensitive to pharmacological concentrations of rapamycin [50-61]. Unlike rapalogs, ATP-competitive kinase inhibitors, also known as dual mTORC1/C2 or pan-mTOR inhibitors, directly inhibit the mTOR kinase in both mTORC1 and mTORC2 complexes [56, 59, 62-65].

In cell culture, induction of senescence requires two events: cell cycle arrest and mTOR-dependent geroconversion from arrest to senescence [66-75]. In proliferating cells, mTOR is highly active, driving cellular mass growth. When the cell cycle gets arrested, then still active mTOR drives geroconversion: growth without division (hypertrophy) and a compensatory lysosomal hyperfunction (beta-Gal staining) [76]. So senescence can be caused by forced arrest in the presence of an active mTOR [76]. Senescent cells lose re-proliferative potential (RPP): the ability to regenerate cell culture after cell cycle arrest is lifted. Quiescence or reversible arrest, in contrast, is caused by deactivation of mTOR. When arrest is released, quiescent cells re-proliferate [66, 67].

In one cellular model of senescence (cells with IPTG-inducible p21), IPTG forces cell cycle arrest without affecting mTOR. During IPTG-induced arrest, the cells become hypertrophic, flat, SA-beta-Gal positive and lose RPP. When IPTG is washed out, such cells cannot resume proliferation. Loss of RPP is a simple quantitative test of geroconversion. Treatment with rapamycin during IPTG-induced arrest preserves RPP. When IPTG and rapamycin are washed out, cells re-proliferate [68-73, 77]. Recently, we have shown that Torin 1 and PP242 suppresses geroconversion, preventing senescent morphology and loss of RPP [78, 79]. In agreement, reversal of senescent phenotype was shown by another pan-mTOR inhibitor, AZD8085 [80].

Pan-mTOR inhibitors have been developed as cytostatics to inhibit cancer cell proliferation. Cytostatic side effects in normal cells are generally acceptable for anti-cancer drugs. However, cytostatic side effects may not be acceptable for anti-aging drugs. Gerosuppressive (anti-aging) effects at drug concentrations that only mildly cytostatic are desirable. Pan-mTOR inhibitors differ by their affinity for mTOR complexes and other kinases. Here we studied 6 pan-mTOR inhibitors (in comparison with rapamycin) and investigated effects of 6 pan-mTOR inhibitors on rapamycin-sensitive and -insensitive activities of mTOR, cell proliferation and geroconversion.

RESULTS

First we investigated the relationship between cytostatic and gerosuppressive activities of 6 pan-mTOR inhibitors: Torin1, Torin 2, AZD8055, PP242, KU-006379 and GSK1059615. All inhibitors inhibited proliferation in a dose-dependent manner (Fig. 1A). Inhibitory concentrations 50 (IC50) varied: Torin1 (22 nM), Torin 2 (8 nM), AZD8055 (20 nM), PP242 (285 nM), KU-006379 (230 nM) and GSK1059615 (>300 nM). At IC50, no cell death was observed. The inhibitory

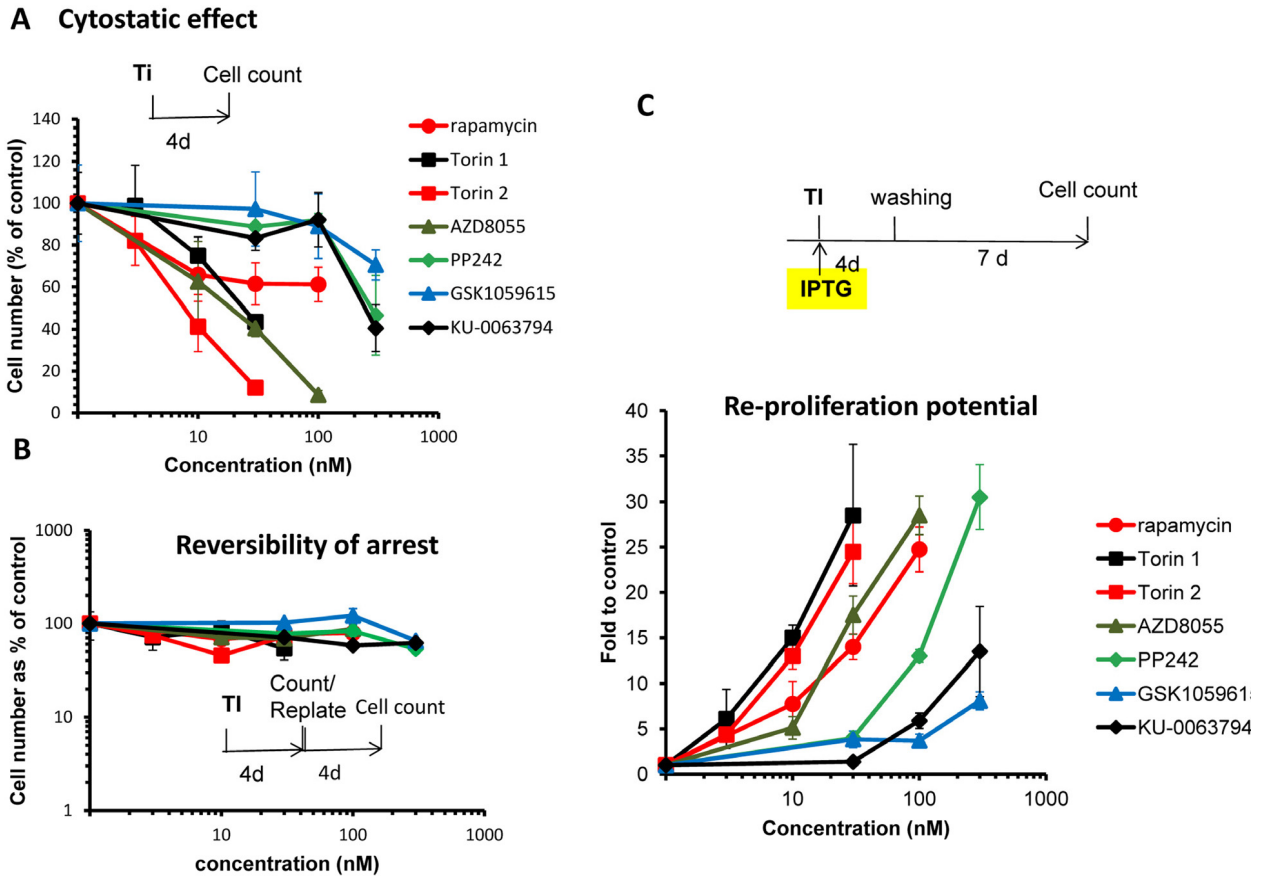

Figure 1. (**A**) Cytostatic effect. Effect of TOR inhibitors (Ti) on proliferation. HT-p21 cells were treated with serial dilutions of indicated Ti for 4 days and counted in triplicates. Data presented as mean ± SD. (**B**) Reversibility. Cells were treated as in A. After 4 day-treatment cells were counted and re-plated at 1000/well in 6-well plates in drug-free medium. Cells were allowed to re-proliferate for 4 days and counted. Cytostatic arrest was fully reversible. (**C**) Gerosuppression. Effect of TOR inhibitors on re-proliferative potential. HT-p21 cells were treated with IPTG in the presence of different concentrations of indicated Ti in triplicates. After 4 day-treatment, cells were washed off the drugs and allowed to regrow in drug-free medium for 7 days and counted. Data presented as mean ± SD.

effect was cytostatic rather than cytotoxic and, furthermore, reversible (Fig. 1B). When cells were treated with pan-mTOR inhibitors for 4 days and then re-plated and incubated in drug-free medium, the cells re-proliferated as efficiently as untreated control cells (Fig. 1B).

In the same cell line, HT-p21, we also measured gerosuppressive activities of mTOR inhibitors, by measuring re-proliferative potential (RPP) after induction of senescence with IPTG (Fig. 1C and Suppl. Fig. S1). In HT-p21 cells, IPTG induces p21, which in turn causes cell cycle arrest [76]. During cell cycle arrest, mTOR drives geroconversion to senescence, characterized by loss of RPP [68-73, 77]. Loss of RPP becomes evident after washing IPTG out. Although cells re-enter cell cycle, they cannot proliferate [81].

Inhibitors of mTOR preserved RPP in IPTG-treated cells. When IPTG and inhibitors of mTOR were washed out, the cells re-proliferated. By counting cell numbers after IPTG is washed out, we can measure gero-suppressive effects of mTOR inhibitors.

As shown in figure 1C and S1, all TOR inhibitors demonstrated equal maximal gerosuppressive activity, however, at different concentrations. Therefore, they have equal efficacy and different potency. (Note: Efficacy: maximum effect that mTOR inhibitor can cause regardless of concentration. Potency: concentration that is needed to cause this effect.) When we compared cytostatic versus gerosuppressive effects for each compound (Fig S2), we noticed that the gero-suppressive effect mirrored the cytostatic effect.

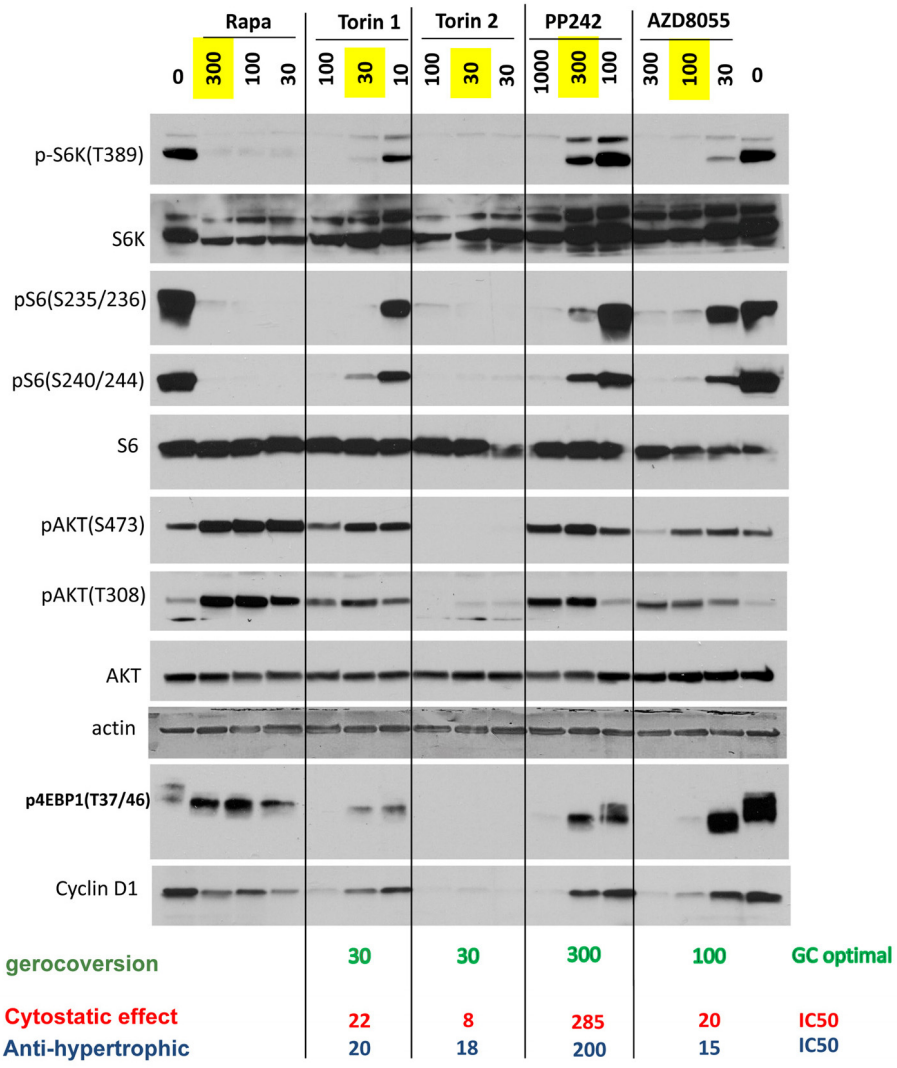

Figure 2. Effect of TOR inhibitors on mTOR-pathway in HT-p21 cells. Cells were treated with IPTG and different concentrations of indicated inhibitors for 24h and lysed. Immunoblotting was performed with indicated antibodies. Maximal optimal gerosuppressive concentrations are highlighted in yellow.

The lower concentration was required to inhibit proliferation, the lower concentration was required to suppress geroconversion (Suppl. Fig. S2). We estimated concentration at which compounds exerted maximum gerosuppressive effect (Fig. 1C and Suppl. Fig. S1). Torins 1 and 2 turned out to be the most potent and GSK1059615 was the least potent. Torin 1 and 2 showed the same maximal effect in suppressing geroconversion at 30 nM (Fig.1C and Suppl. Fig. S1). Maximal gerosuppressive effect was achieved by GSK1059615 and KU-0063794 at 1000 nM (Suppl. Fig. S1). AZD8055 displayed maximum gerosuppressive effect at 100 nM. As seen in figure S1, gerosuppressive effects reached the plateau and then decreased at higher concentrations, due to toxicity.

Preservation of RPP correlated with inhibition of mTORC1

MTOR complex 1 (mTORC1) phosphorylates S6 kinase (S6K) at T389, which in turn phosphorylates S6 at S235/236 and S240/244. This S6K/S6 axis is rapamycin-sensitive. Phosphorylation of 4EBP1 at T37/46 is rapamycin-insensitive. Function of mTORC2, which is rapamycin-insensitive, can be measured by phospho-AKT (S473), albeit it is not the only kinase that phosphorylates Akt at that site.

At optimal gerosuppressive concentrations, pan-mTOR inhibitors decreased phosphorylation of S6K at T389 (target of mTORC1) and its downstream targets S6 (S235/236) and (S240/244) (Fig. 2 and Suppl. Fig. S3). At optimal concentration (30 nM), Torin 2 inhibited phosphorylation of AKT at S473 and T308. Other inhibitors, at optimal gerosuppressive concentrations, did not decrease phosphorylation of AKT or even caused an increase in level of pAKT(S473) and/or pAKT(T308) similar to the effect of rapamycin, which induces phosphorylation of AKT in HT-p21 cells (Fig. 2). We conclude that mTORC2 and/or AKT in particular are not essential for geroconversion, as measured by RPP, in HT-p21 cells. Phosphorylation status of 4EBP1, a substrate of TORC1, was revealing. Rapamycin caused mobility shift but did not inhibit phosphorylation at the particular T37/46 sites. Torin 2 inhibited 4EBP1 phosphorylation at T37/46 sites. At optimal gerosuppressive concentrations, all other pan-mTOR inhibitors caused mobility shift and only marginally decreased T37/46 phosphorylation, which however was inhibited at higher concentrations (Fig. 2 and Suppl. Fig. S3).

Pan-mTOR inhibitors prevent cellular hypertrophy

We next determined effects of mTOR inhibitors on senescence-associated hypertrophy in IPTG-arrested HT-p21 cells. Hypertrophy can be measured as protein per cell [82]. IPTG induces cell cycle arrest, so that cells do not proliferate and the number of plated cells stays the same throughout the treatment [82]. Therefore, hypertrophy can be easily determined by measuring protein per well. We treated cells with IPTG and its combination with mTOR inhibitors. After a 4 day-treatment, cells were lysed and protein was measured. Pan-mTOR inhibitors decreased cellular hypertrophy in a dose-dependent manner. Rapamycin was an exception, i.e. its inhibitory effect on cellular hypertrophy was moderate and reached a plateau. IC50 values were as follows: 20, 18, 15, 200 and 400 nM for Torin 1, Torin 2, AZD8085, PP242 and GSK1059615, respectively (Fig. 3). All inhibitors reduced amount of protein by more than 50% at concentrations corresponding to their optimal gerosuppressive concentrations measured by RPP.

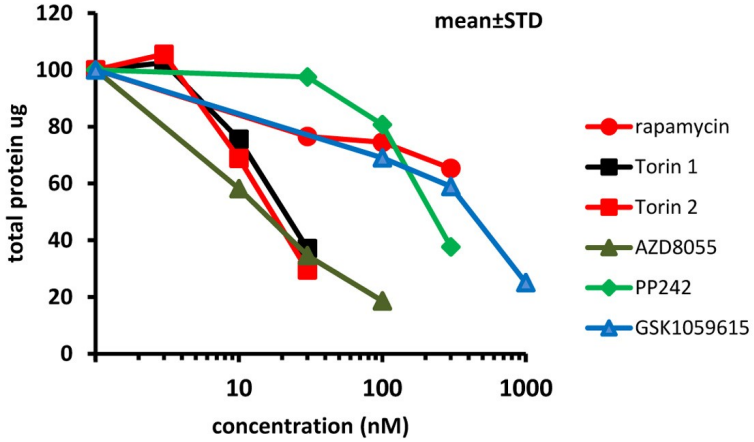

Figure 3. Effect of TORINs on protein level in senescent HT-p21 cells. Cells were treated with IPTG and different concentrations of TORINs for 4 days and protein amounts were measured. Data are mean ± SD.

We next employed additional method of measuring cellular hypertrophy by measuring GFP under CMV-constitutive promoter in HT-p21 cells. (HT-p21 cells are stably transfected with GFP-CMV). It was previously shown that GFP accumulation is a marker of hypertrophy [82]. Torin 2 was more potent anti-hypertrophic agent than Torin 1 (Fig. 4A). IC50 values were 3 nM and 10 nM for torn 1 and 2, respectively (Fig. 4A). At 30 nM, both Torins were more anti-hypertrophic than rapamycin (Fig. 4A, rapamycin was used at 500 nM). Anti-hypertrophic effect of Torins was independent of the nature of senescence-inducing agent, i.e. IPTG-inducible ectopic p21 or inhibitor of CDK4/6 PD0332991 (Fig. 4B, C). We conclude that Torins blocked senescence-associated hypertrophy more effectively compared with rapamycin. Furthermore, Torin 1, which is more rapamycin-like than Torin 2, was less potent as anti-hypertrophic agent than Torin 2.

Torins 1 and 2 decrease lipid accumulation in senescing cells

One of the features of senescent HT-p21 cells is accumulation of lipids, which is detected as positive Oil Red O staining in perinuclear region (Fig. 5, IPTG). When these cells were co-treated with IPTG and Torins 1 or 2, cells remained small and Oil Red O negative (Fig. 5). As in the case of SA-beta-Gal staining, rapamycin was less effective than Torins in decreasing this marker of senescent HT-p21 cells.

Pan-mTOR inhibitors prolongs CLS in HT-p21 cells

The yeast is commonly used as a model of aging. In particular, rapamycin extends chronological lifespan (CLS) [2]. In stationary culture, yeast cells lose viability measured as re-proliferative potential in fresh culture [1-7]. It is erroneously believed that "chronological

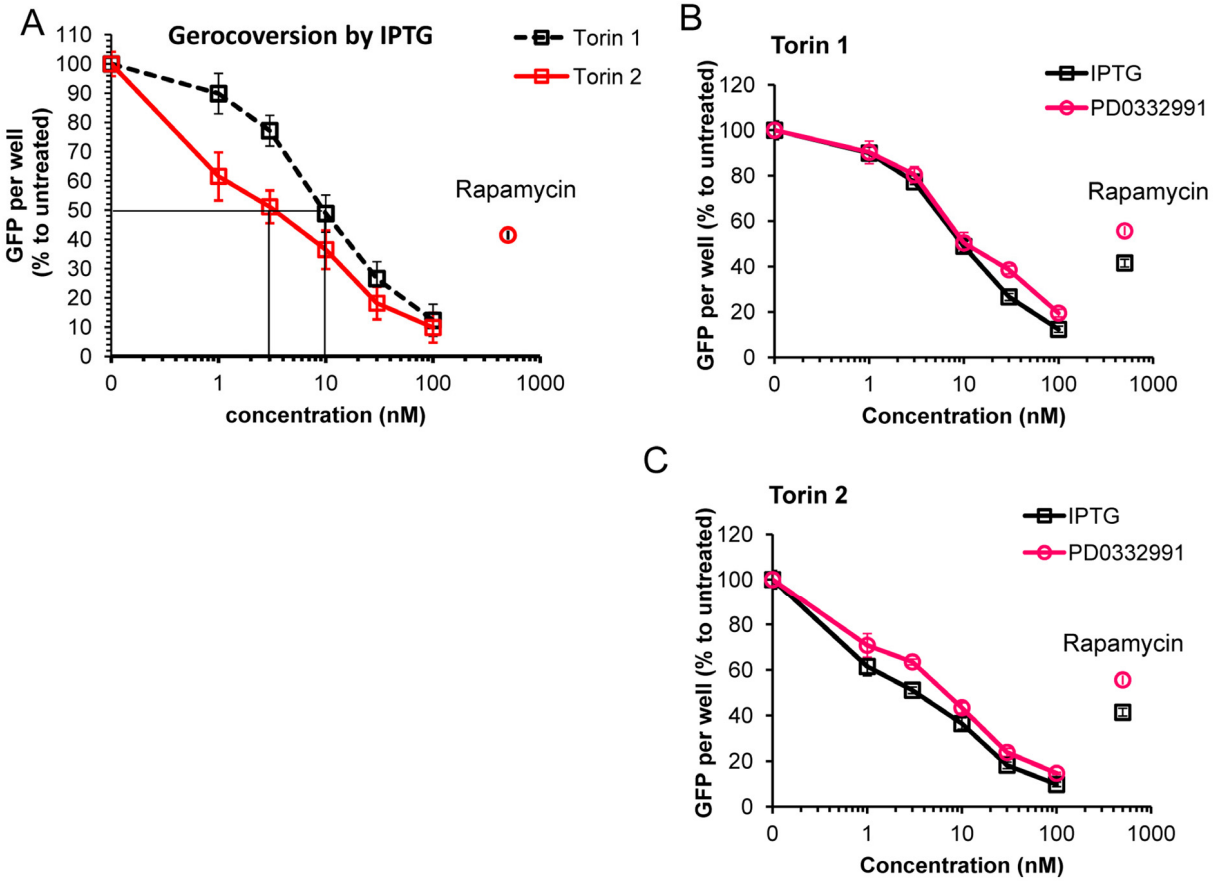

Figure 4. Effect of torins 1 and 2 on hypertrophy of senescent HT-p21 cells measured by constitutive GFP fluorescence of these cells. (**A**) HT-p21 cells were treated with IPTG and concentration range of torin1 or torin 2, rapamycin (500 nM) was included for comparison as additional control. After 4 day-treatment GFP fluorescence was quantified using Typhoon scanner (Amersham Biosciences variable mode imager) and ImageQuantTL software. (**B**) and (**C**) HT-p21 cells were induce to senesce by treatment with either IPTG (3 days) or PD0332991 (0.5 μM, for 4 days) and concentration range of torin 1 (**B**) or torin 2 (**C**). Effect of torins on hypertrophy was assessed by measuring GFP fluorescence as described in (**A**). GFP per well is presented as % to IPTG or PD0332991 only treated cells for each set. Data are means ± SE of 8 replicates from one out of three independent experiments.

aging" is an equivalent of aging of post-mitotic cells in multicellular organism. In reality, this phenomenon is an equivalent of lose of cancer cell viability in overcrowded culture [83]. Both yeast and cancer cells acidify the culture medium and lose viability, as measured for example by re-proliferation in fresh low-density culture. When plated at very high cell density, HT-p21 cells produce high levels of lactic acid, acidifying medium ("yellow color"). This causes loss of re-proliferative potential [83]. Rapamycin extends CLS by decreasing lactate production [83]. Here we tested whether pan-mTOR inhibitors can extend CLS of HT-p21 cells. After 3 days in a high-density culture, HT-p21 cells remained alive, but could not re-proliferate and form colonies when re-plated in fresh medium (Fig. 6, control). When high-density cultures were treated with mTOR inhibitors, these cells produced less lactic acid as seen by the color of the medium (Fig. 6; yellow indicates low pH and high levels of lactic acid) [84]. They maintained re-proliferative potential and formed colonies when re-plated in fresh medium in low density (Fig. 6). Rapamycin was less effective than pan-mTOR inhibitors. At equipotent (optimal) concentrations, all pan-mTOR inhibitors showed similar efficacy in prolonging chronological life span.

Pan-mTOR inhibitors suppress senescent morphology of SKBR3 and MEL10 cells

We next investigated gerosupressive effects of mTOR inhibitors in SKBR3 and MEL10 cells undergoing geroconversion after treatment with CDK4/6 inhibitor PD0332991 and nutlin-3a, respectively **[72]**. As shown in Fig 7, treatment with PD0332991 caused senescent morphology in SKBR3 cells. Co-treatment with pan-mTOR inhibitors prevented senescent morphology and hypertrophy (Fig.7 and Suppl. Fig. S4A). Pan-mTOR inhibitors also prevented senescent morphology of MEL10 cells induced to senesce by treatment with low concentration of nutlin-3a (Fig. 8 and Suppl. Fig. S4B).

DISCUSSION

As predicted by theory of TOR-driven aging [29, 85-97], rapamycin extends life span and prevents age-related diseases (see Introduction). Yet, rapamycin (and other rapalogs such as everolimus) does not inhibit all functions of mTOR. Inhibition of both rapamycin-sensitive and --insensitive functions of mTOR may be translated in superior anti-aging effects. However, potential benefits may be limited by undesirable effects

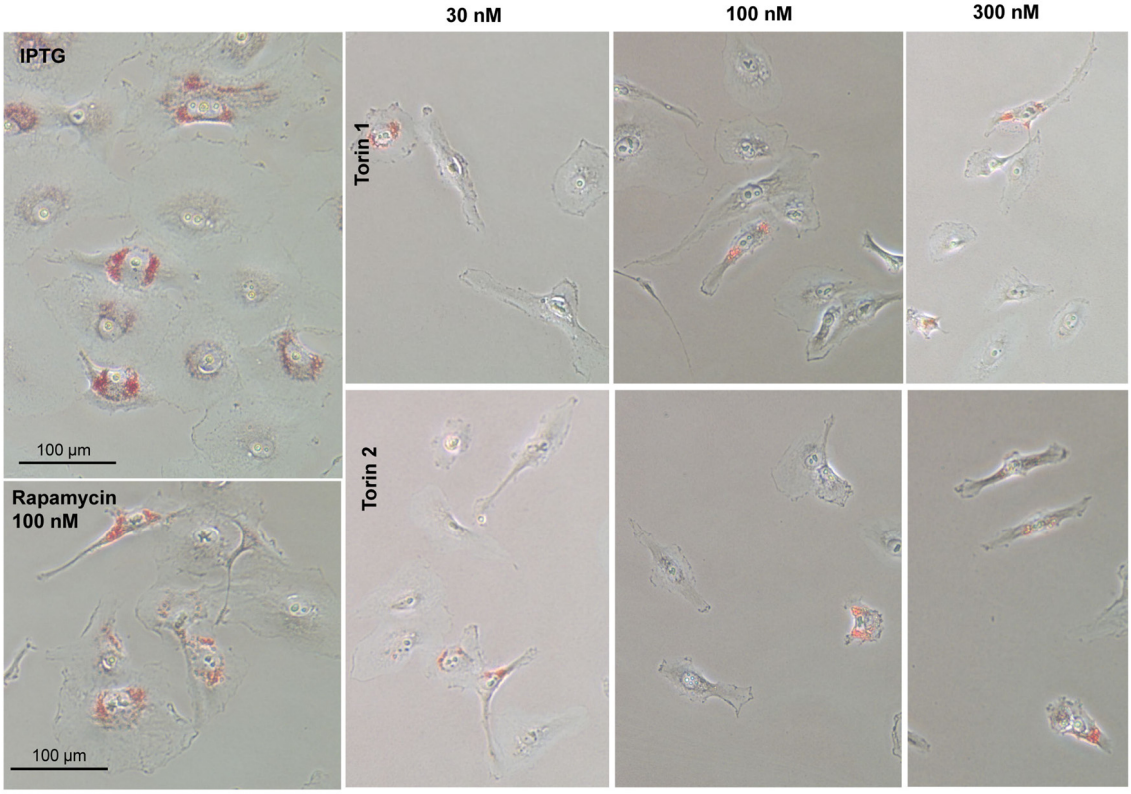

Figure 5. Effect of torin analogs on lipid accumulation in senescent HT-p21 cells. Cells were treated with IPTG and concentrations range of torin 1or torin 2 for 4 days and stained with Oil Red O. Bar – 100 µm.

such as inhibition of cell proliferation (cytostatic effect) and cell death (cytotoxic effect). In fact, pan-mTOR inhibitors have been developed to treat cancer, so they are cytostatic and cytotoxic at intended anti-cancer concentrations. Yet, the window between gero-supressive and cytotoxic effects exists. At optimal gerosuppressive concentrations, pan-mTOR inhibitors caused only mild cytostatic effect. For Torin 1 and PP242, the ratio of gerosuppressive (measured by RPP) to cytostatic concentrations was the most favorable. The ratio of anti-hypertrophic to cytostatic concentration was similar for all pan-mTOR inhibitors.

Gerosuppressive effect of pan-mTOR inhibitors (as measured by RPP) was equal to that of rapamycin because it is mostly associated with inhibition of the S6K/S6 axis. Yet anti-hypertrophic effect as well as prevention of SA-beta-Gal staining and large cell morphology was more pronounced with pan-mTOR inhibitors than with rapamycin. Also, at optimal concentrations, all pan-mTOR inhibitors extended loss of re-proliferative potential in stationary cell culture more potently than rapamycin. This test determines hyper-metabolism and lactic acid production and is an equivalent of "yeast CLS" (see [83]. One conclusion is that pan-mTOR inhibitors may be superior to rapamycin.

At low concentrations, pan-mTOR inhibitors acted like rapamycin, inhibiting the S6K/S6 axis and causing mobility shift of 4EBP1 (Fig. 2). With increasing concentrations, these drugs inhibited phospho-4EBP1 (T37/46) followed by inhibition of phospho-AKT (S473) (Fig. 2) and thereby further contributed to anti-hypertrophic effects (and cytostatic effect), prevention of senescent morphology as well as inhibition of CLS. Importantly, effects of pan-mTOR inhibitors varied in their resemblance to rapamycin effects. In particular, Torin 1 and PP242 were rapamycin-like. The window between inhibition of pS6K/S6 versus p4EBP1 and AKT was narrower for Torin 2 and AZD8085 than for other 4 pan-mTOR inhibitors. In general, maximal gerosuppression (as measured by RPP) was achieved at concentrations that inhibited phosphorylation of S6K and S6 and only partially inhibited rapamycin-insensitive functions of mTOR. Rapamycin-like effects achieved at lower concentrations of pan-mTOR inhi-

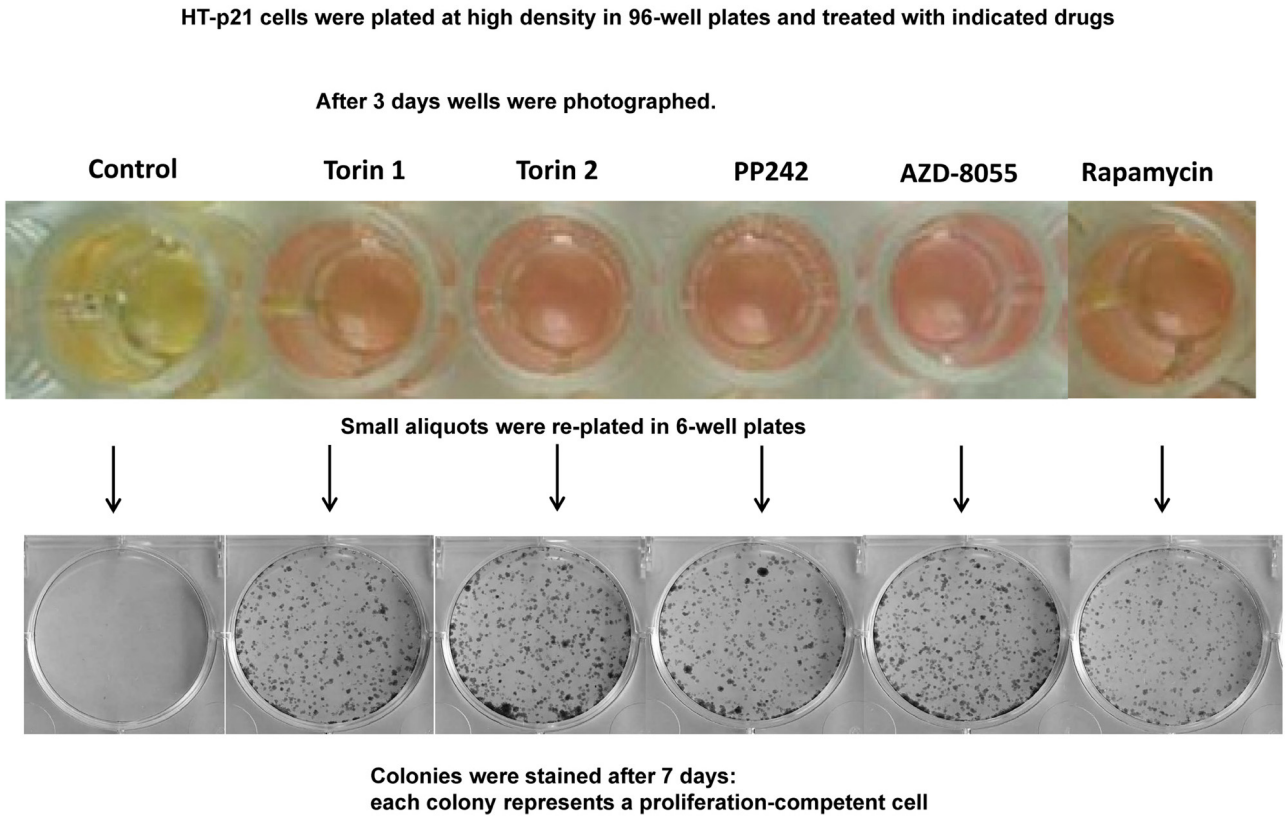

Figure 6. Effect of TOR inhibitors on chronological senescence of cancer HT-p21 cells. Cells were plated at high density in 96-well plates and treated with TOR inhibitors or rapamycin at selected optimal concentrations. After 3 days in culture cells were photographed (color manifests pH of medium), trypsinized and small aliquots were re-plated in 6-well plates. Formed colonies were stained after 7 days in culture with Crystal Violet.

bitors than rapamycin–unlike effects. Preservation of RPP depends on rapamycin-sensitive functions. Inhibition of senescent morphology (SA - beta - Gal staining, hypertrophy, flat morphology) and CLS depends on both rapamycin-sensitive and -insensitive functions of mTOR.

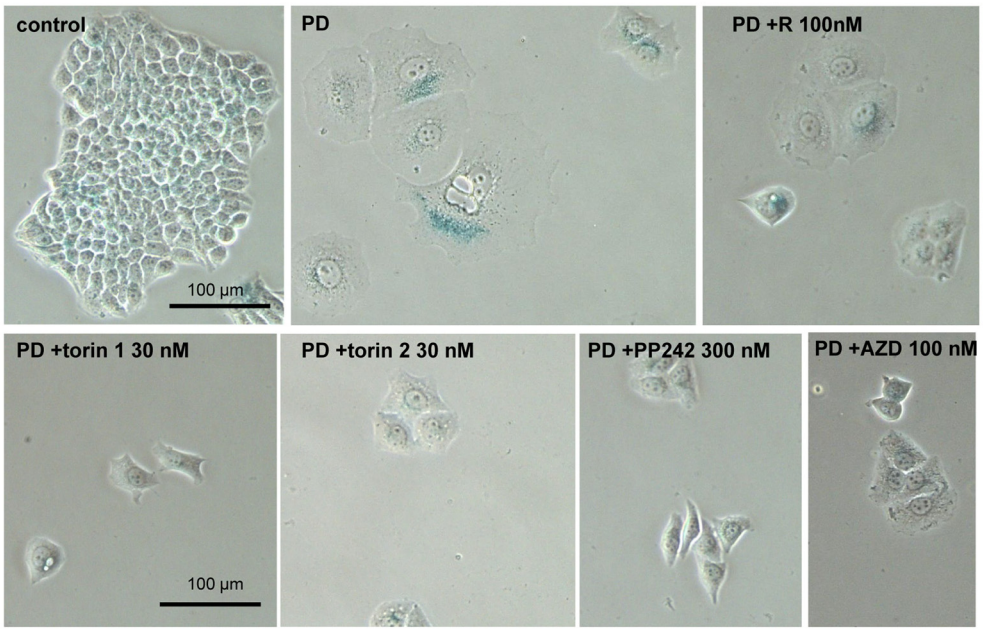

Figure 7. Effect of TORINs on senescent morphology of SKBR3 cells induced to senesce by treatment with PD0332991. Cells were treated with selected concentrations of TORINs and 10 µM PD0332991 (PD). After 4-day treatment drugs were washed out and cells were incubated in drug free medium for 2 days and stained for SA-beta-gal. Bar – 100 µm.

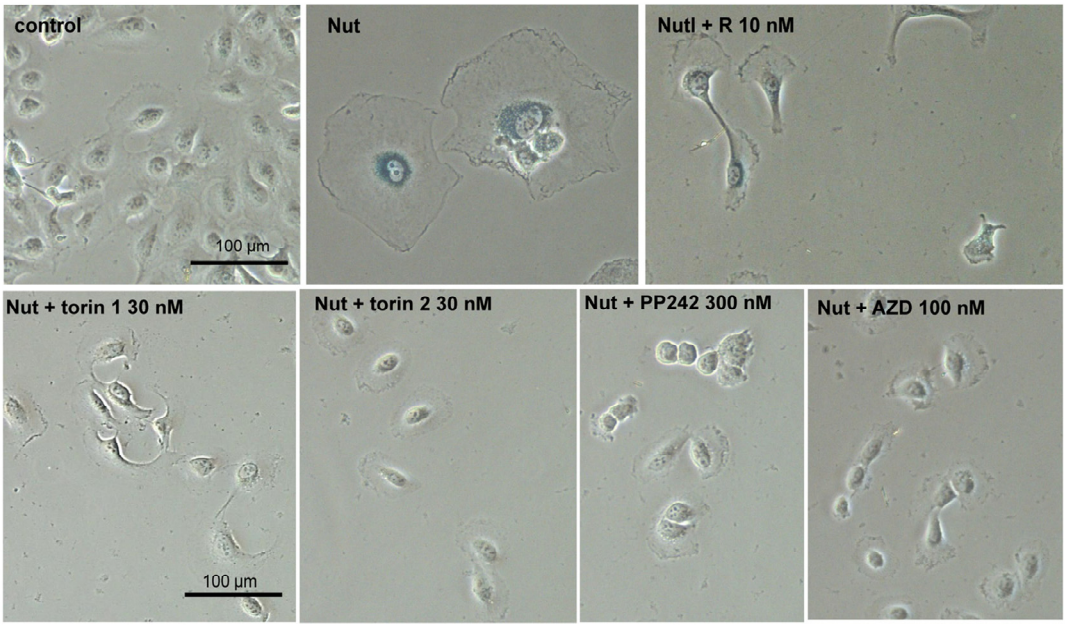

Figure 8. Effect of TORINs on senescent morphology of MEL10 cells undergoing senescence by treatment with nutlin 3a. Cells were treated with nutlin 3a (2.5 µM) and TORINs at selected concentrations or rapamycin (R). After 4-day treatment drugs were washed out and cells were incubated in drug-free medium for another 2 days and stained for SA-beta-gal. Bar – 100 µm. Nut – nutlin 3a; AZD – AZD8085.

At gerosuppressive concentrations, pan-mTOR inhibitors should be tested as anti-aging drugs. Life-long administration of pan-mTOR inhibitors to mice will take several years. Yet, administration of pan-mTOR inhibitors can be started late in life, thus shortening the experiment. In fact, rapamycin is effective when started late in life in mice [9]. Optimal doses and schedules of administration could be selected by administration of pan-mTOR inhibitors to prevent obesity in mice on high fat diet (HFD). It was shown that high doses of rapamycin prevented obesity in mice on HFD even when administrated intermittently [21, 98-100]. Testing anti-obesity effects of pan-mTOR inhibitors will allow investigators to determine their effective doses and schedules within several months. It would be important to test both rapamycin-like agents such as Torin 1 and rapamycin-unlike agent such as Torin 2 or AZD8085. Selected doses and schedules can then be used to extend life-span in both short-lived mice, normal and heterogeneous mice as well as mice on high fat diet. These experiments will address questions of theoretical and practical importance: (a) role of rapamycin-insensitive functions of mTOR in aging. We would learn more about aging and age-related diseases. (b) can pan-mTOR inhibitors extend life span beyond the limits achievable by rapamycin. If successful, such experiments may reveal new causes of death in the absence of mTOR-driven aging, a post-aging syndrome, as mentioned previously [101]. Given that pan-mTOR inhibitors are already undergoing clinical trials for cancer therapy, one can envision their fast application for prevention of age-related diseases by slowing down aging.

MATERIALS AND METHODS

Cell lines and reagents

HT-p21 cells, derived from human fibrosarcoma HT1080, were described previously [69, 76, 81, 102, 103]. In HT-p21 cells, p21 expression can be turned on and off using IPTG (isopropyl-thio-galactosidase). These cells express GFP under CMV promoter. HT-p21 cells were cultured in DMEM/10% FC2 serum (HyClone FetaClone II; Thermo Scientific). Melanoma cell line MEL10 and breast adenocarcinoma SKBR3 (ATCC, Manassas, VA) were maintained in DMEM/10% FBS.

Rapamycin was purchased from LC Laboratories (Woburn, MA). Pan-mTOR inhibitors (torin 1, torin 2, PP242, AZD8085, KU-0063794, GSK1059615) and PD0332991 were from Selleckchem (Houston, TX). Stock solutions were prepared in DMSO.

Re-proliferative potential (RPP)

HT-p21 cells were plated at low densities and treated with IPTG alone or in combination with mTOR inhibitors as described in figure legends. After 3-4 days, IPTG and drugs were washed out and cells were allowed to re-proliferate in drug free medium for 7 days and counted in triplicates.

Immunoblot analysis

Cells were lysed using boiling lysis buffer (1% SDS, 10 mM Tris.HCl, pH7.4). Protein concentrations were measured using BCA protein reagent (Thermo Scientific) and equal amounts of protein were separated on 10% or gradient polyacrylamide gels and transferred onto PVDF membranes [69, 81]. The following antibodies were used: rabbit antibodies against phospho-pS6K(T389), phospho-S6(S235/236) and phospho-S6(S240/244), S6K, phospho-4EBP1(T37/46), phospho-AKT(S473) and phospho-AKT(T308), AKT and mouse anti-S6 – from Cell Signaling Technology (Danvers, MA); mouse monoclonal antibodies against cyclin D1 and rabbit anti-actin were from Santa Cruz Biotechnology (Paso Robles, CA) and Sigma-Aldrich (St. Louis, MO), respectively.

SA-β-galactosidase staining

β-gal staining was performed using Senescence-galactosidase staining kit from Cell Signaling Technology according to manufacturer's protocol. Cells were microphotographed under light microscope [69, 73].

CLS in mammalian cells

Cells were plated at high density in 96-well plates. After 3 days, cells were trypsinized and a small aliquot of attached cells was re-plated at low density in 6-well plates in fresh medium. After 7 days in culture colonies were stained with 1% Crystal Violet (Sigma-Aldrich) [83].

Oil Red O staining

0.35% Oil Red O (Sigma-Aldrich) stock was prepared in isopropanol. Working solution was prepared fresh before use by mixing 3 parts of Oil Red O stock with 2 parts of water and incubating it at RT for 20 min followed by filtering through 0.2 μm filter. Cells were washed with PBS and incubated in 10% formalin at RT for 10 min and then with refreshed formalin for another 1 h followed by two washes in ddH_2O. Fixed cells were incubated in 60% isopropanol for 5 min at RT followed

by incubation with working solution of Oil Red O for 20 min. After extensive washes in ddH_2O, cells were microphotographed under light microscope.

CONFLICTS OF INTEREST

The authors have no conflict of interests to declare.

FUNDING

This work was supported by Roswell Park Cancer Institute fund.

REFERENCES

1. Kaeberlein M, Powers RW 3rd, Steffen KK, Westman EA, Hu D, Dang N, Kerr EO, Kirkland KT, Fields S, Kennedy BK. Regulation of yeast replicative life span by TOR and Sch9 in response to nutrients. Science. 2005; 310:1193–96. doi: 10.1126/science.1115535

2. Powers RW 3rd, Kaeberlein M, Caldwell SD, Kennedy BK, Fields S. Extension of chronological life span in yeast by decreased TOR pathway signaling. Genes Dev. 2006; 20:174–84. doi: 10.1101/gad.1381406

3. Kapahi P, Zid BM, Harper T, Koslover D, Sapin V, Benzer S. Regulation of lifespan in Drosophila by modulation of genes in the TOR signaling pathway. Curr Biol. 2004; 14:885–90. doi: 10.1016/j.cub.2004.03.059

4. Scialò F, Sriram A, Naudí A, Ayala V, Jové M, Pamplona R, Sanz A. Target of rapamycin activation predicts lifespan in fruit flies. Cell Cycle. 2015; 14:2949–58. doi: 10.1080/15384101.2015.1071745

5. Moskalev AA, Shaposhnikov MV. Pharmacological inhibition of phosphoinositide 3 and TOR kinases improves survival of Drosophila melanogaster. Rejuvenation Res. 2010; 13:246–47. doi: 10.1089/rej.2009.0903

6. Bjedov I, Toivonen JM, Kerr F, Slack C, Jacobson J, Foley A, Partridge L. Mechanisms of life span extension by rapamycin in the fruit fly Drosophila melanogaster. Cell Metab. 2010; 11:35–46. doi: 10.1016/j.cmet.2009.11.010

7. Danilov A, Shaposhnikov M, Plyusnina E, Kogan V, Fedichev P, Moskalev A. Selective anticancer agents suppress aging in Drosophila. Oncotarget. 2013; 4:1507–26. doi: 10.18632/oncotarget.1272

8. Robida-Stubbs S, Glover-Cutter K, Lamming DW, Mizunuma M, Narasimhan SD, Neumann-Haefelin E, Sabatini DM, Blackwell TK. TOR signaling and rapamycin influence longevity by regulating SKN-1/Nrf and DAF-16/FoxO. Cell Metab. 2012; 15:713–24. doi: 10.1016/j.cmet.2012.04.007

9. Harrison DE, Strong R, Sharp ZD, Nelson JF, Astle CM, Flurkey K, Nadon NL, Wilkinson JE, Frenkel K, Carter CS, Pahor M, Javors MA, Fernandez E, Miller RA. Rapamycin fed late in life extends lifespan in genetically heterogeneous mice. Nature. 2009; 460:392–95. doi: 10.1038/nature08221

10. Anisimov VN, Zabezhinski MA, Popovich IG, Piskunova TS, Semenchenko AV, Tyndyk ML, Yurova MN, Antoch MP, Blagosklonny MV. Rapamycin extends maximal lifespan in cancer-prone mice. Am J Pathol. 2010; 176:2092–97. doi: 10.2353/ajpath.2010.091050

11. Anisimov VN, Zabezhinski MA, Popovich IG, Piskunova TS, Semenchenko AV, Tyndyk ML, Yurova MN, Rosenfeld SV, Blagosklonny MV. Rapamycin increases lifespan and inhibits spontaneous tumorigenesis in inbred female mice. Cell Cycle. 2011; 10:4230–36. doi: 10.4161/cc.10.24.18486

12. Wilkinson JE, Burmeister L, Brooks SV, Chan CC, Friedline S, Harrison DE, Hejtmancik JF, Nadon N, Strong R, Wood LK, Woodward MA, Miller RA. Rapamycin slows aging in mice. Aging Cell. 2012; 11:675–82. doi: 10.1111/j.1474-9726.2012.00832.x

13. Comas M, Toshkov I, Kuropatwinski KK, Chernova OB, Polinsky A, Blagosklonny MV, Gudkov AV, Antoch MP. New nanoformulation of rapamycin Rapatar extends lifespan in homozygous p53-/- mice by delaying carcinogenesis. Aging (Albany NY). 2012; 4:715–22. doi: 10.18632/aging.100496

14. Komarova EA, Antoch MP, Novototskaya LR, Chernova OB, Paszkiewicz G, Leontieva OV, Blagosklonny MV, Gudkov AV. Rapamycin extends lifespan and delays tumorigenesis in heterozygous p53+/- mice. Aging (Albany NY). 2012; 4:709–14. doi: 10.18632/aging.100498

15. Ramos FJ, Chen SC, Garelick MG, Dai DF, Liao CY, Schreiber KH, MacKay VL, An EH, Strong R, Ladiges WC, Rabinovitch PS, Kaeberlein M, Kennedy BK. Rapamycin reverses elevated mTORC1 signaling in lamin A/C-deficient mice, rescues cardiac and skeletal muscle function, and extends survival. Sci Transl Med. 2012; 4:144ra103. doi: 10.1126/scitranslmed.3003802

16. Livi CB, Hardman RL, Christy BA, Dodds SG, Jones D, Williams C, Strong R, Bokov A, Javors MA, Ikeno Y, Hubbard G, Hasty P, Sharp ZD. Rapamycin extends life span of Rb1+/- mice by inhibiting neuroendocrine tumors. Aging (Albany NY). 2013; 5:100–10. doi: 10.18632/aging.100533

17. Miller RA, Harrison DE, Astle CM, Fernandez E, Flurkey K, Han M, Javors MA, Li X, Nadon NL, Nelson JF, Pletcher S, Salmon AB, Sharp ZD, et al. Rapamycin-

mediated lifespan increase in mice is dose and sex dependent and metabolically distinct from dietary restriction. Aging Cell. 2014; 13:468–77. doi: 10.1111/acel.12194

18. Popovich IG, Anisimov VN, Zabezhinski MA, Semenchenko AV, Tyndyk ML, Yurova MN, Blagosklonny MV. Lifespan extension and cancer prevention in HER-2/neu transgenic mice treated with low intermittent doses of rapamycin. Cancer Biol Ther. 2014; 15:586–92. doi: 10.4161/cbt.28164

19. Zhang Y, Bokov A, Gelfond J, Soto V, Ikeno Y, Hubbard G, Diaz V, Sloane L, Maslin K, Treaster S, Réndon S, van Remmen H, Ward W, et al. Rapamycin extends life and health in C57BL/6 mice. J Gerontol A Biol Sci Med Sci. 2014; 69:119–30. doi: 10.1093/gerona/glt056

20. Fok WC, Chen Y, Bokov A, Zhang Y, Salmon AB, Diaz V, Javors M, Wood WH 3rd, Zhang Y, Becker KG, Pérez VI, Richardson A. Mice fed rapamycin have an increase in lifespan associated with major changes in the liver transcriptome. PLoS One. 2014; 9:e83988. doi: 10.1371/journal.pone.0083988

21. Leontieva OV, Paszkiewicz GM, Blagosklonny MV. Weekly administration of rapamycin improves survival and biomarkers in obese male mice on high-fat diet. Aging Cell. 2014; 13:616–22. doi: 10.1111/acel.12211

22. Hasty P, Livi CB, Dodds SG, Jones D, Strong R, Javors M, Fischer KE, Sloane L, Murthy K, Hubbard G, Sun L, Hurez V, Curiel TJ, Sharp ZD. eRapa restores a normal life span in a FAP mouse model. Cancer Prev Res (Phila). 2014; 7:169–78. doi: 10.1158/1940-6207.CAPR-13-0299

23. Fischer KE, Gelfond JA, Soto VY, Han C, Someya S, Richardson A, Austad SN. Health Effects of Long-Term Rapamycin Treatment: The Impact on Mouse Health of Enteric Rapamycin Treatment from Four Months of Age throughout Life. PLoS One. 2015; 10:e0126644. doi: 10.1371/journal.pone.0126644

24. Ye L, Widlund AL, Sims CA, Lamming DW, Guan Y, Davis JG, Sabatini DM, Harrison DE, Vang O, Baur JA. Rapamycin doses sufficient to extend lifespan do not compromise muscle mitochondrial content or endurance. Aging (Albany NY). 2013; 5:539–50. doi: 10.18632/aging.100576

25. Johnson SC, Rabinovitch PS, Kaeberlein M. mTOR is a key modulator of ageing and age-related disease. Nature. 2013; 493:338–45. doi: 10.1038/nature11861

26. Johnson SC, Yanos ME, Kayser EB, Quintana A, Sangesland M, Castanza A, Uhde L, Hui J, Wall VZ, Gagnidze A, Oh K, Wasko BM, Ramos FJ, et al. mTOR inhibition alleviates mitochondrial disease in a mouse model of Leigh syndrome. Science. 2013; 342:1524–28. doi: 10.1126/science.1244360

27. Fang Y, Bartke A. Prolonged rapamycin treatment led to beneficial metabolic switch. Aging (Albany NY). 2013; 5:328–29. doi: 10.18632/aging.100554

28. Spong A, Bartke A. Rapamycin slows aging in mice. Cell Cycle. 2012; 11:845. doi: 10.4161/cc.11.5.19607

29. Blagosklonny MV. Rapamycin extends life- and health span because it slows aging. Aging (Albany NY). 2013; 5:592–98. doi: 10.18632/aging.100591

30. Hurez V, Dao V, Liu A, Pandeswara S, Gelfond J, Sun L, Bergman M, Orihuela CJ, Galvan V, Padrón Á, Drerup J, Liu Y, Hasty P, et al. Chronic mTOR inhibition in mice with rapamycin alters T, B, myeloid, and innate lymphoid cells and gut flora and prolongs life of immune-deficient mice. Aging Cell. 2015; 14:945–56. doi: 10.1111/acel.12380

31. Verlingue L, Dugourd A, Stoll G, Barillot E, Calzone L, Londoño-Vallejo A. A comprehensive approach to the molecular determinants of lifespan using a Boolean model of geroconversion. Aging Cell. 2016; 15:1018–26. doi: 10.1111/acel.12504

32. Stanfel MN, Shamieh LS, Kaeberlein M, Kennedy BK. The TOR pathway comes of age. Biochim Biophys Acta. 2009; 1790:1067–74. doi: 10.1016/j.bbagen.2009.06.007

33. Campistol JM, Eris J, Oberbauer R, Friend P, Hutchison B, Morales JM, Claesson K, Stallone G, Russ G, Rostaing L, Kreis H, Burke JT, Brault Y, et al. Sirolimus therapy after early cyclosporine withdrawal reduces the risk for cancer in adult renal transplantation. J Am Soc Nephrol. 2006; 17:581–89. doi: 10.1681/ASN.2005090993

34. Kauffman HM, Cherikh WS, Cheng Y, Hanto DW, Kahan BD. Maintenance immunosuppression with target-of-rapamycin inhibitors is associated with a reduced incidence of de novo malignancies. Transplantation. 2005; 80:883–89. doi: 10.1097/01.TP.0000184006.43152.8D

35. Euvrard S, Morelon E, Rostaing L, Goffin E, Brocard A, Tromme I, Broeders N, del Marmol V, Chatelet V, Dompmartin A, Kessler M, Serra AL, Hofbauer GF, et al, and TUMORAPA Study Group. Sirolimus and secondary skin-cancer prevention in kidney transplantation. N Engl J Med. 2012; 367:329–39. doi: 10.1056/NEJMoa1204166

36. Bravo-San Pedro JM, Senovilla L. Immunostimulatory activity of lifespan-extending agents. Aging (Albany NY). 2013; 5:793–801. doi: 10.18632/aging.100619

37. Mannick JB, Del Giudice G, Lattanzi M, Valiante NM,

Praestgaard J, Huang B, Lonetto MA, Maecker HT, Kovarik J, Carson S, Glass DJ, Klickstein LB. mTOR inhibition improves immune function in the elderly. Sci Transl Med. 2014; 6:268ra179. doi: 10.1126/scitranslmed.3009892

38. Kennedy BK, Pennypacker JK. Aging interventions get human. Oncotarget. 2015; 6:590–91. doi: 10.18632/oncotarget.3173

39. Blagosklonny MV. Rejuvenating immunity: "anti-aging drug today" eight years later. Oncotarget. 2015; 6:19405–12. doi: 10.18632/oncotarget.3740

40. Ross C, Salmon A, Strong R, Fernandez E, Javors M, Richardson A, Tardif S. Metabolic consequences of long-term rapamycin exposure on common marmoset monkeys (Callithrix jacchus). Aging (Albany NY). 2015; 7:964–73. doi: 10.18632/aging.100843

41. Fan X, Liang Q, Lian T, Wu Q, Gaur U, Li D, Yang D, Mao X, Jin Z, Li Y, Yang M. Rapamycin preserves gut homeostasis during Drosophila aging. Oncotarget. 2015; 6:35274–83.

42. Johnson SC, Yanos ME, Bitto A, Castanza A, Gagnidze A, Gonzalez B, Gupta K, Hui J, Jarvie C, Johnson BM, Letexier N, McCanta L, Sangesland M, et al. Dose-dependent effects of mTOR inhibition on weight and mitochondrial disease in mice. Front Genet. 2015; 6:247. doi: 10.3389/fgene.2015.00247

43. Zaseck LW, Miller RA, Brooks SV. Rapamycin Attenuates Age-associated Changes in Tibialis Anterior Tendon Viscoelastic Properties. J Gerontol A Biol Sci Med Sci. 2016; 71:858–65. doi: 10.1093/gerona/glv307

44. Xue QL, Yang H, Li HF, Abadir PM, Burks TN, Koch LG, Britton SL, Carlson J, Chen L, Walston JD, Leng SX. Rapamycin increases grip strength and attenuates age-related decline in maximal running distance in old low capacity runner rats. Aging (Albany NY). 2016; 8:769–76. doi: 10.18632/aging.100929

45. Bitto A, Ito TK, Pineda VV, LeTexier NJ, Huang HZ, Sutlief E, Tung H, Vizzini N, Chen B, Smith K, Meza D, Yajima M, Beyer RP, et al. Transient rapamycin treatment can increase lifespan and healthspan in middle-aged mice. eLife. 2016; 5:e16351. doi: 10.7554/eLife.16351

46. Lelegren M, Liu Y, Ross C, Tardif S, Salmon AB. Pharmaceutical inhibition of mTOR in the common marmoset: effect of rapamycin on regulators of proteostasis in a non-human primate. Pathobiol Aging Age Relat Dis. 2016; 6:31793. doi: 10.3402/pba.v6.31793

47. Halloran J, Hussong SA, Burbank R, Podlutskaya N, Fischer KE, Sloane LB, Austad SN, Strong R, Richardson A, Hart MJ, Galvan V. Chronic inhibition of mammalian target of rapamycin by rapamycin modulates cognitive and non-cognitive components of behavior throughout lifespan in mice. Neuroscience. 2012; 223:102–13. doi: 10.1016/j.neuroscience.2012.06.054

48. Lesovaya EA, Kirsanov KI, Antoshina EE, Trukhanova LS, Gorkova TG, Shipaeva EV, Salimov RM, Belitsky GA, Blagosklonny MV, Yakubovskaya MG, Chernova OB. Rapatar, a nanoformulation of rapamycin, decreases chemically-induced benign prostate hyperplasia in rats. Oncotarget. 2015; 6:9718–27. doi: 10.18632/oncotarget.3929

49. Kaeberlein M. Rapamycin and ageing: when, for how long, and how much? J Genet Genomics. 2014; 41:459–63. doi: 10.1016/j.jgg.2014.06.009

50. Tuhácková Z, Sovová V, Sloncová E, Proud CG. Rapamycin-resistant phosphorylation of the initiation factor-4E-binding protein (4E-BP1) in v-SRC-transformed hamster fibroblasts. Int J Cancer. 1999; 81:963–69. doi: 10.1002/(SICI)1097-0215(19990611)81:6<963::AID-IJC20>3.0.CO;2-C

51. Diggle TA, Moule SK, Avison MB, Flynn A, Foulstone EJ, Proud CG, Denton RM. Both rapamycin-sensitive and -insensitive pathways are involved in the phosphorylation of the initiation factor-4E-binding protein (4E-BP1) in response to insulin in rat epididymal fat-cells. Biochem J. 1996; 316:447–53. doi: 10.1042/bj3160447

52. Choo AY, Yoon SO, Kim SG, Roux PP, Blenis J. Rapamycin differentially inhibits S6Ks and 4E-BP1 to mediate cell-type-specific repression of mRNA translation. Proc Natl Acad Sci USA. 2008; 105:17414–19. doi: 10.1073/pnas.0809136105

53. Choo AY, Blenis J. Not all substrates are treated equally: implications for mTOR, rapamycin-resistance and cancer therapy. Cell Cycle. 2009; 8:567–72. doi: 10.4161/cc.8.4.7659

54. Kang SA, Pacold ME, Cervantes CL, Lim D, Lou HJ, Ottina K, Gray NS, Turk BE, Yaffe MB, Sabatini DM. mTORC1 phosphorylation sites encode their sensitivity to starvation and rapamycin. Science. 2013; 341:1236566. doi: 10.1126/science.1236566

55. Liu Y, Vertommen D, Rider MH, Lai YC. Mammalian target of rapamycin-independent S6K1 and 4E-BP1 phosphorylation during contraction in rat skeletal muscle. Cell Signal. 2013; 25:1877–86. doi: 10.1016/j.cellsig.2013.05.005

56. Thoreen CC, Kang SA, Chang JW, Liu Q, Zhang J, Gao Y, Reichling LJ, Sim T, Sabatini DM, Gray NS. An ATP-competitive mammalian target of rapamycin inhibitor

reveals rapamycin-resistant functions of mTORC1. J Biol Chem. 2009; 284:8023–32. doi: 10.1074/jbc.M900301200

57. Yellen P, Saqcena M, Salloum D, Feng J, Preda A, Xu L, Rodrik-Outmezguine V, Foster DA. High-dose rapamycin induces apoptosis in human cancer cells by dissociating mTOR complex 1 and suppressing phosphorylation of 4E-BP1. Cell Cycle. 2011; 10:3948–56. doi: 10.4161/cc.10.22.18124

58. Jiang YP, Ballou LM, Lin RZ. Rapamycin-insensitive regulation of 4e-BP1 in regenerating rat liver. J Biol Chem. 2001; 276:10943–51. doi: 10.1074/jbc.M007758200

59. Benjamin D, Colombi M, Moroni C, Hall MN. Rapamycin passes the torch: a new generation of mTOR inhibitors. Nat Rev Drug Discov. 2011; 10:868–80. doi: 10.1038/nrd3531

60. Hassan B, Akcakanat A, Sangai T, Evans KW, Adkins F, Eterovic AK, Zhao H, Chen K, Chen H, Do KA, Xie SM, Holder AM, Naing A, et al. Catalytic mTOR inhibitors can overcome intrinsic and acquired resistance to allosteric mTOR inhibitors. Oncotarget. 2014; 5:8544–57. doi: 10.18632/oncotarget.2337

61. Jacinto E, Loewith R, Schmidt A, Lin S, Rüegg MA, Hall A, Hall MN. Mammalian TOR complex 2 controls the actin cytoskeleton and is rapamycin insensitive. Nat Cell Biol. 2004; 6:1122–28. doi: 10.1038/ncb1183

62. Markman B, Dienstmann R, Tabernero J. Targeting the PI3K/Akt/mTOR pathway--beyond rapalogs. Oncotarget. 2010; 1:530–43. doi: 10.18632/oncotarget.188

63. Chresta CM, Davies BR, Hickson I, Harding T, Cosulich S, Critchlow SE, Vincent JP, Ellston R, Jones D, Sini P, James D, Howard Z, Dudley P, et al. AZD8055 is a potent, selective, and orally bioavailable ATP-competitive mammalian target of rapamycin kinase inhibitor with in vitro and in vivo antitumor activity. Cancer Res. 2010; 70:288–98. doi: 10.1158/0008-5472.CAN-09-1751

64. Guo Y, Kwiatkowski DJ. Equivalent benefit of rapamycin and a potent mTOR ATP-competitive inhibitor, MLN0128 (INK128), in a mouse model of tuberous sclerosis. Mol Cancer Res. 2013; 11:467–73. doi: 10.1158/1541-7786.MCR-12-0605

65. Yu K, Toral-Barza L, Shi C, Zhang WG, Lucas J, Shor B, Kim J, Verheijen J, Curran K, Malwitz DJ, Cole DC, Ellingboe J, Ayral-Kaloustian S, et al. Biochemical, cellular, and in vivo activity of novel ATP-competitive and selective inhibitors of the mammalian target of rapamycin. Cancer Res. 2009; 69:6232–40. doi: 10.1158/0008-5472.CAN-09-0299

66. Blagosklonny MV. Cell cycle arrest is not yet senescence, which is not just cell cycle arrest: terminology for TOR-driven aging. Aging (Albany NY). 2012; 4:159–65. doi: 10.18632/aging.100443

67. Blagosklonny MV. Geroconversion: irreversible step to cellular senescence. Cell Cycle. 2014; 13:3628–35. doi: 10.4161/15384101.2014.985507

68. Demidenko ZN, Korotchkina LG, Gudkov AV, Blagosklonny MV. Paradoxical suppression of cellular senescence by p53. Proc Natl Acad Sci USA. 2010; 107:9660–64. doi: 10.1073/pnas.1002298107

69. Leontieva OV, Natarajan V, Demidenko ZN, Burdelya LG, Gudkov AV, Blagosklonny MV. Hypoxia suppresses conversion from proliferative arrest to cellular senescence. Proc Natl Acad Sci USA. 2012; 109:13314–18. doi: 10.1073/pnas.1205690109

70. Leontieva OV, Demidenko ZN, Blagosklonny MV. S6K in geroconversion. Cell Cycle. 2013; 12:3249–52. doi: 10.4161/cc.26248

71. Leontieva OV, Blagosklonny MV. CDK4/6-inhibiting drug substitutes for p21 and p16 in senescence: duration of cell cycle arrest and MTOR activity determine geroconversion. Cell Cycle. 2013; 12:3063–69. doi: 10.4161/cc.26130

72. Leontieva OV, Blagosklonny MV. Tumor promoter-induced cellular senescence: cell cycle arrest followed by geroconversion. Oncotarget. 2014; 5:12715–27. doi: 10.18632/oncotarget.3011

73. Leontieva OV, Demidenko ZN, Blagosklonny MV. Contact inhibition and high cell density deactivate the mammalian target of rapamycin pathway, thus suppressing the senescence program. Proc Natl Acad Sci USA. 2014; 111:8832–37. doi: 10.1073/pnas.1405723111

74. Zhao H, Halicka HD, Li J, Darzynkiewicz Z. Berberine suppresses gero-conversion from cell cycle arrest to senescence. Aging (Albany NY). 2013; 5:623–36. doi: 10.18632/aging.100593

75. Sousa-Victor P, Gutarra S, García-Prat L, Rodriguez-Ubreva J, Ortet L, Ruiz-Bonilla V, Jardí M, Ballestar E, González S, Serrano AL, Perdiguero E, Muñoz-Cánoves P. Geriatric muscle stem cells switch reversible quiescence into senescence. Nature. 2014; 506:316–21. doi: 10.1038/nature13013

76. Demidenko ZN, Blagosklonny MV. Growth stimulation leads to cellular senescence when the cell cycle is blocked. Cell Cycle. 2008; 7:3355–61. doi: 10.4161/cc.7.21.6919

77. Demidenko ZN, Zubova SG, Bukreeva EI, Pospelov VA, Pospelova TV, Blagosklonny MV. Rapamycin

decelerates cellular senescence. Cell Cycle. 2009; 8:1888–95. doi: 10.4161/cc.8.12.8606

78. Leontieva OV, Demidenko ZN, Blagosklonny MV. Dual mTORC1/C2 inhibitors suppress cellular geroconversion (a senescence program). Oncotarget. 2015; 6:23238–48. doi: 10.18632/oncotarget.4836

79. Sousa-Victor P, García-Prat L, Muñoz-Cánoves P. Dual mTORC1/C2 inhibitors: gerosuppressors with potential anti-aging effect. Oncotarget. 2015; 6:23052–54. doi: 10.18632/oncotarget.5563

80. Walters HE, Deneka-Hannemann S, Cox LS. Reversal of phenotypes of cellular senescence by pan-mTOR inhibition. Aging (Albany NY). 2016; 8:231–44. doi: 10.18632/aging.100872

81. Leontieva OV, Lenzo F, Demidenko ZN, Blagosklonny MV. Hyper-mitogenic drive coexists with mitotic incompetence in senescent cells. Cell Cycle. 2012; 11:4642–49. doi: 10.4161/cc.22937

82. Demidenko ZN, Blagosklonny MV. Quantifying pharmacologic suppression of cellular senescence: prevention of cellular hypertrophy versus preservation of proliferative potential. Aging (Albany NY). 2009; 1:1008–16. doi: 10.18632/aging.100115

83. Leontieva OV, Blagosklonny MV. Yeast-like chronological senescence in mammalian cells: phenomenon, mechanism and pharmacological suppression. Aging (Albany NY). 2011; 3:1078–91. doi: 10.18632/aging.100402

84. Leontieva OV, Blagosklonny MV. M(o)TOR of pseudo-hypoxic state in aging: rapamycin to the rescue. Cell Cycle. 2014; 13:509–15. doi: 10.4161/cc.27973

85. Blagosklonny MV. Aging and immortality: quasi-programmed senescence and its pharmacologic inhibition. Cell Cycle. 2006; 5:2087–102. doi: 10.4161/cc.5.18.3288

86. Blagosklonny MV. An anti-aging drug today: from senescence-promoting genes to anti-aging pill. Drug Discov Today. 2007; 12:218–24. doi: 10.1016/j.drudis.2007.01.004

87. Blagosklonny MV. Paradoxes of aging. Cell Cycle. 2007; 6:2997–3003. doi: 10.4161/cc.6.24.5124

88. Blagosklonny MV. Aging: ROS or TOR. Cell Cycle. 2008; 7:3344–54. doi: 10.4161/cc.7.21.6965

89. Blagosklonny MV. Validation of anti-aging drugs by treating age-related diseases. Aging (Albany NY). 2009; 1:281–88. doi: 10.18632/aging.100034

90. Blagosklonny MV, Hall MN. Growth and aging: a common molecular mechanism. Aging (Albany NY). 2009; 1:357–62. doi: 10.18632/aging.100040

91. Blagosklonny MV. Calorie restriction: decelerating mTOR-driven aging from cells to organisms (including humans). Cell Cycle. 2010; 9:683–88. doi: 10.4161/cc.9.4.10766

92. Blagosklonny MV. Rapamycin and quasi-programmed aging: four years later. Cell Cycle. 2010; 9:1859–62. doi: 10.4161/cc.9.10.11872

93. Blagosklonny MV. Answering the ultimate question "what is the proximal cause of aging?". Aging (Albany NY). 2012; 4:861–77. doi: 10.18632/aging.100525

94. Blagosklonny MV. Aging is not programmed: genetic pseudo-program is a shadow of developmental growth. Cell Cycle. 2013; 12:3736–42. doi: 10.4161/cc.27188

95. Gems D, de la Guardia Y. Alternative Perspectives on Aging in Caenorhabditis elegans: Reactive Oxygen Species or Hyperfunction? Antioxid Redox Signal. 2013; 19:321–29. doi: 10.1089/ars.2012.4840

96. Gems D, Partridge L. Genetics of longevity in model organisms: debates and paradigm shifts. Annu Rev Physiol. 2013; 75:621–44. doi: 10.1146/annurev-physiol-030212-183712

97. Stipp D. A new path to longevity. Sci Am. 2012; 306:32–39. doi: 10.1038/scientificamerican0112-32

98. Chang GR, Chiu YS, Wu YY, Chen WY, Liao JW, Chao TH, Mao FC. Rapamycin protects against high fat diet-induced obesity in C57BL/6J mice. J Pharmacol Sci. 2009; 109:496–503. doi: 10.1254/jphs.08215FP

99. Leontieva OV, Paszkiewicz GM, Blagosklonny MV. Comparison of rapamycin schedules in mice on high-fat diet. Cell Cycle. 2014; 13:3350–56. doi: 10.4161/15384101.2014.970491

100. Makki K, Taront S, Molendi-Coste O, Bouchaert E, Neve B, Eury E, Lobbens S, Labalette M, Duez H, Staels B, Dombrowicz D, Froguel P, Wolowczuk I. Beneficial metabolic effects of rapamycin are associated with enhanced regulatory cells in diet-induced obese mice. PLoS One. 2014; 9:e92684. doi: 10.1371/journal.pone.0092684

101. Blagosklonny MV. Koschei the immortal and anti-aging drugs. Cell Death Dis. 2014; 5:e1552. doi: 10.1038/cddis.2014.520

102. Chang BD, Broude EV, Fang J, Kalinichenko TV, Abdryashitov R, Poole JC, Roninson IB. p21Waf1/Cip1/Sdi1-induced growth arrest is associated with depletion of mitosis-control proteins and leads to abnormal mitosis and endo-reduplication in recovering cells. Oncogene. 2000; 19:2165–70. doi: 10.1038/sj.onc.1203573

103. Broude EV, Swift ME, Vivo C, Chang BD, Davis BM, Kalurupalle S, Blagosklonny MV, Roninson IB. p21(Waf1/Cip1/Sdi1) mediates retinoblastoma

protein degradation. Oncogene. 2007; 26:6954–58.
doi: 10.1038/sj.onc.1210516

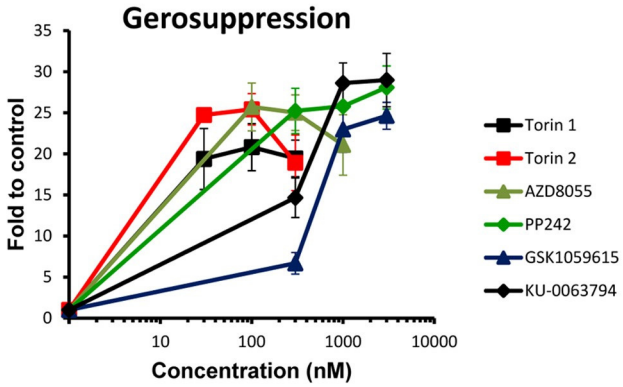

Supplementary Figure S1. Extended concentration ranges of TOR inhibitors to determine maximal optimal dose for gerosuppression in HT-p21 cellular model of senescence. HT-p21 cells were treated with IPTG and different concentrations of indicated TOR inhibitors. After 4 day-treatment, drugs were washed out and cells were incubated in drug-free medium For 7 days and counted. Data are mean ± SD from triplicate wells.

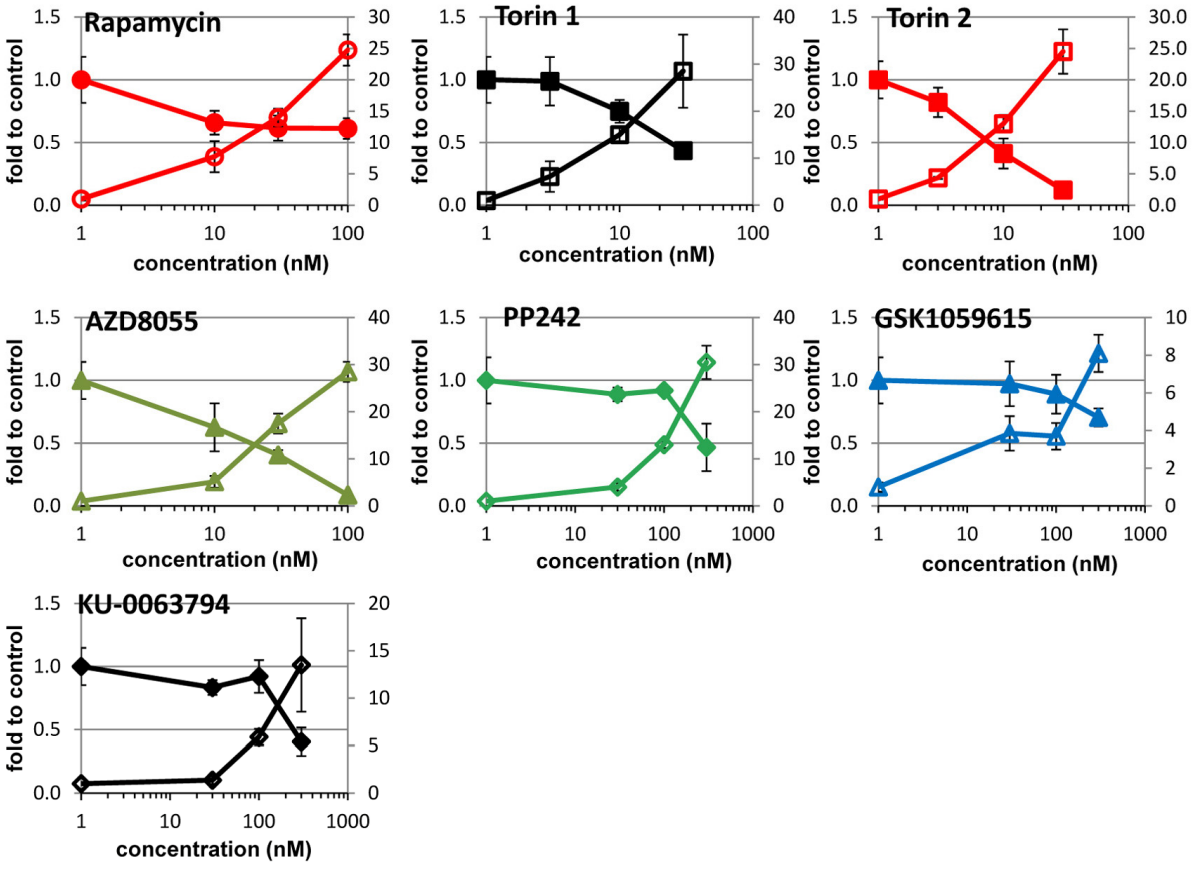

Supplementary Figure S2. Gerosuppressive effect mirrors cytostatic effect. of TOR inhibitors**.** HT-p21 cells were treated with serial dilutions of indicated drugs as described in Figure 1 A (for cytostatic effect, shown as filled markers) and in Fig. 1C (for gerosuppressive effect, shown as empty markers).

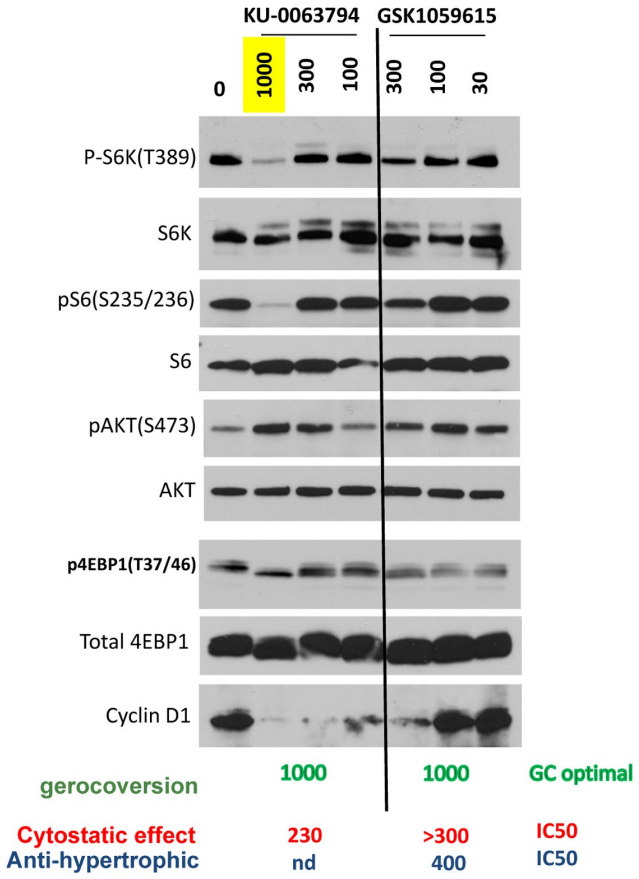

Supplementary Figure S3. HT-p21 cells were treated with range of concentrations of KU-0063794 and GSK1059615 for 24 h and lysed. Data present Immunoblotting with indicated antibodies.

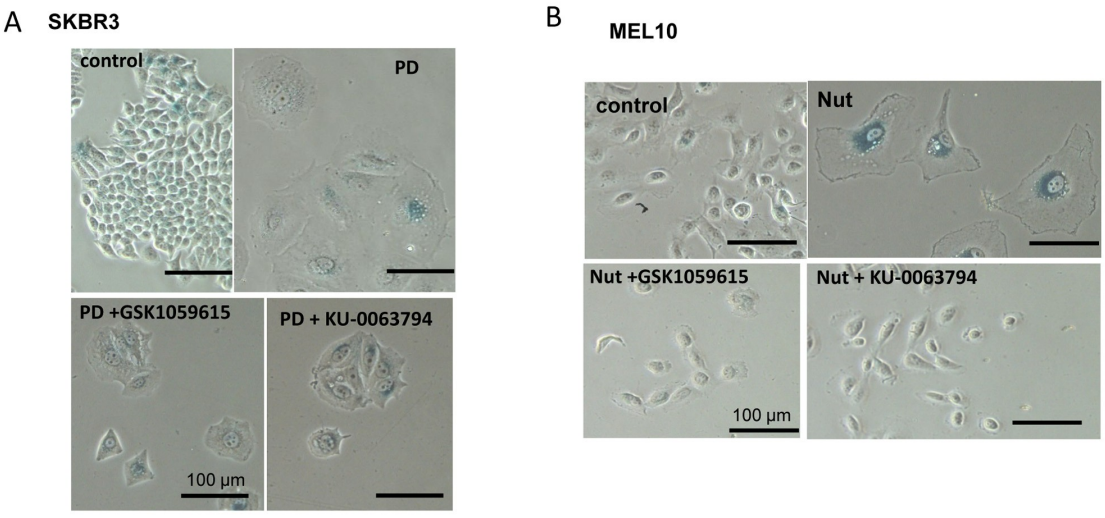

Supplementary Figure S4. Effect of GSK1059615 and KU-0063794 on senescent morphology of SKBR3 (A) and MEL10 (B) cells. SKBR3 and MEL10 cells were induced to senesce by treatment with 10 µM PD0332991 (PD) or 2.5 µM nutlin 3a (Nut), respectively. Co-treatment with either 1000 nM of GSK1059615 or KU-0063794 prevent senescent morphology in these cells.

Research Paper

Identification of *Salvia haenkei* as gerosuppressant agent by using an integrated senescence-screening assay

Ivana Matic[1,3], Ajinkya Revandkar[8], Jingjing Chen[8], Angela Bisio[2], Stefano Dall'Acqua[5], Veronica Cocetta[5], Paola Brun[6], Giorgio Mancino[3], Martina Milanese[7], Maurizio Mattei[4], Monica Montopoli[5], Andrea Alimonti[1,8]

[1]Laboratory for Research and Development in Aging, Atrahasis S.r.l., 00189 Rome, Italy
[2]Department of Chemistry and Pharmaceutical Technologies, University of Genova, 16126 Genova, Italy
[3]Research Center, San Pietro "Fatebenefratelli", 00189 Rome, Italy
[4]Animal Technology Facility of University Tor Vergata, 00173 Rome, Italy
[5]Department of Pharmaceutical and Pharmacological Sciences, University of Padova, 35121 Padova, Italy
[6]Department of Molecular Medicine, University of Padova, 35121 Padova, Italy
[7]Studio Associato Gaia Snc, 16121 Genova, Italy
[8]Institute of Oncology Research (IOR), Bellinzona CH 6500, Switzerland

Correspondence to: Andrea Alimonti; Monica Montopoli; **email:** andrea.alimonti@ior.iosi.ch ; monica.montopoli@unipd.it
Keywords: senescence-screening assay, senescence, *Salvia haenkei*, PICS, gerosuppressant
Received: August 1, 2016 **Accepted:** November 14, 2016 **Published:** December 1, 2016 doi:10.18632/aging.101076

ABSTRACT

Cellular senescence is a stable cell cycle arrest that is the causative process of aging. The PI3K/AKT/mTOR pathway is implicated in the control of cellular senescence and inhibitors of this pathway have been successfully used for life span prolongation experiments in mammals. PTEN is the major regulator of the PI3K/AKT/mTOR pathway and loss of PTEN promotes a senescence response termed PICS. Here we report a novel-screening assay, for the identification of compounds that block different types of senescence response. By testing a library of more than 3000 natural and chemical compounds in PTEN deficient cells we have found that an extract from *Salvia haenkei* (SH), a native plant of Bolivia is a potent inhibitor of PICS. SH also decreases replicative and UV-mediated senescence in human primary fibroblasts and in a model of *in vitro* reconstructed human epidermis. Mechanistically, SH treatment affects senescence driven by UV by interfering with IL1-α signalling. Pre-clinical and clinical testing of this extract by performing toxicity and irritability evaluation *in vitro* also demonstrate the safety of SH extract for clinical use as anti-aging skin treatment.

INTRODUCTION

Cells continually experience stress and damage from exogenous and endogenous sources, and their responses range from complete recovery to senescence and cell death [1]. Proliferating cells cannot divide indefinitely due to the progressive shortness of their telomeres and after almost 60 population doublings (Hayflick limit) they stop to grow while remaining metabolically active [1]. Cells can also become senescent prematurely as a result of stressful events such as oncogene over-expression and exposure to DNA damage (for example induced by UV radiation), or oxidative stress (ROS). This phenomenon, referred as premature senescence, occurs rapidly after the triggering event and is a mechanism implicated in cancer and aging. Recent studies have identified a novel type of cellular senescence response that occurs rapidly after inactivation of PTEN, the major regulator of the PI3K/AKT/mTOR pathway in both mouse and human primary cells [2]. Senescence driven by loss of PTEN is mediated by activation of mTOR that actively translate

p53, a potent inducer of senescence [2]. Activation of the PI3K/AKT/mTOR pathway independent of PTEN loss is also implicated in replicative senescence, and inhibition of mTOR was shown to prevent ageing in different experimental *in vivo* models [3-6]. Interestingly, rapamycin and metformin two potent mTOR inhibitors, suppress geroconversion, prevent cancer and have minor side effects when administered long-term in anti-aging doses [7-22]. Activation of the PI3K/AKT pathway is also implicated in UV induced cellular senescence, a phenomenon known as photo ageing. Recent findings show that UV irradiation can activate AKT and mTOR, thus boosting senescence and photo aging [23-26]. Considering the need for cost effective active agents that prevent or arrest cellular senescence, efforts have been made to develop an assay for the identification of novel anti-senescence compounds [27, 28]. Natural compounds represent an extraordinary inventory of high diversity structural scaffolds that can offer promising candidates in the major healthcare challenge of delaying ageing [29]. Plant extracts provide a substantial source of potentially active compounds, however so far only few natural compounds have been reported to have anti-senescence effects [30-34]. Based on our previous research results [2], we developed an assay that uses *Pten* null cells as a tool to rapidly identify compounds that decrease senescence in primary cells. Positive hits are later on tested in human primary cells to validate their anti-senescence efficacy in replicative and UV-mediated senescence assays.

Here, we report the results of the screening of more than 3000 substances of both natural (plants and marine extracts) and chemical source. Our data demonstrate that an extract derived from the *Salvia haenkei* (SH) plant is a strong inhibitor of senescence driven by loss of *Pten*, senescence associated to replicative stress and photo aging, both in mouse and human primary cells. Furthermore, we have evaluated *in vitro* the toxicity and irritability of SH on a model of reconstructed human epidermis (EpiSkin) demonstrating SH safety for the human skin and anti-senescence activity.

RESULTS

A screening platform for the identification of anti-senescence compounds

Loss of *Pten* drives a cellular senescence response in primary cells termed *Pten* loss induced cellular senescence (PICS) [2]. We have recently developed an effective method for identification of pro-senescence compounds to be used for cancer therapy [35]. By modifying this screening assay, we developed a screening platform, for identification of compounds with anti-senescence activity for the treatment of aging and aging-related disorders (Fig. 1). As previously reported [2], upon inactivation of *Pten*, 30-40% of the cells undergo to senescence within 4 days. This provides a screening window to identify hits that affect senescence in a short time frame, something that would be complicated by using a different senescence assay (e.g. replicative senescence). Compounds that decreased the percentage of senescent cells in the screening platform were designated as anti-senescence compounds based on two parameters: 1) cell proliferation and 2) inhibition of SA-β-galactosidase staining (SA-β-gal), a prototypical senescence marker [36]. For the identification of new anti-senescence hits, the library was created from 3065 substances comprising 1) chemical molecules (2500) 2) blue marine extracts (252) 3) plant extracts (313) as reported in Fig. 1a. *Pten* lx/lx MEFs were infected with a retro-viral Cre vector to delete *Pten* and selected for two days with puromycin to obtain *Pten-/-* MEFs (t0). Experimentally, the screening was carried out in three steps using *Pten-/-* MEFs (Fig. 1b and Supplementary Fig. S1a). In the first step, compounds were studied in triplicates using a single concentration (10 μg/ml). Cells were treated for 5 days from t0. Candidate compounds that increased the cell growth rate of more than 30% compared to control (n=80/3065), were considered as potentially anti-senescent hits and were retested in triplicate. Validated hits (n=54/80) were tested for SA-β-galactivity subsequently. Compounds that decreased the SA-β-gal staining more than 30% (compared to DMSO treated *Pten*$^{-/-}$ cells), passed this filter. Among these hits there were 11 extracts from plants, sponges and marine bacteria and 5 chemical compounds, demonstrating that nature is a valuable source of biologically active phytochemicals that can slow down senescence (Fig. 1c, d). Interestingly, 1/16 hit was plant extract of Angelica whereas, 8/16 hits were plant extracts of Salvias, the largest genus of plants in the family Lamiaceae, with the number of species estimated to range from 700 to nearly 1,000 members. 2/16 hits were from a sponge extract and a marine bacterium associated to a sponge respectively, whereas 5/16 hits were small molecule inhibitors (Supplementary Table S1a). The most potent of these hits was an extract of *Salvia haenkei* (SH) a member of the family of Salvias, native of Bolivia. SH decreased senescence of 50% when compared to untreated control, by-passing the growth arrest promoted by *Pten* loss (Fig. 2a-d). Interestingly, *Pten* null cells treated with SH had a growth rate similar to *Pten* wt cells. *Pten* wt cells also, did not significantly increase proliferation after SH treatment when compared to vehicle treated control (Supplementary Fig. S1b). HPLC analysis revealed that SH extract contained high levels of apigenin and luteolin glycosides, two flavonoids with anti-cancer

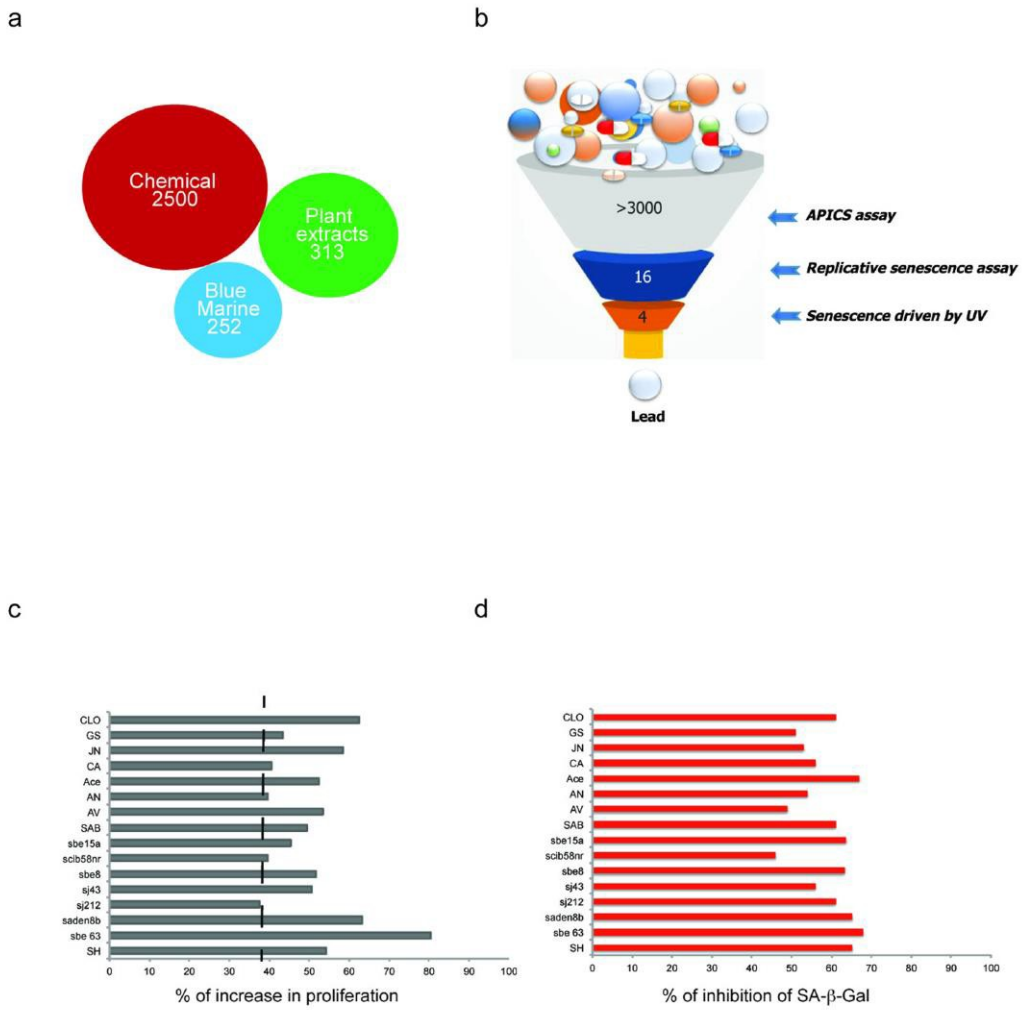

Figure 1. Schematic representation of the platform for the *in vitro* identification of anti-senescent compounds. (**a**) Number of chemical and natural extracts from the plants and blue marine ecosystem used for the screening. (**b**) Schematic representation of the screening steps. (**c-d**) Cytostatic and cytotoxic compounds were excluded from the screening and only anti-senescence hits progressed. Compounds that induced a statistically significant increase (of 40% or more) in cell growth were considered potential anti-senescent candidates. Instead, compounds that induced a statistically significant decrease in cell number were considered pro-senescent (40% to 60% decrease), and cytotoxic (more than 60% decrease).

properties [37] (Supplementary Fig. S1c and Supplementary Table S1b).

Identification of compounds that prevent replicative and radiation-driven senescence

To assess whether identified hits decrease replicative senescence *in vitro*, we used human dermal fibroblasts. To this extent we carried on a series of experiments using the 3T3 protocol in the WI38-CCL75 cells for a period of over 3 months. Cells were plated and subsequently passed and re-plated in the same number every 3 days, in the presence or absence of selected hits. Only four out of 16 hits (2 plants and 2 marine extracts) were able to decrease replicative senescence and were further developed in our screening cascade. Among these extracts, SH showed again the most relevant activity (Supplementary Fig. S2a). As represented in Fig. 3a, while untreated cells stopped growing at passage 30, cells treated with SH continued to proliferate. Moreover, senescence in treated cells was significantly decreased when compared to control as assessed by the SA-β-Gal staining (Fig. 3b). The reduction in the percentage of SA-β-Gal staining in these cells was comparable to the one observed in *Pten* null MEFs showing a correspondence between these two models. Importantly, treatment of cells with SH for a period of three months was not associated to increased cell death, as demonstrated by the cell viability assay (Fig. 3c). Taken together, these data demonstrate that

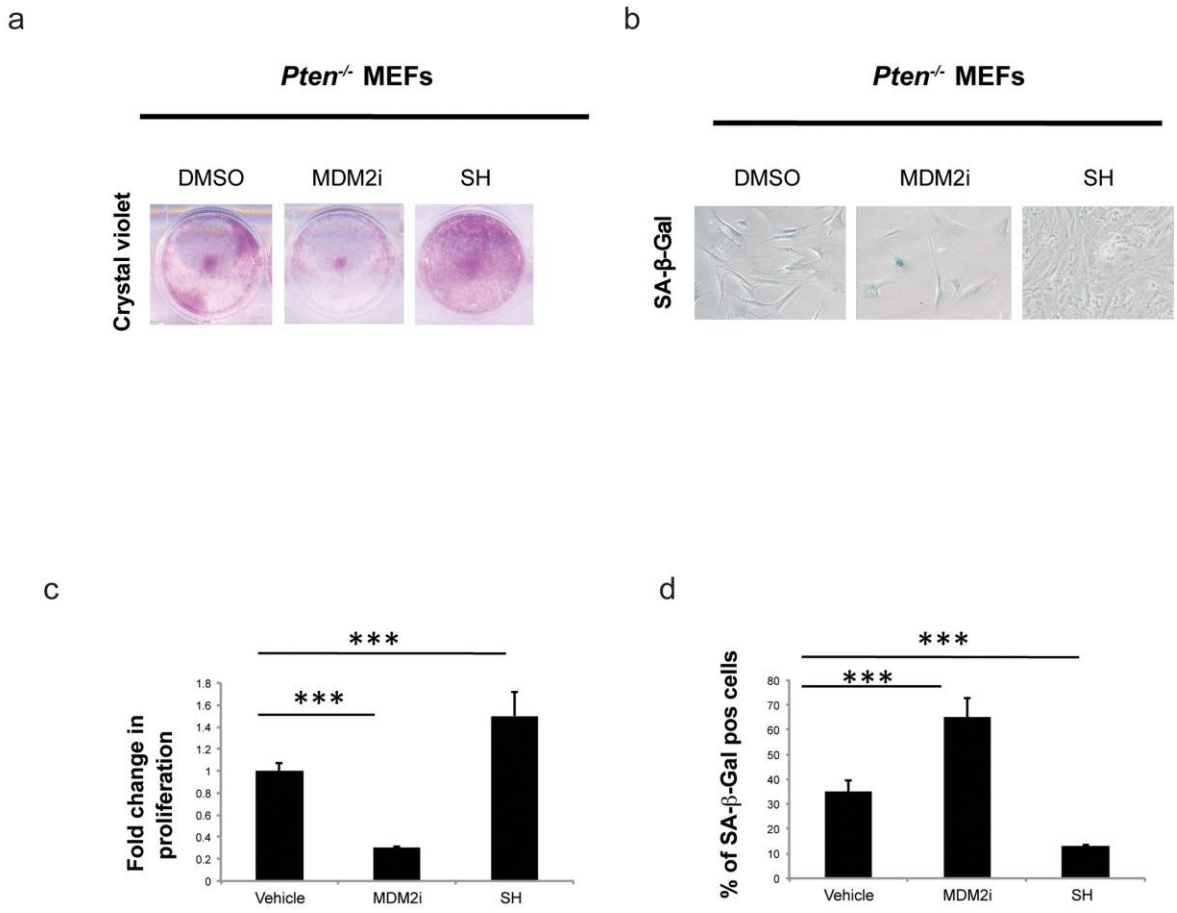

Figure 2. Effect of *S. haenkei* treatment on growth arrest and senescence in Pten-/- MEFs. (**a**) Proliferation of Pten-/- MEFs in culture after 5 days of treatment with *S. haenkei* extract. Pten -/- MEFs were plated in concentration of $2x10^4$ cells/ml and treated for 5 days with 10μM MDM2i (Nutlin-3) or 10μg/ml SH extract. After this period, the proliferation was determined using Crystal violet staining. (**c**) Results are expressed as mean values (+SEM) of absorbance at 590nm for duplicates treated with SH and triplicate for control and Nutlin-3 treated groups, from one representative experiment out of 3 independent experiments. (**b-d**) Senescence of Pten-/- MEFs in culture after 5 days of treatment with *S. haenkei* extract. The graph represents percentage of β-galactosidase positive cells revealed in culture upon 5 day treatment with 10μM MDM2i (Nutlin-3) or 10μg/ml *S. haenkei* extract. Quantifications were done on 4 images (roughly 500 cells) per experiment by determining the ratio of perinuclear blue–positive to perinuclear blue–negative cells. Results are expressed as mean values (+SEM) of cell count in three independent experiments.

SH extract is a potent suppressor of PICS and replicative senescence in human primary dermal fibroblasts. Next, we assessed the anti-senescence activity of SH in an assay of senescence driven by UV irradiation. We set up experimental conditions to induce premature senescence using UV irradiation in WI38-CCL75 human fibroblasts and assess senescence by performing SA-β–Gal staining at 24 and 48 hours after irradiation. SH treatment was able to prevent growth arrest and senescence in irradiated fibroblasts already at 24h after treatment (Fig. 4a, b). At a later time point (48h) the effect of SH resulted even more efficient, mildly stimulating the proliferation of the control cells as well. Taken together, these data demonstrate that SH is a powerful anti-senescence agent in PICS, replicative senescence and cells treated with UV irradiation.

Salvia haenkei extract reduce oxidative stress mediated by H_2O_2

Next, we assessed the efficacy of SH in cells undergoing to oxidative stress. While ROS are produced as a product of normal cellular functioning, excessive amounts can cause deleterious effects. Oxidative stress also promotes cellular senescence and premature aging in the skin [38]. MEFs and human dermal fibroblasts were treated with H_2O_2 - a potent inducer of ROS. The antioxidant activity of SH (0.1-10μg/ml) was assayed in

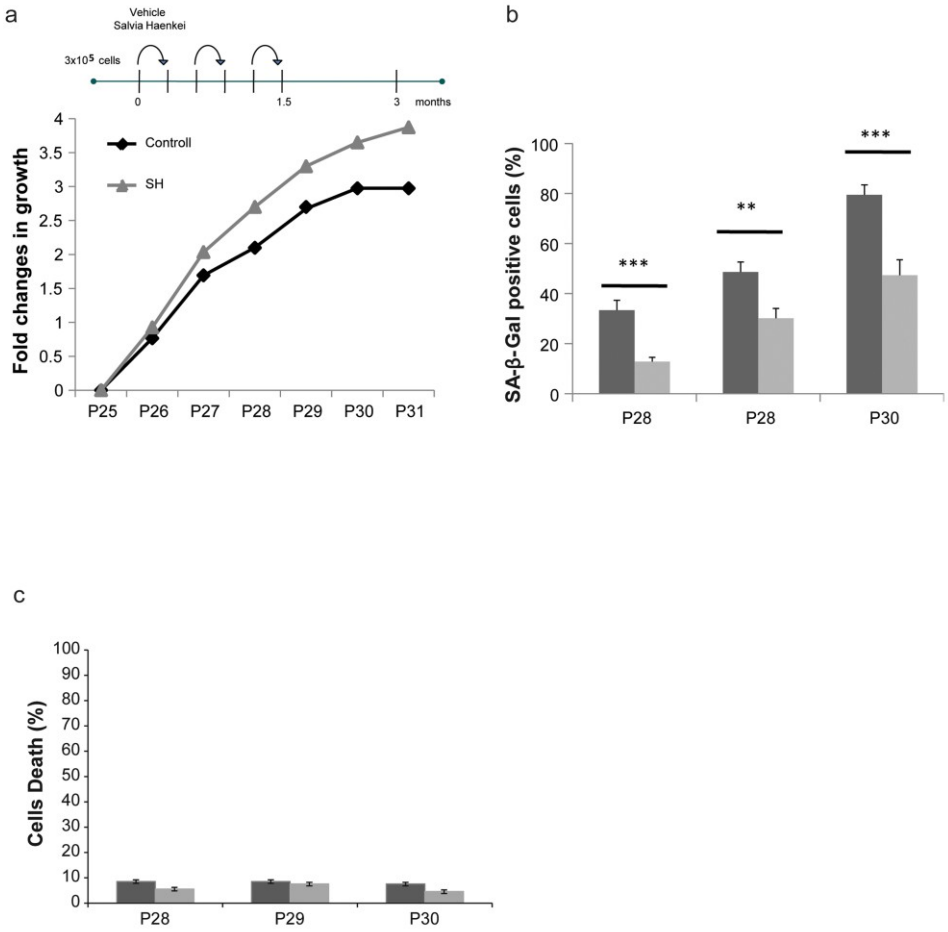

Figure 3. Effect of *S. haenkei* treatment on replicative senescence in human fibroblasts. (**a**) Growth curve of human WI38 fibroblasts treated with *S. haenkei* extract. WI-CCL75 human fibroblasts were plated 300.000 cells per 10cm dish, and subsequently passed and replated in the same number every 3 days for total of 24 passages up to the point when treatment with *S. haenkei* was initiated. At passage 25, cells were plated at the same number 300.000 cells per plate, and treated with 10μg/ml SH extract. Every 3 days cell number was determined by Trypan blue staining and cells replated 300.000 per plate and re-treated. Results are expressed as fold change in cell number from one representative experiment out of 4 independent experiments. (**b**) Senescence of human WI38 fibroblasts treated with *S. haenkei* extract. The graph represents percentage of β-galactosidase positive cells revealed in culture at each passage. Quantifications were done on 4 images (roughly 500 cells) per experiment by determining the ratio of perinuclear blue–positive to perinuclear blue–negative cells. Results are expressed as mean values (+SEM) of cell count in four independent experiments. (**c**) Cell death in culture of human WI38 fibroblasts upon treatment with *S. haenkei* extract. The graph represents percentage of Trypan blue positive (dead) cells revealed in culture at each passage. Quantifications were done on one experimental image (roughly 100 cells) in one representative experiment.

MEFs and human fibroblasts immediately after the exposure to H_2O_2. Interestingly, SH treatment in MEFs reduced the intracellular levels of ROS both in untreated cells and in cells treated with H_2O_2. The effect of SH in these cells was similar to that of N-acetylcysteine (NAC), a known antioxidant compound clinically used to prevent the accumulation of ROS in different inflammatory conditions [39] (Fig. 5a, b). A similar effect was also observed in human fibroblasts treated with and without H_2O_2 (Fig. 5c, d). Taken together, these data demonstrate that SH treatment decreases the intracellular levels of ROS thereby explaining its efficacy in preventing different types of senescence.

Salvia haenkei treatment decreases senescence in a human 3-D skin model (EpiSkin), by interfering with IL1α secretion

To assess the efficacy and safety of SH in a human skin model we took advantage of the EpiSkin model that has been recognized as a valid alternative to animal test procedures [40]. EpiSkin is an *in vitro* reconstructed

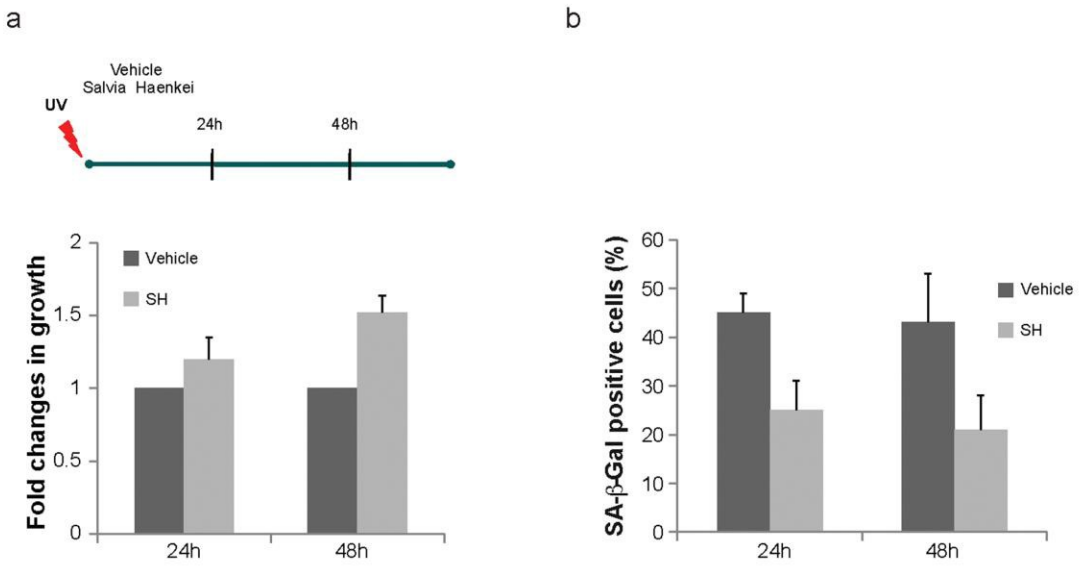

Figure 4. Effect of S. *haenkei* treatment on photo ageing of human fibroblasts. WICCL75 human fibroblasts were irradiated with 30J/m^2 UVB and 3h later treated with 10µg/ml *S. haenkei* extract. (**a**) Proliferation of irradiated human WI38 fibroblasts treated with *S. haenkei* extract. Cell proliferation was measured by Crystal violet staining at time points treatment (10µg/ml) 24h and 48h and represented as fold change in growth (compared to untreated control). Results are expressed as mean values (+SEM) for duplicate in each group in one representative experiment out of three independent experiments. (**b**) Senescence of irradiated human WI38 fibroblasts treated with *S. haenkei* extract. The graph represents percentage of β-galactosidase positive cells revealed in culture at time points 24h and 48h. Quantifications were done on 4 images (roughly 500 cells) per experiment by determining the ratio of perinuclear blue–positive to perinuclear blue–negative cells. Results are expressed as mean values (+SEM) of cell count in three independent experiments.

human epidermis from normal human keratinocytes cultured on a collagen matrix at the air-liquid interface. This model is histologically similar to the *in vivo* human epidermis [41]. To assess the anti-senescence potential and toxicity of SH extract following topical treatment we delivered SH in an oil-in-water conventional skin care vehicle. Human epidermis was treated with UV in the presence or absence of SH (10µg/ml) and SA-β-Gal staining was assessed 42h after treatment. Quantification of SA-β-Gal staining showed that SH decreased the number of senescent cells in the human epidermis validating our previous results (Fig. 6a). Next, we checked the levels of IL-α secreted by the human epidermis in the culture media of samples treated with UV +/- SH. Recent findings demonstrate that IL1α is an essential regulator of paracrine senescence since it can control the senescence-associated secretory phenotype (SASP) [42]. Indeed, senescent cells can release IL1α in the microenvironment to promote senescence in normal cells. This phenomenon has been proposed as the cause of the progressive increase of senescent cells in normal tissues during aging. Surprisingly, SH treatment suppressed also the levels of IL1α released by the human epidermis after treatment with UV and this correlated with a decreased SA-β-Gal staining (Fig. 6a and b). Taken together, these data demonstrate that SH treatment decreases paracrine senescence by interfering with IL1α released by senescent cells. A cell viability assay excluded any cytotoxic activity of SH in cells treated with this compound also in this model (data not shown). Note that as control for this experiment, we used SDS treatment. SDS is an irritant known to promote the secretion of IL1α. Therefore, these data also demonstrate that SH treatment does not irritate human skin at the concentration of 10µg/ml.

DISCUSSION

Cellular senescence is a stable cell growth arrest that occurs in almost all the cells of human tissues during aging [1]. By definition, senescent cells remain arrested even in the presence of growth factors, but are metabolically active and stain positive for SA-β-gal at pH6, a marker of enhanced lysosomal activity [36]. Senescent cells can also release in the tissue microenvironment several factors known collectively as the senescence associated secretory phenotype (SASP)

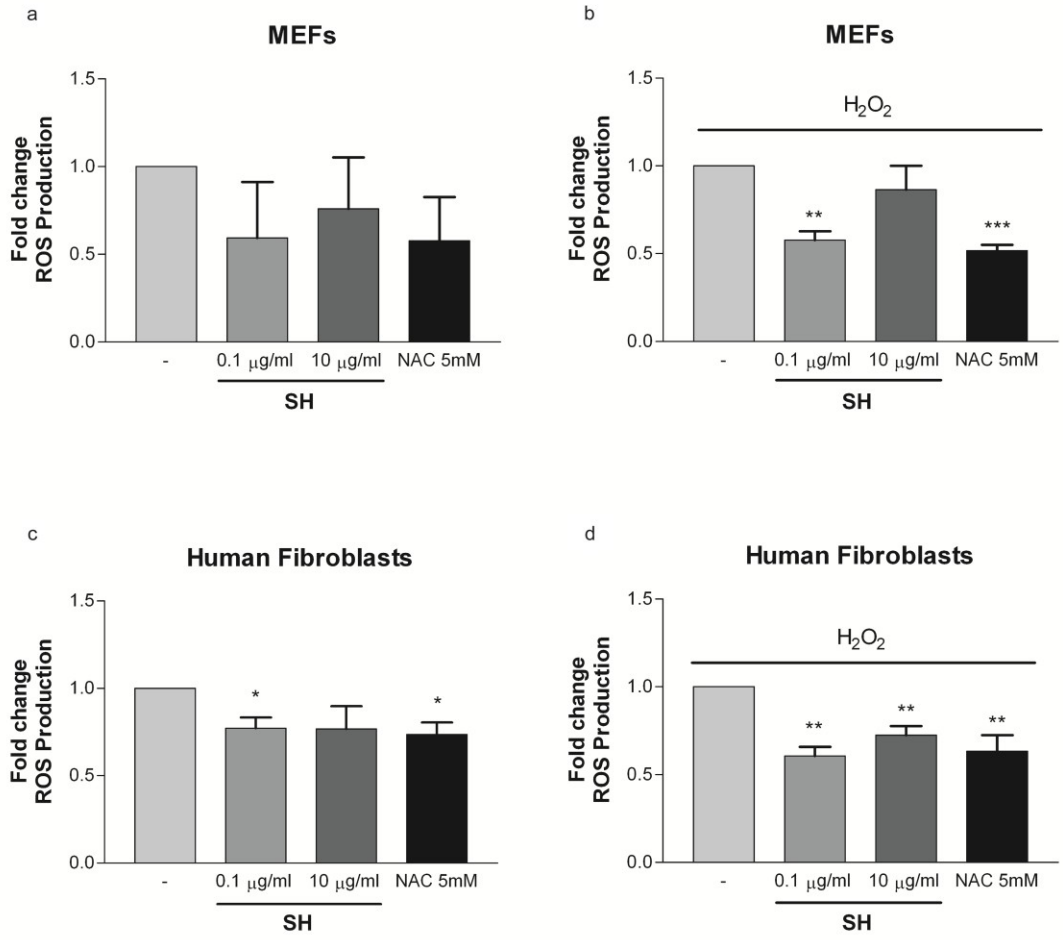

Figure 5. Effect of S. *haenkei* treatment on ROS production on MEFs and human fibroblasts. ROS generation were measured after 3 hours of incubation in untreated cells and after H_2O_2 exposure. Treatment with NAC was used as positive control. Data are expressed as mean ± SEM percentage of basal (100%) DCF fluorescence intensity (FI) of three independent experiments. **p<0.05 treated *vs* untreated. (**a**) ROS production in unstressed MEFs; (**b**) ROS production in MEFs after exposure to H_2O_2; (**c**) ROS production in unstressed human fibroblasts; (**d**) ROS production in human fibroblasts after exposure to H_2O_2.

[1]. These factors can also propagate senescence to neighboring cells, a process known as paracrine senescence. Through the SASP, senescent cells can induce deleterious effects on normal tissues. Mice, whose senescent cells were killed off, were healthier than transgenic mice in which these cells accumulated as effect of aging. Kidneys and heart function in these mice were enhanced; moreover, they were less prone to develop cancers than control animals [43]. Thus, therapies that prevent the accumulation of senescence cells in normal tissues or that selectively kill senescent cells (senolytic therapies) could be used for the treatment of aging and aging associated disorders such as cancer, neurodegenerative and cardiovascular diseases. Eliminating senescent cells could also extend the lifespans of health subjects as recently demonstrated in the mice [43]. We have previously identified a novel type of senescence response, which occurs rapidly after inactivation of PTEN, an essential regulator of the PI3K/AKT/mTOR pathway in both mouse and human cells [2, 44]. Several evidence demonstrates that the PI3K/AKT pathway is implicated in different types of cellular senescence response, including replicative senescence, oncogene-induced senescence (OIS) and photoaging [2, 44, 45]. Inhibition of mTOR, a crucial downstream component of this pathway, attenuates senescence and prolongs the life span of mice [7, 46]. This effect is probably due to the attenuation of the SASP rather than to telomeres preservation as demonstrated by recent findings. Indeed, mTOR inhibition blocks some of the negative effects of the SASP and these compounds may therefore be clinically developed for the prevention of aging or aging related disorders [47, 48]. Currently, there is a high demand for compounds of natural origin that can block senescence to be used as gerosuppressants. Using *Pten* null cells as

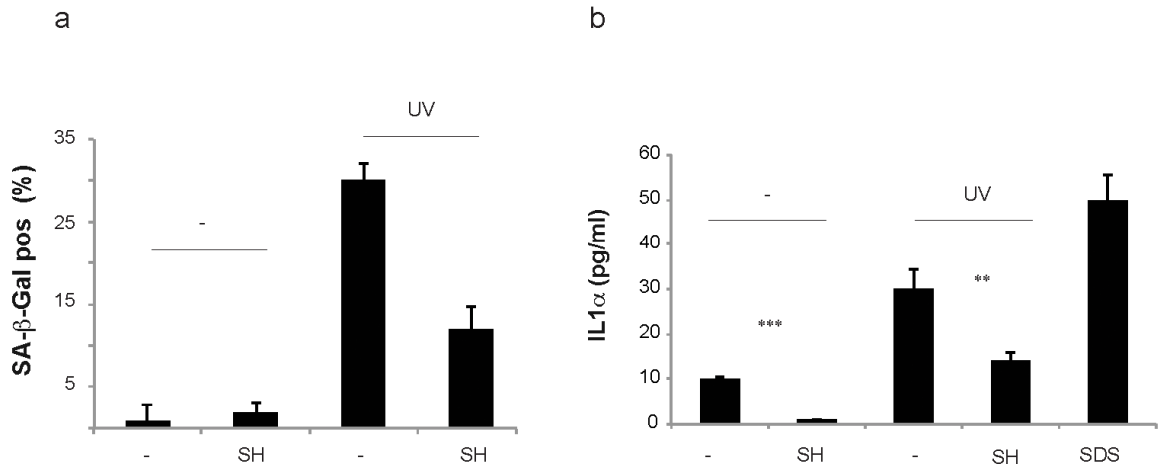

Figure 6. Toxicity and irritability evaluation of *S. haenkei* extract in reconstituted human epidermis. Skin issues were cultured in 12 well plates containing 37°C pre-warmed maintenance media (2 ml/well) and incubated overnight at 37°C, 5% CO_2 and 95% humidity, prior to the experiment. EpiSkin tissues were irradiated with UVB (30J/m^2) and 3 hours later treated by topical application with 10μg/ml *Salvia haenkei* extract and 5% SDS for positive control. 4h later, the epidermis was washed with PBS and left for incubation at 37^{0}C, 5% CO_2. (**a**) 22h after topical application of 10μg/ml of SH on EpiSkin tissues, senescence (bars) was calculated as a percentage of the control for β-galactosidase positive cells. Here, the treatment with UV was used as positive control. Results are expressed as the mean (+SEM) of triplicates in one representative experiment. (**b**) IL1α production by EpiSkin tissue in response to *S. haenkei* treatment in the presence or absence of UV irradiation. Treatment with SDS was used as positive control. 22h after topical application of 10μg/ml of S. *haenkei* extract on EpiSkin tissues, supernatants were collected and samples stored at -80°C. The levels of IL1α were tested by ELISA. Results are represented in logarithmic values (pg/ml) and expressed as mean value±SEM, from triplicates in one experiment.

a model, we have developed a screening assay to identify compounds that block senescence. Inactivation of the tumor suppressor PTEN promotes a strong cellular senescence response that limits the replicative lifespan of primary cells, which exhibit a characteristic enlarged and flattened morphology and increased SA-β-Gal activity. Without ideal means to develop a completely automated screen, we developed a pragmatic semi-automated approach using a high-throughput screening followed by visual assessment of cells of interest, achieved by crystal violet and SA-β-Gal , two standard and accepted assays used to identify senescent cells [49]. The use of these 2 assays in Pten null cells greatly reduces the time and resources required to make the initial identification of potential hits, and although not completely automated, these methods are nonetheless rapid. Herein, we confirm that in contrast to chemical compounds, which showed very little percentage of active anti-senescence compounds, natural compounds affected cellular senescence with much higher rate. The identification of natural compounds as regulators of anti-senescence and anti-oxidant is critical in the discovery of novel therapeutics. Using this screening platform, we have identified *Salvia haenkei* as anti-senescent plant extract and tested it for replicative senescence and photo ageing prevention. Importantly, our experiments in a model of skin human epidermis (EpiSkin) demonstrate that SH extract can decrease the levels of senescence cells by affecting the secretion of IL1α. IL1α is considered the master regulator of the SASP and a recent paper demonstrates that compounds that interfere with IL1 signaling blocks replicative senescence, OIS and PICS [49,50]. Taken together, these data suggest that SH extract may be safely used in a skin-care preparation to prevent skin aging also in consideration of the found SH anti-microbial activity (Supplementary Fig. S2b). Replicative and UV-mediated senescence in skin are responsible of wrinkling, pigment changes, cracking and loss of elasticity among others. Acute dermal overexposure to UV radiation also causes an inflammatory response, erythema and leukocyte infiltration [51]. Oxidative stress initiated by ROS generation is also an important mediator of cellular aging, including skin aging. As demonstrated here, SH treatment also decreased ROS levels in cells treated with H_2O_2 at early and late time points. Finally, experiments in the EpiSkin model also demonstrate that

a skin care preparation containing SH extract is safe and not irritant for the human skin. In sum, our findings describe novel screening assays for the identification of gerosuppressant agents. Previous screenings have reported the identification of anti-aging compounds using different biological systems (e.g. yeast) and assays (e.g. in vitro assays, computer screening). Since the pathways that control aging in mammals have homologs in yeast, flies, and worms, several of these screenings have been performed in invertebrates instead that in mammalian cells [52-54]. These screenings have contributed to the identification of several gerosuppressants active compounds such as rapamycin, metformin and resveratrol whose efficacy have been later on validated in mammalian cells. Our screening based on the use of PTEN deficient mouse embryonic fibroblasts in a first step and in the consecutive validation of positive HITs in human cells offers a promising alternative to these models for the rapid identification of effective gerosuppressants.

MATERIALS AND METHODS

Plant material and preparation of plant extract

The extract of *Salvia haenkei* was kindly provided by Dr. Bisio from Dept. of Chemistry and Pharmaceutical Technologies, University of Genoa, Italy. The plant material was harvested and leaves were put in a ventilated stove at 45°C for 24 hours, and then ground as fine powder using a mixer IKA universal M20. A quantity of 20.0g of powdered dried plant was weighed in a 100ml conical flask to which 70ml of hexane (purity 99%) was added for the pre-extraction. The flask was placed in a bath sonicator (Branson 8210) and sonicated at a temperature of 40°C for 30 minutes. The mixture was filtered with filter paper, followed by washing with 20ml of hexane and then with 50ml of hexane. The filtrate was poured into a flask and the solvent was concentrated under vacuum (about 11mmHg) up to 5-10 ml by rotavapor, using a water bath at 40°C. This residue as poured into a glass container followed by evaporation of the solvent. The filtrate was left open overnight in a well-ventilated hood until complete evaporation of the last traces of solvent. The solids collected on the filter, were divided and air-dried overnight in the hood. The dried material is extracted in the same way with methanol-water (90:10). The dried material from the filters was dissolved in 70ml of 90% methanol. The mixture was sonicated at 40°C for 30 minutes, after being filtered, then washed with 20 ml of 90% methanol. The filtrate was poured into a flask and the solvent completely evaporated under vacuum. The dry extract was dissolved in 90% methanol in the least possible amount of absolute methanol, using sonication and poured into a glass container to evaporate overnight in the hood. The extract was reconstituted with pure DMSO at a concentration of 10mg/ml and kept at -20°C until dilution for the treatment of cell cultures. The SH extract was analysed by HPLC-DAD and HPLC-MS obtaining a phytochemical fingerprint. The identified constituents are summarized in supplementary data (Supplementary Fig. S1c and Supplementary Table S1b).

MEFs isolation

$Pten^{lx/lx}$ MEFs were prepared as previously described [36]. Briefly, pregnant female mice at day 13 postcoitum (assuming as day one the first day the plug was observed) were sacrificed by cervical dislocation. The uterine horns were dissected out, briefly rinsed in 70% (v/v) ethanol and placed into a petri dish containing PBS (Gibco 14190-169, without bivalent cations). Each embryo was separated from its placenta and surrounding membranes, the brain and dark red organs were cut out. Embryos were washed with fresh PBS, removing as much blood as possible. Using a minimal amount of PBS and razor blades, the embryos were finely minced into a suspension of cells to which several ml of trypsin-EDTA (about 1-2ml per embryo, Gibco 25300-096) was added. Following incubation with gentle shaking at 37°C for 15min the resulting cell suspension was pelleted and resuspended in fresh DMEM (ReadyMix, PAA) containing 10% FCS, 2mM L-glutamine, 2mM penicillin, 50µg/ml streptomycin. Cells were plated out at 1 embryo equivalent per 10cm dish ("passage No. 0"). The adherent fibroblasts reached confluence at day 4 when they were collected and stored at -80°C prior to use in the APICS assay (for details of this assay see also Fig. 1 and Supplementary Fig. S1a)

Cell cultures and infections

$Pten^{lx/lx}$ MEFs were isolated as described previously [36]. To produce $Pten^{-/-}$ MEFs, $Pten^{lx/lx}$ MEFs were subsequently infected with a viral vector retro- Cre - recombinase (Adgene Plasmid pMSCV PIG Cre (Cre IRES Puro vector)). This retro-Cre was produced by transfection of Phoenix cells (Eco and Ampho from Life Technologies) at 70-80% confluence using Lipofectamine 2000 (Invitrogen). At 70% confluence, $Pten^{lx/lx}$ MEFs were infected with supernatant from Phoenix cells, collected after 48h of transfection with retro-Cre vector. To increase the efficiency of infection 5µg/ml Polybrene (Santa Cruz) was used. 12h after the first infection, $Pten^{lx/lx}$ MEFs infection was repeated. 24h later, infected $Pten^{lx/lx}$ MEFs were selected with 3µg/ml puromycin. 48h later, $Pten^{-/-}$ were plated and treated with compounds within APICS molecular

screening assay. As control ($Pten^{wt}$) cells in APICS assay we used $Pten^{lx/lx}$MEFs infected with a viral vector retro- PIG (Adgene plasmid pMSCVPIG (Pure IRESGFPvector)), resistant to puromycin, by following the same protocol as described for $Pten^{-/-}$ MEFs. Human WI38-CCL75 fibroblast cell line (ATCC) was used for 3T3 assay and UV irradiation experiments. All cell cultures were maintained in fresh DMEM (ReadyMix, PAA) containing 10% FCS, 2mM L-glutamine, 2mM penicillin, 50µg/ml streptomycin.

Cell proliferation and viability

Cell proliferation was measured using staining with Crystal violet colour (Sigma Aldrich). Cells were per-fixed with 4% formaldehyde for 15min., washed with PBS and stained with 0.1% Crystal violet for 20 minutes. After 3 wash cycles with PBS, cells were lysed in 10% acetic acid and color intensity read at 590nm on SUNRISE ELISA reader (Tecan, Switzerland). Growth curve analysis was carried out as previously described in literature [55]. Cell viability was assessed using Trypan blue exclusion.

SA-β-galactosidase assay

Senescence staining was performed using the commercial Senescence Detection Kit (Calbiochem, #JA7633), designed to histochemically detect β-gal activity in cultured cells at pH 6.0. β-gal at pH 6.0 is present only in senescent cells and is not found in presenescent, quiescent, or immortal cells. Standard protocols were followed [56], and quantifications were done on 4 images (roughly 500 cells) per experiment by determining the ratio of perinuclear blue–positive to perinuclear blue–negative cells. Fluorescent nuclear staining was performed using 4',6-diamidino-2-phenylindole (DAPI), purchased from Sigma Aldrich.

3T3 protocol

Human primary fibroblasts WI38-CCL75 were plated in $10cm^2$ dishes ($3x10^5$cells/dish), and subsequently passed and re-plated in the same number every 3 days for total of 24 passages up to the point when treatment was initiated. At passage 25, cells were plated at the same number and treated with the SH extract in single concentration (10µg/ml). Every 3 days cell number was determined by Trypan blue counting, cells re-plated and re-treated. At passages 28, 29 and 30 senescence was evaluated by measuring β-gal expression.

UV irradiation assay

We tested SH extract for the ability to prevent senescence in a model of UVB irradiated human fibroblast primary cells. To this purpose, WI38-CCL75 human fibroblasts were irradiated with the optimized non cytotoxic dose ($30J/m^2$) of UVB irradiation that causes senescence. 3h after irradiation, positive hits were added in single concentration (10µg/ml). Cell proliferation was determined at different time points using crystal violet assay. Senescence was measured by β-gal expression.

ROS production

ROS were quantified using 2′,7′-dichlorofluorescin-diacetate (H_2-DCF-DA, Sigma-Aldrich), as previously described [57]. Upon cleavage of the acetate groups by intracellular esterase and oxidation, the H_2-DCF-DA is converted to the fluorescent 2',7'-dichlorofluorescein (DCF). Briefly, the cells (5×10^3) were seeded into 96-well plates and allowed to adhere overnight. ROS level was measured after the exposure to SH extract for 3 hours in the absence or presence of H_2O_2, and subsequent addition of 50 µM H_2-DCF-DA, further incubation for 30 min at 37°C and washing with phosphate-buffered saline (PBS). DCF fluorescence intensity was measured at excitation 485 nm—emission 535 nm, using a Multilabel Plate Reader VICTOR X3 (PerkinElmer). Fold increase in ROS production was calculated using the equation: $(F_{treatment}—F_{blank})/(F_{control}—F_{blank})$, where F is the fluorescence reading.

EpiSkinLM

The EpiSkinLM model (LM: large model; manufactured by EPISKIN S.N.C., Lyon, France) is a reconstructed organotypic culture of human adult keratinocytes that reproduce a multilayered and differentiated human epidermis. Briefly, human adult keratinocytes were seeded on a dermal substitute consisting of a collagen I matrix coated with a layer of collagen IV fixed to the bottom of a plastic chamber. Epithelial differentiation was obtained by an air-exposed step leading to a 3-dimensional epidermis construct ($1.07cm^2$ surface), with basal, spinous, granular layers (with specific markers) and a stratum corneum. EpiSkinLM units were delivered to the laboratory within 24 hours after preparation. Upon arrival, tissues were transferred to 12 well plates containing 37°C pre-warmed maintenance media (2 ml/well) and incubated overnight at 37°C, 5% CO_2 and 95% humidity. Skin units were treated with $30J/m^2$ of UVB irradiation. SH extract (10µg/ml) was formulated in a standard oil emulsion and applied topically to the surface of the epidermis. 4h after UV irradiation, the epidermis was washed with PBS and left for incubation at 37°C, 5% CO_2. 42h later, supernatants were collected and stored at -80°C. To assess toxicity of the extract,

cell viability test was performed using MTT assay (In Vitro Toxicology Assay Kit, Sigma Aldrich) (data not shown) and to assess the release of IL-1α, we analysed collected supernatants by ELISA (Abcam) for presence of IL-1α. For the quantification of senescence in the EpiSkinLM modelfrozen sections of skin units (6μm thick) were stained for SA-β-Gal as described above, 42h after irradiation +/- SH treatment at (10μg/ml).

Cytokine assay

Supernatants of EpiSkin epidermis, derived in different conditions (negative control-PBS, positive control-SDS and treatment with SH extract 10μg/ml) were collected and stored at -80^{0}C. IL-1α (limit of sensitivity < 10 pg/ml) levels were determined by ELISA kit (Abcam) according to the manufacturer's specifications. Results are expressed as pg/ml and reported as means from three independent experiments.

Statistical analysis

All values obtained are means of at least three independent experiments performed in duplicate or triplicate. Results are presented as mean value ± SEM. Control and treated groups were compared using the analysis of variance (ANOVA) test. In all analyses, a p-value of <0.05 was considered statistically significant. Data were processed using Assistat (version 7.6b) and Microsoft Excel software.

ACKNOWLEDGEMENTS

The authors wish to thank J. Cadau and Dr. A. Pagetta for their technical and software assistance.

AUTHOR CONTRIBUTIONS

Conceived and designed the experiments: IM, MM, AA. Performed the experiments: IM, AR, JC, AB, MaM, VC, PB, SDA, SC, MI. Analyzed the data: IM, MM, AA. Wrote the paper: IM, MM, AA.

CONFLICTS OF INTEREST

Andrea Alimonti, MD has stock options in Juvenor LLC a skin care company that has developed *Salvia haenkei* extracts as skin care products.

FUNDING

This work was supported by ERC starting grant to AA (nr. 261342). I.M is supported by Grant within the EU project SPECIAL (FP7-KBBE-2010-4-266033). MM is supported from the University of Padova (CPDA124517/12).

REFERENCES

1. Campisi J, d'Adda di Fagagna F. Cellular senescence: when bad things happen to good cells. Nat Rev Mol Cell Biol. 2007; 8:729–40. doi: 10.1038/nrm2233

2. Alimonti A, Nardella C, Chen Z, Clohessy JG, Carracedo A, Trotman LC, Cheng K, Varmeh S, Kozma SC, Thomas G, Rosivatz E, Woscholski R, Cognetti F, et al. A novel type of cellular sense-cence that can be enhanced in mouse models and human tumor xenografts to suppress prostate tumorigenesis. J Clin Invest. 2010; 120:681–93. doi: 10.1172/JCI40535

3. Powers RW 3rd, Kaeberlein M, Caldwell SD, Kennedy BK, Fields S. Extension of chronological life span in yeast by decreased TOR pathway signaling. Genes Dev. 2006; 20:174–84. doi: 10.1101/gad.1381406

4. Jia K, Chen D, Riddle DL. The TOR pathway interacts with the insulin signaling pathway to regulate C. elegans larval development, meta-bolism and life span. Development. 2004; 131:3897–906. doi: 10.1242/dev.01255

5. Kapahi P, Zid BM, Harper T, Koslover D, Sapin V, Benzer S. Regulation of lifespan in Drosophila by modulation of genes in the TOR signaling pathway. Curr Biol. 2004; 14:885–90. doi: 10.1016/j.cub.2004.03.059

6. Vellai T, Takacs-Vellai K, Zhang Y, Kovacs AL, Orosz L, Müller F. Genetics: influence of TOR kinase on lifespan in C. elegans. Nature. 2003; 426:620. doi: 10.1038/426620a

7. Harrison DE, Strong R, Sharp ZD, Nelson JF, Astle CM, Flurkey K, Nadon NL, Wilkinson JE, Frenkel K, Carter CS, Pahor M, Javors MA, Fernandez E, Miller RA. Rapamycin fed late in life extends lifespan in genetically heterogeneous mice. Nature. 2009; 460:392–95. doi: 10.1038/nature08221.

8. Blagosklonny MV. Immunosuppressants in cancer prevention and therapy. OncoImmunology. 2013; 2:e26961. doi: 10.4161/onci.26961

9. Blagosklonny MV. Rejuvenating immunity: "anti-aging drug today" eight years later. Oncotarget. 2015; 6:19405–12. doi: 10.18632/oncotarget.3740

10. Bravo-San Pedro JM, Senovilla L. Immunostimulatory activity of lifespan-extending agents. Aging (Albany NY). 2013; 5:793–801. doi: 10.18632/aging.100619

11. Ross C, Salmon A, Strong R, Fernandez E, Javors M, Richardson A, Tardif S. Metabolic consequences of long-term rapamycin exposure on common marmoset monkeys (Callithrix jacchus). Aging (Albany NY). 2015; 7:964–73.

doi: 10.18632/aging.100843

12. Liu Y, Diaz V, Fernandez E, Strong R, Ye L, Baur JA, Lamming DW, Richardson A, Salmon AB. Rapamycin-induced metabolic defects are reversible in both lean and obese mice. Aging (Albany NY). 2014; 6:742–54. doi: 10.18632/aging.100688

13. Kondratov RV, Kondratova AA. Rapamycin in preventive (very low) doses. Aging (Albany NY). 2014; 6:158–59. doi: 10.18632/aging.100645

14. Fang Y, Bartke A. Prolonged rapamycin treatment led to beneficial metabolic switch. Aging (Albany NY). 2013; 5:328–29. doi: 10.18632/aging.100554

15. Pospelova TV, Leontieva OV, Bykova TV, Zubova SG, Pospelov VA, Blagosklonny MV. Suppression of replicative senescence by rapamycin in rodent embryonic cells. Cell Cycle. 2012; 11:2402–07. doi: 10.4161/cc.20882

16. Blagosklonny MV. TOR-centric view on insulin resistance and diabetic complications: perspective for endocrinologists and gerontologists. Cell Death Dis. 2013; 4:e964. doi: 10.1038/cddis.2013.506

17. Dodds SG, Livi CB, Parihar M, Hsu HK, Benavides AD, Morris J, Javors M, Strong R, Christy B, Hasty P, Sharp ZD. Adaptations to chronic rapamycin in mice. Pathobiol Aging Age Relat Dis. 2016; 6:31688. doi: 10.3402/pba.v6.31688

18. Pellegrini C, Columbaro M, Capanni C, D'Apice MR, Cavallo C, Murdocca M, Lattanzi G, Squarzoni S. All-trans retinoic acid and rapamycin normalize Hutchinson Gilford progeria fibroblast phenotype. Oncotarget. 2015; 6:29914–28. doi: 10.18632/oncotarget.4939.

19. Menendez JA, Joven J. One-carbon metabolism: an aging-cancer crossroad for the gerosup-pressant metformin. Aging (Albany NY). 2012; 4:894–98. doi: 10.18632/aging.100523

20. Verlingue L, Dugourd A, Stoll G, Barillot E, Calzone L, Londono-Vallejo A. A comprehensive approach to the molecular determinants of lifespan using a Boolean model of geroconversion. Aging Cell. 2016; 15:1018–26; Epub ahead of print. doi: 10.1111/acel.12504

21. Kolesnichenko M, Hong L, Liao R, Vogt PK, Sun P. Attenuation of TORC1 signaling delays replicative and oncogenic RAS-induced sense-cence. Cell Cycle. 2012; 11:2391–401. doi: 10.4161/cc.20683

22. Sousa-Victor P, García-Prat L, Muñoz-Cánoves P. Dual mTORC1/C2 inhibitors: gerosuppressors with potential anti-aging effect. Oncotarget. 2015; 6:23052–54. doi: 10.18632/oncotarget.5563

23. Syed DN, Afaq F, Mukhtar H. Differential activation of signaling pathways by UVA and UVB radiation in normal human epidermal keratinocytes. Photochem Photobiol. 2012; 88:1184–90. doi: 10.1111/j.1751-1097.2012.01115.x

24. Zhang QS, Maddock DA, Chen JP, Heo S, Chiu C, Lai D, Souza K, Mehta S, Wan YS. Cytokine-induced p38 activation feedback regulates the prolonged activation of AKT cell survival pathway initiated by reactive oxygen species in response to UV irradiation in human keratinocytes. Int J Oncol. 2001; 19:1057–61.

25. Cao C, Wan Y. Parameters of protection against ultraviolet radiation-induced skin cell damage. J Cell Physiol. 2009; 220:277–84. doi: 10.1002/jcp.21780

26. Strozyk E, Kulms D. The role of AKT/mTOR pathway in stress response to UV-irradiation: implication in skin carcinogenesis by regulation of apoptosis, autophagy and senescence. Int J Mol Sci. 2013; 14:15260–85. doi: 10.3390/ijms140815260

27. Dabhade P, Kotwal S. Tackling the Aging Process With Bio-Molecules: A possible role for caloric restriction, food-derived nutrients, vitamins, amino acids, peptides, and minerals. J Nutr Gerontol Geriatr. 2013; 32:24–40. doi: 10.1080/21551197.2012.753777

28. Mik V, Szüčová L, Smehilová M, Zatloukal M, Doležal K, Nisler J, Grúz J, Galuszka P, Strnad M, Spíchal L. N9-substituted derivatives of kinetin: effective anti-senescence agents. Phytochemistry. 2011; 72:821–31. doi: 10.1016/j.phytochem.2011.02.002

29. Argyropoulou A, Aligiannis N, Trougakos IP, Skaltsounis AL. Natural compounds with anti-ageing activity. Nat Prod Rep. 2013; 30:1412–37. doi: 10.1039/c3np70031c

30. Xie H, Zhu H, Cheng C, Liang Y, Wang Z. Echinacoside retards cellular senescence of human fibroblastic cells MRC-5. Pharmazie. 2009; 64:752–54.

31. Gupta, Shyam K. Walker, Linda (CARDIFF, CA, US) Prevention of Cellular Senescence in Mammals by Natural Peptide Complexes United States Patent Application 20110190202

32. Gruber, James Vincent Composition For Delaying Cellular Senescence US Patent Application 20110052676

33. Jin J, Liang Y, Xie H, Zhang X, Yao X, Wang Z. Dendroflorin retards the senescence of MRC-5 cells. Pharmazie. 2008; 63:321–23.

34. Corominas-Faja B, Santangelo E, Cuyàs E, Micol V, Joven J, Ariza X, Segura-Carretero A, García J,

Menendez JA. Computer-aided discovery of biological activity spectra for anti-aging and anti-cancer olive oil oleuropeins. Aging (Albany NY). 2014; 6:731–41. doi: 10.18632/aging.100691

35. Kalathur M, Toso A, Chen J, Revandkar A, Danzer-Baltzer C, Guccini I, Alajati A, Sarti M, Pinton S, Brambilla L, Di Mitri D, Carbone G, Garcia-Escudero R, et al. A chemogenomic screening identifies CK2 as a target for pro-senescence therapy in PTEN-deficient tumours. Nat Commun. 2015; 6:7227. doi: 10.1038/ncomms8227

36. Dimri GP, Lee X, Basile G, Acosta M, Scott G, Roskelley C, Medrano EE, Linskens M, Rubelj I, Pereira-Smith O. A biomarker that identifies senescent human cells in culture and in aging skin in vivo. Proc Natl Acad Sci USA. 1995; 92:9363–67. doi: 10.1073/pnas.92.20.9363

37. Lin Y, Shi R, Wang X, Shen HM. Luteolin, a flavonoid with potential for cancer prevention and therapy. Curr Cancer Drug Targets. 2008; 8:634–46. doi: 10.2174/156800908786241050

38. Velarde MC, Flynn JM, Day NU, Melov S, Campisi J. Mitochondrial oxidative stress caused by Sod2 deficiency promotes cellular senescence and aging phenotypes in the skin. Aging (Albany NY). 2012; 4:3–12. doi: 10.18632/aging.100423

39. Lan CC, Ho PY, Wu CS, Yang RC, Yu HS. LED 590 nm photomodulation reduces UVA-induced metalloproteinase-1 expression via upregula-tion of antioxidant enzyme catalase. J Dermatol Sci. 2015; 78:125–32. doi: 10.1016/j.jdermsci.2015.02.018

40. Spielmann H, Hoffmann S, Liebsch M, Botham P, Fentem JH, Eskes C, Roguet R, Cotovio J, Cole T, Worth A, Heylings J, Jones P, Robles C, et al. The ECVAM international validation study on in vitro tests for acute skin irritation: report on the validity of the EPISKIN and EpiDerm assays and on the Skin Integrity Function Test. Altern Lab Anim. 2007; 35:559–601.

41. EpiSkin skin irritation test, ECVAM ESAC statement in 2007 · OECD TG 439 published in 2010.

42. Laberge RM, Sun Y, Orjalo AV, Patil CK, Freund A, Zhou L, Curran SC, Davalos AR, Wilson-Edell KA, Liu S, Limbad C, Demaria M, Li P, et al. MTOR regulates the pro-tumorigenic senes-cence-associated secretory phenotype by promoting IL1A translation. Nat Cell Biol. 2015; 17:1049–61. doi: 10.1038/ncb3195

43. Childs BG, Durik M, Baker DJ, van Deursen JM. Cellular senescence in aging and age-related disease: from mechanisms to therapy. Nat Med. 2015; 21:1424–35. doi: 10.1038/nm.4000

44. Astle MV, Hannan KM, Ng PY, Lee RS, George AJ, Hsu AK, Haupt Y, Hannan RD, Pearson RB. AKT induces senescence in human cells via mTORC1 and p53 in the absence of DNA damage: implications for targeting mTOR during malignancy. Oncogene. 2012; 31:1949–62. doi: 10.1038/onc.2011.394

45. Strozyk E, Kulms D. The role of AKT/mTOR pathway in stress response to UV-irradiation: implication in skin carcinogenesis by regulation of apoptosis, autophagy and senescence. Int J Mol Sci. 2013; 14:15260–85. doi: 10.3390/ijms140815260

46. Popovich IG, Anisimov VN, Zabezhinski MA, Semenchenko AV, Tyndyk ML, Yurova MN, Blagosklonny MV. Lifespan extension and cancer prevention in HER-2/neu transgenic mice treated with low intermittent doses of rapamycin. Cancer Biol Ther. 2014; 15:586–92. doi: 10.4161/cbt.28164

47. Herranz N, Gallage S, Mellone M, Wuestefeld T, Klotz S, Hanley CJ, Raguz S, Acosta JC, Innes AJ, Banito A, Georgilis A, Montoya A, Wolter K, et al. mTOR regulates MAPKAPK2 translation to control the senescence-associated secretory phenotype. Nat Cell Biol. 2015; 17:1205–17. doi: 10.1038/ncb3225

48. Laberge RM, Sun Y, Orjalo AV, Patil CK, Freund A, Zhou L, Curran SC, Davalos AR, Wilson-Edell KA, Liu S, Limbad C, Demaria M, Li P, et al. MTOR regulates the pro-tumorigenic sense-cence-associated secretory phenotype by promoting IL1A translation. Nat Cell Biol. 2015; 17:1049–61. doi: 10.1038/ncb3195

49. Kalathur M, Toso A, Chen J, Revandkar A, Danzer-Baltzer C, Guccini I, Alajati A, Sarti M, Pinton S, Brambilla L, Di Mitri D, Carbone G, Garcia-Escudero R, et al. A chemogenomic screening identifies CK2 as a target for pro-senescence therapy in PTEN-deficient tumours. Nat Commun. 2015; 6:7227. doi: 10.1038/ncomms8227

50. Acosta JC, Banito A, Wuestefeld T, Georgilis A, Janich P, Morton JP, Athineos D, Kang TW, Lasitschka F, Andrulis M, Pascual G, Morris KJ, Khan S, et al. A complex secretory program orchestrated by the inflammasome controls paracrine senescence. Nat Cell Biol. 2013; 15:978–90. doi: 10.1038/ncb2784

51. Alimonti A, Carracedo A, Clohessy JG, Trotman LC, Nardella C, Egia A, Salmena L, Sampieri K, Haveman WJ, Brogi E, Richardson AL, Zhang J, Pandolfi PP. Subtle variations in Pten dose determine cancer susceptibility. Nat Genet. 2010; 42:454–58. doi: 10.1038/ng.556

52. Petrascheck M, Ye X, Buck LB. An antidepres-sant that extends lifespan in adult Caenorhab-ditis elegans. Nature. 2007; 450:553–56. doi: 10.1038/nature05991

53. Alavez S, Vantipalli MC, Zucker DJ, Klang IM, Lithgow GJ. Amyloid-binding compounds maintain protein homeostasis during ageing and extend lifespan. Nature. 2011; 472:226–29.
doi: 10.1038/nature09873

54. Alavez S, Vantipalli MC, Zucker DJ, Klang IM, Lithgow GJ. Amyloid-binding compounds maintain protein homeostasis during ageing and extend lifespan. Nature. 2011; 472:226–29.
doi: 10.1038/nature09873

55. Ishiyama M, Tominaga H, Shiga M, Sasamoto K, Ohkura Y, Ueno K. A combined assay of cell viability and in vitro cytotoxicity with a highly water-soluble tetrazolium salt, neutral red and crystal violet. Biol Pharm Bull. 1996; 19:1518–20.
doi: 10.1248/bpb.19.1518

56. Debacq-Chainiaux F, Erusalimsky JD, Campisi J, Toussaint O. Protocols to detect senescence-associated beta-galactosidase (SA-betagal) activity, a biomarker of senescent cells in culture and in vivo. Nat Protoc. 2009; 4:1798–806.
doi: 10.1038/nprot.2009.191

57. Catanzaro D, Rancan S, Orso G, Dall'Acqua S, Brun P, Giron MC, Carrara M, Castagliuolo I, Ragazzi E, Caparrotta L, Montopoli M. Boswellia serrata prevents intestinal epithelial barrier from oxidative and inflammatory damage. PLoS One. 2015; 10:e0125375. doi: 10.1371/journal.pone.0125375

SUPPLEMENTARY MATERIALS

Supplementary Methods

HPLC-MS and HPLC-DAD-ELSD quali-quantitative analysis

Qualitative and quantitative constituents of *Salvia haenkeii* were performed by high-performance liquid chromatography-tandem mass spectrometry (HPLC-MS) and high-performance liquid chromatography coupled with a diode array detector and an evaporative light scattering detector (HPLC-DAD-ELSD). For HPLC-MS analysis a Varian 212 binary chromatograph equipped with 500MS ion trap and Prostar 430 autosampler was used (Varian Inc., USA). For the HPLC-DAD-ELSD analysis an Agilent 1100 Series chromatograph with 1100 Diode Array detector and Sedex LX 60 Evaporative Light Scattering Detector (ELSD) was used. As stationary phase an Agilent Eclipse XDB-C8 2.1 x 150 mm, 3.5 μm (Agilent Tecnologies, USA) was used. Quantification of phenolic constituents was obtained with the method of calibration curve: rutin (Sigma Aldrich, St. Louis, MO, USA) was used as external standard for flavonoid quantification. Calibration curves were Y = 144232X + 112 (R2 = 0.9998) for rutin.

Microbiological assessments

Streptococcus pyogenes and Staphylococcus aureus were isolated from clinical specimens of human skin, cultured on agar plates and identified according to the appearance of colonies, growth conditions and metabolic enzymatic activities. Bacteria were grown in lysogeny broth (LB) at 37°C until mid-log phase determined by spectrophotometric analysis, reading the optical density (O.D.) at 600 nm. Bacterial cultures were then diluted in LB to reach concentration of $1x10^6$ colony-forming units (CFU)/mL and incubated at 37°C for 16 hours with SH at the indicated concentrations. At the end of incubation, bacterial load was estimated by reading the O.D. using a spectrophotometer (Sunrise, Tecan; Switzerland). Data were expressed as mean ± standard error of the percentage of O.D. calculated versus the respective untreated samples.

a

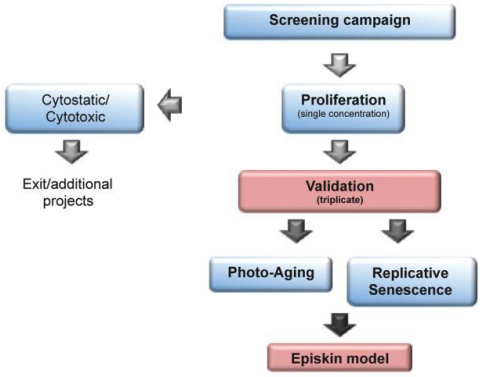

b

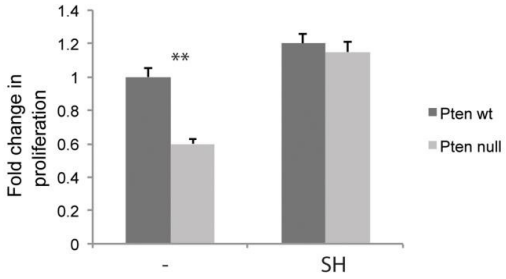

c

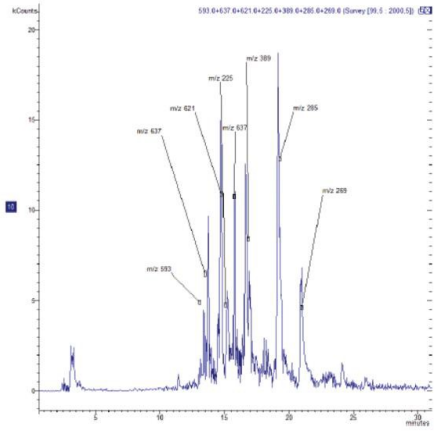

Supplementary Figure S1. (**a**) Schematic representation of PICS assay First step is the identification of candidate compounds that have an anti-senescent effect in the in vitro PICS assay (screening campaign). Compounds are tested for their effect on proliferation and b-gal expression in primary murine embryonal fibroblasts (MEFs) lacking *Pten* gene (*Pten* null). The candidate compounds that are able to increase growth rate more than 40% compared to control and at the same time block senescence (determined by less b-gal positive cells), are selected for testing their ability to block photo-induced and replicative senescence in human fibroblasts (validation). Cytotoxic compounds instead, are selected for external projects on anti-tumor therapy. Candidate compounds that demonstrate efficiency in prevention of replicative and photo ageing are tested in reconstituted skin model as part of preclinical development. Successful (non toxic and non irritant) candidates are formulated into topical products and proceed to clinical trials. (**b**) Proliferation of *Pten* null MEFs in culture after 5 days of treatment with *S. haenkei* extract. *Pten* null MEFs were plated in concentration of $2x10^4$ cells/ml and treated for 5 days with 10µM Nutlin-3 or 10µg/ml SH extract. After this period, the proliferation was determined using Crystal violet staining. (**c**) An exemplificative chromatogram is reported with the indication of twelve compounds identified on the basis of MSn fragmentations.

a

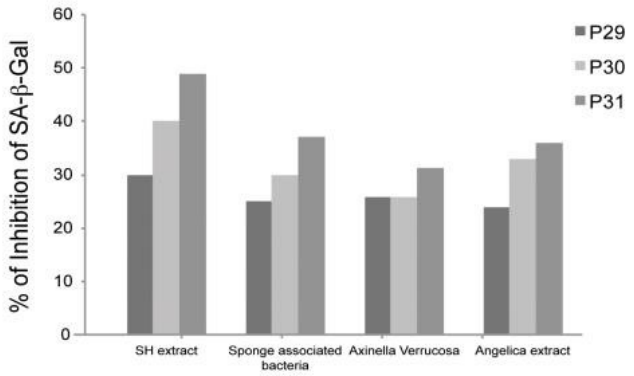

b

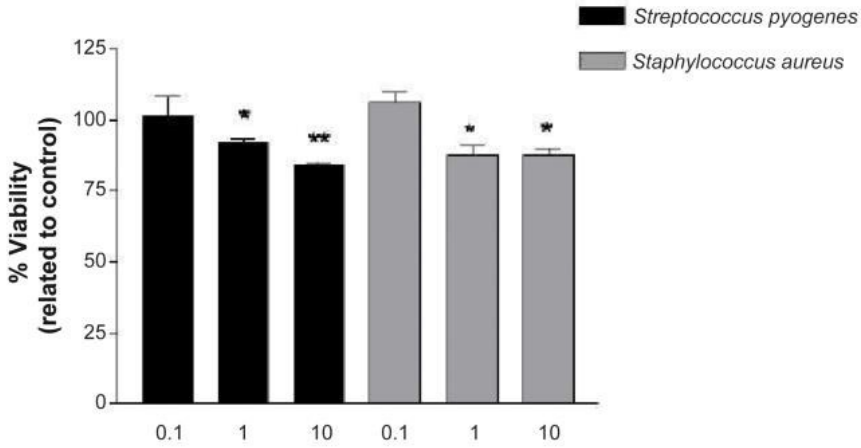

Supplementary Figure S2. (**a**) To assess replicative senescence *in vitro*, 3T3 protocol was performed on human dermal fibroblasts (WI38-CCL75 cells, ATCC). Cells were plated and subsequently passed and re-plated (step called passage) in the same number every 3 days, for a period of over 3 months. From passage 25, 3T3 protocol was continued, but in the presence or absence of selected hits (represented here SH extract, sponge associated bacteria, *Axinella Verrucosa* and *Angelica* extract). The graph represents percentage of β-galactosidase positive cells revealed in culture on passages 29, 30 and 31. Results are expressed as mean values (+SEM) of cell count in three independent experiments. (**b**) Antimicrobic effect of *Salvia haenkeii* treatment on Streptococcus pyogenes and Staphylococcus aureus. Antimicrobic activity was measured after 16 hours of exposure. At the end of incubation, bacterial load was estimated by reading the O.D. using a spectrophotometer. Data were expressed as mean ± standard error of the percentage of O.D. calculated versus the respective untreated samples. *p<0.05 treated vs untreated.

a

Code	Hit description
SH	crude extract of Salvia haenkei
sbe 63	pure extract of Salvia blepharophylla
saden8b	pure extract of Salvia adenophora
sj212	pure extract of Salvia jamensis
sj43	pure extract of Salvia jamensis
sbe8	pure extract of Salvia blepharophylla
scib58nr	pure extract of Salvia cinnabarina
sbe15a	pure extract of Salvia blepharophylla
SAB	Sponge associated bacteria
AV	Axinella verrucosa crude extract
AN	pure extract of Angelica
Ace	Small molecule inhibitor
CA	Small molecule inhibitor
JN	Small molecule inhibitor
GS	Small molecule inhibitor
CLO	Small molecule inhibitor

b

Compound	$[M-H]^-$	MS^2	MS^3
6,8-di-C-glucosyl-apigenin	593	503-473-413-353	325
Diglucuronyl-luteolin isomer I	637	351-285	
Glucoronyl-apigenin	621	351-285	
Genipin	225	207-181-165	
Diglucuronyl-luteolin isomer II	637	593-549	505-411
Rosmanol/epirosmanol derivative	389	359-315	
Apigenin derivative	591	560-503-383-268	
Luteolin	285	241-217-199-175-151	147-133-119
Apigenin	269	255-249	
Betulinic acid	455	407	

Supplementary Table S1. (**a**) Codes and description of hits utilized in the platform for the *in vitro* identification of anti-senescent compounds. (**b**) The identified constituents of SH are summarized in table and are mainly apigenin and luteolin glycosides.

Research Paper

Rapamycin reverses the senescent phenotype and improves immuno-regulation of mesenchymal stem cells from MRL/lpr mice and systemic lupus erythematosus patients through inhibition of the mTOR signaling pathway

Zhifeng Gu[1*], Wei Tan[1,2*], Juan Ji[1*], Guijian Feng[3], Yan Meng[1], Zhanyun Da[1], Genkai Guo[1], Yunfei Xia[1], Xinhang Zhu[1], Guixiu Shi[1,4], and Chun Cheng[1,5]

[1]Department of Rheumatology, Affiliated Hospital of Nantong University, Nantong, Jiangsu Province 226001, China
[2]Department of Emergency Medicine, The Yangzhou First People's Hospital, Yangzhou, Jiangsu Province 225001, China
[3]Department of Stomatology, Affiliated Hospital of Nantong University, Nantong, Jiangsu Province 226001, China
[4]Department of Rheumatology, Affiliated First Hospital of Xiamen University, Xiamen, Fujian Province 361000, China
[5]Jiangsu Province Key Laboratory for Inflammation and Molecular Drug Target, Medical College of Nantong University, Nantong, Jiangsu Province 226001, China
*Equally contributed to this work

Key words: *rapamycin (RAPA), mesenchymal stem cells (MSCs), systemic lupus erythematosus (SLE), senescence, immunoregulation*
Received: *12/04/15; Accepted: 02/13/16; Published: 04/02/16* doi:10.18632/aging.100925
Correspondence to: *Chun Cheng, PhD; Guixiu Shi, PhD;* ***E-mail:*** *chengc@ntu.edu.cn; guixiu.shi@gmail.com*

Abstract: We have shown that bone marrow (BM)-derived mesenchymal stem cells (BM-MSCs) from SLE patients exhibit senescent behavior and are involved in the pathogenesis of SLE. The aim of this study was to investigate the effects of rapamycin (RAPA) on the senescences and immunoregulatory ability of MSCs of MRL/lpr mice and SLE patients and the underlying mechanisms. Cell morphology, senescence associated β-galactosidase (SA-β-gal) staining, F-actin staining were used to detect the senescence of cells. BM-MSCs and purified CD4+ T cells were co-cultured indirectly. Flow cytometry was used to inspect the proportion of regulatory T (Treg) /T helper type 17 (Th17). We used small interfering RNA (siRNA) to interfere the expression of mTOR, and detect the effects by RT-PCR, WB and immunofluorescence. Finally, 1×10^6 of SLE BM-MSCs treated with RAPA were transplanted to cure the 8 MRL/lpr mice aged 16 weeks for 12 weeks. We demonstrated that RAPA alleviated the clinical symptoms of lupus nephritis and prolonged survival in MRL/lpr mice. RAPA reversed the senescent phenotype and improved immunoregulation of MSCs from MRL/lpr mice and SLE patients through inhibition of the mTOR signaling pathway. Marked therapeutic effects were observed in MRL/lpr mice following transplantation of BM-MSCs from SLE patients pretreated with RAPA.

INTRODUCTION

Systemic lupus erythematosus (SLE) is a chronic autoimmune inflammatory disease characterized by multi-organ involvement and a remarkable variability in clinical presentation [1]. It is a typical autoimmune disease based on the variety of its proposed pathogenesis, including abnormalities of T and B

lymphocytes. Current treatments of severe SLE flares consist of toxic immunosuppressive drugs, most commonly cyclophosphamide, mycophenolate mofetil, and leflunomide [2]. However, the therapeutic options in SLE patients who are refractory to standard treatments are extremely limited, and the disease remains potentially fatal in some patients[3]. With recent advances in our understanding of the underlying pathology, several new strategies have been developed to target specific activation pathways relevant to the pathogenesis of SLE [4, 5]. For example, B-cell-depleting therapies using the monoclonal antibody rituximab and the B lymphocyte stimulator (BLyS) inhibitor belimumab, have been shown be beneficial in a specific subpopulation of lupus patients [6, 7].

Mesenchymal stem cells (MSCs) are widely identified as a promising cell source because of their clonogenic, self-renewal and pluripotent differentiation ability [8]. MSCs have been found to possess immunomodulatory effects on various activated immune cells, such as T cells, B cells, natural killer cells and dendritic cells [9-11]. Additionally, MSCs are able to escape alloantigen recognition because of their low immunogenicity and accompanying lack of expression of costimulatory molecules [12, 13]. These properties make MSCs promising candidate cells for preventing rejection in organ transplantation and in the treatment of autoimmune disease.

Our studies and those of others have revealed that SLE BM-MSCs exhibit slow growth with early signs of senescence, as well as some immunoregulatory abnormalities [14-17]. Accumulating evidence confirms the safety and efficacy of allogeneic MSC transplantation in treating drug-resistant SLE patients and animal models [18-24]. However, Carrion and coworkers reported that autologous BM-MSC transplantation (MSCT) had no effect on disease activity in two SLE patients [25]. These findings suggested that the senescence of MSCs from SLE patients may contribute to the disease pathogenesis. Therefore, a complete understanding of the mechanisms underlying early senescence of MSCs in SLE patients is required.

Mammalian target of rapamycin (mTOR) integrates nutrient and hormonal signals to function as a central regulator of diverse cellular processes including cell growth [26-29]. It is a phosphatidylinositol kinase-related kinase (phosphatidylinositol kinase-related kinase, PIKK) protein family member, and regulates protein translation and cell growth and proliferation via phosphorylation of the downstream target proteins p70 ribosomal protein S6 kinase (p70S6K) and eukaryotic initiation factor 4E binding protein1 (4EBP1) [30, 31]. Previous studies revealed that the mTOR signaling pathway is involved in a variety of biological processes including cell senescence *in vivo* [32-36]. Rapamycin (RAPA), which is an inhibitor of the mTOR signaling pathway, is a macrolide antibiotic with potent immunosuppressive properties [37, 38]. Recent studies have shown that RAPA can decelerate certain aspects of cellular senescence [39-42]. In addition, the therapeutic use of RAPA in SLE patients and animal models is clinically effective. RAPA has been shown to normalize T cell activation-induced calcium flux in patients with SLE [43]. However, the ability of RAPA to alleviate LN by influencing the senescence of BM-MSCs from SLE patients and the therapeutic potential of MSCs *in vitro* autotransplantation have not yet been reported.

In this study, we further confirmed that RAPA alleviates LN and prolongs the survival of MRL/lpr mice. Interestingly, we have found that RAPA reversed the senescent phenotype and improved the immuno-regulatory ability of MSCs from MRL/lpr mice. Furthermore, we report, for the first time, the involvement of the activated mTOR pathway in the senescence of MSCs from SLE patients and demonstrated marked therapeutic effects of MRL/lpr mice following transplantation of RAPA-pretreated BM-MSC obtained from SLE patients.

RESULTS

RAPA improves lupus nephritis by influencing cellular senescence in BM-MSCs from MRL/lpr mice

Previous studies have demonstrated the clinical efficacy of RAPA for the treatment of SLE patients and in animal models of lupus. The scheme of RAPA treatment procedures used in the present study is shown in Figure 1A. RAPA increased the survival rate of MRL/lpr mice (Fig. 1B) and alleviated symptoms of LN, including 24-h urinary protein, serum anti-ds-DNA antibody levels, and glomerular sclerosis (Fig. 1C–E). MSCs from MRL/lpr mice showed senescent behavior, characterized by flattened and enlarged cell morphology, increased SA-β-gal activity, and disordered cytoskeletal distribution. Interestingly, we observed decelerated cell hypertrophy in BM-MSCs in the RAPA-treated group (Fig. 1F) and the number of SA-β-gal-positive cells (Fig. 1G). The disordered distribution of F-actin was also reversed by RAPA treatment (Fig. 1H). In contrast, proliferation of BM-MSCs was not affected by RAPA treatment (Fig. 1 I–K).

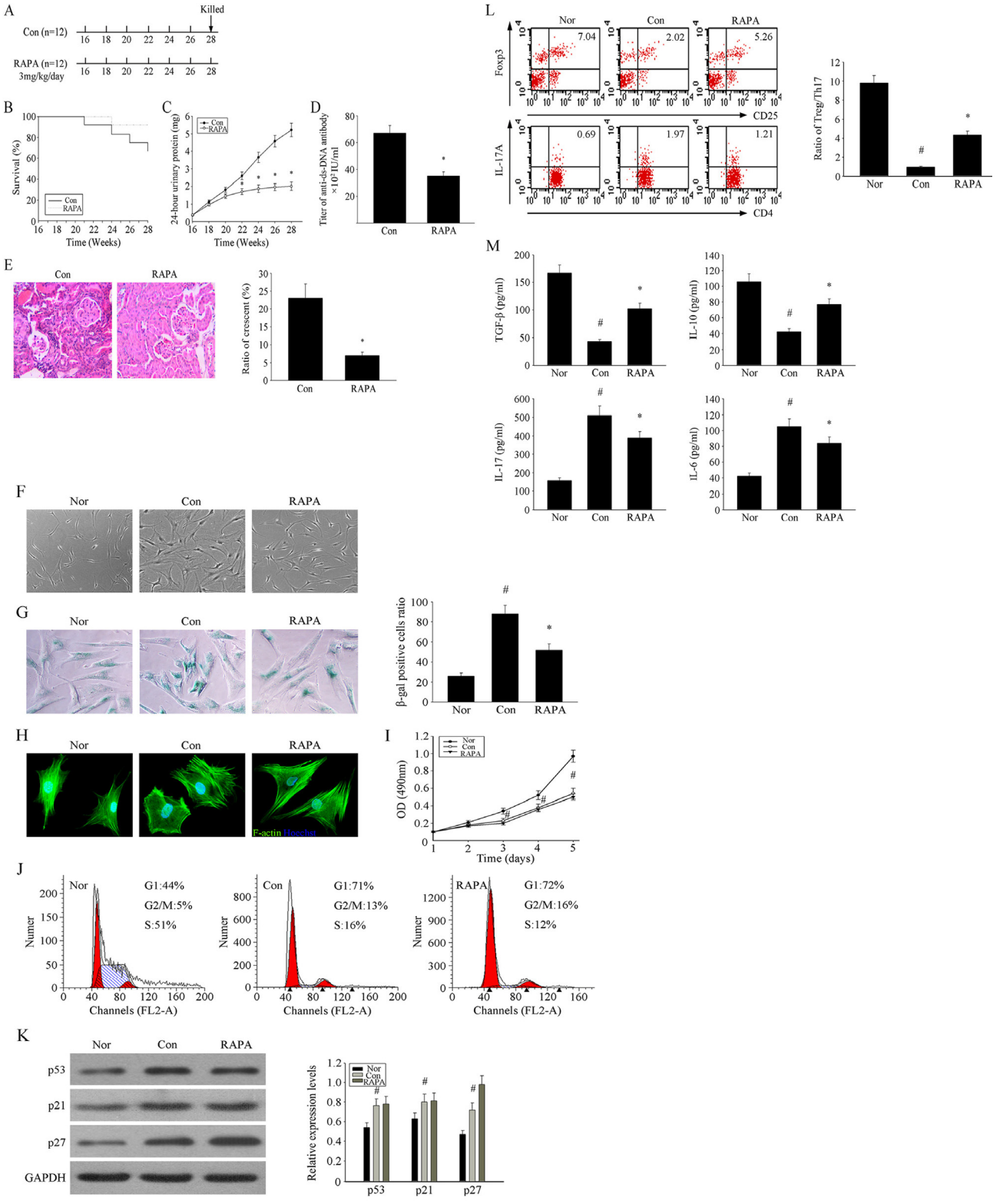

Figure 1. RAPA improves lupus nephritis by influencing the cellular senescence of BM-MSCs from MRL/lpr mice. (**A**) The treatment group had intragastric administration of RAPA 3mg/kg/day between 16 and 28 weeks of ages. Survival curves observed that The survival rate of the RAPA-treated MRL/lpr mice was higher than that of control group. (**B**-**E**) We recorded the survival rate and the weight of mice. 24-hours urinary protein was measured by coomassie brilliant blue method. Mice were killed and were taken peripheral

blood in orbit. Elisa showed that anti-ds-DNA antibody titer in serum in RAPA -treated group is lower than control group. HE-staining showed that renal pathological changes of control group is significant,including glomerular sclerosis, mesangial cell proliferation,matrix widened, and formation of crescent, a number of lymphocytes infiltrating the interstitium (HE×300).However, histopathological changes of RAPA -treated group were remarkable alleviated. **(F)** Cellular morphology observed that the RAPA-treated MSCs from MRL/lpr mice were less hypertrophic than untreated group (magnification; ×200). (**G**) MSCs were fixed and stained for β-gal. The number of SA-β-gal-positive cells among treated groups decreased in comparison with untreated group. (**H**) Immunofluorescence showed that the abnormal F-actin distribution in MSCs from MRL/lpr mice was reversed by RAPA treatment. (**I**) Cell Counting Kit (CCK)-8 method was used to detect the cell proliferation rate. (**J**) Flow cytometry was used to detect the distribution of cell cycle. (**K**) Western Blotting was used to detect the changes of cell cycle-related proteins. However, no remarkably differences were found between treated and untreated MSCs. (**L**) P4 MSCs transwell cultured with CD4+ T cells for 72 h. The count of Treg cells decreased and Th17 cells increased in MSCs from MRL/ lpr mice compared to the normal group by flow cytometry analysis. MSCs from RAPA-treated group could reverse the abnormal changes.The statistical results revealed that the treatment of RAPA could up-regulated the ratio of Treg/Th17 from MRL/lpr mice MSCs. (**M**) The supernatants of MSCs were collected. RAPA-treated group induced the secretion of IL-10 and TGF-β but reduced IL-17 and IL-6 by ELISA. All data were expressed as the mean±SEM (n = 3, *P＜0.05 compared with normal group, #P＜0.05 compared with the untreated group).

Previous studies have shown abnormalities in the immunoregulatory ability of that MSCs from MRL/lpr mice

In the present study, we examined the influence of BM-MSCs on the production of Treg and Th17 cells. BM-MSCs from MRL/lpr mice were cultured in transwells with BALB/c splenic CD4+T cells for 72 h. We found that RAPA-treated MSCs from MRL/lpr mice upregulated the number of Treg cells and down-regulated the number of Th17 cells to increase the ratio of Treg/Th17 (Fig. 1L). At the same time, RAPA treatment increased the secretion of regulatory cytokines TGF-β and IL-10, but decreased that of the proinflammatory cytokines IL-17 and IL-6 in these cultures (Fig. 1M). These results implied that RAPA treatment decelerated the senescence of BM-MSCs from MRL/lpr mice but had no effect on cell cycle arrest and promoted the immunoregulatory ability of MSCs from MRL/lpr mice by enhancing the ratio of Treg/Th17 cells and influencing the profile of related cytokine secretion. Reversing MSC senescence may be an effective approach to SLE therapy.

RAPA inhibited the overactivation mTOR pathway to reverse the senescence of BM-MSCs from MRL/lpr mice

Previous studies have shown that the mTOR signaling pathway is a central mechanism of cellular senescence [26-28]. Activated mTOR phosphorylates S6K, which in turn phosphorylates S6 [30, 31]. Therefore, we investigated the expression of p-mTOR, p-S6K and p-S6 in MSCs from MRL/lpr mice, normal group and RAPA-treated group by Western blot analysis. We found higher levels of phosphorylated mTOR, S6K and S6 in MSCs from MRL/lpr mice compared to the normal group; this difference was reversed in the RAPA-treated group (Fig. 2A). Similarly, immunofluorescence analysis showed that RAPA reversed the high intracellular expression of p-mTOR, p-S6K and p-S6 in MRL/lpr mice MSCs (Fig.2B). These results confirmed that RAPA played an inhibitory role in the mTOR pathway of MSCs from MRL/lpr mice.

Overactivation of the mTOR pathway is involved in the senescence of MSCs from SLE patients

To further confirm its role in the senescence of MSCs from SLE patients, we examined the expression of components of the mTOR pathway. As shown in Figure 3A, the phosphorylation levels of mTOR and its proteins expressed by its downstream regulated genes were higher in SLE MSCs compared to the normal group. Furthermore, immunofluorescence analysis confirmed higher expression of intracellular p-mTOR, p-S6K and p-S6 levels in SLE MSCs compared with the normal group (Fig. 3B). To confirm the role of the mTOR pathway in the senescence of MSCs in SLE patients, we investigated the dose- and time-dependent inhibitory effects of RAPA on the mTOR pathway by measuring S6 phosphorylation, which is a significant marker of mTOR activity. Results showed that RAPA inhibited S6 phosphorylation at concentrations 20 nM or higher, achieving maximal effects at 100 nM–500 nM (Fig. 3C). Furthermore, 500 nM RAPA achieved maximal effects at 72 h (Fig. 3D). Thus, all subsequent experiments were performed using RAPA at 500 nM for 72 h; S6 phosphorylation was completely inhibited under these conditions.

To further determine the effects of the mTOR signaling pathway on senescence and the immunoregulatory ability of MSC, we depleted MSC of mTOR by RNAi treatment. As shown in Figures 3E–F, by comparing interference effects of three RNAi sequences, we chose the third one to do the following experiments. We found that both RNAi and RAPA treatment reversed the

senescent behavior of MSCs from SLE patients. The MSCs from SLE patients were larger than those in the normal group, and exhibited more numerous and longer podia. Morphological evaluation showed that RAPA and siRNA decelerated the hypertrophy of MSCs from SLE patients (Fig. 3G). It is noteworthy that, compared with normal MSCs, RAPA was less effective at preventing hypertrophy than siRNA, indicating that mTOR-dependent and independent components influence cell size and growth. SA-β-gal was usually used to examine cellular senescence. The number of SA-β-gal-positive cells was notably increased in SLE MSCs and this number was decreased by RAPA and knockdown of mTOR (Fig. 3H). Immunofluorescence analysis showed that the F-actin distribution was disorderly and assembled around the nuclear region in MSCs from SLE patients. This abnormal distribution of F-actin was effectively reversed by RAPA and si-mTOR treatment (Fig. 3I); however, the proliferation rate of MSCs was not affected (data not shown).

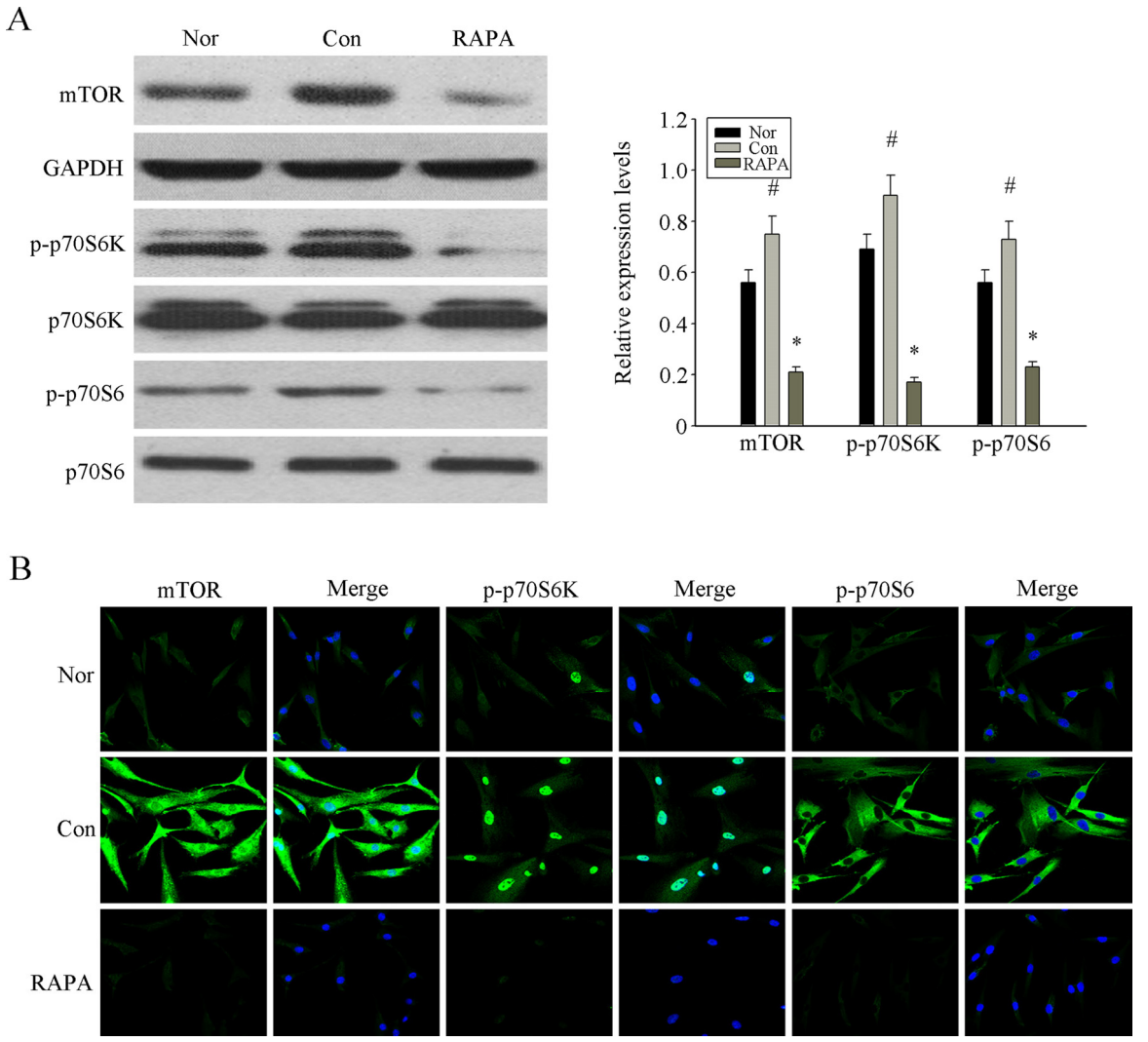

Figure 2. RAPA inhibited the over-activation mTOR pathway to revers the senescence of MSCs from MRL/lpr mice. (**A**) The over-expression of p-mTOR, p-S6K and p-S6 in p4 MSCs from MRL/lpr mice compared with normal group were determined by western blot analysis. The treatment of RAPA could obviously inhibit the expression of those proteins. GAPDH was used as the internal control. (**B**) P4 MSCs cultured into 24-well plates. The expression of p-mTOR, p-S6K and p-S6 analyzed by immunofluorescence staining showed that their over-activation in MSCs from MRL/lpr mice could be inhibited by RAPA treatment. Counterstaining with DAPI displays the localization of the nucleus (Scale bar = 50 μm). All data were expressed as the mean±SEM (n = 3,*P＜0.05 compared with normal group, #P＜0.05 compared with the untreated group).

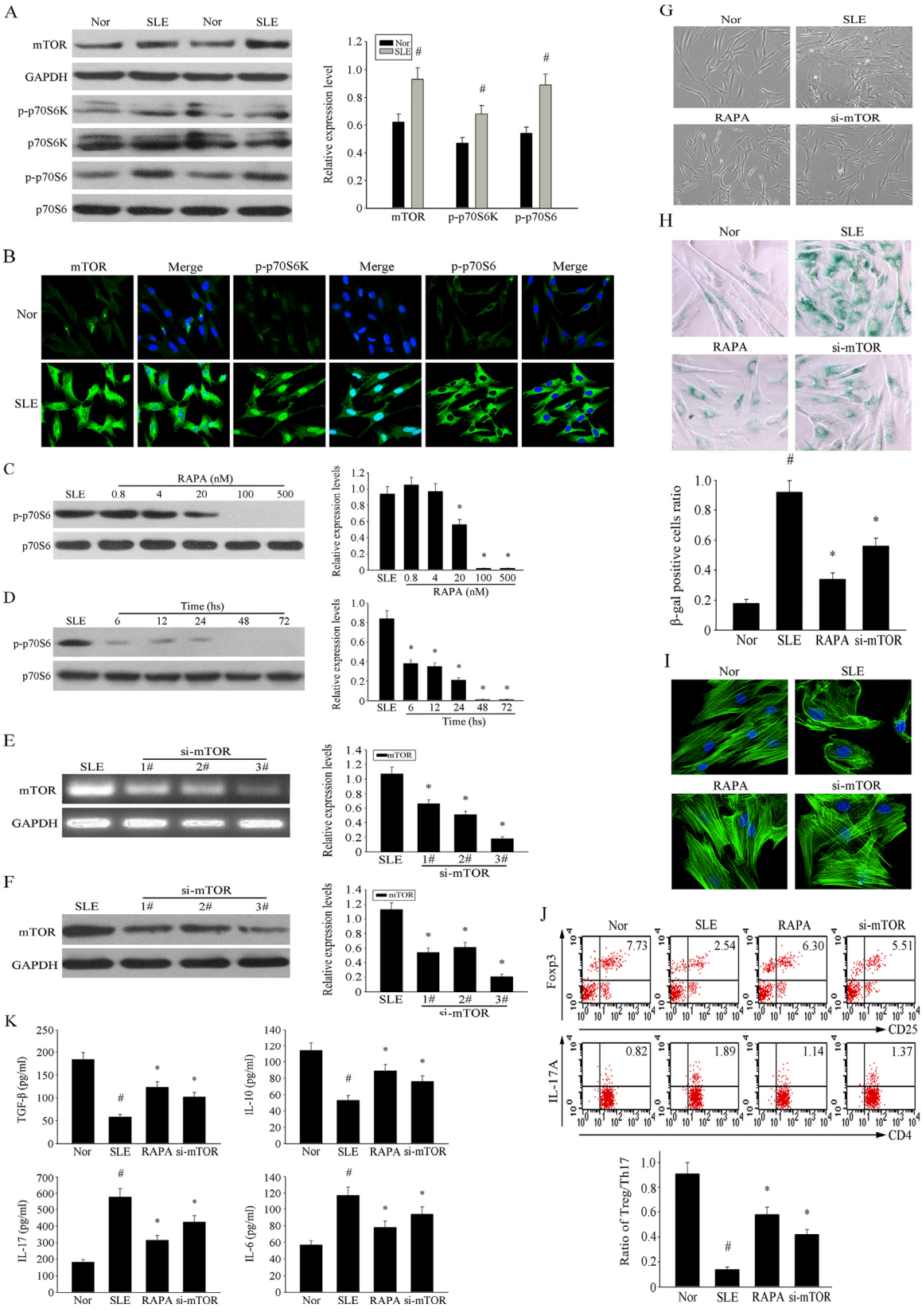

Figure 3. Over-activation of mTOR pathway was involved in the senescence of MSCs from SLE patients. (**A**) The over-expression of p-mTOR, p-S6K and p-S6 in MSCs from SLE compared with normal group were determined by western blot analysis. GAPDH was used as the internal control. (**B**) P4 MSCs from SLE patients and normal group were cultured in 24-well plates. Immunofluorescence

staining of p-mTOR, p-S6K and p-S6 verified their over-activation in SLE MSCs. Counterstaining with DAPI displays the localization of the nucleus (Scale bar = 50 μm). (**C**-**D**) P4 MSCs from SLE patients cultured at the different concentration of RAPA for 72 h. RAPA achieved maximal effects at about 500 nM by assaying the inhibition of p-70S6. (E-F) BMMSCs were depleted of mTOR by RNAi. The third one was chosen as the best siRNA by western blotting. (**G**) P4 MSCs from SLE patients were treated with 500 nM RAPA and si-mTOR or not for 72 h. Cellular morphology showed that the RAPA and si-mTOR treated SLE MSCs were less hypertrophic than untreated group (magnification; ×200). (**H**) MSCs were fixed and stained for β-gal. The number of SA-β-gal- positive cells obviously decreased among treated SLE MSCs in comparison with untreated group. (**I**) Immunofluorescence showed that RAPA and si-mTOR reversed abnormal F-actin distribution in MSCs from SLE patients. (**J**) P4 SLE MSCs were treated with 500 nM RAPA and the third si-mTOR or not, then transwell cultured with CD4+T cells for 72 h. The count of Treg cells decreased and Th17 cells increased in SLE MSCs compared to the normal group by flow cytometry analysis. But si-mTOR and RAPA-treated MSCs could reverse the abnormal changes. The statistical results revealed that RAPA could up-regulated the ratio of Treg/Th17 from SLE MSCs, which was down-regulated compared with normal group. (**K**) The supernatants of MSCs were collected. si-mTOR RAPA-treated SLE MSCs induced the secretion of IL-10 and TGF-β but reduced IL-17 and IL-6 by ELISA. All data were expressed as the mean±SEM (n = 3, *P＜0.05 compared with normal group, #P＜0.05 compared with the untreated group).

We investigated the immunoregulatory ability of SLE MSCs on CD4+T cells using a transwell culture system. We found that RAPA treatment and knockdown of mTOR increased the number of Treg cells and decreased the number of Th17 cells generated in transwell cultures; thus, increasing the Treg/Th17 ratio. Our data revealed that RAPA increased the ratio of Treg/Th17 generated in the presence of SLE MSCs, but was lower than that in the normal control group (Fig. 3J). Furthermore, both treatments increased the secretion of regulatory cytokines TGF-β and IL-10, but reduced the levels of the proinflammatory cytokines IL-17 and IL-6 in MSCs from SLE patients (Fig. 3K). Taken together, these results demonstrated the involvement of the mTOR pathway in the senescence of MSCs from SLE patients. RAPA decelerated the senescence of MSCs from SLE patients and increased the Treg/Th17 cell ratio stimulated by MSCs from SLE patients by affecting the secretion of cytokines.

MSCs from SLE patients pretreated with RAPA have a significant therapeutic effect on LN of MRL/lpr mice

Recent studies have indicated that allogenic MSCT is a feasible and safe therapeutic strategy in lupus-prone mice and SLE patients[18-24]. However, syngeneic BM-MSCT was ineffective [22]. Therefore, we investigated this issue in transplantation experiments conducted in MRL/lpr mice (Fig. 4A). As shown in Figure 4B, the survival rates in the RAPA-pretreated SLE MSCs transplantation group (G2) and normal MSCs transplantation group (G3) were higher than that in the SLE MSCs transplantation group (G1). The weight of the mice in G2 and G3 gradually increased (Fig. 4C). The 24-hours urinary protein (Fig. 4D) and serum anti-ds-DNA antibody levels in G2 and G3 were lower than those in G1 (Fig.4E). In terms of pathology, glomerular sclerosis and interstitial fibrosis (Fig. 4F) and pulmonary inflammation (Fig. 4G) were ameliorated in G2 and G3 MRL/lpr mice. These results demonstrated that transplantation of MSCs from SLE patients pretreated with RAPA and normal MSCs have a significant therapeutic effect on LN in MRL/lpr mice.

DISCUSSION

Since 1994, when the significant reduction or prevention of the many pathologic features of lupus normally seen in the MRL/l mouse mediated by RAPA were first reported [44], there have been an increasing number of studies focusing on RAPA treatment of lupus. In 2006, Fernandez et al. reported that RAPA appeared to be a safe and effective therapy for SLE in patients who proved refractory to traditional medications. This group showed that RAPA normalized T cell activation-induced calcium flux in patients with SLE[43]. In the study, we confirmed that RAPA attenuated the severity of established nephritis. Furthermore, we demonstrated for the first time that RAPA reversed the senescent phenotype and improved the regulatory ability of MSCs from MRL/lpr mice and SLE patients by inhibition of the mTOR signaling pathway. Therefore, reversal of the senescence of MSC may be an effective approach to SLE therapy.

The mTOR signaling pathway plays an important role in cellular senescence [26-29]. Yentrapalli and others have shown that the PI3K/AKT/mTOR signaling pathway is involved in senescence of primary human endothelial cells induced by long-term radiation [35]. In addition, Gharibi reported that the AKT/mTOR signaling pathway promoted MSC senescence and reduced osteogenic differentiation [36]. Our study shows that the mTOR signaling pathway of MSCs from SLE patients is considerably more active than that of the normal group as demonstrated by the upregulated phosphorylation of mTOR, S6K and S6. Furthermore, siRNA-mediated mTOR knockdown inhibited the senescence of MSCs and restored their immunomodulatory capacity. This evidence suggests that the mTOR pathway is involved in the accelerated senescence of MSCs in SLE patients.

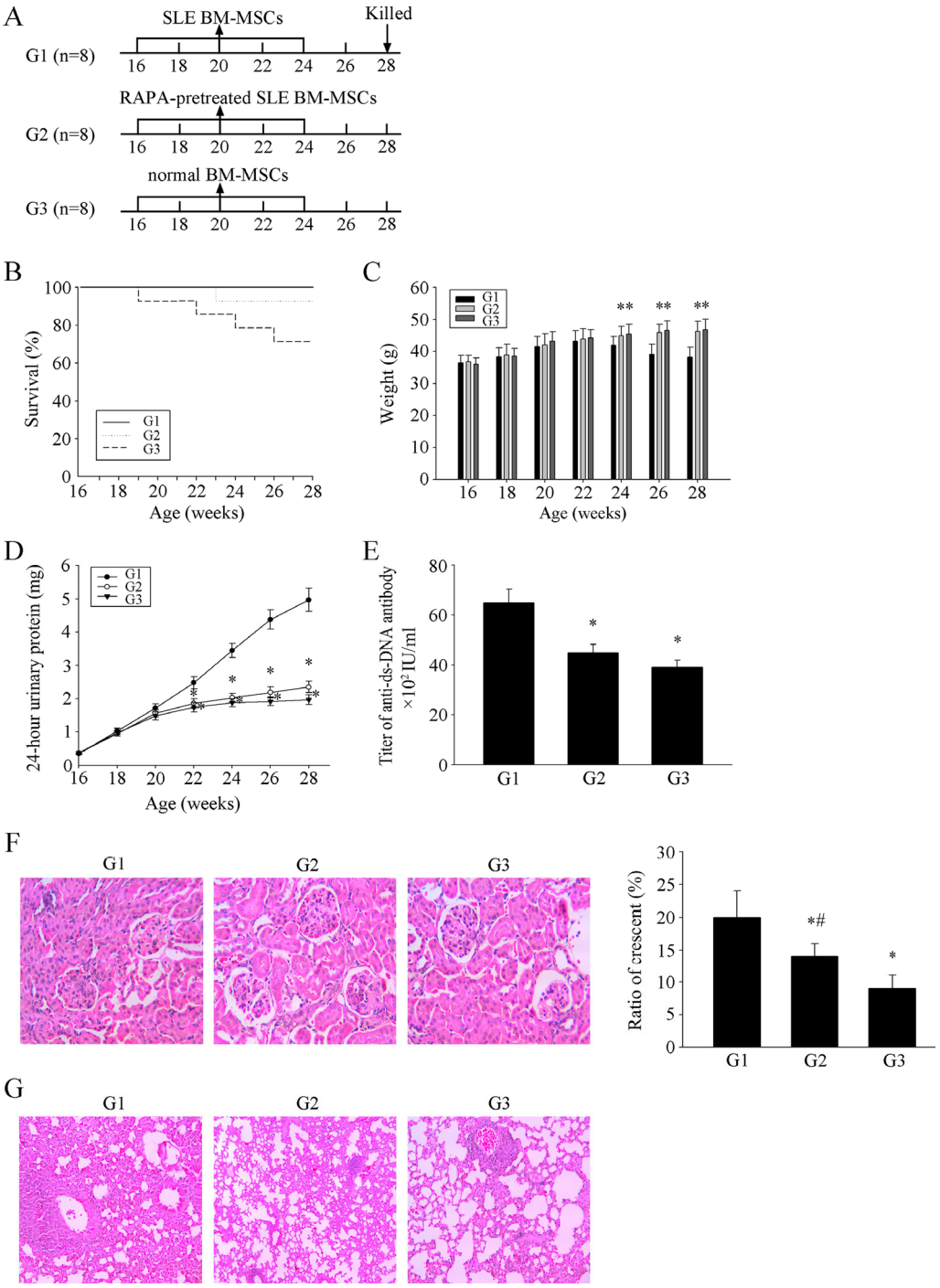

Figure 4. MSCs from SLE patients pretreated with RAPA have a significant effect on LN of MRL/lpr mice. (**A**) 24 MRL / lpr mice were divided into three groups: SLE BM-MSCs transplantation group (G1), RAPA-pretreated SLE BM-MSCs transplantation group (G2), normal BM-MSCs transplantation group (G3). Three groups were injected with BM-MSC in tail vein. (**B**) Survival curves observed that The survival rate of G2 and G3 MRL/lpr mice was higher than that of control group. (**C**) Three groups MRL/lpr mice were weighed one time two weeks. Weight between G2, G3 and G1 had obvious difference from 24 weeks. (**D**) 24-hours urinary protein was measured by coomassie brilliant blue method. (**E**) mice were killed and were taken peripheral blood in orbit. Elisa showed that anti-ds-DNA antibody titer in serum in G2 and G3 is lower than G1. (**F**) HE-staining showed that renal pathological changes of G1 is significant, including glomerular sclerosis, mesangial cell proliferation, matrix widened, and formation of crescent, a number of lymphocytes infiltrating the interstitium (HE×300). However, histopathological changes of other groups were remarkable alleviated. (**G**) HE-staining showed that pulmonary pathological changes of G1 is significant, including Pulmonary vascular congestion and edema, lymphocyte and mononuclear cell infiltration , and consolidation of lung (HE×300). However, histopathological changes of other groups were remarkable alleviated. There is not statistical difference between G2 and G3. All data were expressed as the mean±SEM (n = 3, *P＜0.05 compared with normal group, #P＜0.05 compared with the untreated group).

Emerging evidence indicates the potential of RAPA to alleviate cellular senescence [45, 46]. Chen et al. confirmed that RAPA-mediated suppression of the mTORC1 prevented the appearance of senescence markers in retinal pigment epithelium [41]. Cao et al. showed that RAPA abolished nuclear blebbing, delayed the onset of cellular senescence, and enhanced the degradation of progerin (an abnormal form of the lamin A protein) in Hutchinson-Gilford Progeria Syndrome (HGPS) cells [39]. In our study, we found that RAPA decelerated senescence of SLE BM-MSCs by inhibiting excessive cellular growth caused by the mTOR pathway. Furthermore, the cellular morphology became progressively less hypertrophic in comparison with untreated SLE BM-MSCs, which exhibited more numerous and extensive podia, which contained more actin stress fibers. In addition, fewer SA-β-gal-positive cells were detected among RAPA-treated SLE BM-MSCs, while the F-actin was distributed in a disordered pattern and assembled mainly in the nuclear region. Remarkably, we also demonstrated that RAPA did not stimulate the proliferation of BM-MSCs from SLE, did not abrogate cell cycle arrest caused by $p21^{Cip1}$ and p27, and did not force cells to bypass cell cycle arrest.

More importantly, we found that after transwell culture CD4+ T cells with MSCs for 72 h, the ratio of Treg/Th17 generated in the presence of the RAPA and si-mTOR treated SLE MSCs was increased compared to those cultured in the presence of the untreated SLE MSCs. Defects in Treg and/or Th17 development, maintenance or function have been found to be associated with several human autoimmune diseases[47-49]. Moreover, Sun et al. demonstrated that MSCs from NZBW/F1 lupus mice and SLE human patients had defective immunoregulatory function compared with healthy controls [50-52]. It has been reported that SLE flares might be linked to the expansion of the Th17 cell population and the depletion of the natural Treg cell subpopulations. In contrast to the role of Th17 cells, Treg cells play an essential role in maintaining immune homeostasis and preventing autoimmunity [53]. TGF-β and IL-10 are critical differentiation factor for the generation of Treg cells [54], while IL-6 and IL-17 have been shown to be the main factors responsible for the reciprocal regulating proinflammatory Th17 cell development[55]. Our results showed that RAPA and si-mTOR treated SLE MSCs induced the secretion of IL-10 and TGF-β, but downregulated IL-17 and IL-6. Thus, our data demonstrates that RAPA improves the immuno- regulatory capacity of MSCs from SLE patients and indicates the involvement of the mTOR signaling pathway in the immune disorders of SLE patients.

Although syngeneic BM-MSCT has proved ineffective, previous reports have shown the clinical efficacy of allogeneic MSCT in SLE[18-24]. However, several barriers to the application of allogeneic transplantation exist, such as ethical considerations, the scarcity of donors and the risk of contamination. In this study, we showed that transplantation RAPA-pretreated SLE MSCs into MRL/lpr mice alleviated LN and improved the survival rate in recipients. These results suggest that RAPA reverses the senescence of MSCs in SLE patients.

In conclusion, we have demonstrated for the first time that mTOR plays a key role in senescence and immune disorders of MSC from SLE patients and MRL/lpr mice. Furthermore, we show that RAPA reverses the senescence and immune disorders by mTOR signaling pathway. Moreover, these observations indicate the therapeutic potential of autologous MSCT following *in vitro* intervention to treat SLE. Our findings indicate that targeting mTOR in MSCs may provide a new therapeutic strategy for the treatment of SLE patients.

MATERIALS AND METHODS

Patients. Twelve SLE patients aged 15 to 38 years (mean 25.43±5.75 years) were enrolled in the study. The SLE diagnosis was made based on the criteria proposed by the American College of Rheumatology. Twelve healthy subjects (all female), with a similar age distribution (mean 24.86±4.22 years) were enrolled as the normal control group. All individuals gave informed consent to participation in the study, which was approved by the Ethics Committee of the Affiliated Hospital of Nantong University (China).

Isolation, culture and identification of BM-MSCs from SLE patients and normal subjects. MSCs were isolated and expanded from the iliac crest BM of all SLE patients and normal subjects. Five milliliters of heparinized BM were mixed with an equal volume of phosphate-buffered saline (PBS). The resuspended cells were then layered over Ficoll solution (1.077 g/mL) and centrifuged at 2,000 ×*g* for 25 min at room temperature. The mononuclear cells were collected from the interface and resuspended in low-glucose Dulbecco Modified Eagle Medium (L-DMEM) supplemented with 10% heat inactivated fetal bovine serum (FBS). The cells were then plated at a density of 2×10^7 cells per 25 cm^2 dish and cultured at 37ºC in a 5% CO_2 incubator. After 5 days, the medium was replaced and non-adherent cells were removed; this process was repeated every three days thereafter. When the MSCs became nearly confluent, the adherent cells were released from the dishes with 0.25% trypsin-EDTA (Gibco, USA), and

then replated at a density of 1×10^6 cells per 25 cm^2 dish. Flow cytometric analysis showed that the cells were positive for CD29, CD44, CD105, and CD166, but negative for CD14, CD34, CD38, CD45 and HLA-DR (data not shown). After passage 4 (p4), cells were used for the following studies.

Mice and treatments. Eight-week-old female MRL/lpr mice (n = 48) and BALB/c mice (n = 14) (Slyke Experimental Animals Company, China) were divided into five groups. One group of MRL/lpr mice (n = 12) was treated with RAPA (3 mg/kg/day, Sigma-Aldrich, USA) by oral gavage from 16 to 28 weeks. Another group (n = 12) of control MRL/lpr mice received an equal volume of normal saline using the same schedule. The remaining MRL/lpr mice were randomly divided into the following three groups: Group 1 (G1, n = 8) were transplanted with BM-MSCs from SLE patients; Group 2 (G2, n = 8) were transplanted with 500 nM RAPA-pretreated BM-MSCs from SLE patients; Group 3 (G3, n = 8) were transplanted with normal BM-MSCs. The experimental protocols conformed to the animal care guidelines of the China Physiologic Society and were approved by our Institutional Animal Research Committee.

Albuminuria. 24-h urine samples were collected from each mouse by metabolic cages method once every two weeks. Urinary albumin levels were measured using a commercially available ELISA kit (BioAssay Systems, Hayward, CA, USA) according to the manufacturer's instructions.

Anti-dsDNA antibody measurements. Blood was collected from the mice by cardiac puncture under anesthesia at the time of euthanization. Serum levels of anti-dsDNA (IgG) antibody were determined using a commercially available ELISA kit (Alpha Diagnostic International, San Antonio, TX, USA) according to the manufacturer's instructions.

Renal and pulmonary histology studies. At the time of euthanization, kidney and lung specimens were obtained, fixed in 10% formaldehyde and embedded in paraffin. Sections (4 μm thickness) were prepared and then stained with haematoxylin and eosin (H&E). The kidney and lung sections were coded and examined by two independent observers who were blinded to the treatment groups. At least 50 glomeruli were examined for each sample.

Isolation, culture and identification of BM-MSCs from MRL/lpr mice. The BM was flushed out of the femurs and tibias removed from MRL/lpr and BALB/c mice using 10 ml PBS with 100 U/ml heparin in a syringe. The cells were centrifuged at 1000 ×*g* for 10 min. The cell pellet was resuspended in 5 ml L-DMEM supplemented with 10% FBS (Gibco, USA) and plated in a 25 cm^2 dish to allow the MSCs to adhere. Cultures were maintained in a humidified atmosphere with 5% CO_2 at 37°C. Flow cytometric analysis showed that the cells were positive for CD29, CD44, CD105, and CD166, but negative for CD14, CD34, CD38, CD45 and HLA-DR (data not shown). MSCs were cultured using the same method as that used for human MSCs. All experiments were conducted with MSCs at p4.

Western blotting**.** BM-MSCs were washed in cold-buffered PBS and were then lysed in RIPA buffer (150 mM NaCl, 1%TritonX-100, 0.5%NaDOD, 0.1%SDS and 50 mM Tris, pH 8.0). After centrifugation (12,000 rpm, 5 min) at 4C, the protein supernate was transferred into new tubes. The protein concentration of the samples was determined with a bicinchoninic acid protein assay (Pierce, USA). Equal amounts of proteins were separated by 10% SDS polyacrylamide gel electrophoresis (PAGE) and electrophoretically transferred to polyvinylidene difluoride (PDVF) membranes. Membranes were blocked with 5% non-fat milk in TBST (20 mM Tris, 150 mM NaCl, 0.05% Tween-20) and incubated with primary antibodies (1:500) at 4°C overnight. Subsequently, the membranes were incubated with horseradish peroxidase conjugated mouse anti-rabbit secondary antibody for 2 h at room temperature. The blots were developed using an enhanced chemiluminescence kit (NEN Life Science Products, Boston, MA, USA). GAPDH was used as a reference protein. The following primary antibodies were used: GAPDH (anti-rabbit, Santa Cruz), p-mTOR (anti-rabbit, Sigma), mTOR (anti-rabbit, Sigma), p-S6K (anti-rabbit, Santa Cruz), S6K (anti-rabbit, Santa Cruz), p-S6 (anti-rabbit, Sigma), S6 (anti-rabbit, Sigma), p53 (anti-rabbit, Cell Signaling), p21 (anti-rabbit, Sigma), p27 (anti-rabbit, Cell Signaling).

Immunofluorescence. BM-MSCs were fixed with 4% paraformaldehyde (PFA) for 1 h, washed with PBS containing 0.1% Triton X-100 (PBST), and blocked for 30 min in PBST supplemented with 10% FBS. Cells were then incubated with one of the following primary antibodies (1:100) in the same solution overnight at 4°C: p-mTOR (anti-rabbit, Sigma), p-S6K (anti-rabbit, Santa Cruz), p-S6 (anti-rabbit, Sigma), washed and incubated in the dark with goat anti-rabbit- (cy3-) conjugated antibodies (1 : 300, ICN Cappel, USA) for 2 h at room temperature. Nuclei were stained with DAPI (1:800, Santa Cruz). The cells were examined with a Leica fluorescence microscope (Germany). For visualization of the MSC cytoskeleton, cells were washed twice with PBS and fixed in 4% PFA for 1 h.

After permeabilization and blocking, they were then incubated with fluorescein isothiocyanate-conjugated phalloidin, which is a high-affinity filamentous probe. The stained cells were then examined under a Zeiss Confocal Laser Scanning Microscope.

Senescence-associated-β-galactosidase assay. The SA-β-gal activity was determined using the in situ β-galactosidase staining kit from the Beyotime Institute of Biotechnology following the manufacturer's instructions. MSCs treated with or without RAPA were passaged into 6-well culture plates at a density of 5×10^4 cells per well for 72 h. The cells were then washed twice with PBS and fixed with the 4% paraformaldehyde for 15 min. After incubation with the SA-β-gal detection solution at 37°C without CO_2 overnight, the cells were washed and analyzed under the microscope (Leica company, Germany). We counted at a minimum of 500 cells to determine the percentage of SA-β-gal-positive cells.

Cell number assay. MSCs were seeded at 0.7×10^4 cells/well in 6-well plates in triplicate for each condition. RAPA (500 nM) was added to the cultures of SLE BM-MSCs, and dimethylsulfoxide (DMSO) was added to the untreated control cells. Cells were collected at 1 to 4 days after plating, dissociated, and the total cell numbers were counted.

CD4+ T cell isolation and transwell culture with MSCs. Single-cell suspensions of spleens collected from the BALB/c mice were prepared by mechanical disruption in PBS. CD4+ T cells were isolated by magnetic sorting of Dynabead-bound mouse CD4+ cells according to the manufacturer's directions (Dynal Biotech). Positively selected cells contained an average of 99% CD4+ T cells as assessed by flow cytometric analysis with CD4 monoclonal antibody. Cells were cultured in RPMI 1640 medium supplemented with 10% FCS, 1×nonessential amino acids and 1 mM sodium pyruvate.The purified CD4+ T cells (1×10^5) were obtained and cultured in the lower chamber of the 24-well diameter transwell plate with a 0.3-μm pore size membrane (Corning, NY, USA). MSCs (1×10^6) were seeded onto the transwell membrane of the inner chamber for 72 hours of transwell culture.

Flow cytometry. For cell cycle analysis, MSCs treated with or without 500 nM RAPA were collected and fixed with 70% ethanol at 4°C for 24 h. After being washed with PBS and then treated with 100 μg/ml RNase (Sigma, USA) for 30 min, the cells were stained with 50 μg/ml propidium iodide (PI) solution (Sigma, USA) for 30 minutes and analyzed by flow cytometry (FACS Calibur, BD Biosciences, USA). The fraction of cells in the G0/G1, S, and G2/M phases were quantified with the ModFit LT system. Three separate experiments were performed.

For regulatory T (Treg) and T helper type 17 (Th17) cell analysis, the ratio of Treg/Th17 among the CD4+ T cell population was analyzed using Treg and Th17 assay kits (Santa Cruz, USA). After 72 h of transwell culture, CD4+ cells were harvested and washed with PBS, resuspended in 100 μl staining buffer and divided into two aliquots (one for detection and another for the isotype control). The CD4+ T cells were stained with anti-CD25-APC or anti-IL-17-PE mAbs to assay the Treg and Th17 cells, respectively. IgG_{2a}-PE rat was used as the isotype control. All procedures were performed according to the manufacturer's protocol and cells were analyzed by flow cytometry (FACS Calibur, BD Biosciences, USA).

Cytokine determination by ELISA. The concentrations of transforming growth factor (TGF)-β, interleukin (IL)-10, IL-17 and IL-6 cytokines released in the transwell culture supernatants were measured by enzyme-linked immunosorbent assay (ELISA) using commercially available kits (R&D Systems, Abingdon, Oxon, UK), according to the manufacturer's instructions. Briefly, 10^6 cells in 100 μl of medium were seeded onto transwell membrane of the inner chamber. After 72 h, 100 μl of supernatants were harvested for ELISA assay.

Cell transfection. Transfections were performed using Lipofectamine™ 2000 (Ambion) according to the manufacturer's instructions. mTOR small interfering RNA (siRNA) (Ambion) was used to knock down mTOR expression in MSCs. siRNA was mixed with Lipofectamine transfection reagent in serum-free medium according to the manufacturer's instructions. Subsequently, MSCs cultured in 6-well plates to a confluence of 60% were transfected with siRNA in culture medium. The cells were cultivated for a further 48 h at 37°C.

Statistical analysis. All data were shown as the mean±standard deviation (SD) of at least three independent experiments. All statistical analyses were performed using SPSS 11.0 software, and were analyzed by ANOVA followed by post-hoc Bonferroni tests. $P < 0.05$ was considered to indicate statistically significance.

ACKNOWLEDGEMENTS

We thank the laboratory members for helpful discussions.

Funding

This work was supported by Natural Science Foundation of China, Grant (No.81172841), Natural Science Foundation of China, Grant (No. 81202368 and 81471603), Natural Science Foundation of Jiangsu Colleges and Universities Grant (09KJB320010) (10KJB320012); "Top Six Types of Talents'' Financial Assistance of Jiangsu Province Grant (No. 6 and NO.7), Jiangsu province's outstanding medical academic leader program (LJ201136); Graduate Student Innovation of Science and Technology Projects in Jiangsu Province and in Nantong University (Grants No.13025045).

Conflict of interest statement

No potential conflicts of interest were disclosed.

REFERENCES

1. Rahman A and Isenberg DA. Systemic lupus erythematosus. The New England journal of medicine. 2008; 358:929-939.

2. Jehl F, Quoix E, Leveque D, Pauli G, Breillout F, Krikorian A and Monteil H. Pharmacokinetic and preliminary metabolic fate of navelbine in humans as determined by high performance liquid chromatography. Cancer research. 1991; 51:2073-2076.

3. Rosado MM, Diamanti AP, Capolunghi F and Carsetti R. B cell modulation strategies in autoimmunity: the SLE example. Current pharmaceutical design. 2011; 17:3155-3165.

4. Smith KG, Jones RB, Burns SM and Jayne DR. Long-term comparison of rituximab treatment for refractory systemic lupus erythematosus and vasculitis: Remission, relapse, and re-treatment. Arthritis and rheumatism. 2006; 54:2970-2982.

5. Blagosklonny MV. Validation of anti-aging drugs by treating age-related diseases. Aging (Albany NY). 2009; 1:281-288. doi:10.18632/aging.100034.

6. Ramos-Casals M, Sanz I, Bosch X, Stone JH and Khamashta MA. B-cell-depleting therapy in systemic lupus erythematosus. The American journal of medicine. 2012; 125:327-336.

7. Charbord P. Bone marrow mesenchymal stem cells: historical overview and concepts. Human gene therapy. 2010; 21:1045-1056.

8. Deng W, Han Q, Liao L, You S, Deng H and Zhao RC. Effects of allogeneic bone marrow-derived mesenchymal stem cells on T and B lymphocytes from BXSB mice. DNA and cell biology. 2005; 24:458-463.

9. Sotiropoulou PA, Perez SA, Gritzapis AD, Baxevanis CN and Papamichail M. Interactions between human mesenchymal stem cells and natural killer cells. Stem cells. 2006; 24:74-85.

10. Nauta AJ and Fibbe WE. Immunomodulatory properties of mesenchymal stromal cells. Blood. 2007; 110:3499-3506.

11. Nauta AJ, Westerhuis G, Kruisselbrink AB, Lurvink EG, Willemze R and Fibbe WE. Donor-derived mesenchymal stem cells are immunogenic in an allogeneic host and stimulate donor graft rejection in a nonmyeloablative setting. Blood. 2006; 108:2114-2120.

12. Chan JL, Tang KC, Patel AP, Bonilla LM, Pierobon N, Ponzio NM and Rameshwar P. Antigen-presenting property of mesenchymal stem cells occurs during a narrow window at low levels of interferon-gamma. Blood. 2006; 107:4817-4824.

13. Nie Y, Lau C, Lie A, Chan G and Mok M. Defective phenotype of mesenchymal stem cells in patients with systemic lupus erythematosus. Lupus. 2010; 19:850-859.

14. Gu Z, Cao X, Jiang J, Li L, Da Z, Liu H and Cheng C. Upregulation of p16INK4A promotes cellular senescence of bone marrow-derived mesenchymal stem cells from systemic lupus erythematosus patients. Cellular signalling. 2012; 24:2307-2314.

15. Li X, Liu L, Meng D, Wang D, Zhang J, Shi D, Liu H, Xu H, Lu L and Sun L. Enhanced apoptosis and senescence of bone-marrow-derived mesenchymal stem cells in patients with systemic lupus erythematosus. Stem cells and development. 2012; 21:2387-2394.

16. Gu Z, Jiang J, Tan W, Xia Y, Cao H, Meng Y, Da Z, Liu H and Cheng C. p53/p21 Pathway involved in mediating cellular senescence of bone marrow-derived mesenchymal stem cells from systemic lupus erythematosus patients. Clinical & developmental immunology. 2013; 2013:134243.

17. Wang D, Zhang H, Liang J, Li X, Feng X, Wang H, Hua B, Liu B, Lu L, Gilkeson GS, Silver RM, Chen W, Shi S, et al. Allogeneic mesenchymal stem cell transplantation in severe and refractory systemic lupus erythematosus: 4 years of experience. Cell transplantation. 2013; 22:2267-2277.

18. Sun L, Akiyama K, Zhang H, Yamaza T, Hou Y, Zhao S, Xu T, Le A and Shi S. Mesenchymal stem cell transplantation reverses multiorgan dysfunction in systemic lupus erythematosus mice and humans. Stem cells. 2009; 27:1421-1432.

19. Gu Z, Akiyama K, Ma X, Zhang H, Feng X, Yao G, Hou Y, Lu L, Gilkeson GS, Silver RM, Zeng X, Shi S and Sun L. Transplantation of umbilical cord mesenchymal stem cells alleviates lupus nephritis in MRL/lpr mice. Lupus. 2010; 19:1502-1514.

20. Zhou K, Zhang H, Jin O, Feng X, Yao G, Hou Y and Sun L. Transplantation of human bone marrow mesenchymal stem cell ameliorates the autoimmune pathogenesis in MRL/lpr mice. Cellular & molecular immunology. 2008; 5:417-424.

21. Sun L, Wang D, Liang J, Zhang H, Feng X, Wang H, Hua B, Liu B, Ye S, Hu X, Xu W, Zeng X, Hou Y, et al. Umbilical cord mesenchymal stem cell transplantation in severe and refractory systemic lupus erythematosus. Arthritis and rheumatism. 2010; 62:2467-2475.

22. Gu F, Molano I, Ruiz P, Sun L and Gilkeson GS. Differential effect of allogeneic versus syngeneic mesenchymal stem cell transplantation in MRL/lpr and (NZB/NZW)F1 mice. Clinical immunology. 2012; 145:142-152.

23. Chang JW, Hung SP, Wu HH, Wu WM, Yang AH, Tsai HL, Yang LY and Lee OK. Therapeutic effects of umbilical cord blood-derived mesenchymal stem cell transplantation in experimental lupus nephritis. Cell transplantation. 2011; 20:245-257.

24. Carrion F, Nova E, Ruiz C, Diaz F, Inostroza C, Rojo D, Monckeberg G and Figueroa FE. Autologous mesenchymal stem cell treatment increased T regulatory cells with no effect on disease activity in two systemic lupus erythematosus patients. Lupus. 2010; 19:317-322.

25. Johnson SC, Rabinovitch PS and Kaeberlein M. mTOR is a key modulator of ageing and age-related disease. Nature. 2013; 493:338-345.

26. Xu S, Cai Y and Wei Y. mTOR Signaling from Cellular Senescence to Organismal Aging. Aging and disease. 2014; 5:263-273.

27. Blagosklonny MV. Aging: ROS or TOR. Cell cycle. 2008; 7:3344-3354.

28. Sethe S, Scutt A and Stolzing A. Aging of mesenchymal stem cells. Ageing research reviews. 2006; 5:91-116.

29. Korotchkina LG, Leontieva OV, Bukreeva EI, Demidenko ZN, Gudkov AV and Blagosklonny MV. The choice between p53-induced senescence and quiescence is determined in part by the mTOR pathway. Aging (Albany NY). 2010; 2:344-352. doi: 10.18632/aging.100160.

30. Sabatini DM. mTOR and cancer: insights into a complex relationship. Nature reviews Cancer. 2006; 6:729-734.

31. Yentrapalli R, Azimzadeh O, Sriharshan A, Malinowsky K, Merl J, Wojcik A, Harms-Ringdahl M, Atkinson MJ, Becker KF, Haghdoost S and Tapio S. The PI3K/Akt/mTOR pathway is implicated in the premature senescence of primary human endothelial cells exposed to chronic radiation. PloS one. 2013; 8:e70024.

32. Leontieva OV, Demidenko ZN and Blagosklonny MV. Contact inhibition and high cell density deactivate the mammalian target of rapamycin pathway, thus suppressing the senescence program. Proceedings of the National Academy of Sciences of the United States of America. 2014; 111:8832-8837.

33. Demidenko ZN and Blagosklonny MV. Growth stimulation leads to cellular senescence when the cell cycle is blocked. Cell cycle. 2008; 7:3355-3361.

34. Blagosklonny MV and Hall MN. Growth and aging: a common molecular mechanism. Aging (Albany NY). 2009; 1:357-362. doi: 10.18632/aging.100040.

35. Gharibi B, Farzadi S, Ghuman M and Hughes FJ. Inhibition of Akt/mTOR attenuates age-related changes in mesenchymal stem cells. Stem cells. 2014; 32:2256-2266.

36. Cao K, Graziotto JJ, Blair CD, Mazzulli JR, Erdos MR, Krainc D and Collins FS. Rapamycin reverses cellular phenotypes and enhances mutant protein clearance in Hutchinson-Gilford progeria syndrome cells. Science translational medicine. 2011; 3:89ra58.

37. Lesovaya EA, Kirsanov KI, Antoshina EE, Trukhanova LS, Gorkova TG, Shipaeva EV, Salimov RM, Belitsky GA, Blagosklonny MV, Yakubovskaya MG and Chernova OB. Rapatar, a nanoformulation of rapamycin, decreases chemically-induced benign prostate hyperplasia in rats. Oncotarget. 2015; 6:9718-9727. doi: 10.18632/oncotarget.3929.

38. Blagosklonny MV. Rejuvenating immunity: "anti-aging drug today" eight years later. Oncotarget. 2015; 6:19405-19412. doi: 10.18632/oncotarget.3740.

39. Demidenko ZN, Zubova SG, Bukreeva EI, Pospelov VA, Pospelova TV and Blagosklonny MV. Rapamycin decelerates cellular senescence. Cell cycle. 2009; 8:1888-1895.

40. Chen Y, Wang J, Cai J and Sternberg P. Altered mTOR signaling in senescent retinal pigment epithelium. Investigative ophthalmology & visual science. 2010; 51:5314-5319.

41. Fernandez D, Bonilla E, Mirza N, Niland B and Perl A. Rapamycin reduces disease activity and normalizes T cell activation-induced calcium fluxing in patients with systemic lupus erythematosus. Arthritis and rheumatism. 2006; 54:2983-2988.

42. Mercier I, Camacho J, Titchen K, Gonzales DM, Quann K, Bryant KG, Molchansky A, Milliman JN, Whitaker-Menezes D, Sotgia F, Jasmin JF, Schwarting R, Pestell RG, et al. Caveolin-1 and accelerated host aging in the breast tumor microenvironment: chemoprevention with rapamycin, an mTOR inhibitor and anti-aging drug. The American journal of pathology. 2012; 181:278-293.

43. Warner LM, Adams LM and Sehgal SN. Rapamycin prolongs survival and arrests pathophysiologic changes in murine systemic lupus erythematosus. Arthritis and rheumatism. 1994; 37:289-297.

44. Grant CR, Liberal R, Mieli-Vergani G, Vergani D and Longhi MS. Regulatory T-cells in autoimmune diseases: challenges, controversies and--yet--unanswered questions. Autoimmunity reviews. 2015; 14:105-116.

45. Donehower LA. Rapamycin as longevity enhancer and cancer preventative agent in the context of p53 deficiency. Aging (Albany NY). 2012; 4:660-661. doi: 10.18632/aging.100494.

46. Komarova EA, Antoch MP, Novototskaya LR, Chernova OB, Paszkiewicz G, Leontieva OV, Blagosklonny MV and Gudkov AV. Rapamycin extends lifespan and delays tumorigenesis in heterozygous p53+/- mice. Aging (Albany NY). 2012; 4:709-714. doi: 10.18632/aging.100498.

47. Ohl K and Tenbrock K. Regulatory T cells in systemic lupus erythematosus. European journal of immunology. 2015; 45:344-355.

48. Reinert-Hartwall L, Honkanen J, Salo HM, Nieminen JK, Luopajarvi K, Harkonen T, Veijola R, Simell O, Ilonen J, Peet A, Tillmann V, Knip M, Vaarala O, et al. Th1/Th17 plasticity is a marker of advanced beta cell autoimmunity and impaired glucose tolerance in humans. Journal of immunology. 2015; 194:68-75.

49. Sun LY, Zhang HY, Feng XB, Hou YY, Lu LW and Fan LM. Abnormality of bone marrow-derived mesenchymal stem cells in patients with systemic lupus erythematosus. Lupus. 2007; 16:121-128.

50. Gu Z, Tan W, Feng G, Meng Y, Shen B, Liu H and Cheng C. Wnt/beta-catenin signaling mediates the senescence of bone marrow-mesenchymal stem cells from systemic lupus erythematosus patients through the p53/p21 pathway. Molecular and cellular biochemistry. 2014; 387:27-37.

51. Lu L, Wang DD, Li X, Zeng XF and Sun LY. [Mechanism of umbilical cord mesenchymal stem cells in the up-regulation of regulatory T cells by transforming growth factor beta1 in systemic lupus erythematosus]. Zhonghua yi xue za zhi. 2013; 93:980-983.

52. Duhen T, Duhen R, Lanzavecchia A, Sallusto F and Campbell DJ. Functionally distinct subsets of human FOXP3+ Treg cells that phenotypically mirror effector Th cells. Blood. 2012; 119:4430-4440.

53. Liu H, Hu B, Xu D and Liew FY. CD4+CD25+ regulatory T cells cure murine colitis: the role of IL-10, TGF-beta, and CTLA4. Journal of immunology. 2003; 171:5012-5017.

54. Mills KH. Induction, function and regulation of IL-17-producing T cells. European journal of immunology. 2008; 38:2636-2649.

55. Zhao R. Immune regulation of bone loss by Th17 cells in oestrogen-deficient osteoporosis. European journal of clinical investigation. 2013; 43:1195-1202.

Research Paper

Reversal of phenotypes of cellular senescence by pan-mTOR inhibition

Hannah E. Walters[1], Sylwia Deneka-Hannemann[1,2], and Lynne S. Cox[1]

[1]Department of Biochemistry, University of Oxford, South Parks Road, Oxford, OX1 3QU, United Kingdom
[2]Current address: Oxford BioMedica Plc, Oxford, OX4 6LT, United Kingdom

Key words: *cellular senescence, aging, mTORC1, mTORC2, rapamycin, AZD8055*
Received: *7/1/15; Accepted: 1/15/16; Published: 2/5/16*
Correspondence to: *Lynne Cox, PhD; E-mail: lynne.cox@bioch.ox.ac.uk* doi:10.18632/aging.100872

Abstract: **Cellular senescence, a state of essentially irreversible proliferation arrest, serves as a potent tumour suppressor mechanism. However, accumulation of senescent cells with chronological age is likely to contribute to loss of tissue and organ function and organismal aging. A crucial biochemical modulator of aging is mTOR; here, we have addressed the question of whether acute mTORC inhibition in near-senescent cells can modify phenotypes of senescence. We show that acute short term treatment of human skin fibroblasts with low dose ATP mimetic pan-mTORC inhibitor AZD8055 leads to reversal of many phenotypes that develop as cells near replicative senescence, including reduction in cell size and granularity, loss of SA-β-gal staining and reacquisition of fibroblastic spindle morphology. AZD8055 treatment also induced rearrangement of the actin cytoskeleton, providing a possible mechanism of action for the observed rejuvenation. Importantly, short-term drug exposure had no detrimental effects on cell proliferation control across the life-course of the fibroblasts. Our findings suggest that combined inhibition of both mTORC1 and mTORC2 may provide a promising strategy to reverse the development of senescence-associated features in near-senescent cells.**

INTRODUCTION

Cellular senescence is a hallmark of aging [1] and senescent cells accumulate with age *in vivo* in mammals [2, 3]; this is thought to drive aging by limiting tissue replicative capacity and causing tissue dysfunction (reviewed in [4]). Senescent cells can be characterized by significant alterations in phenotype: they exhibit a large, flat, vacuolated and granular morphology with accumulation of lipid droplets and visible stress fibers, together with increased lysosomal content [5]. Proliferative arrest accompanies senescence, shown by down-regulation of proliferative markers such as Ki67 as well as increased expression of mediators of senescence, such as the cyclin kinase inhibitors $p16^{INK4A}$ and $p21^{CDKN1}$ [6-9]. Deletion of the p21 gene can prolong lifespan in telomerase-null mice [10] and clearance of p16-expressing senescent cells *in vivo* can rejuvenate aged mice [11]. Moreover, telomerase re-activation suppresses premature aging phenotypes in telomerase knock-out mice [12-14]. Taken together these key findings strongly support the argument that senescent cells are detrimental in older animals. Developing strategies to delay the onset of senescence or remove senescent cells therefore may provide a route to preventing age-related disease.

Targeting senescence as a means to combat aging and age-related diseases is, however, challenging due to its antagonistically pleiotropic nature – any treatment needs to limit the deleterious impacts of senescent cells without impacting the potent barrier against tumorigenesis. While caloric restriction has been reported to extend healthspan in macaques [15], the most promising candidate for a longevity therapeutic in mammals is rapamycin [16]; (reviewed [17, 18]). Rapamycin is a macrolide antibiotic produced by *Streptomyces hygroscopius*, discovered in the soil of

Easter Island [19]. It is clinically licensed for immunosuppression in kidney transplant patients and for renal cell carcinoma treatment due to its broad inhibitory effects on cell growth and proliferation [20]. As discovered through *S. cerevisiae* genetic screens [21], rapamycin mechanistically acts by binding the protein FKBP12, producing a complex which can bind and inhibit mTOR, a conserved eukaryotic Ser/Thr kinase. mTOR constitutes the point at which diverse environmental signals are coordinated into a cellular response, regulating pathways including cell growth, proliferation, survival, motility and protein synthesis [22-24]. mTOR is present in two complexes in metazoa, mTORC1 and mTORC2, which have different components and functions [22]. Rapamycin inhibits mTORC1, but chronic treatment may also disrupt mTORC2. Rapamycin does not inhibit the phosphorylation of all mTORC1 substrates equally: it completely inhibits phosphorylation of S6K1 while only partially blocking the phosphorylation of 4EBP1 [25]. A crystal structure of mTOR, rapamycin and FKBP12 [26] suggests that this may be due to differential substrate access to the kinase active site; this is supported by further crystallography data [27]. While rapamycin extends lifespan in mice even when administered in middle age [16], it has significant side-effects that may limit its use in humans. We have therefore explored the potential of second generation rapalogs i.e. pharmacological agents that inhibit mTORC but act not through binding to FKBP12 but instead as mTORC-specific ATP mimetics [28]. AZD8055 is an ATP-competitive inhibitor of mTOR kinase in both mTORC1 and mTORC2, with an IC_{50} of 0.8 nmol/L, with ~1000-fold selectivity for mTOR over other PI3K family members and no significant activity against a large panel of other cellular kinases [29]. AZD8055 has anti-proliferative effects similar to those of rapamycin and has been taken forward into clinical trials against various forms of cancer [30].

To date, studies examining the impact of rapalogs on aging has required chronic drug administration (e.g. [16]), an approach that may not be acceptable for prophylactic avoidance of age-related disease in the general human population. Here, we test whether acute mTORC inhibition can alter features of senescence in cells that have already undergone a large number of population doublings (PD) – as they are about to undergo senescence but are currently still proliferating, we term these populations 'near-senescent'. Such high cumulative PD (CPD) near-senescent cells show many signs characteristic of senescence including increased size and granularity, SA-β-gal staining, high lysosomal content and accumulation of actin stress fibers. They are still capable of cell proliferation, albeit with a reduced rate of proliferation compared with cells at lower CPD. Here, we test the effect of inhibiting both mTORC1 and mTORC2 using the TOR-specific ATP mimetic AZD8055. Remarkably, we demonstrate significant reversal of major phenotypes of senescence on short term low dose pan-TOR inhibition. We therefore suggest that AZD8055 may prove useful in modulating health outcomes in late life.

RESULTS

Morphological rejuvenation of near-senescent cells

We first set out to test the impact of AZD8055 treatment on cell morphology, as this represents a very useful biomarker of cellular senescence in fibroblasts [31]. Near-senescent diploid human neonatal foreskin fibroblasts (HF043) were obtained by serial passaging in the absence of any drug treatment until they started to show signs characteristic of early senescence (such as enlarged cell size, decreased proliferation rate and elevated p21 levels – see supplementary Fig 1). Cell populations showing senescent-like phenotypes were harvested and seeded into parallel culture flasks/plates and then treated with AZD8055 (or DMSO vehicle control) for 7 days. Drug doses were chosen to mimic serum concentrations of animals treated with rapalogs (e.g. [16]); these doses were found to have little or no toxicity, though they did slow down the rate of cell proliferation (data not shown). Overall morphology was observed by phase contrast microscopy. As expected, control cells demonstrated increased size, vacuolization and granularity typical of cells as they approach senescence (DMSO, Fig 1A, B). By contrast, one week's treatment with 35 nM AZD8055 led to marked alteration in morphology, with cells re-acquiring the classical spindle morphology characteristic of low CPD proliferating fibroblasts (Fig 1A, B). This result has been verified in several other populations of high CPD HF043 cells, including cells at CPD 88 (note that this fibroblast line HF043 reaches replicative senescence at ~CPD 95).

To determine whether these apparent cell size changes are quantifiably different following AZD8055 treatment, we harvested cells by gentle trypsinization so that cells detach from the substrate and round up to ovoid/spherical shapes (Fig 1C). Cell diameters in these harvested populations were measured using a Cellometer T4 (see Methods). Low CPD cells (CPD 36) showed a slight though not significant effect of AZD8055 in decreasing diameter (Table 1). However, consistent with the changes observed by phase contrast microscopy (Fig 1C), we found a highly significant reduction in cell diameter of cells at CPD 73 from a

mean of 27.7 µm (DMSO control) to 24.7 µm on AZD8055 treatment (unpaired t-test, $p<0.02$, Table 1), a cell diameter highly similar to that of low CPD untreated cells. Again, this was replicated in several other populations of near-senescent HF043 cells, producing highly similar results.

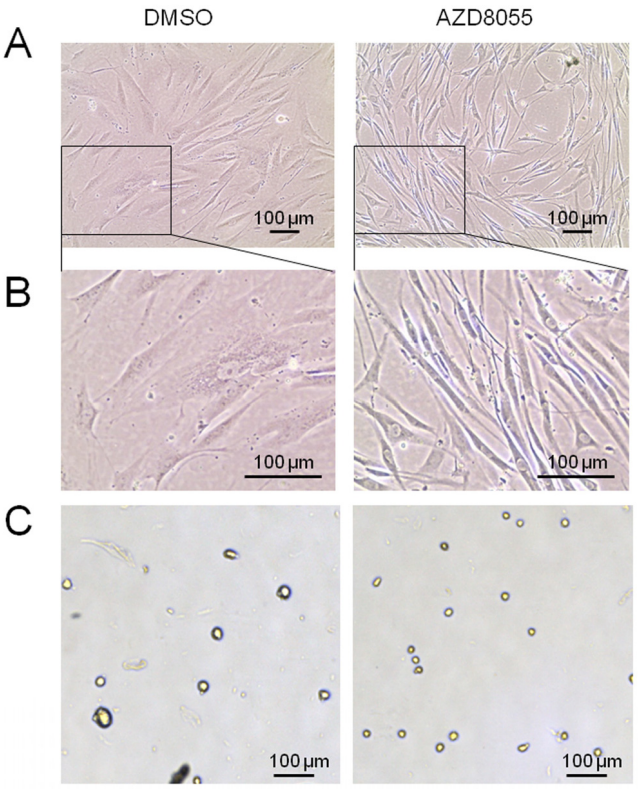

Figure 1. AZD8055 causes major changes in near-senescent fibroblast morphology and size. HF043 fibroblasts at high CPD were incubated with AZD8055 or equivalent volume of DMSO for 7 days. (**A**) Cells were observed *in situ* by phase contrast microscopy. (**B**) Magnified images from (**A**). (**C**) Cells were harvested by trypsinization and cell suspension analysed using a Cellometer T4; images were obtained at x20 magnification.

Loss of Mitotracker signal on AZD8055 treatment

Mitochondrial biomass increases as cells approach senescence [32] possibly as a compensatory mechanism for increasingly inefficient mitochondrial activity. We therefore used a mitochondrial-specific probe, Mitotracker Red, to label mitochondria in low and high CPD cells with acute mTORC inhibition. Mitochondria were detected as reticular networks throughout the fibroblasts, though at low population doublings the signal was relatively weak both without (Fig 2A) and with (Fig 2B) AZD8055 exposure. By contrast, a high Mitotracker signal was detected in near-senescent cells at CPD 73 (Fig 2C, E), consistent with increased ROS in the mitochondria of aged cells. This signal was dramatically reduced on AZD8055 treatment (Fig 2D, F), to levels similar to those detected in cells early in their proliferative lifespan (ie at low CPD (Fig 2A, B)).

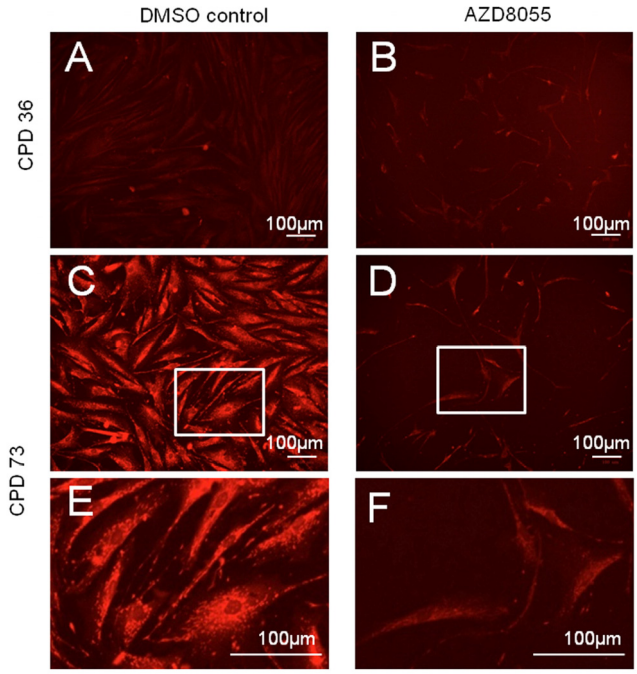

Figure 2. Decreased senescence-related mitochondrial signal on AZD8055 treatment. Fibroblasts were incubated with DMSO (**A, C, E**) or AZD8055 (B, D, F) for 7 days prior to staining with MitoTracker Red and imaging with a BioRad Zoe fluorescent imager. (**A, B**) show cells at early stages of culture (CPD 36), while C-F show cells at CPD 73 at time of drug treatment. (**E, F**) are magnified from **C, D** (respectively, region magnified shown by white box). Scale bar 100 µm. Note that gain and exposure time were the same in all photomicrographs.

Effects of AZD8055 on lysosomes and SA-β-galactosidase

The cellular lysosomal content increases gradually with biological age of cells and can be used as a biomarker of senescence [5]. To assess the effect of mTORC inhibition on lysosomal content, near-senescent fibroblasts were treated with AZD8055 or DMSO for 7 days and then lysosomes were labelled using Lysotracker Red. Notably, treatment of near-senescent cells with AZD8055 led to a marked redistribution of

the lysosomal signal, from a diffuse perinuclear pattern seen in control cells to a more intense pattern distributed along the axis of the cell on drug treatment (Fig 3A), highlighting the overall shift in near-senescent cell shape on AZD8055 treatment to a more spindle-like morphology. As anticipated, lysosomal content increased as control cells reached late passage compared with early passage (assessed quantitatively using Image J, Fig 3B). The lysosomal signal was elevated in early passage cells treated with AZD8055 and this did not alter on cell ageing (Fig 3B).

In addition to increased lysosomal loading, senescent cells - as well as those nearing senescence [31] - also show a major shift in biochemical activity within lysosomes, reflected by the canonical marker SA-β-gal (senescence-associated-β-galactosidase) [5]. We therefore assessed the percentage of near-senescent cells staining positive for SA-β-gal upon treatment (Fig 3C, D). On average, more than 56% of control cells at high CPD stain positive for SA-β-gal, while this was markedly reduced to only 12% after 7 days of AZD8055 treatment (Fig 3D). The difference is highly significant ($p<0.005$, one-tailed student t test, n= 3 independent biological replicates). This marker of senescence is therefore lost on AZD8055 treatment, suggesting a reversal of specific cellular metabolic features associated with senescence.

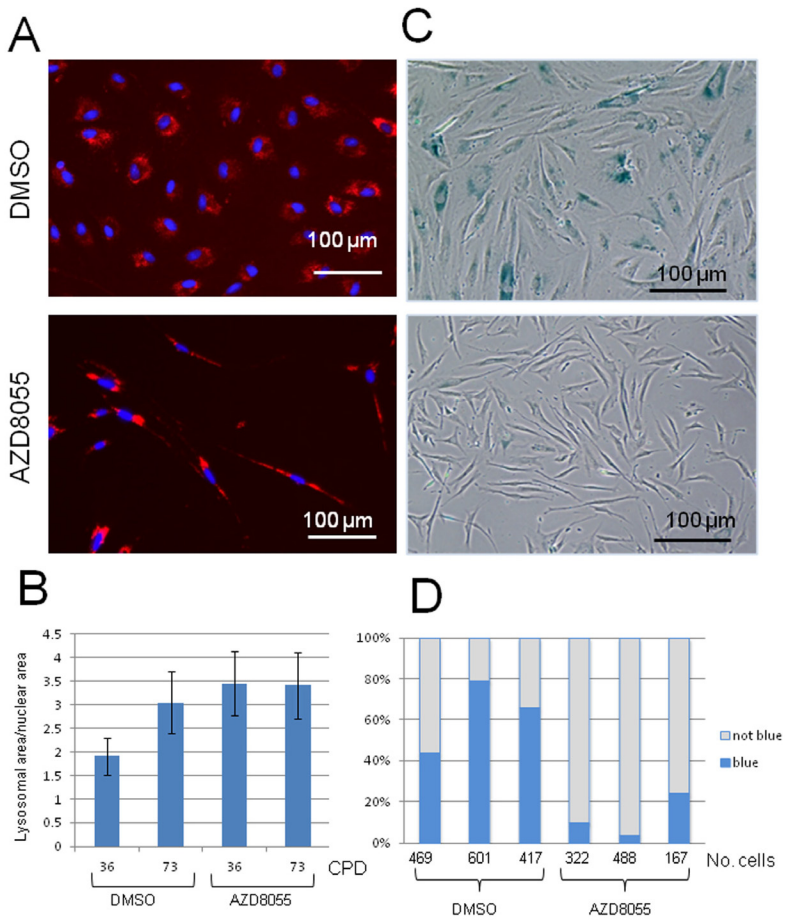

Figure 3. Lysosomal distribution and function are altered on AZD8055 treatment. Fibroblasts at CPD 73 were treated with AZD8055 or DMSO for 7 days then imaged for (**A**) lysosomes using LysoTracker Red. (**B**) Quantification of lysosomal signal over nuclear signal was conducted using ImageJ analysis, for cells at early CPD (36) and those nearing senescence (CPD73) with either AZD8055 treatment at 35 nM or DMSO control. (**C**) SA-β-gal staining of fibroblasts following one week of AZD8055 treatment. (**D**) Three independent biological replicates were each assayed by manually scoring SA-β-gal positive cells - numbers scored for each sample are shown under the graph. Difference between the means of the AZD8055-treated and DMSO controls are significant at $p<0.005$ using one tailed student t test.

Table 1. Mean cell diameter on AZD8055 treatment.

	DMSO	AZD8055	
CPD 36	25.7 (148)	24.5 (49)	NS
CPD 73	27.7 (120)	24.7 (64)	*
	*	NS	

Cells were grown with and without 7 day exposure to 70 nM AZD8055 compared with DMSO control at CPD 36 (low CPD) or CPD 73 (near-senescent). Unpaired t tests were used to assess significance (>40 cells analyzed per sample). NS = not significant. n values for number of cells measured are given in parentheses below each diameter value. * denotes significant at p<0.02.

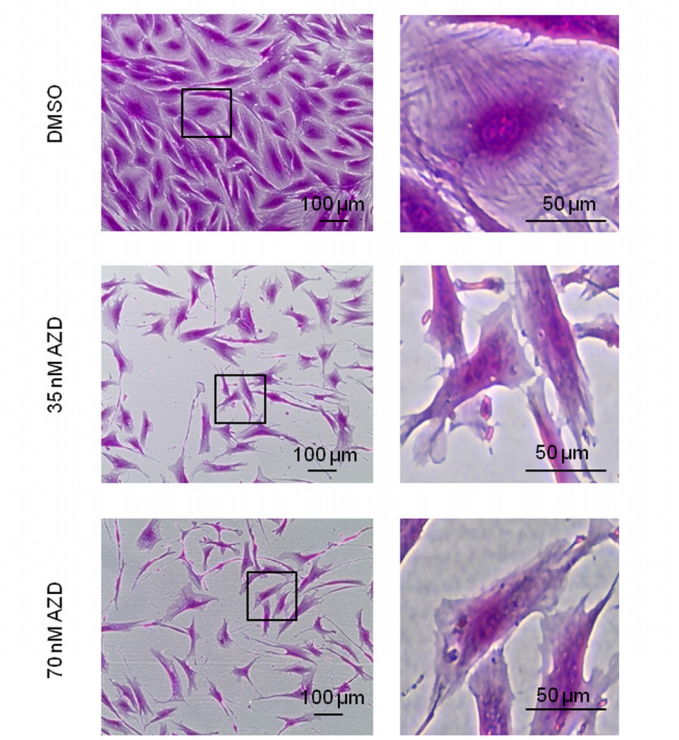

Figure 4. Loss of filamentous structures in AZD8055-treated cells. Fibroblasts at CPD 73 exposed to 35 nM or 70 nM AZD8055 or equivalent volume of DMSO for 1 week were fixed and stained using sulforhodamine B, then imaged by phase contrast microscopy. Left panel imaged with X40 objective; right panel magnification of regions outlined by black boxes.

Major rearrangement of the actin cytoskeleton accompanies reversal of other senescent biomarkers

To further analyze these morphological differences, we stained near-senescent cells with sulforhodamine B with and without prior exposure to AZD8055 for 7 days; this dye is more usually utilized for cytotoxicity screening and biomass measurements [36] but we also find it very informative for microscopic analysis, by either phase contrast (Fig 4) or fluorescence microscopy (Ex480 Em520, not shown). At the molecular level, SRB binds basic amino acid residues under mild acidic conditions, thus staining the cellular protein content. The negative impact on cell proliferation of mTORC inhibition is obvious here as cell density after 7 days of drug exposure is much lower than in the control, even though identical cell numbers were seeded. As consistently observed, AZD8055 treatment again produced a notable decrease in cell size compared with control cells (Fig 4). Additionally, SRB staining highlights filamentous structures which are particularly visible in the control near-senescent cells (Fig 4, DMSO) and which disperse upon AZD8055 treatment (Fig 4, 35nM and 70 nM AZD8055).

To determine whether these filamentous structures observed by SRB staining were indeed actin stress fibers, we stained cells using the actin-specific fluorescent dye FITC-phalloidin. While stress fibers were clearly visible in control late passage fibroblasts (Fig 5A), after 7 days of AZD8055 treatment such fibers became much less prominent and actin instead appeared more centrally distributed (Fig 5B), suggestive of a shift from filamentous to globular conformation. Most notably, the cells changed morphology from enlarged amorphous cells to much smaller, thinner and spindle shapes characteristic of low CPD fibroblasts. Thus AZD8055 appears to trigger a rearrangement of the actin cytoskeleton in late passage cells to a state more usually seen in proliferating cells at low CPD.

Protein changes on short term AZD8055 treatment

The phenotypic and morphological changes we observe on AZD8055 treatment are highly suggestive of rejuvenation. We therefore asked whether such changes are accompanied by alterations in protein levels or modification, particularly addressing components of the mTOR signaling pathway (Fig 6A) and cell proliferation associated proteins (Fig 6B) by immunoblotting cell lysates from low CPD (CPD 36) or near-senescent (CPD 73) fibroblasts. We find that at low CPD, there is little apparent difference in total levels of mTOR, but phospho-mTOR increased upon AZD8055 treatment (Fig 6). The antibody used to

detect total mTOR recognises a doublet in control cells; the lower band of the doublet is decreased in both low and high CPD drug-exposed cells. In near-senescent fibroblasts, an additional high molecular weight smear is detected both with anti-mTORC and anti-phospho-mTORC antibodies – this higher molecular weight form is also detected in DMSO control cells at low CPD but not on AZD8055 treatment.

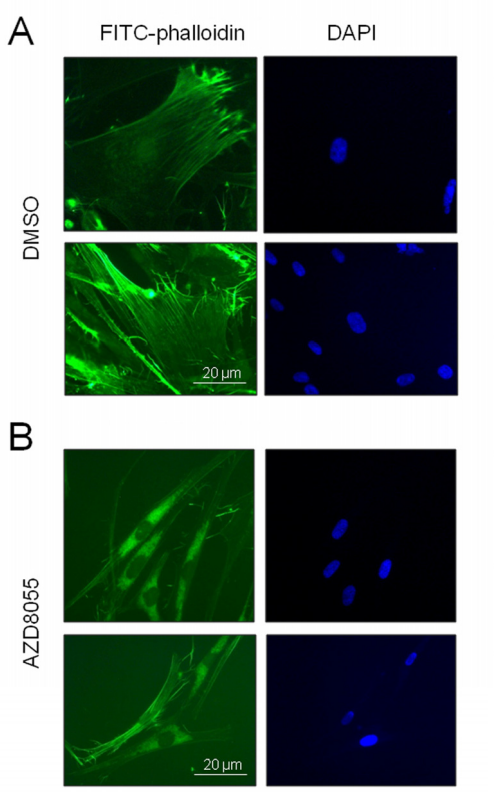

Figure 5. AZD8055 treatment reverses stress fiber formation in near-senescent cells. Late CPD HF043 fibroblasts were exposed to (**A**) DMSO vehicle control or (**B**) AZD8055 for 7 days then fixed and stained for actin using FITC-phalloidin. Imaging was carried out using a Zeiss AxioSkop II with x100 oil immersion lens. Representative images are shown for each treatment condition.

The translation initiation inhibitor 4EBP-1 is a well-documented target of mTORC1 kinase. On Western blotting we observe a marked impact on phospho-rylation of translation initiation inhibitor 4EBP-1 with AZD8055 treatment, such that phosphovariants α and β [37] were detected at lower levels in cells on treatment with AZD8055, particularly for those near senescence (Fig 6A), – note that these differences are not due to uneven loading as they are strips taken from the same gel lane of the same membrane as the phospho-mTOR blots (and this finding was replicated over several experiments, not shown). We also find that levels of the replication clamp PCNA and the cell cycle regulator p27 are both diminished on AZD8055 treatment (Fig 6B).

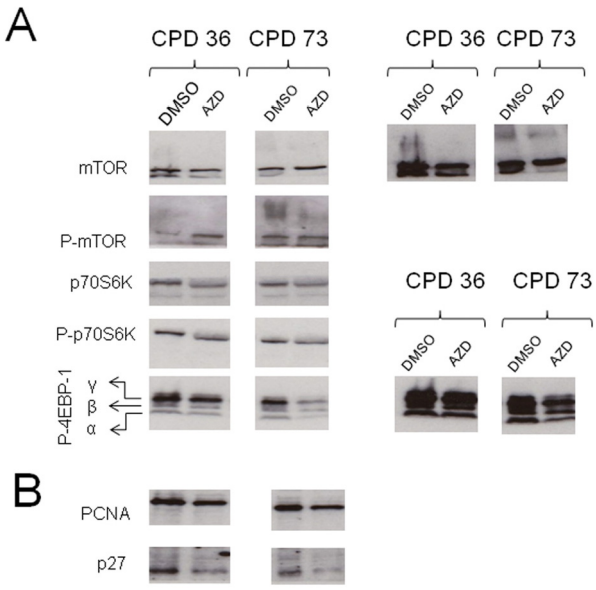

Figure 6. Alteration in protein levels and phosphorylation on short term AZD8055 treatment. Cells at CPD 36 or CPD 73 were seeded into T25 flasks and grown in medium containing AZD8055 or DMSO for one week. After harvesting, cells were pelleted and lysed in RIPA with protease and phosphatase inhibitors, separated on SDS-PAGE then immunoblotted for the indicated proteins. (**A**) Components of the mTOR signaling pathway, (**B**) Cell cycle proteins. The panels on the right show longer exposure images of the same panels on the left, to highlight bands that are faint in the shorter exposure images.

Release of drug treatment leads to normal senescence trajectory

Given the significant impact of AZD8055 in apparently reversing senescence phenotypes, it was important to address whether release from drug treatment might result in unanticipated changes in cell behaviour such as hyper-proliferation, immortalisation or even neoplastic change. We therefore treated cells at 'middle age' (CPD 55) with 35 nM AZD8055 and maintained drug treatment continuously or released cells from drug at CPD 60 (black arrow in Fig 7A). Cells were then grown under standard tissue culture conditions (see Methods) until replicative senescence. Proliferation rates rapidly returned to those of control cells on release from

AZD8055 treatment (Fig 7A, compare blue diamonds with orange circles). Released cells reached senescence at almost the same cumulative population doubling as DMSO controls and showed no long term alteration in growth characteristics or morphology compared with DMSO controls. By contrast, continuous dosing of cells with AZD8055 did restrain proliferation (green triangles, Fig 7A), consistent with inhibition of mTORC1 and negative effects on translation, presumably through blocking inactivation of 4EBP-1 (see also Fig 6). This was further studied by observing cell morphology *in situ*. Shortly after the time of release from drug treatment (8 days in Fig 7B), there is little difference in cell size or shape between the 'recovery' population and those under continuous drug treatment. By contrast, at very late cumulative population doublings (CPD94), released cells showed a classic senescent morphology with greatly enlarged cell size and many cells were rounded in shape (Fig 7B, CPD94), while continuous AZD8055 exposure from mid-CPD resulted in maintenance of a spindle cell morphology characteristic of low CPD cells- notably, cells at extremely high population doublings (CPD99) that were continuously exposed long term to AZD8055 were very similar morphologically to the appearance of near-senescent cells after only one week of drug treatment (compare Fig 7B CPD 99 'Continuous' with Fig 1B). From these findings, we conclude that brief exposure to AZD8055 does not have any long-lasting adverse effects on proliferative properties of skin fibroblasts, an important finding if AZD8055 is to proceed further into whole animal aging studies.

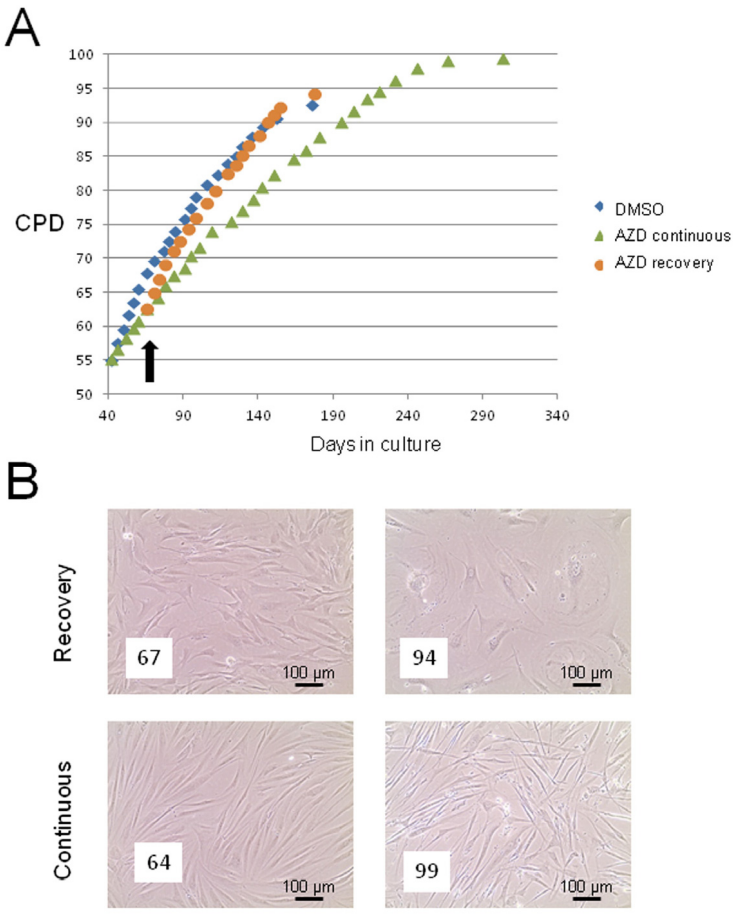

Figure 7. Short term AZD8055 exposure does not immortalise or transform primary human skin fibroblasts. (**A**) HF043 fibroblasts at CDP55 were treated with 35nM AZD8055 either continuously (green triangles) or for 5 population doublings followed by release from drug (black arrow indicates time of drug removal; growth curve shown by orange circles) compared with cells incubated with DMSO as control (blue diamonds). The end point of the growth curve denotes when cells ceased proliferation and became fully senescent (NB cells under continuous AZD80055 treatment continued for several PDs beyond the graph shown but also eventually died). (**B**) Phase contrast photomicrographs of cells in culture either following release from AZD8055 ('Recovery') or under continuous drug treatment ('Continuous'). The left panel shows cells 8 days after drug release and the right panel shows cells at very late CPD: CPDs are shown in white boxes within the micrographs.

DISCUSSION

In this paper, we report that short-term inhibition of mTORC1 and mTORC2 by administration of AZD8055 can reverse morphological and biochemical phenotypes of senescence in near-senescent human fibroblasts, including reduction in cell size and granularity, loss of SA-β-gal staining and reacquisition of fibroblastic spindle morphology. Previous use of mTORC1 inhibitors such as rapamycin has required continuous drug exposure to delay the onset of senescence and hence delay organismal aging (e.g. [16, 39]), so this represents a significant new means of altering senescence in primary cells. Cellular senescence provides an important barrier to tumorigenesis, but senescent cells indirectly contribute to a pro-neoplastic environment ('good citizens, bad neighbors' [38]). As a non-proliferating component of the tissue, senescent cells are also unable to contribute to tissue maintenance and repair. Hence pharmacologic strategies to relieve senescence are likely to have beneficial consequences for organismal health during aging.

mTORC inhibition provides a highly promising route to improving health span of older mammals. As well as increasing overall lifespan of mice [16], many measures of health are improved on administration of the mTORC1 inhibitor rapamycin [39]. Given the huge projected increase in age-related dementias with demographic change in Western populations [40], it is of particular importance that rapamycin increases blood brain flow, reduces amyloid tangles and plaques and improves cognitive function in mouse models of Alzheimer's disease [41-43]; it also shows promise in Parkinson's disease [44], other neurodegenerative disorders [45] and potentially age-related decline in cognitive function distinct from disease [46]. Far from its original role as an immunosuppressant (at high dose), rapamycin actually improves immune function in response to antigenic challenges when used at lower doses [47]. An orally available derivative, everolimus, shows good bioavailability and has shown promise in stimulating anti-viral immunity in older people on challenge with influenza vaccine [48], though the dose that improves immune memory may negatively impact on response to acute infection [49]. Furthermore, AZD8055 may be immunostimulatory [50].

Autophagy has been suggested as a potential mode of action by which mTORC1 inhibitors exert putative anti-aging effects, as mTORC1 phosphorylates and inactivates the autophagy-initiating kinase ULK1. Other approaches that stimulate autophagy can also improve health outcomes on aging, such as spermidine suppression of immunosenescence in mice [51]. While we investigated whether stimulation of autophagy could be responsible for the rejuvenated phenotypes seen upon AZD8055 treatment of late passage cells, our results are as yet inconclusive.

While rapamycin and similar molecules all act through binding to the FKBP12 protein - which then associates with the mTOR kinase and partially occludes the active site in mTORC1 [26], altering substrate recognition - second generation mTOR inhibitors have been designed instead to act as ATP mimetics that are highly specific for mTOR above other PI3K-family kinases and all other cellular kinases [29, 52]. Here, we find that administration of one such ATP mimetic, AZD8055, used at low concentration for as little as 7 days can markedly alter aging phenotypes in primary human skin fibroblasts, including redistribution of lysosomes and alteration in metabolism. Importantly, levels of senescence-associated β galactosidase, a marker of cellular senescence [5] drop in a highly significant manner, suggesting that lysosomal metabolism has shifted away from that characteristic of senescent cells.

Furthermore, we find a very robust reversal of morphological phenotypes of senescence, from enlarged, flattened, amorphous cells to an elongated spindle morphology characteristic of low CPD proliferating skin fibroblasts. The cell sizes we observe are entirely consistent with those previously reported for normal low CPD fibroblasts [57] and appear to be cell-intrinsic in both low CPD fibroblasts and higher CPD drug-treated cells, i.e. AZD8055 administration appears to reset the endogenous cell size regulation reported in [57]. In order to achieve this marked alteration in size and shape, a significant change in the organisation of the cytoskeleton must be taking place – we observe loss of filamentous structures (Fig 4) together with complete rearrangement of actin microfilaments from prominent stress fibers in control near-senescent cells to a central diffuse distribution more reminiscent of pools of globular actin (Fig 5). We suggest that this might be accompanied by an increase in cell motility as the AZD8055 treated cells show leading edge lamellae with some associated actin filaments (Figs 4 and 5) indicative of highly motile cells [57].

So how is AZD8055 causing such a major reorganisation of cellular structure? AZD8055 inhibits mTOR not only in mTORC1 but also when in complex with Rictor and PRR5 i.e. within mTORC2 [22]. Whilst rapamycin can lead to unwanted side effects such as decreased glucose homeostasis and increased diabetes risk [58] it is likely that this is caused by activation of a feedback loop with AKT on chronic (and high dose)

rapamycin inhibition of mTORC1 [59] and Ying-Yang1 interaction [58] rather than via mTORC2 inhibition. Abrogation of mTORC2 activity leads to loss of phosphorylation of Rac/Cdc42 and downstream PAK; the consequence is relief of inhibition of cofilin, resulting in a shift in the equilibrium of actin from f-actin to g-actin [60]. Unlike the aberrant cell sizes caused by actin-disrupting drugs such as cytochalasin [57], we observe cell lengths typical of normal fibroblasts on AZD8055 treatment. Hence AZD8055 allows the cell to reorganise actin and restores the ability of cells to regulate size and shape. It has been suggested that f-actin polymerisation is critical for both short-term memory and long term potentiation in the brain [60]. This does raise the worrying prospect that long term AZD8055 administration may impact on cognitive function, though such fears associated with use of rapamycin have proven groundless; rapamycin actually improves learning and memory in older mice [46]. It remains to be seen whether AZD8055 is similarly beneficial to cognitive function.

Any intervention designed to tackle the problem of senescent cells during aging must not cause long-term harm, particularly neoplastic change. As such, it will be crucial to investigate whether AZD8055 treatment can reverse features of oncogene-induced senescence and senescence induced by other stresses such as DNA damage, as well as the replicative senescence investigated here. Other mooted anti-aging strategies such as telomerase reactivation carry huge cancer risk; indeed pre-neoplastic lesions become highly aggressive in telomerase-reactivated mice [61]. Drugs and potential nutraceuticals that activate sirtuins show promise in terms of improved tissue function [62]; however, the strong association of some of the sirtuin protein deacetylases with cancer [63] has to be carefully considered, especially since epigenetic shifts in senescent cells are associated with increased neoplastic transformation [64]. Other approaches include targeting the SASP (senescence-associated secretory phenotype), and recent evidence indicates that rapamycin may disrupt the SASP by preventing IL1A translation [70]. Furthermore, inhibition of stress signaling through p38 MAPK kinases looks promising in Werner syndrome progeroid models of aging [65] though the therapeutic window is extremely narrow, which may limit clinical use. Since AZD8055 is already in clinical trials as an anti-cancer therapeutic [30], we were optimistic that it may be less risky in terms of possible adverse effects in stimulating cell proliferation and/or neoplastic change. However, it was essential to test whether the drug had negative effects on cell cycle control.

The rate of proliferation of fibroblasts treated with AZD8055 is greatly diminished compared with controls. This is likely to be a consequence, at least in part, of AZD8055 inhibition of protein synthesis, as its inhibition of mTORC1 then blocks relief of translational inhibition by downstream target 4EBP-1. AZD8055 has been reported to alter the profile of translated mRNAs in the cell. In particular, a subset of mRNAs with a 5' terminal oligopyridine tract are affected [55], including a host of ribosomal protein mRNAs together with those encoding cell cycle factors such as the replicative helicases MCMs and the sliding clamp PCNA [56]. Hence factors needed both for increasing cellular mass through ribosomal biogenesis, and those directly involved in critical cell cycle processes such as DNA replication, are kept at lower levels in mTORC-inhibited cells. Consistent with this, we find significant alteration in phospho-4EBP-1 isoforms and decreased PCNA levels on AZD8055 treatment that correlate with the decreased growth rates of treated cells. At first sight, this finding is counterintuitive: a treatment that reverses features of senescence leads to decreased PCNA, but low PCNA levels are characteristic of cells undergoing cell cycle arrest and geroconversion to the senescent state [71, 72]. However, the important point is that the AZD8055 treated cells (unlike senescent cells) have not lost proliferative potential - on release from drug treatment, they regain normal proliferative capacity. While rapamycin treatment of cultured rat cells (that do not show telomere-dependent senescence) has been reported to switch cells to a non-senescing state [66], we believe it is critically important that the short term AZD8055 dosing used here does not immortalize human fibroblasts. Upon drug release, we find that AZD8055-exposed fibroblasts regain normal proliferation kinetics and reach senescence at the normal stage (Fig 7). Furthermore, we find that neither continuous AZD8055 exposure nor treatment followed by release results in any signs of either immortalization or transformation. It will be interesting to determine the effects of pulsed dosing, which may elicit beneficial senescence-reversal effects without triggering side effects such as activation of feedback loops that results from chronic mTORC inhibition [59]. Such pulsed therapies have already been reported in caloric restriction studies and most recently in use of a fasting-mimicking diet (FMD), where repeated short-term intervention led to long-term benefit [67]. Our findings overall suggest that inhibition of both mTORC1 and mTORC2 may be necessary to elicit maximal cellular changes necessary to reverse senescent phenotypes and that AZD8055 is a promising therapeutic candidate to reverse the detrimental effects of cellular senescence during aging.

MATERIALS AND METHODS

Human neonatal foreskin fibroblast line HF043 (Dundee CELL products) was cultured in DMEM (Sigma) supplemented with 10% fetal calf serum (Gibco) in the absence of any added antibiotics, at 37°C in a humidified incubator with 5% CO_2. Cells were monitored microscopically using an EVOS digital microscope (Life Technologies) and harvested when ~80% confluent using TrypleExpress (Invitrogen). Following resuspension in DMEM with FCS, 20 µl of the cell suspension was counted and cell diameters measured using a Cellometer T4 (Nexelcom). Cells were seeded at $2x10^5$ per T25 flask (Greiner), or at $1x10^4$ in 24 well plates (Greiner). Population doublings (PD) were calculated as:

$$PD = \frac{\log_{10}(\text{total cells harvested} / \text{total cells seeded})}{\log_{10} 2}$$

Cumulative population doublings (CPD) were calculated as the sum of PD values.

AZD8055 (Selleckchem) was reconstituted to 1mM in DMSO and stored in aliquots at -20°C protected from light. Prior to drug treatment, medium was removed, cells washed with PBS, then fresh medium supplemented with drug was added. Total volume of drug or DMSO added to the culture medium never exceeded 1:10,000 v/v. Doses of 35 nM and 70 nM were chosen as effective but non-toxic based on our preliminary studies (not shown).

Fluorescence microscopy. To assess lysosomal content, cells were incubated with medium containing 50 nM Lysotracker red (Life Technologies) for 30 minutes at 37°C. Cells were imaged live using a Zoe microscope (BioRad). To account for differences in cell density arising from AZD8055 inhibition of cell proliferation, fluorescent signal (determined using Image J) was normalised against nuclear signal (DAPI). Mitochondrial content was assessed by adding 1µM Mitotracker Red (Molecular Probes) to cells in medium for 30 minutes at 37°C, washing twice with PBS and fixing with ice-cold methanol:acetone (1:1 v/v) for 10 min. Fixative was aspirated and cells washed with PBS prior to imaging. Stress fibers were detected by incubating for 40 min with 1µg/ml FITC-phalloidin (Sigma Aldrich) on cells that had been fixed with 3.7% formaldehyde (Sigma-Aldrich) in PBS for 5 minutes and washed twice with PBS prior to addition of FITC-phalloidin. Cells were then washed twice in PBS prior to imaging with either a BioRad Zoe or a Zeiss Axioskop II microscope. Images were quantified by Image J. Where appropriate, DNA was counterstained with NucBlue Live ReadyProbes Reagent (Life Technologies) (for live cell imaging) or ProLong® Gold Antifade Reagent with DAPI (Life Technologies) for fixed cells.

Scale bars for micrographs were determined using the appropriate microcopy software (BioRad SOFT-ZOE-Cell-Imager-UI-FW on Android operating system; Zeiss Axiovision SE64 Release 4.9.1 adjusted for Zeiss AxioCam Hr resolution), or by manual calculation from imaged rulers (Cellometer T4 and EVOS Core).

SRB staining. Sulforhodamine B staining was performed as described in [36], but cells were photographed using an EVOS microscope (phase contrast), without dye solubilisation.

SA-β-gal. Staining for (SA-β-gal) was performed using a Cell Signaling senescence-associated beta-galactosidase kit according to manufacturer's instructions.

Immunoblotting. Cells were seeded at $2x10^5$ in T25 culture flasks (Greiner) and harvested by trypsinization as above, then pelleted by gentle centrifugation, washed in PBS and re-pelleted, then lysed in 30 µl RIPA buffer containing 1:100 Halt™ protease and phosphatase inhibitors (Thermo Scientific). Lysates representing $2x10^4$ cells were heated for 5 minutes (95°C) in 1X NuPAGE LDS buffer (Novagen) containing 100 mM DTT prior to loading onto BioRad TGX 10% SDS-PAGE, blotted onto nitrocellulose (7 min 25V, 1.3A using a BioRad TurboBlot) then processed for immunoprobing as described previously [68], with the exception that primary antibodies were incubated with membrane at 1:500 dilution overnight at 4°C and secondary Ab (HRP-anti-rabbit or HRP-anti-mouse, both from Dako) were incubated at 1:1000 dilution for 30 mins at 37°C. Bound antibody was visualised by incubation with ECL solution for one minute at room temperature then exposure to HyperFilm MP (GE Healthcare) and development in an Xograph Compact 4 film processor. Anti-PCNA antibody was a polyclonal 3009 raised against the C terminus of PCNA [69]; all other primary antibodies used were purchased from Cell Signaling: anti mTOR phospho S2448 (D9C2) # 5536P; anti-mTOR (7C10) #2983A; anti-p70S6K-phospho T389 (108D2) #9234P; anti-p70 S6K #9202BC; anti-p27 #2552P; anti-phospho T37/46 4EBP-1 (236B4) #2855P. Note that all blots shown were of samples run on the same gel and the nitrocellulose filter was cut horizontally into sections prior to probing to avoid issues with non-equal loading or transfer. (Note that blots shown are representative of several replicates).

Statistical analysis. Comparison of means between different populations (of different total cell number) used the student t test (one or two tailed according to the null hypothesis) where standard errors were similar. t was calculated according to

$$t^2 = \frac{(\mu 1 - \mu 2)}{\sqrt{(\frac{1}{n1} + \frac{1}{n2})}}$$

and t compared with values from t tables using degrees of freedom $v = (n1 + n2 - 2)$.

ACKNOWLEDGEMENTS

We thank Candice Ashmore-Harris for technical support and Sophie Riddell for critical reading of the manuscript.

Funding

We are extremely grateful to an anonymous donor (via the University of Oxford Legacies Office) and to the Glenn Foundation for Medical Research for funding this work through a Glenn Award to LSC. LSC is supported by BBSRC grant BB/M006727/1.

Author contributions

HW and S D-H designed and conducted experiments and performed some data analysis; LSC designed and conducted experiments, analyzed data and wrote the manuscript.

Conflict of interest statement

We declare no conflicts of interest.

REFERENCES

1. Lopez-Otin C, Blasco MA, Partridge L, Serrano M and Kroemer G. The hallmarks of aging. Cell. 2013; 153: 1194-1217.

2. Herbig U, Ferreira M, Condel L, Carey D and Sedivy JM. Cellular senescence in aging primates. Science. 2006; 311:1257.

3. Jeyapalan JC, Ferreira M, Sedivy JM and Herbig U. Accumulation of senescent cells in mitotic tissue of aging primates. Mech Aging Dev. 2007; 128: 36-44.

4. van Deursen JM. The role of senescent cells in aging. Nature. 2014; 509: 439-446.

5. Dimri GP et al. A biomarker that identifies senescent human cells in culture and in aging skin in vivo. Proc Natl Acad Sci U S A. 1995; 92: 9363-9367.

6. Noda A, Ning Y, Venable SF, Pereira-Smith OM and Smith JR. Cloning of senescent cell-derived inhibitors of DNA synthesis using an expression screen. Exp. Cell Res. 1994; 211: 90-98.

7. Sato S, et al. Ablation of the p16(INK4a) tumour suppressor reverses aging phenotypes of klotho mice. Nat Commun. 2015; 6: 7035.

8. Quereda V, Martinalbo J, Dubus P, Carnero A and Malumbres M. Genetic cooperation between p21Cip1 and INK4 inhibitors in cellular senescence and tumor suppression. Oncogene. 2007; 26: 7665-7674.

9. Alcorta DA, Xiong Y, Phelps D, Hannon G, Beach D and Barrett JC. Involvement of the cyclin-dependent kinase inhibitor p16 (INK4a) in replicative senescence of normal human fibroblasts. Proc Natl Acad Sci U S A. 1996; 93: 13742-13747.

10. Choudhury AR, et al. Cdkn1a deletion improves stem cell function and lifespan of mice with dysfunctional telomeres without accelerating cancer formation. Nat Genet. 2007; 39: 99-105.

11. Baker DJ, Wijshake T, Tchkonia T, LeBrasseur NK, Childs BG, van de Sluis B, Kirkland JL and van Deursen JM. Clearance of p16Ink4a-positive senescent cells delays aging-associated disorders. Nature. 2011; 479: 232-236.

12. Rudolph KL, Chang S, Millard M, Schreiber-Agus N and DePinho RA. Inhibition of experimental liver cirrhosis in mice by telomerase gene delivery. Science. 2000; 287: 1253-1258.

13. Jaskelioff M, et al. Telomerase reactivation reverses tissue degeneration in aged telomerase-deficient mice. Nature. 2010; 469: 102-106.

14. Cox LS and Mason PA. Prospects for rejuvenation of aged tissue by telomerase reactivation. Rejuvenation Res. 2010; 13: 749-754.

15. Colman RJ, Anderson RM, Johnson SC, Kastman EK, Kosmatka KJ, Beasley TM, Allison DB, Cruzen C, Simmons HA, Kemnitz JW and Weindruch R. Caloric restriction delays disease onset and mortality in rhesus monkeys. Science. 2009; 325: 201-204.

16. Harrison DE, et al. Rapamycin fed late in life extends lifespan in genetically heterogeneous mice. Nature. 2009; 460: 392-395.

17. Cox LS and Mattison JA. Increasing longevity through caloric restriction or rapamycin feeding in mammals: common mechanisms for common outcomes? Aging Cell. 2009; 8: 607-13

18. Cox LS. Live fast, die young: new lessons in mammalian longevity. Rejuvenation Res. 2009; 12: 283-288.

19. Vezina C, Kudelski A and Sehgal SN. Rapamycin (AY-22,989), a new antifungal antibiotic. I. Taxonomy of the producing streptomycete and isolation of the active principle. J Antibiot (Tokyo). 1975; 28: 721-726.

20. Calne RY, Collier DS, Lim S, Pollard SG, Samaan A, White DJ and Thiru S. Rapamycin for immunosuppression in organ allografting. Lancet. 1989; 2: 227.

21. Heitman J, Movva NR and Hall MN. Targets for cell cycle arrest by the immunosuppressant rapamycin in yeast. Science. 1991; 253: 905-909.

22. Huang K and Fingar DC. Growing knowledge of the mTOR signaling network. Semin Cell Dev Biol. 2014; 36: 79-90.

23. Johnson SC, Sangesland M, Kaeberlein M and Rabinovitch PS. Modulating mTOR in aging and health. Interdiscip Top Gerontol. 2015; 40: 107-127.

24. Johnson SC, Rabinovitch PS and Kaeberlein M. mTOR is a key modulator of aging and age-related disease. Nature. 2013; 493: 338-345.

25. Choo AY, Yoon SO, Kim SG, Roux PP and Blenis J. Rapamycin differentially inhibits S6Ks and 4E-BP1 to mediate cell-type-specific repression of mRNA translation. Proc Natl Acad Sci U S A. 2008; 105: 17414-17419.

26. Yang H, Rudge DG, Koos JD, Vaidialingam B, Yang HJ and Pavletich NP. mTOR kinase structure, mechanism and regulation. Nature. 2013; 497: 217-223.

27. Yip CK, Murata K, Walz T, Sabatini DM and Kang SA. Structure of the human mTOR complex I and its implications for rapamycin inhibition. Mol Cell. 2010; 38: 768-774.

28. Benjamin D, Colombi M, Moroni C and Hall MN. Rapamycin passes the torch: a new generation of mTOR inhibitors. Nat Rev Drug Discov. 2011; 10: 868-880.

29. Chresta CM, et al. AZD8055 is a potent, selective and orally bioavailable ATP-competitive mammalian target of rapamycin kinase inhibitor with in vitro and in vivo antitumor activity. Cancer Res. 2009; 70: 288-298.

30. Naing A, Aghajanian C, Raymond E, Olmos D, Schwartz G, Oelmann E, Grinsted L, Burke W, Taylor R, Kaye S, Kurzrock R and Banerji U. Safety, tolerability, pharmacokinetics and pharmacodynamics of AZD8055 in advanced solid tumours and lymphoma. Br J Cancer. 2012; 107: 1093-1099.

31. Kim YM, Byun HO, Jee BA, Cho H, Seo YH, Kim YS, Park MH, Chung HY, Woo HG and Yoon G. Implications of time-series gene expression profiles of replicative senescence. Aging Cell. 2013; 12: 622-634.

32. Yoon YS, Yoon DS, Lim IK, Yoon SH, Chung HY, Rojo M, Malka F, Jou MJ, Martinou JC and Yoon G. Formation of elongated giant mitochondria in DFO-induced cellular senescence: involvement of enhanced fusion process through modulation of Fis1. J Cell Physiol. 2006; 209: 468-480.

33. Cao K, Graziotto JJ, Blair CD, Mazzulli JR, Erdos MR, Krainc D and Collins FS. Rapamycin reverses cellular phenotypes and enhances mutant protein clearance in Hutchinson-Gilford progeria syndrome cells. Sci Transl Med. 2011; 3: 89ra58.

34. Noda T and Ohsumi Y. Tor, a phosphatidylinositol kinase homologue, controls autophagy in yeast. J Biol Chem. 1998; 273: 3963-3966.

35. Kim J, Kundu M, Viollet B and Guan KL. AMPK and mTOR regulate autophagy through direct phosphorylation of Ulk1. Nat Cell Biol. 2011; 13: 132-141.

36. Vichai V and Kirtikara K. Sulforhodamine B colorimetric assay for cytotoxicity screening. Nat Protoc. 2006; 1: 1112-1116.

37. Gingras AC, Kennedy SG, O'Leary MA, Sonenberg N and Hay N. 4E-BP1, a repressor of mRNA translation, is phosphorylated and inactivated by the Akt(PKB) signaling pathway. Genes Dev. 1998; 12: 502-513.

38. Campisi J. Senescent cells, tumor suppression and organismal aging: good citizens, bad neighbors. Cell. 2005; 120: 513-522.

39. Wilkinson JE, Burmeister L, Brooks SV, Chan CC, Friedline S, Harrison DE, Hejtmancik JF, Nadon N, Strong R, Wood LK, Woodward MA and Miller RA. Rapamycin slows aging in mice. Aging Cell. 2012; 11: 675-682.

40. Alzheimer's Disease International and World Health Organisation. Dementia: a public health priority. 2012; ISBN 978 4 156445 8

41. Lin AL, et al. Chronic rapamycin restores brain vascular integrity and function through NO synthase activation and improves memory in symptomatic mice modeling Alzheimer's disease. J Cereb Blood Flow Metab. 2013; 33: 1412-1421.

42. Spilman P, Podlutskaya N, Hart MJ, Debnath J, Gorostiza O, Bredesen D, Richardson A, Strong R and Galvan V Inhibition of mTOR by rapamycin abolishes cognitive deficits and reduces amyloid-beta levels in a mouse model of Alzheimer's disease. PLoS One. 2010; 5: e9979.

43. Richardson A, Galvan V, Lin AL and Oddo S. How longevity research can lead to therapies for Alzheimer's disease: The rapamycin story. Exp Gerontol. 2014; 68: 51-8

44. Malagelada C, Jin ZH, Jackson-Lewis V, Przedborski S and Greene LA. Rapamycin protects against neuron death in in vitro and in vivo models of Parkinson's disease. J Neurosci. 2010; 30: 1166-1175.

45. Chong ZZ, Shang YC, Wang S and Maiese K. Shedding new light on neurodegenerative diseases through the mammalian target of rapamycin. Prog Neurobiol. 2012; 99: 128-148.

46. Majumder S, Caccamo A, Medina DX, Benavides AD, Javors MA, Kraig E, Strong R, Richardson A and Oddo S, Lifelong rapamycin administration ameliorates age-dependent cognitive deficits by reducing IL-1beta and enhancing NMDA signaling. Aging Cell. 2012; 11: 326-335.

47. Ferrer IR, Wagener ME, Robertson JM, Turner AP, Araki K, Ahmed R, Kirk AD, Larsen CP and Ford ML, Cutting edge: Rapamycin augments pathogen-specific but not graft-reactive CD8+ T cell responses. J Immunol. 2010; 185: 2004-2008.

48. Mannick JB, Del Giudice G, Lattanzi M, Valiante NM, Praestgaard J, Huang B, Lonetto MA, Maecker HT, Kovarik J, Carson S, Glass DJ and Klickstein LB, mTOR inhibition improves immune function in the elderly. Sci Transl Med. 2014; 6: 268ra179.

49. Goldberg EL, Smithey MJ, Lutes LK, Uhrlaub JL and Nikolich-Zugich J, Immune memory-boosting dose of rapamycin impairs macrophage vesicle acidification and curtails glycolysis in effector CD8 cells, impairing defense against acute infections. J Immunol. 2014; 193: 757-763.

50. Jiang Q, Weiss JM, Back T, Chan T, Ortaldo JR, Guichard S and Wiltrout RH, mTOR kinase inhibitor AZD8055 enhances the immunotherapeutic activity of an agonist CD40 antibody in cancer treatment. Cancer Res. 2011; 71: 4074-4084.

51. Puleston DJ, Zhang H, Powell TJ, Lipina E, Sims S, Panse I, Watson AS, Cerundolo V, Townsend AR, Klenerman P and Simon AK, Autophagy is a critical regulator of memory CD8(+) T cell formation. Elife. 2014; 3.

52. Pike KG, Malagu K, Hummersone MG, Menear KA, Duggan HM, Gomez S, Martin NM, Ruston L, Pass SL and Pass M, Optimization of potent and selective dual mTORC1 and mTORC2 inhibitors: the discovery of AZD8055 and AZD2014. Bioorg Med Chem Lett. 2013; 23: 1212-1216.

53. Vellai T, Takacs-Vellai K, Sass M and Klionsky DJ, The regulation of aging: does autophagy underlie longevity? Trends Cell Biol. 2009; 19: 487-494.

54. He C and Klionsky DJ, Regulation mechanisms and signaling pathways of autophagy. Annu Rev Genet. 2009; 43: 67-93.

55. Huo Y, Iadevaia V, Yao Z, Kelly I, Cosulich S, Guichard S, Foster LJ and Proud CG, Stable isotope-labelling analysis of the impact of inhibition of the mammalian target of rapamycin on protein synthesis. Biochem J. 2012; 444: 141-151.

56. Thoreen CC, Chantranupong L, Keys HR, Wang T, Gray NS and Sabatini DM, A unifying model for mTORC1-mediated regulation of mRNA translation. Nature. 2012; 485: 109-113.

57. Levina EM, Kharitonova MA, Rovensky YA and Vasiliev JM, Cytoskeletal control of fibroblast length: experiments with linear strips of substrate. J Cell Sci. 2001; 114: 4335-4341.

58. Blattler SM, Cunningham JT, Verdeguer F, Chim H, Haas W, Liu H, Romanino K, Ruegg MA, Gygi SP, Shi Y and Puigserver P,

Yin Yang 1 deficiency in skeletal muscle protects against rapamycin-induced diabetic-like symptoms through activation of insulin/IGF signaling. Cell Metab. 2012; 15: 505-517.

59. Wan X, Harkavy B, Shen N, Grohar P and Helman LJ, Rapamycin induces feedback activation of Akt signaling through an IGF-1R-dependent mechanism. Oncogene. 2007; 26: 1932-1940.

60. Josselyn SA and Frankland PW, mTORC2: actin on your memory. Nat Neurosci. 2013; 16: 379-380.

61. Ding Z, et al., Telomerase reactivation following telomere dysfunction yields murine prostate tumors with bone metastases. Cell. 2012; 148: 896-907.

62. Gomes AP, et al., Declining NAD(+) induces a pseudohypoxic state disrupting nuclear-mitochondrial communication during aging. Cell. 2013; 155: 1624-1638.

63. Saunders LR and Verdin E, Sirtuins: critical regulators at the crossroads between cancer and aging. Oncogene. 2007; 26: 5489-5504.

64. Cruickshanks HA, et al., Senescent cells harbour features of the cancer epigenome. Nat Cell Biol. 2013; 15: 1495-1506.

65. Davis T, Bachler MA, Wyllie FS, Bagley MC and Kipling D, Evaluating the role of p38 MAP kinase in growth of Werner syndrome fibroblasts. Ann N Y Acad Sci. 2010; 1197: 45-48.

66. Pospelova TV, Leontieva OV, Bykova TV, Zubova SG, Pospelov VA and Blagosklonny MV, Suppression of replicative senescence by rapamycin in rodent embryonic cells. Cell Cycle. 2012; 11: 2402-2407.

67. Brandhorst S, et al. A Periodic Diet that Mimics Fasting Promotes Multi-System Regeneration, Enhanced Cognitive Performance and Healthspan. Cell Metabolism. 2015; 22:86-99.

68. Cox LS, Midgley CA and Lane DP, Xenopus p53 is biochemically similar to the human tumour suppressor protein p53 and is induced upon DNA damage in somatic cells. Oncogene. 1994; 9: 2951-2959.

69. Warbrick E, Lane DP, Glover DM and Cox LS, A small peptide inhibitor of DNA replication defines the site of interaction between the cyclin-dependent kinase inhibitor p21WAF1 and proliferating cell nuclear antigen. Curr Biol. 1995; 5: 275-282.

70. Laberge RM, Sun Y, Orjalo AV, Patil CK, Freund A, Zhou L, Curran SC, Davalos AR, Wilson-Edell KA, Liu S, Limbad C, Demaria M, Li P, Hubbard GB, Ikeno Y, Javors M, Desprez PY, Benz CC, Kapahi P, Nelson PS and Campisi J, MTOR regulates the pro-tumorigenic senescence-associated secretory phenotype by promoting IL1A translation. Nat Cell Biol. 2015;17:1049-1061.

71. Goukassian D1, Gad F, Yaar M, Eller MS, Nehal US, and Gilchrest BA, Mechanisms and implications of the age-associated decrease in DNA repair capacity. FASEB J. 2000; 14:1325-1334.

72. Blagosklonny MV, Cell cycle arrest is not yet senescence, which is not just cell cycle arrest: terminology for TOR-driven aging. Aging (Albany, NY). 2012; 4:159-165.

Research Paper

A novel autosomal recessive TERT T1129P mutation in a dyskeratosis congenita family leads to cellular senescence and loss of CD34+ hematopoietic stem cells not reversible by mTOR-inhibition

Clemens Stockklausner[1*], Simon Raffel[2, 3, 4*], Julia Klermund[5], Obul Reddy Bandapalli[1], Fabian Beier[6], Tim H. Brümmendorf[6], Friederike Bürger[7], Sven W. Sauer[7], Georg F. Hoffmann[7], Holger Lorenz[5], Laura Tagliaferri[1], Daniel Nowak[8], Wolf-Karsten Hofmann[8], Rebecca Buergermeister[1, 5], Carolin Kerber[1], Tobias Rausch[9, 10], Jan O. Korbel[10], Brian Luke[5, 11*], Andreas Trumpp[2, 3, 4*] and Andreas E. Kulozik[1*]

[1]Department of Pediatric Oncology, Hematology and Immunology, University of Heidelberg and Molecular Medicine Partnership Unit, 69120 Heidelberg, Germany;
[2]Division of Stem Cells and Cancer, German Cancer Research Center (DKFZ), Im Neuenheimer Feld 280, 69120 Heidelberg, Germany;
[3]Heidelberg Institute for Stem Cell Technology and Experimental Medicine (HI-STEM gGmbH), Im Neuenheimer Feld 280, 69120 Heidelberg, Germany;
[4]German Cancer Consortium (DKTK), 69120 Heidelberg, Germany;
[5]Zentrum für Molekulare Biologie der Universität Heidelberg (ZMBH), DKFZ-ZMBH Alliance, 69120 Heidelberg, Germany;
[6]Department of Hematology, Oncology, Hemostaseology and Stem Cell Transplantation, Medical Faculty of the RWTH Aachen University, 52062 Aachen, Germany;
[7]Center for Pediatric and Adolescent Medicine, Heidelberg University Hospital, Im Neuenheimer Feld 430, 69120 Heidelberg, Germany;
[8]Department of Hematology and Oncology, University Hospital Mannheim, Medical Faculty Mannheim of the University of Heidelberg, 68167 Mannheim, Germany;
[9]European Molecular Biology Laboratory (EMBL), Genomics Core Facility, D 69117 Heidelberg, Germany;
[10]European Molecular Biology Laboratory (EMBL), Genome Biology Unit and Molecular Medicine Partnership Unit, D 69117 Heidelberg, Germany;
[11]Institute of Molecular Biology gGmbH, gefördert durch die Böhringer Ingelheim Stiftung, 55128 Mainz, Germany;
*Equally contributed

Key words: *TERT, TERC, mTOR, rapamycin, sirolimus, senescence*
Received: *09/24/15; Accepted: 10/30/15; Published: 11/06/15* doi:10.18632/aging.100835
Correspondence to: *Andreas E. Kulozik, MD/PhD;* ***E-mail:*** *andreas.kulozik@med.uni-heidelberg.de*

Abstract: **The TERT gene encodes for the reverse transcriptase activity of the telomerase complex and mutations in TERT can lead to dysfunctional telomerase activity resulting in diseases such as dyskeratosis congenita (DKC). Here, we describe a novel TERT mutation at position T1129P leading to DKC with progressive bone marrow (BM) failure in homozygous members of a consanguineous family. BM hematopoietic stem cells (HSCs) of an affected family member were 300-fold reduced associated with a significantly impaired colony forming capacity in vitro and impaired repopulation activity in**

mouse xenografts. Recent data in yeast suggested improved cellular checkpoint controls by mTOR inhibition preventing cells with short telomeres or DNA damage from dividing. To evaluate a potential therapeutic option for the patient, we treated her primary skin fibroblasts and BM HSCs with the mTOR inhibitor rapamycin. This led to prolonged survival and decreased levels of senescence in T1129P mutant fibroblasts. In contrast, the impaired HSC function could not be improved by mTOR inhibition, as colony forming capacity and multilineage engraftment potential in xenotransplanted mice remained severely impaired. Thus, rapamycin treatment did not rescue the compromised stem cell function of TERT^{T1129P} mutant patient HSCs and outlines limitations of a potential DKC therapy based on rapamycin.

INTRODUCTION

Telomeres, the protective nucleoprotein structures at chromosome ends, shorten upon each cell division due to the so-called "end-replication problem" [1, 2]. The end-replication problem is compensated for by the reverse transcriptase, telomerase, which is active in germ cells, cancer cells and, to an extent in somatic stem cells [3]. Accelerated telomere shortening leads to the premature replicative senescence of cells and can be caused by mutations of the telomerase components DKC1 (dyskerin), TERC and TERT, among other genes involved in telomere maintenance [4-7]. TERC and TERT represent the RNA and catalytic protein moieties of the telomerase reverse transcriptase, respectively. Mutations affecting the function of these genes may lead to dyskeratosis congenita (DKC), a disease with a highly heterogeneous phenotype [8-11]. Affected patients suffer from a variable combination of skin, nail and mucosal dystrophies, but also life-threatening conditions such as progressive bone marrow failure, pulmonary fibrosis and an increased propensity to develop malignant tumors [12-16]. Telomere loss has been proposed to eliminate cells with a long proliferative history, and in this manner, acts as a tumor suppressor to limit replicative capacity. Telomere attrition also occurs with age and the associated accumulation of senescent cells may contribute to the aging process [13]. In disease states with reduced stem cell replicative reserve, substantially increased stem cell turnover or in the absence of telomerase activity short telomeres accumulate in hematopoietic stem cells [17]. Critically short telomeres are dysfunctional in terms of chromosome end protection and hence upon nucleolytic processing the DNA damage checkpoint is unleashed, thereby driving the onset of replicative senescence [18]. Dysfunctional telomeres are also prone to unscheduled repair events leading to chromosomal rearrangements. Therefore, in the absence of a functional DNA damage checkpoint, chronic telomere shortening could also potentially lead to pathogenic chromosomal instability.

Current treatment for patients affected by dyskeratosis congenita includes the androgen danazol [19-21]. The use of androgens can lead to virilization in female patients and thereby limits its therapeutic range [22, 23].

Stem cell transplantation to cure the progressive bone marrow failure is challenging, and DKC patients have a poor tolerance for conditioning regiments and frequently suffer from life threatening side effects [24-26]. Future therapy options include the utilization of induced pluripotent stem cells that might be beneficial for patients that have defined mutations in telomerase components such as TERC [5].

mTOR is a protein kinase that promotes cell growth in response to nutrient supplies and growth signals, and can be specifically inhibited by rapamycin [27]. As it has been shown that inhibiting the mTOR pathway with rapamycin reduces the rate of cellular senescence onset, we hypothesized that rapamycin might have a therapeutic potential for patients suffering from mutations of the telomerase complex where senescent cells accumulate [28, 29].

In this work we describe a consanguineous Libyan family in which we identify a novel T1129P TERT mutation leading to progressive bone marrow failure in homozygous family members. In order to test our hypothesis that rapamycin may rescue or at least improve the physiology of TERT^{T1129P} patient cells, we analyzed the effect of the mTOR inhibitor rapamycin on growth and senescence of skin fibroblasts and on hematopoietic stem cells using in vitro cultures and xenograft mouse models.

RESULTS

The novel TERT T1129P mutation leads to pathological telomere shortening causing progressive bone marrow failure in homozygous patients

Progressive bone marrow failure including transfusion dependent anemia und thrombocytopenia was first diagnosed in patient II-1 at the age of six years in a consanguineous Libyan family when a blood count was obtained to address symptoms of anemia including weak-

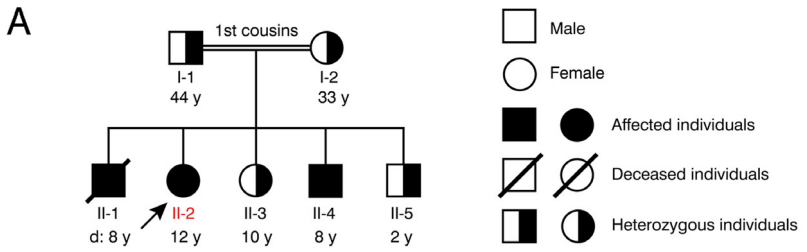

B

Parameter	I-1	I-2	II-2	II-3	II-4	II-5
WBC in n/nl (Normal range)	9.45 (4-10)	7.63 (4-10)	2.16 (4.5-13.0)	9.76 (4.5-13.0)	3.09 (4.5-13.0)	13.9 (5-17.5)
ANC in % (Normal range)	55 (50-80)	60.6 (50-80)	14 (50-80)	55.3 (50-80)	22.7 (50-80)	59 (50-80)
RBC in n/pl (Normal range)	4.9 (4.3-6.1)	3.64 (4-5.2)	2.44 (4.0-5.2)	4.79 (4.0-5.2)	1.71 (4.0-5.2)	4.3 (3.7-5.2)
Hemoglobin in g/dl (Normal range)	15.1 (13-17)	12.1 (12-15)	7.3 * (11.5-15)	12.8 (11.5-15)	6.2 (11.5-15)	11.7 (9.5-13.5)
Platelets in n/nl (Normal range)	181 (150-440)	195 (150-440)	9 (180-530)	280 (180-530)	13 (180-530)	279 (200-480)
MCV in fl (Normal range)	88.4 (83-97)	94.5 (83-97)	81.6 * (69-95)	80.2 (69-95)	106.4 (69-95)	76.3 (74-108)
Reticulocytes in ‰ (Normal range)	14 (5-15)	24.4 (5-15)	1.6 (5-15)	11.4 (5-15)	28.9 (5-15)	8.5 (5-15)

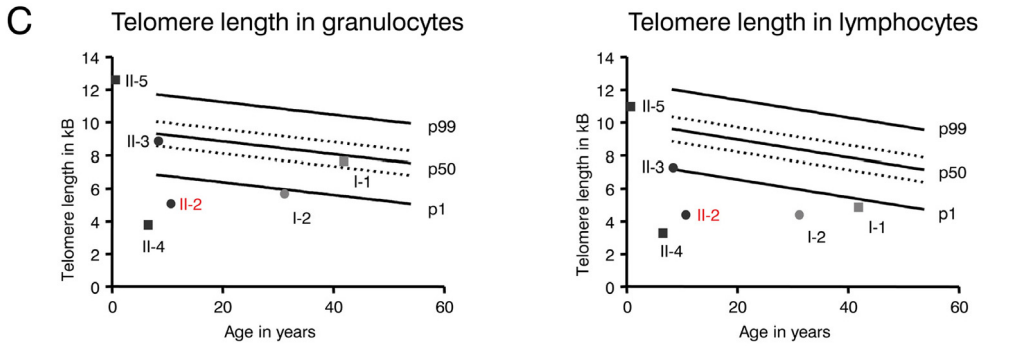

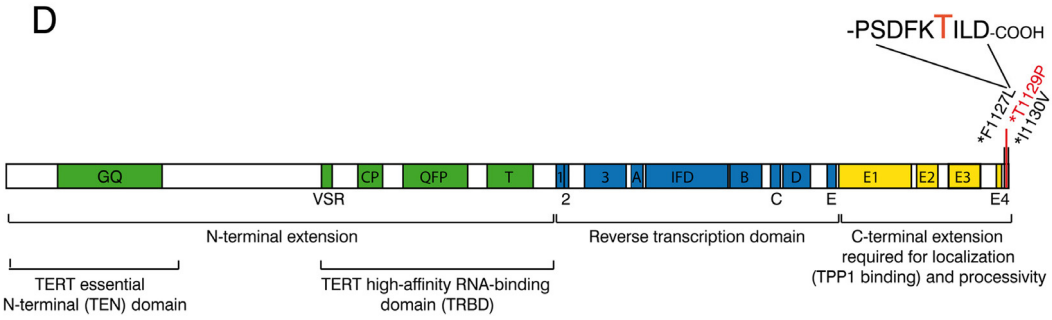

Figure 1. Clinical features and telomere length of the DKC family with the novel T1129P TERT mutation. (**A**) Family tree of the consanguineous Libyan family. Family members affected by dyskeratosis congenita (son II-1 (deceased), daughter II-2, son II-4) are indicated in black. Marked in red: patient II-2 who was analyzed in detail in the following figures. (**B**) Table showing complete blood counts (WBC=white blood cells (n/nl), ANC= absolute neutrophil count (% of WBC), RBC= red blood cells (n/pl), Hb=hemoglobin (g/dl), Plt=platelet count, mean corpuscular volume (MCV in fl) and reticulocytes (‰ of RBC) and the respective age dependent normal values in brackets of the family members I-1, I-2, II-2, II-3, II-4 and II-5 shown in (A). Family members II-2 and II-4 that were diagnosed with dyskeratosis congenita and were homozygous for the $TERT^{T1129P}$ mutation are highlighted with grey color. Indicated with *: Patient II-2 was on a 3-weekly red cell transfusion regimen and had a red cell transfusion of 15 ml/kg erythrocytes 20 days before the sample was taken; patient II-4 had no history of red blood cell or platelet transfusions. (**C**) Telomere lengths of the described family determined in lymphocytes and granulocytes of the peripheral blood. Absolute telomere lengths in kb of lymphocytes and granulocytes of the patient II-2, her affected brother II-4, her siblings II-3, II-5 and her parents I-1 and I-2 are shown in the context of age-dependent percentiles (Females: circle, males: square. Parents: light grey, children: black. Marked in red: patient II-2 who was analyzed in detail). The solid lines represent the respective 1%, 50%, 99% percentile curves. The dashed lines represent the 25% and 75% percentile. (**D**) Schematic representation of the TERT gene with functional domains and known mutations at the C-terminus. Our novel T1129P mutation is depicted in red.

ness and pallor. There was no history of transfusions in the family before. The parents of II-1 were first degree cousins and family studies showed similar thrombocytopenia and anemia in two of their other offspring (II-2 and II-4) (Figure 1 A and B). Normal white blood counts, hemoglobin and platelet counts were observed from the father (I-1), mother (I-2) as well as in the second sister (II-3) and in the third brother (II-5). No family member showed any indication of nail dystrophy or skin alterations.

II-1 died at the age of eight years during conditioning regimen for intended stem cell transplantation that was performed abroad under the suspected diagnosis of aplastic anemia. His aplastic anemia was not diagnosed on a molecular basis and blood samples are no longer available.

The patient II-2 presented at our center at the age of 12 years with progressive bone marrow failure including transfusion dependent anemia and thrombocytopenia, leukopenia (Figure 1B) and hypermenorrhea. Fanconi anemia was excluded as normal results were obtained for the analysis of DNA breakage. Suspected dyskeratosis congenita was confirmed by telomere length analysis in lymphocytes and granulocytes as determined by Flow-FISH (Figure 1C). The telomere lengths in lymphocytes and granulocytes in patients II-2 and II-4 and the mother I-2 corresponded to less than the 1st percentile of age matched controls. Telomere length of the father (I-1) in lymphocytes (right panel) also corresponded to less than the 1st percentile of age-matched controls, whereas it was normal in granulocytes (left panel). The healthy sibling II-3 also displayed a decreased telomere length when compared to age matched controls, although not below the 1st percentile (Figure 1C). Pulmonary function was normal in patient II-2 and not determined in other family members.

Whole exome sequencing and validation by Sanger sequencing revealed a novel homozygous c. 3385 A>C mutation (nucleotide entry NM_198253), resulting in the novel p.Thr1129Pro or T1129P mutation (Figure 1D) of the TERT gene in the 12-year-old patient II-2. No other homozygous mutation was found in the patient. This mutation was absent from public SNP databases (dbSNP, 1000 Genome variant catalogue), conserved and was predicted to be damaging using SIFT and PolyPhen-2 [30, 31]. The unaffected family members were heterozygous carriers of this mutation. The 8-year-old brother II-4 was detected with the same homozygous mutation by Sanger sequencing from peripheral blood.

The T1129P mutated TERT does not show nuclear clustering together with TERC in a ST-cell culture model

The novel T1129P mutation is located at the C-terminus of TERT altering the 4th last amino acid (Figure 1D). This region of normal TERT was shown to bind the telomeric protein TPP1, and has therefore been suggested to be required for the telomeric localization of TERT [32]. To investigate if this novel mutation would influence recruitment of the telomerase complex, we employed a modified "supertelomerase" assay (ST) that used transient, plasmid based expression of the central scaffold protein of the telomerase ribonucleo-protein TERC and hemagglutinin (HA)-tagged TERT in HeLa cells [32-35]. As shown in Figure 2, transfection of N-terminally HA-tagged TERT into HeLa cells resulted in a nucleoplasmic pattern. In line with previous findings, expression of TERC together with HA-TERT resulted in nuclear clusters that have been described as clusters with the telomeres at the chromosomal ends (Figure 2A, compare b with e) [32]. Interestingly, the mutant HA-TERT T1129P protein was detected in the cytoplasm in the absence of co-expressed TERC. When co-expressed with TERC, a nucleoplasmic pattern was observed, but it lacked the typical nuclear clustering of wild type TERT (Figure 2A, compare e to h, k, quantified in B and C) suggesting a failure to be recruited to chromosome ends. Taken together, these results strongly further support the hypothesis that the T1129P mutation impairs the recruitment of TERT to the telomerase complex located at its site of action at the chromosome ends.

mTOR inhibition with rapamycin influences population doublings and senescence of patient skin fibroblast cultures

The proliferative capacity of cells can by quantified by calculating the population doublings that cells undergo during the culturing process as a function of time. Population doublings are defined as the number of times that the cell number is doubled. As telomeres shorten, the proliferative potential decreases. Generally, population doublings can be recorded in skin fibroblast cultures by plating a specific number of cells and then counting those cells after a defined period of growth as described in Material and Methods. Skin fibroblasts represent an easily accessible cell type that can be cultivated over a long time period, and were treated with either 5 nM rapamycin or DMSO as a vehicle control. Fibroblast cultures obtained from the father (I-1) fulfilled criteria of senescence from the beginning, as they did not show population doublings within 4 weeks despite frequent changes of cell culture media (not shown).

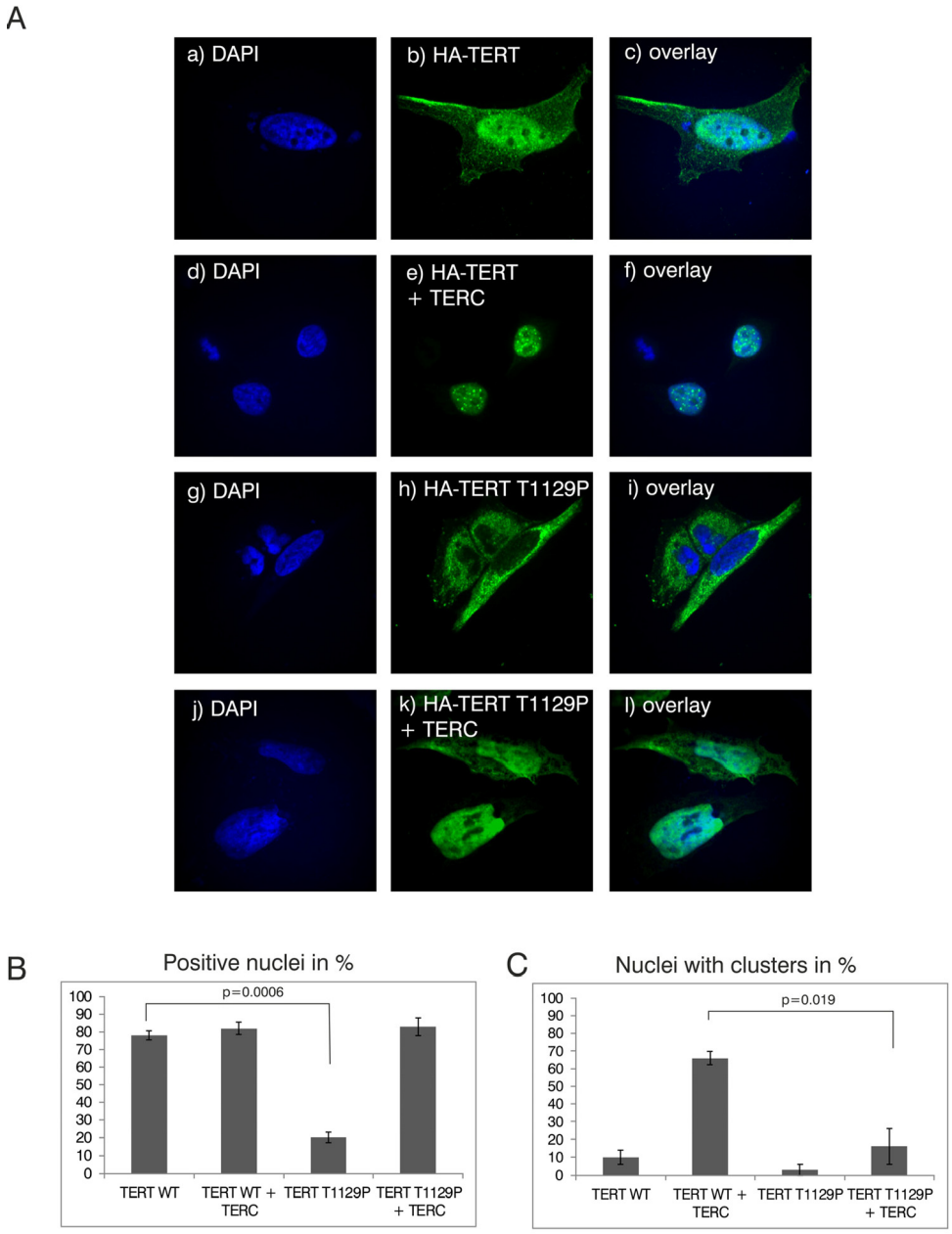

Figure 2. Analysis of nuclear clustering of the TERT T1129P mutation in a cell culture model. (**A**) Representative confocal images of transiently co-transfected HeLa-cells. HA-TERT or HA-TERT T1129P, respectively, harboring 3 HA-tag sequences in frame at the N-terminus were transfected and fixed 48h later. On the indicated pictures e) and k) equal amounts of the TERC minigene was co-transfected together with the respective TERT minigene. The HA-tag was visualized with a mouse monoclonal anti-HA antibody and an anti-mouse secondary antibody linked to Alexa 488 as described in Materials and Methods. The nucleus was visualized by DAPI staining. The panels on the right represent overlays of the TERT wild type or the T1129P mutations, respectively, with the nucleus stained with DAPI. Cells depicted represent the subcellular distribution pattern seen in >90% of the transfected cells. (**B**) and (**C**) Quantification of nuclear accumulation and clustering. For quantification of nuclear accumulation and clustering in the nuclei, 100 cells each from 3 independent transfections have been assessed and counted visually for the presence of nuclear staining and/or nuclear clustering. For statistical analysis a student's unpaired two-tailed t-test was used.

Skin fibroblast cultures of the TERT T1129P homozygous patient II-2 but also from the heterozygous mother I-2 showed impaired population doublings when compared to fibroblasts from a healthy age matched control (Figure 3A). Treatment of the control and mother (I-2) fibroblasts with rapamycin did not influence the proliferative potential measured by population doublings over time (Figure 3A). The fibroblast culture of the patient II-2 did not show a comparable proliferation potential after day 48 and had no vital cells after day 97. In contrast, the rapamycin treated fibroblast culture of patient II-2 still divided (albeit slowly) after day 97 and showed prolonged survival until day 182 (Figure 3A).

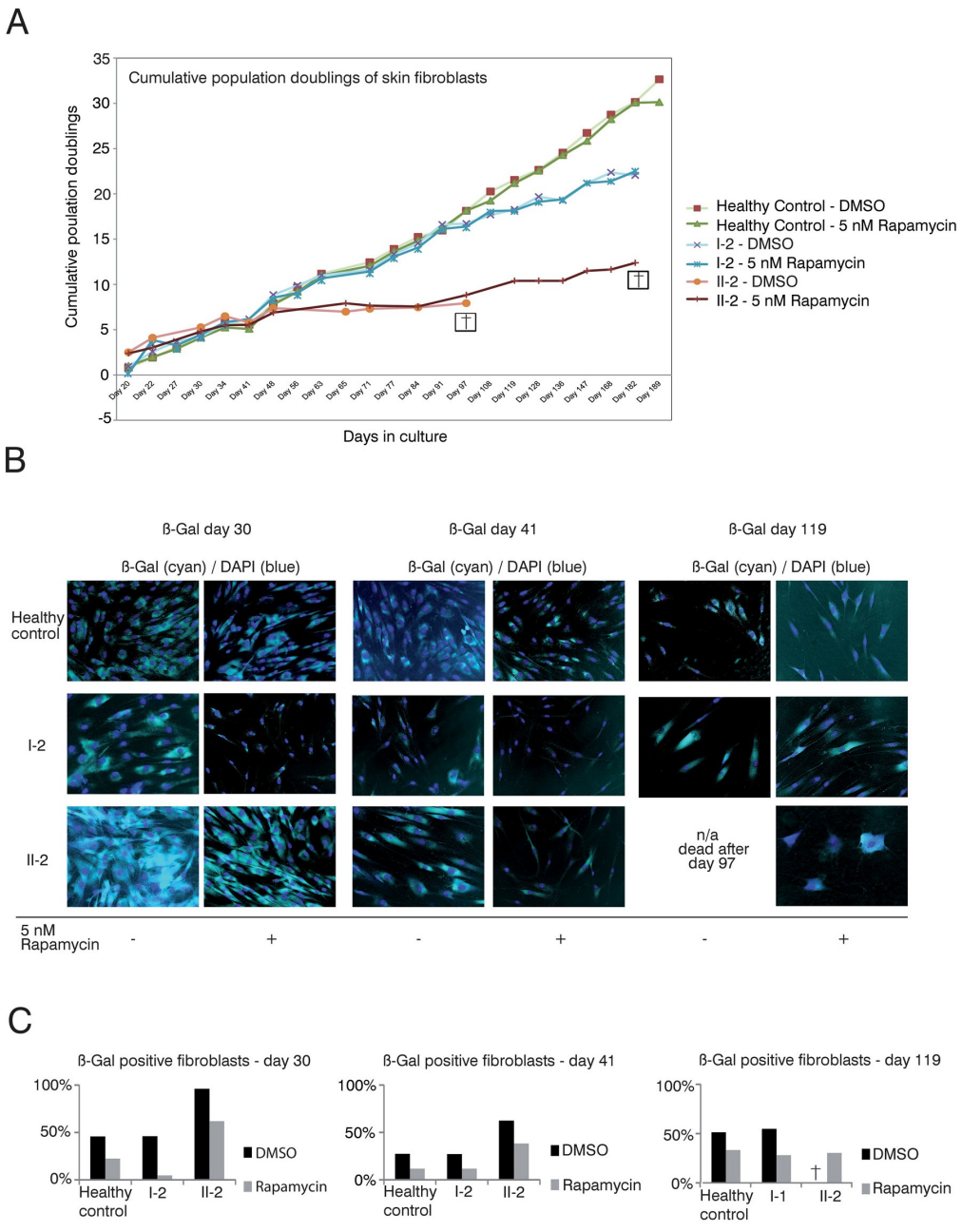

Figure 3. Rapamycin treatment of DKC skin fibroblast cultures. (**A**) Cumulative population doublings of skin fibroblasts. Fibroblast cultures from the mother I-2, the daughter II-2 and a healthy control were trypsinized and viable cells determined by trypan blue staining. Viable cells remained unstained. Population doublings were calculated using the following equation: PD=X + log2(Y/I) where: X = initial PD I = cell inoculum (number of cells plated in the flask) Y = final cell yield (number of cells at the end of the growth period). Cell were defined as dead (indicated with a cross) if no remaining viable cells were detected.

(**B**) ß-gal senescence assay of skin fibroblasts. Fibroblasts were cultured in DMEM/10% FCS/1%PenStrep containing either 5nM rapamycin dissolved in DMSO or the equal volume of DMSO as negative control (equivalent to a 1:1,000 dilution). For the indicated timepoints, cells were fixed after 24h with 0.1% glutaraldehyde and stained for ß-galactosidase (ß-Gal) at pH 6 as described in Materials and Methods. Nuclei were visualized by staining with DAPI (Sigma-Aldrich), diluted 1:10,000. Coverglasses were embedded in moviol 4-88 (Carl Roth) on slides. Cells were observed at 20-fold magnification and pictures taken at brightfield and fluorescent light with a filter set suitable for DAPI on an Olympus CellR microscope. Depicted overlays of brightfield and fluorescence were merged in ImageJ. Images are representative of the indicated time points. (**C**) Quantification of ß-gal assay. ß-Gal-positive cells were detected at the indicated time points using a programmed plugin for the image editing program ImageJ as described in Materials and Methods. The quantified images were representative of the indicated time points. 200 cells counted by DAPI staining were analyzed for each time point and measurement. The fibroblasts were determined as ß-Gal positive when blue staining in the brightfield reached a defined intensity and surrounding area of the core that was detected in the fluorescence light (Ex 330-385, Em LP420 filter set for DAPI detection).

The limited capacity of cells to divide culminates in senescence, a status that is characterized by decreased viability, enlarged cell size, altered pattern of gene expression and expression of pH dependent beta-galactosidase activity [36-38]. ß-galactosidase activity is present only in senescent cells and is not found in pre-senescent, quiescent or immortal cells [37]. Therefore, we performed ß-galactosidase assays to test if the prolonged survival in the rapamycin treated fibroblast cultures of the patient (II-2) correlated with decreased senescence (Figure 3B and C). We detected decreased senescence in the control fibroblasts, fibroblasts of the mother I-2 and the affected patient II- 2 at day 30 when treated with rapamycin (Figure 3B and C). The same effect was observed at day 41 of this experiment. At day 119 the DMSO treated fibroblast culture of our patient II-2 did not show any vital cells (no viability after day 97). In healthy control fibroblasts and the mother's fibroblasts, the rapamycin treated cultures still showed decreased senescence when compared to the respective DMSO treated cultures (Figure 3B). Taken together, these data reveal a positive correlation between proliferative potential and a decrease of the senescence marker, beta-galactosidase activity, in DC patient cells.

CD34+ HSPCs are reduced more than 300-fold in patient bone marrow

Next, we sought to investigate the effect of rapamycin treatment on hematopoietic stem and progenitor cells (HSPCs), hypothesizing that in line with our previous results with fibroblasts (Figure 3), a prolonged survival of HSPCs could improve the patient's blood counts. If so, rapamycin might offer a therapeutic treatment to reduce transfusion dependence of the affected family members. Patient bone marrow derived HSPCs were characterized and quantified by flow cytometry and functionally characterized in vitro by colony forming unit (CFU) assays as well as in vivo by xeno-transplantation into immunocompromized NOD/SCID/ interleukin 2 receptor γ^{null} (NSG) mice. Rapamycin treatment and control groups were included in all experiments (Figure 4A). As shown in Figure 4B cellularity and HSPC frequency were strongly reduced in the bone marrow of patient II-2. Compared to a healthy female donor the patient had a 4-fold reduced bone marrow mononuclear cell count ($1.53x10^6$/ml vs. $0.4x10^6$/ml) with reduced viability after gradient centrifugation (98.1 percent vs. 84.3 percent viable cells). A dramatic 300-fold reduction was observed in CD34+ HSPCs per ml bone marrow. Only 0.034 percent of all lineage negative cells were CD34+ in the patient II-2 compared to 7.04 percent in the healthy control sample, highlighting a severe HSPC depletion phenotype (Figure 4B and C). Using magnetic bead enrichment for CD34, less than 10,000 CD34+ cells could be isolated from 100 ml bone marrow aspirate, limiting functional studies with these cells.

Impaired clonogenic growth potential of patient II-2 HSPCs in vitro was not improved by rapamycin

To evaluate clonogenicity and lineage differentiation potential of the patient's HSPCs and the influence of rapamycin treatment we performed colony forming unit (CFU) assays (see Figure 4A for experimental design). Plating 3,000 CD34+ cells resulted in approx. 80 colonies per plate in the healthy control. In contrast, the patient's HSPC colony forming potential was significantly reduced, revealing on average only 4 colonies in the DMSO treatment group and 2 colonies in the rapamycin treatment group (Figure 5A). Although colonies treated with rapamycin were reduced in size in both patient and healthy control, this effect was more pronounced in the patient HSPCs (Figure 5B). Furthermore, patient HSPCs showed no long-term self-renewing potential as no colonies were detected anymore in secondary CFU assays, irrespective of rapamycin treatment. In addition to a reduced abundance of HSPCs in the patient's bone marrow, results from the CFU assays indicate a severe functional

impairment including self-renewal potential of mutant progenitors. However, in contrast to our observation in fibroblasts, rapamycin treatment showed no beneficial effect on colony number, size and self-renewal activity.

Xenotransplantation of remaining CD34-negative HSPCs from patient II-2 does not result in multilineage engraftment

Xenotransplantation of human HSPCs into immunocompromized NSG mice is considered the gold standard to evaluate hematopoietic stem cell function. We have recently shown that co-transplantation of mesenchymal stromal cells (MSCs) can enable engraftment of functionally impaired and usually non-transplantable HSPCs derived from Myelodysplastic Syndrome patients [39]. Lacking sufficient amounts of CD34+ HSPCs and to rule out the possibility that the patient's HSPCs are "hidden" within the CD34-negative fraction we co-injected CD34-negative BM MNCs together with healthy human MSCs infra-femorally into sub-lethally irradiated NSG recipient mice. As control, CD34+ healthy HSPCs and MSCs were co-transplanted. In addition, 90-day slow release rapamycin or placebo pellets were implanted subcutaneously. Engraftment of human blood cells was measured by the chimerism for human CD45+ cells 90 days after transplantation. Expression of human CD19 determined lymphoid lineage output, while human CD33 expression was indicative of myeloid differentiation. As expected, healthy HSPCs reconstituted multi-lineage human hematopoiesis in bone marrow (Figure 6A, D), spleen (Figure 6B) and peripheral blood (Figure 6C) of recipient mice. Although not statistically significant, there was a clear trend showing that human CD45+ engraftment was impaired in the rapamycin treatment group in all organs analyzed. In contrast, patient II-2 derived CD34-negative bone marrow MNCs failed to engraft in both rapamycin and placebo treated animals as neither myeloid nor lymphoid cell engraftment was observed.

A

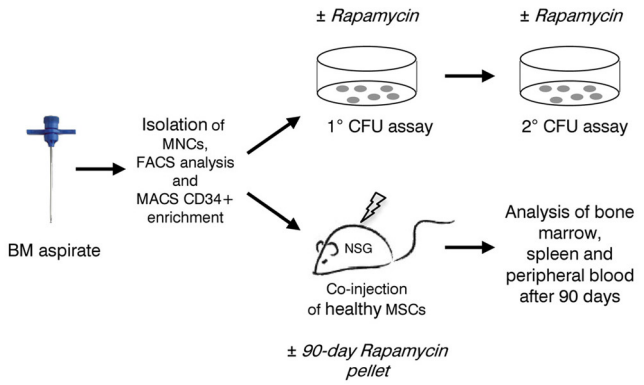

B

	Control	Patient II-2
MNC per ml BM	1.53x10^6	0.4x10^6
Viability (%)	98,1	84,3
CD34+ per ml BM	31900	100

C

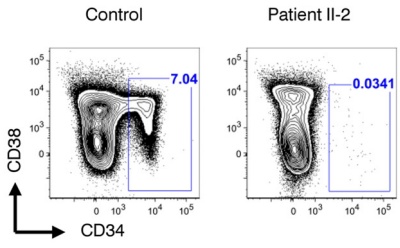

Figure 4. Analysis of patient II-2 bone marrow. (**A**) Experimental setup: Bone marrow mononuclear cells were isolated by gradient centrifugation from patient II-2 and healthy control, analyzed by FACS and either plated in colony forming unit assays (see Figure 5) or transplanted into NSG females (see Figure 6). (**B**) Bone marrow characteristics at time of sampling. (**C**) FACS plots showing CD34 and CD38 levels gated on live, lineage-negative cells. Gates show frequencies of CD34+ cells in percent.

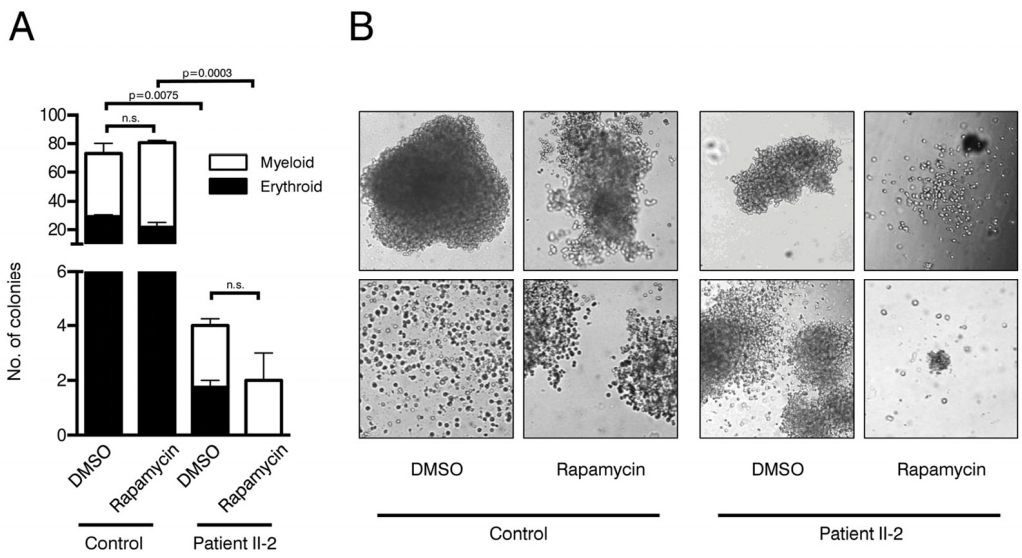

Figure 5. Colony forming unit assays. (**A**) Number of colonies in patient and control CFU assays treated with rapamycin or DMSO. Cells were plated in duplicates. Student's t-test was performed on total number of colonies, n.s. not significant. (**B**) Representative pictures of colonies.

However, CD3+ T cells, which were present in the transplanted CD34-negative cell fraction of patient II-2, expanded over the course of 90 days under placebo treatment leading to a clinically inapparent graft-versus-host disease. Rapamycin almost completely suppressed T cell expansion in the recipient mice, confirming the activity of the rapamycin pellets and being in line with its known mode of action as an immunosuppressive drug (Figure 6A-D).

Taken together, our experiments with bone marrow MNCs from the dyskeratosis congenita patient II-2 revealed a striking reduction in HSPCs associated with a severe functional impairment of stem cell activity that could not be improved by rapamycin treatment.

DISCUSSION

Members of the telomerase complex such as TERC, TERT or DKC1 play fundamental roles in aging processes [4-7]. Mutations in these genes may lead to diseases associated with premature aging such as DKC and cancers. Therefore, a refined knowledge of the effects of these mutations may prove useful for understanding pathways that lead to, or mitigate, long-term health, prevention of cancer and late-stage disease. The novel germline T1129P mutation in the TERT gene identified in a consanguineous Libyan family leads to DKC with progressive bone marrow failure in all homozygous individuals. Patients II-2 and II-4 showed significantly shortened telomeres below the 1st percentile when compared to healthy controls or to heterozygous family members. The pronounced telomere loss for lymphocytes in comparison to granulocytes is consistent with previous findings in healthy individuals as well as in patients with reduced telomere activity [40, 41]. Only homozygous family members showed progressive bone marrow failure. Heterozygous family members showed normal blood results. Heterozygosity of TERC- and most TERT-mutations can lead to haploinsufficiency and to the clinical phenotype of dyskeratosis congenita, although some TERT mutations cause recessive DKC with heterozygous carriers showing normal blood counts [42]. The heterozygous family members described here are phenotypically healthy despite the presence of shortened telomeres indicating a recessive mode of inheritance of the TERT T1129P mutation. This is consistent with the observation that disease severity cannot be predicted by telomere length alone [43]. However, a late onset of clinical symptoms cannot, of course, be ruled out. Strikingly, the phenotype of affected, homozygous family members only showed progressive bone marrow failure with an absence of other DKC related symptoms such as skin or nail dystrophy or pulmonary fibrosis. The localization of the mutation within the gene does not necessarily predict the phenotype, which is highly variable in various muta-

tions described throughout the TERT gene [4]. Our novel autosomal recessive T1129P mutation is in close proximity to the previously described mutations at positions 1127 and 1130 [43, 44]. When comparing the phenotypes and modes of inheritance of these two near-by mutations, it is striking that the mutation F1127L resembles Hoyeraal-Hreidarsson-syndrome and causes autosomal dominant dyskeratosis congenita whereas the somatic I1130V mutation leads to non-severe aplastic anemia [43, 44].

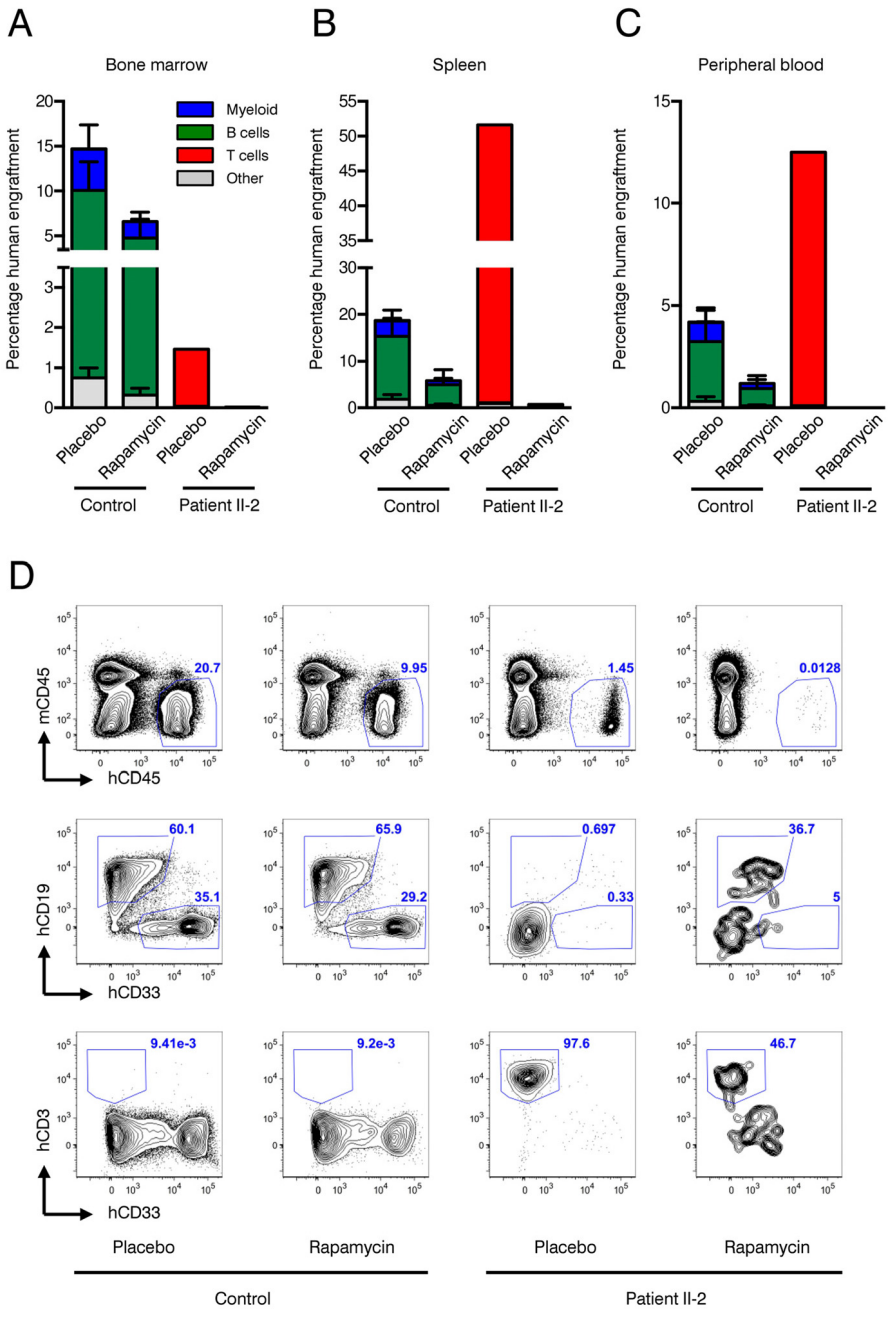

Figure 6. **Xenotransplantation experiments.** (**A**-**C**) Frequencies of human engraftment with respect to lineage differentiation in bone marrow (**A**), spleen (**B**) and peripheral blood (**C**) 90 days after transplantation of patient II-2 or healthy bone marrow. Mice were treated either with rapamycin or placebo. n=2 per condition in healthy donor, n=1 per condition in patient (**D**) Representative FACS plots depicting human (h)CD45 versus mouse (ms)CD45 for blood cell chimerism (upper panel), human (h)CD19 for lymphoid differentiation and human (h)CD33 for myeloid differentiation (middle panel) and human (h)CD3 for T cell expansion. Upper panel is gated on live cells, middle and lower panels are gated on live, hCD45+ cells. Numbers represent percentage of gated events.

It still needs to be elucidated how the T1129P TERT mutation exerts its effect causing aplastic anemia in affected patients. In HeLa cell cultures the T1129P mutated TERT did not efficiently enter the nucleus without co-transfected TERC (Figure 2A and B). Together with the lack of nuclear clustering upon co-transfection with TERC, this indicates an inefficient recruitment of the telomerase complex to telomeres within the nucleus for T1129P mutated TERT. As the postulated binding site of TPP1 is within the C-terminus, binding to TPP1 or other members of the telomerase recruitment complex might be impaired by the novel T1129P mutation. A mutant of the three amino acid sequence F1127/K1128/T1129 has been shown before to display only slightly compromised telomerase catalytic activity in vitro, but its in vivo ability to elongate telomeres was highly compromised [45]. In another study, this mutant was further analyzed for its ability to localize to telomeres and to TPP1. While it did not localize to telomeres, it could still localize with TPP1 in Cajal bodies, even though the association with TPP1 was weaker compared to wild type [32].

As androgens harbor various side effects especially for female patients with DKC including virilization, there is need for substances that are safe and well tolerated antagonizing pre-mature aging processes [22, 39]. mTOR inhibition, by rapamycin, has been demonstrated to extend lifespan in a host of model organisms as well as reduce the onset of cellular senescence in cell culture [46, 47]. Moreover, recent data obtained in yeast suggest that mTOR inhibition by rapamycin can strengthen the DNA damage checkpoint and thereby increase the likelihood that cell division only occurs when damaged chromosomes are repaired [48].

Therefore, rapamycin, a substance well characterized in the clinical setting, might be an attractive target to treat DKC patients as they harbor increased numbers of senescent cells which contain dysfunctional chromosome ends. Before administering rapamycin to the patient, we assessed its effect on skin fibroblasts and on HSPCs – the cells that are most severely affected in our patient. Rapamycin had no effect on enhancing the proliferation of normal skin fibroblasts but did prolong the survival of the fibroblasts from the affected patient II-2 (Figure 3A). In our functional analysis, senescence of skin fibroblasts of patient II-2 was increased, as expected. Rapamycin showed an effect on decreasing cellular senescence in treated skin fibroblast cultures of patient II-2. Strikingly, cellular senescence was also reduced in the fibroblast culture of the mother I-2 and the fibroblasts of the healthy control (Figure 3B and C). As mTOR inhibition regulates cellular pathways that affect senescence and aging, this might show the influence of mTOR on fundamental senescence steps even in healthy cells [47]. All fibroblast cultures showed a higher initial senescence at day 30 when compared to day 41. This can be explained by an increased senescence of the newly plated cells and later a reduced senescence of the increasingly dense cell cultures at day 41 that could have been caused by contact inhibition of geroconversion [49, 50].

Decreased frequency of HSPCs and severe impairment of these cells in functional tests such as colony-forming unit assays and xenotransplantation into immuno-compromized NSG mice highlight a fundamental HSC defect in patient II-2 (Figures 4 and 5).

In contrast to fibroblasts, rapamycin treatment did not improve HSC function in these assays. The fact that rapamycin treatment resulted in a trend towards fewer and smaller colonies argues against a possible improvement of the patient's blood counts by inhibiting mTOR. However, we cannot exclude that long-term rapamycin treatment of CD34+ HSPCs may ultimately lead to restoration of HSC function as CFU assays cover only a few weeks. Due to limited availability of diseased CD34+ HSPCs (only 10,000 CD34+ cells in 100ml bone marrow aspirate) xenotransplantation had to be performed using MNCs not selected for CD34. The data thus exclude the possibility that the patient's HSCs in the diseased BM down-regulated CD34 expression. Even co-transplantation of MSCs, which typically enhance engraftment of stem cells usually not capable of initiating human hematopoiesis in NSG mice, showed no beneficial effect [39].

Interestingly, T cells present in the CD34-negative MNCs expanded in the non-treated xenografts, while the immunosuppressive agent rapamycin blocked their expansion efficiently in the treated animals (Figure 6).

Due to the nature of our biological samples (skin biopsy and bone marrow aspirate from patient II-2) repetitive sampling was not possible or useful.

Previous studies in yeast demonstrated that rapamycin was beneficial for cells with dysfunctional telomeres when cells were given the chance to repair the telomeres and eventually proliferate in the absence of rapamycin [48]. Indeed when telomere dysfunction and rapamycin treatment were chronic, there was an initial lag in growth and only at very late time points the rapamycin treatment appeared to be beneficial (J.K. and B.L unpublished results). In the mouse experiments, rapamycin was constantly released from the pellets. In contrast, rapamycin was added to the fibroblast cultures

at the time of the splitting procedure and a possible degradation of the drug over time might have limited the toxic effects in our fibroblast experiments. Fine-tuning of rapamycin dosage might therefore be required for the anti-senescent effect and to avoid toxic effects [51]. Therefore it may be necessary to re-evaluate the dosage of rapamycin and the effects of cyclic dosing in order to see stronger effects.

The observed difference between fibroblasts and hematopoietic cells might also be explained by the different growth characteristics of the cell types studied: Fibroblasts divide much more slowly than hemato-poietic cells and it is possible that hematopoietic DKC T1129P cells require a stronger therapeutic effect than DKC T1129P fibroblasts for an improvement in survival. This difference of the effect of this mutation in either fibroblast or hematopoietic cells might also be reflected by the most severely affected hematopoiesis of the homozygous TERT T1129P patients, whereas the skin and other epithelial tissues were not clinically affected.

Furthermore, the severity of the telomerase mutation may render cells completely unable to re-elongate telomeres. It should also be considered that continuous presence of rapamycin in our experiment might have had additional toxic effects preventing cell division.

In summary, we report a novel hereditary T1129P TERT mutation that leads to DKC with aplastic anemia that can be attributed to a severe reduction and functional impairment of CD34+ hematopoietic stem cells. Functional analyses to find a therapeutic alternative for this serious condition revealed that rapamycin treatment prolonged survival and decreased levels of cellular senescence in treated skin fibroblasts. However, impaired HSC function could not be restored by rapamycin mediated mTOR inhibition, as colony forming capacity in vitro and multilineage engraftment potential in xenotransplanted mice was unchanged in the presence of rapamycin. Our data argue against a therapeutic use of mTOR inhibitors to treat aplastic anemia in DKC patients with TERT mutations.

MATERIALS AND METHODS

Ethics statement. Investigation has been conducted in accordance with the ethical standards and according to the Declaration of Helsinki and according to national and international guidelines and has been approved by the authors' institutional review board.

Genotype analysis. EDTA-blood samples of the patients and their family were obtained after informed consent had been given. DNA was prepared according to standard protocols (QIAampDNA Blood Mini Kit, Qiagen, Germany). The genebank accession number used was NM_198253 for the cDNA and amino acid sequences.

Telomere length measurement via flow-FISH. Telomere length in lymphocytes and granulocytes from the peripheral blood of our patients was analyzed using flow-FISH as previously described [40, 52, 53]. Briefly, samples were analyzed in triplicates with and without Alexa488-(C3TA2) PNA staining (Panagene, Daejeon, South Korea). Granulocytes, lymphocytes and cow thymocytes were identified based on forward scatter and LDS 751 staining. Cow thymocytes with known telomere length were used as an internal control to calculate telomere length in kilobases. To determine the percentiles, linear regression on 104 blood samples from healthy donors was carried out [54, 55].

Exome capture and Illumina sequencing**.** Exome capture was carried out with the SureSelect Target Enrichment Kit v4 (Agilent, Santa Clara, CA) according to manufacturer's instructions (version 1.7, July, 2014). DNA concentration was determined with the Qubit fluorometer using the BR dsDNA Assay (Qubit 2.0, Invitrogen Life Technologies, Grand Island, NY). 3 µg of genomic DNA was sheared using Covaris S2 instrument (Covaris, Woburn, Mass, USA) to a mean size of 150-200bp. 500 ng of the library was subjected to hybridization with the SureSelect baits for 16 hours at 65 °C. Fragments captured in hybridization were indexed, amplified and sequenced in a paired end 100-bp mode using an Illumina HiSeq2000 deep sequencing instrument (v3 sequencing chemistry; Illumina, San Diego, CA).

Analysis of the whole exome sequencing data. Single nucleotide variant (SNV) calling was performed with the Genome Analysis Toolkit (GATK) and SAMtools mpileup [56, 57]. For GATK, the data were recalibrated with dbSNP v132 and the 1000 Genomes Project Indel release from July 5, 2011 (http://1000genomes.org). Subsequently, SNVs were called by using GATK's Unified Genotyper on the recalibrated data. All GATK calls were annotated for strand bias, low mapping quality, and SNV clusters. The GATK resulting SNV calls were intersected with the SAMtools mpileup SNV calls. All SNVs were intersected with information on gene coding regions by using the Annotation of Genetic Variants framework (ANNOVAR) [58]. By using RefSeq gene annotations, the SNVs were classified as nonsynonymous SNVs affecting protein-coding regions. ANNOVAR was also used to compute the overlap with dbSNP v132 (www.ncbi.nlm.nih.gov/projects/SNP), and

the October 2011 SNV releases of the 1000 Genomes Project (http://1000genomes.org). Additionally the SNVs were filtered using an in-house database, which is based on more than 25 deeply sequenced (>30x coverage) human genomes and which includes sites that are commonly identified as false-positive SNVs by using GATK and SAMtools mpileup. Following these additional filtering steps, candidate SNVs were evaluated computationally to assess the possible effect of an amino acid substitution on the structure and function of the respective protein by using SIFT and PolyPhen-2 [30, 59].

To verify the results obtained by whole exome sequencing, the coding regions of the TERT gene were PCR-amplified and sequenced (GATC Biotech AG, Germany). Primer sequences used for fragment amplification and sequencing are available on request.

Plasmid constructs. The 3xHA-TERT in pCDNA-minigene was kindly provided by Steven Artandi over addgene (pCDNA-3xHA-hTERT, addgene plasmid #51637) [60]. Functionality of this TERT construct with 3xHA at the N-terminus has been previously shown by immortalization of human fibroblasts that lack TERT expression [60].

The 3xHA-TERT T1129P minigene was constructed using the following primers:
forward primer Asc1Tert: CGGGGGCGCGCCCCGCG CGCTCCCCG
reverse primer Pac1Tert: AGACTTAATTAATCAGTC CAGGATGGGCTTGAAGTCTG.

After PCR amplification, the PCR products were digested with AscI and PacI and inserted in an AscI and PacI digested pCDNA vector. The identity of all constructs was confirmed by DNA sequencing (GATC Biotech AG, Germany).

The TERC minigene (pBS U3-hTR-500, addgene plasmid #28170) was kindly provided by Kathleen Collins over addgene [61].

Cell culture and transient transfection. HeLa-cells were grown in Dulbecco's modified Eagle's medium (DMEM) supplemented with 10% FCS and 1% P/S at 37°C and 5% CO_2. Cells were transiently transfected by calcium phosphate precipitation in 6-well plates using 3µg of the test construct DNA as described before [62].

Immunocytochemistry. For immunocytochemical detection of the HA-epitope, transfected cells that had been grown on coverslips in 6-well plates were fixed in 4% paraformaldehyde in phosphate-buffered saline (PBS) for 20min at 4°C and pre-treated with 5% FCS in PBS+/-T (0.1% Triton X-100 in PBS) for 20min at RT to block unspecific antibody binding and to permeabilize the cells. The cells were then incubated with a mouse monoclonal anti-HA antibody (Sigma-Aldrich) at 1:1,000 in 3% FCS/PBS. Immunoreactivity was visualized by a goat anti-mouse secondary antibody conjugated to AlexaFluor488 (CellSignaling) (1.1,000 in 3% FCS/PBS). Before mounting the coverslips upside down in moviol 4-88 (Carl Roth) on slides, cells were washed 3x with PBS and nuclei were visualized by staining with DAPI (4'-6-Diamidino-2-phenylindole, 10mg/ml stock solution, Sigma-Aldrich), diluted 1:10,000 in PBS for 10min at RT.

Microscopy and quantification. Cells were imaged in the 405 and 488nm laser channels (DAPI excitation 405nm, emission 455nm; AlexaFluor excitation 488nm, emission 525nm) using a spinning-disk confocal microscope (Perkin Elmer ERS-6 with a Hamamatsu C9100-50 camera).The system incorporated a Nikon Eclipse TE2000-U inverted microscope using a Nikon 100x objective. Perkin-Elmer Ultraview ERS software and Volocity 6.3 software (Improvision, Lexington, MA) were used for acquisition. Images were subsequently cropped in Adobe Photoshop CS2. Cropped images were imported into Corel Draw X5 for the final figures presented.

For quantification of nuclear accumulation and clustering in the nuclei, 100 cells each from 3 independent transfections have been assessed and counted visually for the presence of nuclear staining and/or nuclear clustering. For statistical analysis a student's unpaired two-sided t-test was used.

Patient data and material. Patient data and samples were acquired and the patient was treated in accordance with the Helsinki Declaration of 1975.

After written consent, the bone marrow sample was taken according to standard procedures as a necessary routine assessment in bone marrow failure patients to determine cellularity and further cytogenetic aberrations.

Skin fibroblasts were obtained by standard procedures from underarm skin under local anesthesia and grown in DMEM (LifeTechnologies) media supplemented with 10% FCS, 1% P/S and 1% fungizone (LifeTechnologies) at 37°C in 5% CO_2.

Determination of population doublings in skin fibroblast cultures. Monolayers were dissociated with trypsin/EDTA and resuspended cells in complete

medium. To check for viability, cells were diluted 1:2 with trypan blue (LifeTechnologies). Viable cells remained unstained. Viability and number were determined using a hemacytometer (improved Neubauer). Population doublings were calculated using the following equation: PD=X + log2(Y/I) where: X = initial PD I = cell inoculum (number of cells plated in the flask) Y = final cell yield (number of cells at the end of the growth period).

Beta-galactosidase (ß-Gal) Staining + DAPI. Fibroblasts were cultured in DMEM/10% FCS/1%PenStrep containing either DMSO (negative control) or 5 nM rapamycin dissolved in DMSO. For several time points cells were semi-confluently seeded on 18mm-coverslips in DMEM/10%FCS/1%PenStrep at 37°C and 5% CO^2. Senescence associated ß-Gal staining was performed according to a modified published protocol [63]. After 24h cells were washed twice with PBS and fixed with 0.1% glutaraldehyde at room temperature for 15 minutes. Following two washing steps with PBS, fibroblasts were stained for ß-galactosidase using a 0.1%ß-Gal / 5 mM Potassium hexacyano-ferrate (II)/5 mM Potassium hexacyano-ferrate (III)/2 mM $MgCl_2$ / 7.4mM Citric Acid / 150 mM NaCl- solution at pH6 for 14-16 hours at 37°C. Nuclei were visualized by staining with DAPI (4'-6-Diamidino-2-phenylindole, 10mg/ml stock solution, Sigma-Aldrich), diluted 1:10,000 in PBS for 20min at RT. Two additional washings with PBS were performed before embedding coverslips upside down in moviol 4-88 (Carl Roth) on slides. Cells were observed at 20-fold magnification on an Olympus CellR microscope and pictures taken at brightfield and fluorescent light (Ex 330-385, Em LP420), respectively. Depicted overlays of brightfield and fluorescence were merged in Fiji.

Quantification of ß-Gal positive cells. The self-written macro Nuclei_PeripheryMeasure was used to count the number of cells with a cytosolic signal above a user-defined threshold within a cell population. As output, the number of criteria-matching cell counts with respect to the total number of cells is provided. The macro works on images or image stacks with at least two channels. In short, the macro takes the nuclear signal (here DAPI) in one channel as reference for individual cells. Segmentation of nuclei is done by intensity thresholding. The corresponding nuclear areas are registered and used to create binary images as masks. In order to measure the cytosolic signal of the second channel (here ß-Gal), dilations are performed on the binary images in a user-defined manner to match cell dimensions. The resulting mask images with intensity values 0 (background) and 1 (foreground) are multiplied with the images of the second channel to select the areas for measurement. For the analysis, the user can specify both a general signal intensity threshold and a minimal number of pixels required above that threshold for positive counts. The software is available as ImageJ macro and can be downloaded from http://www.zmbh.uniheidelberg.de/Central_Services/Imaging_Facility/2D_ImageJ_Macros.html [64]. The following settings were used to define ß-Gal positive cells in the programmed plugin: Find and add nuclei to the ROI manger (yes). Substract background (yes), maximum nuclei radius 80 pixels, minimum nuclei size 300 pixels, maximum nuclei size 4000 pixels, minimum circularity 0, maximum circularity 1. Clear ROI manager (yes). Surrounding analysis: surrounding distance (dilation) 5, threshold to detect intensity: 120, amount of pixels over threshold: 100. For quantification an average number of 200 DAPI stained cells were counted.

FACS analysis, CD34+ magnetic bead enrichment and colony forming unit assays. Bone marrow mononuclear cells were isolated by gradient centrifugation using Histopaque-1077 (Sigma) and labeled with APC-eFluor780-conjugated anti-CD34 (4H11, eBioscience), Alexa-Fluor 700-conjugated anti-CD38 (HIT2, eBioscience), a cocktail of APC-conjugated lineage antibodies consisting of anti-CD4 (RPA-T4), anti-CD8 (RPA-T8), anti-CD11b (ICRF44), anti-CD20 (2H7), anti-CD56 (B159, all BD Biosciences), anti-CD14 (61D3), anti-CD19 (HIB19) and anti-CD235a (HIR2, all eBiocience) and DAPI (Sigma). FACS analysis was performed on LSR Fortessa (BD Biosciences).

CD34+ cells from MNC were isolated using MACS enrichment columns (Miltenyi Biotec) according to the manufacturer's instructions. CD34+ cells were plated in methylcellulose medium (MethoCult H4434; StemCell Technologies) with 5nM rapamycin or DMSO. Colonies were counted after 14 days and pictures were taken with a Nikon Eclipse Ti microscope.

Mouse transplantation and in-vivo rapamycin treatment. Animals were housed under specific pathogen-free conditions at the central animal facility of the German Cancer Research Center (DKFZ). All animal experiments were approved by the Regierungspräsidium Karlsruhe under "Tierversuchsantrag G210/12".

Female NSG mice with 8 weeks of age were sub-lethally irradiated (175 cGy) one day before the cells were injected in the femoral bone marrow cavity. For the healthy control 10^5 CD34+ cells were injected along with 5 $x10^5$ MSCs. For the patient 10^6 CD34-negative MNCs cells were injected along with 5 $x10^5$ MSCs. 90 day slow release implantable pellets (Innovative

Research of America, USA) with 9mg rapamycin/pellet or placebo were implanted subcutaneously on the day of transplantation.

Recipient mice were analyzed 12 weeks post transplantation. Bone marrow cells were labeled with PE-conjugated anti-human CD45 (2D1), APC-eFluor780-conjugated anti-mouse CD45 (30-F11), PE-Cy5-conjugated anti-human CD3 (UCHT1), APC-labeled anti-human CD19 (HIB19), PE-Cy7-conjugated anti-human CD33 (WM-53, all from ebioscience) to assess multilineage human hematopoietic engraftment.

ACKNOWLEDGEMENT

The authors acknowledge the staff at the Nikon Imaging Center at the University of Heidelberg for their assistance and for providing their excellent facility for imaging. We thank Dr. Michaela Socher and A. Rathgeb from the DKFZ Central Animal Facility for excellent mouse husbandry, and the EMBL GeneCore and EMBL IT for technical support.

Funding

C.S. was supported by the Frontier program of the University of Heidelberg. This work was supported by the SFB 1036 of the Deutsche Forschungsgemeinschaft (DFG) and the Forschergruppe NicHem (FOR 2033) of the DFG and by the Dietmar Hopp Stiftung.

Conflict of interest statement

The authors have no relevant conflicts of interest to disclose.

REFERENCES

1. Hug N and Lingner J. Telomere length homeostasis. Chromosoma. 2006; 115:413-425.

2. Lingner J, Cooper JP and Cech TR. Telomerase and DNA end replication: no longer a lagging strand problem? Science. 1995; 269:1533-1534.

3. Shay JW and Wright WE. Telomeres and telomerase in normal and cancer stem cells. FEBS Lett. 2010; 584:3819-3825.

4. Diaz de Leon A, Cronkhite JT, Katzenstein AL, Godwin JD, Raghu G, Glazer CS, Rosenblatt RL, Girod CE, Garrity ER, Xing C and Garcia CK. Telomere lengths, pulmonary fibrosis and telomerase (TERT) mutations. PloS one. 2010; 5:e10680.

5. Batista LF, Pech MF, Zhong FL, Nguyen HN, Xie KT, Zaug AJ, Crary SM, Choi J, Sebastiano V, Cherry A, Giri N, Wernig M, Alter BP, et al. Telomere shortening and loss of self-renewal in dyskeratosis congenita induced pluripotent stem cells. Nature. 2011; 474:399-402.

6. Agarwal S, Loh YH, McLoughlin EM, Huang J, Park IH, Miller JD, Huo H, Okuka M, Dos Reis RM, Loewer S, Ng HH, Keefe DL, Goldman FD, et al. Telomere elongation in induced pluripotent stem cells from dyskeratosis congenita patients. Nature. 2010; 464:292-296.

7. Du HY, Pumbo E, Ivanovich J, An P, Maziarz RT, Reiss UM, Chirnomas D, Shimamura A, Vlachos A, Lipton JM, Goyal RK, Goldman F, Wilson DB, et al. TERC and TERT gene mutations in patients with bone marrow failure and the significance of telomere length measurements. Blood. 2009; 113:309-316.

8. Dokal I. Dyskeratosis congenita in all its forms. British journal of haematology. 2000; 110:768-779.

9. Armanios M and Blackburn EH. The telomere syndromes. Nat Rev Genet. 2012; 13:693-704.

10. Mason PJ and Bessler M. The genetics of dyskeratosis congenita. Cancer Genet. 2011; 204:635-645.

11. Tummala H and Walne AJ. Long tails, short telomeres: Dyskeratosis congenita. Oncotarget. 2015; 6:13856-13857.

12. Calado RT and Young NS. Telomere maintenance and human bone marrow failure. Blood. 2008; 111:4446-4455.

13. Townsley DM, Dumitriu B and Young NS. Bone marrow failure and the telomeropathies. Blood. 2014; 124:2775-2783.

14. Savage SA and Alter BP. The role of telomere biology in bone marrow failure and other disorders. Mechanisms of ageing and development. 2008; 129:35-47.

15. Calado RT. Telomeres and marrow failure. Hematology / the Education Program of the American Society of Hematology American Society of Hematology Education Program. 2009:338-343.

16. Gadalla SM, Cawthon R, Giri N, Alter BP and Savage SA. Telomere length in blood, buccal cells, and fibroblasts from patients with inherited bone marrow failure syndromes. Aging (Albany NY). 2010; 2:867-874.

17. Brummendorf TH and Balabanov S. Telomere length dynamics in normal hematopoiesis and in disease states characterized by increased stem cell turnover. Leukemia. 2006; 20:1706-1716.

18. Karlseder J, Smogorzewska A and de Lange T. Senescence induced by altered telomere state, not telomere loss. Science. 2002; 295:2446-2449.

19. Islam A, Rafiq S, Kirwan M, Walne A, Cavenagh J, Vulliamy T and Dokal I. Haematological recovery in dyskeratosis congenita patients treated with danazol. British journal of haematology. 2013; 162:854-856.

20. Ziegler P, Schrezenmeier H, Akkad J, Brassat U, Vankann L, Panse J, Wilop S, Balabanov S, Schwarz K, Martens UM and Brummendorf TH. Telomere elongation and clinical response to androgen treatment in a patient with aplastic anemia and a heterozygous hTERT gene mutation. Ann Hematol. 2012; 91:1115-1120.

21. Zlateska B, Ciccolini A and Dror Y. Treatment of dyskeratosis congenita-associated pulmonary fibrosis with danazol. Pediatric pulmonology. 2015.

22. Zawar V and Sankalecha C. Facial hirsutism following danazol therapy. Cutis. 2004; 74:301-303.

23. Riedl MA. Critical appraisal of androgen use in hereditary angioedema: a systematic review. Ann Allergy Asthma Immunol. 2015; 114:281-288 e287.

24. Yabe M, Yabe H, Hattori K, Morimoto T, Hinohara T, Takakura I, Shimizu T, Shimamura K, Tang X and Kato S. Fatal interstitial pulmonary disease in a patient with dyskeratosis congenita after allogeneic bone marrow transplantation. Bone marrow transplantation. 1997; 19:389-392.

25. Amarasinghe K, Dalley C, Dokal I, Laurie A, Gupta V and Marsh J. Late death after unrelated-BMT for dyskeratosis congenita following conditioning with alemtuzumab, fludarabine and melphalan. Bone marrow transplantation. 2007; 40:913-914.

26. Giri N, Lee R, Faro A, Huddleston CB, White FV, Alter BP and Savage SA. Lung transplantation for pulmonary fibrosis in dyskeratosis congenita: Case Report and systematic literature review. BMC Blood Disord. 2011; 11:3.

27. Laplante M and Sabatini DM. mTOR signaling in growth control and disease. Cell. 2012; 149:274-293.

28. Demidenko ZN and Blagosklonny MV. Growth stimulation leads to cellular senescence when the cell cycle is blocked. Cell Cycle. 2008; 7:3355-3361.

29. Demidenko ZN, Zubova SG, Bukreeva EI, Pospelov VA, Pospelova TV and Blagosklonny MV. Rapamycin decelerates cellular senescence. Cell Cycle. 2009; 8:1888-1895.

30. Adzhubei IA, Schmidt S, Peshkin L, Ramensky VE, Gerasimova A, Bork P, Kondrashov AS and Sunyaev SR. A method and server for predicting damaging missense mutations. Nature methods. 2010; 7:248-249.

31. Ng PC and Henikoff S. SIFT: Predicting amino acid changes that affect protein function. Nucleic acids research. 2003; 31:3812-3814.

32. Zhong FL, Batista LF, Freund A, Pech MF, Venteicher AS and Artandi SE. TPP1 OB-fold domain controls telomere maintenance by recruiting telomerase to chromosome ends. Cell. 2012; 150:481-494.

33. Abreu E, Aritonovska E, Reichenbach P, Cristofari G, Culp B, Terns RM, Lingner J and Terns MP. TIN2-tethered TPP1 recruits human telomerase to telomeres in vivo. Molecular and cellular biology. 2010; 30:2971-2982.

34. Cristofari G, Adolf E, Reichenbach P, Sikora K, Terns RM, Terns MP and Lingner J. Human telomerase RNA accumulation in Cajal bodies facilitates telomerase recruitment to telomeres and telomere elongation. Molecular cell. 2007; 27:882-889.

35. Cristofari G and Lingner J. Telomere length homeostasis requires that telomerase levels are limiting. The EMBO journal. 2006; 25:565-574.

36. Goldstein S. Replicative senescence: the human fibroblast comes of age. Science. 1990; 249:1129-1133.

37. Dimri GP, Lee X, Basile G, Acosta M, Scott G, Roskelley C, Medrano EE, Linskens M, Rubelj I, Pereira-Smith O and et al. A biomarker that identifies senescent human cells in culture and in aging skin in vivo. Proceedings of the National Academy of Sciences of the United States of America. 1995; 92:9363-9367.

38. Cristofalo VJ, Volker C, Francis MK and Tresini M. Age-dependent modifications of gene expression in human fibroblasts. Critical reviews in eukaryotic gene expression. 1998; 8:43-80.

39. Medyouf H, Mossner M, Jann JC, Nolte F, Raffel S, Herrmann C, Lier A, Eisen C, Nowak V, Zens B, Mudder K, Klein C, Oblander J, et al. Myelodysplastic cells in patients reprogram mesenchymal stromal cells to establish a transplantable stem cell niche disease unit. Cell stem cell. 2014; 14:824-837.

40. Rufer N, Brummendorf TH, Kolvraa S, Bischoff C, Christensen K, Wadsworth L, Schulzer M and Lansdorp PM. Telomere fluorescence measurements in granulocytes and T lymphocyte subsets point to a high turnover of hematopoietic stem cells and memory T cells in early childhood. J Exp Med. 1999; 190:157-167.

41. Aubert G, Baerlocher GM, Vulto I, Poon SS and Lansdorp PM. Collapse of telomere homeostasis in hematopoietic cells caused by heterozygous mutations in telomerase genes. PLoS Genet. 2012; 8:e1002696.

42. Marrone A, Walne A, Tamary H, Masunari Y, Kirwan M, Beswick R, Vulliamy T and Dokal I. Telomerase reverse-transcriptase homozygous mutations in autosomal recessive dyskeratosis congenita and Hoyeraal-Hreidarsson syndrome. Blood. 2007; 110:4198-4205.

43. Vulliamy TJ, Kirwan MJ, Beswick R, Hossain U, Baqai C, Ratcliffe A, Marsh J, Walne A and Dokal I. Differences in disease severity but similar telomere lengths in genetic subgroups of patients with telomerase and shelterin mutations. PloS one. 2011; 6:e24383.

44. Vulliamy TJ, Walne A, Baskaradas A, Mason PJ, Marrone A and Dokal I. Mutations in the reverse transcriptase component of telomerase (TERT) in patients with bone marrow failure. Blood Cells Mol Dis. 2005; 34:257-263.

45. Banik SS, Guo C, Smith AC, Margolis SS, Richardson DA, Tirado CA and Counter CM. C-terminal regions of the human telomerase catalytic subunit essential for in vivo enzyme activity. Molecular and cellular biology. 2002; 22:6234-6246.

46. Blagosklonny MV. Geroconversion: irreversible step to cellular senescence. Cell Cycle. 2014; 13:3628-3635.

47. Komarova EA, Antoch MP, Novototskaya LR, Chernova OB, Paszkiewicz G, Leontieva OV, Blagosklonny MV and Gudkov AV. Rapamycin extends lifespan and delays tumorigenesis in heterozygous p53+/- mice. Aging (Albany NY). 2012; 4:709-714.

48. Klermund J, Bender K and Luke B. High nutrient levels and TORC1 activity reduce cell viability following prolonged telomere dysfunction and cell cycle arrest. Cell Rep. 2014; 9:324-335.

49. Leontieva OV and Blagosklonny MV. Gerosuppression in confluent cells. Aging (Albany NY). 2014; 6:1010-1018.

50. Leontieva OV, Demidenko ZN and Blagosklonny MV. Contact inhibition and high cell density deactivate the mammalian target of rapamycin pathway, thus suppressing the senescence program. Proceedings of the National Academy of Sciences of the United States of America. 2014; 111:8832-8837.

51. Qi H, Su FY, Wan S, Chen Y, Cheng YQ and Liu AJ. The antiaging activity and cerebral protection of rapamycin at micro-doses. CNS Neurosci Ther. 2014; 20:991-998.

52. Beier F, Balabanov S, Buckley T, Dietz K, Hartmann U, Rojewski M, Kanz L, Schrezenmeier H and Brummendorf TH. Accelerated telomere shortening in glycosylphosphatidylinositol (GPI)-negative compared with GPI-positive granulocytes from patients with paroxysmal nocturnal hemoglobinuria (PNH) detected by proaerolysin flow-FISH. Blood. 2005; 106:531-533.

53. Beier F, Masouleh BK, Buesche G, Ventura Ferreira MS, Schneider RK, Ziegler P, Wilop S, Vankann L, Gattermann N, Platzbecker U, Giagounidis A, Götze KS, Nolte F, et al. Telomere dynamics in patients with del (5q) MDS before and under treatment with lenalidomide. Leukemia Research. 2015.

54. Weidner CI, Lin Q, Koch CM, Eisele L, Beier F, Ziegler P, Bauerschlag DO, Jockel KH, Erbel R, Muhleisen TW, Zenke M, Brummendorf TH and Wagner W. Aging of blood can be tracked by DNA methylation changes at just three CpG sites. Genome Biol. 2014; 15:R24.

55. Stepensky P, Rensing-Ehl A, Gather R, Revel-Vilk S, Fischer U, Nabhani S, Beier F, Brummendorf TH, Fuchs S, Zenke S, Firat E, Pessach VM, Borkhardt A, et al. Early-onset Evans syndrome, immunodeficiency, and premature immunosenescence

associated with tripeptidyl-peptidase II deficiency. Blood. 2015; 125:753-761.

56. DePristo MA, Banks E, Poplin R, Garimella KV, Maguire JR, Hartl C, Philippakis AA, del Angel G, Rivas MA, Hanna M, McKenna A, Fennell TJ, Kernytsky AM, et al. A framework for variation discovery and genotyping using next-generation DNA sequencing data. Nature genetics. 2011; 43:491-498.

57. Li H, Handsaker B, Wysoker A, Fennell T, Ruan J, Homer N, Marth G, Abecasis G, Durbin R and Genome Project Data Processing S. The Sequence Alignment/Map format and SAMtools. Bioinformatics. 2009; 25:2078-2079.

58. Wang K, Li M and Hakonarson H. ANNOVAR: functional annotation of genetic variants from high-throughput sequencing data. Nucleic acids research. 2010; 38:e164.

59. Kumar P, Henikoff S and Ng PC. Predicting the effects of coding non-synonymous variants on protein function using the SIFT algorithm. Nature protocols. 2009; 4:1073-1081.

60. Venteicher AS, Meng Z, Mason PJ, Veenstra TD and Artandi SE. Identification of ATPases pontin and reptin as telomerase components essential for holoenzyme assembly. Cell. 2008; 132:945-957.

61. Fu D and Collins K. Distinct biogenesis pathways for human telomerase RNA and H/ACA small nucleolar RNAs. Molecular cell. 2003; 11(5):1361-1372.

62. Stockklausner C, Breit S, Neu-Yilik G, Echner N, Hentze MW, Kulozik AE and Gehring NH. The uORF-containing thrombopoietin mRNA escapes nonsense-mediated decay (NMD). Nucleic acids research. 2006; 34:2355-2363.

63. Debacq-Chainiaux F, Erusalimsky JD, Campisi J and Toussaint O. Protocols to detect senescence-associated beta-galactosidase (SA-betagal) activity, a biomarker of senescent cells in culture and in vivo. Nature protocols. 2009; 4:1798-1806.

64. Schneider CA, Rasband WS and Eliceiri KW. NIH Image to ImageJ: 25 years of image analysis. Nature methods. 2012; 9:671-675.

Research Perspective

Gerosuppression in confluent cells

Olga V. Leontieva and Mikhail V. Blagosklonny

Department of Cell Stress Biology, Roswell Park Cancer Institute, Elms and Carlson Streets, Buffalo, NY 14263, USA

Key words: *MTOR, rapalogs, sirolimus, aging, cancer, senescence*
Received: *11/18/14; Accepted: 12/27/14; Published: 12/31/14* doi:10.18632/aging.100714
Correspondence to: *Mikhail V. Blagosklonny MD/PhD* ***E-mail:*** *Mikhail.blagosklonny@roswellpark.org*

Abstract: The most physiological type of cell cycle arrest – namely, contact inhibition in dense culture - is the least densely studied. Despite cell cycle arrest, confluent cells do not become senescent. We recently described that mTOR (target of rapamycin) is inactive in contact-inhibited cells. Therefore, conversion from reversible arrest to senescence (geroconversion) is suppressed. I this Perspective, we further extended the gerosuppression model. While causing senescence in regular cell density, etoposide failed to cause senescence in contact-inhibited cells. A transient reactivation of mTOR favored geroconversion in etoposide-treated confluent cells. Like p21, p16 did not cause senescence in high cell density. We discuss that suppression of geroconversion in confluent and contact-inhibited cultures mimics gerosuppression in the organism. We confirmed that levels of p-S6 were low in murine tissues in the organism compared with mouse embryonic fibroblasts in cell culture, whereas p-Akt was reciprocally high in the organism.

Preface

When normal cells become confluent, they get arrested: a phenomenon known as contact inhibition [1-7]. Certainly, this is the most physiologically relevant type of cell cycle arrest. In the organism, cells are predominantly contact-inhibited. Yet, contact inhibition is the least studied type of cell cycle arrest. Instead, scientific attention has been attracted to two types of arrest: (a) starvation-induced arrest and (b) Cyclin Dependent Kinase-inhibitor (CDKi)-induced arrest.
As a classic example of starvation-induced arrest, serum withdrawal causes reversible quiescence in normal cells. During serum-starvation, mitogen-activated pathways become silent [8]. Cells neither grow in size nor cycle. Re-addition of serum causes cell activation and proliferation.

As an example of CDKi-induced arrest, DNA damage and telomere shortening induce p53, which in turn induces p21 and p16, inhibiting CDKs. In other cases, stresses induce both p21 and p16 [8-23]. When serum growth factors and nutrients stimulate growth, then inhibition of CDKs leads to senescence [8]. All stresses that induce senescence inhibit CDKs in part by inducing CDKi such as p21, p16, p15. Oncogenic Ras and Raf activate MAPK and mTOR pathways and induce p21 and p16, causing senescence [9, 24-27].

Numerous studies have been aimed to pinpoint the difference between quiescence and senescence based on either the point of arrest, the nature of stresses or peculiarities of CDKi (p21 versus p16). Yet, despite all efforts, the distinction remained elusive.

In fact, the difference between quiescence and senescence lies outside the cell cycle [8, 28, 29]. A senescent program consists of two steps: cell cycle arrest and gerogenic conversion or geroconversion, for brevity [29]. It is geroconversion that distinguishes quiescence from senescence. Geroconversion is "futile cellular growth" driven by mTOR as well as related mitogen-activated and growth-promoting signaling pathways [29-31]. Rapamycin suppresses gero-conversion, maintaining quiescence instead [32-38]. Furthermore, any condition that directly or indirectly inhibits mTOR in turn suppresses geroconversion [39-49]. Two-step model of senescence is applicable to all forms of senescence: from replicative and stress-induced to physiological cellular aging in the organism [29]. Senescent cells are hyper-active, hyper-functional

(for example, hyper-secretory phenotype or SASP) compensatory signal-resistant, secondary malfunctional and eventually atrophic [28, 36-38, 50-55]. Hyper-function and secondary malfunction lead to age-related diseases from cancer and atherosclerosis to diabetes and Alzheimer's disease [54, 56-73]. MTOR-driven gero-conversion activates stem cells, eventually leading to their exhaustion [34, 46, 74-82].

Rapamycin extends life span and prevents age-related diseases, including cancer in mice and humans [33, 57-73, 83-110].

The two-step model is applicable to contact inhibition. Given that contact inhibition is reversible, we predicted that mTOR is inhibited. In fact, we found that mTORC1 targets - S6K and S6 – are dephosphorylated in CI cells [41]. Furthermore, activation of mTOR (by depletion of TSC2) shifts reversible contact inhibition towards senescence [41]. Thus, it is deactivation of mTOR that suppresses geroconversion in contact inhibited cells. Deactivation of mTOR was associated with induction of p27. In cancer cells, there is no induction of p27 in high cell density. Accordingly, cancer cells do not get arrested in confluent cultures. There is a complex relationship between p27 and mTOR [111-113].

To cause arrest of cancer cells, we induced ectopic p21. Remarkably, p21-mediated arrest, which leads to senescence of HT-p21 cells in regular density, did not cause senescence in confluent cultures [41]. Why? It turned out that the mTOR pathway was inhibited in dense cultures of cancer cells. Yet, cancer cells do not induce p27 and do not undergo contact inhibition. mTOR is constitutively activated in cancer, [114-118]. And induction of p21 by itself does not inhibit mTOR. So why mTOR is deactivated not only in contact-inhibited but also in confluent cancer cells? The answer is that cancer cells with highly increased metabolism rapidly exhaust and acidify the medium, thus inhibiting mTOR by starvation-like mechanism [41]. In fact, change of the medium restored mTOR activity. Therefore, in normal cells with low metabolism, mTOR is deactivated by contact inhibition and the change of the medium only marginally affects mTOR. In cancer cells, mTOR is inhibited due to exhaustion of the medium. And some cell lines are somewhere in between.

Illustrations

In agreement with previous report, pS6 was barely detectable in contact inhibited cells (Fig. 1A). Inhibition of pS6 was associated with induction of p27. Treatment of contact-inhibited (CI) cells with etoposide did not affect either pS6 or p27. Change of the medium also did not affect pS6, as measured on second day after the change. Yet, the change of the medium transiently activated pS6 up to 6 hours (Fig. 1 B). This transient activation was not result in medium exhation, because CM by itseld did not inhibit pS6 in sparse culture [41]. Transient induction was in part due to hyper-sensitivity of CI-cells to slight signals.

We treated CI-culture and regular (exponentially growing) culture with etoposide for 3 days (Fig. 1C). In regular culture, WI-38 cells acquired a large flat morphology with beta-Gal staining. This senescent morphology was prevented by rapamycin (Fig. 1C). So etopiside caused mTOR-dependent senescence in regular culture conditions.

In CI-culture, cells were beta-Gal positive to start with. In fact, beta-Gal-staining is a marker of both contact inhibition, senescence and serum-starvation [119-130]. In contact-inhibition, beta-Gal staining, a marker of lysosomal overactivation, is mTOR-independent [41] and Figure 1 C. We next, employed two non-morphological tests to evaluate senescence: (a) cellular hypertrophy, measured as protein per cell and (b) the reversibility potential (RP) or the potential to restart proliferation and to regenerate cell culture after splitting in drug-free media. (Note: the reversibility also means that regenerated culture consists of cells identical to initial regular culture).

In regular culture, etoposide induced hypertrophy, which was prevented by rapamycin (Fig. 1D). In CI-culture, the cells were small and etoposide failed to cause any increase in cellular size. A small cell morphology is due to deactivated mTOR pathway in CI-culture. As expected, rapamycin did not decrease cell size further. Thus, etoposide caused mTOR-dependent hypertrophy only in regular but not in CI-culture.

The regenerative/reversibility potential can be tested after washing etoposide out. It is importantly that etoposide is easily washable [131].

In regular culture, etoposide dramatically eliminated the reversibility potential (RP), meaning that etoposide-treated cells did not proliferate after re- plating in low density in drug-free culture. This effect was in part mTOR dependent, because co-addition of rapamycin and etoposide caused a lesser loss of RP (Fig. 1E).

In CI-culture, etoposide did not cause loss of RP. Etoposide-pretreated cells resumed proliferation, similar to untreated cells. Noteworthy, when treatment with

rapamycin was combined with a daily-change of the medium, which caused transient mTOR activation in CI-culture, the cells indeed lost some RP (Fig. 1 E, low panel). This loss was m-TOR-dependent, reversed by rapamycin (Fig. 1E). Therefore, we confirmed that, due to deactivation mTOR, etoposide did not cause senescence in CI-cultures. Also, etoposide did not cause hypertrophy in CI-cultures of RPE cells, while causing hypertrophy in regular density RPE cells (Fig. 2A). Etoposide-pretreated CI- cells retained RP, capable to proliferate and regenerate culture after splitting in low cell density (Fig. 2B).

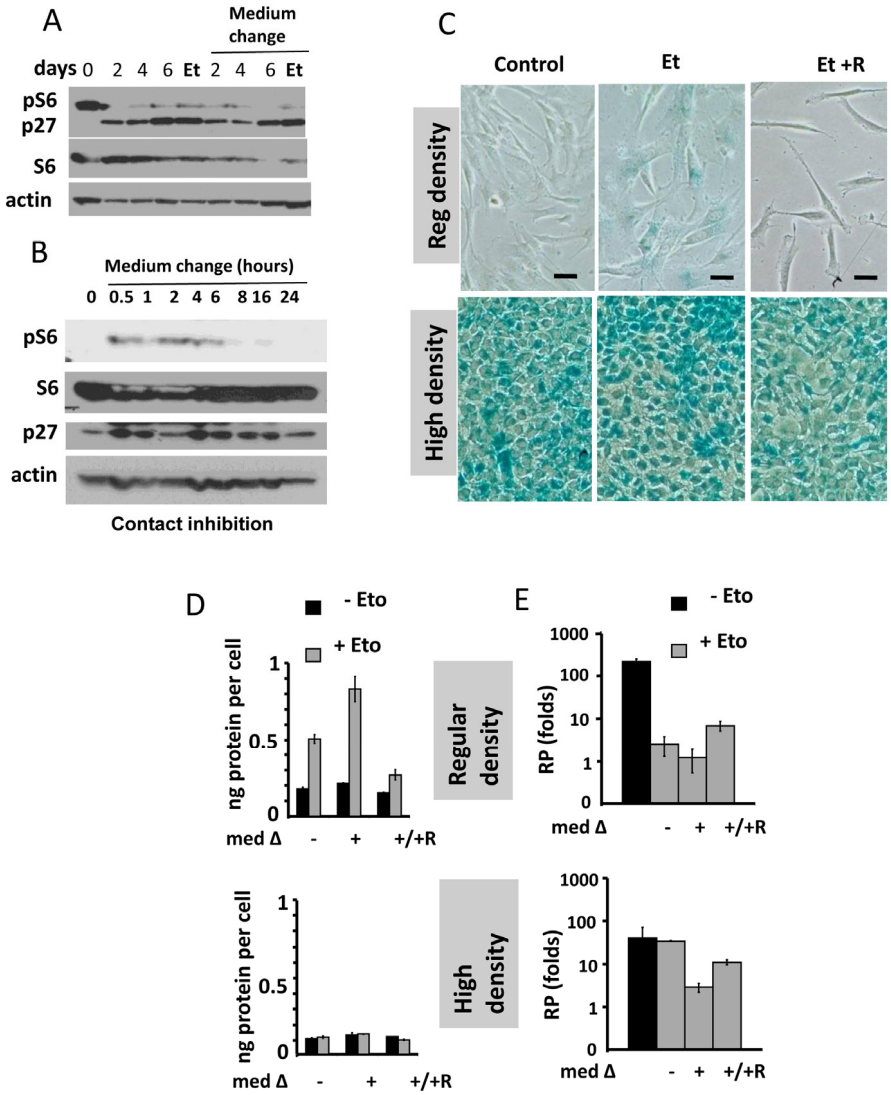

Figure 1. Contact inhibition suppresses etoposide-induced senescence in WI-38t cells. (A-B) Immunoblot analysis [41]. (A) WI-38t cells [41] were plated at high density and lysed on the days indicated. When indicated "Medium change", the medium was changed to fresh one every day. Et: cells were treated with 0.5 μg/ml etoposide on day 3 and lysed on day 6. p-S6(S240/244). (**B**) The effect of medium change on Contact Inhibited cells, measured in hours. (**C**) Beta-gal staining. WI38t cells were plated at regular or high density. After 3 days, 0.5 μg/ml etoposide (Et) and +/- 10 nM rapamycin (R) was added, if indicated. After 3 days, cells were stained for beta-Gal. Bar – 100 μm. (**D-E**) Cells were treated as described in panel C. Data are mean ± SD. (**D**) Cell size, protein per cell. (**E**) Reversibility potential or Replicative potential (RP). On day 6, cells were counted and re-plated at 1000/well in 12-well plates in fresh drug-free medium. Cells were counted after 9 days of growth. Fold increase in cell numbers were calculated. Mean ± SD.

Importantly, senescence could be induced in CI-cultures by wounding in the presence of rapamycin. At the edge of wounds, mTOR is reactivated [41]. When CI-monolayer was wounded, cells acquired senescent morphology in the presence of the same medium, containing etoposide (Fig. 2C). We emphasize that failure of etoposide to induce senescence in CI-cultures cannot be explained by cell cycle arrest in CI-cultures. It was extensively studied and shown that etoposide caused DNA damage in G1 phase of the cell cycle [132-134]. Furthermore its toxicity is high in non-cycling cells [132-134].

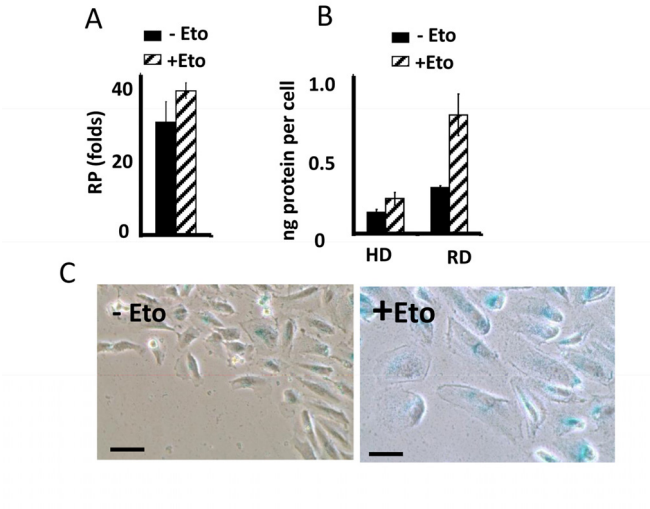

Figure 2. Suppression of etoposide-induced senescence in RPE cells. (**A**) Reversibility potential (RP) in RPE cells [41] treated with 0.5 μg/ml etoposide (+Eto) in high cell density. After 2 day-treatment with etoposide (total 6 days in culture), cells were counted and re-plated in fresh medium at 1000/well in 24-well plates. After 7 days, cells were re-counted. Fold increase in cell numbers mean ± SD. (**B**) Protein per cell in regular (RD) versus high cell density (HD). RPE cells were plated at regular or high density. If indicated, cells were treated with 0.5 μg/ml etoposide (+Eto). After 2 days, cells were counted and lysed, protein amount was determined and protein (ng) amounts per cell was calculated. Data are mean ± SD. (**C**) Wounding. RPE cells were plated at high density. 0.5 μg/ml etoposide (+Eto) was added, if indicated "+". Wounds were made in cell monolayer without changing the medium. After 3 days, cells were stained for beta-Gal.

Previously we showed that geroconversion is suppressed in p21-arrested cancer cells in very high density [41]. This gerosuppression was associated with deactivated mTOR in exhausted media, [41]. Here we confirmed this observation and extended it to p16-induced arrest (Fig. 3). This indicated that high density suppresses geroconversion regardless of whether p21 or p16 caused arrest.

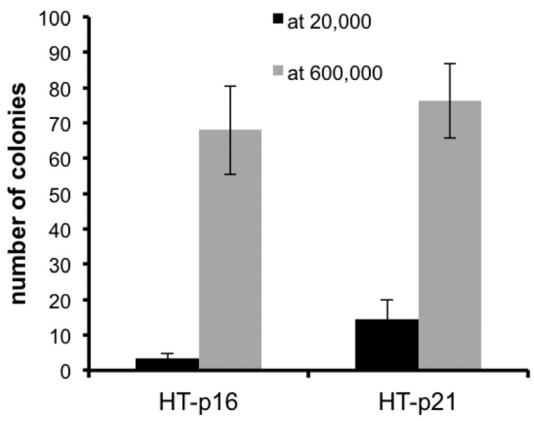

Figure 3. Effect of high density (HD) on p21- and p16-induced senescence. HT-p21 and HT-p16 cells (see [37]) were plated at 20,000 (low density) and 600,000 (high density) cells in 6 well plates and then treated with IPTG to induce p21 and p16. After 3 days, cells were trypsinized, counted and 1000 cells were re-plated in IPTG-free medium in 6 well plates. Colonies were stained and counted after 8 days.

Low basal activation of mTOR in vivo

In the organism, cells are predominantly contact inhibited. Our in vitro data predict that mTOR activity should be low in the organism compared with cells in vitro. We compared levels of p-S6 (a marker of mTOR activity) in the organs (the heart and the liver) with the levels in mouse embrionyc fibroblasts (MEF). Use of the same species (mouse) ensures that there is no species-dependent differences in detection of p-S6 by antibody. Due to extra-cell matrix in vivo, we loaded a lesser amount of MEF protein (5 microg) than tissue-extracted protein (30 microM). What was important is a ratio between pS6 and S6 and between p-Akt and Akt (Fig. 4). In the livers and the hearts, pS6/S6 ratios were lower (approximately 4-100 fold) compared to MEF.

In contrast, the ratio p-Akt/Akt was much higher in the tissues than in MEF in culture (Fig. 4).

Physiological and clinical applications

Contact inhibition suppresses geroconversion. In the organism, most cells are contact inhibited. Even proliferating cellular pools exist in a relatively high cell density, albeit they may occupy special niches. Also, near-anoxia suppresses mTOR, thus exerting gerosuppression during cell cycle arrest [40, 130, 135, 136]. Low glucose and amino-acid levels in the organism (compared with cell culture in vitro culture conditions [137]) are also gerosuppressive. Therefore,

normal cells senesce slowly in the organism. In vivo, physiological geroconversion may take decades, culminating in age-related diseases.

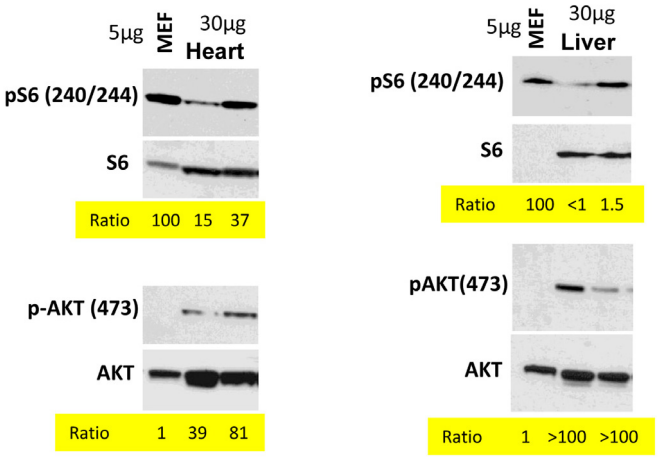

Figure 4. Comparison of p-S6(S240/244) and pAKT(S473) levels in murine heart and liver vs cultured MEFs. Immunoblot analysis. 5 µg protein MEF lysate and 30 µg protein mice tissue were separated on the same gel and blotted for pS6/S6 and pAKT(S473)/AKT. Signal intensities were quantified using ImageJ program and normalized levels of p-S6 and p-AKT in mice organs were estimated. Ratio in MEFs is 100 and 1 (indicated as numbers). Methods are described previously and corresponding tissues samples blots published [103, 138-140].

The gerosuppression model shed light on the treatment with DNA damaging agents. Despite DNA damage, if the organism survives, it does not become old. One of explanations is that contact inhibition is gero-suppressive. This further supports the notion that accumulation of DNA damage is not a cause of aging, which instead is driven by the mTOR pathway.

Also, the model is applicable to tumors. In tumors, necrotic regions coincide with exhaustion of the medium. Thus in large tumors (and any detectable tumors are already large), geroconversion is suppressed. This may explain lack of senescence by conventional drugs, which easily cause senescence in cell culture. Also, solitary cancer cells, trapped among contact-inhibited normal cells, such as epithelial cells are resistant to therapy-induced senescence [41]. This is a subject of our ongoing investigation.

Conflict of interest statement

The authors of this manuscript declare no conflict of interests.

REFERENCES

1. Abercrombie M. Contact inhibition and malignancy. Nature. 1979; 281: 259-262.

2. Polyak K, Kato JY, Solomon MJ, Sherr CJ, Massague J, Roberts JM, Koff A. p27Kip1, a cyclin-Cdk inhibitor, links transforming growth factor-beta and contact inhibition to cell cycle arrest. Genes Dev. 1994; 8: 9-22.

3. Dietrich C, Wallenfang K, Oesch F, Wieser R. Differences in the mechanisms of growth control in contact-inhibited and serum-deprived human fibroblasts. Oncogene. 1997; 15: 2743-2747.

4. Levenberg S, Yarden A, Kam Z, Geiger B. p27 is involved in N-cadherin-mediated contact inhibition of cell growth and S-phase entry. Oncogene. 1999; 18: 869-876.

5. Faust D, Dolado I, Cuadrado A, Oesch F, Weiss C, Nebreda AR, Dietrich C. p38alpha MAPK is required for contact inhibition. Oncogene. 2005; 24: 7941-7945.

6. Slisz M, Rothenberger E, Hutter D. Attenuation of p38 MAPK activity upon contact inhibition in fibroblasts. Mol Cell Biochem. 2008; 308: 65-73.

7. Seluanov A, Hine C, Azpurua J, Feigenson M, Bozzella M, Mao Z, Catania KC, Gorbunova V. Hypersensitivity to contact inhibition provides a clue to cancer resistance of naked mole-rat. Proc Natl Acad Sci U S A. 2009; 106: 19352-19357.

8. Blagosklonny MV. Cell senescence and hypermitogenic arrest. EMBO Rep. 2003; 4: 358-362.

9. Serrano M, Lim AW, McCurrach ME, Beach D, Lowe SW. Oncogenic ras provokes premature cell senescence associated with accumulation of p53 and p16INK1A. Cell. 1997; 88: 593-602.

10. McConnell BB, Starborg M, Brookes S, Peters G. Inhibitors of cyclin-dependent kinases induce features of replicative senescence in early passage human diploid fibroblasts. Curr Biol. 1998; 8: 351-354.

11. Serrano M, Blasco MA. Putting the stress on senescence. Curr Opin Cell Biol. 2001; 13: 748-753.

12. Chen QM, Prowse KR, Tu VC, Purdom S, Linskens MH. Uncoupling the senescent phenotype from telomere shortening in hydrogen peroxide-treated fibroblasts. Exp Cell Res. 2001; 265: 294-303.

13. Campisi J, Kim SH, Lim CS, Rubio M. Cellular senescence, cancer and aging: the telomere connection. Exp Gerontol. 2001; 36: 1619-1637.

14. Itahana K, Zou Y, Itahana Y, Martinez JL, Beausejour C, Jacobs JJ, Van Lohuizen M, Band V, Campisi J, Dimri GP. Control of the replicative life span of human fibroblasts by p16 and the polycomb protein Bmi-1. Mol Cell Biol. 2003; 23: 389-401.

15. Parrinello S, Samper E, Krtolica A, Goldstein J, Melov S, Campisi J. Oxygen sensitivity severely limits the replicative lifespan of murine fibroblasts. Nat Cell Biol. 2003; 5: 741-747.

16. Itahana K, Campisi J, Dimri GP. Mechanisms of cellular senescence in human and mouse cells. Biogerontology. 2004; 5: 1-10.

17. Satyanarayana A, Greenberg RA, Schaetzlein S, Buer J, Masutomi K, Hahn WC, Zimmermann S, Martens U, Manns MP, Rudolph KL. Mitogen stimulation cooperates with telomere shortening to activate DNA damage responses and senescence signaling. Mol Cell Biol. 2004; 24: 5459-5474.

18. Jacobs JJ, de Lange T. p16INK4a as a second effector of the telomere damage pathway. Cell Cycle. 2005; 4: 1364-1368.

19. Jeyapalan JC, Sedivy JM. How to measure RNA expression in rare senescent cells expressing any specific protein such as p16Ink4a. Aging (Albany NY). 2013; 5: 120-129.

20. Salama R, Sadaie M, Hoare M, Narita M. Cellular senescence and its effector programs. Genes Dev. 2014; 28: 99-114.

21. Georgakopoulou EA, Tsimaratou K, Evangelou K, Fernandez Marcos PJ, Zoumpourlis V, Trougakos IP, Kletsas D, Bartek J, Serrano M, Gorgoulis VG. Specific lipofuscin staining as a novel biomarker to detect replicative and stress-induced senescence. A method applicable in cryo-preserved and archival tissues. Aging (Albany NY). 2013; 5: 37-50.

22. Burd CE, Sorrentino JA, Clark KS, Darr DB, Krishnamurthy J, Deal AM, Bardeesy N, Castrillon DH, Beach DH, Sharpless NE. Monitoring tumorigenesis and senescence in vivo with a p16(INK4a)-luciferase model. Cell. 2013; 152: 340-351.

23. Leontieva OV, Blagosklonny MV. CDK4/6-inhibiting drug substitutes for p21 and p16 in senescence: duration of cell cycle arrest and MTOR activity determine geroconversion. Cell Cycle. 2013; 12: 3063-3069.

24. Zhu JY, Woods D, McMahon M, Bishop JM. Senescence of human fibroblasts induced by oncogenic Raf. Genes Dev. 1998; 12: 2997-3007.

25. Lin AW, Barradas M, Stone JC, van Aelst L, Serrano M, Lowe SW. Premature senescence involving p53 and p16 is activated in response to constitutive MEK/MAPK mitogenic signaling. Genes Dev. 1998; 12: 3008-3019.

26. Benanti JA, Galloway DA. The normal response to RAS: senescence or transformation? Cell Cycle. 2004; 3: 715-717.

27. Malumbres M, De Castro IP, Hernandez MI, Jimenez M, Corral T, Pellicer A. Cellular response to oncogenic Ras involves induction of the Cdk4 and Cdk6 inhibitor p15(INK4b). Mol Cell Biol. 2000; 20: 2915-2925.

28. Blagosklonny MV. Cell cycle arrest is not yet senescence, which is not just cell cycle arrest: terminology for TOR-driven aging. Aging (Albany NY). 2012; 4: 159-165.

29. Blagosklonny MV. Geroconversion: irreversible step to cellular senescence. Cell Cycle. 2014: in press.

30. Demidenko ZN, Blagosklonny MV. Growth stimulation leads to cellular senescence when the cell cycle is blocked. Cell Cycle. 2008; 7: 3355-3361.

31. Cho S, Hwang ES. Status of mTOR activity may phenotypically differentiate senescence and quiescence. Mol Cells. 2012; 33: 597-604.

32. Demidenko ZN, Zubova SG, Bukreeva EI, Pospelov VA, Pospelova TV, Blagosklonny MV. Rapamycin decelerates cellular senescence. Cell Cycle. 2009; 8: 1888-1895.

33. Chen C, Liu Y, Zheng P. mTOR regulation and therapeutic rejuvenation of aging hematopoietic stem cells. Sci Signal. 2009; 2: ra75.

34. Luo Y, Li L, Zou P, Wang J, Shao L, Zhou D, Liu L. Rapamycin enhances long-term hematopoietic reconstitution of ex vivo expanded mouse hematopoietic stem cells by inhibiting senescence. Transplantation. 2014; 97: 20-29.

35. Mercier I, Camacho J, Titchen K, Gonzales DM, Quann K, Bryant KG, Molchansky A, Milliman JN, Whitaker-Menezes D, Sotgia F, Jasmin JF, Schwarting R, Pestell RG, Blagosklonny MV, Lisanti MP. Caveolin-1 and accelerated host aging in the breast tumor microenvironment: chemoprevention with rapamycin, an mTOR inhibitor and anti-aging drug. Am J Pathol. 2012; 181: 278-293.

36. Pospelova TV, Leontieva OV, Bykova TV, Zubova SG, Pospelov VA, Blagosklonny MV. Suppression of replicative senescence by rapamycin in rodent embryonic cells. Cell Cycle. 2012; 11: 2402-2407.

37. Leontieva OV, Lenzo F, Demidenko ZN, Blagosklonny MV. Hyper-mitogenic drive coexists with mitotic incompetence in senescent cells. Cell Cycle. 2012; 11: 4642 - 4649.

38. Leontieva OV, Demidenko ZN, Blagosklonny MV. MEK drives cyclin D1 hyperelevation during geroconversion. Cell Deth Diff. 2013; 20: 1241-1249.

39. Demidenko ZN, Korotchkina LG, Gudkov AV, Blagosklonny MV. Paradoxical suppression of cellular senescence by p53. Proc Natl Acad Sci U S A. 2010; 107: 9660-9664.

40. Leontieva OV, Natarajan V, Demidenko ZN, Burdelya LG, Gudkov AV, Blagosklonny MV. Hypoxia suppresses conversion from proliferative arrest to cellular senescence. Proc Natl Acad Sci U S A. 2012; 109: 13314-13318.

41. Leontieva OV, Demidenko ZN, Blagosklonny MV. Contact inhibition and high cell density deactivate the mammalian target of rapamycin pathway, thus suppressing the senescence program. Proc Natl Acad Sci U S A. 2014; 111: 8832-8837.

42. Zhao H, Halicka HD, Li J, Darzynkiewicz Z. Berberine suppresses gero-conversion from cell cycle arrest to senescence. Aging (Albany NY). 2013; 5: 623-636.

43. Dulic V. Senescence regulation by mTOR. Methods Mol Biol. 2013; 965: 15-35.

44. Iglesias-Bartolome R, Patel V, Cotrim A, Leelahavanichkul K, Molinolo AA, Mitchell JB, Gutkind JS. mTOR inhibition prevents epithelial stem cell senescence and protects from radiation-induced mucositis. Cell Stem Cell. 2012; 11: 401-414.

45. Halicka HD, Zhao H, Li J, Lee YS, Hsieh TC, Wu JM, Darzynkiewicz Z. Potential anti-aging agents suppress the level of constitutive mTOR- and DNA damage- signaling. Aging (Albany NY). 2012; 4: 952-965.

46. Menendez JA, Vellon L, Oliveras-Ferraros C, Cufi S, Vazquez-Martin A. mTOR-regulated senescence and autophagy during reprogramming of somatic cells to pluripotency: a roadmap from energy metabolism to stem cell renewal and aging. Cell Cycle. 2011; 10: 3658-3677.

47. CoppŽ JP, Patil CK, Rodier F, Sun Y, Mu–oz DP, Goldstein J, Nelson PS, Desprez PY, Campisi J. Senescence-associated secretory phenotypes reveal cell-nonautonomous functions of oncogenic RAS and the p53 tumor suppressor. PLoS Biol. 2008; 6: 2853-2868.

48. Serrano M. Dissecting the role of mTOR complexes in cellular senescence. Cell Cycle. 2012; 11: 2231-2232.

49. Loayza-Puch F, Drost J, Rooijers K, Lopes R, Elkon R, Agami R. p53 induces transcriptional and translational programs to suppress cell proliferation and growth. Genome Biol. 2013; 14: R32.

50. Rodier F, Coppe JP, Patil CK, Hoeijmakers WA, Munoz DP, Raza SR, Freund A, Campeau E, Davalos AR, Campisi J. Persistent DNA damage signalling triggers senescence-associated inflammatory cytokine secretion. Nat Cell Biol. 2009; 11: 973-979.

51. Hubackova S, Krejcikova K, Bartek J, Hodny Z. IL1- and TGFbeta-Nox4 signaling, oxidative stress and DNA damage response are shared features of replicative, oncogene-induced, and drug-induced paracrine 'bystander senescence'. Aging (Albany NY). 2012; 4: 932-951.

52. Ohanna M, Cheli Y, Bonet C, Bonazzi VF, Allegra M, Giuliano S, Bille K, Bahadoran P, Giacchero D, Lacour JP, Boyle GM,

Hayward NF, Bertolotto C, Ballotti R. Secretome from senescent melanoma engages the STAT3 pathway to favor reprogramming of naive melanoma towards a tumor-initiating cell phenotype. Oncotarget. 2013; 4: 2212-2224.

53. Berman AE, Leontieva OV, Natarajan V, McCubrey JA, Demidenko ZN, Nikiforov MA. Recent progress in genetics of aging, senescence and longevity: focusing on cancer-related genes. Oncotarget. 2012; 3: 1522-1532.

54. Blagosklonny MV. Answering the ultimate question "what is the proximal cause of aging?" Aging (Albany NY). 2012; 4: 861-877.

55. Vizioli MG, Santos J, Pilotti S, Mazzoni M, Anania MC, Miranda C, Pagliardini S, Pierotti MA, Gil J, Greco A. Oncogenic RAS-induced senescence in human primary thyrocytes: molecular effectors and inflammatory secretome involved. Oncotarget. 2014; 5: 8270-8283.

56. Blagosklonny MV. Validation of anti-aging drugs by treating age-related diseases. Aging (Albany NY). 2009; 1: 281-288.

57. Blagosklonny MV. Prospective treatment of age-related diseases by slowing down aging. Am J Pathol. 2012; 181: 1142-1146.

58. Blagosklonny MV. Once again on rapamycin-induced insulin resistance and longevity: despite of or owing to. Aging (Albany NY). 2012; 4: 350-358.

59. Blagosklonny MV. How to save Medicare: the anti-aging remedy. Aging (Albany NY). 2012; 4: 547-552.

60. Blagosklonny MV. Rapalogs in cancer prevention: Anti-aging or anticancer? Cancer Biol Ther. 2012; 13: 1349-1354.

61. Blagosklonny MV. TOR-centric view on insulin resistance and diabetic complications: perspective for endocrinologists and gerontologists. Cell Death Dis. 2013; 4: e964.

62. Blagosklonny MV. MTOR-driven quasi-programmed aging as a disposable soma theory: blind watchmaker vs. intelligent designer. Cell Cycle. 2013; 12: 1842-1847.

63. Blagosklonny MV. M(o)TOR of aging: MTOR as a universal molecular hypothalamus. Aging (Albany NY). 2013; 5: 490-494.

64. Wilkinson JE, Burmeister L, Brooks SV, Chan CC, Friedline S, Harrison DE, Hejtmancik JF, Nadon N, Strong R, Wood LK, Woodward MA, Miller RA. Rapamycin slows aging in mice. Aging Cell. 2012; 11: 675-682.

65. Gems DH, de la Guardia YI. Alternative Perspectives on Aging in C. elegans: Reactive Oxygen Species or Hyperfunction? Antioxid Redox Signal. 2013; 19: 321-329.

66. Cai D, Liu T. Inflammatory cause of metabolic syndrome via brain stress and NF-kappaB. Aging (Albany NY). 2012; 4: 98-115.

67. Kennedy BK, Pennypacker JK. Drugs that modulate aging: the promising yet difficult path ahead. Transl Res. 2014;163:456-465

68. Kaeberlein M. mTOR Inhibition: From Aging to Autism and Beyond. Scientifica (Cairo). 2013; 2013: 849186.

69. Kaeberlein M. Longevity and aging. F1000Prime Rep. 2013; 5: 5.

70. Johnson SC, Yanos ME, Kayser EB, Quintana A, Sangesland M, Castanza A, Uhde L, Hui J, Wall VZ, Gagnidze A, Oh K, Wasko BM, Ramos FJ, Palmiter RD, Rabinovitch PS, Morgan PG et al. mTOR inhibition alleviates mitochondrial disease in a mouse model of Leigh syndrome. Science. 2013; 342: 1524-1528.

71. Johnson SC, Rabinovitch PS, Kaeberlein M. mTOR is a key modulator of ageing and age-related disease. Nature. 2013; 493: 338-345.

72. Cornu M, Albert V, Hall MN. mTOR in aging, metabolism, and cancer. Curr Opin Genet Dev. 2013; 23: 53-62.

73. Kolosova NG, Muraleva NA, Zhdankina AA, Stefanova NA, Fursova AZ, Blagosklonny MV. Prevention of age-related macular degeneration-like retinopathy by rapamycin in rats. Am J Pathol. 2012; 181: 472-477.

74. Blagosklonny MV. Aging, stem cells, and mammalian target of rapamycin: a prospect of pharmacologic rejuvenation of aging stem cells. Rejuvenation Res. 2008; 11: 801-808.

75. Castilho RM, Squarize CH, Chodosh LA, Williams BO, Gutkind JS. mTOR mediates Wnt-induced epidermal stem cell exhaustion and aging. Cell Stem Cell. 2009; 5: 279-289.

76. Gan B, DePinho RA. mTORC1 signaling governs hematopoietic stem cell quiescence. Cell Cycle. 2009; 8: 1003-1006.

77. Hinojosa CA, Mgbemena V, Van Roekel S, Austad SN, Miller RA, Bose S, Orihuela CJ. Enteric-delivered rapamycin enhances resistance of aged mice to pneumococcal pneumonia through reduced cellular senescence. Exp Gerontol. 2012; 47: 958-965.

78. Sousa-Victor P, Gutarra S, Garcia-Prat L, Rodriguez-Ubreva J, Ortet L, Ruiz-Bonilla V, Jardi M, Ballestar E, Gonzalez S, Serrano AL, Perdiguero E, Munoz-Canoves P. Geriatric muscle stem cells switch reversible quiescence into senescence. Nature. 2014; 506: 316-321.

79. Iglesias-Bartolome R, Gutkind SJ. Exploiting the mTOR paradox for disease prevention. Oncotarget. 2012; 3: 1061-1063.

80. Blagosklonny MV. Why men age faster but reproduce longer than women: mTOR and evolutionary perspectives. Aging (Albany NY). 2010; 2: 265-273.

81. Zhang XM, Li L, Xu JJ, Wang N, Liu WJ, Lin XH, Fu YC, Luo LL. Rapamycin preserves the follicle pool reserve and prolongs the ovarian lifespan of female rats via modulating mTOR activation and sirtuin expression. Gene. 2013; 523: 82-87.

82. Adhikari D, Zheng W, Shen Y, Gorre N, Hamalainen T, Cooney AJ, Huhtaniemi I, Lan ZJ, Liu K. Tsc/mTORC1 signaling in oocytes governs the quiescence and activation of primordial follicles. Hum Mol Genet. 2010; 19: 397-410.

83. Harrison DE, Strong R, Sharp ZD, Nelson JF, Astle CM, Flurkey K, Nadon NL, Wilkinson JE, Frenkel K, Carter CS, Pahor M, Javors MA, Fernandezr E, Miller RA. Rapamycin fed late in life extends lifespan in genetically heterogenous mice. Nature. 2009; 460: 392-396.

84. Miller RA, Harrison DE, Astle CM, Baur JA, Boyd AR, de Cabo R, Fernandez E, Flurkey K, Javors MA, Nelson JF, Orihuela CJ, Pletcher S, Sharp ZD, Sinclair D, Starnes JW, Wilkinson JE et al. Rapamycin, but not resveratrol or simvastatin, extends life span of genetically heterogeneous mice. J Gerontol A Biol Sci Med Sci. 2011; 66: 191-201.

85. Anisimov VN, Zabezhinski MA, Popovich IG, Piskunova TS, Semenchenko AV, Tyndyk ML, Yurova MN, Antoch MP, Blagosklonny MV. Rapamycin extends maximal lifespan in cancer-prone mice. Am J Pathol. 2010; 176: 2092-2097.

86. Anisimov VN, Zabezhinski MA, Popovich IG, Piskunova TS, Semenchenko AV, Tyndyk ML, Yurova MN, Rosenfeld SV, Blagosklonny MV. Rapamycin increases lifespan and inhibits spontaneous tumorigenesis in inbred female mice. Cell Cycle. 2011; 10: 4230-4236.

87. Ramos FJ, Chen SC, Garelick MG, Dai DF, Liao CY, Schreiber KH, MacKay VL, An EH, Strong R, Ladiges WC, Rabinovitch PS, Kaeberlein M, Kennedy BK. Rapamycin reverses elevated mTORC1 signaling in lamin A/C-deficient mice, rescues cardiac and skeletal muscle function, and extends survival. Sci Transl Med. 2012; 4: 144ra103.

88. Comas M, Toshkov I, Kuropatwinski KK, Chernova OB, Polinsky A, Blagosklonny MV, Gudkov AV, Antoch MP. New nanoformulation of rapamycin Rapatar extends lifespan in homozygous p53-/- mice by delaying carcinogenesis. Aging (Albany NY). 2012; 4: 715-722.

89. Komarova EA, Antoch MP, Novototskaya LR, Chernova OB, Paszkiewicz G, Leontieva OV, Blagosklonny MV, Gudkov AV. Rapamycin extends lifespan and delays tumorigenesis in heterozygous p53+/- mice. Aging (Albany NY). 2012; 4: 709-714.

90. Donehower LA. Rapamycin as longevity enhancer and cancer preventative agent in the context of p53 deficiency. Aging (Albany NY). 2012; 4: 660-661.

91. Danilov A, Shaposhnikov M, Plyusnina E, Kogan V, Fedichev P, Moskalev A. Selective anticancer agents suppress aging in Drosophila. Oncotarget. 2013; 4: 1507-1526.

92. Livi CB, Hardman RL, Christy BA, Dodds SG, Jones D, Williams C, Strong R, Bokov A, Javors MA, Ikeno Y, Hubbard G, Hasty P, Sharp ZD. Rapamycin extends life span of Rb1+/- mice by inhibiting neuroendocrine tumors. Aging (Albany NY). 2013; 5: 100-110.

93. Zhang Y, Bokov A, Gelfond J, Soto V, Ikeno Y, Hubbard G, Diaz V, Sloane L, Maslin K, Treaster S, Rendon S, van Remmen H, Ward W, Javors M, Richardson A, Austad SN et al. Rapamycin extends life and health in C57BL/6 mice. J Gerontol A Biol Sci Med Sci. 2014; 69: 119-130.

94. Neff F, Flores-Dominguez D, Ryan DP, Horsch M, Schroder S, Adler T, Afonso LC, Aguilar-Pimentel JA, Becker L, Garrett L, Hans W, Hettich MM, Holtmeier R, Holter SM, Moreth K, Prehn C et al. Rapamycin extends murine lifespan but has limited effects on aging. J Clin Invest. 2013; 123: 3272-3291.

95. Miller RA, Harrison DE, Astle CM, Fernandez E, Flurkey K, Han M, Javors MA, Li X, Nadon NL, Nelson JF, Pletcher S, Salmon AB, Sharp ZD, Van Roekel S, Winkleman L, Strong R. Rapamycin-Mediated Lifespan Increase in Mice is Dose and Sex-Dependent and Appears Metabolically Distinct from Dietary Restriction. Aging Cell. 2014; 13:468-477

96. Ye L, Widlund AL, Sims CA, Lamming DW, Guan Y, Davis JG, Sabatini DM, Harrison DE, Vang O, Baur JA. Rapamycin doses sufficient to extend lifespan do not compromise muscle mitochondrial content or endurance. Aging (Albany NY). 2013; 5: 539-550.

97. Fok WC, Chen Y, Bokov A, Zhang Y, Salmon AB, Diaz V, Javors M, Wood WH, 3rd, Becker KG, Perez VI, Richardson A. Mice fed rapamycin have an increase in lifespan associated with major changes in the liver transcriptome. PLoS One. 2013; 9: e83988.

98. Hasty P, Livi CB, Dodds SG, Jones D, Strong R, Javors M, Fischer KE, Sloane L, Murthy K, Hubbard G, Sun L, Hurez V, Curiel TJ, Sharp ZD. eRapa Restores a Normal Life Span in a FAP Mouse Model. Cancer Prev Res (Phila). 2014; 7: 169-178.

99. Fang Y, Bartke A. Prolonged rapamycin treatment led to beneficial metabolic switch. Aging (Albany NY). 2013; 5: 328-329.

100. Luo LL, Xu JJ, Fu YC. Rapamycin prolongs female reproductive lifespan. Cell Cycle. 2013; 12: 3353-3354.

101. Spong A, Bartke A. Rapamycin slows aging in mice. Cell Cycle. 2012; 11: 845.

102. Selman C, Partridge L. A double whammy for aging? Rapamycin extends lifespan and inhibits cancer in inbred female mice. Cell Cycle. 2012; 11: 17-18.

103. Leontieva OV, Paszkiewicz GM, Blagosklonny MV. Weekly administration of rapamycin improves survival and biomarkers in obese male mice on high-fat diet. Aging Cell. 2014; 13: 616-622.

104. Khapre RV, Kondratova AA, Patel S, Dubrovsky Y, Wrobel M, Antoch MP, Kondratov RV. BMAL1-dependent regulation of the mTOR signaling pathway delays aging. Aging (Albany NY). 2014; 6: 48-57.

105. Kondratov RV, Kondratova AA. Rapamycin in preventive (very low) doses. Aging (Albany NY). 2014; 6: 158-159.

106. Popovich IG, Anisimov VN, Zabezhinski MA, Semenchenko AV, Tyndyk ML, Yurova MN, Blagosklonny MV. Lifespan extension and cancer prevention in HER-2/neu transgenic mice treated with low intermittent doses of rapamycin. Cancer Biol Ther. 2014; 15: 586-592.

107. Mabuchi S, Altomare DA, Connolly DC, Klein-Szanto A, Litwin S, Hoelzle MK, Hensley HH, Hamilton TC, Testa JR. RAD001 (Everolimus) delays tumor onset and progression in a transgenic mouse model of ovarian cancer. Cancer Res. 2007; 67: 2408-2413.

108. Levine AJ, Harris CR, Puzio-Kuter AM. The interfaces between signal transduction pathways: IGF-1/mTor, p53 and the Parkinson Disease pathway. Oncotarget. 2012; 3: 1301-1307.

109. Law BK. Rapamycin: an anti-cancer immunosuppressant? Crit Rev Oncol Hematol. 2005; 56: 47-60.

110. Campistol JM, Eris J, Oberbauer R, Friend P, Hutchison B, Morales JM, Claesson K, Stallone G, Russ G, Rostaing L, Kreis H, Burke JT, Brault Y, Scarola JA, Neylan JF. Sirolimus Therapy after Early Cyclosporine Withdrawal Reduces the Risk for Cancer in Adult Renal Transplantation. J Am Soc Nephrol. 2006; 17: 581-589.

111. Nakayama K, Ishida N, Shirane M, Inomata A, Inoue T, Shishido N, Horii I, Loh DY. Mice lacking p27(Kip1) display increased body size, multiple organ hyperplasia, retinal dysplasia, and pituitary tumors. Cell. 1996; 85: 707-720.

112. Roque M, Reis ED, Cordon-Cardo C, Taubman MB, Fallon JT, Fuster V, Badimon JJ. Effect of p27 deficiency and rapamycin on intimal hyperplasia: in vivo and in vitro studies using a p27 knockout mouse model. Lab Invest. 2001; 81: 895-903.

113. Diersch S, Wenzel P, Szameitat M, Eser P, Paul MC, Seidler B, Eser S, Messer M, Reichert M, Pagel P, Esposito I, Schmid RM, Saur D, Schneider G. Efemp1 and p27(Kip1) modulate responsiveness of pancreatic cancer cells towards a dual PI3K/mTOR inhibitor in preclinical models. Oncotarget. 2013; 4: 277-288.

114. Blagosklonny MV. Molecular damage in cancer: an argument for mTOR-driven aging. Aging (Albany NY). 2011; 3: 1130-1141.

115. Francipane MG, Lagasse E. Selective targeting of human colon cancer stem-like cells by the mTOR inhibitor Torin-1. Oncotarget. 2013; 4: 1948-1962.

116. Cornu M, Albert V, Hall MN. mTOR in aging, metabolism, and cancer. Curr Opin Genet Dev. 2013; 23: 53-62

117. McCubrey JA, Steelman LS, Chappell WH, Abrams SL, Montalto G, Cervello M, Nicoletti F, Fagone P, Malaponte G, Mazzarino MC, Candido S, Libra M, Basecke J, Mijatovic S, Maksimovic-Ivanic D, Milella M et al. Mutations and deregulation of Ras/Raf/MEK/ERK and PI3K/PTEN/Akt/mTOR cascades which alter therapy response. Oncotarget. 2012; 3: 954-987.

118. Dann SG, Selvaraj A, Thomas G. mTOR Complex1-S6K1 signaling: at the crossroads of obesity, diabetes and cancer. Trends Mol Med. 2007; 13: 252-259.

119. Knecht E, Hernandez-Yago J, Grisolia S. Regulation of lysosomal autophagy in transformed and non-transformed

mouse fibroblasts under several growth conditions. Exp Cell Res. 1984; 154: 224-232.

120. Severino J, Allen RG, Balin S, Balin A, Cristofalo VJ. Is beta-galactosidase staining a marker of senescence in vitro and in vivo? Exp Cell Res. 2000; 257: 162-171.

121. Kurz DJ, Decary S, Hong Y, Erusalimsky JD. Senescence-associated (beta)-galactosidase reflects an increase in lysosomal mass during replicative ageing of human endothelial cells. J Cell Sci. 2000; 113 (Pt 20): 3613-3622.

122. Yang NC, Hu ML. The limitations and validities of senescence associated-beta-galactosidase activity as an aging marker for human foreskin fibroblast Hs68 cells. Exp Gerontol. 2005; 40: 813-819.

123. Gary RK, Kindell SM. Quantitative assay of senescence-associated beta-galactosidase activity in mammalian cell extracts. Anal Biochem. 2005; 343: 329-334.

124. Coates PJ. Markers of senescence? J Pathol. 2002; 196: 371-373.

125. Krishna DR, Sperker B, Fritz P, Klotz U. Does pH 6 beta-galactosidase activity indicate cell senescence? Mech Ageing Dev. 1999; 109: 113-123.

126. Yegorov YE, Akimov SS, Hass R, Zelenin AV, Prudovsky IA. Endogenous beta-galactosidase activity in continuously nonproliferating cells. Exp Cell Res. 1998; 243: 207-211.

127. Papadopoulos T, Pfeifer U. Protein turnover and cellular autophagy in growing and growth-inhibited 3T3 cells. Exp Cell Res. 1987; 171: 110-121.

128. Lee BY, Han JA, Im JS, Morrone A, Johung K, Goodwin EC, Kleijer WJ, DiMaio D, Hwang ES. Senescence-associated beta-galactosidase is lysosomal beta-galactosidase. Aging Cell. 2006; 5: 187-195.

129. Dimri GP, Lee X, Basile G, Acosta M, Scott G, Roskelley C, Medrano EE, Linskens M, Rubelj I, Pereira-Smith O, et al. A biomarker that identifies senescent human cells in culture and in aging skin in vivo. Proc Natl Acad Sci U S A. 1995; 92: 9363-9367.

130. Blagosklonny MV. Hypoxia, MTOR and autophagy: converging on senescence or quiescence. Autophagy. 2013; 9: 260-262.

131. Soubeyrand S, Pope L, Hache RJ. Topoisomerase IIalpha-dependent induction of a persistent DNA damage response in response to transient etoposide exposure. Mol Oncol. 2010; 4: 38-51.

132. Wang L, Roy SK, Eastmond DA. Differential cell cycle-specificity for chromosomal damage induced by merbarone and etoposide in V79 cells. Mutat Res. 2007; 616: 70-82.

133. Tanaka T, Halicka HD, Traganos F, Seiter K, Darzynkiewicz Z. Induction of ATM activation, histone H2AX phosphorylation and apoptosis by etoposide: relation to cell cycle phase. Cell Cycle. 2007; 6: 371-376.

134. Robison JG, Dixon K, Bissler JJ. Cell cycle-and proteasome-dependent formation of etoposide-induced replication protein A (RPA) or Mre11/Rad50/Nbs1 (MRN) complex repair foci. Cell Cycle. 2007; 6: 2399-2407.

135. Leontieva OV, Blagosklonny MV. Hypoxia and gerosuppression: the mTOR saga continues. Cell Cycle. 2012; 11: 3926-3931.

136. Demaria M, Campisi J. Matters of life and breath: A role for hypoxia in determining cell state. Aging (Albany NY). 2012; 4: 523-524.

137. Leontieva OV, Demidenko ZN, Blagosklonny MV. Rapamycin reverses insulin resistance (IR) in high-glucose medium without causing IR in normoglycemic medium. Cell Death Dis. 2014; 5: e1214.

138. Leontieva OV, Geraldine M. Paszkiewicz GM, Blagosklonny MV. Mechanistic or mammalian target of rapamycin (mTOR) may determine robustness in young male mice at the cost of accelerated aging. Aging (Albany NY). 2012; 4: 899-916.

139. Leontieva OV, Paszkiewicz GM, Blagosklonny MV. Fasting levels of hepatic p-S6 are increased in old mice. Cell Cycle. 2014; 13: 2656-2659.

140. Leontieva OV, Paszkiewicz GM, Blagosklonny MV. Comparison of rapamycin schedules in mice on high-fat diet. Cell Cycle. 2014; 13: 3350-3356.

Research Paper

Berberine suppresses gero-conversion from cell cycle arrest to senescence

Hong Zhao, H Dorota Halicka, Jiangwei Li, and Zbigniew Darzynkiewicz

Brander Cancer Research Institute and Department of Pathology, New York Medical College, Valhalla, NY 10595, USA

Key words: *Berberine, Cellular senescence, H2AX phosphorylation, ROS, ribosomal protein S6, calorie restriction, metformin, rapamycin, 2-deoxyglucose, replication stress, cell cycle*
Received: *7/31/13; Accepted: 8/20/13; Published: 8/21/13* doi:10.18632/aging.100593
Correspondence to: *Zbigniew Darzynkiewicz, MD/PhD;* ***E-mail:*** *darzynk@nymc.edu*

Abstract: Berberine (BRB), a natural alkaloid, has a long history of medicinal use in both Ayurvedic and old Chinese medicine. Recently, available as a dietary supplement, Berberine is reported to have application in treatment of variety diseases. Previously we observed that BRB inhibited mTOR/S6 signaling concurrently with reduction of the level of endogenous oxidants and constitutive DNA damage response. We currently tested whether Berberine can affect premature, stress-induced cellular senescence caused by mitoxantrone. The depth of senescence was quantitatively measured by morphometric parameters, senescence-associated β-galactosidase, induction of $p21^{WAF1}$, replication stress (γH2AX expression), and mTOR signaling; the latter revealed by ribosomal S6 protein (rpS6) phosphorylation. All these markers of senescence were distinctly diminished, in a concentration-dependent manner, by Berberine. In view of the evidence that BRB localizes in mitochondria, inhibits respiratory electron chain and activates AMPK, the observed attenuation of the replication stress-induced cellular senescence most likely is mediated by AMPK that leads to inhibition of mTOR signaling. In support of this mechanism is the observation that rhodamine123, the cationic probe targeting mitochondrial electron chain, also suppressed rpS6 phosphorylation. The present findings reveal that: (a) in cells induced to senescence BRB exhibits gero-suppressive properties by means of mTOR/S6 inhibition; (b) in parallel, BRB reduces the level of constitutive DNA damage response, previously shown to report oxidative DNA damage by endogenous ROS; (c) there appears to a causal linkage between the (a) and (b) activities; (d) the *in vitro* model of premature stress-induced senescence can be used to assess effectiveness of potential gero-suppressive agents targeting mTOR/S6 and ROS signaling; (e) since most of the reported beneficial effects of BRB are in age-relate diseases, it is likely that gero-suppression is the primary activity of this traditional medicine.

INTRODUCTION

Cellular senescence can be categorized in two groups. The replicative senescence, seen after certain rounds of cell division in cultures ("Hayflick's limit") [1], is a consequence of a progressive erosion of telomeres at each division which leads to a telomere dysfunction and irreversible cell cycle arrest [2]. The second category defined as premature cellular senescence is unrelated to telomere shortening [review, 3]. Persistent cellular stress including replicative stress caused by oxidative DNA damage [4,5], activation of oncogenes [6] and loss of tumor suppressor genes [7] are among mechanisms inducing premature senescence. While in certain malignancies, particularly in acute leukemia, chemo- or radio- therapy induces apoptosis, the mechanism of elimination of cancer cells in some solid tumors often relies on irreversible impairment of cell reproductive capability defined as a drug- or radiation-induced senescence, that also belongs to the category of premature senescence [8,9]. Likewise, premature senescence of induced pluripotent stem cells (iPSCs) is a barrier in tumor development [10]. The stress-induced premature senescence of normal cells *in vivo* is considered to be a critical mechanism affecting organismal aging and longevity [11-14].

Extensive attempts have been made to develop gero-suppressive modalities that can slow down processes of senescence and aging extending longevity. Assessment of their effectiveness by analysis of animals' life span, especially when it involves vertebrates [15,16], is cumbersome and time consuming. It is therefore desirable to have relatively rapid *in vitro* approach that can be used for this purpose. Cumulative DNA damage caused by reactive oxygen species (ROS) produced during oxidative phosphorylation for long time was thought to be the major factor promoting aging (ROS mechanism) [17-19]. More recently, however, the persistent stimulation of the mitogen- and nutrient-sensing pathways including mammalian target of rapamycin (mTOR) signaling mechanism has been advanced as an alternative to ROS mechanism [20-28]. Activation of these pathways enhances translation and leads to cell growth in size/mass resulting in cell hypertrophy and senescence. Activation of mTOR/S6K pathway when combined with oxidative DNA damage that leads to replication stress appears to be particularly effective factor promoting aging and senescence [29].

The background level of constitutive activation of ATM and expression of γH2AX seen in untreated normal or cancer cells reports the ongoing DNA oxidative damage and replication stress induced by endogenous ROS [30-32]. Using flow- and laser scanning- cytometry as major methodologies we have recently shown that several reported gero-suppressive agents, namely, rapamycin, metformin, berberine (BRB), 1,25-dihydroxyvitamin D3, the calorie-restriction mimetic 2-deoxyglucose, and acetylsalicylic acid (ASA; aspirin), all depressed the level of constitutive DNA damage signaling [33-35]. Specifically, these substances reduced expression of γH2AX and activation of ATM in a variety of cell types, including tumor A549 and TK6 cells, as well as normal WI-38 cells or mitogenically stimulated human lymphocytes [33]. These agents also decreased the level of intracellular ROS and mitochondrial trans-membrane potential ΔΨm, the marker of mitochondrial energizing [33-35]. The above observations would be consistent with the ROS mechanism of aging. However, all these agents also distinctly reduced the constitutive level of phosphorylation of Ser235/236 of ribosomal S6 protein (rpS6), Ser2448 of mTOR and Ser65 of 4EBP1 [33], the major elements of the mTOR signaling [27,36-38]. Collectively, these data indicated that the reduction of mTOR/S6K signaling, that in turn reduces the translation rate, was coupled with a decrease in oxidative phosphorylation (revealed by ΔΨm) that led to reduction of ROS and attenuated oxidative DNA damage [33]. Thus, while the decreased rate of translation induced by these agents may slow down cells hypertrophy and alleviate other features of cell aging/senescence reduction of oxidative DNA damage may lower predisposition to neoplastic transformation. The latter may result from damage to DNA sites coding for oncogenes or tumor suppressor genes. Our data suggested that combined assessment of constitutive γH2AX expression, mitochondrial activity (ROS, ΔΨm) and mTOR signaling by cytometry can provide an adequate gamut of cell responses to evaluate effectiveness of potential gero-suppressive agents [33]. In continuation of these studies we attempted to explore whether gero-suppressive agents can also attenuate the level of premature, stress-induced cellular senescence. Toward this end we initiated experiments designed to reveal possible effects of these agents on induction of cellular senescence upon exposure of A549 cells to very low concentration of the DNA damaging drugs, shown by us before to trigger DNA replication stress manifesting by ATM activation and induction of γH2AX, that leads to senescence [39,40]. In preliminary experiments we observed that one of the gero-suppressive agents, the isoquinoline alkaloid berberine (BRB), was the most effective, suppressing the induction of cellular senescence at its low, clinically relevant, concentration. The present study, therefore, was designed to explore this effect of BRB in more detail and at the same time to demonstrate utility of flow- and laser scanning- cytometry in multiparametric analysis [41] of the depth of cellular senescence and its modulation by this alkaloid.

RESULTS

One of the most characteristic features of cells undergoing senescence is change in their morphology revealed by an increase in cellular and nuclear size. In the case of cells growing attached this manifests by their dramatic "flattening" appearance combined with markedly reduced cell density at confluence [42,43]. The morphometric analysis of cell nucleus by laser scanning cytometry (LSC) is a sensitive detector of such a change [39,40]. Premature senescence of A549 cells was induced by their exposure to 2 nM DNA topoisomerase inhibitor mitoxantrone (Mxt), the drug that interacts with DNA by intercalation and is a type II DNA topoisomerase inhibitor [44]. Fig. 1 illustrates the features of these cells undergoing senescence, including their morphological changes that were measured by LSC. The morphometric analysis of the nucleus stained with the DNA fluorochrome DAPI shows an increase in nuclear area concomitant with the decrease in intensity of DAPI maximal pixel fluorescence [39]. The integral of intensity of DAPI fluorescence over the nucleus reports DNA content and thus the cell cycle phase, which as seen Fig. 1 (insets), indicates cell arrest in G_1 and G_2M with paucity of S-phase cells in the Mxt-

treated cultures. Since nuclear area in senescent cells is increased and DAPI maximal pixel decreased the ratio of maximal pixel to the area (Mp:area) provides an even more sensitive marker reporting this change in cell morphology than either of these measurements alone (Fig. 1B). The cells arrested in G_1 and G_2M in the Mxt-treated cultures show 10 to19-fold increase in expression of the CDK inhibitor $p21^{WAF1}$, the another marker of cellular senescence [42,43]. Activation of the senescense-associated β-galactosidase A-β-gal), another hallmark of cellular senescence [42,43] is also markedly elevated in cells growing in the presence of Mxt. The rise in SA-β-gal activity measured by LSC is expressed either as percent of the enzyme-positive cells, which is augmented from 1.4 to 23% and 44%, or the mean value of the light absorption of the SA-β-gal product, increased 8.4- and 17.7-fold, in cells from cultures growing with Mxt for 48 and 72 h respectively (Fig. 1; D,E).

Induction of senescence of A549 cells growing in the presence of Mxt is distinctly suppressed, in a concentration-dependent fashion, by BRB (Fig. 2). Thus, the morphometric parameter reporting the nuclear change (Mp:area) which in the presence of Mxt alone is decreased from 1.0 to 0.28, in cultures treated with Mxt and 5 μM BRB is decreased to only 0.56, which is a 100% reduction compared to Mxt alone. At higher BRB concentration this effect is more pronounced, and at 60 μM BRB the reduction is 182% vis-à-vis Mxt alone. The attenuation of the Mxt-induced senescence by BRB, when measured by the induction of SA-β-gal activity, is also quite evident, and BRB-concentration dependent. The BRB-induced decrease of SA-β-gal activity in Mxt-treated cells was 26% at 5 μM BRB and further decreased to 75% at 60 μM concentration (Fig. 2).

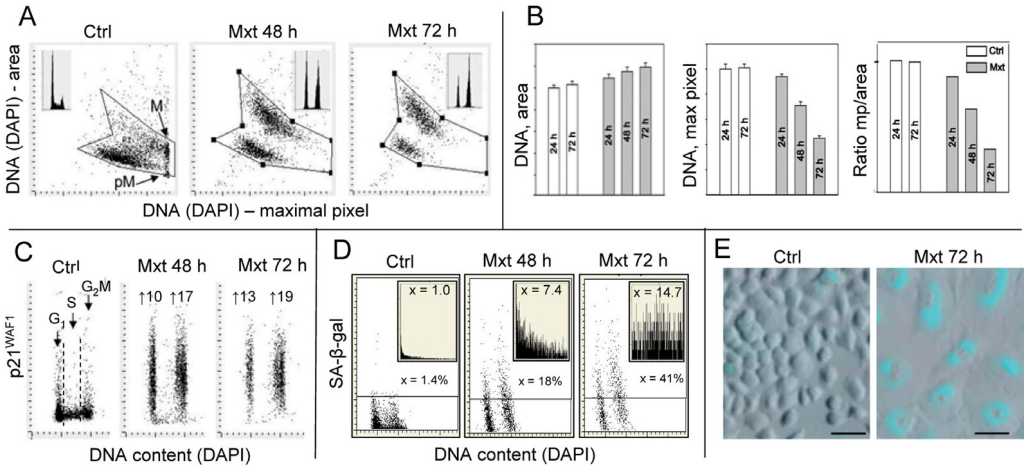

Figure 1. Induction of premature cellular senescence of A549 cells measured by laser scanning cytometry. Human pulmonary non-small cell lung carcinoma A549 were untreated (Ctrl) or treated with 2 nM DNA topoisomerase II inhibitor mitoxantrone (Mxt) for 48 or 72 h. Panel **A** shows morphometric features of the cells revealed by measurement of nuclear DNA (DAPI) fluorescence reporting on the bivariate distributions (scatterplots) nuclear area versus intensity of maximal pixel of fluorescence, respectively. Intensity of maximal pixel is correlated with chromatin condensation and in the untreated cells has the highest value and marks mitotic (M) and immediately post-mitotic (pM) G_1 cells, which also have low value of DAPI area [41]. In the senescing cells, while nuclear area increases, the intensity of maximal pixel decreases [39,40,64]. These morphometric changes reflect enlargement of the projected nuclear area and decreased DAPI local staining per unit area, due to "flattened" cellular appearance, the hallmark of cellular senescence [42,43]. The insets show DNA content frequency histograms of cells from the respective cultures. Panel **B**: Bar plots reporting mean values (+SD) of nuclear (DNA, DAPI) area, DNA (DAPI) maximal pixel, and ratio of maximal pixel to nuclear area, respectively, of cells from control and Mxt treated cultures. Panel **C**: Bivariate distributions (DNA content vs p21) reporting expression of $p21^{WAF1}$ with respect to the cell cycle phase; the figures show the n-fold increase in mean expression of p21 of G_1 and G_2M cells from the Mxt-treated cultures with respect to respective cells in Ctrl. Panel **D**: Bivariate distributions of DNA content versus senescence-associated galactosidase (SA-β-gal) activity. Figures indicate percent of SA-β-gal positive (above the threshold marked by the horizontal lines) cells. Insets show the frequency distribution of SA-β-gal positive cells; the figures in insets show the n-fold increase in the mean activity of SA-β-gal in Mxt-treated cultures over Ctrl (1.0). Panel **E**: Images of cells growing in the absence (left) and presence of 2 nM Mxt for 72 h (right) stained to detect activation of SA-β-gal activity recorded by laser scanning cytometer (Research Imaging Cytometer iCys); 50 μm bars mark the length scale.

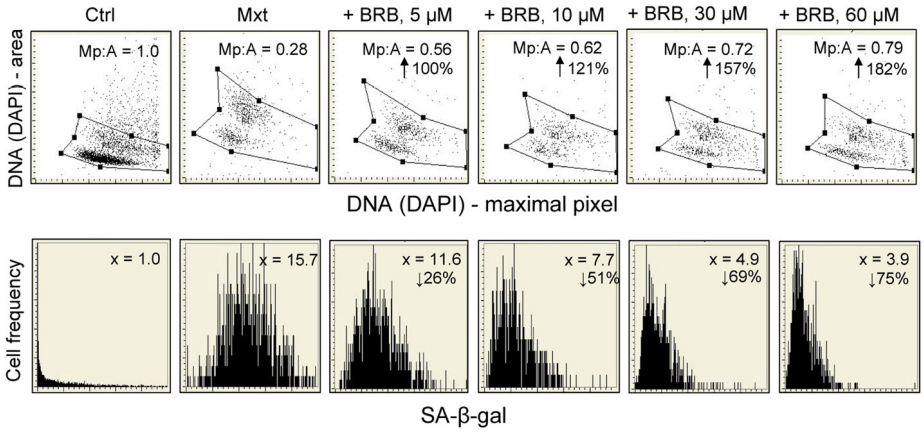

Figure 2. Attenuation of Mxt-induced senescence of A549 cells by berberine (BRB) as measured by cell morphometric features and SA-β-gal activity. Exponentially growing A549 cells were untreated (Ctrl) or treated with 2 nm Mxt in the absence and presence of BRB at concentration as shown, for 5 days. Top panels: Morphometric analysis, reporting changes in nuclear area (DNA–DAPI) versus maximal pixel of DAPI fluorescence. The ratio of maximal pixel to nuclear area (Mp:A) is expressed as a fraction of that of the untreated cells; shown is the percent increase in Mp:A in the BRB-treated cultures with respect to cells growing with Mxt alone, with the arrows. Bottom panels: The frequency histograms reporting SA-β-gal activity. The figures present the increase (n-fold) in the enzyme activity with respect to the Ctrl (1.0), measured as the mean intensity of SA-β-gal absorption of cells in the respective cultures.

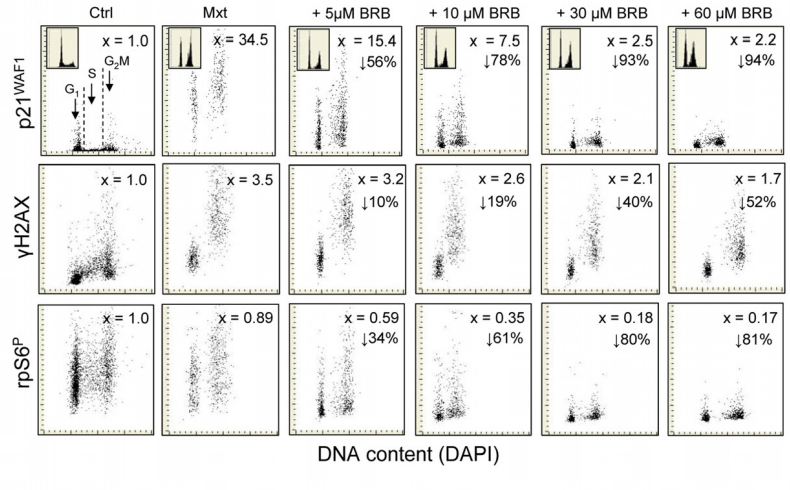

Figure 3. Attenuation of Mxt-induced senescence of A549 cells by BRB as measured by reduction in expression of $p21^{WAF1}$, γH2AX and $rpS6^{P}$. Exponentially growing A549 cells were untreated (Ctrl) or treated with Mxt in the absence and presence of BRB at concentrations as shown, for 5 days. Top panels: bivariate distributions of p21 versus cellular DNA content; the figures (x) present the increase (n-fold) in the mean expression for all cells of p21 with respect to the untreated cells, the percent reduction in p21 in cultures with BRB with respect to Mxt alone, is shown with the arrows. Mid-panels: expression of γH2AX versus DNA content; the figures (x) represent the increase (n-fold) in the mean expression of γH2AX with respect to untreated cells (1.0); the percent reduction in expression of γH2AX in cultures grown with BRB with respect to cells growing in the presence of Mxt alone is presented with the arrows. Bottom panels: expression of $rpS6^{P}$ versus DNA content. The figures illustrate the change (n-fold) with respect to the untreated cells; the percent reduction in expression of $rpS6^{P}$ in cultures with BRB with respect to cells treated with Mxt alone is shown with the arrows.

Fig. 3 illustrates the effect of BRB on expression of $p21^{WAF1}$, γH2AX and ribosomal protein (rpS6) phosphorylated on Ser235/236 ($rpS6^P$) in A549 cells, detected by phospho-specific Ab, induced to senescence by treatment with Mxt for 5 days. The Mxt-induced senescence of these cells manifests in dramatic increase in expression of p21 (34.5-fold), which is more pronounced than after 3 days of treatment with Mxt (Fig. 1). However, the increase in expression of p21 is markedly reduced in cells treated with Mxt in the presence of BRB and the reduction is BRB-dose dependent, starting with 56% at 5 μM and decreasing by 94% at 60 μM concentration. The induction of p21 by Mxt is paralleled by cell arrest in G_1 and G_2M phases of the cell cycle, and the arrest in G_2M is to some extent reduced at 5 and 10 μM BRB (top panels, insets). The Mxt-induced senescence is also marked by 3.5-fold rise in expression of γH2AX and this rise is also attenuated, in a concentration-dependent fashion, by BRB, varying from 10% to 52% at 5 to 60 μM concentration of this isoquinoline. Phosphorylation of rpS6 on Ser235/236 is reduced by 11% in cells induced to senescence by Mxt alone. However, there is a dramatic further reduction in expression of this phosphorylated protein in cells growing in the presence of Mxt and BRB compared with Mxt alone, also in the dose-dependent mode, from 34% at 5 μM, to as much as 81% at 60 μM BRB concentration.

The results shown in Figs. 1-3 demonstrate that the induction of premature cellular senescence of A549 cell by treatment with Mxt is distinctly attenuated by BRB and the attenuation is already evident at its 5 μM concentration. In our prior study we observed that treatment of several cell types including A549, TK6, WI-38 cells and normal proliferating lymphocytes with different potential gero-suppressive agents reduced both, the mTOR- as well as DNA damage- signaling [33]. Among these agents was BRB which at 60 μM concentration was seen to markedly suppress the level of constitutive phosphorylation of mTOR, rpS6 and 4EBP1 as well as of H2AX. These findings were consistent with the notion that BRB had potential gero-suppressive properties combined with the ability protect DNA from endogenous oxidants [33]. In light of the current observation that 5-60 μM BRB suppresses induction of the premature senescence we have tested its ability at these lower concentrations to affect the level of constitutive mTOR signaling in cells not induced to premature senescence. Such low BRB concentrations are relevant in terms of the drug pharmacokinetics and its *in vivo* effects [45-48]. To this end we treated human lymphoblastoid TK6 cells, the cells which we explored in the prior study [33], with the range of BRB concentration as used for A549 cells. As is evident from the data in Fig. 4 growth of these cells in the presence of 5 – 60 μM BRB led to a distinct reduction of rpS6 phosphorylation. The reduction was evident already at 5 μM BRB and at that concentration its extent showed distinct cell cycle phase specificity. Namely at 5 μM the reduction was more pronounced in G_2M- and S- phase cells, lowering expression of $rpS6^P$ in these cells by 60% and 49%, respectively, compared with 39% for G_1 cells. The degree of suppression of rpS6 phosphorylation was BRB-concentration dependent, reaching over 80% for the G_2M and S-phase cells at its 60 μM concentration. The BRB concentration-dependency was quite apparent from the $rpS6^P$ frequency histograms (Fig. 4 top panels, insets).

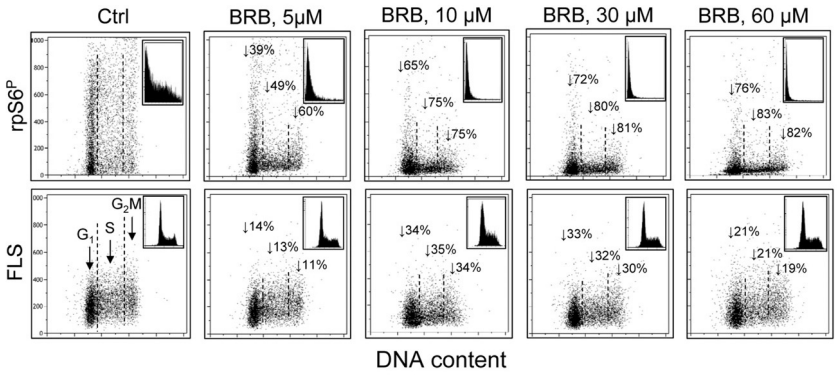

Figure 4. Suppression of rpS6 phosphorylation and reduction of size of human lymphoblastoid TK6 cells grown in the presence of BRB at 5 μM – 60 μM concentration. Exponentially growing TK6 cells were untreated (Ctrl) or treated with BRB at concentrations as shown, for 24 h. Top panels: the bivariate distributions of $rpS6^P$ expression versus DNA content. Figures show percent decrease in expression of the mean $rpS6^P$ for cells at G_1, S and G_2M phases of the cell cycle, respectively, growing in the presence of BRB vis-à-vis to the untreated cells. Insets show the frequency histograms of $rpS6^P$ expression for all cells in culture. Bottom panels: Bivariate distributions of cellular forward light scatter (FLS) versus DNA content. Percent decrease in of mean value of FLS, considered to represent cellular size [49,50], of G_1, S and G_2M of cells growing in the presence of BRB with respect to the untreated cells is shown with the arrows. Insets illustrate DNA content frequency histograms of cells from the respective cultures.

Interestingly, growth of TK6 cells in the presence of 5 - 60 μM of BRB for 24 h led to reduction of their size (Fig. 4, bottom panels). The reduction was estimated from analysis of the forward light scatter (FLS), which when measured by flow cytometry is considered to be a marker of cell size [49,50]. The diminished size of TK6 cells was evident already at 5 μM concentration of BRB and it was approximately of similar extent for cells in different phases of the cell cycle. The cell size reduction was more extensive at 10 μM and 30 μM than at 5 μM BRB concentration. No significant changes in the cell cycle distribution were seen at these BRB concentrations, as reflected by the DNA content frequency histograms (insets).

BRB is fluorescent and its fluorescence and localization in mitochondria in live cells was initially reported by Borodina and Zelenin in 1977 [51]. Its fluorescence is maximally induced by UV light at 421-431 nm and emission is within a wide range of green to yellow (514-555 nm) wavelength [52]. In binding to mitochondria BRB has an affinity to respiratory electron transport chain and the extent of its binding appears to correlate with mitochondrial potential $\Delta\Psi m$ [53-55]. This is in analogy to another mitochondrial probe rhodamine123 (Rh123) which is a widely used marker of mitochondrial energizing [56,57]. We have presently observed that 60 min exposure of A549 cells to BRB distinctly labels mitochondria (Fig. 6). This can be seen however for only for short period of time after exposure to blue light (< 3 min) or even shorter (< 1 min) to UV light. With longer exposures the BRB fluorescence disappears from mitochondria and undergoes translocation to nuclei and nucleoli (Fig. 5). It should be noted that BRB fluorescence was not apparent in cells that were fixed and subsequently rinsed, and thus it did not interfere with the subsequent measurement of fluorescent markers reporting mTOR/S6- and DNA damage- signaling.

The evidence in literature [53-55] and our observation (Fig. 5) indicate that in live cells BRB localizes in mitochondria where most likely it interferes with the electron transport chain. It may be suspected therefore that its presently measured effect namely attenuation of phosphorylation of rpS6 may be mediated by targeting electron transport in mitochondria. We have tested therefore the effect of a classical mitochondrial potential probe Rh123 [56,57] on rpS6 phosphorylation. As is evident from the data in Fig. 6 exposure of A549 cells in the presence of Rh123 leads to a decline in the level of constitutive phosphorylation of rpS6. The effect is not cell cycle-phase specific but related to time of exposure to Rh123, as 31% decrease is noted after 6 h and 59% after 24 h of treatment with Rh123, respectively.

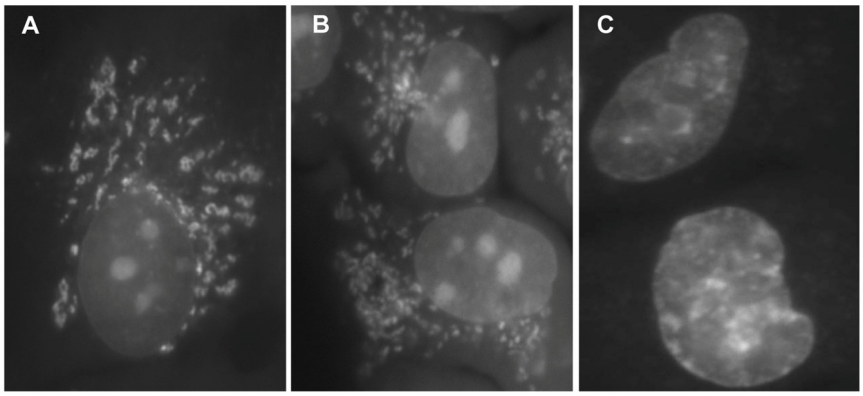

Figure 5. Detection of BRB fluorescence in live A549 cells exposed to this isoquinoline. Exponentially growing A549 cells were treated with 5 μM BRB for 60 min, rinsed with PBS and examined under fluorescence microscopy. Immediately after illumination (the first min after exposure to UV) the BRB yellow fluorescence was localized almost exclusively in mitochondria (**A**). With extended time of illumination (2 min) intensity of fluorescence of mitochondria declined while nuclear and nucleolar fluorescence become more apparent (**B**). After 5 min exposure to UV no mitochondrial fluorescence was evident whereas intensity of nuclear and nucleolar fluorescence was distinctly increased (**C**). Images taken with the Nikon Microphot FXA; objective Fluor 40X.

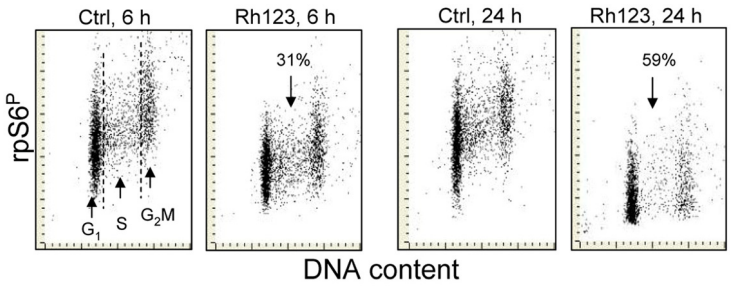

Figure 6. Effect of treatment of A549 cells with Rh123 on the level of expression of phosphorylated rpS6. Exponentially growing A549 cells were treated for 6 h or 24 h with 1 μM Rh123. Expression of $rpS6^P$ in cytoplasm was detected by phosphospecific Ab and measured by the iCys laser scanning cytometry. The figures indicate percent decree in expression of RP-S6P in the Rh123 treated cells vis-à-vis the respective control (Ctrl) cells.

DISCUSSION

Potential gero-suppressive properties of berberine

Several elements of stress-induced premature cellular senescence are relevant to aging. The key element, considered to be the major driving force of aging, is persistent activation of mTOR and its downstream target rpS6 kinase (p70S6 kinase; p70S6K), a serine/threonine kinase that phosphorylates rpS6. Phosphorylation of rpS6 induces protein synthesis at the ribosome [27,36,38]. When equilibrium between protein synthesis and its degradation (including by autophagy) is broken and synthesis prevails, cells become hypertrophic acquiring senescent ("growth imbalance") phenotype, the phenomenon described nearly five decades ago [59]. There is an extensive and rapidly accumulating evidence in support of this mechanism as the primary inducer of premature cellular senescence as well as major contributor to organismal aging [20-28,59-63]. As mentioned in the Introduction we have tested seven different potential gero-suppressive agents in terms of their ability to attenuate the level of constitutive mTOR/S6 signaling in normal cell types and cell lines. Each of these agents was quite effective in causing the decline of this signaling [33]. Interestingly, they all also reduced the level of constitutive DNA damage response, considered to be a reporter of DNA damage by endogenous oxidants [30-32]. In continuation of these studies we initiated to assess whether these agents can modulate the induction of premature cellular senescence. The senescence was instigated by low level of persistent DNA damage maintained by cell exposure to DNA-targeting drugs mitoxantrone [39] or mitomycin C [40]. Such treatment was seen to induce replication stress manifesting by low level of DNA replication activity combined with the induction of DNA damage signaling viz. ATM activation and H2AX phosphorylation, and development of characteristic features of cellular senescence [39,40,64,65]. In the pilot experiments we observed that one of the investigated gero-suppressive agents, namely BRB, was particularly effective in attenuation of premature cell senescence. The present studies were designed to investigate this phenomenon in more detail, using BRB concentrations that are relevant to its potential pharmacological *in vivo* doses [45-48].

The present results clearly indicate that administration of BRB into cultures of A549 cells undergoing premature senescence reduced the development of senescent phenotype as revealed by analysis of cells morphometric features, activation of SA-β-gal and induction of CDK inhibitor $p21^{WAF1}$. BRB also attenuated the level of mTOR/S6 signaling by lowering the level of phosphorylation of rpS6, as well as expression of γH2AX. All these effects were BRB-concentration-dependent and already evident at its lowest, 5 μM concentration. In parallel experiments, we observed that BRB also decreased rpS6 phosphorylation and reduced the size of TK6 cells (Fig. 4). In the prior study 60 μM BRB was seen to attenuate the level of constitutive mTOR/S6 and DNA damage signaling, and to reduce both the mitochondrial potential (ΔΨm) as well as the abundance of ROS [33]. Since as mentioned, the mechanisms of stress-induced cellular senescence and aging have much in common, collectively these data suggest that BRB can be effective at an *in vivo* achievable concentration [45-48,66,67] as a gero-suppressive agent.

The mechanism by which BRB exerts these effects may be through targeting mitochondria. Its localization in mitochondria was reported before [53-55] and presently shown in the case of A549 cells (Fig. 5). BRB in mitochondria is photolabile; even the short exposure to UV light results in a loss of its mitochondrial localization and apparent translocation into nuclei. The specific target appears to be the respiratory electron transport chain [53,54]; inhibition of the electron transport results in a decrease of ATP production which leads to an increase of AMP to ATP ratio which in turn triggers the AMP-activated protein kinase (AMPK) [68]. The inhibition of mTOR/S6 signaling, the event presently observed (Fig. 3), is one of the key effects of AMPK activation [27,28,36-38]. This mechanism is essentially identical to that induced by metformin, which also targets electron transport in complex 1 of mitochondria and in this way activates AMPK [69]. In fact, among its many clinical applications BRB, similar to metformin, has been promoted as an anti-diabetic supplement [70-72]. Since metformin was shown to extend lifespan of *C. elegans* [73,74] and even rodents [15,75,76] (although not of *Drosophila* [77]), it is reasonable to expect that BRB may demonstrate gero-suppressive properties as well.

In the present study we observed that exposure of A549 cells to the classic cationic mitochondrial probe Rh123, which also targets electron transport chain and monitors mitochondrial electrochemical potential $\Delta\Psi m$ [56,57], led to reduction of rpS6 phosphorylation (Fig. 6). It is thus possible that inhibition of the mitochondrial respiratory chain by other modalities, *via* similar mechanism of activation of AMPK and mTOR inhibition as in the case of metformin or BRB, may have potential gero-suppressive properties as well. It should be noted however, that these potential gero-suppressive agents may differ in other properties and may have different side effects. Thus, for example, whereas rapamycin extends lifespan of various organisms including vertebrates [16,78], it does not ameliorate some traits of animal aging [79,80]. The possibility of induction of autophagy as an additional mechanism counteracting cellular senescence and providing anti-aging benefits should be estimated in parallel with the inhibitory activity on the mTOR/S6 signaling [81-83]. The choice of an agent or perhaps a combination of several agents differing in primary binding site and/or mechanism of action that, would have maximal gero-suppressive properties and minimal side effects, has to be explored to assess the advantages of their use for attenuation of aging processes. Their analysis *in vitro* such as exploring potential in preventing the premature, stress-induced, cellular senescence as presently shown in the case of BRB, may offer an advantage over *in vivo* experiments testing animals' longevity, by yielding the data rapidly and economically.

BRB has a long history of medicinal use in both Ayurvedic and old Chinese medicine. More recently, BRB has found wide application to treat a variety of different maladies. However, because it has been used primarily as a dietary nutritional supplement the evidence of its clinical toxicity or side effects such as is generally being obtained from well monitored clinical trials is scarce but forthcoming [72,84]. Interestingly, many applications at which BRB was reported to have positive health effects relate to age-related diseases [84-89], including metabolic and cardiovascular risks [84], type 2 diabetes [45-47,70-72], atherosclerosis [68], senile osteoporosis [87], Alzheimer's disease [88], hypercholesterolemia [89] and diabetes-induced renal inflammation [90]. It is tempting to speculate that this diversity of medical benefits reportedly provided by BRB, having one common denominator namely organismal aging, stems from the gero-suppressive properties of this isoquinoline, as presently detected. It should be noted, however that BRB [91,92], similar as metformin [93-95], was shown to exert anticancer properties, suppressing growth and/or sensitizing cancer cells to various other anticancer modalities.

In vitro assessment of gero-suppressive agents

Our prior studies [32-35,64] and the present results indicate that evaluation of effectiveness of potential anti-aging modalities can be achieved *in vitro* by monitoring their effect on mTOR/S6- and ROS-DNA damage signaling pathways that leads to attenuation of the stress-induced cellular senescence. Quantification of these effects is carried on using phospho-specific Abs that detect critical phosphorylation of the mTOR targets such as rpS6 and 4EBP1 concurrently with the level of ROS, $\Delta\Psi m$, constitutive expression of γH2AX and activation of ATM, all measured in individual cells by multiparametric flow- or laser scanning- cytometry.

Fig. 7 presents key pathways associated with cellular senescence and aging linking mTOR/S6- and DNA damage- signaling, the targets of potential gero-suppressive agents that can be assessed this way. Reduction of signals activating m-TOR (raptor) pathway such as mitogens, growth factors and amino acids, triggering MAPK, Rsgs, MAP4K3, RaIA and hVps34, provide the outmost target for gero-suppression. These signals are suppressed by 2-deoxyglucose and other calorie restriction mimetics as well as by inhibitors of growth factors, primarily of IGF-1. Downstream of these signals, the mTOR

activation is directly suppressed by its specific inhibitor rapamycin, and indirectly by activation of AMP-PK. Among effective activators of AMP-PK is metformin, as well as BRB. While the gero-suppressive effects of metformin are well documented [15,16] the present data demonstrate strongly suppressive effect of BRB on induction of the stress-induced premature cellular senescence. As mentioned, activation of AMP-PK can be achieved by targeting mitochondrial energy production, as it was shown with Rh123 (Fig. 6).

Since the increased rate of translation driven by rpS6 phosphorylation is the primary motor of cell growth in size (hypertrophy, "growth imbalance", which is a characteristic phenotype of senescence) it is expected that inhibition of the translation rate through other means, downstream of mTOR activation, can also have gero-suppressive effects. For example, mimetics of amino acids that are not incorporated into protein but lower the rate of translation may have similar gero-suppressive effect. Likewise, reduction of ribosomal activity by such means as modification of the mRNA with the mRNA 5'-cap analogs [97, 98] or other approaches [99] may be gero-suppressive as well. Attenuation of the senescence phenotype that may be independent of translation is mediated by autophagy (Fig. 7) [100-102]. Specific inducers of autophagy, therefore, may have an additive effect with the mTOR inhibitors in terms of suppression of aging. However, most mTOR inhibitors are also activators of autophagy [100-102].

Our observation that the gero-suppressive agents inhibit constitutive level of mTOR activation concurrently with reduction of DNA damage signaling [33] provides evidence of a direct linkage between mTOR activation and oxidative DNA damage (Fig. 7). This is expected since translation requires production of energy (ATP) through oxidative phosphorylation which generates ROS; the increased ROS production (translation) leads to a greater oxidative DNA damage. It should be noted however that when ROS induce damage to telomeric sections of DNA this has an effect in promoting replicative senescence (Fig. 7). Likewise, the ROS-mediated lipid peroxidation is another marker of cellular senescence and aging.

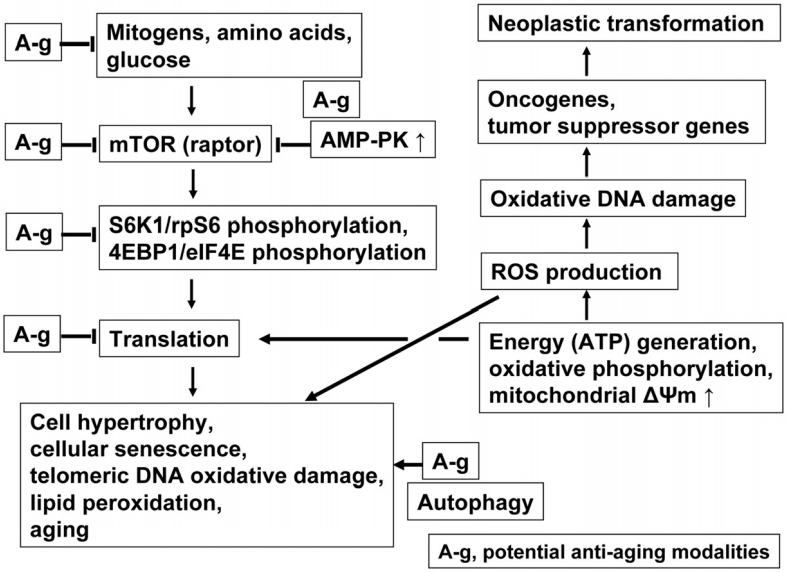

Figure 7. Schematic presentation of key pathways associated with cellular senescence and aging linking mTOR- and DNA damage- signaling. The ongoing translation particularly during perturbed cell cycle progression (replication stress), is considered to be the major factor leading to senescence. Suppression of translation that may have anti-aging effect can be achieved at several steps along the mTOR signaling pathway (marked A-g), as discussed in the text. Activation of autophagy provides an additional gero-suppressive effect. The translation requires production of ATP and thus generates ROS that cause oxidative DNA damage, which when occurs at sites of oncogenes and tumor suppressor genes, may lead to neoplasia. The damage of telomeric DNA and lipid peroxidation by ROS further contributes to the senescent phenotype. The *in vitro* model of stress-induced cellular senescence as presently described can be used to evaluate potential gero-suppressive agents in terms of their effect in reduction of mTOR/S6- and DNA- damage signaling. See text for further details.

Whereas mTOR/S6 signaling is the primary basis for induction of premature cell senescence and aging the endogenous ROS when cause DNA damage at sites coding for oncogenes or tumor suppressor genes predispose to neoplastic transformation (Fig. 7). Anti-oxidants (ROS scavengers) therefore are expected to be more effective in terms of chemo-prevention rather than as anti-aging modalities, and this indeed appears to be the case [103-106]. The attempts to attenuate aging processes including the increase in organismal longevity by antioxidants were largely unsuccessful [reviewed in 20]. On the other hand, most gero-suppressive agents were shown to have chemopreventive properties as well [106-112].

MATERIALS AND METHODS

Cells, Cell Treatment. *Human non-small cell lung carcinoma A549 cells,* obtained from American Type Culture Collection (ATCC; Manassas, VA), were grown in Ham's F-12K Nutrient Mixture (Mediatech, Inc., Manassas, VA) supplemented with 10% fetal bovine serum, 100 units/ml penicillin, 100 μg/ml streptomycin and 2 mM L-glutamine (GIBCO/BRL; Grand Island, NY) in 25 ml FALCON flasks (Becton Dickinson Co., Franklin Lakes, NJ) at 37.5 ^{o}C in an atmosphere of 95 % air and 5% CO_2. The cells were maintained in exponential and asynchronous phase of growth by repeated trypsinization and reseeding prior to reaching sub-confluency. The cells were then trypsinized and seeded at about $1x10^4$ cells per chamber in 2-chambered Falcon Culture Slides (Beckton Dickinson). To induce cellular senescence A549 cells were treated with 2 nM mitoxantrone (Mxt; Sigma-Aldrich, St. Louis, MO) as described before [39]. Concurrently with Mxt berberine (BRB; Sigma-Aldrich) was included into cultures at a final concentration as shown in Figure legends. At the end of incubation medium from each chamber was aspirated, 1 ml of 1% methanol-free formaldehyde in phosphate buffered saline (PBS) was added and the cells fixed by gently rocking the slides at room temperature for 15 min. Following aspiration of the formaldehyde the chamber slides were disassembled and the slides submerged in 70% ethanol. The fixed slides were stored at 4^0C before staining and analysis. *Human lymphoblastoid TK6 cells*, kindly provided by Dr. Howard Liber [96], were maintained in suspension in RPMI 1640 medium (GIBCO/Life Technologies) supplemented with L-glutamine (2 mM) and fetal bovine serum (10%), as described [33-35]. These cells were also exposed to 1 μM rhodamine 123 (Rh123; Sigma-Aldrich) to be assessed for expression of $rpS6^P$ and forward light scatter by flow cytometry. Other details on cultures' treatment are presented in figure legends.

Detection of γH2AX, $rpS6^P$, $p21^{WAF1}$ and activity of senescence-associated β-galactosidase. After fixation the cells were washed twice in PBS and with 0.1% Triton X-100 (Sigma-Aldrich) in PBS for 15 min and with a 1% (w/v) solution of bovine serum albumin (BSA; Sigma-Aldrich in PBS for 30 min to suppress nonspecific antibody (Ab) binding. The cells were then incubated in 1% BSA containing a 1:300 dilution of phospho-specific (Ser139) γH2AX mAb (Biolegend, San Diego, CA) and/or with a 1: 200 dilution of phosphospecific (Ser235/236), rpS6 Ab (Epitomics, Burlingame, CA) or 1;100 dilution of $p21^{WAF1}$ Ab (Cell Signaling, Danvers, MA) at 4^{o}C overnight. The secondary Ab was tagged either with AlexaFluor 488 or 647 fluorochrome (Invitrogen/Molecular Probes, used at 1:100 dilution in 1% BSA). The incubation was at room temperature for 45 min. Cellular DNA was counterstained with 2.8 μg/ml 4,6-diamidino-2-phenylindole (DAPI; Sigma-Aldrich) at room temperature for 15 minutes. Activity of senescence-associate β-galactosidase (SA-β-gal) was detected using the protocol provided by Chemicon's® Cellular Senescence Assay Kit (Millipore, Billerica, MA). After adding of Antifade (for fluorescence-labeled cells) or 50% glycerol in PBS (for (SA-β-gal) the slides were subjected to quantitative study by laser scanning cytometry. The protocol for measuring the chromatic (SA-β-gal) dye staining was provided by CompuCyte (Westwood, MA). The fixation, rinsing and labeling of A549 cells was carried out on slides, and TK6 cells in suspension. Other details have been described previously [64,112].

Analysis of Cells by Cytometry. *A549 cells:* Cellular immunofluorescence representing the binding of the respective phospho-specific Abs as well as the blue emission of DAPI stained DNA was measured by laser scanning cytometer [39-41] iCys (CompuCyte) utilizing standard filter settings; fluorescence was excited with 488-nm argon, helium neon (633 nm) and violet (405 nm) lasers. Intensities of maximal pixel and integrated fluorescence were measured and recorded for each cell. At least 3,000 cells were measured per sample. Gating analysis was carried out as described in Figure legends. *TK6cells:* Intensity of cellular fluorescence was measured using a MoFlo XDP (Beckman-Coulter, Brea, CA) high speed flow cytometer/sorter. DAPI fluorescence was excited with the UV laser (355-nm), AlexaFluor 488, DCF and Rh123 with the argon ion (488-nm) laser. Although BRB is fluorescent [Fig. 5] it was not retained by the cells following their fixation and repeated washings and control experiments excluded the possibility that its fluorescence significantly contributed to analysis of the measured cells that could lead to a bias. Analysis of forward light

scatter by flow cytometry provides information on cell size [49,50]. All experiments were repeated at least three times, representative data are presented. Other details of the particular experimental procedures were described before [64,112].

ACKNOWLEDGEMENTS

Supported by: NCI, CA RO1 28704 and Robert A. Welke Cancer Research Foundation.

Conflicts of Interest Statement

The authors have no conflicting interest to declare.

REFERENCES

1. Hayflick L. The limited in vitro lifetime of human diploid cell strains. Exp Cell Res 1965; 37:614–636.

2. Harley CB, Futcher AB, Greider CW. Telomeres shorten during ageing of human fibroblasts. Nature1990; 345:458–460.

3. Kuilman T, Michaloglou C, Mooi W, Peeper DS. The essence of senescence. Genes Dev 2010; 24:2463-2479.

4. Parrinello S, Samper E, Krtolica A, Goldstein J, Melov S, Campisi J. Oxygen sensitivity severely limits the replicative lifespan of murine fibroblasts. Nat Cell Biol 2003; 5:741–747.

5. Sherr CJ, DePinho RA. Cellular senescence: Mitotic clock or culture shock? Cell 2000; 102:407–410.

6. Serrano M, Lin AW, McCurrach ME, Beach D, Lowe SW. Oncogenic ras provokes premature cell senescence associated with accumulation of p53 and p16INK4a. Cell 1997; 88:593–602.

7. Chen Z, Trotman LC, Shaffer D, Lin H-K, Dotan ZA, Niki M, Koutcher JA, Scher HI, Ludwig T, Gerald W, et al. Crucial role of p53-dependent cellular senescence in suppression of Pten-deficient tumorigenesis. Nature 2005; 436:725–730.

8. Gerwitz DA, Holt SE, Elmore LW Accelerated senescence: An emerging role in tumor cell response to chemotherapy and radiation. Biochem Pharmacol 2008; 76:947–957.

9. Litwiniec A, Grzanka A, Helmin-Basa A, Gackowska L, Grzanka D. Features of senescence and cell death induced by doxorubicin in A549 cells: Organization and level of selected cytoskeletal proteins. J Canc Res Clin Oncol 2010; 36:717–736.

10. Banito A, Gil J. Induced pluripotent stem cells and senescence: Learning the biology to improve the technology. EMBO Reports 2010; 11:353–359.

11. Sikora E, Arendt T, Bennett M, Narita M. Impact of cellular senescence signature on ageing research. Ageing Res Rev 2011; 10:146-152.

12. Zou H, Stoppani E, Volonte D, Galbiati F**.** Caveolin-1, cellular senescence and age-related diseases. Mech Ageing Dev 2011; 132:533-542.

13. Salminen A, Kaarniranta K. Control of p53 and NF-κB signaling by WIP1 and MIF: role in cellular senescence and organismal aging. Cell Signal 2011; 23:747-752.

14. Rufini A, Tucci P, Celardo I, Melino G. Senescence and aging. Oncogene 2013 EpubFeb 18.

15. Anisimov VN, Berstein LM, Popovich IG, Zabezhinski MA, Egormin PA, Piskunova TS, Semenchenko AV, Tyndyk ML, Yurova MN, Kovalenko IG, Poroshina TE. If started early in life, metformin treatment increases life span and postpones tumors in female SHR mice. Aging (Albany NY). 2011; 3:148-157.

16. Anisimov VN, Zabezhinski MA, Popovich IG, Piskunova TS, Semenchenko AV, Tyndyk ML, Yurova MN, Antoch MP, Blagosklonny MV. Rapamycin extends maximal lifespan in cancer-prone mice. Am J Pathol 2010;176:2092-2097.

17. Barzilai A, Yamamoto K. DNA damage responses to oxidative stress. DNA repair (Amst) 2004; 3:1109-1115.

18. Beckman KB, Ames BN. Oxidative decay of DNA. J Biol Chem 1997;272:13300-13305.

19. Karanjawala ZE, Lieber MR. DNA damage and aging. Mech Ageing Dev 2004; 125:405-416.

20. Blagosklonny MV. Aging: ROS or TOR. Cell Cycle. 2008; 7:3344-3354.

21. Blagosklonny MV. mTOR-driven aging: speeding car without brakes. Cell Cycle 2009; 8:4055-4059.

22. Blagosklonny MV. Revisiting the antagonistic pleiotropy theory of aging: TOR-driven program and quasi-program. Cell Cycle 2010; 9:3151-3156.

23. Cabreiro F, Ackerman D, Doonan R, Araiz C, Back P, Papp D, Braeckman BP, Gems D. Increased life span from overexpression of superoxide dismutase in *Caenorhabditis elegans* is not caused by decreased oxidative damage. Free Radic Biol Med 2011; 51:1575-1582.

24. Lapointe J, Hekimi S. When a theory of aging ages badly. Cell Mol Life Sci. 2009; 67:1-8.

25. Hands SL, Proud CG, Wyttenbach A. mTOR's role in ageing: protein synthesis or autophagy? Aging (Albany) 2009; 1:586-597.

26. Blagosklonny MV, Hall MN. Growth and aging: a common molecular mechanism. Aging (Albany) 2009; 1:357-362.

27. Magnuson B, Ekim B, Fingar DC. Regulation and function of ribosomal protein S6 kinase (S6K) within mTOR signaling networks. Biochem J 2012; 441:1-21.

28. Zoncu R, Efeyan A, Sabatini DM. mTOR: from growth signal integration to cancer, diabetes and ageing. Nat Rev Mol Cell Biol 2010; 12:21-35.

29. Burhans WC, Weinberger M. DNA replication stress, genome instability and aging. Nucleic Acids Res 2007; 33:7545-7556.

30. Huang X, Tanaka T, Kurose A, Traganos F, Darzynkiewicz Z. Constitutive histone H2AX phosphorylation on *Ser*-139 in cells untreated by genotoxic agents is cell-cycle phase specific and attenuated by scavenging reactive oxygen species. Int J Oncol 2006; 29:495-501.

31. Tanaka T, Halicka HD, Huang X, Traganos F, Darzynkiewicz Z. Constitutive histone H2AX phosphorylation and ATM activation, the reporters of DNA damage by endogenous oxidants. Cell Cycle 2006; 5:1940-1945.

32. Zhao H, Tanaka T, Halicka HD, Traganos F, Zarebski M, Dobrucki J, Darzynkiewicz Z. Cytometric assessment of DNA damage by exogenous and endogenous oxidants reports the aging-related processes**.** Cytometry A 2007; 71A:905-914.

33. Halicka HD, Zhao H, Li J, Lee Y-S, Hsieh T-C, Wu JM, Darzynkiewicz Z. Potential anti-aging agents suppress the level of constitutive DNA mage and mTOR- signaling. Aging (Albany NY). 2012; 4:952-965.

34. Halicka HD, Zhao H, Li J, Traganos DF, Studzinski G, Darzynkiewicz Z. Attenuation of constitutive DNA damage signaling by1,25-dihydroxyvitamin D3. Aging (Albany) 2012; 4;270-278.

35. Halicka HD, Zhao H, Li J, Traganos F, Zhang S, Lee M, Darzynkiewicz Z Genome protective effect of metformin as

revealed by reduced level of constitutive DNA damage signaling. Aging (Albany) 2011; 3:1028-1038.
36. Hay N, Sonenberg N. Upstream and downstream of mTOR. Genes Dev 2004; :1926-1945.
37. Wullschleger S, Loewith R, Hall MN. TOR signaling in growth and metabolism. Cell 2006; 124:471-484.
38. Ma XM, Blenis J. Molecular mechanisms of mTOR-mediated translational control. Nat Rev Mol Cell Biol 2009; 10:307-318.
39. Zhao H, Halicka HD, Jorgensen E, Traganos F, Darzynkiewicz Z. New biomarkers probing the depth of cell senescence assessed by laser scanning cytometry. Cytometry A, 2010; 77A:999-1007.
40. McKenna E, Traganos F, Zhao H, Darzynkiewicz Z. Persistent DNA damage caused by low levels of mitomycin C induces irreversible senescence of A549 cells. Cell Cycle 2012; 12:3132-3140.
41. Pozarowski P, Holden E, Darzynkiewicz Z. Laser scanning cytometry: Principles and applications. An update. Meth Molec Biol 2013; 913:187-212.
42. Rodier F, Campisi J. Four faces of cellular senescence. J Cell Biol 2011; 192:547-556.
43. Kuilman T, Michaloglou C, Mooi WJ, Peeper DS. The essence of senescence. Genes Dev 2010; 24:2463-2479.
44. Kapuscinski J, Darzynkiewicz Z. Interactions of antitumor agents ametantrone and mitoxantrone (novantrone) with double-stranded DNA. Biochem Pharmacol 1985; 34:4203-4213.
45. Guo Y, Pope C, Cheng X, Zhou H, Klaassen CD. Dose-response of berberine on hepatic cytochromes P450 mRNA expression and activities in mice. J Ethnopharmacol 2011; 138:111-118.
46. Liu L, Yu YL, Yang JS, Li Y, Liu YW, Liang Y, Liu XD, Xie L, Wang GJ. Berberine suppresses intestinal disaccharidases with beneficial metabolic effects in diabetic states, evidences from in vivo and in vitro study. Naunyn Schmiedebergs Arch Pharmacol 2010; 381:371-381
47. Cicero AF, Tartagani E. Antidiabetic properties of berberine: from cellular pharmacology to clinical effects. Hosp Pract (Minneap) 2012; 40:56-63.
48. Xu LN, Lu BN, Hu MM, Xu YW, Han X, Qi Y, Peng JY. Mechanisms involved in the cytotoxic effects of berberine on human colon cancer HCT-8 cells. Biocell 2012; 36:113-20
49. Wlodkowic D, Telford W, Skommer J, Darzynkiewicz Z. Apoptosis and beyond: Cytometry in studies of programmed cell death. Methods Cell Biol 2011; 103:55-98.
50. Darzynkiewicz Z, Bruno S, Del Bino G, Gorczyca W, Hotz MA, Lassota P, Traganos F. Features of apoptotic cells measured by flow cytometry. Cytometry 1992; 13:795-808
51. Borodina VM, Zelenin AV. Fluorescence microscopy demonstration of mitochondria in tissue culture cells using berberine. Tsitologiia 1977; 19:1067-1068.
52. Díaz MS, Freile ML, Gutiérrez MI. Solvent effect on the UV/Vis absorption and fluorescence spectroscopic properties of berberine. Photochem Photobiol Sci 2009; 8:970-974.
53. Mikes V, Dadák V. Berberine derivatives as cationic fluorescent probes for the investigation of the energized state of mitochondria. Biochim Biophys Acta 1983; 723:231-239.
54. Mikes V, Yaguzhinskij LS. Interaction of fluorescent berberine alkyl derivatives with respiratory chain of rat liver mitochondria. J Bioenerg Biomembr 1985; 17:23-32.
55. Turner N, Li J-Y, Gosby A, To SWC, Cheng Z, Myoshi H, Taketo MM, Cooney GJ, Kraegen EW, James DE, Hu L-H, Li J, Ye J-M. Berberine and its more biologically available derivative, dihydroberberine, inhibit mitochondrial respiratory complex I Diabetes 2008; 57:1414-1425.
56. Darzynkiewicz Z, Staiano-Coico L, Melamed MR. Increased mitochondrial uptake of rhodamine 123 during lymphocyte stimulation. Proc Natl Acad Sci USA 1981; 78:2383-2387.
57. Darzynkiewicz Z, Traganos F, Staiano-Coico L, Kapuscinski J, Melamed MR. Interactions of rhodamine 123 with living cells studied by flow cytometry. Cancer Res 1982; 42:799-806.
58. Cohen LS, Studzinski GP. Correlation between cell enlargement and nucleic acid and protein content of HeLa cells in unbalanced growth produced by inhibitors of DNA synthesis. J Cell Physiol 1967; 69:331-339.
59. Blagosklonny MV. mTOR-driven quasi-programmed aging as a disposable soma theory: Blind watchmaker vs. intelligent designer. Cell Cycle 2013; 12:1842-1847.
60. Demidenko ZN, Blagosklonny MV. Growth stimulation leads to cellular senescence when the cell cycle is blocked. Cell Cycle 2008; 7:3355-3361.
61. Demidenko ZN, Blagosklonny MV. At concentrations that inhibit mTOR, resveratrol suppresses cellular senescence. Cell Cycle 2009; 8:1901-1904.
62. Demidenko ZN, Shtutman M, Blagosklonny MV. Pharmacologic inhibition of MEK and PI-3K converges on the mTOR/S6 pathway to decelerate cellular senescence. Cell Cycle 2009; 8:1896-1900.
63. Demidenko ZN, Korotchkina LG, Gudkov AV, Blagosklonny MV. Paradoxical suppression of cellular senescence by p53. Proc Natl Acad Sci U S A 2010; 107:9660-9664.
64. Zhao H, Darzynkiewicz Z. Biomarkers of cell senescence assessed by imaging cytometry. Meth Molec Biol 2013; 965:83-92.
65. Seifrtova M, Havelek R, Soukup T, Filipova A, Mokry J, Rezacova M. Mitoxantrone ability to induce premature senescence in human dental pulp stem cells and human dermal fibroblasts J Physiol Pharmacol 2013; 64:255-266.
66. Zhou Y, He P, Liu A, Zhang L, Liu Y, Dai R. Drug-drug interactions between ketoconazole and berberine in rats: pharmacokinetic effects benefit pharmacodynamic synergism. Phytother Res 2012; 26:772-777.
67. Zhou H, Mineshita S The effect of berberine chloride on experimental colitis in rats in vivo and in vitro.J Pharmacol Exp Ther 2000; 294:822-829.
68. Wang Q, Zhang M, Liang B, Shirwany N, Zhu Y, Zou MH. Activation of AMP-activated protein kinase is required for berberine-induced reduction of atherosclerosis in mice: the role of uncoupling protein 2. PLoS One 2011; e25436.
69. Owen MR, Doran E, Halestrap AP. Evidence that metformin exerts its anti-diabetic effects through inhibition of complex 1 of the mitochondrial respiratory chain. Biochem J 2000; 348:607-614.
70. Lee YS, Kim WS, Yoon MJ, Cho HJ, Shen Y, Ye JM, Lee CH, Oh WK, Kim CT, Hohnen-Behrens C, Gosby A, Kraegen EW, James DE, Kim JB. Berberine, a natural plant product, activates AMP-Activated protein kinase with beneficial metabolic effects in diabetic and insulin-resistant states. Diabetes. 2006; 55:1006;2256–2264.
71. Shen N, Huan Y, Shen ZF. Berberine inhibits mouse insulin gene promoter through activation of AMP activated protein kinase and may exert beneficial effect on pancreatic β-cell. Eur J Pharmacol 2012; 694:120-126.
72. Dong H, Wang N, Zhao L, Lu F. Berberine in the treatment of type 2 diabetes mellitus: a systemic review and meta-analysis.

Evid Based Complement Alternat Med. 2012; 2012:591654. Epub 2012 Oct 15.

73. Cabreiro F, Au C, Leung KY, Vergara-Irigaray N, Cochemé HM, Noori T, Weinkove D, Schuster E, Greene ND, Gems D. Metformin retards aging in C. elegans by altering microbial folate and methionine metabolism. Cell 2013; 153:228-239.

74. Onken B, Driscoll M. Metformin induces a dietary restriction-like state and the oxidative stress response to extend *C. elegans* Healthspan via AMPK, LKB1, and SKN-1. PLoS ONE 2010; 5:e8758.

75. Anisimov VN, Piskunova TS, Popovich IG, Zabezhinski MA, Tyndyk ML, Egormin PA, Yurova MV, Rosenfeld SV, Semenchenko AV, Kovalenko IG, Poroshina TE, Berstein LM. Gender differences in metformin effect on aging, life span and spontaneous tumorigenesis in 129/Sv mice. Aging (Albany NY) 2010; 2:945-958.

76. Anisimov VN, Metformin for aging and cancer prevention. Aging (Albany NY) 2010; 2:760-774.

77. Slack C, Foley A, Partridge L. Activation of AMPK by the putative dietary restriction mimetic metformin is insufficient to extend lifespan in Drosophila. PLoS One 2012; 7:e47699. Epub 2012 Oct 16.

78. Harrison DE, Strong R, Sharp ZD, Nelson JF, Astle CM, Flurkey K, Nadon NL, Wilkinson JE, Frenkel K, Carter CS, Pahor M, Javors MA, Fernandez E, Miller RA. Rapamycin fed late in life extends lifespan in genetically heterogeneous mice. Nature 2009; 460:392-395.

79. Wilkinson E, Burmeister L, Brooks SV, Chan CC, Friedline S, Harrison DE, Hejtmancik JF, Nadon N, Strong R, Wood LK, Woodward MA, Miller RA. Rapamycin slows aging in mice. Aging Cell. 2012; 11:675-82.

80. Neff F, Flores-Dominguez D, Ryan DP, Horsch M, Schröder S, Adler T, Afonso LC et al., Rapamycin extends murine lifespan but has limited effects on aging. J Clin Invest 2013 Jul 25. pii: 67674. [Epub ahead of print]

81. Nair S, Ren J Autophagy and cardiovascular aging lesson learned from rapamycin. Cell Cycle 2012; 11:2092-2099.

82. Rubinsztein DC, Mariño G, Kroemer G. Autophagy and aging. Cell 2011; 146:682-695.

83. Leontieva OV, Blagosklonny MV. Hypoxia and gerosuppression: the mTOR saga continues. Cell Cycle. 2012; 11: 3926-3931.

84. Derosa G, Maffioli P, Cicero AF. Berberine on metabolic and cardiovascular risk factors: an analysis from preclinical evidences to clinical trials. Expert Opin Biol Ther 2012; 12:1113-1124.

85. Yu HH, Kim KJ, Cha JD Kim HK, Lee YE, Choi NY, You YO. Antimicrobial activity of berberine alone and in combination with ampicillin or oxacillin against methicillin-resistant Staphylococcus aureus. Journal of Medicinal Food 2005; 8:454–461.

86. Kuo CL, Chi CW, Liu TY. The anti-inflammatory potential of berberine in vitro and in vivo. Cancer Lett 2004; 203:127–137.

87. Li H, Miyahara T, Tezuka Y, Tran OL, Seto H, Kadota S. Effect of berberine on bone mineral density in SAMP6 as a senile osteoporosis model. Biol Pharma Bull 2003; 26:130-131.

88. Ki HF, Shen L. Berberine: a potential multipotent natural product to combat Alzheimer's Disease. Molecules 2011; 16:6732-6740.

89. Kong W, Wei J, Abidi P, Lin M, Inaba S, Li C, Wang Y, Wang Z, Si S, Pan H, Wang S, Wu J, Wang Y, Li Z, Liu J, Jiang J-D. Berberine is a novel cholesterol-lowering drug working through a unique mechanism distinct from statins. Nature Medicine 2004;10:1344-1351.

90. Xie X, Chang X, Chen L, Huang K, Huang J, Wang S, Shen X, Liu P, Huang H. Berberine ameliorates experimental diabetes-induced renal inflammation and fibronectin by inhibiting the activation of RhoA/ROCK signaling. Mol Cell Endocrinol 2013; Epub Jul 26.

91. Chappell WH, Abrams SL, Franklin RA, LaHair MM, Montalto G, Cervello M, Martelli AM, Nicoletti F, Candido S, Libra M, Polesel J, Talamini R, Milella M, Tafuri A, Steelman LS, McCubrey JA. Ectopic NGAL expression can alter sensitivity of breast cancer cells to EGFR, Bcl-2, CaM-K inhibitors and the plant natural product berberine. Cell Cycle 2012; 11:4447-4461

92. Cai Y, Xia Q, Luo R, Huang P, Sun Y, Shi Y, Jiang W. Berberine inhibits the growth of human colorectal adenocarcinoma in vitro and in vivo. J Nat Med 2013 Apr 21. [Epub ahead of print].

93. Würth R, Pattarozzi A, Gatti M, Bajetto A, Corsaro A, Parodi A, Sirito R, Massollo M, Marini C, Zona G, Fenoglio D, Sambuceti G, Filaci G, Daga A, Barbieri F, Florio T. Metformin selectively affects human glioblastoma tumor-initiating cell viability: A role for metformin-induced inhibition of Akt. Cell Cycle 2013; 12:145-156.

94. Menendez JA, Oliveras-Ferraros C, Cufí S, Corominas-Faja B, Joven J, Martin-Castillo B, Vazquez-Martin A. Metformin is synthetically lethal with glucose withdrawal in cancer cells. Cell Cycle 2012; 11:2782-2792.

95. Pan J, Chen C, Jin Y, Fuentes-Mattei E, Velazquez-Tores G, Benito JM, Konopleva M, Andreeff M, Lee MH, Yeung SC. Differential impact of structurally different anti-diabetic drugs on proliferation and chemosensitivity of acute lymphoblastic leukemia cells. Cell Cycle 2012; 11:2314-2326.

96. Schwartz JL, Jordan E, Evans HH, Lenarczyk M, Liber H. The TP53 dependence of radiation–induced chromosome instability in human lymphoblastoid lines. Radiat Res 2003; 159:730–736.

97. Zuberek J, Kubacka D, Jablonowska A, Jemielity J, Stepinski J, Sonenberg N, Darzynkiewicz E. Weak binding affinity of human 4EHP for mRNA cap analogs RNA 2007; 13:691-697.

98. Mathonnet G, Fabian MR, Svitkin YV, Parsyan A, Huck L, Murata T, Biffo S, Merrick WC, Darzynkiewicz E, Pillai RS, Filipowicz W, Duchaine TF, Sonenberg N. MicroRNA inhibition of translation initiation in vitro by targeting the cap-binding complex eIF4F. Science 2007; 317:1764-1767.

99. Pan KZ, Palter JE, Rogers AN, Olsen A, Chen D, Lithgow GJ, Kapahi P. Inhibition of mRNA translation extends lifespan in *Caenohabditis elegans.* Ageing Cell 2007; 6:111-119.

100. Blagosklonny MV. Hypoxia, mTOR and autophagy: converging on senescence or quiescence. Autophagy 2013; 9:260-262.

101. Nair S, Ren J. Autophagy and cardiovascular aging: lesson learned from rapamycin. Cell Cycle 2012; 11:2092-2099.

102. Bennetzen MV, Mariño G, Pultz D, Morselli E, Færgeman NJ, Kroemer G, Andersen JS. Phosphoproteomic analysis of cells treated with longevity-related autophagy inducers. Cell Cycle 2012; 11:1827-1840.

103. Blagosklonny MV. Rapalogs in cancer prevention: anti-aging or anticancer? Cancer Biol Ther. 2012; 13:1349-1354.

104. Martinez-Outschoorn UE, Balliet R, Lin Z, Whitaker-Menezes D, Birbe RC, Bombonati A, Pavlides S, Lamb R, Sneddon S, Howell A, Sotgia F, Lisanti MP. BRCA1 mutations drive oxidative stress and glycolysis in the tumor microenvironment: implications for breast cancer prevention with antioxidant therapies. Cell Cycle 2012; 11:4402-4413.

105. BRCA1 mutations drive oxidative stress and glycolysis in the tumor microenvironment: implications for breast cancer prevention with antioxidant therapies. Cell Cycle 2012; 11:4402-4413.

106. Thapa D, Ghosh R. Antioxidants for prostate cancer chemoprevention: challenges and opportunities. Biochem Pharmacol 2012; 83:1319-1330.

107. Li D. Metformin as an antitumor agent in cancer prevention and treatment. J Diabetes 2011; 3:320-327.

108. Buitrago-Molina LE, Vogel A. mTOR as a potential target for the prevention and tratment of hepatocellular carcinoma. Curr Cancer Drug Target 2012; Aug 7 Epub.

109. Kajser J. Will an aspirin a day keep cancer away? Science 2012; 337: 1471-1473.

110. Anis KV, Rajeshkumar NV, Kuttan R. Inhibition of chemical carcinogenesis by berberine in rats and mice. J Pharm Pharmacol 2001; 53:763-768.

111. Zhu Z, Jiang W, McGinley JN, Thompson HJ. 2-Deoxyglucose as an energy restriction mimetic agent: effects on mammary carcinogenesis and on mammary tumor cell growth in vitro. Cancer Res 2005; 65:7023-7030.

112. Juan ME, Alfaras I, Planas JM. Colorectal cancer chemoprevention by trans-resveratrol. Pharmacol Res 2012; 65:584-5891.

113. Darzynkiewicz Z, Zhao H, Halicka HD, Rybak P, Dobrucki J, Wlodkowic D. DNA damage signaling assessed in individual cells in relation to the cell cycle phase and induction of apoptosis. Crit Rev Clin Lab Sci 2012; 49:199-217

Research Paper

mTOR pathway and Ca^{2+} stores mobilization in aged smooth muscle cells

Francisco E Martín-Cano, Cristina Camello-Almaraz, David Hernandez, Maria J Pozo, and Pedro J Camello

Department of Physiology, Faculty of Nursing and Faculty of Veterinary Sciences, University of Extremadura, 10003 Cáceres, Spain

Key words: *mTOR, Ca^{2+} signal, FKBP12, colon, smooth muscle*
Received: *4/9/13; Accepted: 5/7/13; Published: 5/8/13* doi:10.18632/aging.100555
Correspondence to: *Pedro J Camello, PhD;* ***E-mail:*** *pcamello@unex.es*

Abstract: Aging is considered to be driven by the so called senescence pathways, especially the mTOR route, although there is almost no information on its activity in aged tissues. Aging also induces Ca^{2+} signal alterations, but information regarding the mechanisms for these changes is almost inexistent. We investigated the possible involvement of the mTOR pathway in the age-dependent changes on Ca^{2+} stores mobilization in colonic smooth muscle cells of young (4 month old) and aged (24 month old) guinea pigs. mTORC1 activity was enhanced in aged smooth muscle, as revealed by phosphorylation of mTOR and its direct substrates S6K1 and 4E-BP1. Mobilization of intracellular Ca^{2+} stores through IP_3R or RyR channels was impaired in aged cells, and it was facilitated by mTOR and by FKBP12, as indicated by the inhibitory effects of KU0063794 (a direct mTOR inhibitor), rapamycin (a FKBP12-mediated mTOR inhibitor) and FK506 (an FKBP12 binding immunosuppressant). Aging suppressed the facilitation of the Ca^{2+} mobilization by FKBP12 but not by mTOR, without changing the total expression of FKBP12 protein. In conclusion, or study shows that in smooth muscle aging enhances the constitutive activity of mTORC1 pathway and impairs Ca^{2+} stores mobilization by suppression of the FKBP12-induced facilitation of Ca^{2+} release.

INTRODUCTION

Aging can be viewed as a quasi-programmed process driven by changes in signaling pathways, among which the mTOR pathway stands out as a key factor [1; 2]. This kinase forms part of a energy-sensing signaling pathway and can assemble two types of heteromeres, mTORC1 and mTORC2, the former involved in aging based on the lifespan-extending effects of the mTOR inhibitor rapamycin (reviewed in [3]). mTORC1 is activated by nutrients, insulin and the PI_3K/Akt pathway, and can be inhibited by nutrients deprivation, AMPK activation [4] and FKBP12 [5; 6], the target for the immunosuppressant rapamycin. mTOR has been proposed to convert arrest to senescence (gero-conversion) [7; 8]. In spite of this, there is very little information regarding the mTOR pathway status in aged tissues [9; 10].

One of the functional consequences of aging is the alteration of different aspects of calcium signals, which play a key role in multiple cellular functions, from contraction or secretion to gene regulation and cell fate and proliferation. Therefore, these changes are the basis for important alterations linked to aging [11-15]. Calcium signals consist of cytosolic Ca^{2+} concentration ($[Ca^{2+}]_i$) increases due either to activation of Ca^{2+} entry from extracellular space (through Ca^{2+} channels activated by voltage, Ca^{2+} stores depletion or receptors), or to Ca^{2+} release from intracellular stores. Mobilization of intracellular stores is mediated by IP_3R and RyR channels, activated respectively by the intracellular messengers IP_3 and cADPribose. The subsequent $[Ca^{2+}]_i$ decrease to resting levels is operated by active extrusion to extracellular medium or reuptake into intracellular organelles.

Most of available evidence on the effects of aging on $[Ca^{2+}]_i$ has focused on Ca^{2+} clearing mechanisms [15-17] and influx of extracellular Ca^{2+} [15; 18; 19], but it is rather limited and controversial for Ca^{2+} release. In neurons, the most studied model for age-related changes in Ca^{2+} signals, there is evidence that aging enhances Ca^{2+} release from intracellular stores through RyR and IP_3R calcium channels [13], similar to reports in cardiomyocytes [20]. In aged smooth muscle cells both inhibition [21] and enhancement [22; 23] have been reported.

Regarding the mechanisms underlying the effects of age on $[Ca^{2+}]_i$ signals, knowledge is rather superficial, most of the studies addressing only a description of the signal alterations. Some authors have proposed that mitochondrial modifications or redox imbalance are the origin for Ca^{2+} signal disfunction [14; 24]. Interactions between some mTOR pathway elements and Ca^{2+} release imply that the mTOR pathway could be involved in the age-related $[Ca^{2+}]_i$ modifications: Ca^{2+} release from intracellular stores can be modulated by mTOR kinase [25-28], and its inhibitor FKBP12 is a known modulator of Ca^{2+} release channels [29]. More explicit, a recent study hypothesizes that in aging neurons down-regulation of FKBP12 activates mTOR and enhances RyR mediated Ca^{2+} release [5], explaining the Ca^{2+} signal phenotype typical of aged neurons [12]. The aim of this study was to investigate the involvement of mTOR and FKBP12 in the age-induced changes in Ca^{2+} release in smooth muscle cells. Our data indicate that aging reduces the intracellular Ca^{2+} release, an effect accompanied by loss of a facilitatory effect of FKBP12 on Ca^{2+} mobilization which was independent on the expression of this protein. mTOR facilitated Ca^{2+} release both in young and aged cells and showed enhanced activity in aged cells.

RESULTS

Effect of aging on mTOR pathway activation

Since changes in the mTOR route have been proposed to be associated to the aging process [30], we investigated the constitutive activation of this pathway in the non stimulated smooth muscle layer of guinea pig colon. Activation of mTORC1 can be reliably determined by phosphorylation of Ser 2448 [31]. Figure 1 shows that Ser2448 phosphorylation was significantly enhanced in the aged colon muscle layer compared to the young colon ($p < 0.05$). To confirm that mTOR pathway was enhanced in aged muscle, we determined the level of phosphorylation of two direct substrates of mTOR, p70S6K1 and 4E-BP1, which are respectively activated and inhibited upon phosphorylation by mTORC1 kinase activity. We found that aged muscle showed higher levels of the phosphorylated forms of both 4E-BP1 and p70S6K1, the latter including phosphorylation of two different residues specific for mTOR kinase activity [32] (Fig. 1).

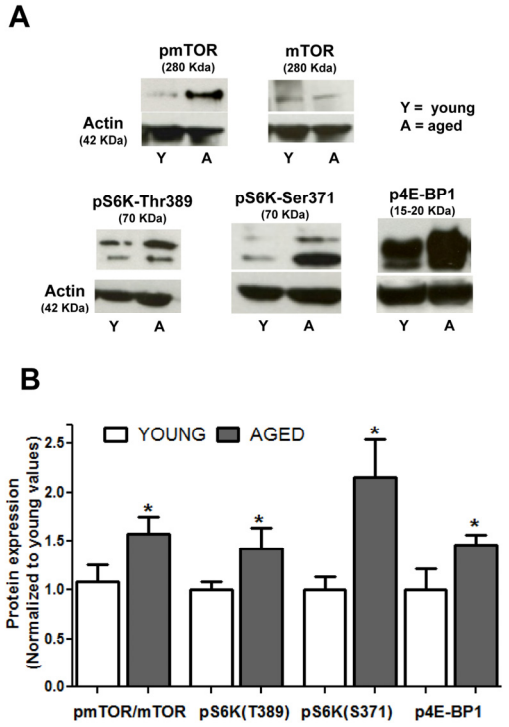

Figure 1. Aging enhances the constitutive activity of the mTOR pathway in colon smooth muscle. (**A**) Representative immunoblotts showing expression of mTOR and phosphorylated (active) forms of mTOR, p70S6K1 (at Thr389 and Ser371) and 4E-BP1 in non stimulated muscular layer of colon. Figures in parenthesis are the molecular weight of each band as judged from the molecular weight marker run in each assay. (**B**) Histogram depicting phosphorylation of mTOR and its substrates in young and aged colon. Values are average ± sem of arbitrary units normalized to mean average values of young colon. * $p < 0.05$, $n = 6$.

Modification of Ca^{2+} signals in aged smooth muscle cells

To study the effects of aging in the mobilization of Ca^{2+} from intracellular stores we challenged colon smooth muscle cells with bethanechol, known to release Ca^{2+} through IP_3R in this cell type [33; 34], or with caffeine, which releases Ca^{2+} through RyR [35]. $[Ca^{2+}]_i$ signals

induced by mobilization of intracellular Ca^{2+} pools in smooth muscle cells are characterized by an initial $[Ca^{2+}]_i$ peak followed by gradual decline towards pre-stimulus levels, as shown in Figure 2. Bethanechol caused a transient $[Ca^{2+}]_i$ increase which was smaller in aged (0.418 ± 0.024 $\Delta F_{340}/F_{380}$, n =1 88) than in young cells (0.546 ±0 .028 $\Delta F_{340}/F_{380}$, n = 117, p <0.005). Compared to bethanechol, the effect of caffeine in young cells was also transient but larger in amplitude (0.588 ± 0.027 $\Delta F_{340}/F_{380}$, n = 165, p < 0.05), and showed a similar decrease in aged cells (0.450 ± 0.018 $\Delta F_{340}/F_{380}$, n = 286, p <0.005).

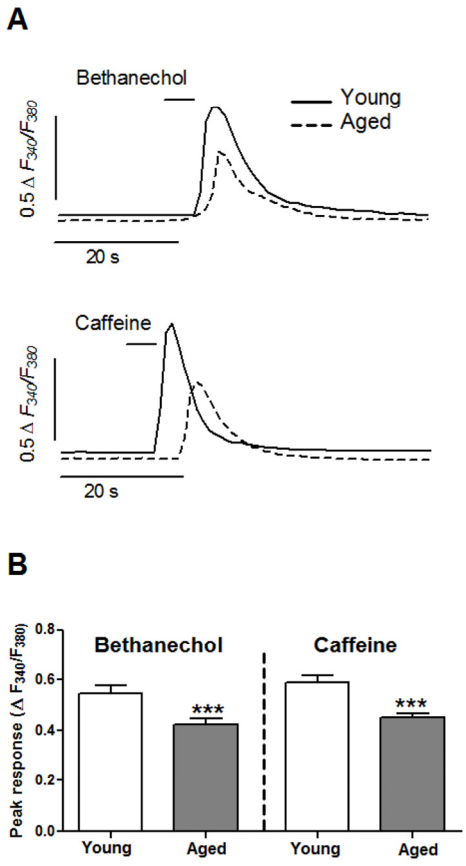

Figure 2. Aging inhibits the mobilization of Ca^{2+} stores in colonic smooth muscle cells. (**A**) Isolated cells were challenged with a short pulse of bethanechol (0.1 mM) or caffeine (10 mM) to release Ca^{2+} from intracellular pools through IP_3R and RyR channels, respectively. Traces are representative of average responses in young and aged cells. (**B**) Average ± sem response ($\Delta F_{340}/F_{380}$) from young (8 animals, 117 and 165 cells) and aged (6 animals, 188 and 286 cells) guinea pigs.

To assess a possible role of mTOR in Ca^{2+} pools mobilization, we used a double pulse protocol: either bethanechol or caffeine was applied twice separated by a 15 minutes interval to allow for recovery of the response and acute application of inhibitors (see Fig. 3). In control experiments the amplitude of the second stimulus was close to 90 % respect to the first one in young cells (bethanechol: 85.60 ± 4.82 % respect to the first pulse, n = 54; caffeine: 88.10 ± 4.16 %, n = 74), and close to 80% in aged cells (bethanechol: 81.13 ± 3.59 %, n = 89; caffeine: 74.24 ± 2.87 %, n= 130) (Fig. 3).

To inhibit mTOR we used two different types of compounds: rapamycin, a frequently used mTOR inhibitor which binds to FKBP12 protein to inhibit mTOR kinase, and KU0063794, a second generation inhibitor acting directly at the kinase domain of mTOR. When applied to cells from young guinea pigs, KU0063794 (5 μM) significantly decreased ($p < 0.005$) the responses to bethanechol and to caffeine (by around 50% each, see Fig. 3). This inhibition was also present in aged cells, indicating that mTOR kinase activity has a facilitating role on IP_3R- and RyR-mediated Ca^{2+} release and that this facilitation is not affected by aging. In the case of rapamycin (5 μM), its inhibitory effect in young cells was qualitatively similar to that of KU0063794 though smaller in amplitude (around 23 and 30% for bethanechol and caffeine, respectively; Fig. 3). On the contrary, in aged cells the inhibition was strongly attenuated or even suppressed, suggesting that the mechanisms of action of rapamycin on the Ca^{2+} mobilization are altered in aged cells.

To explore the differential influence of age on KU0063794 and rapamycin effects on Ca^{2+} mobilization, we treated colon muscle cells with the compound FK506, which binds FKBP12 without inhibiting mTOR activity. In young cells FK506 (10 μM) reduced clearly ($p < 0.005$) the responses to bethanechol and caffeine by approximately 50 and 60% respectively (Fig. 3). Similar to rapamycin, FK506 failed to inhibit significantly the responses in aged cells. Therefore, our data strongly suggest that aging alters the FKBP12-mediated facilitation of calcium signal, but not the facilitation induced by mTOR.

In view of our data, and given that a recent report shows an age-related decrease in FKBP12 expression [5], we explored a possible down-regulation of FKBP12 expression in the colonic smooth muscle layer of aged guinea pigs. Figure 4 shows, however, that in the aged colon there is a slight and non-significant ($p < 0.09$) increase in FKBP12 rather than a decrease in the expression of this protein.

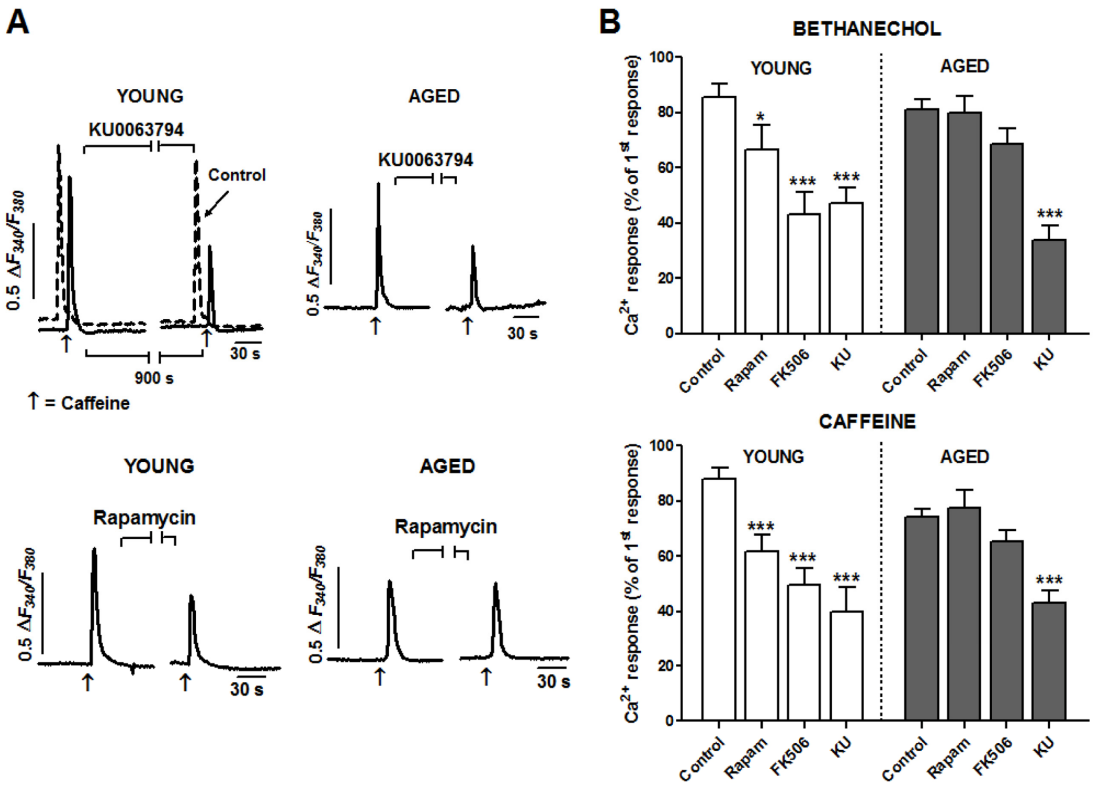

Figure 3. Aging reduces facilitation of Ca^{2+} release by FKBP12 but not by mTOR kinase in smooth muscle cells. (**A**) Cells were stimulated with two pulses of caffeine (10 mM) separated by a 15 min interval to apply inhibitors (indicated by horizontal lines) or normal medium (control trace). For the sake of comparison, the control trace in top left panel is shifted to the left .Traces are representative of the effects of KU0063794 (5 μM) or rapamycin (5 μM) on young (left column) or aged cells (right column). (**B**) Histogram summarizing the effects of the three inhibitors (KU: KU0063794, 5 μM; rapamycin 5 μM; FK506 10 μM) on the bethanechol (0.1 mM) and caffeine (10 mM) evoked Ca^{2+} responses in young and aged cells. Two-ways ANOVA showed significant effect for treatment (bethanechol: $F = 22.4$, $p < 0.005$; caffeine: $F = 21.9$, $p < 0.005$), which was modified by age (bethanechol: $F = 4.0$, $p < 0.01$; caffeine: $F = 5.0$, $p < 0.01$). Asterisks denote significance for planned comparisons between groups of interest. * $p<0.05$, ** $p< 0.01$, *** $p< 0.005$. n= 17-130 cells from 6 (aged) or 8 (young) animals.

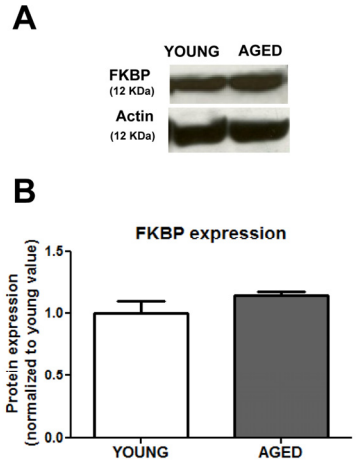

Figure 4. Aging does not change significantly the expression of FKBP12 protein. (**A**) Representative immunoblotts and (**B**) average ± sem values (arbitrary units) (n=6) of the FKBP12 expression in muscular layer of colon from young and aged guinea pigs.

DISCUSSION

The present study shows that in colonic smooth muscle aging enhances the activity of the mTOR pathway and inhibits the mobilization of Ca^{2+} stores, an effect likely associated to the alteration of the facilitating effect of FKBP12 protein on Ca^{2+} mobilization.

Aging is considered a process regulated by longevity pathways among other factors. The mTOR route is an energy-sensing system whose inhibition with rapamycin prolongs lifespan in a number of models, resembling the effect of caloric restriction [3], hitherto the most successful intervention to extend lifespan. We describe here that in resting conditions aged smooth muscle cells show a significant increase in the expression and phosphorylation of mTOR, and in the phosphorylation of its targets p70S6K1 and 4B-EP1. To our knowledge, the only precedent of age-induced mTOR constitutive activity are hippocampal neurons in mice [9] and an enhancement of pS6 phosphorylation in male mice heart compared to females [10]. In human heart no effect of age has been reported [36]. Our findings are in keeping with a previous report showing increased mTOR pathway responses in senescent cultured cells [30]. Data from gene expression studies are conflicting. Rat hippocampus shows enhanced mTOR gene expression ([37], their supplementary data), but recent array studies on the expression of genes linked to the mTOR pathway in blood samples from human cohorts suggest that aging down-regulates this route [38], although this report found no decrease in mTOR gene expression for and Protor1, a protein forming mTOR complexes, was actually up-regulated. Another study in a cohort of long-lived nonagenarians [39] reported that increased longevity was associated to slightly reduced expression of mTOR gene, but the pattern of the gene expression for the mTOR complex proteins was unclear: for mTORC1 complex, protein Raptor was impaired but PRAS40 was enhanced, and for mTORC2 complexes only Protor2 was enhanced. Whether these discrepancies are due to methodological or to tissue-specific differences (see [9]) is unclear and need further investigation. In any case, our findings support the theory that aging is a quasi-programmed process driven by signaling routes [1]: enhanced mTOR levels would drive and accompany aging, so that the more long-lived individuals display lower levels [10; 38]. As inhibition of mTOR had the same influence in aged and young cells, it is unlikely, however, that our finding of an age-mediated decrease of Ca^{2+} release is due to the activation of mTOR pathway.

Given that Ca^{2+} signals are a key regulator in multiple cellular functions, age–related changes in this parameter are relevant for the aging process [15]. For example, age-related changes in Ca^{2+} influx [18; 19; 40] could reduce Ca^{2+} content of the stores, a condition known to alter several cellular functions [41], and can change gene expression [42; 43]. Although in striated muscle the effects of aging on Ca^{2+} signals seem to be relatively settled (enhanced Ca^{2+} sparks and impaired Ca^{2+} release upon stimulation; reviewed in [44]), reports in smooth muscle are very limited and somewhat conflicting. Initial contractility studies proposed enhanced release from intracellular stores in colon and arterial strips [22; 23] but not in gallbladder [45]. Results from $[Ca^{2+}]_i$ determination in isolated cells showed that aging decreases intracellular Ca^{2+} release in arterial and detrusor muscle cells [21; 46] but not in gallbladder cells [18]. We report here that in colonic smooth muscle cells aging impairs IP_3R- and RyR-mediated Ca^{2+} release, suggesting that age influences this signaling system in a tissue-specific way.

At the moment there is very little information regarding the mechanisms causing age-related changes in Ca^{2+} signals. Because its facilitator role in Ca^{2+} release through IP_3R and RyR channels [25; 27-29], modifications of mTOR and FKBP12 function are plausible candidates to mediate the age-induced Ca^{2+} signal changes. While there is no information regarding the mechanism of action of mTOR on Ca^{2+} release, the complex effects of FKBP12 are due to direct interaction with the channels and/or to inhibition of calcineurin, a known regulator of Ca^{2+} release. In fact, we describe here that both IP_3 and RyR signals are impaired by inhibitors targeted to mTOR kinase (KU0063794), to FKBP12 (FK506) or to both (rapamycin, that binds FKBP12 to a regulatory domain of mTOR kinase). Our results agree with a previous work in colon myocytes for IP_3-mediated signals [28], but are opposite for RyR-mediated signal [35]. The discrepancy could be due to differences in the age of the animals (we use 5 months old, more mature than other reports [35]) or to the experimental design (we use single pulses of stimulation instead of choosing cells responding to repetitive stimulation).

The finding that aging does reduce only the effect of the FKBP12-targeted inhibitors rapamycyin and FK506, indicates for the first time that aging could impair Ca^{2+} signals by alteration of the facilitation of Ca^{2+} release by FKBP12. On the contrary, the enhanced activity of mTOR and its facilitating effect on the Ca^{2+} signal in aged cells rules out an involvement of mTOR in the impairment of the Ca^{2+} mobilization. Although a recent report in hippocampus [37] describes that age-related Ca^{2+} deregulation is due to down-regulation of FKBP12, which operates there as an inhibitor of RyR-

mediated Ca^{2+} release [5], we found that FKBP12 expression was not decreased in aged cells. Assuming that FKBP12 interaction to mTOR was normal in aged cells one would expect an inhibition of the signal comparable to that of KU0063794, which was not the case. It his therefore likely that aging simply alters the functional association of FKBP12 with Ca^{2+} release channels and even with mTOR activity. The differences in the effects of experimental manipulations of the mTOR pathway could be due to cell-specific changes in the regulation of aging. For example, in aged hypothalamus only some neuronal populations show enhanced mTOR activity in aged rodents [9]. The exact link between changes in FKBP12 expression and functional facilitation of Ca^{2+} release, out of the scope of the present study, deserves further investigation and could be related to the constitutive activation of mTOR pathway in aged cells.

In conclusion, this study shows that in smooth muscle the mTOR kinase activity is increased by aging, but although mTOR facilitates Ca^{2+} mobilization, aged cells present lower responses to agonists as the result of the loss of FKBP12-induced facilitation of Ca^{2+} release.

METHODS

Animals and cell isolation. Female guinea pigs (Dunkin–Hartley), housed in light (12 h light–dark cycle) and temperature (20ºC) controlled conditions and with *ad libitum* access to water and food, were divided into two groups according to age: young adults (5 months old, average weight 1048.3 ± 82.7 g) and aged (28 month old, average weight 912.9 ± 22.6 g). The experiments were performed according to European guidelines for animal research and approved by the Animal Ethics Committees of the University of Extremadura.

Approximately 20 mg of the circular and longitudinal smooth muscle layer of the colon was cut into small pieces and incubated for 35 min at 37ºC in enzyme solution (ES, for composition see *Solutions and drugs*) supplemented with 1 mg/mL BSA, 1 mg/mL papain and 1 mg/mL dithioerythritol. The tissue was then transferred to fresh ES containing 1 mg/mL BSA, 1 mg/mL collagenase and 100 µm $CaCl_2$ and incubated for 10 min at 37ºC. After washing with cold ES, single smooth muscle cells were mechanically isolated using a fire-polished pipette. Cell suspensions were kept in ES at 4ºC until use, generally within 6 h. Cell viability (90%), as assessed by trypan blue staining was the same in all groups of animals.

Cell loading and [Ca2+]i determination. $[Ca^{2+}]_i$ was determined by epifluorescence microscopy (Eclipse TE2000-S; Nikon, Melville, NY, USA) at room temperature using the ratiometric Ca^{2+} indicator fura-2. Isolated cells were loaded with 4 µM fura 2-AM at room temperature for 15 min. After loading, cells were perfused with Na^+-HEPES solution in the absence or presence of the experimental agents. Cells were illuminated with a monochromator (Optoscan; Cairn Research, Faversham, UK) at 340-380 nm 1 Hz cycles, and the emitted fluorescence was captured with a digital camera (ORCAII-ERG; Hamamatsu Spain, Barcelona, Spain) and recorded using dedicated software (Metafluor; Universal Imaging, Molecular Devices, Downingtown, PA, USA). After background subtraction, fluorescence ratio (F340/F380) was calculated pixel by pixel and used to estimate the changes in $[Ca^{2+}]_i$. A calibration of the ratio for $[Ca^{2+}]_i$ was not performed in view of the many uncertainties related to the binding properties of fura 2 with Ca^{2+} inside of smooth muscle cells.

Analysis of protein expression and phosphorylation by Western blot. Small pieces (~2 mg of dry weight) were quickly frozen, pulverized in liquid nitrogen, extracted in lysis buffer (for composition see *Solutions and drugs*) and then sonicated for 5 s. Lysates were centrifuged at 10000 g for 15 min at 4ºC to remove nuclei and intact cells and the protein concentration was measured. Protein extracts (30 µg) were heat-denatured at 95ºC for 5 min with DTT, electrophoresed on 7.5% and 15% polyacrylamide-SDS gels and then transferred to nitrocellulose membranes. Membranes were blocked for 1 h at room temperature using 10% bovine serum albumin (BSA) and incubated overnight at 4ºC with affinity-purified polyclonal antibodies against mTOR, phospho-mTOR (Ser2448), phospho-4E-BP1, phospho-p70 S6 kinase (Ser371 and Thr389) (Cat#9862, Cell Signaling, Boston, MA, USA) and FKBP12 (#PA1-026A, Thermo Scientific, MA, USA).

A mouse anti-actin antibody (A2066, Sigma-Aldrich) was used to control for protein loading and to normalize expression of proteins of interest. After washing, the membranes were incubated for 1 h at room temperature with anti-mouse (1:10000; Amersham Biosciences, Bucks, UK) or anti-rabbit (1:7000; Santa Cruz Biotechnology) IgG-horseradish peroxidase conjugated secondary antibodies.

Bands were visualized using the supersignal west pico chemiluminescent substrate (Pierce, Rockford, IL, USA), quantified using the software gel-pro analyzer (4.0, Media Cybernetics, Bethesda, MD, USA) and normalized to α-tubulin content. For comparison purposes between young and aged samples, all the α-

tubulin-corrected values were normalized to the average of young samples of the same assay.

In mTOR phosphorylation assay, two similar gels were run and one membrane was incubated with the antibody against the total protein and the other with an antiphospho-protein of interest.

Solutions and drugs. Na^+-HEPES solution (in mM): 10 HEPES, 140 NaCl, 4.7 KCl, 2 $CaCl_2$, 2 $MgCl_2$ and 10 D-glucose (pH 7.3). The Ca^{2+} -free Na^+-HEPES solution included EGTA (1 mm) instead of $CaCl_2$. ES (in mM): 10 HEPES, 55 NaCl, 5.6 KCl, 80 sodium glutamate, 2 $MgCl_2$ and 10 D-glucose (pH 7.3). Lysis buffer (in mM): Tris–HCl 40, NaCl 400, 0.2% SDS and 10% glycerol supplemented with protease and phosphatase inhibitors (4-(2-aminoethyl) benzenesulfonyl fluoride, E-64, bestatin, leupeptin, aprotinin and sodium vanadate).

Drugs and chemicals were obtained from the following sources: bethanechol, caffeine and phosphatase inhbitors from Sigma-Aldrich (Madrid, Spain); fura 2-AM from Molecular Probes (Life Technologies, Madrid, Spain), rapamycin and KU-63794 from Calbiochem (VWR, Madrid, Spain), FK-506 from Cayman (VWR, Madrid, Spain), collagenase from Fluka (Madrid, Spain) and papain from Worthington Biochemical (Lakewood, NJ,USA).

Quantification and statistics. Results are expressed as means ± standard error of the mean (sem) of n cells or blots. $[Ca^{2+}]_i$ responses are expressed as increases in the ratio of fura-2 fluorescence ($\Delta F_{340}/F_{380}$). To compare two groups, paired *t* test was used to assess the effect of treatment. The effects of age and experimental treatments were tested using a two-way analysis of variance, followed by planned comparisons between selected groups. Differences were considered significant at $p < 0.05$.

ACKNOWLEDGEMENTS

Supported by BFU2011-24365, RETICEF RD12/0043/0016, FEDER and Junta de Extremadura (GR10009).

Conflict of Interest Statement

The authors declare no conflicts of interest.

REFERENCES

1. Blagosklonny MV. Answering the ultimate question "What is the Proximal Cause of Aging?". Aging (Albany. NY). 2012; 4:899-916.

2. Blagosklonny MV. Aging: ROS or TOR. Cell Cycle. 2008; 7:3344-3354.

3. Camello PJ, Camello-Almaraz C, and Pozo MJ, Pharmacological approaches to improve ageing. In: Pharmacology,(Ed. Gallelli L), pp. 257-282. InTech, 2012.

4. Laplante M and Sabatini DM. mTOR signaling at a glance. J. Cell Sci. 2009; 122:3589-3594.

5. Gant JC, Chen KC, Norris CM, Kadish I, Thibault O, Blalock EM, Porter NM, and Landfield PW. Disrupting function of FK506-binding protein 1b/12.6 induces the $Ca^{(2)+}$-dysregulation aging phenotype in hippocampal neurons. J. Neurosci. 2011; 31:1693-1703.

6. Hoeffer CA, Tang W, Wong H, Santillan A, Patterson RJ, Martinez LA, Tejada-Simon MV, Paylor R, Hamilton SL, and Klann E. Removal of FKBP12 enhances mTOR-Raptor interactions, LTP, memory, and perseverative/repetitive behavior. Neuron. 2008; 60:832-845.

7. Leontieva OV and Blagosklonny MV. DNA damaging agents and p53 do not cause senescence in quiescent cells, while consecutive re-activation of mTOR is associated with conversion to senescence. Aging (Albany. NY). 2010; 2:924-935.

8. Blagosklonny MV. Cell cycle arrest is not yet senescence, which is not just cell cycle arrest: terminology for TOR-driven aging. Aging (Albany. NY). 2012; 4:159-165.

9. Yang SB, Tien AC, Boddupalli G, Xu AW, Jan YN, and Jan LY. Rapamycin ameliorates age-dependent obesity associated with increased mTOR signaling in hypothalamic POMC neurons. Neuron. 2012; 75:425-436.

10. Leontieva OV, Paszkiewicz GM, and Blagosklonny MV. Mechanistic or mammalian target of rapamycin (mTOR) may determine robustness in young male mice at the cost of accelerated aging. Aging (Albany. NY). 2012; 4:899-916.

11. Toescu EC and Verkhratsky A. Parameters of calcium homeostasis in normal neuronal ageing. J. Anat. 2000; 197 Pt 4:563-569.

12. Gant JC, Sama MM, Landfield PW, and Thibault O. Early and simultaneous emergence of multiple hippocampal biomarkers of aging is mediated by Ca^{2+}-induced Ca^{2+} release. J. Neurosci. 2006; 26:3482-3490.

13. Thibault O, Gant JC, and Landfield PW. Expansion of the calcium hypothesis of brain aging and Alzheimer's disease: minding the store. Aging Cell. 2007; 6:307-317.

14. Toescu EC and Verkhratsky A. Ca^{2+} and mitochondria as substrates for deficits in synaptic plasticity in normal brain ageing. J. Cell Mol. Med. 2004; 8:181-190.

15. Toescu EC and Vreugdenhil M. Calcium and normal brain ageing. Cell Calcium. 2010; 47:158-164.

16. Martinez-Serrano A, Blanco P, and Satrustegui J. Calcium binding to the cytosol and calcium extrusion mechanisms in intact synaptosomes and their alterations with aging. J. Biol. Chem. 1992; 267:4672-4679.

17. Gomez-Pinilla PJ, Pozo MJ, Baba A, Matsuda T, and Camello PJ. Ca^{2+} extrusion in aged smooth muscle cells. Biochem. Pharmacol. 2007; 74:860-869.

18. Gomez-Pinilla PJ, Camello-Almaraz C, Moreno R, Camello PJ, and Pozo MJ. Melatonin treatment reverts age-related changes in Guinea pig gallbladder neuromuscular transmission and contractility. J. Pharmacol. Exp. Ther. 2006; 319:847-856.

19. Xiong Z, Sperelakis N, Noffsinger A, and Fenoglio-Preiser C. Changes in calcium channel current densities in rat colonic

smooth muscle cells during development and aging. Am. J. Physiol. 1993; 265:C617-C625.

20. Howlett SE, Grandy SA, and Ferrier GR. Calcium spark properties in ventricular myocytes are altered in aged mice. Am. J. Physiol Heart Circ. Physiol. 2006; 290:H1566-H1574.

21. Del CC, Ostrovskaya O, McAllister CE, Murray K, Hatton WJ, Gurney AM, Spencer NJ, and Wilson SM. Effects of aging on Ca^{2+} signaling in murine mesenteric arterial smooth muscle cells. Mech. Ageing Dev. 2006; 127:315-323.

22. Rubio C, Moreno A, Briones A, Ivorra MD, D'Ocon P, and Vila E. Alterations by age of calcium handling in rat resistance arteries. J. Cardiovasc. Pharmacol. 2002; 40:832-840.

23. Lopes GS, Ferreira AT, Oshiro ME, Vladimirova I, Jurkiewicz NH, Jurkiewicz A, and Smaili SS. Aging-related changes of intracellular Ca^{2+} stores and contractile response of intestinal smooth muscle. Exp. Gerontol. 2006; 41:55-62.

24. Xiong J, Camello PJ, Verkhratsky A, and Toescu EC. Mitochondrial polarisation status and $[Ca^{2+}]$i signalling in rat cerebellar granule neurones aged in vitro. Neurobiol. Aging. 2004; 25:349-359.

25. Fregeau MO, Regimbald-Dumas Y, and Guillemette G. Positive regulation of inositol 1,4,5-trisphosphate-induced Ca^{2+} release by mammalian target of rapamycin (mTOR) in RINm5F cells. J. Cell Biochem. 2011; 112:723-733.

26. Dargan SL, Lea EJ, and Dawson AP. Modulation of type-1 Ins(1,4,5)P3 receptor channels by the FK506-binding protein, FKBP12. Biochem. J. 2002; 361:401-407.

27. Macmillan D and McCarron JG. Regulation by FK506 and rapamycin of Ca^{2+} release from the sarcoplasmic reticulum in vascular smooth muscle: the role of FK506 binding proteins and mTOR. Br. J. Pharmacol. 2009; 158:1112-1120.

28. Macmillan D, Currie S, Bradley KN, Muir TC, and McCarron JG. In smooth muscle, FK506-binding protein modulates IP3 receptor-evoked Ca^{2+} release by mTOR and calcineurin. J. Cell Sci. 2005; 118:5443-5451.

29. Macmillan D. FK506 binding proteins: Cellular regulators of intracellular Ca(2+) signalling. Eur J. Pharmacol. 2013; 700:181-193.

30. Chen Y, Wang J, Cai J, and Sternberg P. Altered mTOR signaling in senescent retinal pigment epithelium. Invest Ophthalmol. Vis. Sci. 2010; 51:5314-5319.

31. Copp J, Manning G, and Hunter T. TORC-specific phosphorylation of mammalian target of rapamycin (mTOR): phospho-Ser2481 is a marker for intact mTOR signaling complex 2. Cancer Res. 2009; 69:1821-1827.

32. Saitoh M, Pullen N, Brennan P, Cantrell D, Dennis PB, and Thomas G. Regulation of an activated S6 kinase 1 variant reveals a novel mammalian target of rapamycin phosphorylation site. J. Biol. Chem. 2002; 277:20104-20112.

33. Macmillan D, Chalmers S, Muir TC, and McCarron JG. IP3-mediated Ca^{2+} increases do not involve the ryanodine receptor, but ryanodine receptor antagonists reduce IP3-mediated Ca^{2+} increases in guinea-pig colonic smooth muscle cells. J. Physiol. 2005; 569:533-544.

34. Zhang LB and Buxton IL. Muscarinic receptors in canine colonic circular smooth muscle. II. Signal transduction pathways. Mol. Pharmacol. 1991; 40:952-959.

35. Macmillan D, Currie S, and McCarron JG. FK506-binding protein (FKBP12) regulates ryanodine receptor-evoked Ca^{2+} release in colonic but not aortic smooth muscle. Cell Calcium. 2008; 43:539-549.

36. Niemann B, Pan R, Teschner M, Boening A, Silber RE, and Rohrbach S. Age and obesity-associated changes in the expression and activation of components of the AMPK signaling pathway in human right atrial tissue. Exp. Gerontol. 2013; 48:55-63.

37. Kadish I, Thibault O, Blalock EM, Chen KC, Gant JC, Porter NM, and Landfield PW. Hippocampal and cognitive aging across the lifespan: a bioenergetic shift precedes and increased cholesterol trafficking parallels memory impairment. J. Neurosci. 2009; 29:1805-1816.

38. Harries LW, Fellows AD, Pilling LC, Hernandez D, Singleton A, Bandinelli S, Guralnik J, Powell J, Ferrucci L, and Melzer D. Advancing age is associated with gene expression changes resembling mTOR inhibition: evidence from two human populations. Mech. Ageing Dev. 2012; 133:556-562.

39. Passtoors WM, Beekman M, Deelen J, van der BR, Maier AB, Guigas B, Derhovanessian E, van HD, de Craen AJ, Gunn DA, Pawelec G, and Slagboom PE. Gene expression analysis of mTOR pathway: association with human longevity. Aging Cell. 2013; 12:24-31.

40. Xiong Z, Sperelakis N, Noffsinger A, and Fenoglio-Preiser C. Ca^{2+} currents in human colonic smooth muscle cells. Am. J. Physiol. 1995; 269:G378-G385.

41. Mekahli D, Bultynck G, Parys JB, De SH, and Missiaen L. Endoplasmic-reticulum calcium depletion and disease. Cold Spring Harb. Perspect. Biol. 2011; 3.

42. Kuribara M, Eijsink VD, Roubos EW, Jenks BG, and Scheenen WJ. BDNF stimulates Ca^{2+} oscillation frequency in melanotrope cells of Xenopus laevis: contribution of IP3-receptor-mediated release of intracellular Ca^{2+} to gene expression. Gen. Comp Endocrinol. 2010; 169:123-129.

43. Morales S, Diez A, Puyet A, Camello P, Camello-Almaraz C, Bautista J, and Pozo MJ. Calcium controls smooth muscle TRPC gene transcription via the CAMK/calcineurin-dependent pathways. Am. J. Physiol Cell Physiol. 2006.

44. Weisleder N and Ma J. Altered Ca^{2+} sparks in aging skeletal and cardiac muscle. Ageing Res. Rev. 2008; 7:177-188.

45. Ishizuka J, Murakami M, Nichols GA, Cooper CW, Greeley GH, Jr., and Thompson JC. Age-related changes in gallbladder contractility and cytoplasmic Ca^{2+} concentration in the guinea pig. Am. J. Physiol. 1993; 264:G624-G629.

46. Gomez-Pinilla PJ, Pozo MJ, and Camello PJ. Aging differentially modifies agonist-evoked mouse detrusor contraction and calcium signals. Age (Dordr.). 2011; 33:81-88.

Research Paper

Potential anti-aging agents suppress the level of constitutive mTOR- and DNA damage- signaling

H. Dorota Halicka[1], Hong Zhao[1], Jiangwei Li[1], Yong-Syu Lee[2], Tze-Chen Hsieh[2], Joseph M.Wu[2], and Zbigniew Darzynkiewicz[1]

[1] Brander Cancer Research Institute, Department of Pathology, New York Medical College, Valhalla, NY 10595, USA
[2] Department of Biochemistry and Molecular Biology, New York Medical College, Valhalla, NY 10595, USA

Key words: *H2AX phosphorylation, ROS, ribosomal protein S6, calorie restriction, metformin, rapamycin, 2-deoxyglucose, rapamycin, berberine, vitamin D3, resveratrol, aspirin, replication stress, senescence, cell cycle, 4EBP1*
Received: *12/6/12; Accepted: 12/28/12; Published: 12/30/12* doi:10.18632/aging.100521
Correspondence to: *Zbigniew Darzynkiewic, PhD;* ***E-mail:*** *darzynk@nymc.edu*

Abstract: Two different mechanisms are considered to be the primary cause of aging. Cumulative DNA damage caused by reactive oxygen species (ROS), the by-products of oxidative phosphorylation, is one of these mechanisms (ROS concept). Constitutive stimulation of mitogen- and nutrient-sensing mTOR/S6 signaling is the second mechanism (TOR concept). The flow- and laser scanning- cytometric methods were developed to measure the level of the constitutive DNA damage/ROS- as well as of mTOR/S6- signaling in individual cells. Specifically, persistent activation of ATM and expression of γH2AX in untreated cells appears to report constitutive DNA damage induced by endogenous ROS. The level of phosphorylation of Ser235/236-ribosomal protein (RP), of Ser2448-mTOR and of Ser65-4EBP1, informs on constitutive signaling along the mTOR/S6 pathway. Potential gero-suppressive agents rapamycin, metformin, 2-deoxyglucose, berberine, resveratrol, vitamin D3 and aspirin, all decreased the level of constitutive DNA damage signaling as seen by the reduced expression of γH2AX in proliferating A549, TK6, WI-38 cells and in mitogenically stimulated human lymphocytes. They all also decreased the level of intracellular ROS and mitochondrial trans-membrane potential ΔΨm, the marker of mitochondrial energizing as well as reduced phosphorylation of mTOR, RP-S6 and 4EBP1. The most effective was rapamycin. Although the primary target of each on these agents may be different the data are consistent with the downstream mechanism in which the decline in mTOR/S6K signaling and translation rate is coupled with a decrease in oxidative phosphorylation, (revealed by ΔΨm) that leads to reduction of ROS and oxidative DNA damage. The decreased rate of translation induced by these agents may slow down cells hypertrophy and alleviate other features of cell aging/senescence. Reduction of oxidative DNA damage may lower predisposition to neoplastic transformation which otherwise may result from errors in repair of DNA sites coding for oncogenes or tumor suppressor genes. The data suggest that combined assessment of constitutive γH2AX expression, mitochondrial activity (ROS, ΔΨm) and mTOR signaling provides an adequate gamut of cell responses to evaluate effectiveness of gero-suppressive agents.

INTRODUCTION

The cumulative DNA damage caused by reactive oxygen species (ROS), by-products of oxidative phosphorylation, for long time has been considered to be a key factor contributing both to cell aging as well as predisposing to neoplastic transformation [1-12]. Oxidative DNA damage generates significant number of DNA double-strand breaks (DSBs), the potentially deleterious lesions. DSBs can be repaired either by the homologous recombination or nonhomologous DNA-end joining (NHEJ) mechanism. Recombinatorial repair which uses newly replicated DNA as a template restores DNA rather faithfully. It can take place however when cells have already the template, namely during late-S and G_2 phase. In the cells that lack a template (G_1, early-S) DNA repair relies on the NHEJ which is error- prone due to a possibility of a deletion or rearrangement

of some base pairs [13-17]. If the erroneously repaired DSBs are at sites of oncogenes or tumor suppressor genes this may result in somatic mutations that predispose cell to oncogenic transformation. Oxidative damage of telomeric DNA may lead to dysfunction of telomeres thereby driving cells to undergo replicative senescence [18-30].

Whereas DNA damage induced by endogenous (and exogenous) oxidants may indeed significantly contribute to cancer development its role as being the key factor accountable either for cellular or organismal aging is debatable [31-40]. There is growing body of evidence in support of the notion that the primary culprit of aging is the constitutive stimulation of the mitogen- and nutrient-sensing signaling pathways. Activation of these pathways enhances translation, leads to cell growth in size/mass and ultimately results in cell hypertrophy and senescence. Among these culprit pathways the mammalian target of rapamycin (mTOR) and its downstream target S6 protein kinase (S6K) play the key role [41-49]. Constitutive replication stress likely resulting from the ongoing oxidative DNA damage when combined with activation of mTOR/S6K appears to be the driving force leading to aging and senescence both at the cellular as well as organismal level [43-51].

We have recently reported that constitutive DNA damage signaling (CDDS) observed in the untreated normal or tumor cells, assessed as the level of expression of histone H2AX phosphorylated on Ser139 (γH2AX) and of activated (Ser1981 phosphorylated) *Ataxia Telangiectasia mutated* protein kinase (ATM), is an indication of the ongoing DNA damage induced by endogenous ROS [52-55]. These phosphorylation events were detected with phospho-specific antibodies (Ab) and measured in individual cells by flow- or laser scanning- cytometry. Using this approach we have assessed several agents reported to have anti-oxidant and DNA-protective properties with respect to their ability to attenuate the level of CDDS [52-58]. In the present study we test effectiveness of several reported anti-aging modalities to attenuate the level of CDDS in individual TK6 and A549 tumor cell lines as well as in WI-38 and mitogenically stimulated normal lymphocytes.

In parallel, we also assess their effect on the level of constitutive state of activation of the critical mTOR downstream targets. Specifically, using phospho-specific Abs detecting activated status of ribosomal protein S6 (RP-S6) phosphorylated on Ser235/236 we measure effectiveness of these gero-suppressive agents along the mTOR/S6K signaling. We have also tested effects of these agents on the level of endogenous reactive oxidants as well as mitochondrial electrochemical potential ΔΨm. The following agents, reported as having anti-aging and/or chemopreventive properties, were chosen in the present study: 2-deoxy-D-glucose (2dG) [59-62], metformin (MF) [63-71], rapamycin (RAP) [72-80], berberine (BRB) [81-85], vitamin D3 (Vit. D3) [86- 91], resveratrol (RSV) [92-97] and acetylsalicylic acid (aspirin) (ASA) [98-103].

RESULTS

Fig. 1 illustrates the effect of exposure of human lymphoblastoid TK6 cells for 24 h to the investigated presumed anti-aging agents on the level of constitutive expression of γH2AX. Consistent with our prior findings [52-54] the expression γH2AX in S and G_2M cells is distinctly higher than in the cells of G_1 phase. This is the case for both, the untreated (Ctrl) cells as well as the cells treated with these agents. It is also apparent that exposure of cells to each of the studied drugs led to the decrease in expression of γH2AX in all phases of the cell cycle. In most treated cells, however, the decline in the mean expression γH2AX was somewhat more pronounced in the S- compared to G_1 - or G_2M- phase cells. Analysis of DNA content frequency histograms reveals that the 24 h treatment with most of the drugs had no effect on the cell cycle distribution. The exception are the cells treated with 50 nM RP which show about 50% reduction in frequency of cells in S and G_2M which would indicate partial cells arrest in G_1 phase of the cell cycle. It should be noted that exposure of cells to these agents for 4 h led to rather minor (<15%) decrease in expression of γH2AX whereas the treatment for 48 h had similar effect as for 24 h (data not shown).

The effect of exposure of TK6 cells to the investigated gero-suppressive agents on state of phosphorylation of ribosomal S6 protein is shown in Fig. 2. Unlike expression of γH2AX the level of phosphorylation of RP-S6 shows no significant cell cycle phase-related differences, neither in control nor in the treated cultures. Somewhat higher expression of RP-$S6^P$ in S- and G_2M- compared to G_1- cells is proportional to an overall increase in cell size during cell cycle progression. It is quite evident however that the treatment with each of these anti-aging agents led to a decrease in the level of phosphorylation of S6 protein. The most dramatic decrease (>95%) was seen in the cells treated with RAP. The cells treated with 2dG showed the smallest (32-38%) decrease. There was no evidence that treatment of TK6 cells with all these drugs for 4 h had any distinct effect on the cell cycle progression as detected by analysis of DNA content frequency histograms (not shown).

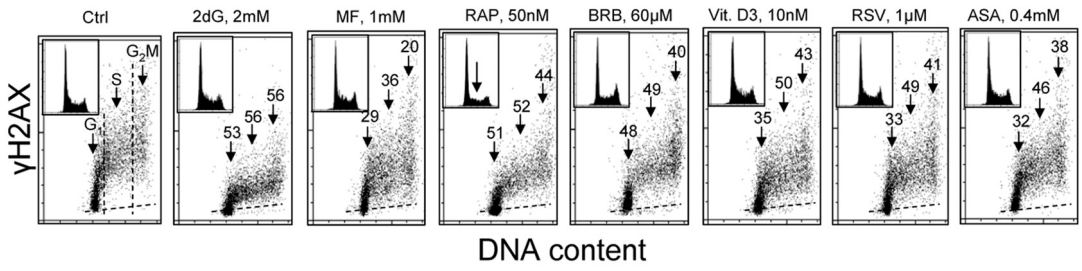

Figure 1. Effect of exposure of TK6 cells to different presumed anti-aging drugs on the level of constitutive expression of γH2AX. Exponentially growing TK6 cells were untreated (Ctrl) or treated with the respective agents for 24 h at concentrations as shown. Expression of γH2AX in individual cells was detected immunocytochemically with the phospho-specific Ab (AlexaFluor647), DNA was stained with DAPI; cellular fluorescence was measured by flow cytometry. Based on differences in DNA content cells were gated in the respective phases of the cell cycle, as marked by the dashed vertical lines. The percent decrease in mean fluorescence intensity of the treated cells in particular phases of the cell cycle, with respect to the respective untreated controls, is shown above the arrows. Inserts present DNA content frequency histograms from the individual cultures. The dashed skewed lines show the background level, the mean fluorescence intensity of the cells stained with secondary Ab only.

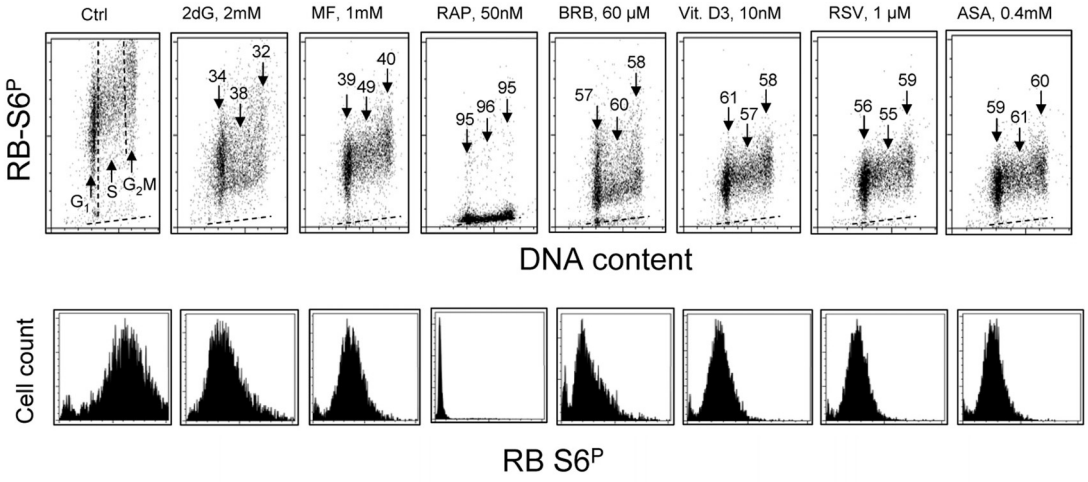

Figure 2. **Effect of treatment of TK6 cells with different presumed anti-aging drugs for 4 h on the level of constitutive phosphorylation of ribosomal protein S6 (RP-S6).** Exponentially growing TK6 cells were untreated (Ctrl) or treated with the respective agents at concentrations as shown. Phosphorylation status of ribosomal S6 protein was detected immunocytochemically with the phospho-specific Ab (AlexaFluor647), DNA was stained with DAPI; cellular fluorescence was measured by flow cytometry. **Top panels:** Based on differences in DNA content cells were gated in the respective phases of the cell cycle, as marked by the dashed vertical lines (Ctrl). The percent decrease in mean fluorescence intensity of the treated cells in particular phases of the cell cycle, with respect to the to the same phases of the untreated cells, is shown above the arrows. The dashed skewed lines show the background level, the mean fluorescence intensity of the cells stained with secondary Ab only. **Bottom panels:** Single parameter frequency histograms showing expression of phosphorylated ribosomal S6 protein (RB-$S6^P$) in all (G_1+S+G_2M) cells of the respective cultures.

Fig. 3 presents the effect of exposure of TK6 cells to MF, RAP or RSV at somewhat lower concentration for 24 h on the level of expression of RP-S6^{P}. Compared with cells exposed for 4 h (Fig. 1) the effect of MF, even at the lower concentration (50 μM), was more pronounced after 24 h. Also, after that time of exposure, more pronounced was the effect of RAP and RSV.

Analysis of the DNA content frequency histograms indicates that neither 50 – 500 μM MF nor RSV had an effect on the cell cycle progression. However, exposure to 0.1 μM RAP (similar to 50 nM, see Fig. 1) resulted in about 50% decrease in frequency of S and G_2M cells (insets, marked by arrows).

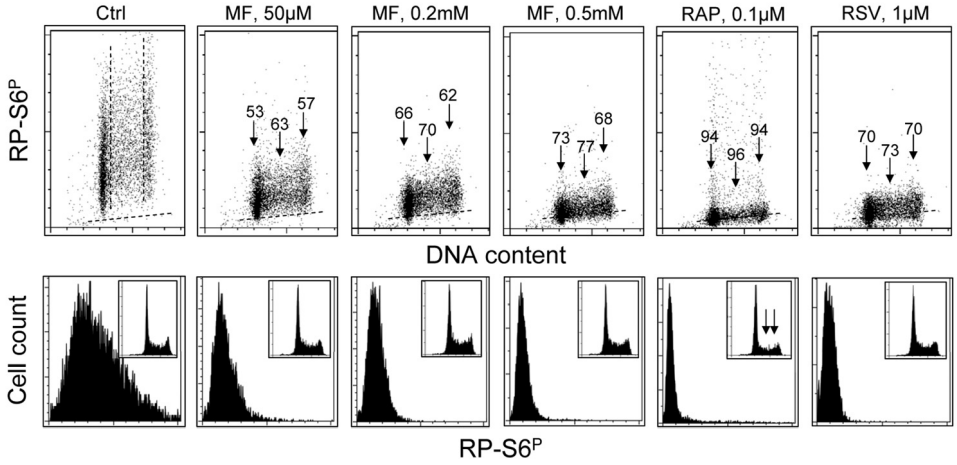

Figure 3. Effect of treatment of TK6 cells with MF, RAP or RSV for 24 h on the level of constitutive phosphorylation of S6 protein. TK6 cells were untreated (Ctrl) or treated with different concentrations of MF as well as with RAP or RSV for 24 h. Phosphorylation status of S6 was assessed as described in legend to Fig. 2. **Top panels:** The percent decrease in mean fluorescence intensity of the drug-treated cells in particular phases of the cell cycle is shown above the arrows. **Bottom panels:** Frequency histograms showing expression of RP-S6^{P} in all cells of the respective cultures. Insets show cellular DNA content histograms of cells in these cultures.

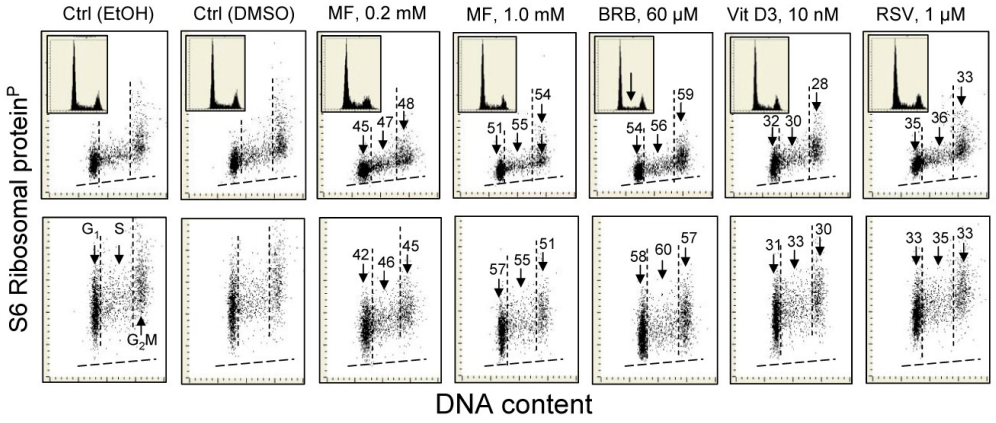

Figure 4. Reduction of the level of constitutive expression of RP-S6^{P} in A549 cells exposed to MF, BRB, Vit. D3 or RSV for 24 h. Exponentially growing in chamber slides A549 cells, were treated with the respective agents and their fluorescence was measured the laser scanning cytometry (LSC).[75] Top panels show RP-S6^{P} immunofluorescence integrated over the nuclei (reporting expression of RP-S6^{P} in the cytoplasm located over and below the nucleus); bottom panels present RP-S6^{P} immunofluorescence integrated over the cytoplasm aside of the nucleus. The percent decrease in expression of RP-S6^{P} in cells in particular phases of the cell cycle (mean values) is shown above the arrows. Because stock solutions of some of these agents were made in DMSO, other in MeOH or EtOH, the equivalent quantities of these solvents were included in the respective control culture and the percent decrease shown in the panels refers to the decrease compared to these controls shown are the cells from EtOH and DMSO containing controls. The insets present DNA content frequency histograms from the respective cultures.

The effect of some of these gero-suppressive drugs was also studied on human pulmonary adenocarcinoma A549 cells (Fig. 4). These cells grow attached and their fluorescence intensity was measured by imaging cytometry (laser scanning cytometer; LSC) [104]. The decrease in expression of RP-S6^{P} was seen in the cells treated with each of the drugs. The effect was essentially of similar degree whether measured in cytoplasm over- and underlying the nucleus (Fig. 4 top panels) or in the cytoplasm at the nuclear periphery (bottom panels). The most pronounced decrease was induced by BRB. Also affected was the cell cycle progression, as evidenced by the decline in frequency of S-phase cells on the DNA histogram in BRB treated cells (inset, marked by arrow).

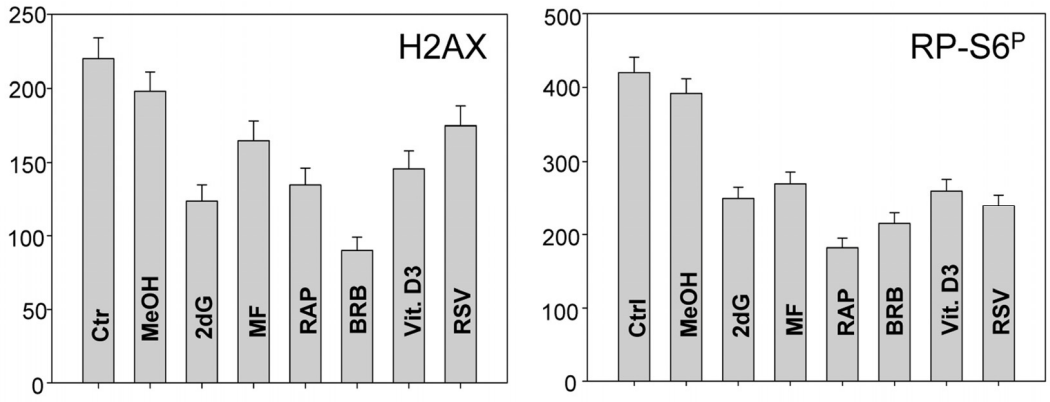

Figure 5. Effect of treatment of WI-38 cells with 2dG, MF, RAP, BRB, Vit. D3 or RSV for 24 h on the level of constitutive expression of γH2AX (left panel) and RP-S6^{P} (right panel). Exponentially growing cells, were treated with the respective agents at concentrations as shown in Figs. 1 and 2, RP-S6^{P} was detected immunocytochemically and cell fluorescence was measured with the laser scanning cytometry (LSC). The bar graphs present the mean fluorescence intensity measured as an integral over the nucleus (γH2AX) or over cytoplasm (PR-S6^{P}).

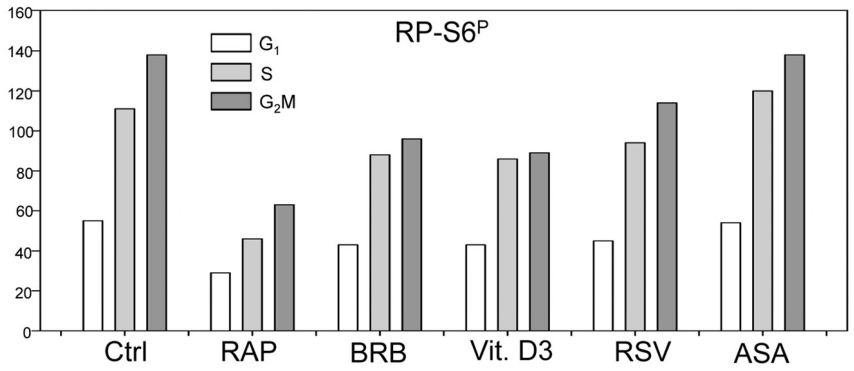

Figure 6. Effect of treatment of mitogenically stimulated human lymphocytes with RAP, BRB, Vit. D3, RSV or ASA for 4 h on the level of constitutive expression of RP-S6^{P}. Peripheral blood lymphocytes were mitogenically stimulated with phytohemagglutinin (PHA) for 72 h, the cells were then treated with the respective drugs at concentrations as shown in Figs. 1 and 2 for 4 h, RP-S^{6} was detected immunocytochemically and cellular fluorescence measured by flow cytometry. The bar graphs present the mean values (+SD) of RP-S6^{P} immunofluorescence for G_1, S and G_2M cell subpopulations identified by differences in DNA content (intensity of DAPI fluorescence).

In addition to tumor cell lines we have also tested effects of the presumed gero-suppressive agents on non-tumor cells. Fig. 5 illustrates their effect on the WI-38 cells and Fig. 6 on mitogenically-stimulated human lymphocytes. A decrease in expression of γH2AX was observed in WI-38 cells treated with each of the tested agents, the most pronounced reduction (>50%) showed cells treated with BRB while the least affected (<10%) were cells growing in the presence of RSV. A reduction in the level of phosphorylated RB-S6 was also evident in WI-38 cells exposed to each of these agents, the most pronounced (>50%) after treatment with RAP. Because stock solutions of some of these agents were made in DMSO or MeOH equivalent quantities of these solvents were included in the respective control cultures. A minor suppressive effect of MeOH on expression of γH2AX and RB-S6^{P} was observed (Fig. 5). Likewise, DMSO exerted also minor (~5%) but repeatable suppressive effect (not shown). As is evident RAP, BRB, Vit. D3 and RSV reduced the level of RP-S6^{P} in mitogenically stimulated human lymphocytes, in all phases of the cell cycle, while the effect of ASA on these cells was minimal (Fig. 6).

To confirm the findings obtained by the flow- and laser scanning- cytometry based on measurement of individual cells we assessed effects of the gero-suppressive agents by measurement mTOR signaling in bulk, by western blotting. In this experiment, having available phospho-specific Abs that detect phosphorylation of mTOR, RP-S6 and the eukaryotic translation initiation factor 4E-binding protein (4EBP1) applicable to western blotting (not yet available for cytometry) we have been able to test effects of the studied gero-preventive agents on the level of constitutive phosphorylation of these proteins as well. As is evident in Fig. 7 and Table 1 exposure of TK6 cells to the gero-preventive agents lowered the level of phosphorylation status of mTOR, as well as its downstream targets RP-S6 and 4EBP1. The most pronounced effect was seen in the case of RAP, BRB and 2dG which lowered expression of RP-S6^{P} by 95%,78 and 70%, respectively. RAP, BRB and 2dG were also quite effective in lowering the level of 4EBP1^{P}, by 52%, 51% and 51%.

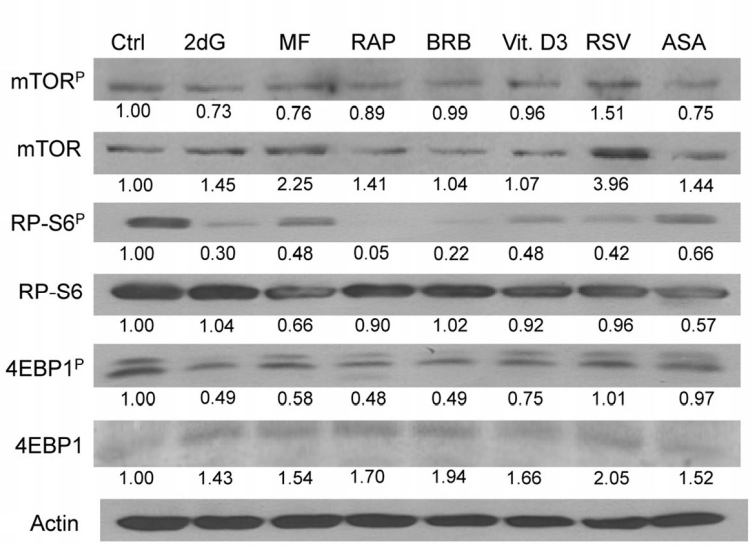

Figure 7. Effect of the studied gero-preventive agents on constitutive level of expression of mTOR-Ser2448^{P}, RP-S6-Ser235/236^{P} and 4EBP1-Ser65^{P} and their corresponding unphosphorylated forms in TK6 cells, detected by western blotting. TK6 cells were exposed to the studied agents at concentrations as shown in Figs 1 and 2 for 4 h. The protein expression level were determined by western blot analysis and the intensity of the specific immunoreactive bands were quantified by densitometry and normalized to actin (loading control). The numbers indicate the n-fold change in expression of the respective phospho-proteins in the drug-treated cultures with respect to the untreated cells (Ctrl).

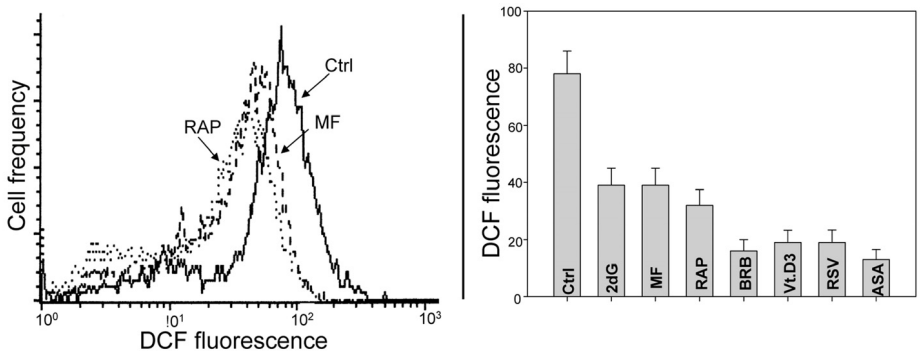

Figure 8. Effects of the studied gero-preventive agents on the intercellular level of ROS. TK6 cells, untreated (Ctrl) or treated for 24 h with the investigated agents, were exposed for 30 min to H_2DCF-DA and their fluorescence intensity was measured by flow cytometry. The cell-permeant non-fluorescent H_2DCF-DA upon cleavage of the acetate moiety by intercellular esterases and oxidation by ROS is converted to strongly fluorescent DCF and thus reports the ROS abundance. Left panel shows the frequency histograms of the untreated (Ctrl) as well MF and RAP-treated cells (note exponential scale of the DCF fluorescence). Right panel presents the mean values (+SD) of DCF fluorescence of the untreated (Ctrl) and treated cells.

Table 1. Effect of the studied gero-preventive agents on constitutive level of expression of mTOR-Ser2448^P, RP-S6-Ser235/236^P and 4EBP1-Ser65^P and their corresponding unphosphorylated forms, detected by western blotting (Fig. 7)

Agent	Ctrl	2dG	MF	RAP	BRB	Vit. D3	RSV	ASA
mTOR^P	1.00	0.73	0.76	0.89	0.99	0.96	1.51	0.75
m-TOR	1.00	1.45	2.25	1.41	1.04	1.07	3.96	1.44
RATIO	**1.00**	**0.50**	**0.34**	**0.63**	**0.95**	**0.90**	**0.38**	**0.52**
RP-S6^P	1.00	0.30	0.48	0.05	0.22	0.48	0.42	0.66
S6	1.00	1.04	0.66	0.9	1.02	0.92	0.96	0.57
RATIO	**1.00**	**0.29**	**0.73**	**0.06**	**0.22**	**0.52**	**0.44**	**1.16**
4EBP1^P	1.00	0.49	0.58	0.48	0.49	0.75	1.01	0.97
4EBP1	1.00	1.43	1.54	1.7	1.94	1.66	2.05	1.52
RATIO	**1.00**	**0.38**	**0.38**	**0.28**	**0.25**	**0.45**	**0.45**	**0.64**

The numbers indicate the change in expression of the respective proteins in the dug-treated cultures with respect to the untreated ones. Densitometric quantification of phosphorylated and total proteins for mTOR, RP-S6 and 4EBP1 are presented as the ***ratio*** of actin-normalized phosphorylated to total protein level of expression (**Bold font**).

Most interesting, however, were the results reporting effects of the studied drugs on the total mTOR, RP-S6 and 4EBP1 protein content and on the ratios of the phosphorylated protein fractions to the total content of the respective proteins (Table 1). These data show that exposure of cells to each drug led to a distinct up-regulation of mTOR and 4EBP1 expression. This was not the case of RP-S6, which, with an exception of 2dG and BRB, showed a minor decline. However, compared with the apparent increase of total proteins content, the level of the phosphorylated fractions of the respective proteins was more severely reduced. This over-compensated the upregulation and is expressed as the reduction of the ratio of phosphorylated to total content of the respective proteins. In the case of RP-S6 and 4EBP1, the downstream effectors of mTOR and the agents directly affecting the translation rate, the most effective was BRB and RAP, reducing proportion of the phosphorylated to total protein content by 75% and 72% respectively (Table 1).

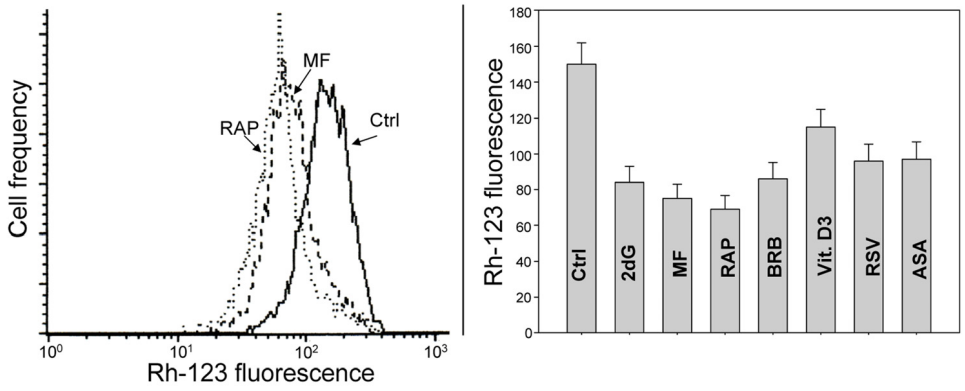

Figure 9. Effect of the studied gero-preventive agents on the mitochondrial transmembrane potential (ΔΨm). TK6 cells, untreated (Ctrl) or treated for 24 h with the investigated agents were exposed for 30 min to the mitochondrial probe rhodamine 123 (Rh-123) and their fluorescence intensity was measured by flow cytometry. Left panel shows the frequency histograms of the untreated (Ctrl) as well MF and RAP-treated cells (note exponential scale of the DCF fluorescence). Right panel presents the mean values (+SD) of Rh-123 fluorescence of the investigated cells.

In other set of experiments we assessed the effect of the studied gero-preventive agents on the level of endogenous ROS. As is evident in Fig. 8 exposure of TK6 cells to each of these agents led to a marked reduction of cells ability to oxidize H_2DCF-DA; its oxidation by ROS results in formation of the strongly fluorescent DCF which is considered to be a marker of ROS abundance. In this respect more effective appeared to be BRB, Vit. D3, RSV and ASA compared to RAP, MF or 2dG.

Fig. 9 illustrates changes in electrochemical transmembrane potential of mitochondria detected by cells capability to accumulate the mitochondrial probe rhodamine 123 (Rh-123) in TK6 cells treated with the investigated gero-preventive agents. The data show a reduction in the ability to accumulate Rh-123 in cells treated with each of these agents, the most pronounced in the case of treatment with RAP.

DISCUSSION

In the prior studies we have already observed that MF at concentrations 0.1 mM – 20 mM [55] and Vit. D (2 nM - 10 nM) [56] effectively reduced constitutive level of H2AX-Ser139 and ATM-Ser1981 phosphorylation. In the present study all seven agents, all reportedly having anti-aging and/or chemopreventive properties, including MF and Vit D3[59-103], have been tested with respect of their ability to affect both the level of constitutive DNA damage signaling as monitored γH2AX expression as well as constitutive level of phosphorylation of ribosomal S6 protein (RP-S6^P). The data show that each of the drugs reduced both, the level of phosphorylation of both H2AX on Ser139 and RP-S6 on Ser235/236. RP-S6, a component of the 40S ribosomal subunit and the most downstream effector of mTOR signaling, is directly involved in regulation of translation [46] and considered to be a determinant of cell size [105,106]. As is evident from the western blotting data (Fig. 7) with an exception of RSV all the studied drugs reduced also the level of phosphorylation of mTOR, RP-S6 and 4EBP1. The latter protein is also considered to be a critical regulator of translation and cell size determinant [105-108].

Analysis of the mTOR vs. mTOR^P, RP-S6 vs. RP-S6^P and 4EBP1 vs. 4EBP1^P revealed up-regulation of mTOR and 4EBP1 in cells treated with each of the studied drugs (Table 1). The increase of total content of these proteins was overcompensated by the reduction in the extent of their phosphorylation, which led to decrease in the ratios of mTOR^P/mTOR, RP-S6^P/RP-S6 and 4EB1^P/4EB1. The upregulation of these proteins was unexpected but it suggests that the reduction of their phosphorylation status by the studied drugs may trigger compensatory synthesis (or reduced turnover rate) that leads to increase in their content. The distinctly reduced ratios of mTOR^P/mTOR, RP-S6^P/RP-S6 and 4EB1^P/4EB1, however, may provide a novel biomarker useful to assess the potential mTOR-inhibitory activities that relate to reduction of translation rate, cell size and thus may be of value in assessing anti-aging properties of the studied agents.

The reduction of RP-S6 phosphorylation by each of the gero-suppressive drugs was presently observed in all types of the cells, including tumor TK6 (Fig. 1-3,7) and A549 (Fig. 4) cell lines as well as in normal WI-38 (Fig. 5) and mitogenically stimulated human lymphocytes (Fig. 6). The results obtained by flow and laser scanning cytometry were confirmed by measurement in bulk, by western blotting. The western blotting approach allowed us also to measure phosphorylation level of mTOR and 4EBP1 to which the commercially available phospho-specific Abs are not fully applicable for flow or laser scanning cytometry. The cytometric approach has an advantage that it provides information regarding the cell cycle phase specificity of expression of γH2AX or RP-S6. Furthermore, the cytometric approach has no potential risk of an artifact that the level of phosphorylation of the studied proteins may be altered as a result of disruption of cell integrity in preparation for blotting, which may provide contact of these proteins with active phosphatases and kinases. We observed, for example that when inhibitors of phosphatases were not rigorously used during cell preparation for western blotting the results (not shown) were entirely different than in Fig. 7.

According to the mTOR concept of the mechanism of aging the observed reduction of the level of phosphorylation of mTOR, 4EBP1 and RP-S6 by the studied agents would be consistent with their reported anti-aging properties. The gero-preventive mechanism of these agents thus would be similar to that of the calorie restriction which was definitely proven to extent life span of a variety of organisms [94-97,109].

Parallel to the reduction of constitutive mTOR/S6 signaling each of the investigated gero-suppressive agents also reduced CDDS, as seen by the decline in γH2AX expression (Fig. 1). This corresponding response to these agents, concurrently by both the DNA damage- and mTOR- signaling pathways, suggests on mechanistic association between these two pathways that may converge on the aging-related processes. One of the mechanisms linking these pathways is straightforward as it may involve a decrease of intensity of oxidative phosphorylation in mitochondria. Namely, because the declined translation rate requires less energy the intensity of oxidative phosphorylation that generates ROS is reduced which results in attenuation of CDDS. Consistent with this mechanism is our prior observation that exposure of lymphocytes to Vit. D3 led to a three-fold decline in abundance of ROS [55]. Likewise, treatment of TK6 cells with MF resulted in a significant decrease in the level of ROS [56]. In the present study we confirmed these earlier findings as we observed that all studied drugs markedly lowered abundance of ROS in TK6 cells (Fig. 8). Accordingly, mitogenic stimulation of lymphocytes known to dramatically enhance transcription and translation rates [110,111] also was seen to boost production of ROS and augment CDDS [112]. There are numerous linkages connecting DNA damage response with mTOR/RP-S6 pathways, primarily involving p53 signaling [113-118]. Of interest, and confirming the involvement of mitochondrial pathways in response to the studied gero-preventive agents, is also the observation that exposure of cells to each of them resulted in a decreased mitochondrial transmembrane potential (ΔΨm). The latter was detected by reduced cells capability to bind rhodamine 123 (Fig. 9), the probe known to be the marker of energized mitochondria [119-121].

Unlike constitutive phosphorylation of RP-S6 which was unrelated to the cell cycle phase, H2AX phosphorylation was cell cycle phase specific, distinctly higher in S- and G_2M- than in G_1- cells. This suggests that DNA replication stress may be a contributing factor to the observed CDDS. DNA lesions resulting from oxidative DNA damage caused by endogenous ROS could be responsible for the replication stress. As mentioned in the Introduction constitutive replication stress when concurrent with mTOR/S6K signaling is considered to be the predominant factor leading to aging and senescence. Thus, the present data that show that the investigated gero-preventive drugs suppress both, the mTOR/RP-S6 signaling and CDDS, would be consistent with the mechanism that involves attenuation of DNA replication stress.

Whereas mTOR/S6 signaling is the primary cause of aging and induction of premature cell senescence the DNA damage by reactive oxidants, since it induces DSBs which cannot always be faithfully repaired, predisposes to neoplastic transformation [1-7]. It is expected therefore that the anti-aging agents that reduce CDDS would have cancer preventive properties as well. Indeed such chemo-preventive properties have been described for each of the presently investigated drugs [122-128]. The present data indicate that the combined analysis of: (i) CDDS measured by γH2AX expression, (ii) mitochondria activity (ROS, ΔΨm) and (iii) mTOR signaling (mTOR, S6K, 4EBP1 phosphorylation) in individual cells [129] may provide an adequate gamut of cell responses to evaluate potential gero- or chemo-preventive properties of suspected agents.

MATERIALS AND METHODS

Cells, Cell Treatment. Human lung carcinoma A549 cells, diploid lung WI-38 fibroblasts and lympho-blastoid TK6 cells were obtained from American Type

Culture Collection (ATCC CCL-185, Manassas, VA). Human peripheral blood lymphocytes were obtained by venipuncture from healthy volunteers and isolated by density gradient centrifugation. A549 cells were cultured in Ham's F12K, TK6, WI-38 and lymphocytes were cultured in RPMI 1640 with 2 mM L-glutamine, 1.5 g/L sodium bicarbonate and 10% fetal bovine serum (GIBCO/Invitrogen, Carlsbad, CA). Adherent A549 and WI-38 cells were grown in dual-chambered slides (Nunc Lab-Tek II), seeded with 10^5 cells/ml suspended in 2 ml medium per chamber. TK6 cells and lymphocytes were grown in suspension; lymphocyte cultures were treated with the polyvalent mitogen phytohemaglutinin (Sigma /Aldrich; St Louis, MO) as described [36]. MF (1,1-dimethylbiguanide) was obtained from Calbiochem, La Jolla, CA, 2dG, RAP, BRB, RSV and ASA from Sigma-Aldrich. The active form of vitamin D3 (1,25-dihydroxyvitamin D3) was kindly provided by Dr Milan Uskokovic [56]. Stock solutions of some of these agents were prepared either in DMSO, MeOH or EtOH as indicated by the vendor. The cells, during exponential phase of growth were treated with these agents, at concentrations and for duration as indicated in the figures or figure legends. Respective control cultures were treated with the equivalent volumes of solvents used for stock solutions. After exposure to the gero-preventive agents the cells were rinsed with phosphate buffered salt solution (PBS) and fixed in 1% methanol-free formaldehyde (Polysciences, Warrington, PA) for 15 min on ice. The cells were then transferred to 70% ethanol and stored at -20 ^{o}C for up to 3 days until staining.

Immunocytochemical Detection of γH2AX and RP-S6^{P}. After fixation the cells were washed twice in PBS and with 0.1% Triton X-100 (Sigma-Aldrich) in PBS for 15 min and with a 1% (w/v) solution of bovine serum albumin (BSA; Sigma-Aldrich in PBS for 30 min to suppress nonspecific antibody (Ab) binding. The cells were then incubated in 1% BSA containing a 1:300 dilution of phospho-specific (Ser139) γH2AX mAb (Biolegend, San Diego, CA) and/or with a 1: 200 dilution of phosphospecific (Ser235/236) RP-S6 Ab (Epitomics, Burlingame, CA) at 4^{o}C overnight. The secondary Ab was tagged with AlexaFluor 488 or 647 fluorochrome (Invitrogen/Molecular Probes, used at 1:100 dilution in 1% BSA). The incubation was at room temperature for 45 min. Cellular DNA was counterstained with 2.8 μg/ml 4,6-diamidino-2-phenylindole (DAPI; Sigma-Aldrich) at room temperature for 15 minutes. Each experiment was performed with an IgG control in which cells were labeled only with the secondary AlexaFluor 488 Ab, without primary Ab incubation to estimate the extent of nonspecific adherence of the secondary Ab to the cells. The fixation, rinsing and labeling of A549 and WI-38cells was carried out on slides, and lymphocytes and TK6 cells in suspension. Other details have been described previously [53-56].

Detection of ROS and Mitochondrial Transmembrane Potential ΔΨm. Untreated cells as well as the gero-protective agents drugs-treated TK6 cells were incubated 60 min with 10 μM 2',7'-dihydrodichlorofluorescein- diacetate (H_2DCF-DA) (Invitrogen/Molecular Probes) at 37°C. Cellular green fluorescence was then measured by flow cytometry. Following oxidation by ROS and peroxides within cells the non-fluorescent substrate H_2DCF-DA is converted to the strongly fluorescent derivative DCF [97]. Mitochondrial potential ΔΨm was assessed by exposure of cells in tissue culture to 1 μM rhodamine 123 (Rh-123; Invitrogen/Molecular Probes) for 30 min prior to measurement of their fluorescence.

Analysis of Cellular Fluorescence**.** *A549 and WI-38 cells:* Cellular immunofluorescence representing the binding of the respective phospho-specific Abs as well as the blue emission of DAPI stained DNA was measured by Laser Scanning Cytometry (LSC) [131] (iCys; CompuCyte, Westwood, MA) utilizing standard filter settings; fluorescence was excited with 488-nm argon, helium neon (633 nm) and violet (405 nm) lasers. Intensities of maximal pixel and integrated fluorescence were measured and recorded for each cell. At least 3,000 cells were measured per sample. Gating analysis was carried out as described in Figure legends. *TK6cells and lymphocytes:* Intensity of cellular fluorescence was measured using a MoFlo XDP (Beckman-Coulter, Brea, CA) high speed flow cytometer/sorter. DAPI fluorescence was excited with the UV laser (355-nm), AlexaFluor 488, DCF and Rh123 with the argon ion (488-nm) laser. Although berberine, one of the studied agents, is fluorescent [132] control experiments excluded the possibility that its fluorescence significantly contributed to analysis of the measured cells that could lead to a bias. Statistical evaluation of individual measurements (SD) was carried out assuming the Poisson distribution in evaluation of populations of cells in particular phases of the cell cycle. All experiments were repeated at least three times, representative data are presented.

Western Blotting. TK6 cells were exposed to the investigated agents at concentrations as shown in Figs. 1 and for 4 h. The cells were then collected and lysed by incubation on ice for 30 min in cold immuno-precipitation (RIPA) buffer, which contained 50 mM Tris, pH 7.4, 150 mM NaCl, 1 mM EDTA, 1% Triton X-100, 1% deoxycholate, 0.1 % SDS, 1 mM

dithiothreitol (DTT) and 10 µl/ml protease inhibitor cocktail and 1% phosphatase inhibitor cocktail 3 (Sigma-Aldrich). The extracts were centrifuged and the clear supernatants were stored in aliquots at –80°C for further analysis. Protein concentrations of cell lysates were determined by Coomassie protein assay kit (Pierce, Rockford, IL) using BSA as standard. Aliquots of lysates (10 µg of protein) were resolved by 10% SDS-PAGE followed by western blot analysis. The primary antibody against total 4EBP1 (C-19) was purchased from Santa Cruz Biotechnology, Inc. (Santa Cruz, CA). The primary antibodies for mTOR-Ser2448^{P}, total mTOR, RP-S6-Ser235/236^{P}, Total RB-S6, and 4EBP1-Ser65^{P} were obtained from Cell Signaling Technology, Inc. (Beverly, CA). The blots were first incubated with specific primary antibodies followed by secondary antibodies. Specific immunoreactive bands was identified and detected by enhanced chemiluminescence (ECL) using protocol provided by the manufacturer (Kirkegaard & Perry Laboratories, Inc., Gaithersburg, MD). The expression of actin was monitored in parallel as loading control. The intensity of specific immunoreactive bands was quantified by densitometry and expressed as a ratio relative to the expression of actin [133].

ACKNOWLEDGEMENTS

Supported by: NCI, CA RO1 28704, 1 S10 RRO26548-1 and Robert A.Welke Cancer Research Foundation.

Conflict of Interest Statement

The authors of this manuscript have no conflict of interests to declare.

REFERENCES

1. Barzilai A, Yamamoto K. DNA damage responses to oxidative stress. DNA repair (Amst) 2004;3:1109-1115.

2. Moller P, Loft S. Interventions with antioxidants and nutrients in relation to oxidative DNA damage and repair. Mutat Res 2004;551:79-89.

3. Beckman KB, Ames BN. Oxidative decay of DNA. J Biol Chem 1997;272:13300-13305.

4. Vilenchik MM, Knudson AG. Endogenous DNA double-strand breaks: Production, fidelity of repair, and induction of cancer. Proc Natl Acad Sci USA 2003;100:12871-12876.

5. Karanjawala ZE, Lieber MR. DNA damage and aging. Mech Ageing Dev 2004;125:405-416.

6. Hudson D, Kovalchuk I, Koturbash I, Kolb B, Martin OA, Kovalchuk O. Induction and persistence of radiation-induced DNA damage is more pronounced in young animals than in old animals. Aging (Albany NY) 2011;609-620.

7. Schriner SE, Linford NJ, Martin GM, Treuting P, Ogburn CE, Emond M, Coskun PE, Ladiges W, Wolf N, Van Remmen H, Wallace DC, Rabinovitch PS. Extension of murine life span by over expression of catalase targeted to mitochondria. Science 2005;308:1875-1878.

8. Parrinello S, Samper E, Krtolica A, Goldstein J, Melov S, Campisi J. Oxygen sensitivity severely limits the replicative lifespan of murine fibroblasts. Nat Cell Biol 2003;5:741-747.

9. Balliet RM, Capparelli C, Guido C, Pestell TG, Martinez-Outschoorn UE, Lin Z, Whitaker-Menezes D, Chiavarina B, Pestell RG, Howell A, Sotgia F, Lisanti MP. Mitochondrial oxidative stress in cancer-associated fibroblasts drives lactate production, promoting breast cancer tumor growth: understanding the aging and cancer connection. Cell Cycle 2011;10:4065-4073.

10. Erol A. Genotoxic stress-mediated cell cycle activities for the decision of cellular fate. Cell Cycle 2011;10:3239-3248.

11. Lisanti MP, Martinez-Outschoorn UE, Pavlides S, Whitaker-Menezes D, Pestell RG, Howell A, Sotgia F. Accelerated aging in the tumor microenvironment: connecting aging, inflammation and cancer metabolism with personalized medicine. Cell Cycle. 2011;10:2059-2063.

12. Redon CE, Nakamura AJ, Martin OA, Parekh PR, Weyemi US, Bonner WM. Recent developments in the use of γ-H2AX as a quantitative DNA double-strand break biomarker. Aging (Albany NY) 2011;3:168-174.

13. Jeggo PA, Lobrich M. Artemis links ATM to double strand end rejoining. Cell Cycle 2005;4:359-362.

14. Seluanov A, Mittelman D, Pereira-Smith OM, Wilson JH, Gorbunova V. DNA end joining becomes less efficient and more error-prone during cellular senescence. Proc Natl Acad Sci USA 2004;101:7624-7629.

15. Bogomazova AN, Lagarkova MA, Tskhovrebova LV, Shutova MV, Kiselev SL. Error-prone nonhomologous end joining repair operates in human pluripotent stem cells during late G2. Aging (Albany NY) 2011;3:584-596.

16. Dever SM, Golding SE, Rosenberg E, Adams BR, Idowu MO, Quillin JM, Valerie N, Xu B, Povirk LF, Valerie K. Mutations in the BRCT binding site of BRCA1 result in hyper-recombination. Aging (Albany) 2011;3:515-532.

17. Dregalla RC, Zhou J, Idate RR, Battaglia CL, Liber HL, Bailey SM. Regulatory roles of tankyrase 1 at telomeres and in DNA repair: suppression of T-SCE and stabilization of DNA-PKcs. Aging (Albany NY). 2010;2:691-708.

18. Liu L, Trimarchi JR, Smith PJ, Keete DL. Mitochondrial dysfunction leads to telomere attrition and genomic instability. Aging Cell 2002;1:40-46.

19. Kurz DJ, Decary S, Hong Y, Trivier E, Akhmedov A, Erusalimsky JD. Chronic oxidative stress comprises telomere integrity and accelerates the onset of senescence in human endorthelial cells. J Cell Sci 2004;117:2417-2426.

20. Passos JF, von Zglinicki T. Mitochondria, telomeres and cell senescence. Exp Gerontol 2005;40:466-472.

21. Richter T, Proctor C. The role of intracellular peroxide levels on the development and maintenance of telomere-dependent senescence. Exp Gerontol 2007;42:1043-1052.

22. Voghel G, Thorin-Trescases N Mamarbachi AM, Villeneaue L, Malette FA, Farbeyre G, Farhat N, Perrault LP, Carrier M, Therin E. Endogenous oxidative stress prevents telomerase-dependent immortalization of human endothelial cells. Mech Ageing Dev 2010;131:354-363.

23. McNeely S, Conti C, Sheikh T, Patel H, Zabludoff S, Pommier Y, Schwartz G, Tse A. Chk1 inhibition after replicative stress activates a double strand break response mediated by ATM and DNA-dependent protein kinase. Cell Cycle. 2010;9:995-1004.

24. Adams BR, Hawkins AJ, Povirk LF, Valerie K ATM-independent, high-fidelity nonhomologous end joining predominates in human embryonic stem cells. Aging (Albany NY) 2010;2:582-596.

25. Li B, Reddy S, Comai L. Depletion of Ku70/80 reduces the levels of extrachromosomal telomeric circles and inhibits proliferation of ALT cells.Aging (Albany NY) 2011;3:395-406.

26. Horikawa I, Fujita K, Harris CC. p53 governs telomere regulation feedback too, via TRF2. Aging (Albany NY). 2011;3:26-32.

27. Mason M, Skordalakes E. Insights into Cdc13 dependent telomere length regulation.Aging (Albany NY) 2010;2:731-734.

28. Sheppard SA, Loayza D. LIM-domain proteins TRIP6 and LPP associate with shelterin to mediate telomere protection. Aging (Albany NY) 2010;2:432-444.

29. Kusumoto-Matsuo R, Opresko PL, Ramsden D, Tahara H, Bohr VA. Cooperation of DNA-PKcs and WRN helicase in the maintenance of telomeric D-loops. Aging (Albany NY) 2010;2:274-284.

30. Jee HJ, Kim AJ, Song N, Kim HJ, Kim M, Koh H, Yun J. Nek6 overexpression antagonizes p53-induced senescence in human cancer cells. Cell Cycle. 2010;9:4703-4710.

31. Doonan R, McElwee JJ, Matthijssens F, Walker GA, Houthoofd K, Back P, Matscheski A, Vanfleteren JR, Gems D. Against the oxidative damage theory of aging: superoxide dismutases protect against oxidative stress but have little or no effect on life span in Caenorhabditis elegans. Genes Dev 2008;22:3236-3241.

32. Gems D, Doonan R. Antioxidant defense and aging in C. elegans: Is the oxidative damage theory of aging wrong? Cell Cycle 2009;8:1681-1687.

33. Blagosklonny MV. Program-like aging and mitochondria: instead of random damage by free radicals. J Cell Biochem 2007;102:1389-1399.

34. Blagosklonny MV. Aging: ROS or TOR. Cell Cycle. 2008;7:3344-3354.

35. Blagosklonny MV. Paradoxes of aging. Cell Cycle 2007;6:2997-3003.

36. Blagosklonny MV. mTOR-driven aging: speeding car without brakes. Cell Cycle 2009;8:4055-4059.

37. Blagosklonny MV. Revisiting the antagonistic pleiotropy theory of aging: TOR-driven program and quasi-program. Cell Cycle 2010;9:3151-3156.

38. Cabreiro F, Ackerman D, Doonan R, Araiz C, Back P, Papp D, Braeckman BP, Gems D. Increased life span from overexpression of superoxide dismutase in Caenorhabditis elegans is not caused by decreased oxidative damage. Free Radic Biol Med 2011;51:1575-1582.

39. Lapointe J, Hekimi S. When a theory of aging ages badly. Cell Mol Life Sci. 2009;67:1-8.

40. Speakman JR, Selman C. The free-radical damage theory: Accumulating evidence against a simple link of oxidative stress to ageing and lifespan. Bioessays 2011;33:255-259.

41. Heeren G, Rinnerthaler M, Laun P, von Seyerl P, Kössler S, Klinger H, Hager M, Bogengruber E, Jarolim S, Simon-Nobbe B, Schüller C, Carmona-Gutierrez D, et al. The mitochondrial ribosomal protein of the large subunit, Afo1p, determines cellular longevity through mitochondrial back-signaling via TOR1. Aging (Albany NY). 2009;1:622-636.

42. Hay N, Sonenberg N. Upstream and downstream of mTOR. Genes Dev 2004;18:1926-1945.

43. Hands SL, Proud CG, Wyttenbach A. mTOR's role in ageing: protein synthesis or autophagy? Aging (Albany NY) 2009;1:586-597.

44. Blagosklonny MV, Hall MN. Growth and aging: a common molecular mechanism. Aging (Albany NY) 2009;1:357-362.

45. Wullschleger S, Loewith R, Hall MN. TOR signaling in growth and metabolism. Cell 2006;124:471-484.

46. Magnuson B, Ekim B, Fingar DC. Regulation and function of ribosomal protein S6 kinase (S6K) within mTOR signalling networks. Biochem J 2012;441:1-21.

47. Loewith R, Hall MN. Target of rapamycin (TOR) in nutrient signaling and growth control. Genetics 2011;189:1177-1201.

48. Zoncu R, Efeyan A, Sabatini DM. mTOR: from growth signal integration to cancer, diabetes and ageing. Nat Rev Mol Cell Biol 2010;12:21-35.

49. Ma XM, Blenis J. Molecular mechanisms of mTOR-mediated translational control. Nat Rev Mol Cell Biol 2009;10:307-318.

50. Burhans WC, Weinberger M. DNA replication stress, genome instability and aging. Nucleic Acids Res 2007;33:7545-7556.

51. McKenna E, Traganos F, Zhao H, Darzynkiewicz Z. Persistent DNA damage caused by low levels of mitomycin C induces irreversible senescence of A549 cells. Cell Cycle 2012;11:3132-3140.

52. Huang X, Tanaka T, Kurose A, Traganos F, Darzynkiewicz Z. Constitutive histone H2AX phosphorylation on *Ser*-139 in cells untreated by genotoxic agents is cell-cycle phase specific and attenuated by scavenging reactive oxygen species. Int J Oncol 2006;29:495-501.

53. Tanaka T, Halicka HD, Huang X, Traganos F, Darzynkiewicz Z. Constitutive histone H2AX phosphorylation and ATM activation, the reporters of DNA damage by endogenous oxidants. Cell Cycle 2006;5:1940-1945.

54. Zhao H, Tanaka T, Halicka HD, Traganos F, Zarebski M, Dobrucki J, Darzynkiewicz Z. Cytometric assessment of DNA damage by exogenous and endogenous oxidants reports the aging-related processes**.** Cytometry A 2007;71A:905-914.

55. Halicka HD, Zhao H, Li J, Traganos F, Zhang S, Lee M, Darzynkiewicz Z Genome protective effect of metformin as revealed by reduced level of constitutive DNA damage signaling. Aging (Albany NY) 2011;3:1028-1038.

56. Halicka HD, Zhao H, Li J, Traganos DF, Studzinski G, Darzynkiewicz Z. Attenuation of constitutive DNA damage signaling by 1,25-dihydroxyvitamin D3. Aging (Albany NY) 2012;4;270-278.

57. Zhao H, Tanaka T, Mitlitski V, Heeter J, Balazs EA, Darzynkiewicz Z. Protective effect of hyaluronate on oxidative DNA damage in WI-38 and A549 cells. Int J Oncol 2008;32:1159-1169.

58. Halicka HD, Ita M, Tanaka T, Kurose A, Darzynkiewicz Z. The biscoclaurine alkaloid cepharanthine protects DNA in TK6 lymphoblastoid cells from constitutive oxidative damage. Pharmacol Rep 2008;60:93-100.

59. Yang NC, Song TY,Chen MY, Hu ML. Effects of 2-deoxyglucose and dehydroepiandrosterone on intracellular NAD(+) level, SIRT1 activity and replicative lifespan of human Hs68 cells. Biogerontology 2011;12:527-536.

60. Ingram DK, Roth GS. Glycolitic inhibition as a strategy for developing calorie restriction mimetics. Exp. Gerontol 2011;46:148-154.

61. Smith DL, Nagy TR, Allison DB. Calorie restriction: what recent results suggest for the future of ageing research. Eur J Clin Invest 2010;40:440-450.

62. Blagosklonny MV. Calorie restriction: decelerating mTOR-driven aging from cells to organisms (including humans) Cell Cycle 2010;9:683–688.
63. Anisimov VN, Berstein LM, Popovich IG, Zabezhinski MA, Egormin PA, Piskunova TS, Semenchenko AV, Tyndyk ML, Yurova MN, Kovalenko IG, Poroshina TE. If started early in life, metformin treatment increases life span and postpones tumors in female SHR mice. Aging (Albany NY). 2011 Feb;3:148-157.
64. Menendez JA, Cufí S, Oliveras-Ferraros C, Vellon L, Joven J, Vazquez-Martin A. Gerosuppressant metformin: less is more. Aging (Albany NY) 2011;3:348-362.
65. Blagosklonny MV Metformin and sex: Why suppression of aging may be harmful to young male mice. Aging (Albany NY) 2010;2:897-899.
66. Anisimov VN, Piskunova TS, Popovich IG, Zabezhinski MA, Tyndyk ML, Egormin PA, Yurova MV, Rosenfeld SV, Semenchenko AV, Kovalenko IG, Poroshina TE, Berstein LM. Gender differences in metformin effect on aging, life span and spontaneous tumorigenesis in 129/Sv mice. Aging (Albany) 2010;2:945-958.
67. Mashhedi H, Blouin MJ, Zakikhani M, David S, Zhao Y, Bazile M, Birman E, Algire C, Aliaga A, Bedell BJ, Pollak M. Metformin abolishes increased tumor (18)F-2-fluoro-2-deoxy-D-glucose uptake associated with a high energy diet. Cell Cycle. 2011 Aug 15;10:2770-2778.
68. Bernstein LM. Metformin in obesity, cancer and aging: addressing controversies. Aging (Albany) 2012;4:320-329.
69. Bulterijs S. Metformin as a geroprotector. Rejuvenation Res 2011;14:469-482.
70. Anisimov VN, Metformin for aging and cancer prevention. Aging (Albany NY) 2010;2:760-774.
71. Pollak MN. Investigating metformin for cancer prevention and treatment: the end of the beginning. Cancer discovery 2012;2:778-790.
72. Zheng XF. Chemoprevention of age-related macular regeneration (AMD) with rapamycin. Aging (Albany). 2012;4:375-376.
73. Blagosklonny MV.Once again on rapamycin-induced insulin resistance and longevity: despite of or owing to. Aging (Albany). 2012;4:350-358.
74. Khanna A, Kapahi P. Rapamycin: killing two birds with one stone. Aging (Albany NY). 2011;3:1043-1044.
75. Leontieva OV, Blagosklonny MV. DNA damaging agents and p53 do not cause senescence in quiescent cells, while consecutive re-activation of mTOR is associated with conversion to senescence. Aging (Albany NY). 2010;2:924-235.
76. Wesierska-Gadek J. mTOR and its link to the picture of Dorian Gray - re-activation of mTOR promotes aging. Aging (Albany NY). 2010;2:892-893.
77. Galluzzi L, Kepp O, Kroemer G. TP53 and MTOR crosstalk to regulate cellular senescence. Aging (Albany NY). 2010;2:535-537.
78. AnisimovVN, Zabezhinski MA, Popovich IG, Piskunova, TS. Semenchenko, AV. Tyndyk ML, Yurova MN,. Antoch MP,. Blagosklonny MV. Rapamycin extends maximal lifespan in cancer-prone mice. Am J Pathol 2010;176:2092-2097
79. Pospelova TV, Leontieva OV, Bykova TV, Zubova SG, Pospelov VA, Blagosklonny MV. Suppression of replicative senescence by rapamycin in rodent embryonic cells. Cell Cycle 2012;11:2402-2407,
80. Wilkinson JE, Burmeister L, Brooks SV, Chan CC, Friedline S, Harrison DE, Hejtmancik JF, Nadon N, Strong R, Wood LK, Woodward MA, Miller RA. Rapamycin slows aging in mice. Aging Cell 2012;11;675-682.
81. Wang Q, Zhang M, Liang B, Shirwany N, Zhu Y, Zou MH. Activation of AMP-activated protein kinase is required for berberine-induced reduction of artheriosclerosis in mice: the role of uncoupling protein 2. PLoS One 2011; e25436.
82. Li H, Miyahara T, Tezuka Y, Tran OL, Seto H, Kadota S. Effect of berberine on bone mineral density in SAMP6 as a senile osteoporosis model. Biol Pharma Bull 2003;26:130-131.
83. Ki HF, Shen L. Berberine: a potential multipotent natural product to combat Alzheimer's Disease. Molecules 2011;16:6732-6740.
84. Cicero AF, Tartagani E. Antidiabetic properties of berberine: from cellular pharmacology to clinical effects. Hosp Pract (Minneap) 2012;40:56-63.
85. Shen N, Huan Y, Shen ZF. Berberine inhibits mouse insulin gene promoter through activation of AMP activated protein kinase and may exert beneficial effect on pancreatic β-cell. Eur J Pharmacol 2012; S0014-2099, 00697-8 (Epub).
86. Klotz B, Mentrup B, Regensburger M, Zeck S, Schneidereit J, Schupp N, Linded C, Merz C, Ebert R, Jakob F. 1,25-dihydroxyvitamin D3 treatment delays cellular aging in human mesenchymal stem cells while maintaining their multipotent capacity. PLoS One 2012;7:e29959 Epub Jan 5.
87. Haussler MR, Haussler CA, Whitfield GK, Hsieh JC, Thompson PD, Barthel TK, Bartik L, Egan JB, Wu Y, Kubicek JL, Lowmiller CL, Moffet EW, Forster RE, Jurutka PW. The nuclear vitamin D receptor controls the expression of genes encoding factors which feed the "Fountain of Youth" to mediate healthful Aging. J Steroid Biochem Mol Biol 2010;121:88-97.
88. Touhimm P. Vitamin D and aging. J Steroid Biochem Mol Biol 2009;114:78-84.
89. Lanske B, Razzaque MS. Vitamin D and aging: old concepts and new insights. J Nutr Biochem 2007;18:771-777.
90. Forster RE, Jurutka PW, Hsieh JC, Haussler CA, Lowmiller CL, Kaneko I, Haussler MR, Kerr WH. Vitamin D receptor controls expression of the anti-aging klotho gene in mouse and human renal cells. Biochem Biophys Res Commun 2011;414:557-562.
91. Yang J, Ikezoe T, Nishioka C, Ni L, Koeffler HP, Yokoyama, A. Inhibition of mTORC1 by RAD001 (everolimus) potentiates the effects of 1,25-dihydroxyvitamin D(3) to induce growth arrest and differentiation of AML cells in vitro and in vivo. Exp Hematol 2010;38:666-676.
92. Vetterli L, Maechler P. Resveratrol-activated SIRT1 in liver and pancreatic β-cells: a Janus head looking to the same direction of metabolic homeostasis. Aging (Albany NY). 2011;3:444-449.
93. Gerhardt E, Graber S, Szego EM, Moisol N, Martins LM, Outeiro TF, Kermer P. Idebebone and resveratrol extend life span and improve motor function of HtrA2 knockout mice. PLoS One 2011;6:e28855. Epub Dec 19.
94. Rascon B, Hubbard BP, Sinclair DA, Amdam GV. The lifespan extension effects of resveratrol are conserved in the honey bee and may be driven by a mechanism related to caloric restriction. Aging (Albany NY) 2012;4:499-508.
95. Chung JH, Manganiello V, Dyck JR. Resveratrol as a calorie restriction mimetic: therapeutic implications. Trends Cell Biol 2012; Aug 9 (Epub).
96. Timmers S, Auwerx J, Schrauwen P. The journey of resveratrol from yeast to human. Aging (Albany NY) 2012;4:146-158.

97. Bass TM, Weinkove G, Hourthoofd K, Gems D, Partridge L. Effects of resveratrol on lifespan in Drosophila melanogaster and Caenorhabditis elegans. Mech Ageing Dev 2007;128:546–552.

98. Ayyadevara S, Bharill P, Dandapat A, Hu C, Khaidakov M, Mitra S, Shmookler Reis RJ, Mehta JL. Aspirin inhibits oxidant stress, reduces age-associated functional declines, and extends lifespan of caenorhabditis elegans. Antioxid Redox Signal 2012 Sept 7 Epub.

99. Bode-Boger SM, Martens-Lobenhoffer J, Tager M, Schroder H, Scalera F. Aspirin reduces endothelial cell senescence. Biochem Biophys Res Commun 2005;334:1226-1232.

100. Strong B, Miller RA, Astie CM, Floyd RA, Flurkey K, Hensley KL, Javors MA, Leeuwenburgh C, Nelson JF, Ongini E, Nadon NL, Warner HR, Harrison DE. Nordihydroguaiaretic acid and aspirin increase lifespan of genetically heterogenous male mice. Aging Cell 2008;7: 641-650.

101. Yi TN, Zhao HY, Zhang JS, Shan HY, Meng X, Zhang J, Effect of aspirin on high glucose-induced senescence of endothelial cells. Chin Med J (Engl) 2009; 20:122:3055-3061.

102. Mcllhatton MA, Tyler J, Kerepesi LA, Bocker-Edmonston T, Kucherlapati MH, Edelmann W, Kucherlapati R, Kopelovich L, Fishel L. Aspirin and low-dose nitric-oxide-donating aspirin increase life span in a Lynch syndrome mouse model. Cancer Prev Res (Phila) 2011;4:684-693.

103. Bulckaen H, Prevost G, Boulanger E, Robitaille G, Roquet V, Gaxatte C, Garcon G, Corman B, Gosset, P, Shirali P, Creusy C, Puisleux F. Low-dose aspirin prevents age-related endothelial dysfunction in a mouse model of physiological aging. Am J Physiol Heart Circ Physiol 2008;294;H1562-70.

104. Pozarowski P, Holden E, Darzynkiewicz Z. Laser scanning cytometry: Principles and applications. An update. Meth Molec Biol 2013;913:187-212.

105. Ruvinsky I, Sharon N, Lerer T, Cohen H, Stolovich-Rain M, Nir T, Dor Y, Zisman O, Meyuhas O. Ribosomal protein S6 phosphorylation is a determinant of cell size and glucose homeostasis. Genes & Dev 2005;19:2199-2211.

106. Fingar, D. Salama C., S., Tsou C., Harlow E.,. Blenis J. Mammalian cell size is controlled by mTOR and its downstream targets S6K1 and 4EBP1/eIF4E. Genes Dev 2002;16:1472–1487.

107. Nyfeler B, Bergman P, Triantafellow E, Wilson CJ, Zhu Y, Radetich B, Finan PM, Klionsky DJ, Murphy LO. Relieving autophagy and E4BP1 from rapamycin resistance. Mol Cell Biol 2011;31:2867-2876.

108. Chao SK, Horwitz SB, McDaid HM. Insights into 4E-bp1 and p53 mediated regulation of accelerated cell senescence. Oncotarget 2011;2:89-98.

109. Bartke A. Insulin and aging. Cell Cycle 2008;3338-3343.

110. Darzynkiewicz. Z, Krassowski T, Skopinska E. Effect of phytohemagglutinin on synthesis of "rapidly labeled" ribonucleic acid in human lymphocytes. Nature 1965;207:1402-1403.

111. Darzynkiewicz Z, Traganos F, Sharpless T, Melamed MR. Lymphocyte stimulation: A rapid multiparameter analysis. Proc Natl Acad Sci USA 1976;73:2881-2884.

112. Tanaka T, Kajstura M, Halicka HD, Traganos F, Darzynkiewicz Z. Constitutive histone H2AX phosphorylation and ATM activation are strongly amplified during mitogenic stimulation of lymphocytes. Cell Prolif 2007;40:1-13.

113. Lai KP, Leong WF, Chau IF, Jia D, Zeng L, Liu H. He L, Hao A, Zhang H, Meek D. Velagapudi C, Habib SL, Li B. S6K1 is a multifaceted regulator of Mdm2 that connects nutrient status and DNA damage response. EMBO J 2010;29:2994-3006.

114. Ditch S, Paull TT. The ATM protein kinase and cellular redox signaling: beyond the DNA damage response. Trends Biochem Sci 2012;37:15-22.

115. Zajkowicz A, Rusin M. The activation of the p553 pathway by the AMP mimetic AICAR is reduces by inhibitors of the ATM or mTOR kinases. Mech Aging Dev 2011;132:543-551.

116. Mukherjee B, Tomimatsu N, Amanchela K, Camacho CV, Pichamoorthy N, Burma S. The dual PI3K/mTOR inhibitor NVP-BEZ235 is a potent inhibitor of ATM- and DNA-PKCs-mediated DNA damage responses. Neoplasia 2012;14:34-43.

117. Darzynkiewicz Z. Another "Janus paradox" of p53: induction of cell senescence versus quiescence. Aging (Albany NY) 2010;2:329-330.

118. Darzynkiewicz Z. Running m(o)TOR with the brakes on leads to catastrophe at mitosis. Cell Cycle 2012, 11.

119. Darzynkiewicz Z, Traganos F, Staiano-Coico L, Kapuscinski J, Melamed MR. Interactions of rhodamine 123 with living cells studied by flow cytometry. Cancer Res 1982;42:799-806.

120. Darzynkiewicz Z, Staiano-Coico L, Melamed MR. Increased mitochondrial uptake of rhodamine 123 during lymphocyte stimulation. Proc Natl Acad Sci USA 1981;78:2383-2387.

121. Smith CP, Thersness PE. Formation of energized inner membrane in mitochondria with a gamma-deficient F1-ATPase. Eukaryot Cell 2005;4:2078-2086.

122. Li D. Metformin as an antitumor agent in cancer prevention and treatment. J Diabetes 2011;3:320-327.

123. Buitrago-Molina LE, Vogel A. mTOR as a potential target for the prevention and tratment of hepatocellular carcinoma. Curr Cancer Drug Target 2012; Aug 7 Epub.

124. Kajser J. Will an aspirin a day keep cancer away? Science 2012; 337: 1471-1473.

125. Anis KV, Rajeshkumar NV, Kuttan R. Inhibition of chemical carcinogenesis by berberine in rats and mice. J Pharm Pharmacol 2001;53:763-768.

126. Zhu Z, Jiang W, McGinley JN, Thompson HJ. 2-Deoxyglucose as an energy restriction mimetic agent: effects on mammary carcinogenesis and on mammary tumor cell growth in vitro. Cancer Res 2005;65:7023-7030.

127. Juan ME, Alfaras I, Planas JM. Colorectal cancer chemoprevention by trans-resveratrol. Pharmacol Res 2012;65:584-5891.

128. Trump DL, Deeb KK, Johnson CS. Vitamin D: considerations in the continued development as an agent for cancer prevention and therapy. Cancer J 2010;16:1-9.

129. Darzynkiewicz Z, Zhao H, Halicka HD, Rybak P, Dobrucki J, Wlodkowic D. DNA damage signaling assessed in individual cells in relation to the cell cycle phase and induction of apoptosis. Crit Rev Clin Lab Sci 2012; 2012;49:199-217.

130. Rothe G, Klouche M. Phagocyte functions. Meth Cell Biol 2004;75:679-708.

131. Darzynkiewicz Z. Bedner E. Gorczyca W, Melamed MR. Laser scanning cytometry. A new instrumentation with many applications. Exp Cell Res 1999; 249:1-12.

132. Mikes V, Dadak V. Berberine derivatives are cationic fluorescent probes for the investigation of the energized state of mitochondria. Biochim Biophys Acta 1983;723:231-239.

133. Hsieh TC, Yang CJ, Lin CY, Lee YS, Wu JM, Control of stability of cyclin D1 by quinine reductase 2 in CWR22Rv1 prostate cancer cells. Carcinogenesis. 2012;33:670-677.

Research perspective

Tumor suppression by p53 without apoptosis and senescence: conundrum or rapalog-like gerosuppression?

Mikhail V. Blagosklonny

Department of Cell Stress Biology, Roswell Park Cancer Institute, Buffalo, NY 14263, USA

Key words: *tumor suppressors, aging, apoptosis, geroconversion*
Received: *7/15/12; Accepted: 7/30/12; Published: 7/31/12* doi:10.18632/aging.100475
Correspondence to: *Mikhail V. Blagosklonny, MD/PhD;* ***E-mail:*** *blagosklonny@oncotarget.com*

Abstract: I discuss a very obscure activity of p53, namely suppression of senescence (gerosuppression), which is also manifested as anti-hypertrophic, anti-hypermetabolic, anti-inflammatory and anti-secretory effects of p53. But can gerossuppression suppress tumors?

INTRODUCTION

Wt p53 can induce apoptosis, cell cycle arrest and senescence, which are sufficient to explain tumor suppression by p53 [1]. A recent paper in *Cell* described that these activities are dispensable for tumor suppression [2]. Mutant p53 ($p53^{3KR}$) that cannot cause arrest, senescence and apoptosis still suppressed tumors in mice [2, 3]. Why do then wt p53 induce apoptosis, cell cycle arrest and senescence? Before entertaining this intriguing question, I will focus on suppression of senescence (gerosuppression) by p53, overlapping with its anti-hypertrophic, anti-hypermetabolic, anti-inflammatory and anti-secretory effects.

P53 suppresses the conversion from arrest to senescence (geroconversion)

How can p53 suppress senescence, if it also can cause senescence? As recently suggested, induction of senescence is not an independent activity of p53 but a consequence of cell-cycle arrest [4-8]. This predicts that any mutant p53 that cannot cause arrest will not cause senescence too. In agreement, $p53^{3KR}$ did not cause senescence [2]. This is not trivial. To create $p53^{3KR}$, wt p53 was altered to abolish apoptosis and cell-cycle arrest only [2]. Li et al did not modify p53 to abolish senescence as an independent activity. It was not needed, simply because p53 does not induce senescence as an independent effect. (Note: Seemingly in contrast, it was reported that mutant p53, which cannot induce arrest in response to DNA damage, can cause senescence [9]. Although this mutant p53 did not cause instant arrest, it still arrested proliferation later and then senescence developed [9]. So there is no exception). p53 cannot induce senescence without inducing arrest. But p53 can induce quiescence, a reversible condition characterized by low protein synthesis and metabolism (see detailed definitions in ref. [7, 8]). It was assumed that when p53 causes quiescence, it simply fails to induce senescence. But another possibility is that in such cases p53 suppresses the conversion from cell-cycle arrest to senescence (geroconversion). How can that be tested? In some cell lines, induction of ectopic p21 causes irreversible senescence, whereas induction of p53 causes quiescence [4]. Does p53 suppresses a senescent program? This question can be answered by simultaneously inducing both p53 and ectopic p21. When both p21 and p53 were induced, then cells become quiescent not senescent [4]. p53 was dominant, actively suppressing senescence caused by p21... or by something else? In fact, p21 merely causes cell cycle arrest and does not inhibit mitogen-activated, nutrient-sensing and growth-promoting pathways such as Target of Rapamycin (mTOR) [4]. During several days, these pathways (gerogenic pathways, for brevity) convert p21-induced arrest into senescence. Rapamycin can decelerate geroconversion [10-13]. Also, p53 can inhibit the mTOR pathway [4-6, 14-17]. In some conditions, p53 can suppress senescence during arrest [4-6]. Wt p53 induces arrest and then if it fails to suppress senescence, then senescence prevails. Rather than p53, gerogenic

pathways drive senescence during cell-cycle arrest [18].

In summary, wt p53 seems to have three independent effects: apoptosis, cell-cycle arrest and gerosuppression. By inducing arrest, wt p53 primes cells for senescence, unless p53 is able or "willing" to suppress geroconversion. At high levels, gerosuppression by p53 is limited by apoptosis [6]. This predicts that $p53^{3KR}$ would potently suppress senescence because gero-suppression by $p53^{3KR}$ will not be limited by apoptosis.

Hyper-metabolic senescent phenotype

Senescent cells are hyper-functional: hypertrophic, hypermetabolic, hyper-secretory and hyper-inflammatory [8]. Also, senescent cells may accumulate lipids, becoming not only large but also "fat" (Figure1). Induction of p53 decreased both cellular hypertrophy and fat accumulation (Figure 1). This is in line with numerous metabolic effects of p53 including inhibition of glycolysis and stimulation of fatty acids oxidation [19-32]. Importantly, $p53^{3KR}$ retained the ability to inhibit glycolysis and reactive oxygen species (ROS) [2]. (Noteworthy, ROS and mTOR co-activate each other [33] and N-Acetyl Cysteine (NAC), which decreases ROS, also inhibits mTOR [34]). Also, p53 decreases hyper-secretory phenotype also known as SASP [35] and suppresses a pro-inflammatory phenotype [36, 37]. How might gerosuppression contribute to tumor suppression? There are several overlapping explanations, from different points of view of the same process.

Gerogenic conversion and oncogenic transformation

In proliferating epithelial cells, pro-gerogenic conversion may contribute to carcinogenesis directly. The PI3K/mTOR pathway is universally activated in cancer [38-49]. p53 can inhibit the PI3K/mTOR pathway [4-6, 14-17, 50]. Like p53, many other tumor suppressors such as PTEN, AMPK, TSC2, LKB1, NF1 inhibit the PI3K/mTOR pathway [51].

Geroconversion of stromal cells creates carcinogenic microenvironment

First, senescence creates a selective disadvantage for normal cells, thus selecting for cancer [52-54]. Also, senescent stromal cells secrete factors that favors pre-cancer and cancer growth [37, 54-62]. Third, the senescent stroma is hyper-metabolic and thus promotes cancer by fueling cancer growth [59, 60, 63-71]. In a model of accelerated host aging, mTOR activity was increased in normal tissues [72]. This pro-senescent microenvironment accelerated growth of implanted tumors. The tumor-promoting effects of pro-senescent microenvironment were abrogated by rapamycin [72].

Cancer is an age-related disease

The incidence of cancer is increased exponentially in aging mammals. Manipulations that slow down aging delay cancer [73]. For example, calorie restriction delays cancer [74-76] including cancer in p53-deficient mice [77, 78]. Rapamycin, which decelerates aging, also postpones cancer in animals [73, 79-81] and in patients after renal transplantation [82-86].

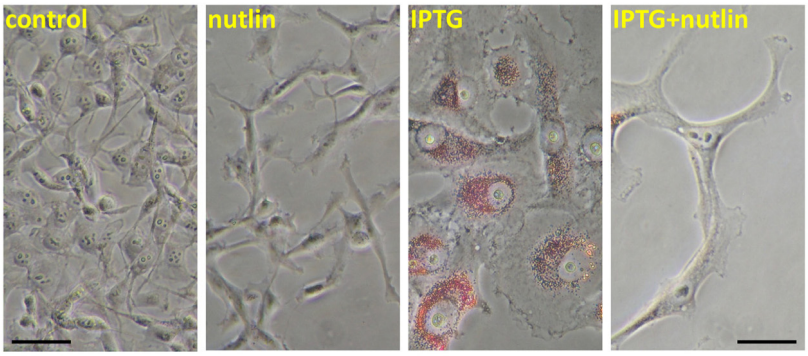

Figure 1. Nutlin-3a decreased lipid accumulation during IPTG-induced senescence. HT-p21 cells were treated with IPTG, nutlin-3a and IPTG+nutlin-3a (as indicated) for 3 days as described previously [4-6] and cells were stained with "oil red O" for lipids. In HT-p21 cells, IPTG induces ectopic p21 and senescence. As described previously, nutlin-3a induces endogenous p53 and suppresses IPTG-induced senescence [4-6].

Is aging accelerated in p53-deficient mice?

Inactivation of tumor suppressors accelerates both aging and cancer [87]. It was thought that p53 is an exception. Yet, given that p53 can suppress geroconversion, it may not be the exception after all. A complex role of p53 in cellular senescence and organismal aging was discussed [88-91]. Mice with increased, but normally regulated, p53 lives longer [92]. p53 knockout mice have both accelerated carcinogenesis and decreased longevity [93-98]. p53-/- mice have a pro-inflammatory phenotype characteristic of accelerated aging [36,37]. Also, atherosclerosis is accelerated in p53-/- animals [99-102]. While loss of p53 by itself makes cells prone to become tumorigenic, an increased rate of organismal aging in the absence of p53 may further accelerate carcinogenesis.

Rapalogs and p53

Rapamycin (sirolimus) and other rapalogs (everolimus and temsirolimus) are pharmacological tumor suppressors. Noteworthy, like p53, rapamycin decreases glycolysis [103] and lactate production [34] and stimulates oxidation of fatty acids [104, 105]. Furthermore, rapamycin slows cellular proliferation, and so, not surprisingly, $p53^{3KR}$ inhibits clonogenicity too [2]. Yet, p53 affects metabolism and aging not only via mTOR but also via direct transactivation of metabolic enzymes, rendering it a more potent tumor suppressor.

Puzzles remain

Still, even if gerosuppression and anti-hypermetabolic effects can in part explain tumor suppression, puzzles remain. Why does wt p53 cause "unneeded" apoptosis and "instant" (p21-dependent) arrest? Why is p53 needed at all? In the wild, most mice die from external/accidental causes and only a few would live long enough to die from cancer, regardless of p53 status. In the wild, starvation (natural calorie restriction) would delay cancer further. Yet, p53 is also needed very early in life, or technically speaking, even before life has begun, because p53 plays role in fertility and reproduction [106-113]. And is tumor suppression a late life function?

Alternatively, tumor suppression is a primary function of p53. And each of the three activities (apoptosis, arrest, gerosuppression) is partially sufficient for cancer prevention. In their combination, these activities are the most effective tumor suppressor. And each activity may be partially dispensable in some mice strains and in some conditions. For example, the gerosuppressive activity of p53 may be preferentially important in peculiar strains of laboratory mice, or mice fed *ad libitum*, which constantly activates mTOR and accelerates aging. In fact, calorie restriction, which deactivates mTOR and decelerates aging, partially substitutes for the loss of p53 in mice.

ACKNOWLEDGEMENTS

I thank Wei Gu, Arnold Levine and Bert Vogelstein for critical reading of the manuscript and excellent suggestions.

CONFLICT OF INTERESTS STATEMENT

The author of this manuscript has no conflict of interest to declare.

REFERENCES

1. Vogelstein B, Lane DP, Levine AJ. Surfing the p53 network. Nature. 2000; 408: 307-310.

2. Li T, Kon N, Jiang L, Tan M, Ludwig T, Zhao Y, Baer R, Gu W. Tumor Suppression in the Absence of p53-Mediated Cell-Cycle Arrest, Apoptosis, and Senescence. Cell. 2012; 149: 1269-1283.

3. Hock AK, Vousden KH. Tumor Suppression by p53: Fall of the Triumvirate? Cell. 2012; 149: 1183-1185.

4. Demidenko ZN, Korotchkina LG, Gudkov AV, Blagosklonny MV. Paradoxical suppression of cellular senescence by p53. Proc Natl Acad Sci U S A. 2010; 107: 9660-9664.

5. Korotchkina LG, Leontieva OV, Bukreeva EI, Demidenko ZN, Gudkov AV, Blagosklonny MV. The choice between p53-induced senescence and quiescence is determined in part by the mTOR pathway. Aging. 2010; 2: 344-352.

6. Leontieva O, Gudkov A, Blagosklonny M. Weak p53 permits senescence during cell cycle arrest. Cell Cycle. 2010; 9: 4323-4327.

7. Blagosklonny MV. Cell cycle arrest is not senescence. Aging. 2011; 3: 94-101.

8. Blagosklonny MV. Cell cycle arrest is not yet senescence, which is not just cell cycle arrest: terminology for TOR-driven aging. Aging. 2012; 4: 159-165.

9. Brady CA, Jiang D, Mello SS, Johnson TM, Jarvis LA, Kozak MM, Kenzelmann Broz D, Basak S, Park EJ, McLaughlin ME, Karnezis AN, Attardi LD. Distinct p53 transcriptional programs dictate acute DNA-damage responses and tumor suppression. Cell. 2011; 145: 571-583.

10. Demidenko ZN, Blagosklonny MV. Growth stimulation leads to cellular senescence when the cell cycle is blocked. Cell Cycle. 2008; 7: 3355-3361.

11. Demidenko ZN, Zubova SG, Bukreeva EI, Pospelov VA, Pospelova TV, Blagosklonny MV. Rapamycin decelerates cellular senescence. Cell Cycle. 2009; 8: 1888-1895.

12. Demidenko ZN, Blagosklonny MV. Quantifying pharmacologic suppression of cellular senescence: prevention of cellular hypertrophy versus preservation of proliferative potential. Aging. 2009; 1: 1008-1016.

13. Pospelova TV, Demidenko ZN, Bukreeva EI, Pospelov VA, Gudkov AV, Blagosklonny MV. Pseudo-DNA damage response in senescent cells. Cell Cycle. 2009; 8: 4112-4118.

14. Feng Z, Levine AJ. The regulation of energy metabolism and the IGF-1/mTOR pathways by the p53 protein. Trends Cell Biol. 2010; 20: 427-434.

15. Feng Z, Hu W, de Stanchina E, Teresky AK, Jin S, Lowe S, Levine AJ. The regulation of AMPK beta1, TSC2, and PTEN expression by p53: stress, cell and tissue specificity, and the role of these gene products in modulating the IGF-1-AKT-mTOR pathways. Cancer Res. 2007; 67: 3043-3053.

16. Levine AJ, Feng Z, Mak TW, You H, Jin S. Coordination and communication between the p53 and IGF-1-AKT-TOR signal transduction pathways. Genes Dev. 2006; 20: 267-275.

17. Budanov AV, Karin M. p53 target genes sestrin1 and sestrin2 connect genotoxic stress and mTOR signaling. Cell. 2008; 134: 451-460.

18. Leontieva OV, Blagosklonny MV. DNA damaging agents and p53 do not cause senescence in quiescent cells, while consecutive re-activation of mTOR is associated with conversion to senescence. Aging. 2010; 2: 924-935.

19. Bensaad K, Tsuruta A, Selak MA, Vidal MN, Nakano K, Bartrons R, Gottlieb E, Vousden KH. TIGAR, a p53-inducible regulator of glycolysis and apoptosis. Cell. 2006; 126: 107-120.

20. Bensaad K, Vousden KH. p53: new roles in metabolism. Trends Cell Biol. 2007; 17: 286-291.

21. Kawauchi K, Araki K, Tobiume K, Tanaka N. p53 regulates glucose metabolism through an IKK-NF-kappaB pathway and inhibits cell transformation. Nat Cell Biol. 2008; 10: 611-618.

22. Vousden KH, Ryan KM. p53 and metabolism. Nat Rev Cancer. 2009; 9: 691-700.

23. Vigneron A, Vousden KH. p53, ROS and senescence in the control of aging. Aging. 2010; 2: 471-474.

24. Cheung EC, Vousden KH. The role of p53 in glucose metabolism. Curr Opin Cell Biol. 2010; 22: 186-191.

25. Suzuki S, Tanaka T, Poyurovsky MV, Nagano H, Mayama T, Ohkubo S, Lokshin M, Hosokawa H, Nakayama T, Suzuki Y, Sugano S, Sato E, Nagao T, Yokote K, Tatsuno I, Prives C. Phosphate-activated glutaminase (GLS2), a p53-inducible regulator of glutamine metabolism and reactive oxygen species. Proc Natl Acad Sci U S A. 2010; 107: 7461-7466.

26. Jiang P, Du W, Wang X, Mancuso A, Gao X, Wu M, Yang X. p53 regulates biosynthesis through direct inactivation of glucose-6-phosphate dehydrogenase. Nat Cell Biol. 2011; 13: 310-316.

27. Zhu Y, Prives C. p53 and Metabolism: The GAMT Connection. Mol Cell. 2009; 36: 351-352.

28. Bensaad K, Cheung EC, Vousden KH. Modulation of intracellular ROS levels by TIGAR controls autophagy. Embo J. 2009; 28: 3015-3026.

29. Hu W, Zhang C, Wu R, Sun Y, Levine A, Feng Z. Glutaminase 2, a novel p53 target gene regulating energy metabolism and antioxidant function. Proc Natl Acad Sci U S A. 2010; 107: 7455-7460.

30. Ide T, Brown-Endres L, Chu K, Ongusaha PP, Ohtsuka T, El-Deiry WS, Aaronson SA, Lee SW. GAMT, a p53-inducible modulator of apoptosis, is critical for the adaptive response to nutrient stress. Mol Cell. 2009; 36: 379-392.

31. Park JY, Wang PY, Matsumoto T, Sung HJ, Ma W, Choi JW, Anderson SA, Leary SC, Balaban RS, Kang JG, Hwang PM. p53 improves aerobic exercise capacity and augments skeletal muscle mitochondrial DNA content. Circ Res. 2009; 105: 705-712.

32. Madan E, Gogna R, Bhatt M, Pati U, Kuppusamy P, Mahdi AA. Regulation of glucose metabolism by p53: emerging new roles for the tumor suppressor. Oncotarget. 2011; 2: 948-957.

33. Blagosklonny MV. Aging: ROS or TOR. Cell Cycle. 2008; 7: 3344-3354.

34. Leontieva OV, Blagosklonny MV. Yeast-like chronological senescence in mammalian cells: phenomenon, mechanism and pharmacological suppression. Aging. 2011; 3: 1078-1091.

35. CoppŽ JP, Patil CK, Rodier F, Sun Y, Mu–oz DP, Goldstein J, Nelson PS, Desprez PY, Campisi J. Senescence-associated secretory phenotypes reveal cell-nonautonomous functions of oncogenic RAS and the p53 tumor suppressor. PLoS Biol. 2008; 6: 2853-2868.

36. Komarova EA, Krivokrysenko V, Wang K, Neznanov N, Chernov MV, Komarov PG, Brennan ML, Golovkina TV, Rokhlin OW, Kuprash DV, Nedospasov SA, Hazen SL, Feinstein E, Gudkov AV. p53 is a suppressor of inflammatory response in mice. Faseb J. 2005; 19: 1030-1032.

37. Gudkov AV, Gurova KV, Komarova EA. Inflammation and p53: A Tale of Two Stresses. Genes Cancer. 2011; 2: 503-516.

38. Vogelstein B, Kinzler KW. Cancer genes and the pathways they control. Nat Med. 2004; 10: 789-799.

39. Shaw RJ, Cantley LC. Ras, PI(3)K and mTOR signalling controls tumour cell growth. Nature. 2006; 441: 424-430.

40. Janes MR, Fruman DA. Targeting TOR dependence in cancer. Oncotarget. 2010; 1: 69-76.

41. Guertin DA, Sabatini DM. Defining the role of mTOR in cancer. Cancer Cell. 2007; 12: 9-22.

42. Schmidt-Kittler O, Zhu J, Yang J, Liu G, Hendricks W, Lengauer C, Gabelli SB, Kinzler KW, Vogelstein B, Huso DL, Zhou S. PI3Kalpha inhibitors that inhibit metastasis. Oncotarget. 2010; 1: 339-348.

43. Martelli AM, Evangelisti C, Chiarini F, McCubrey JA. The phosphatidylinositol 3-kinase/Akt/mTOR signaling network as a therapeutic target in acute myelogenous leukemia patients. Oncotarget. 2010; 1: 89-103.

44. Zawel L. P3Kalpha: a driver of tumor metastasis? Oncotarget. 2010; 1: 315-316.

45. Zhang Z, Stiegler AL, Boggon TJ, Kobayashi S, Halmos B. EGFR-mutated lung cancer: a paradigm of molecular oncology. Oncotarget. 2010; 1: 497-514.

46. Shahbazian D, Parsyan A, Petroulakis E, Hershey J, Sonenberg N. eIF4B controls survival and proliferation and is regulated by proto-oncogenic signaling pathways. Cell Cycle. 2010; 9: 4106-4109.

47. Zhao L, Vogt PK. Hot-spot mutations in p110alpha of phosphatidylinositol 3-kinase (pI3K): differential interactions with the regulatory subunit p85 and with RAS. Cell Cycle. 2010; 9: 596-600.

48. Bhatia B, Nahle Z, Kenney AM. Double trouble: when sonic hedgehog signaling meets TSC inactivation. Cell Cycle. 2010; 9: 456-459.

49. Fujishita T, Aoki M, Taketo MM. The role of mTORC1 pathway in intestinal tumorigenesis. Cell Cycle. 2009; 8: 3684-3687.

50. Galluzzi L, Kepp O, Kroemer G. TP53 and MTOR crosstalk to regulate cellular senescence. Aging. 2010; 2: 535-537.

51. Blagosklonny MV. Molecular damage in cancer: an argument for mTOR-driven aging. Aging. 2011; 3: 1130-1141.

52. Blagosklonny MV. NCI's provocative questions on cancer: some answers to ignite discussion. Oncotarget. 2011; 2: 1352-1367.

53. Henry CJ, Marusyk A, Zaberezhnyy V, Adane B, DeGregori J. Declining lymphoid progenitor fitness promotes aging-

associated leukemogenesis. Proc Natl Acad Sci U S A. 2010; 107: 21713-21718.

54. Henry CJ, Marusyk A, DeGregori J. Aging-associated changes in hematopoiesis and leukemogenesis: what's the connection? Aging. 2011; 3: 643-656.

55. Parrinello S, Coppe JP, Krtolica A, Campisi J. Stromal-epithelial interactions in aging and cancer: senescent fibroblasts alter epithelial cell differentiation. J Cell Sci. 2005; 118: 485-496.

56. Coppe JP, Patil CK, Rodier F, Sun Y, Munoz DP, Goldstein J, Nelson PS, Desprez PY, Campisi J. Senescence-associated secretory phenotypes reveal cell-nonautonomous functions of oncogenic RAS and the p53 tumor suppressor. PLoS Biol. 2008; 6: 2853-2868.

57. Davalos AR, Coppe JP, Campisi J, Desprez PY. Senescent cells as a source of inflammatory factors for tumor progression. Cancer Metastasis Rev. 2011; 29: 273-283.

58. Coussens LM, Werb Z. Inflammation and cancer. Nature. 2002; 420: 860-867.

59. Lisanti MP, Martinez-Outschoorn UE, Pavlides S, Whitaker-Menezes D, Pestell RG, Howell A, Sotgia F. Accelerated aging in the tumor microenvironment: connecting aging, inflammation and cancer metabolism with personalized medicine. Cell Cycle. 2011; 10: 2059-2063.

60. Balliet RM, Capparelli C, Guido C, Pestell TG, Martinez-Outschoorn UE, Lin Z, Whitaker-Menezes D, Chiavarina B, Pestell RG, Howell A, Sotgia F, Lisanti MP. Mitochondrial oxidative stress in cancer-associated fibroblasts drives lactate production, promoting breast cancer tumor growth: understanding the aging and cancer connection. Cell Cycle. 2011; 10: 4065-4073.

61. Campisi J. Senescent cells, tumor suppression, and organismal aging: good citizens, bad neighbors. Cell. 2005; 120: 513-522.

62. Vicente-Duenas C, Abollo-Jimenez F, Ruiz-Roca L, Alonso-Escudero E, Jimenez R, Cenador MB, Criado FJ, Cobaleda C, Sanchez-Garcia I. The age of the target cell affects B-cell leukaemia malignancy. Aging. 2010; 2: 908-913.

63. Bonuccelli G, Whitaker-Menezes D, Castello-Cros R, Pavlides S, Pestell RG, Fatatis A, Witkiewicz AK, Vander Heiden MG, Migneco G, Chiavarina B, Frank PG, Capozza F, Flomenberg N, Martinez-Outschoorn UE, Sotgia F, Lisanti MP. The reverse Warburg effect: glycolysis inhibitors prevent the tumor promoting effects of caveolin-1 deficient cancer associated fibroblasts. Cell Cycle. 2010; 9: 1960-1971.

64. Castello-Cros R, Bonuccelli G, Molchansky A, Capozza F, Witkiewicz AK, Birbe RC, Howell A, Pestell RG, Whitaker-Menezes D, Sotgia F, Lisanti MP. Matrix remodeling stimulates stromal autophagy, "fueling" cancer cell mitochondrial metabolism and metastasis. Cell Cycle. 2011; 10: 2021-2034.

65. Chiavarina B, Whitaker-Menezes D, Martinez-Outschoorn UE, Witkiewicz AK, Birbe RC, Howell A, Pestell RG, Smith J, Daniel R, Sotgia F, Lisanti MP. Pyruvate kinase expression (PKM1 and PKM2) in cancer-associated fibroblasts drives stromal nutrient production and tumor growth. Cancer Biol Ther. 2011; 12.

66. Bonuccelli G, Tsirigos A, Whitaker-Menezes D, Pavlides S, Pestell RG, Chiavarina B, Frank PG, Flomenberg N, Howell A, Martinez-Outschoorn UE, Sotgia F, Lisanti MP. Ketones and lactate "fuel" tumor growth and metastasis: Evidence that epithelial cancer cells use oxidative mitochondrial metabolism. Cell Cycle. 2010; 9: 3506-3514.

67. Migneco G, Whitaker-Menezes D, Chiavarina B, Castello-Cros R, Pavlides S, Pestell RG, Fatatis A, Flomenberg N, Tsirigos A, Howell A, Martinez-Outschoorn UE, Sotgia F, Lisanti MP. Glycolytic cancer associated fibroblasts promote breast cancer tumor growth, without a measurable increase in angiogenesis: evidence for stromal-epithelial metabolic coupling. Cell Cycle. 2010; 9: 2412-2422.

68. Ko YH, Lin Z, Flomenberg N, Pestell RG, Howell A, Sotgia F, Lisanti MP, Martinez-Outschoorn UE. Glutamine fuels a vicious cycle of autophagy in the tumor stroma and oxidative mitochondrial metabolism in epithelial cancer cells: Implications for preventing chemotherapy resistance. Cancer Biol Ther. 2011; 12.

69. Martinez-Outschoorn UE, Pestell RG, Howell A, Tykocinski ML, Nagajyothi F, Machado FS, Tanowitz HB, Sotgia F, Lisanti MP. Energy transfer in "parasitic" cancer metabolism: mitochondria are the powerhouse and Achilles' heel of tumor cells. Cell Cycle. 2011; 10: 4208-4216.

70. Martinez-Outschoorn UE, Whitaker-Menezes D, Lin Z, Flomenberg N, Howell A, Pestell RG, Lisanti MP, Sotgia F. Cytokine production and inflammation drive autophagy in the tumor microenvironment: role of stromal caveolin-1 as a key regulator. Cell Cycle. 2011; 10: 1784-1793.

71. Capparelli C, Guido C, Whitaker-Menezes D, Bonuccelli G, Balliet R, Pestell TG, Goldberg AF, Pestell RG, Howell A, Sneddon S, Birbe R, Tsirigos A, Martinez-Outschoorn U, Sotgia F, Lisanti MP. Autophagy and senescence in cancer-associated fibroblasts metabolically supports tumor growth and metastasis via glycolysis and ketone production. Cell Cycle. 2012; 11: 2285-2302.

72. Mercier I, Camacho J, Titchen K, Gonzales DM, Quann K, Bryant KG, Molchansky A, Milliman JN, Whitaker-Menezes D, Sotgia F, Jasmin JF, Schwarting R, Pestell RG, Blagosklonny MV, Lisanti MP. Caveolin-1 and Accelerated Host Aging in the Breast Tumor Microenvironment: Chemoprevention with Rapamycin, an mTOR Inhibitor and Anti-Aging Drug. Am J Pathol. 2012; 181: 278-293.

73. Blagosklonny MV. Prevention of cancer by inhibiting aging. Cancer Biol Ther. 2008; 7: 1520-1524.

74. Hursting SD, Lavigne JA, Berrigan D, Perkins SN, Barrett JC. Calorie restriction, aging, and cancer prevention: mechanisms of action and applicability to humans. Annu Rev Med. 2003; 54: 131-152.

75. Longo VD, Fontana L. Calorie restriction and cancer prevention: metabolic and molecular mechanisms. Trends Pharmacol Sci. 2010; 31: 89-98.

76. Blagosklonny MV. Calorie restriction: Decelerating mTOR-driven aging from cells to organisms (including humans). Cell Cycle. 2010; 9: 683-688.

77. Hursting SD, Perkins SN, Phang JM. Calorie restriction delays spontaneous tumorigenesis in p53-knockout transgenic mice. Proc Natl Acad Sci U S A. 1994; 91: 7036-7040.

78. Berrigan D, Perkins SN, Haines DC, Hursting SD. Adult-onset calorie restriction and fasting delay spontaneous tumorigenesis in p53-deficient mice. Carcinogenesis. 2002; 23: 817-822.

79. Harrison DE, Strong R, Sharp ZD, Nelson JF, Astle CM, Flurkey K, Nadon NL, Wilkinson JE, Frenkel K, Carter CS, Pahor M, Javors MA, Fernandezr E, Miller RA. Rapamycin fed late in life extends lifespan in genetically heterogenous mice. Nature. 2009; 460: 392-396.

80. Anisimov VN, Zabezhinski MA, Popovich IG, Piskunova TS, Semenchenko AV, Tyndyk ML, Yurova MN, Antoch MP, Blagosklonny MV. Rapamycin extends maximal lifespan in cancer-prone mice. Am J Pathol. 2010; 176: 2092-2097.

81. Anisimov VN, Zabezhinski MA, Popovich IG, Piskunova TS, Semenchenko AV, Tyndyk ML, Yurova MN, Rosenfeld SV, Blagosklonny MV. Rapamycin increases lifespan and inhibits spontaneous tumorigenesis in inbred female mice. Cell Cycle. 2011; 10: 4230-4236.

82. Mathew T, Kreis H, Friend P. Two-year incidence of malignancy in sirolimus-treated renal transplant recipients: results from five multicenter studies. Clin Transplant. 2004; 18: 446-449.

83. Kauffman HM, Cherikh WS, Cheng Y, Hanto DW, Kahan BD. Maintenance immunosuppression with target-of-rapamycin inhibitors is associated with a reduced incidence of de novo malignancies. Transplantation. 2005; 80:883-889.

84. Yakupoglu YK, Buell JF, Woodle S, Kahan BD. Individualization of Immunosuppressive Therapy. III. Sirolimus Associated With a Reduced Incidence of Malignancy. Transplant Proc. 2006; 38: 358-361.

85. Campistol JM, Eris J, Oberbauer R, Friend P, Hutchison B, Morales JM, Claesson K, Stallone G, Russ G, Rostaing L, Kreis H, Burke JT, Brault Y, Scarola JA, Neylan JF. Sirolimus Therapy after Early Cyclosporine Withdrawal Reduces the Risk for Cancer in Adult Renal Transplantation. J Am Soc Nephrol. 2006; 17: 581-589.

86. Stallone G, Schena A, Infante B, Di Paolo S, Loverre A, Maggio G, Ranieri E, Gesualdo L, Schena FP, Grandaliano G. Sirolimus for Kaposi's sarcoma in renal-transplant recipients. N Engl J Med. 2005; 352: 1317-1323.

87. Pinkston JM, Garigan D, Hansen M, Kenyon C. Mutations that increase the life span of C. elegans inhibit tumor growth. Science. 2006; 313: 971-975.

88. Poyurovsky MV, Prives C. P53 and aging: A fresh look at an old paradigm. Aging. 2010; 2: 380-382.

89. Blagosklonny MV. Revisiting the antagonistic pleiotropy theory of aging: TOR-driven program and quasi-program. Cell Cycle. 2010; 9: 3151-3156.

90. de Keizer PL, Laberge RM, Campisi J. p53: Pro-aging or pro-longevity? Aging. 2010; 2: 377-379.

91. Chao SK, Horwitz SB, McDaid HM. Insights into 4E-BP1 and p53 mediated regulation of accelerated cell senescence. Oncotarget. 2011; 2: 89-98.

92. Matheu A, Maraver A, Klatt P, Flores I, Garcia-Cao I, Borras C, Flores JM, Vi–a J, Blasco MA, Serrano M. Delayed ageing through damage protection by the Arf/p53 pathway. Nature. 2007; 448: 375-379.

93. Donehower LA, Harvey M, Slagle BL, McArthur MJ, Montgomery CA, Jr., Butel JS, Bradley A. Mice deficient for p53 are developmentally normal but susceptible to spontaneous tumours. Nature. 1992; 356: 215-221.

94. Harvey M, McArthur MJ, Montgomery CA, Jr., Butel JS, Bradley A, Donehower LA. Spontaneous and carcinogen-induced tumorigenesis in p53-deficient mice. Nat Genet. 1993; 5: 225-229.

95. Jacks T, Remington L, Williams BO, Schmitt EM, Halachmi S, Bronson RT, Weinberg RA. Tumor spectrum analysis in p53-mutant mice. Curr Biol. 1994; 4: 1-7.

96. Donehower LA, Harvey M, Vogel H, McArthur MJ, Montgomery CA, Jr., Park SH, Thompson T, Ford RJ, Bradley A. Effects of genetic background on tumorigenesis in p53-deficient mice. Mol Carcinog. 1995; 14: 16-22.

97. Venkatachalam S, Shi YP, Jones SN, Vogel H, Bradley A, Pinkel D, Donehower LA. Retention of wild-type p53 in tumors from p53 heterozygous mice: reduction of p53 dosage can promote cancer formation. Embo J. 1998; 17: 4657-4667.

98. Hinkal G, Parikh N, Donehower LA. Timed somatic deletion of p53 in mice reveals age-associated differences in tumor progression. PLoS One. 2009; 4: e6654.

99. Guevara NV, Kim HS, Antonova EI, Chan L. The absence of p53 accelerates atherosclerosis by increasing cell proliferation in vivo. Nat Med. 1999; 5: 335-339.

100. Mercer J, Figg N, Stoneman V, Braganza D, Bennett MR. Endogenous p53 protects vascular smooth muscle cells from apoptosis and reduces atherosclerosis in ApoE knockout mice. Circ Res. 2005; 96: 667-674.

101. Mercer J, Bennett M. The role of p53 in atherosclerosis. Cell Cycle. 2006; 5: 1907-1909.

102. van Vlijmen BJ, Gerritsen G, Franken AL, Boesten LS, Kockx MM, Gijbels MJ, Vierboom MP, van Eck M, van De Water B, van Berkel TJ, Havekes LM. Macrophage p53 deficiency leads to enhanced atherosclerosis in APOE*3-Leiden transgenic mice. Circ Res. 2001; 88: 780-786.

103. Edinger AL, Linardic CM, Chiang GG, Thompson CB, Abraham RT. Differential effects of rapamycin on mammalian target of rapamycin signaling functions in mammalian cells. Cancer Res. 2003; 63: 8451-8460.

104. Sipula IJ, Brown NF, Perdomo G. Rapamycin-mediated inhibition of mammalian target of rapamycin in skeletal muscle cells reduces glucose utilization and increases fatty acid oxidation. Metabolism. 2006; 55: 1637-1644.

105. Brown NF, Stefanovic-Racic M, Sipula IJ, Perdomo G. The mammalian target of rapamycin regulates lipid metabolism in primary cultures of rat hepatocytes. Metabolism. 2007; 56: 1500-1507.

106. Hu W, Feng Z, Teresky AK, Levine AJ. p53 regulates maternal reproduction through LIF. Nature. 2007; 450: 721-724.

107. Hu W, Feng Z, Atwal GS, Levine AJ. p53: a new player in reproduction. Cell Cycle. 2008; 7: 848-852.

108. Roemer K. Are the conspicuous interdependences of fecundity, longevity and cognitive abilities in humans caused in part by p53? Cell Cycle. 2010; 9: 3438-3441.

109. Levine AJ, Tomasini R, McKeon FD, Mak TW, Melino G. The p53 family: guardians of maternal reproduction. Nat Rev Mol Cell Biol. 2011; 12: 259-265.

110. Mantovani R. More on the pro-fertility activity of p53: the blastocyst side. Cell Cycle. 2011; 10: 4205.

111. Chen D, Zheng W, Lin A, Uyhazi K, Zhao H, Lin H. Pumilio 1 suppresses multiple activators of p53 to safeguard spermatogenesis. Curr Biol. 2012; 22: 420-425.

112. McGee MD, Day N, Graham J, Melov S. cep-1/p53-dependent dysplastic pathology of the aging C. elegans gonad. Aging. 2012; 4: 256-269.

113. Kang HJ, Feng Z, Sun Y, Atwal G, Murphy ME, Rebbeck TR, Rosenwaks Z, Levine AJ, Hu W. Single-nucleotide polymorphisms in the p53 pathway regulate fertility in humans. Proc Natl Acad Sci U S A. 2009; 106: 9761-9766.

Research Perspective

Cell cycle arrest is not yet senescence, which is not just cell cycle arrest: terminology for TOR-driven aging

Mikhail V. Blagosklonny

Department of Cell Stress Biology, Roswell Park Cancer Institute, BLSC, L3-312, Buffalo, NY, 14263, USA

Key words: *senescence, geroconversion, gerosuppressants, rapamycin, mTOR*
Received: *2/17/12; Accepted: 3/5/12; Published: 3/5/12* doi:10.18632/aging.100443
Correspondence to: *Mikhail V. Blagosklonny, MD/PhD;* ***E-mail:*** *blagosklonny@oncotarget.com*

Abstract: Cell cycle arrest is not yet senescence. When the cell cycle is arrested, an inappropriate growth-promotion converts an arrest into senescence (geroconversion). By inhibiting the growth-promoting mTOR pathway, rapamycin decelerates geroconversion of the arrested cells. And as a striking example, while causing arrest, p53 may decelerate or suppress geroconversion (in some conditions). Here I discuss the meaning of geroconversion and also the terms gerogenes, gerossuppressors, gerosuppressants, gerogenic pathways, gero-promoters, hyperfunction and feedback resistance, regenerative potential, hypertrophy and secondary atrophy, pro-gerogenic and gerogenic cells.

INTRODUCTION

A year ago, I wrote a perspective "Cell cycle arrest is not senescence", intended to clarify a new meaning of cellular senescence [1]. The perspective was not completely understood in part due to its title. The title was missing the word "yet", which is now included. As discussed in the article, cell cycle arrest is not yet senescence and senescence is not just arrest: senescence can be driven by growth-promoting pathways such as mTOR, when actual growth is impossible. (This mechanism connects cellular senescence, organismal aging and age-related diseases, predicting anti-aging agents [2-6]). In brief, senescence can be caused by growth stimulation, when the cell cycle is arrested [7, 8]. As one hallmark, senescent cells loose proliferative potential (PP) - the potential to resume proliferation. Importantly, inhibitors of mTOR suppress hallmarks of senescence during cell cycle arrest so cells stay quiescent but not senescent [9-13]. Such quiescent cells, with inhibited mTOR, retain PP. Once again, cells may be arrested but retain PP, the ability to restart proliferation, when allowed. In certain conditions, p53 causes arrest but can preserve PP by inhibiting the mTOR pathway [14-16]. However, this phenomenon should not be misunderstood to indicate that "p53 induces proliferation or prevents arrest or keeps cells proliferating" or "arrested cells retain proliferation"; rather, p53 instead regulates proliferative potential. Although we tried to explain what p53 does exactly (causes arrest, while preserving PP) misunderstanding nonetheless ensued. One solution is not to use the term PP altogether, substituting for it the term RP (regenerative potential). In the organism, stem cells and wound-healing cells, while quiescent, are capable to regenerate tissues after cell loss. Unlike non-senescent cells, senescent cells cannot divide in response to cell loss and therefore lose the potential to regenerate tissues. In cell culture, quiescent cells preserve RP. If the cell cycle is blocked, activation of mTOR causes loss of RP [17]. New concepts need new terminology. Instead of squeezing novel meaning into the old terms, here we present new terms for a new meaning of the aging process. And a central term is gerogenic conversion or geroconversion.

Geroconversion

Mitogens and growth factors activate growth-promoting pathways, which stimulate (a) growth in size and (b) cell cycle progression. When cells proliferate, an increase in cell mass is balanced by division. Withdrawal of growth factors causes quiescence: the quiescent cell neither grows, nor cycles, and its functions and metabolism are low. In contrast, cell cycle

blockage, in the presence of growth-stimulation leads to senescence (Figure 1). Hallmarks of senescence include a large flat morphology, senescence-associated beta-galactosidase (SA-beta-gal) staining, cellular over-activation and hyper-function, feedback signal resistance and loss of RP (that is, the inability to restart proliferation when the cell cycle inhibitor is removed). For example, in one well-studied cellular model, inducible ectopic expression of p21 causes cycle arrest (day 1) and senescence (after 3 days) [18, 19]. At first, the arrested cells are quiescent-like: they are not hypertrophic, and they are SA-beta-gal negative and retain RP. Thus, they can restart proliferation when p21 expression is switched off. After 3 days, however, the cells acquire a senescent morphology and, if p21 is then switched off, the cells cannot restart proliferation or die in mitosis [19]. Importantly, while inhibiting the cell cycle, p21 does not inhibit the mTOR pathway [8-17, 20, 21]. mTOR and perhaps some other growth-promoting pathways convert quiescence (day 1) into senescence (day 3). Inhibition of mTOR by rapamycin decelerates this 'geroconversion' [8-17, 20, 21].

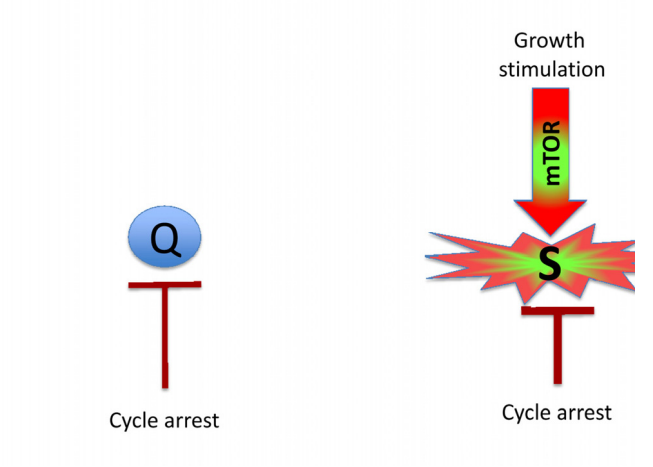

Figure 1. Quiescence versus senescence. Q: quiescent cell. In the absence of the growth factors, normal cells undergo cell cycle arrest. S: senescent cell. When cell cycle is arrested, the growth signal (if it cannot reactivate cycling) drives senescence.

Similarly other inhibitors of mTOR also suppress geroconversion [10, 11]. For example, in some cell lines, induction of p53 inhibits mTOR [22-26] and other anabolic pathways [27-32], thus suppressing geroconversion in cells arrested by ectopic p21 [14]. By itself, p53 causes cell cycle arrest but can suppress geroconversion [14-17, 33-35]. In cell culture, cell cycle arrest and geroconversion are initiated simultaneously.

In proliferating cultured cells (especially cancer cells) mTOR is activated. Many agents cause cell cycle arrest without inhibiting mTOR (or other growth factor-sensing pathways). Once arrested, such cells are rapidly converted to senescent cells. This is accelerated geroconversion. So it may seem that senescence is "caused" by cell cycle arrest. The above examples, however, suggest that senescence is caused by growth-stimulation when the cell cycle is arrested.

In the organism, most cells are arrested and geroconversion can be slow. When chronically stimulated (but still arrested) they can become senescent. This physiological geroconversion can be imitated in cell culture [17].

The terms gerogenic conversion and oncogenic transformation sound alike.This is not a coincidence for choosing the term geroconversion. *Gerogenic conversion and oncogenic transformation are two sides of the same process*.

Gerogenic oncogenes and gerogenes

Activation of growth factor receptors, Ras and Raf family members and members of the MAPK and PI3K/Akt pathways are universal in cancer [36-38]. All these oncogenes activate the mTOR pathway [39-47]. They are gerogenic oncogenes, which drive the geroconversion of arrested cells. Because strong growth-promoting (mitogenic) signals induce cell cycle arrest [48-54], strong mitogenic signaling causes both conditions of senescence: arrest and mTOR/growth signal (Figure 2A). To avoid senescence, cancer cells must disable cell cycle control (Figure 2B) by either loss of p16, p53 and Rb or activation of c-myc, for example [36-38, 48, 55, 56]. In proliferating cells, gerogenic oncogenes render cells malignant and pro-gerogenic (see below). The same gerogenic oncogenes or their analogs accelerate aging and shorten life span in diverse species from worm to mammals. Therefore, these genes can be termed gerogenes [57]. Thus, the mTOR pathway shortens life span, whereas rapamycin extends life span [58-75]. Not coincidentally, Mutations that increase the life span of *C. elegans* inhibit tumor growth [76]. Finally, metabolic self-destruction, known as chronological senescence in yeast [60, 61, 77] is also stimulated by gerogenes and is inhibited by rapamycin [78].

Gerosuppressors

Gerosuppressors are genes (and their products) that suppress geroconversion. Gerosuppressors (for example, PTEN, AMPK, sirtuins, TSC2, NF-1 and p53) antagonize the mTOR pathway (see for ref. [57]). Their inactivation shortens life span in model organisms.

Gerosuppressors are also tumor suppressors. So gero-suppressors suppress both geroconversion and cancer.

Gerosuppressants

Gerosuppressants are small molecules (such as rapamycin) that suppress geroconversion. Not co-incidentally, rapamycin also extends life span in diverse species from yeast to mammals. They can, in theory, be used to treat age-related diseases by slowing down aging, thus extending both maximal and healthy lifespan.

Gero promoters

Small molecules or drugs that can accelerate or promote geroconversion. One potential candidate is phorbol esters, which can activate mTOR in some cells. Not surprisingly, it is also a tumor-promoter.

Gerogenic pathways

Gerogenic signaling pathways promote geroconversion. Whether gerogenic pathways cause or abrogate cell cycle arrest is irrelevant. For example, strong mitogenic/growth signals can induce cell cycle arrest, instead of proliferation [48-54]. Simultaneously, in arrested cells, growth signals cause geroconversion, leading to senescence (Figure 2A). As another example, the effects of p53 on cell cycle and geroconverion can be dissociated [14].

Pro-gerogenic conversion

In proliferating cells, overactivation of the mTOR pathway renders them pro-gerogenic. Cancer cells are proliferating pro-gerogenic cells. When such cells are forcefully arrested, they become senescent. Also, stimulation of mTOR in normal stem cells causes hyper-proliferation, pro-gerogenic conversion and cell exhaustion [79-84], contributing to aging.

Gerogenic cell

Although loss of RP is very useful marker of senescence in cell culture, this marker may not play a key role in age-related pathologies in the organism, because most post-mitotic cells should not be able to restart proliferation anyway. (Notable exceptions are stem, wound-healing and satellite cells). I suggest that active mTOR in arrested cells is a crucial marker of gerogenic cells and early senescence. Gerogenic (senescent) and quiescent cells can be distinguished by the levels of phosphorylated S6 (pS6), the ribosomal protein that is phosphorylated in response to mTOR activation: high in senescent cells and low in quiescent cells. Levels of pS6 in senescent cells may remain similar to the levels of pS6 in proliferating cells. So senescent/gerogenic cells have many features of proliferating cells. Interestingly, basal (fasting) levels pS6 were elevated in old mice [85]. Gerogenic cells could be defined as arrested cell with activated mTOR. The most physiologically relevant features are hypertrophy, hyperfunction and feedback resistance.

Hypertrophy

Growth signals during cell cycle arrest lead to an enlarged cell morphology. From theoretical perspective, hypertrophy will eventually be limited by activation of lysosomes/autophagy [7]. This phenomenon may explain the activity of SA-beta-Gal, which is lysosomal enzyme [86-88] and active autophagy despite active mTOR [89, 90].

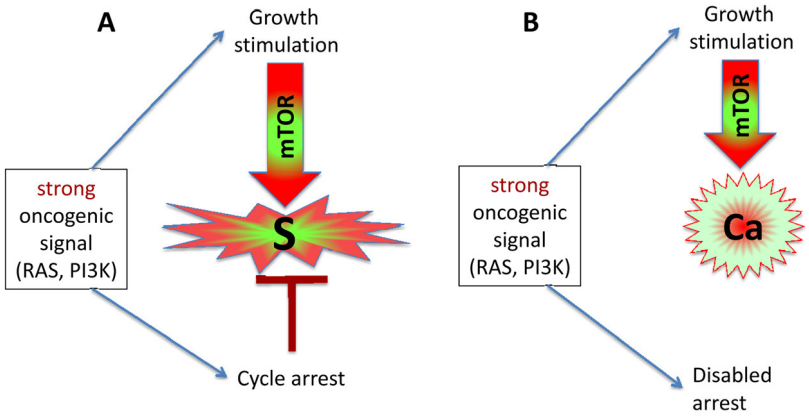

Figure 2. Strong oncogenic signaling, senescence and cancer. (**A**) Strong mitogenic/ oncogenic signal can simultaneously cause arrest and activate mTOR. Cells senesce. **(B)** Disabling of cell cycle control (loss of p16, Rb, p53) can convert senescence to cancer.

Hyperfunction

Due to over-stimulation, senescent cells are hyperfunctional. For example, For example, senescent fibroblasts secrete many cytokines, growth factors and proteases (the hypersecretory senescence-associated secretory phenotype or SASP), senescent osteoclasts resorb bones, smooth muscle cells contract, platelets aggregate, neutrophils generate ROS, neurons charge, endocrine cells produce hormones. Noteworthy, SASP as a marker of senescence [91-99] is an example of hyperfunction.

Feedback resistance

Overactivation of signaling pathways causes signal resistance due to feedback inactivation of the signaling pathway. As an example, mTOR/S6K overactivation causes insulin and GF resistance [100-104].

Secondary atrophy

Hyperfunctions are associated with hypertrophy and hyperplasia. Yet, at the end, cells may fail either to function or to survive, leading to secondary atrophy. When cells fail, conditions become TOR-independent and terminal. This conceals hyperfunction as an initial cause, misleadingly presenting aging as a decline.

From gerogenic cells to organismal aging

You might notice that an accumulation of molecular damage was never mentioned in this article. It was unneeded. Cellular aging and geroconversion is not caused by accumulation of random molecular damage. Although damage accumulates, I suggest that the organism does not live long enough to suffer from this accumulation with one special exception that illuminates the rule [105]. (The weakness of free radical damage theory was discussed in detail [106-114]).

One definition of organismal aging is an increase in the probability of death. Gerogenic cells (due to their hyper-activity and signal-resistance) may slowly cause atherosclerosis, hypertension, insulin-resistance, obesity, cancer, neurodegeneration, age-related macular degeneration, prostate enlargement, menopause, hair loss, osteoporosis, osteoarthritis, benign tumors and skin alterations. These conditions lead to damage -- not molecular damage but organ and system damage. Examples include beta-cell failure [115], ovarian failure (menopause) [116], myocardial infarction, stroke, renal failure, broken hips, cancer metastases and so on [6, 117]. These are acute catastrophes, which cause death. I suggest that by suppressing geroconversion, gerosuppressants will prevent diseases and extend healthy life span.

ACKNOWLEDGMENTS

I thank Judith Campisi (Buck Institute for Age Research, Novato, CA, USA) and Manuel Serrano (Spanish National Cancer Research Center, Madrid, Spain) for reading or editing this manuscript and for excellent suggestions.

CONFLICT OF INTERESTS STATEMENT

The author of this manuscript has no conflict of interest to declare.

REFERENCES

1. Blagosklonny MV. Cell cycle arrest is not senescence. Aging (Albany NY). 2011; 3: 94-101.

2. Blagosklonny MV. Aging and immortality: quasi-programmed senescence and its pharmacologic inhibition. Cell Cycle. 2006; 5: 2087-2102.

3. Blagosklonny MV. An anti-aging drug today: from senescence-promoting genes to anti-aging pill. Drug Disc Today. 2007; 12: 218-224.

4. Blagosklonny MV. Paradoxes of aging. Cell Cycle. 2007; 6: 2997-3003.

5. Blagosklonny MV, Hall MN. Growth and aging: a common molecular mechanism. Aging. 2009; 1: 357-362.

6. Blagosklonny MV. mTOR-driven aging: speeding car without brakes. Cell Cycle. 2009; 8: 4055-4059.

7. Blagosklonny MV. Cell senescence and hypermitogenic arrest. EMBO Rep. 2003; 4: 358-362.

8. Demidenko ZN, Blagosklonny MV. Growth stimulation leads to cellular senescence when the cell cycle is blocked. Cell Cycle. 2008; 7: 3355-3361.

9. Demidenko ZN, Zubova SG, Bukreeva EI, Pospelov VA, Pospelova TV, Blagosklonny MV. Rapamycin decelerates cellular senescence. Cell Cycle. 2009; 8: 1888-1895.

10. Demidenko ZN, Shtutman M, Blagosklonny MV. Pharmacologic inhibition of MEK and PI-3K converges on the mTOR/S6 pathway to decelerate cellular senescence. Cell Cycle. 2009; 8: 1896-1900.

11. Demidenko ZN, Blagosklonny MV. At concentrations that inhibit mTOR, resveratrol suppresses cellular senescence. Cell Cycle. 2009; 8: 1901-1904.

12. Demidenko ZN, Blagosklonny MV. Quantifying pharmacologic suppression of cellular senescence: prevention of cellular hypertrophy versus preservation of proliferative potential. Aging (Albany NY). 2009; 1: 1008-1016.

13. Pospelova TV, Demidenk ZN, Bukreeva EI, Pospelov VA, Gudkov AV, Blagosklonny MV. Pseudo-DNA damage response in senescent cells. Cell Cycle. 2009; 8: 4112-4118.

14. Demidenko ZN, Korotchkina LG, Gudkov AV, Blagosklonny MV. Paradoxical suppression of cellular senescence by p53. Proc Natl Acad Sci U S A. 2010; 107: 9660-9664.

15. Korotchkina LG, Leontieva OV, Bukreeva EI, Demidenko ZN, Gudkov AV, Blagosklonny MV. The choice between p53-induced senescence and quiescence is determined in part by the mTOR pathway. Aging (Albany NY). 2010; 2: 344-352.

16. Leontieva O, Gudkov A, Blagosklonny M. Weak p53 permits senescence during cell cycle arrest. Cell Cycle. 2010; 9: 4323-4327.

17. Leontieva OV, Blagosklonny MV. DNA damaging agents and p53 do not cause senescence in quiescent cells, while consecutive re-activation of mTOR is associated with conversion to senescence. Aging (Albany NY). 2010; 2: 924-935.

18. Chang BD, Xuan Y, Broude EV, Zhu H, Schott B, Fang J, Roninson IB. Role of p53 and p21waf1/cip1 in senescence-like terminal proliferation arrest induced in human tumor cells by chemotherapeutic drugs. Oncogene. 1999; 18: 4808-4818.

19. Chang BD, Broude EV, Fang J, Kalinichenko TV, Abdryashitov R, Poole JC, Roninson IB. p21Waf1/Cip1/Sdi1-induced growth arrest is associated with depletion of mitosis-control proteins and leads to abnormal mitosis and endoreduplication in recovering cells. Oncogene. 2000; 19: 2165-2170.

20. Romanov VS, Abramova MV, Svetlikova SB, Bykova TV, Zubova SG, Aksenov ND, Fornace AJ, Jr., Pospelova TV, Pospelov VA. p21(Waf1) is required for cellular senescence but not for cell cycle arrest induced by the HDAC inhibitor sodium butyrate. Cell Cycle. 2010; 9: 3945-3955.

21. Leontieva OV, Demidenko ZN, Gudkov AV, Blagosklonny MV. Elimination of proliferating cells unmasks the shift from senescence to quiescence caused by rapamycin. PLoS One. 2011; 6: e26126.

22. Stambolic V, MacPherson D, Sas D, Lin Y, Snow B, Jang Y, Benchimol S, Mak TW. Regulation of PTEN transcription by p53. Mol Cell. 2001; 8: 317-325.

23. Levine AJ, Feng Z, Mak TW, You H, Jin S. Coordination and communication between the p53 and IGF-1-AKT-TOR signal transduction pathways. Genes Dev. 2006; 20: 267-275.

24. Feng Z, Zhang H, Levine AJ, Jin S. The coordinate regulation of the p53 and mTOR pathways in cells. Proc Natl Acad Sci U S A. 2005; 102: 8204-8209.

25. Feng Z, Hu W, de Stanchina E, Teresky AK, Jin S, Lowe S, Levine AJ. The regulation of AMPK beta1, TSC2, and PTEN expression by p53: stress, cell and tissue specificity, and the role of these gene products in modulating the IGF-1-AKT-mTOR pathways. Cancer Res. 2007; 67: 3043-3053.

26. Feng Z, Levine AJ. The regulation of energy metabolism and the IGF-1/mTOR pathways by the p53 protein. Trends Cell Biol. 2010; 20: 427-434.

27. Suzuki S, Tanaka T, Poyurovsky MV, Nagano H, Mayama T, Ohkubo S, Lokshin M, Hosokawa H, Nakayama T, Suzuki Y, Sugano S, Sato E, Nagao T, Yokote K, Tatsuno I, Prives C. Phosphate-activated glutaminase (GLS2), a p53-inducible regulator of glutamine metabolism and reactive oxygen species. Proc Natl Acad Sci U S A. 2010; 107: 7461-7466.

28. Poyurovsky MV, Prives C. P53 and aging: A fresh look at an old paradigm. Aging (Albany NY). 2010.

29. Vousden KH, Ryan KM. p53 and metabolism. Nat Rev Cancer. 2009; 9: 691-700.

30. Vigneron A, Vousden KH. p53, ROS and senescence in the control of aging. Aging (Albany NY). 2010; 2: 471-474.

31. Madan E, Gogna R, Bhatt M, Pati U, Kuppusamy P, Mahdi AA. Regulation of glucose metabolism by p53: Emerging new roles for the tumor suppressor. Oncotarget. 2011; 2: 948-957.

32. Zawacka-Pankau J, Grinkevich VV, Hunten S, Nikulenkov F, Gluch A, Li H, Enge M, Kel A, Selivanova G. Inhibition of glycolytic enzymes mediated by pharmacologically activated p53: targeting Warburg effect to fight cancer. J Biol Chem. 2011; 286: 41600-41615.

33. Long JS, Ryan KM. p53 and senescence: a little goes a long way. Cell Cycle. 2010; 9: 4050-4051.

34. Santoro R, Blandino G. p53: The pivot between cell cycle arrest and senescence. Cell Cycle. 2010; 9: 4262-4263.

35. Serrano M. Shifting senescence into quiescence by turning up p53. Cell Cycle. 2010; 9: 4256-4257.

36. Vogelstein B, Kinzler KW. Cancer genes and the pathways they control. Nat Med. 2004; 10: 789-799.

37. Cully M, You H, Levine AJ, Mak TW. Beyond PTEN mutations: the PI3K pathway as an integrator of multiple inputs during tumorigenesis. Nat Rev Cancer. 2006; 6: 184-192.

38. Hanahan D, Weinberg RA. Hallmarks of cancer: the next generation. Cell. 2011; 144: 646-674.

39. Hay N, Sonenberg N. Upstream and downstream of mTOR. Genes Dev. 2004; 18: 1926-1945.

40. Sarbassov dos D, Ali SM, Sabatini DM. Growing roles for the mTOR pathway. Curr Opin Cell Biol. 2005; 17: 596-603.

41. Inoki K, Corradetti MN, Guan KL. Dysregulation of the TSC-mTOR pathway in human disease. Nat Genet. 2005; 37: 19-24.

42. Wullschleger S, Loewith R, Hall MN. TOR signaling in growth and metabolism. Cell. 2006; 124: 471-484.

43. Dann SG, Selvaraj A, Thomas G. mTOR Complex1-S6K1 signaling: at the crossroads of obesity, diabetes and cancer. Trends Mol Med. 2007; 13: 252-259.

44. Dazert E, Hall MN. mTOR signaling in disease. Curr Opin Cell Biol. 2011.

45. Zoncu R, Efeyan A, Sabatini DM. mTOR: from growth signal integration to cancer, diabetes and ageing. Nat Rev Mol Cell Biol. 2010; 12: 21-35.

46. Conn CS, Qian SB. mTOR signaling in protein homeostasis: less is more? Cell Cycle. 2011; 10: 1940-1947.

47. Ma XM, Blenis J. Molecular mechanisms of mTOR-mediated translational control. Nat Rev Mol Cell Biol. 2009; 10: 307-318.

48. Serrano M, Lim AW, McCurrach ME, Beach D, Lowe SW. Oncogenic ras provokes premature cell senescence associated with accumulation of p53 and p16INK1A. Cell. 1997; 88: 593-602.

49. Lloyd AC, Obermuller F, Staddon S, Barth CF, McMahon M, Land H. Cooperating oncogenes converge to regulate cyclin/cdk complexes. Genes Dev. 1997; 11: 663-677.

50. Sewing A, Wiseman B, Lloyd AC, Land H. High-intensity Raf signal causes cell cycle arrest mediated by p21Cip1. Mol Cell Biol. 1997; 17: 5588-5597.

51. Woods D, Parry D, Cherwinski H, Bosch E, Lees E, McMahon M. Raf-induced proliferation or cell cycle arrest is determined by the level of Raf activity with arrest mediated by p21Cip1. Mol Cell Biol. 1997; 17: 5598-5611.

52. Lin AW, Barradas M, Stone JC, van Aelst L, Serrano M, Lowe SW. Premature senescence involving p53 and p16 is activated in response to constitutive MEK/MAPK mitogenic signaling. Genes Dev. 1998; 12: 3008-3019.

53. Zhu JY, Woods D, McMahon M, Bishop JM. Senescence of human fibroblasts induced by oncogenic Raf. Genes Dev. 1998; 12: 2997-3007.

54. Kerkhoff E, Rapp UR. High-intensity Raf signals convert mitotic cell cycling into cellular growth. Cancer Res. 1998; 58: 1636-1640.

55. Beausejour CM, Krtolica A, Galimi F, Narita M, Lowe SW, Yaswen P, Campisi J. Reversal of human cellular senescence: roles of the p53 and p16 pathways. EMBO J. 2003; 22: 4212-4222.

56. Hueber AO, Evan GI. Traps to catch unwary oncogenes. Trends Genet. 1998; 14: 364-367.
57. Blagosklonny MV. Revisiting the antagonistic pleiotropy theory of aging: TOR-driven program and quasi-program. Cell Cycle. 2010; 9: 3151-3156.
58. Stipp D. A new path of longevity. Sci Am. 2012; 306: 32-39.

59. Vellai T, Takacs-Vellai K, Zhang Y, Kovacs AL, Orosz L, Muller F. Genetics: influence of TOR kinase on lifespan in C. elegans. Nature. 2003; 426: 620.
60. Powers RWr, Kaeberlein M, Caldwell SD, Kennedy BK, Fields S. Extension of chronological life span in yeast by decreased TOR pathway signaling. Genes Dev. 2006; 20: 174-184.
61. Kaeberlein M, Powers RWr, K.K. S, Westman EA, Hu D, Dang N, Kerr EO, Kirkland KT, Fields S, Kennedy BK. Regulation of yeast replicative life span by TOR and Sch9 in response to nutrients. Science. 2005; 310: 1193-1196.
62. Jia K, Chen D, Riddle DL. The TOR pathway interacts with the insulin signaling pathway to regulate C. elegans larval development, metabolism and life span. Development. 2004; 131: 3897-3906.
63. Kapahi P, Zid BM, Harper T, Koslover D, Sapin V, Benzer S. Regulation of lifespan in Drosophila by modulation of genes in the TOR signaling pathway. Curr Biol. 2004; 14: 885-890.
64. Hansen M, Taubert S, Crawford D, Libina N, Lee SJ, Kenyon C. Lifespan extension by conditions that inhibit translation in Caenorhabditis elegans. Aging Cell. 2007; 6: 95-110.
65. Harrison DE, Strong R, Sharp ZD, Nelson JF, Astle CM, Flurkey K, Nadon NL, Wilkinson JE, Frenkel K, Carter CS, Pahor M, Javors MA, Fernandezr E, Miller RA. Rapamycin fed late in life extends lifespan in genetically heterogenous mice. Nature. 2009; 460: 392-396.
66. Selman C, Tullet JM, Wieser D, Irvine E, Lingard SJ, Choudhury AI, Claret M, Al-Qassab H, Carmignac D, Ramadani F, Woods A, Robinson IC, Schuster E, Batterham RL, Kozma SC, Thomas G et al. Ribosomal protein S6 kinase 1 signaling regulates mammalian life span. Science. 2009; 326: 140-144.
67. Moskalev AA, Shaposhnikov MV. Pharmacological Inhibition of Phosphoinositide 3 and TOR Kinases Improves Survival of Drosophila melanogaster. Rejuvenation Res. 2010; 13: 246-247.
68. Bjedov I, Toivonen JM, Kerr F, Slack C, Jacobson J, Foley A, Partridge L. Mechanisms of life span extension by rapamycin in the fruit fly Drosophila melanogaster. Cell Metab. 2010; 11: 35-46.
69. Miller RA, Harrison DE, Astle CM, Baur JA, Boyd AR, de Cabo R, Fernandez E, Flurkey K, Javors MA, Nelson JF, Orihuela CJ, Pletcher S, Sharp ZD, Sinclair D, Starnes JW, Wilkinson JE et al. Rapamycin, But Not Resveratrol or Simvastatin, Extends Life Span of Genetically Heterogeneous Mice. J Gerontol A Biol Sci Med Sci. 2011; 66: 191-201.
70. Anisimov VN, Zabezhinski MA, Popovich IG, Piskunova TS, Semenchenko AV, Tyndyk ML, Yurova MN, Antoch MP, Blagosklonny MV. Rapamycin extends maximal lifespan in cancer-prone mice. Am J Pathol. 2010; 176: 2092-2097.
71. Anisimov VN, Zabezhinski MA, Popovich IG, Piskunova TS, Semenchenko AV, Tyndyk ML, Yurova MN, Blagosklonny MV. Rapamycin increases lifespan and inhibits spontaneous tumorigenesis in inbred female mice. Cell Cycle. 2011; 10: 4230-4236.
72. Kapahi P, Chen D, Rogers AN, Katewa SD, Li PW, Thomas EL, Kockel L. With TOR, less is more: a key role for the conserved nutrient-sensing TOR pathway in aging. Cell Metab. 2010; 11: 453-465.
73. Blagosklonny MV. Rapamycin and quasi-programmed aging: Four years later. Cell Cycle. 2010; 9: 1859-1862.
74. Bjedov I, Partridge L. A longer and healthier life with TOR down-regulation: genetics and drugs. Biochem Soc Trans. 2011; 39: 460-465.
75. Katewa SD, Kapahi P. Role of TOR signaling in aging and related biological processes in Drosophila melanogaster. Exp Gerontol. 2011; 46: 382-390.
76. Pinkston JM, Garigan D, Hansen M, Kenyon C. Mutations that increase the life span of C. elegans inhibit tumor growth. Science. 2006; 313: 971-975.
77. Burtner CR, Murakami CJ, Kennedy BK, Kaeberlein M. A molecular mechanism of chronological aging in yeast. Cell Cycle. 2009; 8: 1256-1270.
78. Leontieva OV, Blagosklonny MV. Yeast-like chronological senescence in mammalian cells: phenomenon, mechanism and pharmacological suppression. Aging (Albany NY). 2011; 3: 1078-1091.
79. Blagosklonny MV. Aging, stem cells, and mammalian target of rapamycin: a prospect of pharmacologic rejuvenation of aging stem cells. Rejuvenation Res. 2008; 11: 801-808.
80. Chen C, Liu Y, Zheng P. mTOR regulation and therapeutic rejuvenation of aging hematopoietic stem cells. Sci Signal. 2009; 2: ra75.
81. Gan B, Sahin E, Jiang S, Sanchez-Aguilera A, Scott KL, Chin L, Williams DA, Kwiatkowski DJ, DePinho RA. mTORC1-dependent and -independent regulation of stem cell renewal, differentiation, and mobilization. Proc Natl Acad Sci U S A. 2008; 105: 19384-19389.
82. Gan B, DePinho RA. mTORC1 signaling governs hematopoietic stem cell quiescence. Cell Cycle. 2009; 8: 1003-1006.
83. Castilho RM, Squarize CH, Chodosh LA, Williams BO, Gutkind JS. mTOR mediates Wnt-induced epidermal stem cell exhaustion and aging. Cell Stem Cell. 2009; 5: 279-289.
84. Wang CY, Kim HH, Hiroi Y, Sawada N, Salomone S, Benjamin LE, Walsh K, Moskowitz MA, Liao JK. Obesity increases vascular senescence and susceptibility to ischemic injury through chronic activation of Akt and mTOR. Sci Signal. 2009; 2: ra11.
85. Sengupta S, Peterson TR, Laplante M, Oh S, Sabatini DM. mTORC1 controls fasting-induced ketogenesis and its modulation by ageing. Nature. 2010; 468: 1100-1104.
86. Kurz DJ, Decary S, Hong Y, Erusalimsky JD. Senescence-associated (beta)-galactosidase reflects an increase in lysosomal mass during replicative ageing of human endothelial cells. J Cell Sci. 2000; 113 (Pt 20): 3613-3622.
87. DeJesus V, Rios I, Davis C, Chen Y, Calhoun D, Zakeri Z, Hubbard K. Induction of apoptosis in human replicative senescent fibroblasts. Exp Cell Res. 2002; 274: 92-99.
88. Hampel B, Malisan F, Niederegger H, Testi R, Jansen-Durr P. Differential regulation of apoptotic cell death in senescent human cells. Exp Gerontol. 2004; 39: 1713-1721.
89. Narita M, Young AR, Arakawa S, Samarajiwa SA, Nakashima T, Yoshida S, Hong S, Berry LS, Reichelt S, Ferreira M, Tavare S, Inoki K, Shimizu S. Spatial coupling of mTOR and autophagy augments secretory phenotypes. Science. 2011; 332: 966-970.
90. Narita M, Young AR. Autophagy facilitates oncogene-induced senescence. Autophagy. 2009; 5: 1046-1047.
91. CoppŽ JP, Patil CK, Rodier F, Sun Y, Mu–oz DP, Goldstein J,

Nelson PS, Desprez PY, Campisi J. Senescence-associated secretory phenotypes reveal cell-nonautonomous functions of oncogenic RAS and the p53 tumor suppressor. PLoS Biol. 2008; 6: 2853-2868.

92. Krtolica A, Parrinello S, Lockett S, Desprez PY, Campisi J. Senescent fibroblasts promote epithelial cell growth and tumorigenesis: a link between cancer and aging. Proc Natl Acad Sci U S A. 2001; 98: 12072-12077.

93. Rodier F, Coppe JP, Patil CK, Hoeijmakers WA, Munoz DP, Raza SR, Freund A, Campeau E, Davalos AR, Campisi J. Persistent DNA damage signalling triggers senescence-associated inflammatory cytokine secretion. Nat Cell Biol. 2009; 11: 973-979.

94. Rodier F, Munoz DP, Teachenor R, Chu V, Le O, Bhaumik D, Coppe JP, Campeau E, Beausejour CM, Kim SH, Davalos AR, Campisi J. DNA-SCARS: distinct nuclear structures that sustain damage-induced senescence growth arrest and inflammatory cytokine secretion. J Cell Sci. 2011; 124: 68-81.

95. Komarova EA, Krivokrysenko V, Wang K, Neznanov N, Chernov MV, Komarov PG, Brennan ML, Golovkina TV, Rokhlin OW, Kuprash DV, Nedospasov SA, Hazen SL, Feinstein E, Gudkov AV. p53 is a suppressor of inflammatory response in mice. Faseb J. 2005; 19: 1030-1032.

96. Campisi J, Andersen JK, Kapahi P, Melov S. Cellular senescence: a link between cancer and age-related degenerative disease? Semin Cancer Biol. 2011; 21: 354-359.

97. Chien Y, Scuoppo C, Wang X, Fang X, Balgley B, Bolden JE, Premsrirut P, Luo W, Chicas A, Lee CS, Kogan SC, Lowe SW. Control of the senescence-associated secretory phenotype by NF-κB promotes senescence and enhances chemosensitivity. Genes Dev. 2011; 25: 2125-2136.

98. Pani G. From growing to secreting: new roles for mTOR in aging cells. Cell Cycle. 2011; 10: 2450-2453.

99. Lisanti MP, Martinez-Outschoorn UE, Pavlides S, Whitaker-Menezes D, Pestell RG, Howell A, Sotgia F. Accelerated aging in the tumor microenvironment: connecting aging, inflammation and cancer metabolism with personalized medicine. Cell Cycle. 2011; 10: 2059-2063.

100. Tremblay F, Marette A. Amino acid and insulin signaling via the mTOR/p70 S6 kinase pathway. A negative feedback mechanism leading to insulin resistance in skeletal muscle cells. J Biol Chem. 2001; 276: 38052-38060.

101. Tremblay F, Krebs M, Dombrowski L, Brehm A, Bernroider E, Roth E, Nowotny P, WaldhŠusl W, Marette A, Roden M. Overactivation of S6 kinase 1 as a cause of human insulin resistance during increased amino acid availability. Diabetes. 2005; 54: 2674-2684.

102. Um SH, Frigerio F, Watanabe M, Picard F, Joaquin M, Sticker M, Fumagalli S, Allegrini PR, Kozma SC, Auwerx J, Thomas G. Absence of S6K1 protects against age- and diet-induced obesity while enhancing insulin sensitivity. Nature. 2004; 431: 200-205.

103. Shah OJ, Wang Z, Hunter T. Inappropriate activation of the TSC/Rheb/mTOR/S6K cassette induces IRS1/2 depletion, insulin resistance, and cell survival deficiencies. Curr Biol. 2004; 14: 1650-1656.

104. Zhang H, Bajraszewski N, Wu E, Wang H, Moseman AP, Dabora SL, Griffin JD, Kwiatkowski DJ. PDGFRs are critical for PI3K/Akt activation and negatively regulated by mTOR. J Clin Invest. 2007; 117: 730-738.

105. Blagosklonny MV. Molecular damage in cancer: an argument for mTOR-driven aging. Aging (Albany NY). 2011; 3: 1130-1141.

106. Doonan R, McElwee JJ, Matthijssens F, Walker GA, Houthoofd K, Back P, Matscheski A, Vanfleteren JR, Gems D. Against the oxidative damage theory of aging: superoxide dismutases protect against oxidative stress but have little or no effect on life span in Caenorhabditis elegans. Genes Dev. 2008; 22: 3236-3241.

107. Cabreiro F, Ackerman D, Doonan R, Araiz C, Back P, Papp D, Braeckman BP, Gems D. Increased life span from overexpression of superoxide dismutase in Caenorhabditis elegans is not caused by decreased oxidative damage. Free Radic Biol Med. 2011; 51: 1575-1582.

108. Gems D, Doonan R. Antioxidant defense and aging in C. elegans: Is the oxidative damage theory of aging wrong? Cell Cycle. 2009; 8: 1681-1687.

109. Lapointe J, Hekimi S. When a theory of aging ages badly. Cell Mol Life Sci. 2009; 67: 1-8.

110. Van Raamsdonk JM, Meng Y, Camp D, Yang W, Jia X, Benard C, Hekimi S. Decreased energy metabolism extends life span in Caenorhabditis elegans without reducing oxidative damage. Genetics. 2010; 185: 559-571.

111. Speakman JR, Selman C. The free-radical damage theory: Accumulating evidence against a simple link of oxidative stress to ageing and lifespan. Bioessays. 2011; 33: 255-259.

112. Ristow M, Schmeisser S. Extending life span by increasing oxidative stress. Free Radic Biol Med. 2011; 51: 327-336.

113. Blagosklonny MV. Aging: ROS or TOR. Cell Cycle. 2008; 7: 3344-3354.

114. Blagosklonny MV. Hormesis does not make sense except in the light of TOR-driven aging. Aging (Albany NY). 2011; 3: 1051-1062.

115. Blagosklonny MV. Rapamycin-induced glucose intolerance: Hunger or starvation diabetes. Cell Cycle. 2011; 10: 4217-4224.

116. Blagosklonny MV. Why men age faster but reproduce longer than women: mTOR and evolutionary perspectives. Aging (Albany NY). 2010; 2: 265-273.

117. Blagosklonny MV. Aging-suppressants: cellular senescence (hyperactivation) and its pharmacologic deceleration. Cell Cycle. 2009; 8: 1883-1887.

Editorial Comment

Mitochondrial dysfunction and cell senescence – skin deep into mammalian aging

Joao F. Passos and Thomas von Zglinicki doi:10.18632/aging.100432

Comment on: Velarde MC et al. Mitochondrial oxidative stress caused by SOD2 deficiency promotes cellular senescence and aging phenotypes in the skin. Aging (Albany NY). 2012; 4:3-12.

There is a lively discussion going on as to whether oxidative stress is or is not a cause of (accelerated) aging, fuelled to a significant extent by the finding from Arlan Richardson's group that mice heterozygous for the mitochondrial superoxide dismutase SOD2 showed increased oxidative stress, increased cancer incidence but not accelerated ageing [1]. A new twist to this story was introduced recently when it was shown that connective tissue-specific SOD2 knockouts developed multiple signs of progeria including short lifespan, associated with up-regulation of the cell senescence marker $p16^{INK4A}$ [2]. Mitochondrially generated oxidative stress is both an established cause [3] and a relevant consequence [4] of cell senescence, frequencies of senescent cells in connective tissue increase during mice aging [5], and destruction of senescent cells can 'cure' some age-related tissue dysfunction [6]. A paper by Judith Campisi's and Simon Melov's groups recently published in Aging [7] now further explores the connection between oxidative stress, cell senescence and aging. The authors demonstrate that mitochondrial dysfunction occurs in the epidermis of old (2 years) mice, measured as decreased complex II activity, and correlate this with increased senescence (shown by SA-bGAL activity) in the stratum corneum. Moreover, they observe the same senescence phenotype in skin from young (17 – 20 days old) constitutive SOD2-/- mice, which were treated with the synthetic SOD and catalase mimetic EUK-189 in order to allow sufficient development to take place for a skin phenotype to develop. An increase of various senescence markers in the epidermis, the stratum corneum or the lining of the hair follicles was associated with epidermal thinning (a classical aging marker in skin) and increased expression of a keratinocyte terminal differentiation marker [7]. These data enforce two central hypotheses in the field, namely that of mitochondrial dysfunction as a cause of cell senescence, and of cell senescence as a relevant contributor to mammalian aging *in vivo*.

However, a fascinating question remains: Is it really Reactive Oxygen Species (ROS) arising from mitochondria that promote cellular senescence in this model? Mitochondria from SOD2-/- mice accumulate superoxide in their matrix space which oxidizes and damages multiple mitochondrial enzyme complexes, leading to decreased oxygen uptake and ATP production and lowered complex II activity [8, 9]. However, superoxide cannot cross the mitochondrial inner membrane, and the generation of hydrogen peroxide, which is the only membrane-permeable ROS, is greatly reduced by two factors, the absence of the mitochondrial SOD and the decrease in oxygen uptake. Thus, SOD2-/- mitochondria actually release less ROS than wild-type mitochondria into their environment. This is attenuated by the addition of the superoxide mimetic EUK-189, but even under high drug concentrations the ROS release from heart mitochondria was below wild-type levels [9]. Thus, it is not at all clear that mitochondrial oxidative stress directly produces cellular oxidative stress in the skin of EUK-189 treated SOD2-/- mice. Importantly, studies have shown that mitochondrial dysfunction in SOD2-/- fibroblasts is associated with Ca^{2+} signal transduction, suppression of signals through the mTOR axis and induction of markers of autophagy [8]. All these changes are characteristically associated with cell senescence [3, 10, 11]. Thus, we are again left with a chicken-and egg situation: Is disrupted Ca^{2+} signalling, reduced mTOR activity and increased autophagy found in SOD2-/- cells because there are more senescent cells in the examined population? Or is any of these factors the culprit that triggers senescence in the first place?

While the answer to these questions still eludes us, the study from Campisi and colleagues highlights the importance of mitochondrial dysfunction and cellular senescence in vivo and its impact on the aging process.

ACKNOWLEDGEMENTS

The authors are grateful for support from BBSRC (David Phillips Fellowship to JP, grant BB/I020748/1 to TvZ).

Institute for Ageing and Health, Newcastle University, Newcastle upon Tyne, NE4 5PL, UK
Email: t.vonzglinicki@ncl.ac.uk

Received: 2/8/12; Published: 2/12/12

REFERENCES

1. Van Remmen H, Ikeno Y, Hamilton M et al. Physiol Genomics 2003; 16:29-37.
2. Treiber N, Maity P, Singh K et al. Aging Cell;10:239-254.
3. Passos JF, Saretzki G, Ahmed S et al. PLoS Biol 2007;5:e110.
4. Passos JF, Nelson G, Wang C et al. Mol Syst Biol 2010;6:347.
5. Wang C, Jurk D, Maddick M et al. Aging Cell 2009;8:311-323.
6. Baker DJ, Wijshake T, Tchkonia T et al. submitted 2011.
7. Velarde MC, Flynn JM, Day NU et al. Aging (Albany NY) 2012; 4:3-12.
8. Zhang Y, Zhang HM, Shi Y et al. Free Radical Biology and Medicine 2010; 49:1255-1266.
9. Morten KJ, Ackrell BA, Melov S. J Biol Chem 2006; 281:3354-3359.
10. Korotchkina LG, Leontieva OV, Bukreeva EI et al. Aging (Albany NY) 2010; 2:344-352.
11. Sitte N, Merker K, Grune T et al. Experimental Gerontology 2001; 36:475-486.

Research Paper

Yeast-like chronological senescence in mammalian cells: phenomenon, mechanism and pharmacological suppression

Olga V. Leontieva and Mikhail V. Blagosklonny

Department of Cell Stress Biology, Roswell Park Cancer Institute, BLSC, L3-312, Buffalo, NY, 14263, USA

Key words: *chronological aging, senescence, metabolism, rapamycin, mTOR, lactate*
Received: *09/15/11; Accepted: 12/9/11; Published: 12/10/11* doi:10.18632/aging.100402
Correspondence to: *Mikhail V. Blagosklonny, MD/PhD;* ***E-mail:*** *blagosklonny@oncotarget.com*

Abstract: In yeast, chronological senescence (CS) is defined as loss of viability in stationary culture. Although its relevance to the organismal aging remained unclear, yeast CS was one of the most fruitful models in aging research. Here we described a mammalian replica of yeast CS: loss of viability of overgrown "yellow" cancer cell culture. In a density and time (chronological)-dependent manner, cell culture loses the ability to re-grow in fresh medium. Rapamycin dramatically decelerated CS. Loss of viability was caused by acidification of the medium by lactic acid (lactate). Rapamycin decreased production of lactate, making conditioned medium (CM) less deadly. Both deadly CM and lactate caused loss of viability in low cell density, not preventable by either rapamycin or additional glucose. Also, NAC, LY294002, U0126, GSK733, which all indirectly inhibit mTOR and have been shown to suppress the senescent phenotype in traditional models of mammalian cell senescence, also decreased lactate production and decelerated CS. We discuss that although CS does not mimic organismal aging, the same signal transduction pathways that drive CS also drive aging.

INTRODUCTION

In yeast, chronological senescence (CS) is defined as loss of viability of yeast cells grown in confluent state [1-10]. Viability is determined as the ability to resume replication in fresh medium. CS is genetically regulated and inactivation of numerous genes including TOR (Target of Rapamycin) extends lifespan [2, 11-23]. Furthermore, rapamycin, an inhibitor of TOR, decelerates CS in yeast [24]. Noteworthy, the TOR (target of rapamycin) pathway is involved in aging of variety of species from worm to mammals [25-28]. Some other genes identified in the yeast model turned out to be involved in organismal aging and age-related diseases in mammals [29-38]. CS is often compared to aging of postmitotic cells in the organism. However, as recently discussed, the link between CS and organismal aging is not immediately apparent but indirectly relies on common genetic pathways [39].

Since yeasts are unicellular organisms, CS should be compared with some form of cellular senescence in cell culture. There are two types of senescence of mammalian cells in culture: replicative and accelerated (also known as premature or stress-induced senescence). Yeast replicative senescence corresponds to replicative senescence in rodent cells. Then at first glance, yeast CS is analogous to accelerated cellular senescence. The analogy is seemingly strengthened by the involvement of mTOR in senescent phenotype of mammalian cells [40-46]. In proliferating cells, mTOR is active, thus driving cell growth in size, which is balanced by cell division. When cell cycle is blocked by p21 or p16, for instance, but mTOR is still active, then mTOR drives cellular senescence [40, 46, 47]. By deactivating mTOR, rapamycin prevents conversion of quiescence into senescence or, in other words, prevents gerogenic conversion (geroconversion) during cell cycle arrest [41, 46].

Yet accelerated senescence is not analogous to yeast CS. Accelerated cellular senescence is not caused by medium acidification. Senescent cells are large, flat, highly viable and apoptosis-resistant**.** Furthermore, gero-

conversion occurs in low cell densities, whereas in high density mTOR is spontaneously deactivated thus suppressing geroconversion (manuscript in preparation). So there is no known mammalian analogy to yeast CS. Given that yeast aging research has been so fruitful in identification of pathways involved in organismal aging, [1, 3, 48-51] it is important to recognize relevant mammalian cell model for CS.

We realized that replica of CS is so trivial that it remains unnamed and ignored, although this phenomenon is known to any cancer researcher. If a flask with cancer cells is forgotten (neglected) in the incubator, cells become over-confluent, overgrow, and loose viability. And this is exactly what would be called chronological aging (in yeast). Here we investigated mechanisms of chronological senescence (**CS**) in human cells and its pharmacological suppression.

RESULTS

TOR-dependent CS in HT-p21-9 cells

For initial experiments we chose HT-p21-9 cells, because these cells were extensively studied as a model of conventional cellular senescence [52, 41]. Importantly, these cells rapidly turn media yellow. Acidification of the medium is evident by transition of the color of phenol red (a pH indicator) from pink-red to yellow over the pH range 7.4 to 6.8. The color of phenol red is a convenient measure of pH. In dense cell culture, the medium becomes acidic (yellow) (Fig. 1A: top panel – control (C). Rapamycin renders the color pinkish. After recording the color by photography, media were collected for further analysis (lactate levels, cytotoxicity) and equal volumes of trypsinized cells were re-plated in larger plates in fresh medium (Fig. 1 A, bottom panel) and colonies were allowed to grow for 7 days. In control, cells lost the replicative capacity and did not form colonies in fresh medium (Fig. 1A, bottom panel). Rapamycin prevented loss of viability (Fig. 1A). Loss of viability, over time (Fig. 1B), is chronological senescence (CS). At initial cell densities of 40,000 and 80,000 cells per well (Fig. 1 B), the major drop in viability occurred at day 5 and day 4, respectively (Fig. 1B). The most dramatic effect of rapamycin was observed, when control cultures almost completely lost their viability. To quantify the viability, we counted cells after 7 days of re-growth in fresh culture (Fig. 1C). There was a dramatic decrease in viability after 4 and 5 days in control wells, which was prevented by rapamycin (Fig. 1 C).

Time course of lactate production

At both cell densities, lactic acid (LA) concentrations reached the maximal level of ~30 mM on day 3 and day 4, respectively (Fig. 1D). Noteworthy, these maximal levels of LA were achieved a day before the major loss of viability (Fig. 1 D versus C). Rapamycin decreased levels of LA, so that LA concentration approximated to the maximal level by day 6-7. A comparison of LA levels and CS time points suggests that levels of LA above 30 mM may make medium toxic: then cells loose viability and this prevents further accumulation of LA.

Protection by rapamycin is indirect

Next, we tested the effect of conditioned medium (CM) that was collected from the dense culture and applied to cells plated at low density. Such CM was deadly, causing loss of viability in low cell density. This allowed us to investigate the mechanism of action of rapamycin: direct versus indirect. One possibility is that rapamycin protects cells directly by increasing resistance to cell death caused by deadly CM. Another possibility is that CM produced in the presence of rapamycin would be less deadly. We tested CM produced in the presence of rapamycin (R-CM) versus CM with rapamycin being added after CM collection (CM+R). Both types of CM were added to low density HT-p21-9 and HCT116 cells for 3 days and then the cells were grown in fresh medium. CM+R was as toxic as CM, whereas R-CM was significantly less toxic (Fig. 2). We conclude that rapamycin does not protect cells directly, but instead changes the property of CM. As we have already shown, rapamycin decreased levels of LA (Fig. 1D).

Lactate poisoning

Next we tested whether LA is toxic. Addition of 40 mM lactate to fresh medium rendered it "absolutely deadly" (Fig. 2 A). Viability IC_{50} was around 20-30 mM LA, depending on cell line. Noteworthy, color of the medium containing 30 mM lactate was similar to yellow color of CM in the stationary culture, when cells undergo CS. This was confirmed by measurements of LA in such deadly CM (34.6 ± 1 mM). So LA levels slightly above 30 mM were maximally achievable, killing cells and thus preventing further accumulation of LA.

There are 2 possibilities that are not mutually exclusive: 1) **LA** is toxic by itself and is the only cause of CS. Rapamycin, which decreases levels of LA, simultaneously decreases toxicity of CM; 2) production of 30 mM lactate requires metabolism of 15 mM glucose. In principle, exhaustion of glucose may contribute to CM toxicity. However, addition of glucose to CM did not decrease its toxicity (Fig. 2B).

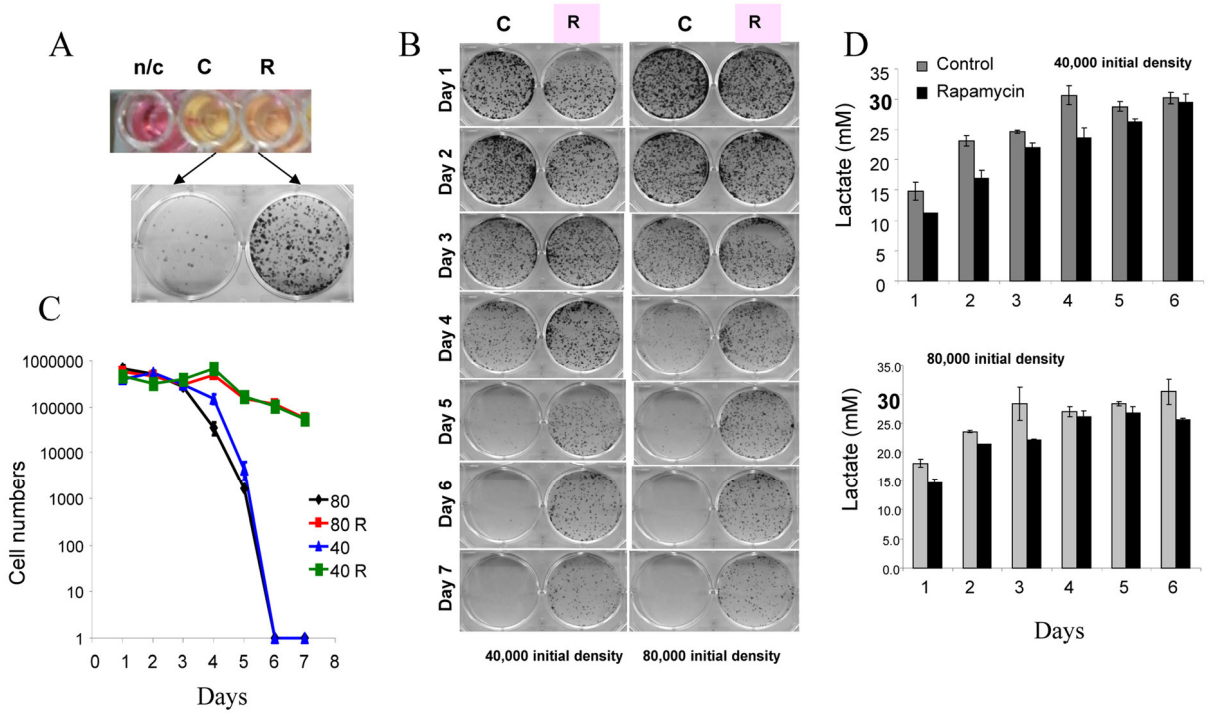

Figure 1. Defining mTOR-dependent CS. (**A**) Measurement of CS. 80000 HT-p21-9 cells were plated in 0.2 ml medium per well in 96-well plate with 500 nM rapamycin (R) or without rapamycin – control (C). After 4 days, the plate was photographed to record color of media (i.e. pH). The color of medium without cells is shown for comparison n/c (no cells). Then cells from each well were split into larger wells of 6-well plates. Detailed description: medium (together with floating cells) was aspirated and adherent cells were trypsinized in 0.2 ml of trypsin. Equal volume (a 4 µl aliquot of cell culture) or 2% of total adherent (live) cells was plated in 4 ml of fresh medium in 6-well plates. After 7 days, colonies were stained and photographed. A number of colonies is a measure of viability of the stationary culture. (**B**) Time-dependent (chronological) loss of replicative viability. Cells were plated at initial density of 40000 and 80000 cells per well in 96-well plates without (C) or with rapamycin (R) as shown in panel A. After indicated time, cells were trypzinised and equal volume of adherent cells (2%) were re-plated in 6 well plates and allowed to form colonies for 7 days. (C) Cells from plates shown in panel B were trypsinized and counted to precisely quantify replicative viability. (**D**) Levels of lactate in conditioned medium. Cells were plated at initial density of 40000 and 80000 cells per well in 96-well plates without (C) or with rapamycin (R) as shown in panel A. After indicated time, concentration of lactate was measured in conditioned media.

Thus, LA was the main cause of toxicity. Next, we tested whether this toxicity was due to LA acidity. To neutralize pH, we added NaOH to cells plated in high density after one day of cultivation. At concentrations (0.5-1 mM) NaOH shifted the medium color from yellow to pink and decreased CS (Fig. S1). We conclude that it is acidity of LA that is deleterious for the cells.

Gerosuppressants decrease lactate levels and CS

Recently we have demonstrated that agents that deactivate the mTOR pathway decelerate premature (p21-induced) senescence in HT-p21-9 cells [41, 53, 54]. Given that these agents suppress the conversion from quiescence to senescence (geroconversion), we named them gero-suppressants [55]. Here we evaluated the effect of gero-suppressants on CS, using rapamycin as a positive control (Fig. 3). Inhibitors of PI-3K and MEK, LY294002 and U0126, respectively, decreased acidosis (Fig. 3 A), lactic acid production (Fig. 3 B) and dramatically decreased CS in HT-p21-9 and HCT116 cells (Fig. 3 C-D). Suppression of CS correlated with inhibition of LA production in both cell lines. The antioxidant N-acetyl-L-cysteine (NAC) decreased LA production preferentially in HT-p21-9 cells and also prevented CS in the same cell line. CGK733, in contrast, was preferentially effective in HCT116 cells (Fig. 3). Finally, metformin did not affect either LA levels or CS in any cell lines (Fig. 3).

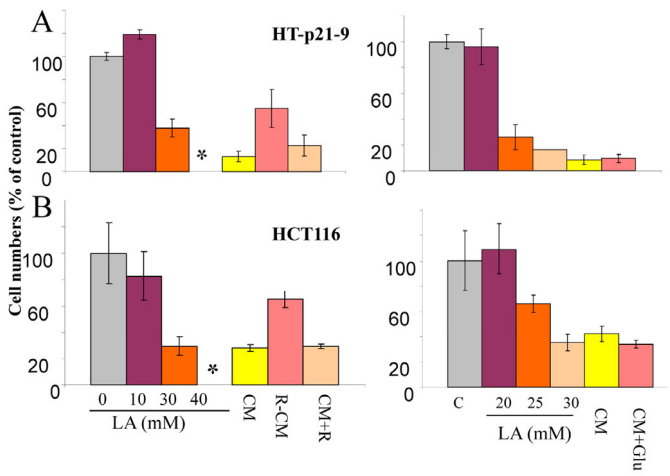

Figure 2. Cytotoxicity of conditioned medium (CM) and lactate. HT-p21-9 cells (A) and HCT116 cells (B) were plated in 96-well plates at low density (2000 cells/well) and treated with a range of lactic acid (LA) concentrations or conditioned medium (CM), collected from overgrown HT-p21-9 cell culture. After 3 days, medium was changed to fresh medium and cells were allowed to proliferate for 5 days and then number of viable cells was determined using MTT assay. CM, R-CM, and CM+R were prepared as described in Methods.

Noteworthy, free radicals and oxidative stress can activate Akt/mTOR and vice versa active TOR may promote ROS [9, 56]. Therefore, inhibition of ROS by NAC is expected to decrease not only ROS levels but also mTOR activity. In fact, NAC inhibited CS in a dose-dependent manner with maximal effect at 20 mM (higher concentrations were toxic) (Fig. 4 A). In high cell density, mTOR was spontaneously deactivated after first day in culture. NAC inhibited the Akt/mTOR pathway by 6 hrs (Fig. 4B, 6 hrs), before mTOR becomes spontaneously deactivated. Noteworthy, the ATM inhibitor CGK733 also inhibited mTOR (Fig. 4B).

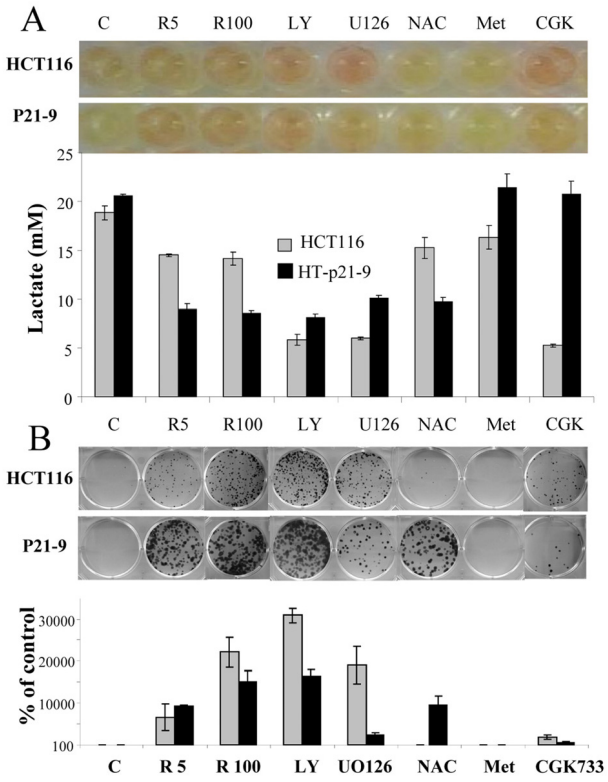

Figure 3. Testing potential gero-suppressants. HCT116 cells and HT-p21-9 cells were plated at 80000 per well in 96 well plates with indicated agents: 5 nM and 100 nM rapamycin (R5 and R 100), 10 μM LY294002 (LY), UO126, and CGK733, 2 mM NAC. (**A)** After 4 days, the plates were photographed (upper panel) and lactate concentrations were measured in media (lower panel). (**B**) An equal volume of attached cells (an aliquot of 2%) was plated in 6 well plates. After 7 days, colonies were stained with Crystal Violet (upper panel) or total numbers of cells per well were determined by counting (low panel).

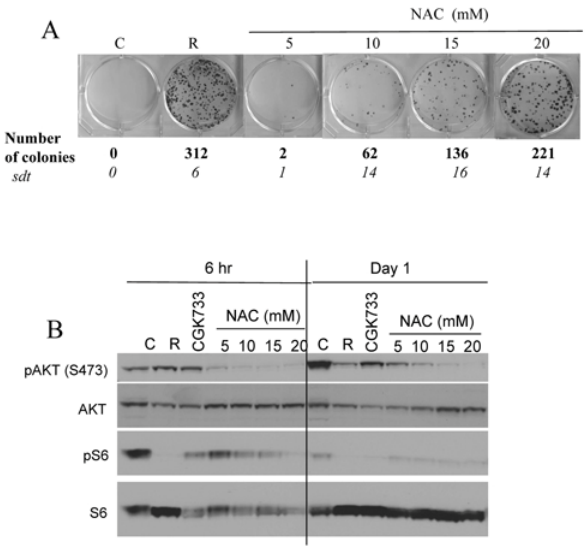

Figure 4. Effects of NAC and CGK733 on CS and mTOR. (A) HT-p21-9 cells were plated at 40000 per well in 96 well plates with indicated agents: 500 nM rapamycin (R), 5-20 mM NAC and incubated for 6 days. On Day 6 replicative viability of cells was measured by colony formation (8 days) as described in legend for Figure 1. (**B**) HT-p21-9 cells were plated at high density with indicated agents or left untreated (C) and allowed to attach for 6 hrs. Then, one set was lysed (Day 0, 6 hr) and second set was lysed after 24 hrs treatment (Day 1). Immunoblot was performed using indicated antibodies.

At high cell density, mTOR is shut down after 1 day in culture (Fig. 4 and Fig. S3). Still, rapamycin and other mTOR inhibitors suppressed CS very effectively. This suggests that the activity of mTOR during the first day (before spontaneous deactivation of mTOR) determines cell fate.

Effects of pre-conditions

We have noticed that time course of CS was slightly variable in different experiments (compare HCT116 cells in Fig. 3 and Fig. 6), even if cells were plated at the same densities and conditions. We reasoned that this may be due to different pre-conditions, given that mTOR becomes spontaneously deactivated in culture over time. This suggests that cells from the fresh culture will lose viability faster compared with those from the old culture. We tested this prediction. 80,000 cells from either old or fresh culture were plated in 96-wells in fresh medium and cultivated for the same time before measuring their viability. In fact, cells derived from "old pre-culture" retained viability longer (Fig. S2). Whereas rapamycin prevented CS in cells derived from fresh pre-culture, its effect was minimal in old pre-culture cells (Fig. S2). This result is in agreement with the data that mTOR is already inhibited in old pre-culture.

Lactate production *vs* apoptosis-reluctance as determinant of CS

We next compared 3 cell lines: HT-p21-9, HCT116 and HCT116-Bax-/-, a clone of HCT116 cells lacking Bax (Fig. 5 and 6). HCT-Bax-/- cells are apoptosis-reluctant [57, 58]. Cells were plated in 2 cell densities (80,000 and 20,000 cells per well). At high cell density on day 4, HT-p21-9 cells lost viability, which was prevented by rapamycin (Fig. 5B). In contrast, HCT116 and HCT-Bax-/- cells retained viability at that time point (in this particular experiment).

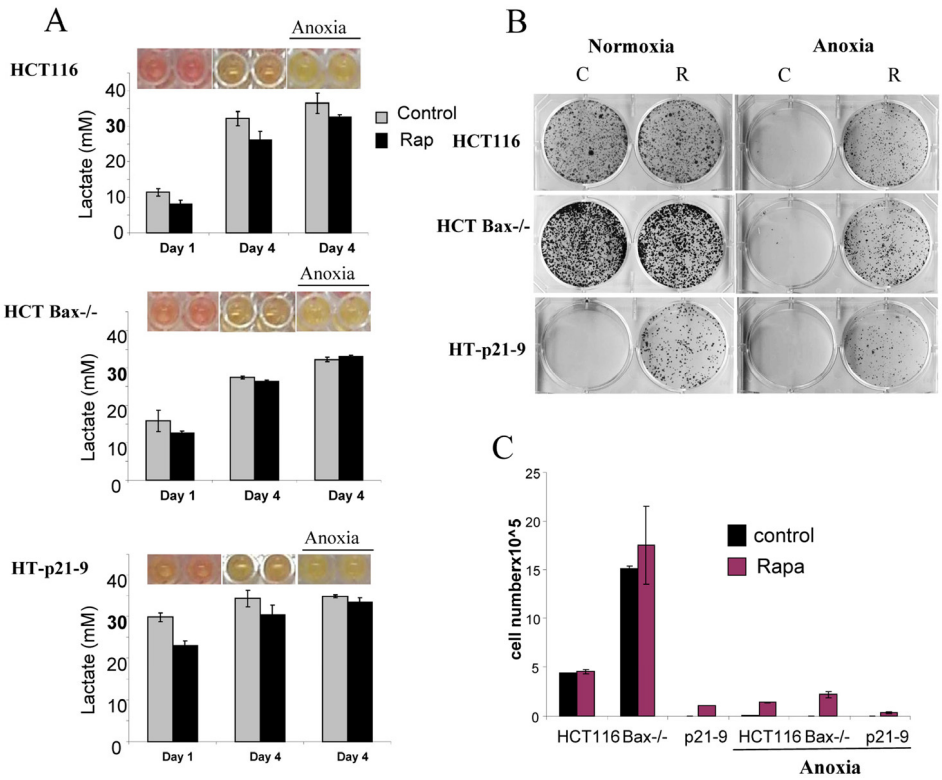

Figure 5. Effects of glycolytic phenotype, apoptosis resistance and anoxia on CS in very high initial cell density. HCT116, HCT-Bax-/- cells and HT-p21-9 cells) were plated at 80000 per well in 96 well plates and next day 1 set of plates was placed under anoxia and 2 nd set was incubated in normoxia. If indicated, cells were treated with 100 nM rapamycin (R). (**A**) Wells were photographed (upper panels) and LA (lower panels) was measured after 1 day (D 1) or on the last 4th day (D 4) of culture. (**B**) Replicative viability. On day 4, equal aliquots of attached cells were plated in 6 well plates. After 7 days, colonies were stained with Crystal Violet (upper panel) or total numbers of cells per well were determined by counting (lower panel).

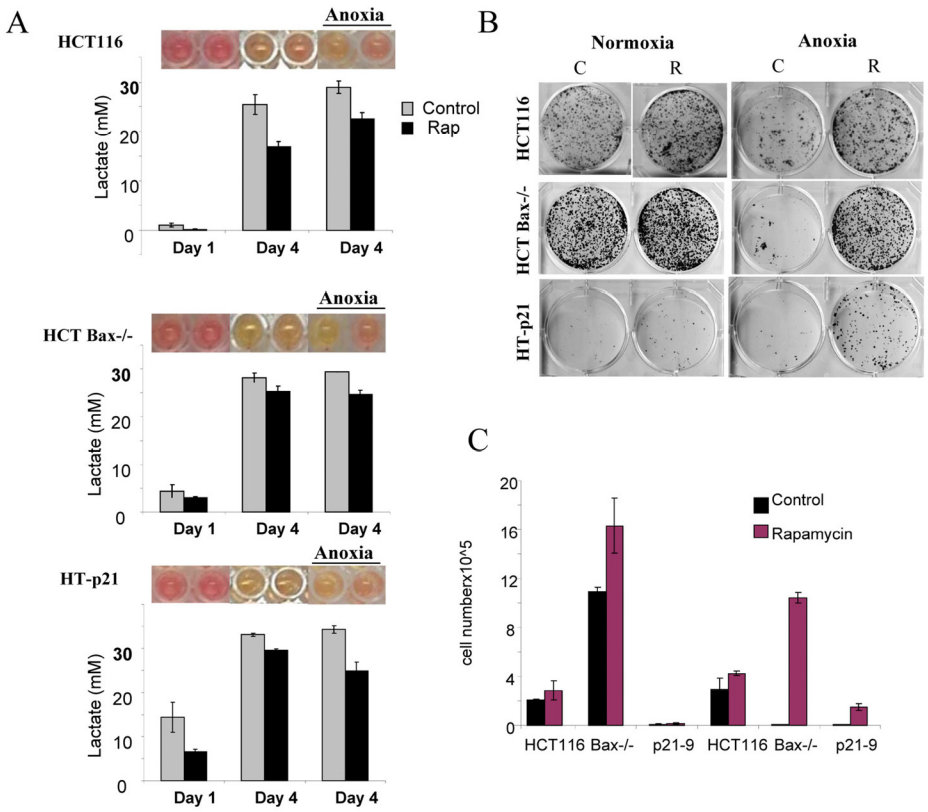

Figure 6. Effects of glycolytic phenotype, apoptosis resistance and anoxia on CS in medium initial cell density. HCT116, HCT Bax-/- cells and HT-p21-9 cells were plated at 20000 per well in 96 well plates and after 1 day were placed in normoxia or anoxia. If indicated, cells were treated with 100 nM rapamycin (R). (**A**) Wells were photographed (upper panels) and LA (lower panels) was measured on 1 day (D 1) and on the last 4th day (D 4) of culture. (**B**) Replicative viability. On day 8, equal aliquots of attached cells were plated in 6 well plates. After 7 days, colonies were stained with Crystal Violet (upper panel) or total numbers of cells per well were determined by counting (lower panel).

In comparison with HCT116 cells, HT-p21-9 cells produced considerably more LA during the first day, which reached sub-lethal levels at that time (Fig. 5A). This demonstrated that levels of LA reached on the first day determine CS. However, HCT-Bax-/- cells, which were less prone to CS produced more lactate than HCT116 parental cells, indicating that resistance to apoptosis can also determine the viability. That was confirmed by direct testing of lactate on cell viability: HCT-Bax-/- cells appeared to be slightly more resistant to 30 mM LA than parental cells (Fig. 7). Still, the difference in resistance was relatively small. The major factor that determined CS was the rate of LA production during the first day in culture (Fig. 5, 6). At low cell density, the difference in LA production was the most prominent (Fig. 6A). HT-p21-9 cells were the most glycolytic, whereas HCT116 cells were the least glycolytic (Fig. 6A, day 1). By day 4, HT-p21-9 cells produced near-lethal levels of lactate (Fig. 6A). Accordingly, HT-p21-9 cells lost viability by day 8 (Fig. 6 B, C).

A forced increase in lactate levels accelerated CS

If mTOR-dependent lactate production (rather than the activity of mTOR per se) is responsible for CS, then anoxia will accelerate CS. Anoxia and hypoxia induce (hypoxia-inducible factor) HIF-1 and this effect is not blocked by rapamycin (Fig. S3). Furthermore, hypoxia/anoxia decreases the activity of the mTOR pathway [59, 60]. So in anoxia LA production is forced by HIF-1. On the other hand, hypoxia/anoxia may

diminish mTOR-dependent glycolysis by deactivating mTOR. Not surprisingly, relationship between aging and hypoxia are complex [61].

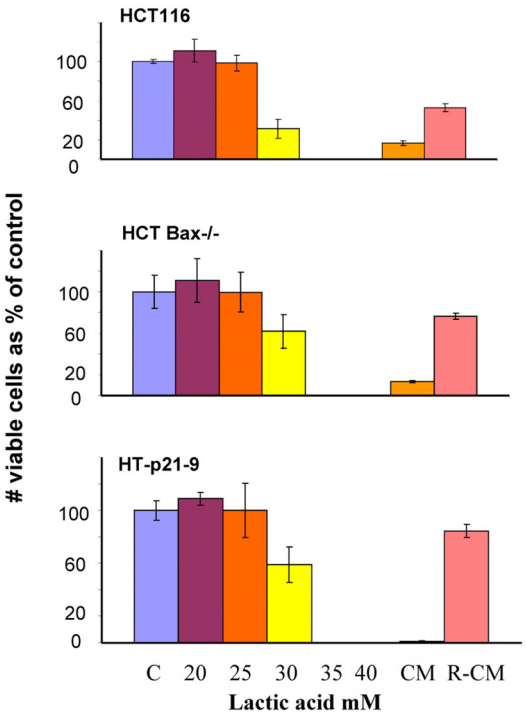

Figure 7. Lactate resistance of HT-p21-9, HCT116 and HCT116-Bax-/- cells. HCT116 cells, HCT-Bax-/- and HT-p21-9 cells were plated in 96-well plates at low density (2000 cells/well) and treated with a range of lactic acid (LA) concentrations or conditioned medium (CM). After 3 days, medium was changed to fresh medium and cells were allowed to proliferate for 5 days and then numbers of live cells were determined using MTT assay. CM and R-CM were prepared as described in Methods.

In anoxia experiments, cells were cultivated without oxygen for 3 days: from day 1 to day 4 (Fig. 5, 6). At high cell density on day 4, HT-p21-9 cells lost viability, which partially was prevented by rapamycin (Fig. 5 B, C). Furthermore, even HCT116 and HCT-Bax-/- cells lost viability in anoxia but not in normoxia (Fig. 5, 6). Yet, final levels of LA were almost identical in both normoxia and anoxia because CS prevented further accumulation of lactate (Fig. 5A, Fig 6A).

Rapamycin decelerated CS under both normoxia and anoxia. This might be due to a decrease in lactate production on the first day (especially in high density cultures, Fig. 5A) before cells were placed in anoxia.

Alternatively, rapamycin may decrease cellular metabolism in anoxia, which would indicate that the effect of rapamycin was not due to its effects on respiration. Experiments here were not intended to determine whether the protective effect of rapamycin was independent of respiration. Further studies are under way to determine the effect of rapamycin on glycolysis under anoxia versus normoxia.

Suppression of CS by rapamycin was not due to its cytostatic effect

Rapamycin is moderately cytostatic in some cell lines including HT-p21-9 cells. However, the cytostatic effect in low cell density cannot account for deceleration of CS in high cell density. First, at high cell densities with a limited proliferation window, the cytostatic effect of rapamycin was undetectable. We plated HT-p21-9 cells in a wide range of initial cell densities (Fig. 8) from 35000 to 560000 cells per well with and without IPTG. In HT-p21-9 cells, IPTG induces ectopic p21 and causes cell cycle arrest [52], thus ensuring a constant number of cells.

The acidity (yellow color) of the medium was proportional to initial cell numbers up to 140000 (Fig. 8 A) and corresponded to deadly levels of LA (Fig. 8 B). Rapamycin decreased levels of lactate. Noteworthy, highest levels of lactate were achieved at initial density 140000 (Fig. 8 B), but not at higher densities. At initial density of 280000 and 560000, all cells died within several days (Fig. 9, upper panel). These cells were floating and did not produce any colonies (Fig. 9, lower panel). On day 4, numbers of adherent (alive) cells were approximately identical at initial plating densities between 35000 and 140000 (Fig. 9, upper panel). This means that cells underwent 2, 1, and 0 divisions when plated at initial densities of 35000, 70000 and 140000, respectively. Most importantly, rapamycin did not affect the number of live cells (Fig. 9, upper panel); even though it decreased LA levels (Fig. 8 B). Despite rapamycin did not have an effect on the number of live cells, it dramatically increased the number of cells with replicative potential (Fig. 9, lower panel).

At initial density of 140000 cells, cells did not proliferate and did not die (Fig. 9). At this density, the level of lactate was maximal as well as the effect of rapamycin on CS (Fig. 8). Furthermore, we excluded the cytostatic effect of rapamycin by mixing IPTG-arrested HT-p21-9 (GFP-positive) cells with a few HCT116 cells, termed here as indicator cells. Since HT-p21-9 cells were already arrested by IPTG, rapamycin could not possibly arrest them further. The indicator HCT116 cells are not sensitive to cytostatic effects of

rapamycin. Even if rapamycin could decrease proliferation of the indicator HCT116 cells, the small number of indicator cells could not significantly contribute to lactate production. We treated the cell mixture (80000 HT-p21-9 cells mixed with 2000 indicator cells) with IPTG (Fig. 10). After 4 days of incubation, small aliquots of cells were re-plated in fresh medium with IPTG to preclude proliferation of HT-p21-9 cells. As shown in Figure 10A, rapamycin dramatically increased a number of colonies. It was confirmed by microscopy that only HCT116 cells formed colonies, whereas IPTG-arrested HT-p21-9 (green) cells became senescent (large morphology of green cells) (Fig. 10B).

DISCUSSION

Here we described a mammalian model of yeast-like chronological senescence (CS). Regardless of how trivial this phenomenon is, it is the replica of yeast CS.

For both yeast and cancer cells, CS can be defined as loss of replicative viability in a stationary culture.

Cancer cells with high glycolysis resemble yeast cells [62-65]. The most predictive sign of CS is yellow color of the medium, which indicates pH. Lactate and conditioned medium (CM) by were deadly in cells plated in low density. Furthermore, levels of lactate that caused CS coincided with maximally reachable lactate levels in the culture. Neutralization of the acidity prevented CS. Similarly, in some studies in yeast, loss of replicative ability was attributed to acidosis [39, 66-68]. The only difference is that mammalian cells produce lactic acid instead of acetic acid. Rapamycin decelerated CS. Rapamycin decreased lactate accumulation, keeping lactate levels below deadly levels. In other words, CS is a metabolic self-destruction or hypermetabolism-induced loss of replicative ability. By producing lactate, cells poison themselves and cannot resume replication in the fresh medium.

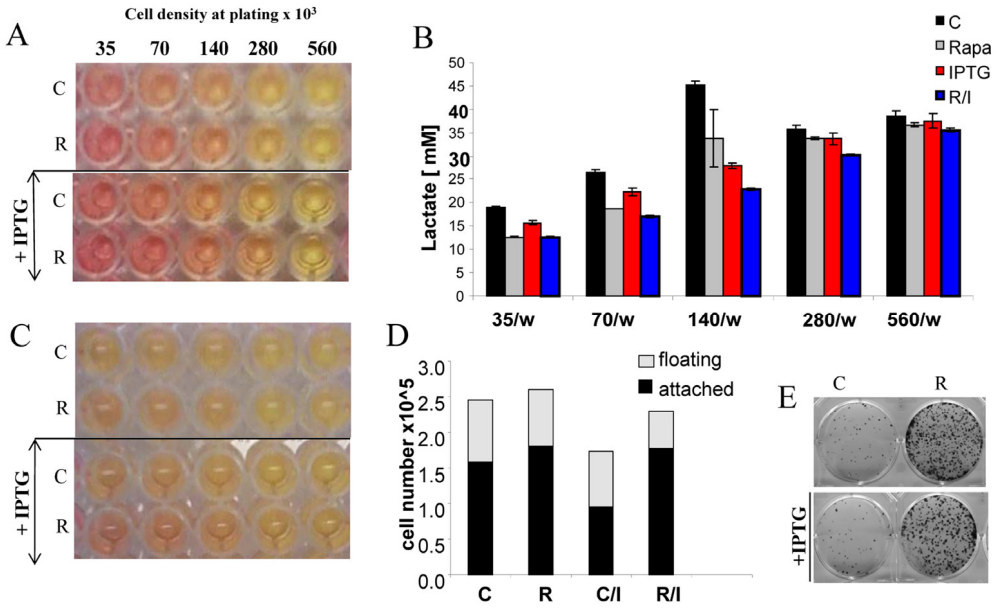

Figure 8. Effects of IPTG, rapamycin and initial cell densities on CS. HT-p21-9 cells were plated at indicated densities (x10^3) in 96-well plates in the presence of IPTG and/or 500 nM rapamycin (R) or left untreated (C). (**A**) On day 1, plates were photographed. (**B**) On Day 1 lactate concentrations were measured in media. (**C**) On day 4 plates were photographed. (**D**) On Day 4 alive (attached) and dead (floating) cells were counted in wells with initial plating density of 140,000 cells/well. (**E**) Replicative viability of attached cells was measured as described in Materials and Methods and legend for Figure 1.

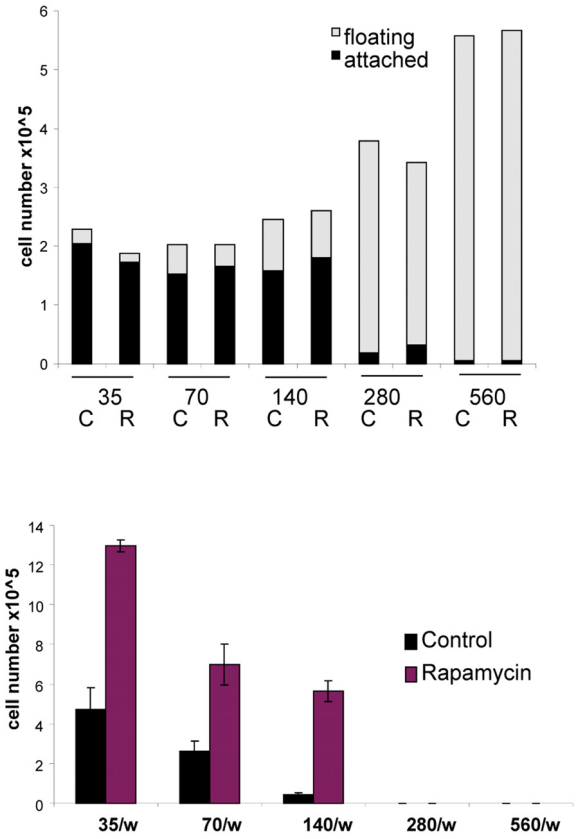

Figure 9. Effects of initial density and rapamycin on cell proliferation, survival and replicative viability. Experiment was performed as described in the legend for Figure 8 (Upper panel). Cell survival. Alive (attached) and dead (floating) cells were counted in all wells on Day 4. (Lower panel). Replicative viability. In all samples, attached cells were replated in the fresh medium in low density and viability was measured by trypsinizing colonies and counting cells.

Still mechanisms of yeast CS are widely disputed and may depend on culture conditions [9, 18, 19, 22, 66-68]. Perhaps, mechanisms of mammalian CS may vary depending on initial cell densities, cell line, the propensity to apoptosis, levels of nutrients in the medium, initial mTOR activity, levels of oxygen and culture conditions prior to experiment. Also, we emphasize that our study was not intended to address the mechanisms of yeast CS. It neither resolves nor complicates the current debate in yeast aging research. The main goal of this study was to characterize "yeast-like" senescence in human cells and its pharmacological manipulation and also to address the question whether CS mimics cellular aging in the organism. CS mimics tumor necrosis rather than aging of post-mitotic cells.

So, literally, CS is not a physiological model of organismal aging. But the same signaling pathways (such as TOR) are involved in CS and aging (Fig. 11), making the model useful for drug and gene discovery. We have shown that agents that decrease lactate production decelerate CS. Specifically, agents that directly or indirectly inhibit mTOR such as rapamycin, LY294002, U106 and to a lesser extend NAC, all suppressed CS. What all these agents have in common is that they inhibit the mTOR pathway. Thus, the same agents that suppress CS also were shown to suppress the senescent phenotype or conversion from quiescence to senescence during cell cycle arrest in traditional models of cellular senescence [46, 53].

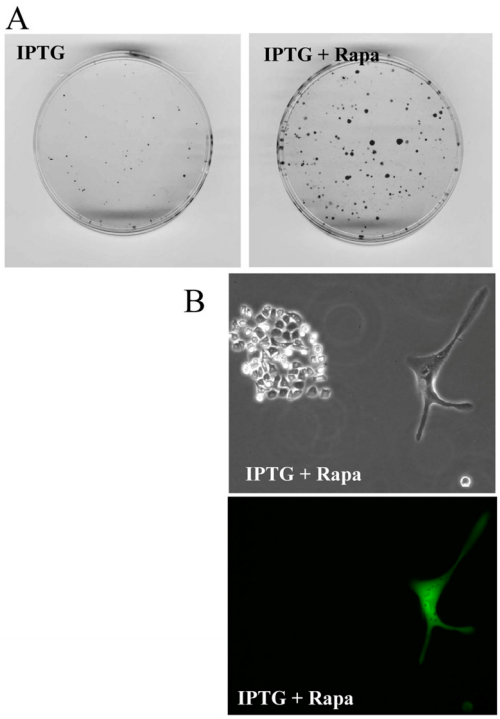

Figure 10. Rapamycin prevents CS of a few indicator cells by indirect effects on abundant cells. A mixture of 2000 HCT116 cells (indicator, non-green cells) and 80000 HT-p21-9 (GFP-expressing, green cells) were plated in 96-well plate with 50 μg/ml IPTG with or without 500 nM rapamycin. After 4 days, equal aliquots of attached cells were re-plated in 60 mm dishes in fresh medium with IPTG to prevent proliferation of HT-p21-9 cells and to allow only viable indicator cells to form colonies. (**A**) After 7 days, colonies were stained. (**B**) Microphotograph of live cells before staining. A colony of HCT116 cells with a solitary large HT-p21-9 cell (labeled with GFP) is shown.

Activation of growth factor receptors, Ras, Raf, PI3K, Akt, which all activate mTOR, are most common

alterations in cancer [69-83]. These growth-promoting pathways also drive senescent phenotype, when the cell cycle is blocked [40, 53, 55]. The same pathways confirm highly glycolytic phenotype [84, 85], rendering cells prone to lactate-induced CS. And the same oncogenic pathways are involved in aging from yeast to mammals [11, 86-88]. And tumor suppressors (including p53) that inhibit the mTOR pathway are aging-suppressors [44, 89-93].

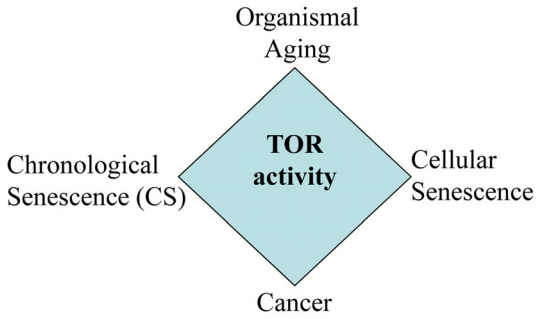

Figure 11. The relationship between CS and other TOR-dependent phenomena. Common signaling pathways such as TOR are involved in cancer, aging, cellular senescence and CS.

In line with previous proposals [11, 39], our work suggests that the same signaling pathways that are known to drive aging are also involved in glycolytic phenotype, which determines CS. Therefore, genetic and pharmacological manipulations that decelerate CS may also affect physiological aging. The same pathways (Ras, MEK and PI-3 K/Akt/mTOR) that render cells malignant and glycolytic are involved in aging. So the same agents that inhibit CS can also suppress malignant metabolism and organismal aging. In addition such agents may be beneficial during acute ischemia (as well as re-oxygenation) to prevent necrosis. Lactic acidosis is one of the complications of diabetes. Also, overproduction of lactate by tumors can lead to fatal lactic acidosis in cancer patients [94-96]. We suggest that rapamycin may be used to treat lactic acidosis both in diabetes and in cancer patients. Interestingly, stromal cells also overproduced lactate, thereby feeding the tumor [97-99]. We suggest that systemic rapamycin may decrease lactate production in the stroma.

Pro-aging pathways are conserved in evolution. This may explain why screening for agents that decelerate yeast CS could be useful against age-related diseases, aging and cancer. In comparison with yeast, human cells are more relevant to human aging and drug discovery.

In conclusion, CS is relevant to aging not because CS happens during physiological aging in the organism, but because the common genes and signaling pathways determine both CS and aging (Fig. 11). Here we discussed CS from the point of view of the aging research, as an analogy to yeast CS. From the cancer research point of view, we will discuss the implication of CS for tumor progression, aggressiveness and cancer therapy (Leontieva et al, Oncotarget, in press).

MATERIALS AND METHODS

Cell lines and reagents. HT-p21-9 cells, derived from HT1080 human fibrosarcoma cells (ATCC, Manassas, VA), provided by Igor Roninson, were previously described [52, 41]. HT1080-p21-9 cells were cultured in high-glucose DMEM without pyruvate supplemented with FC2 serum (HyClone FetalClone II from Thermo Scientific, Logan, Utah). In HT-p21-9 cells, p21 expression can be turned on or off using isopropyl-thio-galactosidase (IPTG) [52, 41]. MCF-7 and HCT116 cell lines were obtained from ATCC (Manassas, VA). MCF-7, breast cancer cell line was cultured in high-glucose DMEM (plus pyruvate) with 10% FBS. HCT-Bax/- cells were derived from HCT116, colorectal adenocarcinoma cell line, and were provided by Bert Vogelstein. Rapamycin was obtained from LC Laboratories (MA, USA) and dissolved in DMSO as 5 mM solution. IPTG (Invitrogen) was dissolved in water as 50 mg/ml stock solution and used in cell culture at final concentration of 1.25-50 μg/ml. LY294002, CGK733, metformin, NAC, UO126 were obtained from Sigma-Aldrich.

Immunoblot analysis. Whole cell lysates were prepared using boiling lysis buffer (1%SDS, 10 mM Tris.HCl, pH 74.). Equal amounts of proteins were separated on 10% or gradient polyacrylamide gels and transferred to nitrocellulose membranes. The following antibodies were used: rabbit anti-phospho-S6 (Ser235/236) and mouse anti-S6, rabbit anti-phospho AKT and anti-Akt from Cell Signaling Biotechnology; anti-actin antibody from Sigma-Aldrich and mouse anti-HIF-1a from BD Biosciences. Secondary anti-rabbit and anti-mouse HRP conjugated antibodies were from Cell Signaling Biotechnology.

Preparation of conditioned medium. Conditioned medium (CM) from HT-p21-9 cells plated at high density (10^6 cells per 60 mm dish) and cultured for 4 days. R-CM, cells were cultured in the presence of 500 nM rapamycin. CM+R: 500 nM rapamycin was added to CM after collection of CM.

Lactate assay was performed using L-Lactate assay kit from Eton Bioscience Inc (San Diego, CA) according to

manufacture's instructions.

Replicative viability as measure of CS. Cells were plated at high initial density (see Fig. 1A) and cultured for 4-8 days. Then media with floating (dead cells) were removed, cells trypsinized and a small aliquot of attached cells was replated at low cell density in 6 well plates in fresh medium. After 6-8 days, colonies were stained with 1.0 % crystal violet and in replicate wells cells were trypzinised and counted.

CONFLICT OF INTERESTS STATEMENT

The authors of this manuscript have no conflict of interest to declare.

REFERENCES

1. Kaeberlein M, McVey M, Guarente L. Using yeast to discover the fountain of youth. Sci Aging Knowledge Environ. 2001; 2001:pe1.

2. Fabrizio P, Pozza F, Pletcher SD, Gendron CM, Longo VD. Regulation of longevity and stress resistance by Sch9 in yeast. Science. 2001; 292:288-290.

3. Sinclair DA. Paradigms and pitfalls of yeast longevity research. Mech Ageing Dev. 2002; 123:857-867.

4. Fabrizio P, Longo VD. The chronological life span of Saccharomyces cerevisiae. Aging Cell. 2003; 2:73-81.

5. Fabrizio P, Longo VD. The chronological life span of Saccharomyces cerevisiae. Methods Mol Biol. 2007; 371:89-95.

6. Kaeberlein M, Kennedy BK. Large-scale identification in yeast of conserved ageing genes. Mech Ageing Dev. 2005; 126:17-21.

7. Murakami CJ, Burtner CR, Kennedy BK, Kaeberlein M. A method for high-throughput quantitative analysis of yeast chronological life span. J Gerontol A Biol Sci Med Sci. 2008; 63:113-121.

8. Kaeberlein M. Lessons on longevity from budding yeast. Nature. 2010; 464:513-519.

9. Weinberger M, Mesquita A, Caroll T, Marks L, Yang H, Zhang Z, Ludovico P, Burhans WC. Growth signaling promotes chronological aging in budding yeast by inducing superoxide anions that inhibit quiescence. Aging. 2010; 2:709-726.

10. Ruckenstuhl C, Carmona-Gutierrez D, Madeo F. The sweet taste of death: glucose triggers apoptosis during yeast chronological aging. Aging. 2010; 2:643-649.

11. Longo VD. Ras: the other pro-aging pathway. Sci Aging Knowledge Environ. 2004; 2004:pe36.

12. Bonawitz ND, Chatenay-Lapointe M, Pan Y, Shadel GS. Reduced TOR signaling extends chronological life span via increased respiration and upregulation of mitochondrial gene expression. Cell Metab. 2007; 5:265-277.

13. Boer VM, Amini S, Botstein D. Influence of genotype and nutrition on survival and metabolism of starving yeast. Proc Natl Acad Sci U S A. 2008; 105:6930-6935.

14. Wei M, Fabrizio P, Hu J, Ge H, Cheng C, Li L, Longo VD. Life span extension by calorie restriction depends on Rim15 and transcription factors downstream of Ras/PKA, Tor, and Sch9. PLoS Genet. 2008; 4:e13.

15. Wei M, Fabrizio P, Madia F, Hu J, Ge H, Li LM, Longo VD. Tor1/Sch9-regulated carbon source substitution is as effective as calorie restriction in life span extension. PLoS Genet. 2009; 5:e1000467.

16. Stanfel MN, Shamieh LS, Kaeberlein M, Kennedy BK. The TOR pathway comes of age. Biochim Biophys Acta. 2009; 1790:1067-1074.

17. Heeren G, Rinnerthaler M, Laun P, von Seyerl P, Kossler S, Klinger H, Hager M, Bogengruber E, Jarolim S, Simon-Nobbe B, Schuller C, Carmona-Gutierrez D, Breitenbach-Koller L, Muck C, Jansen-Durr P, Criollo A *et al*. The mitochondrial ribosomal protein of the large subunit, Afo1p, determines cellular longevity through mitochondrial back-signaling via TOR1. Aging. 2009; 1:622-636.

18. Pan Y, Shadel GS. Extension of chronological life span by reduced TOR signaling requires down-regulation of Sch9p and involves increased mitochondrial OXPHOS complex density. Aging. 2009; 1:131-145.

19. Madia F, Wei M, Yuan V, Hu J, Gattazzo C, Pham P, Goodman MF, Longo VD. Oncogene homologue Sch9 promotes age-dependent mutations by a superoxide and Rev1/Polzeta-dependent mechanism. J Cell Biol. 2009; 186:509-523.

20. Alvers AL, Wood MS, Hu D, Kaywell AC, Dunn WA, Jr., Aris JP. Autophagy is required for extension of yeast chronological life span by rapamycin. Autophagy. 2009; 5:847-849.

21. Parrella E, Longo VD. Insulin/IGF-I and related signaling pathways regulate aging in nondividing cells: from yeast to the mammalian brain. ScientificWorldJournal. 2010; 10:161-177.

22. Pan Y, Schroeder EA, Ocampo A, Barrientos A, Shadel GS. Regulation of Yeast Chronological Life Span by TORC1 via Adaptive Mitochondrial ROS Signaling. Cell Metab. 2011; 13:668-678.

23. Delaney JR, Murakami CJ, Olsen B, Kennedy BK, Kaeberlein M. Quantitative evidence for early life fitness defects from 32 longevity-associated alleles in yeast. Cell Cycle. 2011; 10:156-165.

24. Powers RW, 3rd, Kaeberlein M, Caldwell SD, Kennedy BK, Fields S. Extension of chronological life span in yeast by decreased TOR pathway signaling. Genes Dev. 2006; 20:174-184.

25. Kapahi P, Zid BM, Harper T, Koslover D, Sapin V, Benzer S. Regulation of lifespan in Drosophila by modulation of genes in the TOR signaling pathway. Curr Biol. 2004; 14:885-890.

26. Blagosklonny MV. Aging and immortality: quasi-programmed senescence and its pharmacologic inhibition. Cell Cycle. 2006; 5:2087-2102.

27. Kapahi P, Chen D, Rogers AN, Katewa SD, Li PW, Thomas EL, Kockel L. With TOR, less is more: a key role for the conserved nutrient-sensing TOR pathway in aging. Cell Metab. 2010; 11:453-465.

28. Kaeberlein M, Kennedy BK. Hot topics in aging research: protein translation and TOR signaling, 2010. Aging Cell. 2011; 10:185-190.

29. Wood JG, Rogina B, Lavu S, Howitz K, Helfand SL, Tatar M, Sinclair D. Sirtuin activators mimic caloric restriction and delay ageing in metazoans. Nature. 2004; 430:686-689.

30. Medvedik O, Lamming DW, Kim KD, Sinclair DA. MSN2 and MSN4 Link Calorie Restriction and TOR to Sirtuin-Mediated Lifespan Extension in Saccharomyces cerevisiae. PLoS Biol. 2007; 5:e261.

31. Sinclair DA, Guarente L. Unlocking the secrets of longevity genes. Sci Am. 2006; 294:48-51.

32. Kim D, Nguyen MD, Dobbin MM, Fischer A, Sananbenesi F, Rodgers JT, Delalle I, Baur JA, Sui G, Armour SM, Puigserver P, Sinclair DA, Tsai LH. SIRT1 deacetylase protects against neurodegeneration in models for Alzheimer's disease and amyotrophic lateral sclerosis. EMBO J. 2007;26:3169-3179.

33. Longo VD, Kennedy BK. Sirtuins in aging and age-related disease. Cell. 2006; 126:257-268.

34. Firestein R, Blander G, Michan S, Oberdoerffer P, Ogino S, Campbell J, Bhimavarapu A, Luikenhuis S, de Cabo R, Fuchs C, Hahn WC, Guarente LP, Sinclair DA. The SIRT1 deacetylase suppresses intestinal tumorigenesis and colon cancer growth. PLoS One. 2008; 3:e2020.

35. Blagosklonny MV, Campisi J, Sinclair DA, Bartke A, Blasco MA, Bonner WM, Bohr VA, Brosh RM, Jr., Brunet A, Depinho RA, Donehower LA, Finch CE, Finkel T, Gorospe M, Gudkov AV, Hall MN *et al*. Impact papers on aging in 2009. Aging. 2010; 2:111-121.

36. Fontana L, Partridge L, Longo VD. Extending healthy life span--from yeast to humans. Science. 2010; 328:321-326.

37. Baur JA, Chen D, Chini EN, Chua K, Cohen HY, de Cabo R, Deng C, Dimmeler S, Gius D, Guarente LP, Helfand SL, Imai S, Itoh H, Kadowaki T, Koya D, Leeuwenburgh C *et al*. Dietary restriction: standing up for sirtuins. Science. 2010; 329:1012-1013; author reply 1013-1014.

38. Haigis MC, Sinclair DA. Mammalian sirtuins: biological insights and disease relevance. Annu Rev Pathol. 2010; 5:253-295.

39. Burtner CR, Murakami CJ, Kennedy BK, Kaeberlein M. A molecular mechanism of chronological aging in yeast. Cell Cycle. 2009; 8:1256-1270.

40. Demidenko ZN, Blagosklonny MV. Growth stimulation leads to cellular senescence when the cell cycle is blocked. Cell Cycle. 2008; 7:3355-3361.

41. Demidenko ZN, Zubova SG, Bukreeva EI, Pospelov VA, Pospelova TV, Blagosklonny MV. Rapamycin decelerates cellular senescence. Cell Cycle. 2009; 8:1888-1895.

42. Demidenko ZN, Blagosklonny MV. Quantifying pharmacologic suppression of cellular senescence: prevention of cellular hypertrophy versus preservation of proliferative potential. Aging. 2009; 1:1008-1016.

43. Pospelova TV, Demidenko ZN, Bukreeva EI, Pospelov VA, Gudkov AV, Blagosklonny MV. Pseudo-DNA damage response in senescent cells. Cell Cycle. 2009; 8:4112-4118.

44. Demidenko ZN, Korotchkina LG, Gudkov AV, Blagosklonny MV. Paradoxical suppression of cellular senescence by p53. Proc Natl Acad Sci U S A. 2010; 9660-4:9660-9664.

45. Korotchkina LG, Leontieva OV, Bukreeva EI, Demidenko ZN, Gudkov AV, Blagosklonny MV. The choice between p53-induced senescence and quiescence is determined in part by the mTOR pathway. Aging. 2010; 2:344-352.

46. Leontieva OV, Blagosklonny MV. DNA damaging agents and p53 do not cause senescence in quiescent cells, while consecutive re-activation of mTOR is associated with conversion to senescence. Aging. 2010; 2:924-935.

47. Leontieva O, Gudkov A, Blagosklonny M. Weak p53 permits senescence during cell cycle arrest. Cell Cycle. 2010; 9:4323-4327.

48. Gems D. Ageing. Yeast longevity gene goes public. Nature. 2001; 410:154-155.

49. Morselli E, Galluzzi L, Kepp O, Criollo A, Maiuri MC, Tavernarakis N, Madeo F, Kroemer G. Autophagy mediates pharmacological lifespan extension by spermidine and resveratrol. Aging. 2009; 1:961-970.

50. Goldberg AA, Richard VR, Kyryakov P, Bourque SD, Beach A, Burstein MT, Glebov A, Koupaki O, Boukh-Viner T, Gregg C, Juneau M, English AM, Thomas DY, Titorenko VI. Chemical genetic screen identifies lithocholic acid as an anti-aging compound that extends yeast chronological life span in a TOR-independent manner, by modulating housekeeping longevity assurance processes. Aging. 2010; 2:393-414.

51. Mirisola MG, Longo VD. Conserved role of Ras-GEFs in promoting aging: from yeast to mice. Aging. 2011; 3:340-343.

52. Chang BD, Broude EV, Fang J, Kalinichenko TV, Abdryashitov R, Poole JC, Roninson IB. p21Waf1/Cip1/Sdi1-induced growth arrest is associated with depletion of mitosis-control proteins and leads to abnormal mitosis and endoreduplication in recovering cells. Oncogene. 2000; 19:2165-2170.

53. Demidenko ZN, Shtutman M, Blagosklonny MV. Pharmacologic inhibition of MEK and PI-3K converges on the mTOR/S6 pathway to decelerate cellular senescence. Cell Cycle. 2009; 8:1896-1900.

54. Demidenko ZN, Blagosklonny MV. Quantifying pharmacologic suppression of cellular senescence: prevention of cellular hypertrophy versus preservation of proliferative potential. Aging. 2009; 1:1008-1016.

55. Blagosklonny MV. Cell cycle arrest is not senescence. Aging. 2011; 3:94-101.

56. Blagosklonny MV. Aging: ROS or TOR. Cell Cycle. 2008; 7:3344-3354.

57. Zhang L, Yu J, Park BH, Kinzler KW, Vogelstein B. Role of BAX in the apoptotic response to anticancer agents. Science. 2000; 290:989-992.

58. Kuribayashi K, Finnberg N, Jeffers JR, Zambetti GP, El-Deiry WS. The relative contribution of pro-apoptotic p53-target genes in the triggering of apoptosis following DNA damage in vitro and in vivo. Cell Cycle. 2011; 10:2380-2389.

59. Arsham AM, Howell JJ, Simon MC. A novel hypoxia-inducible factor-independent hypoxic response regulating mammalian target of rapamycin and its targets. J Biol Chem. 2003; 278:29655-29660.

60. Brugarolas J, Lei K, Hurley RL, Manning BD, Reiling JH, Hafen E, Witters LA, Ellisen LW, Kaelin WG, Jr. Regulation of mTOR function in response to hypoxia by REDD1 and the TSC1/TSC2 tumor suppressor complex. Genes Dev. 2004; 18:2893-2904.

61. Kaeberlein M, Kapahi P. The hypoxic response and aging. Cell Cycle. 2009; 8:2324.

62. Diaz-Ruiz R, Rigoulet M, Devin A. The Warburg and Crabtree effects: On the origin of cancer cell energy metabolism and of yeast glucose repression. Biochim Biophys Acta. 2011; 1807:568-576.

63. Ruckenstuhl C, Buttner S, Carmona-Gutierrez D, Eisenberg T, Kroemer G, Sigrist SJ, Frohlich KU, Madeo F. The Warburg effect suppresses oxidative stress induced apoptosis in a yeast model for cancer. PLoS One. 2009; 4:e4592.

64. Gatenby RA, Gillies RJ. Why do cancers have high aerobic glycolysis? Nat Rev Cancer. 2004; 4:891-899.

65. Martinez-Outschoorn UE, Lin Z, Ko YH, Goldberg AF, Flomenberg N, Wang C, Pavlides S, Pestell RG, Howell A, Sotgia F, Lisanti MP. Understanding the metabolic basis of drug resistance: Therapeutic induction of the Warburg effect kills cancer cells. Cell Cycle. 2011; 10:2521-2528.

66. Murakami CJ, Wall V, Basisty N, Kaeberlein M. Composition and acidification of the culture medium influences chronological aging similarly in vineyard and laboratory yeast. PLoS One. 2011; 6:e24530.

67. Fabrizio P, Battistella L, Vardavas R, Gattazzo C, Liou LL, Diaspro A, Dossen JW, Gralla EB, Longo VD. Superoxide is a mediator of an altruistic aging program in Saccharomyces cerevisiae. J Cell Biol. 2005; 166: 1055-1067.

68. Fabrizio P, Gattazzo C, Battistella L, Wei M, Cheng C, McGrew K, Longo VD. Sir2 blocks extreme life-span extension. Cell. 2005; 123:655-667.

69. Janes MR, Fruman DA. Targeting TOR dependence in cancer. Oncotarget. 2010; 1:69-76.

70. Martelli AM, Evangelisti C, Chiarini F, McCubrey JA. The phosphatidylinositol 3-kinase/Akt/mTOR signaling network as a therapeutic target in acute myelogenous leukemia patients. Oncotarget. 2010; 1:89-103.

71. Luo J, Manning BD, Cantley LC. Targeting the PI3K-Akt pathway in human cancer: rationale and promise. Cancer Cell. 2003; 4:257-262.

72. Zhang Z, Stiegler AL, Boggon TJ, Kobayashi S, Halmos B. EGFR-mutated lung cancer: a paradigm of molecular oncology. Oncotarget. 2010; 1:497-514.

73. Nucera C, Lawler J, Hodin R, Parangi S. The BRAFV600E mutation: what is it really orchestrating in thyroid cancer? Oncotarget. 2010; 1:751-756.

74. Choo AY, Blenis J. Not all substrates are treated equally: implications for mTOR, rapamycin-resistance and cancer therapy. Cell Cycle. 2009; 8:567-572.

75. Carver BS, Chapinski C, Wongvipat J, Hieronymus H, Chen Y, Chandarlapaty S, Arora VK, Le C, Koutcher J, Scher H, Scardino PT, Rosen N, Sawyers CL. Reciprocal feedback regulation of PI3K and androgen receptor signaling in PTEN-deficient prostate cancer. Cancer Cell. 19:575-586.

76. Rexer BN, Engelman JA, Arteaga CL. Overcoming resistance to tyrosine kinase inhibitors: lessons learned from cancer cells treated with EGFR antagonists. Cell Cycle. 2009; 8:18-22.

77. Schmidt EV, Ravitz MJ, Chen L, Lynch M. Growth controls connect: interactions between c-myc and the tuberous sclerosis complex-mTOR pathway. Cell Cycle. 2009; 8:1344-1351.

78. Markman B, Dienstmann R, Tabernero J. Targeting the PI3K/Akt/mTOR pathway--beyond rapalogs. Oncotarget. 2010; 1:530-543.

79. Abrams SL, Steelman LS, Shelton JG, Wong EW, Chappell WH, Basecke J, Stivala F, Donia M, Nicoletti F, Libra M, Martelli AM, McCubrey JA. The Raf/MEK/ERK pathway can govern drug resistance, apoptosis and sensitivity to targeted therapy. Cell Cycle. 2010; 9:1781-1791.

80. Novosyadlyy R, LeRoith D. Hyperinsulinemia and type 2 diabetes: impact on cancer. Cell Cycle. 2010; 9:1449-1450.

81. Zhao L, Vogt PK. Hot-spot mutations in p110alpha of phosphatidylinositol 3-kinase (pI3K): differential interactions with the regulatory subunit p85 and with RAS. Cell Cycle. 2010; 9:596-600.

82. Shahbazian D, Parsyan A, Petroulakis E, Hershey J, Sonenberg N. eIF4B controls survival and proliferation and is regulated by proto-oncogenic signaling pathways. Cell Cycle. 2010; 9:4106-4109.

83. Hay N. The Akt-mTOR tango and its relevance to cancer. Cancer Cell. 2005; 8:179-183.

84. Sun Q, Chen X, Ma J, Peng H, Wang F, Zha X, Wang Y, Jing Y, Yang H, Chen R, Chang L, Zhang Y, Goto J, Onda H, Chen T, Wang MR *et al*. Mammalian target of rapamycin up-regulation of pyruvate kinase isoenzyme type M2 is critical for aerobic glycolysis and tumor growth. Proc Natl Acad Sci U S A. 2011; 108:4129-4134.

85. Duvel K, Yecies JL, Menon S, Raman P, Lipovsky AI, Souza AL, Triantafellow E, Ma Q, Gorski R, Cleaver S, Vander Heiden MG, MacKeigan JP, Finan PM, Clish CB, Murphy LO, Manning BD. Activation of a metabolic gene regulatory network downstream of mTOR complex 1. Mol Cell. 39:171-183.

86. Pinkston JM, Garigan D, Hansen M, Kenyon C. Mutations that increase the life span of C. elegans inhibit tumor growth. Science. 2006; 313:971-975.

87. Blagosklonny MV, Hall MN. Growth and aging: a common molecular mechanism. Aging. 2009; 1:357-362.

88. Blagosklonny MV. Revisiting the antagonistic pleiotropy theory of aging: TOR-driven program and quasi-program. Cell Cycle. 2010; 9:3151-3156.

89. Matheu A, Maraver A, Klatt P, Flores I, Garcia-Cao I, Borras C, Flores JM, Vina J, Blasco MA, Serrano M. Delayed ageing through damage protection by the Arf/p53 pathway. Nature. 2007; 448:375-379.

90. Vigneron A, Vousden KH. p53, ROS and senescence in the control of aging. Aging. 2010; 2:471-474.

91. Poyurovsky MV, Prives C. P53 and aging: A fresh look at an old paradigm. Aging. 2010; 2: 380-382.

92. Serrano M. Shifting senescence into quiescence by turning up p53. Cell Cycle. 2010; 9: 4256-4257.

93. Galluzzi L, Kepp O, Kroemer G. TP53 and MTOR crosstalk to regulate cellular senescence. Aging. 2010; 2:535-537.

94. Chan FH, Carl D, Lyckholm LJ. Severe lactic acidosis in a patient with B-cell lymphoma: a case report and review of the literature. Case Report Med. 2009; 2009:534561.

95. Dogan E, Erkoc R, Sayarlioglu H, Alici S, Dilek I, Alici O. Fatal lactic acidosis due to leukemic transformation in a patient with non-Hodgkin's lymphoma: case report. Adv Ther. 2005; 22:443-446.

96. Feron O. Pyruvate into lactate and back: from the Warburg effect to symbiotic energy fuel exchange in cancer cells. Radiother Oncol. 2009; 92:329-333.

97. Pavlides S, Whitaker-Menezes D, Castello-Cros R, Flomenberg N, Witkiewicz AK, Frank PG, Casimiro MC, Wang C, Fortina P, Addya S, Pestell RG, Martinez-Outschoorn UE, Sotgia F, Lisanti MP. The reverse Warburg effect: aerobic glycolysis in cancer associated fibroblasts and the tumor stroma. Cell Cycle. 2009; 8:3984-4001.

98. Migneco G, Whitaker-Menezes D, Chiavarina B, Castello-Cros R, Pavlides S, Pestell RG, Fatatis A, Flomenberg N, Tsirigos A, Howell A, Martinez-Outschoorn UE, Sotgia F, Lisanti MP. Glycolytic cancer associated fibroblasts promote breast cancer tumor growth, without a measurable increase in angiogenesis: evidence for stromal-epithelial metabolic coupling. Cell Cycle. 2010; 9:2412-2422.

99. Bonuccelli G, Tsirigos A, Whitaker-Menezes D, Pavlides S, Pestell RG, Chiavarina B, Frank PG, Flomenberg N, Howell A, Martinez-Outschoorn UE, Sotgia F, Lisanti MP. Ketones and lactate "fuel" tumor growth and metastasis: Evidence that epithelial cancer cells use oxidative mitochondrial metabolism. Cell Cycle. 2010; 9:3506-3514.

SUPPLEMENTAL FIGURES

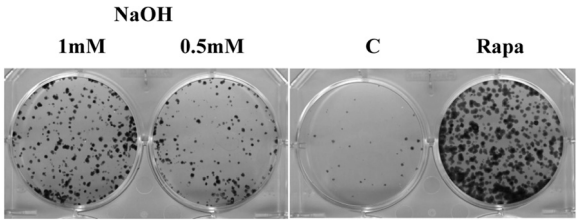

Figure S1. Effect of NaOH on CS. HT-p21-9 cells were plated at 80,000/well in 96 well plates. On day 1, 0.5 mM or 1 mM NaOH was added. 100 nM rapamycin (Rapa) was used as positive control. Cells were split on day 5 (4 µl out of 200 µl culture per well into 6 well plates) as shown in Fig. 1A. Colonies were grown for 9 days and stained with Crystal Violet.

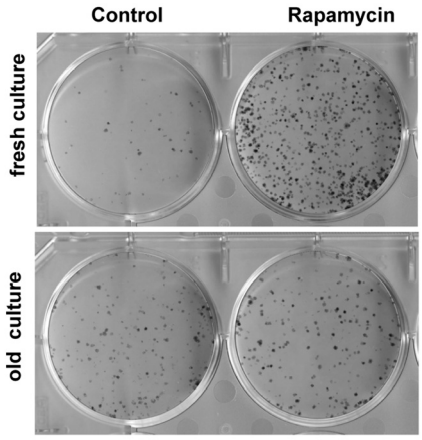

Figure S2. HT1080 p21-9 cells passaged the day before (fresh culture) or cultured for 2 weeks without change of the medium (old culture) plated at 80000 cells/well in 96-well plates with or without 500 nM rapamycin. On day 4, cells were trypsinized and equal volumes of adherent cells (2%) were re-plated in 6 well plates. After 7 days, colonies were stained with Crystal violet.

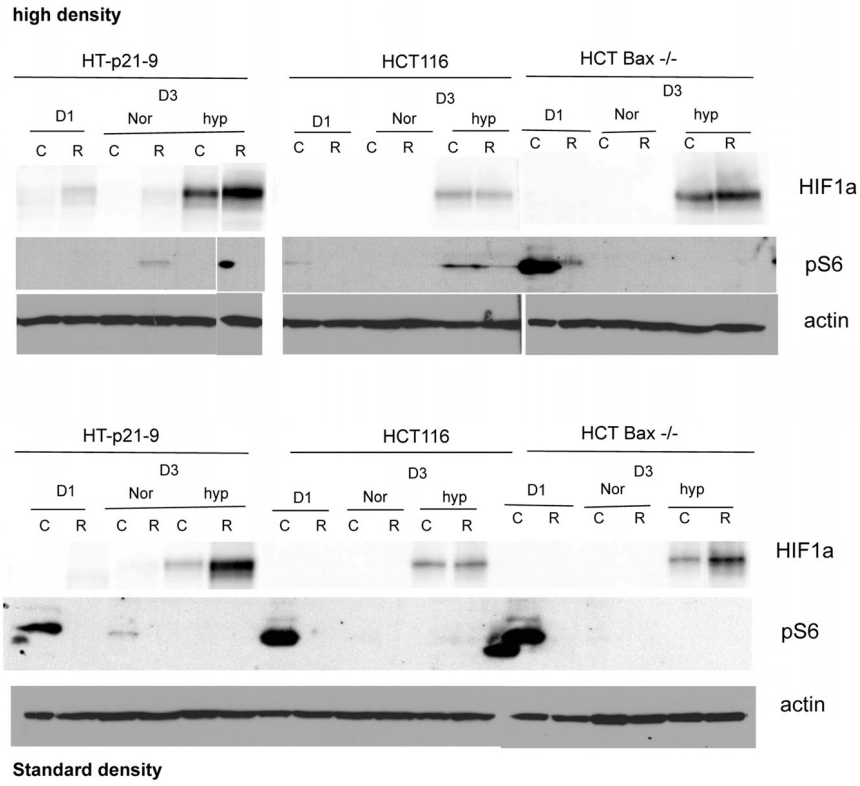

Figure S3. HT-p21-9, HCT116 and HCT Bax-/- cells were plated at high density (upper panel) and regular density (lower panel) and on Day 1 was placed in either normoxia (Nor) or hypoxia (Hyp) with or without 100 nM rapamycin (R) or left untreated (C). Cells were lysed on day 1 (D1) and on day 3 (D3). Immunoblot was performed using indicated antibodies.

Research Paper

Genome protective effect of metformin as revealed by reduced level of constitutive DNA damage signaling

H. Dorota Halicka[1], Hong Zhao[1], Jiangwei Li[1], Frank Traganos[1], Sufang Zhang[2], Marietta Lee[2], and Zbigniew Darzynkiewicz[1]

[1] Brander Cancer Research Institute and Department of Pathology, New York Medical College, Valhalla, NY 10595, USA
[2] Department of Biochemistry and Molecular Biology, New York Medical College, Valhalla, NY 10595, USA

Key words: *DNA replication stress, Reactive oxidant species (ROS), H2AX phosphorylation, ATM activation, cell cycle*
Received: *9/22/11; Accepted: 10/26/11; Published: 10/28/11* doi:10.18632/aging.100397
Correspondence to: *Z. Darzynkiewicz, PhD;* ***E-mail:*** *darzynk@nymc.edu*

Abstract: We have shown before that constitutive DNA damage signaling represented by H2AX-Ser139 phosphorylation and ATM activation in untreated normal and tumor cells is a reporter of the persistent DNA replication stress induced by endogenous oxidants, the by-products of aerobic respiration. In the present study we observed that exposure of normal mitogenically stimulated lymphocytes or tumor cell lines A549, TK6 and A431 to metformin, the specific activator of 5'AMP-activated protein kinase (AMPK) and an inhibitor of mTOR signaling, resulted in attenuation of constitutive H2AX phosphorylation and ATM activation. The effects were metformin-concentration dependent and seen even at the pharmacologically pertinent 0.1 mM drug concentration. The data also show that intracellular levels of endogenous reactive oxidants able to oxidize 2',7'-dihydro-dichlorofluorescein diacetate was reduced in metformin-treated cells. Since persistent constitutive DNA replication stress, particularly when paralleled by mTOR signaling, is considered to be the major cause of aging, the present findings are consistent with the notion that metformin, by reducing both DNA replication stress and mTOR-signaling, slows down aging and/or cell senescence processes.

INTRODUCTION

In live cells, DNA is continuously being damaged by reactive oxygen species (ROS), the by-products of aerobic respiration in mitochondria [1-6]. Exogenous oxidants originating from environmental pollutants [7], phagocyte-oxidative burst [8-10], and even iatrogenic factors [11], additionally contribute to DNA damage. Such DNA damage involves oxidation of the constituent DNA bases, particularly of guanine by formation of 8-oxo-7,8-dihydro-2'-deoxyguanosine (oxo8dG), base ring fragmentation, modification of deoxyglucose, crosslinking of DNA and protein, and induction of DNA double strand breaks (DSBs) [12,13]. Another important injurious effect of endogenous and exogenous oxidants is peroxidation of lipids in cell membranes [14].

The extent of ROS-induced DNA damage varies widely in different studies [1-6]. According to one rather conservative estimate, about 5,000 DNA single-strand lesions (SSLs) are generated per nucleus during a single cell cycle of approximately 24 h duration [6]. About 1% of those lesions become converted to DSBs, mostly during DNA replication. This leads to formation of ~50 "endogenous DSBs", the most severe and potentially mutagenic lesions [6]. DSBs can be repaired by two mechanisms, recombinatorial repair or nonhomologous DNA-end joining (NHEJ). The template-assisted recombinatorial repair is essentially error-free but takes place only when cells have already replicated their DNA which can serve as a template, namely in late-S and G_2 phase of the cell cycle. DNA repair in cells lacking a template such as in G_1 and early S phase occurs via the NHEJ mechanism. The latter is error-prone and may result in deletion of some base pairs [15,16]. When such change occurs at the site of an oncogene or tumor suppressor gene it may promote carcinogenesis [17,18]. It can also lead to translocations and telomere fusion, hallmarks of tumor cells [19]. The

progressive accumulation of DNA damage with each sequential cell cycle has been considered to be the primary cause of cell aging and senescence [20]. However, the notion that persistent stimulation of mTOR-driven pathways (rather than the ROS-induced DNA damage) is the major mechanism responsible for aging appears to have more merit [21-27]. Oxidative DNA damage, on the other hand, by contributing to replication stress may be a factor enhancing the TOR-driven aging or senescence process [28].

Strategies for preventing cancer or slowing down aging are often directed at protecting DNA from oxidative damage. Protective agents can be identified by their ability to reduce formation of "endogenous DSBs". The direct detection of endogenous DSBs in individual cells has been difficult because the leading methodology, single cell electrophoresis (comet) assay [29], lacks the desired sensitivity. The TUNEL assay, developed to label DSBs in apoptotic cells, also lack sufficient sensitivity [30,31]. While the assays of DNA damage measurement in bulk offer greater sensitivity, these approaches do not allow one to relate the damage to individual cells, reveal any heterogeneity within cell populations, or the relationship of DSBs to cell cycle phase or apoptosis.

Among the early and most sensitive reporters of DNA damage, and in particular formation of DSBs, is the activation of the Ataxia Telangiectasia mutated protein kinase (ATM) through its autophosphorylation on Ser1981 [32], and the phosphorylation of histone H2AX on Ser139; the phosphorylated H2AX is designated as γH2AX]33]. Immunocytochemical detection of these events offers high sensitivity in assessment of DSBs formation in individual cells [34-37]. These biosensors of DNA damage have been used in conjunction with flow- or image-cytometry to assess DNA damage in cells exposed to a variety of exogenous genotoxins (reviews, [31,38]). In fact, the high sensitivity of these biomarkers makes it possible to use them to detect and measure the extent of constitutive DNA damage induced by the metabolically generated ROS in untreated cells [39-41]. Furthermore, these markers can be used to explore the effectiveness of factors protecting nuclear DNA from endogenous oxidants [42-45]. Thus, the anti-oxidants (N-acetyl-L-cysteine, ascorbate, Celecoxib), inhibitors of glycolysis and oxidative phosphorylation (2-deoxy-D-glucose and 5-bromo-pyruvate), hypoxia (3-5% O_2), confluency, low serum concentration, were all shown to distinctly reduce the level of constitutive ATM activation and H2AX phosphorylation [40-45]. Conversely, the factors enhancing metabolic activity (aerobic glycolysis) such as cell mitogenic activation, glucose, or dichloroacetate amplified the level of constitutive expression of γH2AX and activated ATM [42-45]. Collectively, these observations provide strong evidence that the extent of the ongoing DNA damage imposed by endogenous oxidants as well as the effectiveness of factors that protect from (or enhance) the damage can be assessed by analysis of the level of constitutive DNA damage signaling.

In the present study we tested whether metformin, a drug widely prescribed to treat type 2 diabetes, has the ability to modulate the level of constitutive DNA damage signaling. Metformin is a specific activator of 5'AMP-activated protein kinase (AMPK), a phylo-genetically conserved serine/threonine kinase that plays a key role in cellular energy homeostasis (reviews, [46-52]). AMPK is the energy sensor ("fuel gauge") monitoring and regulating cellular energy in response to metabolic needs and nutritional environmental variations. This kinase is activated by low cellular energy status (increased AMP/ATP ratio) and responds by: (i) activating ATP-producing catabolic pathways such as glycolysis and fatty acids oxidation and (ii) suppressing the energy (ATP)-consuming anabolic pathways such as lipogenesis, gluconeogenesis and protein synthesis. Another effect of AMPK activation is inhibition of mammalian target of rapamycin (mTOR), the downstream effector of growth factor signaling pathways [51]. AMPK affects these activities by phosphorylating proteins regulating these pathways (instant effect) as well as by modulating transcription of genes encoding proteins of these pathways (delayed effect) [53-55]. AMPK itself is activated by the upstream mediator liver kinase B1 (LKB1) [52]. Activation of AMPK by metformin was shown to reduce intracellular reactive oxygen species (ROS) levels *via* upregulation of expression of the antioxidant thioredoxin through the AMPK-FOXO3 pathway [55].

There is a growing body of evidence that metformin may be considered a promising anti-aging candidate, applicable for life span extension, prevention and even treatment of cancer [22-27,50,56]. Given the above, it is of additional interest to know how metformin affects the level of constitutive DNA signaling in normal and tumor cells. Our present data show that in normal lymphocytes, as well as in cells of tumor lines the level of constitutive ATM activation and γH2AX expression was distinctly attenuated upon exposure to metformin. Also reduced was the level of intracellular ROS.

RESULTS

The effect of metformin was tested on the level of constitutive expression of γH2AX and Ser1981-

phoshorylated ATM in human lung adenocarcinoma A549 cells. The cells were grown attached on slides and the expression of these phospho-proteins was measured by laser scanning cytometry (LSC) [57]. The data provide clear evidence that expression of γH2AX in A549 cells growing in the presence of metformin for 48 h was reduced (Figure 1). The reduction was apparent at 1 mM, and was progressively more pronounced following exposure to 5 and 20 mM concentrations of metformin.

Across all the three metformin concentrations, the degree of reduction in γH2AX expression was more distinct in G_2M- and S- phase cells compared to cells in the G_1-phase of the cycle. The DNA content frequency histograms did not show major changes in the cell cycle distribution following 48 h treatment with up to 10 mM metformin, while only a modest decrease in the proportion of S-phase cells was apparent following exposure to 20mM metformin (Figure 1, insets).

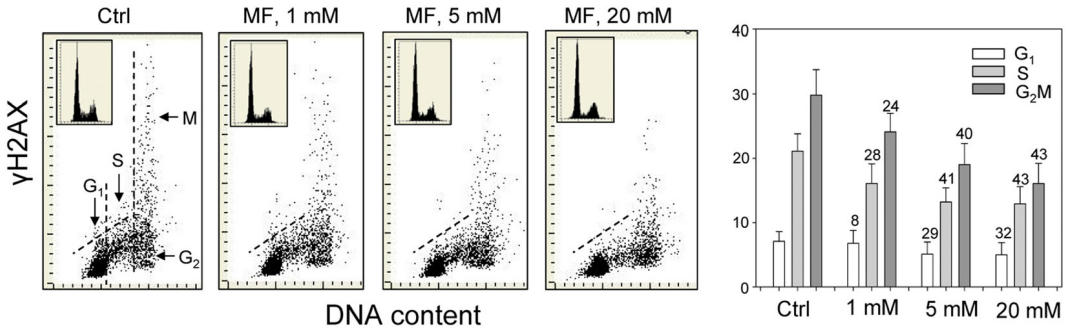

Figure 1. Effect of metformin (MF) on the level of constitutive γH2AX expression in A549 cells. Exponentially growing A549 cells were left untreated (Ctrl) or treated with 1, 5 or 20 mM metformin for 48 h. Left panels present bivariate distributions of cellular DNA content *versus* intensity of γH2AX immunofluorescence (IF) detected with H2AX-Ser139 phospho-specific Ab in cells of these cultures; fluorescence of individual cells was measured by laser scanning cytometry (LSC) [76]. Based on differences in DNA content the cells were gated in G_1, S and G_2M phases of the cell cycle, as shown in the left panel, and the mean values of γH2AX IF for cells in each of these cell cycle phases by were obtained gating analysis. These mean values (+SD) are presented as the bar plots (right panel). The percent decrease in mean values of γH2AX expression of the metformin-treated cells with respect to the same phase of the cell cycle of the untreated cells is shown above the respective bars. The skewed dash line shows the upper level of γH2AX IF intensity for 97% of G_1- and S- phase cells in Ctrl. The insets show cellular DNA content frequency histograms in the respective cultures.

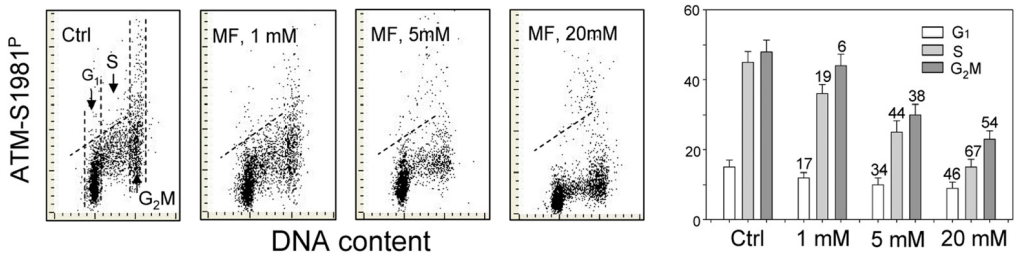

Figure 2. Effect of metformin (MF) on the level of constitutive ATM phosphorylation on Ser1981 in A549 cells. Similar as in Figure 1, the cells were treated with 1, 5 or 20 mM MF for 48 h. Left panels present bivariate distributions of cellular DNA content vs intensity of ATM-S1981^P IF. The mean values of ATM-S1981^P for cells in G_1, S, and G_2M were obtained by gating analysis and are shown (+SD) as the bar plots (right panel). The skewed dash line shows the upper level of ATM-S198^P IF intensity for 97% of G_1- and S- phase cells in Ctrl.

The effect of metformin on the level of constitutive expression of ATM phosphorylated on Ser1981 in A549 cells was strikingly similar to that of γH2AX (Figure 2). The degree of reduction of ATM-S1981^{P} was metformin-concentration dependent. While the decline in ATM activation was seen in all phases of the cell cycle, the most pronounced reduction was evident in S-phase cells (Figure 2).

In the next set of experiments we have tested the effect of metformin on human lymphoblastoid TK6 cells. These cells grow in suspension and their fluorescence, upon staining with phospho-specific Abs, was measured by flow cytometry [57]. The data show that, similar to A549, the expression of γH2AX was also reduced in TK6 cells exposed to metformin (Figure 3). The effect could be seen (7 – 10% decrease) even at a metformin concentration as low as 0.1 mM, and was more pronounced (up to 44% reduction) at higher concentrations. In TK6 cells the reduction in γH2AX was more pronounced in G_1 and S phase than in G_2M phase cells. The level of constitutively activated ATM was also decreased in TK6 cells growing in the presence of metformin (Figure 4).

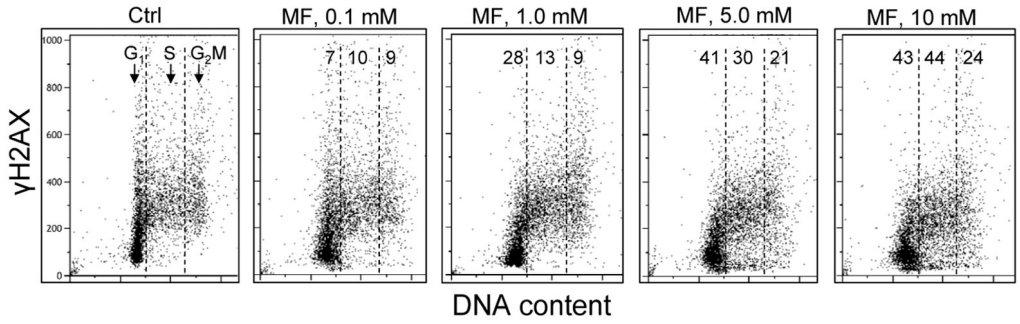

Figure 3. Effect of metformin on the level of constitutive expression of γH2AX in TK6 cells. Exponentially growing TK6 cells were untreated (Ctrl) or were grown in the presence of 0.1, 1.0, 5.0 and 10 mM metformin (MF) for 48 h. The expression of γH2AX was detected with phospho-specific (Ser139-P) Ab and cell fluorescence was measured by flow cytometry. Based on differences in DNA content the cells were gated in G_1, S and G_2M phases of the cell cycle and the mean values of γH2AX IF for cells in each of these cell cycle phases were calculated. The numerical figures show the percent reduction in mean values of γH2AX IF of the metformin-treated cells with respect to the mean values of the untreated cells (Ctrl) in the respective phases of the cell cycle.

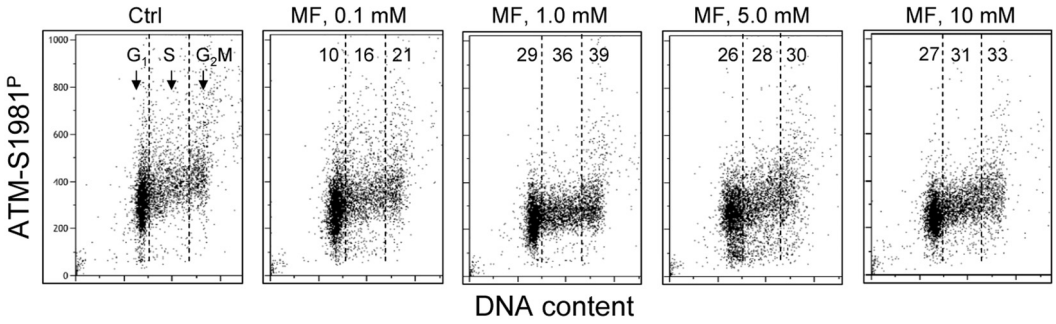

Figure 4. Effect of metformin on the level of constitutive expression of ATM-S1981^{P}. Exponentially growing TK6 cells were untreated (Ctrl) or were grown in the presence of 0.1, 1.0, 5.0 and 10 mM metformin (MF) for 48 h. The expression of ATM-S1981^{P} was detected with phospho-specific Ab. As in Fig. 3, the cells were gated in G_1, S and G_2M phases of the cell cycle and the mean values of ATM-S1981^{P} for cells in each of these cell cycle phases were estimated. The figures show the percent reduction in mean values of ATM-S1981^{P} IF of the metformin-treated cells with respect to the mean values of the untreated cells (Ctrl) in the respective phases of the cell cycle.

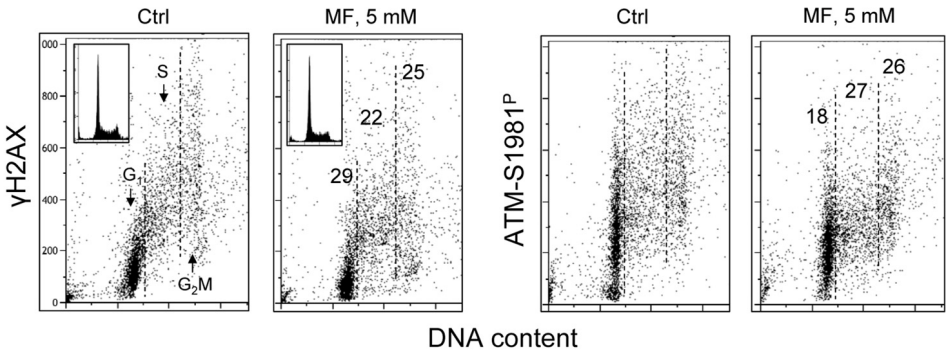

Figure 5. Effect of metformin on constitutive expression γH2AX and ATM-S1981^P in normal human proliferating lymphocytes. Peripheral blood lymphocytes were mitogenically stimulated by phytohemagglutinin for 48 h and then were grown in the absence (Ctrl) or presence of 5 mM metformin (MF) for additional 24 h. The expression of γH2AX and ATM-S1981^P was detected with phospho-specific Abs and cell fluorescence we as measured by flow cytometry. The numerical figures show the percent reduction in expression of γH2AX and ATM-S1981^P of cells treated with metformin with respect to Ctrl, in the respective phases of the cell cycle.

Figure 5 illustrates the effect of metformin on proliferating human lymphocytes. The peripheral blood lymphocytes were stimulated to proliferate by the polyvalent mitogen phytohemagglutinin for 48 h and subsequently were grown in the absence or presence of 5 mM metformin for 24 h. The data show that, as was the case with the tumor cell lines A549 and TK6, growth of lymphocytes in the presence of 5mM metformin distinctly reduced both the level of constitutive expression of γH2AX as well as of ATM-S1981^P.

As mentioned in the Introduction, the decline in the level of constitutive expression of γH2AX and phosphorylation of ATM was observed in cells treated with agents that decrease the level of endogenous oxidants such as ROS scavengers or antioxidants [39-45,58]. Therefore, we assessed the effect of metformin on the abundance of reactive oxidants in human leukemic TK6 cells in the same cultures in which we observed the decline in expression of γH2AX (Figure 3) and ATM-S1981^P (Figure 4). As is quite evident from the data shown in Figure 6, the growth of TK6 cells for 48 h in the presence of metformin led to a decrease in the level of ROS that were detected by their ability to oxidize 2',7'-dihydro-dichlorofluorescein diacetate (H2DCF-DA); following oxidation by ROS the non-fluorescent substrate H2DCF-DA is converted to the highly fluorescent product DCF [59]. The effect was concentration dependent and the oxidation of H2DCF-DA was reduced by nearly two orders of magnitude at a 10 mM concentration of metformin compared to untreated cells (Figure 6).

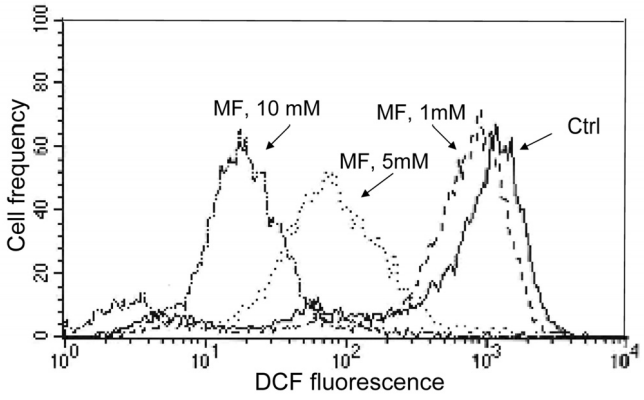

Figure 6. Effect of metformin on ability of TK6 cells to oxidize 2',7'-dihydro-dichlorofluorescein diacetate (H2DCF-DA). TK6 cells were untreated (Ctrl) or treated with 1, 5 or 10 mM metformin (MF) for 48 h. The cells were then incubated for 30 min with 10 μM H2DCF-DA and their fluorescence was measured by flow cytometry. While H2DCF-DA is not fluorescent, the product of its oxidation (DCF) by intracellular ROS shows strong green fluorescence. Note dramatic decline in fluorescence intensity of cells treated with 5 or 10 mM metformin.

DISCUSSION

The present data demonstrate that exposure of either normal, mitogenically activated lymphocytes, or tumor cell lines (A549, TK6) to metformin leads to a decrease in the level of constitutive phosphorylation of H2AX on Ser139 and constitutive activation of ATM. The

observed decrease was evident even at a concentration as low as 0.1 mM metformin (Figures 3 and 4). Pharmacokinetic data indicate that this concentration of metformin is of pharmacological relevance [60]. Since the level of constitutive expression of γH2AX and ATM-S1981^{P} to a large extent reports DNA damage signaling in response to DNA damage by endogenous oxidants generated during aerobic respiration [39-45,58]. the present findings would be consistent with a notion that metformin exerts protective effect on nuclear DNA against oxidative damage. These findings are consistent with the observation that exposure of cells to metformin lowered the extent of reactive oxidants that were able to oxidize the H2DCF-DA substrate (Figure 5). They are also in accordance with numerous studies in which a decrease in the level of ROS in cells treated with metformin has been observed [55,61-65]. It appears that the mechanisms activated by metformin for neutralizing ROS such as upregulation of the antioxidant thioredoxin [55], and/or suppression of NAD(P)H oxidase activity [61] may prevail over the ROS-generating inhibitory effect on mitochondrial respiratory complex I or catabolic processes activated by AMPK [66,67].

It should be noted that DNA damage signaling such as reported by H2AX phosphorylation and ATM activation do not necessarily indicate the actual DNA damage that involves formation of DNA strand breaks [68]. While some breaks may be formed during replication of DNA sections containing the primary oxidative lesions (e.g. oxo8dG) the presence of such lesions by themselves can induce persistent replication stress. The persistent replication stress combined with activation of mTOR pathways is considered to be the main mechanism contributing to aging and senescence [22-27,69,70]. Induction of replication stress by arrest in the cell cycle e.g. by upregulation of the CKI p21, with no evidence of actual DNA damage, elevates the level of constitutive DNA damage signaling ("pseudo-DNA damage response") whereas attenuation of this "pseudo-DNA damage response" can be achieved by reduction in mTOR-signaling [29]. Likewise, the cell senescence induced by the replication stress triggered by low doses (1 – 2 nM) of the DNA damaging agent mitoxantrone, that is also accompanied by elevated levels of DNA damage signaling, was shown to be attenuated by the caloric restriction-mimicking drug 2-deoxy-D-glucose [71]. All this evidence collectively indicates that the observed constitutive DNA damage signaling occurs as a response to persistent DNA replication stress. Thus, by reducing the level of DNA damage signaling, as we presently see, metformin appears to alleviate the extent of the persistent DNA replication stress. Since metformin inhibits mTOR pathways, the reduction of replication stress by metformin may not only be mediated by attenuation of the oxidative stress through reduction of ROS, but also may be mediated by its direct inhibitory effect on mTOR [50-53].

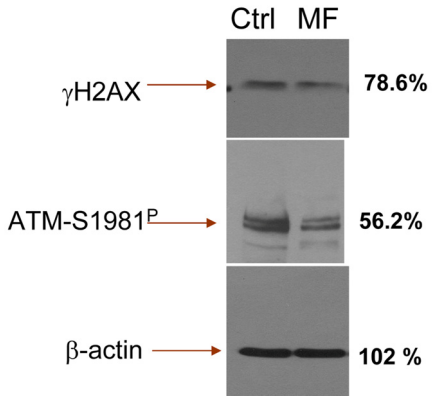

Figure 7. Detection of γH2AX and ATM-S1981^{P} in TK6 cells untreated (Ctrl) and treated with 5 mM metformin (MF) for 48 h, by immunoblotting. The figures on right side of the blot represent the percent intensity of the scanned protein bands of the metformin-treated cells (UN-SCAN-IT gel 6.1) as that of the intensity of the respective protein bands of the untreated (Ctrl) cells.

Our observation that cells exposure to metformin reduces expression of γH2AX and ATM-S1981^{P} remains in contrast to recent data by Vazquez-Martin et al., that show the opposite, namely an activation of ATM and phosphorylation of H2AX in cells treated with metformin [72]. This report prompted us to repeat our experiments numerous times, using a variety of positive and negative controls. Yet in each experiment we observed that treatment of proliferating lymphocytes, TK6 or A549 cells led to a *decline* in expression of γH2AX and ATM-S1981^{P}. We have also tested the A431 epidermoid carcinoma cells used by these authors [72]. The data show that treatment of A431with metformin *decreased* the level of H2AX and ATM phosphorylation (Supplemental data, Figure 1). To exclude the possibility of bias resulting from different methodologies we also assessed the effect of metformin on expression of γH2AX and ATM-S1981^{P} in TK6 cells using immonoblotting, the methodology used by the authors [72]. The results obtained by immunobloting (Figure 7) confirm all our immunocytochemical data (Figs. 1-5) by showing a distinct reduction of γH2AX and ATM-S1981^{P} in cells treated with metformin. In fact, the reduction in expression of ATM-S1981^{P} was nearly 45% related to the control. We have also observed that constitutive

H2AX phosphorylation and ATM activation in quiescent A549 cells, maintained for 5 days at high cells density (>10^6 cells/ml) with no medium change also was reduced by treatment with metformin (Supplemental data Figure 2). The effect of metformin, thus, was unrelated as to whether the cells were in exponential- or stationary- phase of growth. Our data also concur with the findings of Nilsson et al., who did not detect any induction of γH2AX in U2OS or HT1080 cells treated with 40 mM metformin [73]. Actually, careful inspection of their data provides some evidence of a decline in expression of γH2AX upon treatment with metformin [73]. At present we see no explanation for the apparent discrepancy of our results (and the data of Nilsson et al., [73]) versus the data presented by Vazquez-Martin al., [72].

As mentioned, cell aging and senescence appear to be driven by persistent mTOR activation in conjunction with DNA replication stress; the latter can be induced by ROS as well as by inhibition of cell cycle progression, such as activation of CKIs. DNA replication stress and mTOR activation are being reported by the elevated level of constitutive DNA damage signaling ("pseudo-DNA damage response") [29,71]. As shown in the present study, the effectiveness of potential anti-aging factors such as metformin may be tested by monitoring their effect on constitutive DNA damage signaling. This approach offers novel means to assess the anti-aging or aging-promoting properties of different factors suspected of such activities. Assessment of DNA damage signaling may serve to detect both genotoxicity [38,74] as well as genome-protective mechanisms related to attenuation of DNA replication stress.

MATERIALS AND METHODS

Cells, cell treatment. Human lung carcinoma A549 cells, epidermoid carcinoma A431 and lymphoblastoid TK6 cells were obtained from American Type Culture Collection (ATCC CCL-185, Manassas,VA). Human peripheral blood lymphocytes were obtained by venipuncture from healthy volunteers and isolated by density gradient centrifugation. A549 cells were cultured in Ham's F12K, TK6 and lymphocytes were cultured in RPMI 1640 and A431cells in Dulbecco modified Eagle medium, with 2 mM L-glutamine adjusted to contain 1.5 g/L sodium bicarbonate supplemented with 10% fetal bovine serum (GIBCO/Invitrogen, Carlsbad, CA). Adherent A549 and A431 cells were grown in dual-chambered slides (Nunc Lab-Tek II), seeded with 10^5 cells/ml suspended in 2 ml medium per chamber. TK6 cells and lymphocytes were grown in suspension; lymphocyte cultures were treated with the polyvalent mitogen phytohemaglutinin (Sigma /Aldrich; St Louis, MO) as described [75]. During treatment with metformin (1,1-dimethylbiguanide; Calbiochem, La Jolla, CA) the cells were in exponential phase of growth unless indicated otherwise. After exposure to metformin at various concentrations and for specified periods of time (as shown in figure legends) the cells were rinsed with phosphate buffered salt solution (PBS) and fixed in 1% methanol-free formaldehyde (Polysciences, Warrington, PA) for 15 min on ice The cells were then transferred to 70% ethanol and stored at -20 ^{o}C for up to 3 days until staining.

Detection of H2AX phosphorylation and ATM activation. The cells were washed twice in PBS and with 0.1% Triton X-100 (Sigma) in PBS for 15 min and with a 1% (w/v) solution of bovine serum albumin (BSA; Sigma) in PBS for 30 min to suppress nonspecific antibody (Ab) binding. The cells were then incubated in 1% BSA containing a 1:300 dilution of phospho-specific (Ser139) γH2AX mAb (Biolegend, San Diego, CA or with a 1:100 dilution of phospho-specific (Ser1981) ATM mAb (Millipore, Tamecula, CA). The secondary Ab was tagged with AlexaFluor 488 fluorochrome (Invitrogen/Molecular Probes, used at 1:200 dilution). Cellular DNA was counterstained with 28 μg/ml 4,6-diamidino-2-phenylindole (DAPI; Sigma). Each experiment was performed with an IgG control in which cells were labeled only with the secondary AlexaFluor 488 Ab, without primary Ab incubation to estimate the extent of nonspecific adherence of the secondary Ab to the cells. The fixation, rinsing and labeling of A549 or A431 cell was carried out on slides, and lymphocytes and TK6 cells in suspension. Other details have been previously described [38-40].

Analysis of cellular fluorescence. *A549 and A431 cells:* Cellular immunofluorescence representing the binding of the respective phospho-specific Abs as well as the blue emission of DAPI stained DNA was measured with an LSC (iCys; CompuCyte, Westwood, MA) utilizing standard filter settings; fluorescence was excited with 488-nm argon, helium-neon (633 nm) and violet (405 nm) lasers [76]. The intensities of maximal pixel and integrated fluorescence were measured and recorded for each cell. At least 3,000 cells were measured per sample. Gating analysis was carried out as described in Figure legends. *TK6 cells and lymphocytes:* Cellular fluorescence was measured by using a MoFlo XDP (Beckman-Coulter, Brea, CA) high speed flow cytometer/sorter. DAPI fluorescence was excited with the UV laser (355-nm) and AlexaFluor 488 with the argon ion (488-nm) laser.

Protein immonoblotting. Nitrocellulose membrane was blocked with 5% w/v nonfat dry milk in TBST (20 mM TrisHCl, pH 7.4, 150 mM NaCl, 0.05% Tween 20) for 1h at room temperature. The blot was then incubated with the primary antibody either phospho-specific (Ser139) γH2AX mAb (Biolegend) or a phospho-specific (Ser1981) ATM mAb (Millipore) at 1:500 dilution overnight at 4 °C. After three washes in TBST, the blot was incubated with HRP-conjugated goat anti-mouse IgG (Pierce, Rockford, IL) for 1h at room temperature and washed with TBST three times. SuperSignal West Pico chemiluminescence substrate (Pierce) was used for signal production.

CONFLICT OF INTERESTS STATEMENT

The authors of this manuscript have no conflict of interest to declare.

REFERENCES

1. Barzilai A and Yamamoto K: DNA damage responses to oxidative stress. DNA repair (Amst) 2004:3;1109-1115.

2. Nohl H. Generation of superoxide radicals as byproducts of cellular respiration. Ann Biol Clin 1994;52:199-204.

3. Moller P and Loft S. Interventions with antioxidants and nutrients in relation to oxidative DNA damage and repair. Mutat Res 2004;551:79-89.

4. Beckman KB and Ames BN. Oxidative decay of DNA. J Biol Chem 1997;272: 13300-13305.

5. Dianov GL, Parsons JL. Co-ordination of DNA single strand break repair. DNA repair (Amst) 2007;6:454-460.

6. Vilenchik MM and Knudson AG. Endogenous DNA double-strand breaks: Production, fidelity of repair, and induction of cancer. Proc Natl Acad Sci USA 2003;100:12871-12876.

7. Taioli E, Sram RJ, Garte BM, Kalina I, Popov TA and Farmer PB. Effects of polycyclic aromatic hydrocarbons (PAHs) in environmental pollution on exogenous and oxidative DNA damage (EXPAH project): description of the population under study. Mutat Res 2007;620:1-6.

8. Tanaka T, Halicka HD, Traganos F and Darzynkiewicz Z. Phosphorylation of histone H2AX on Ser 139 and activation of ATM during oxidative burst in phorbol ester-treated human leukocytes. Cell Cycle 2006;5:2671-2675.

9. Shacter E, Beecham EJ, Covey JM, Kohn KW and Potter M. Activated neutrophils induce prolonged DNA damage in neighboring cells. Carcinogenesis 1988;9:2297-2304.

10. Chong YC, Heppner GH, Paul LA and Fulton AM. Macrophage-mediated induction of DNA strand breaks in target tumor cells. Cancer Res 1989;49:6652-6657.

11. Demirbag R, Yilmaz R, Kocyigit A and Guzel S. Effect of coronary angiography on oxidative DNA damage observed in circulating lymphocytes. Angiology 2007;58:141-147.

12. Altman SA, Zastawny TH, Randers-Eichorn L, Caciuttolo MA, Akman SA, Disdaroglu M and Rao G. Formation of DNA-protein cross-links in cultured mammalian cells upon treatment with iron ions. Free Radic Biol Med 1995;19:897-902.

13. Cadet J, Delatour T, Douki T, Gasparutto D, Pouget JP, Ravanat JL and Sauvaigo S. Hydroxyl radicals and DNA base damage. Mutat Res 1999;424:9-21.

14. Marnett LJ, Oxy radicals, lipid peroxidation and DNA damage. Toxicology 2002; 219:181-182.

15. Pastwa E and Blasiak J. Non-homologous DNA end joining. Acta Biochim Pol 2003;50:891-908.

16. Jeggo PA and Lobrich M. Artemis links ATM to double strand end rejoining. Cell Cycle 2005;4:359-362.

17. Kryston TB, Georgiev AB, Pissis P, Georgakilas AG. Role of oxidative stress and DNA damage in human carcinogenesis. Mutat Res 2011; Jan7 (Epub)

18. Gorbunova V, Seluanov A. Making ends meet in old age: DSB repair and aging. Mech Ageing Dev 2005;126:621-628.

19. Espejel S, Franco S, Rodriguez-Perales S, Bouffler SD, Cigudosa JC, Blasco MA. Mammalian Ku86 mediates chromosomal fusions and apoptosis caused by critically short telomeres. EMBO J 2002;21:2207-2219.

20. Karanjawala ZE, Lieber MR. DNA damage and aging. Mech Ageing Dev 2004; 125:405-416.

21. Blagosklonny MV. Aging: ROS or TOR. Cell Cycle 2008;7:3344-3354.

22. Blagosklonny MV, Campisi J. Cancer and aging: more puzzles, more promises? Cell Cycle 2008;7:2615-2618.

23. Demidenko ZN, Zubova SG, Bukreeva EI, Pospelov VA, Pospelova TV, Blagosklonny MV. Rapamycin decelerates cellular senescence. Cell Cycle. 2009; 8:1888-1895.

24. Blagosklonny MV. Increasing healthy lifespan by suppressing aging in our lifetime: Preliminary proposal. Cell Cycle 2010;9:4788-4794.

25. Blagosklonny MV. Revisiting the antagonistic pleiotropy theory of aging: TOR-driven program and quasi-program. Cell Cycle. 2010;9:3151-6.

26. Blagosklonny MV. Why human lifespan is rapidly increasing: solving "longevity riddle" with "revealed-slow-aging" hypothesis. Aging. 2010;2:177-182.

27. Blagosklonny MV. Validation of anti-aging drugs by treating age-related diseases. Aging 2009;1:281-288.

28. Pospelova TV, Demidenko ZN, Bukreeva EI, Gudkov VA, Blagosklonny MV. Cell Pseudo-DNA damage response in senescent cells. Cycle 2009;8:4112-4118.

29. Olive PL, Durand RE, Banath JP, Johnston PJ. Analysis of DNA damage in individual cells. Methods Cell Biol 2001;64:235-249.

30. Gorczyca W, Gong J, Darzynkiewicz Z. Detection of DNA strand breaks in individual apoptotic cells by the *in situ* terminal deoxynucleotidyl transferase and nick translation assays. Cancer Res 1993;53:1945-1951.

31. Huang X, Halicka HD, Traganos F, Tanaka T, Kurose A, Darzynkiewicz Z. Cytometric assessment of DNA damage in relation to cell cycle phase and apoptosis. Cell Prolif 2005;38:223-243.

32. Kitagawa R, Kastan MB. The ATM-dependent DNA damage signaling pathway. Cold Spring Harb Symp Quant Biol 2005;70:99-109.

33. Rogakou EP, Pilch DR, Orr AH, Ivanova VS, Bonner WM. DNA double-stranded breaks induce histone H2AX phosphorylation on serine 139. J Biol Chem 1998;273:5858-5868.

34. Bartkova J, Bakkenist CJ, Rajpert-De Meyts E, Skakkebaek NE, Sehested M, Lukas J, Kastan MB, Bartek J. ATM activation in

normal human tissues and testicular cancer. Cell Cycle 2005;4:838-845.

35. Sedelnikova OA, Rogakou EP, Panuytin IG, Bonner W. Quantitive detection of ^{125}IUdr-induced DNA double-strand breaks with γ-H2AX antibody. Ratiation Res 2002;158:486-492.

36. Huang X, Traganos F, Darzynkiewicz Z. DNA damage induced by DNA topoisomerase I- and topoisomerase II- inhibitors detected by histone H2AX phosphorylation in relation to the cell cycle phase and apoptosis. Cell Cycle 2003; 2:614-619.

37. Banath JP, Olive PL. Expression of phosphorylated histone H2AX as a surrogate of cell killing by drugs that create DNA double-strand breaks. Cancer Res 2003; 63:4347-4350.

38. Tanaka T, Huang X, Halicka HD, Zhao H, Traganos F, Albino AP, Dai W, Darzynkiewicz Z. Cytometry of ATM activation and histone H2AX phosphorylation to estimate extent of DNA damage induced by exogenous agents. Cytometry A 2007; 71A:648-661.

39. Tanaka T, Halicka HD, Huang X, Traganos F, Darzynkiewicz Z. Constitutive histone H2AX phosphorylation and ATM activation, the reporters of DNA damage by endogenous oxidants. Cell Cycle 2006;5:1940-1945.

40. Zhao H, Tanaka T, Halicka HD, Traganos F, Zarebski M, Dobrucki J, Darzynkiewicz Z. Cytometric assessment of DNA damage by exogenous and endogenous oxidants reports the aging-related processes. Cytometry A 2007;71A:905-914.

41. Tanaka T, Kajstura M, Halicka HD, Traganos F, Darzynkiewicz Z. Constitutive histone H2AX phosphorylation and ATM activation are strongly amplified during mitogenic stimulation of lymphocytes. Cell Prolif 2007;40:1-13.

42. Tanaka T, Kurose A, Halicka HD, Traganos F, Darzynkiewicz Z. 2-Deoxy-D-glucose reduces the level of constitutive activation of ATM and phosphorylation of histone H2AX. Cell Cycle 2006; 5:878-882.

43. Zhao H, Tanaka T, Mitlitski V, Heeter J, Balazs EA, Darzynkiewicz Z. Protective effect of hyaluronate on oxidative DNA damage in WI-38 and A549 cells. Int J Oncol 2008;32:1159-1169.

44. Halicka HD, Darzynkiewicz Z, Teodori L. Attenuation of constitutive ATM activation and H2AX phosphorylation in human leukemic TK6 cells by their exposure to static magnetic field. Cell Cycle, 2009;8:3236-3238.

45. Halicka HD, Ita M, Tanaka T, Kurose A, Darzynkiewicz Z. The biscoclaurine alkaloid cepharanthine protects DNA in TK6 lymphoblastoid cells from constitutive oxidative damage. Pharmacol Rep 2008;60:93-100.

46. Towler MC, Hardie DG. AMP-activated protein kinase in metabolic control and insulin signaling. Circ Res 2007;100:328-341.

47. Hardie DG. AMP-activated protein kinase: a cellular energy sensor with a key role in metabolic disorders and in cancer. Biochem Soc Trans 2011; 39:1-13.

48. Viollet B, Andreelli F. AMP-activated protein kinase and metabolic control. Handb Exp Pharmacol. 2011; 203:303-330.

49. Carling D, Mayer FV, Sanders MJ, Gamblin SJ. AMP-activated protein kinase: nature's energy sensor. Nat Chem Biol 2011; 7:512-518.

50. Anisimov VN. Metformin for aging and cancer prevention. Aging 2010;2:760-74.

51. Xie Y, Wang Y, Yu L, Hu Q, Ji L, Zhang Y, Liao Q. Metformin promotes progesterone receptor expression via inhibition of mammalian target or rapamycin (mTOR) in endometrial cancer cells. J Ster Biochem Mol Biol 2010; Dec 17 Epub.

52. Shaw RJ, Lamia KA, Vasquez D, Koo SH, Bardeesy N, Depinho RA, Montminy M, Cantley LC. The kinase LKB1 mediates glucose homeostasis in liver and therapeutic effects of metformin. Science 2005;310:1642-1646.

53. Jalving M, Gietema JA, Lefrandt JD, De Jong S, Reyners AKL, Gans ROB, de Vries EGE. Metformin: taking away the candy for cancer? Eur J Cancer 2010; 46:2369-2380.

54. Ouyang J, Parakhia RA, Ochs RS. Metformin activates AMP kinase through inhibition of AMP deaminase. J Biol Chem 2011;286:1-11.

55. Hou X, Song J, Li X-N, Zhang L, Wang XL, Chen L, Shen YH. Metformin reduces intracellular reactive oxygen species levels by upregulating expression of the antioxidant thioredoxin via the AMPK-FOXO3 pathway. Biochem Biophys Res Commun 2010;396:199-205.

56. Anisimov VN, Egormin PA, Piskunova TS, Popovich IG, Tyndyk ML, Yurova MN, Zabezhinski MA, Anikin IV, Karkach AS, Romanyukha AA. Metformin extents life span of HER-2/neu transgenic mice and in combination with melatonin inhibits growth of transplantable tumors. Cell Cycle 2010;9:188-197.

57. Darzynkiewicz Z, Traganos F, Zhao H, Halicka HD, Skommer J, Wlodkowic D. Analysis of individual molecular events of DNA damage response by flow and image-assisted cytometry. Methods Cell Biol 2011;103:115-148.

58. Huang X, Tanaka T, Kurose A, Traganos F, Darzynkiewicz Z. Constitutive histone H2AX phosphorylation on *Ser*-139 in cells untreated by genotoxic agents is cell-cycle phase specific and attenuated by scavenging reactive oxygen species. Int J Oncol 2006;29:495-501.

59. Rothe G, Klouche M. Phagocyte functions. Methods Cell Biol 2004;75:679-708.

60. Graham GG, Punt J, Arora M, Day RO Doogue MP, Duong JK, Furlong JR, Greenfield JR, Greenup LC, Kirkpatrick CM, Ray JE, Timmins P, Williams KM. Clinical pharmacokinetics of metformin. Clin Pharmacokinet 2011;50:81-98.

61. Piwkowska A, Rogacka D, Jankowski M, Dominiczak MH, Stepinski JK, Angielski S. Metformin induces suppression of NAD(P)H oxidase activity in podocytes. Biochem Biophys Res Commun 2010; 393:268-273.

62. Ouslimani, N.; Peynet, J.; Bonnefont-Rousselot, D.; Therond, P.; Legrand, A.; Beaudeux, J. L. Metformin decreases intracellular production of reactive oxygen species in aortic endothelial cells. Metabolism 2005;54:829–834.

63. Kane DA, Andersen EJ, Price III JW, Woodlief TL, Lin C-T, Bikman BT, Cortright RN, Neufer PD. Metformin selectively attenuates mitochondrial H_2O_2 emission without affecting respiratory capacity in skeletal muscle of obese rats. Free Radical Biol Med 2010;49:1082-1087.

64. Piro S, Rabuazzo AM, Renis M, Purello F. Effects of metformin on oxidative stress, adenine nucleotides balance and glucose-induced insulin release impaired by chronic FFA exposure in rat pancreatic islets. J Endocrinol Invest 2011 Jul 12 (Epub).

65. Bellin, C, de Wiza DH, Wiernsperger NF, Rosen P. Generation of reactive oxygen species by endothelial and smooth muscle cells: Influence of hyperglycemia and metformin. Horm Metab Res 2006;38:732-739.

66. Brunmair B, Staniek K, Gras F, Scharf N, Althaym A, Clara R, Roden M, Gnaiger E, Hohl H, Waldhansl W, Furnassin C. Thiazolidinediones, like metformin, inhibit respiratory complex I. A common mechanism contributing to their antidiabetic action. Diabetes 2004;53:1052-1059.

67. Drose S, Hanley PJ, Brandt U. Ambivalent effects of diazoxide on mitochondrial ROS production at respiratory chain complexes I and II. Biochim Biophys Acta 2009;1790:558-565.

68. Cleaver JA, Feeney L, Revet I. Phosphorylated H2Ax is not an unambiguous marker of DNA double strand breaks. Cell Cycle 2011;10:3223-3224.

69. Burhans WC, Weinberger M. DNA replication stress, genome instability and aging. Nucleic Acids Res 2007;33:7545-7556.

70. Bartkova J, Hamerlik P, Stockhausen MT, Ehrman J, Hlobikova A, Laursen H, Kalita O, Kolar Z, Paulsen HS, Broholm H, Lukas J, Bartek J. Replication stress and oxidative damage contributes to aberrant constitutive activation of DNA damage signaling in human gliomas. Oncogene 2010;29:5095-5102.

71. Zhao H, Halicka HD, Jorgensen E, Traganos F, Darzynkiewicz Z. New biomarkers probing the depth of cell senescence assessed by laser scanning cytometry. Cytometry A, 2010, 77A, 999-1007.

72. Vazquez-Martin A, Oliveras-Ferraros C, Cufi S, Martin-Castillo B, Menendez Ja. Metformin activates an Ataxia Telangiectasia Mutated (ATM)/Chk2-regulated DNA damage-like response. Cell Cycle 2011;10:1499-1501.

73. Nilsson S, Huelsenbeck J, Fritz G. Mevalonate pathway inhibitors affect anticancer drug-induced cell death and DNA damage response of human sarcoma cells. Cancer Lett 2011;304:60-69.

74. Smart DJ, Ahmedi KP, Harvey JS, Lynch AM. Genotoxicity screening via the γH2AX by flow assay. Mutat Res 2011;71:21-31

75. Kajstura M, Halicka HD, Pryjma J, Darzynkiewicz Z. Discontinuous fragmentation of nuclear DNA during apoptosis revealed by discrete "sub-G_1" peaks on DNA content histograms.Cytometry A 2007; 71A:125-131.

76. Pozarowski P, Holden E, Darzynkiewicz Z. Laser scanning cytometry: Principles and applications. Meth Molec Biol. 2006; 319:165-192.

SUPPLEMENTARY FIGURES

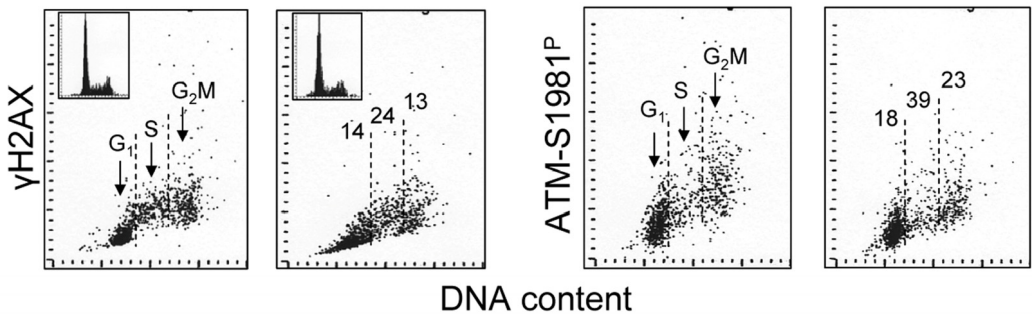

Supplemental Figure 1. Effect of metformin (MF) on the level of constitutive expression of γH2AX and ATM-S1981P in A431 cells. Exponentially growing A431 cells were left untreated (Ctrl) or treated with 5 mM metformin for 48 h. γH2AX and ATM-S1981 immunofluorescence (IF) was detected with the phospho-specific Abs and cells fluorescence was measured by laser scanning cytometry.[75] Based on differences in DNA content the cells were gated in G_1, S and G_2M phases of the cell cycle and the mean values of γH2AX and ATM-S1981^P IF for cells in each of these cell cycle phases by were obtained gating analysis. The percent reduction of these mean values of the metformin-treated related to the untreated (Ctrl) cells is shown in the respective panels (the means of the three separate bands per each protein). The insets show DNA content frequency histograms in the untreated and metformin-treated cultures.

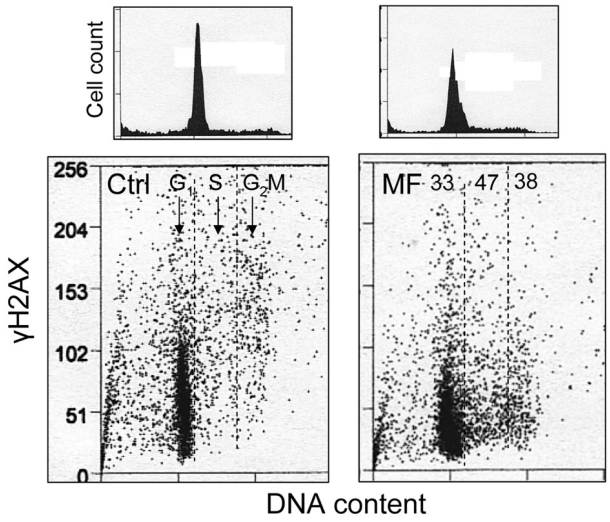

Supplemental Figure 2. Effect of metformin (MF) on the level of expression of γH2AX in TK6 cells in stationary cultures. TK6 cells were maintained at high cell density (>10^6 cells/ml) with no medium change for 5 days, then cells were left untreated (Ctrl) or treated with 5 mM metformin for 24 h (MF) . The percent decline in mean values of γH2AX IF of cells in G_1, S, and G_2M phases of the cycle in the metformin-treated culture is shown in the MF panel.

Commentary

Be quiet and you'll keep young: does mTOR underlie p53 action in protecting against senescence by favoring quiescence?

Vjekoslav Dulic

Institut de Génétique Moléculaire de Montpellier UMR 5535 CNRS-Université Montpellier 1 et 2, 34293 Montpellier, Cedex 5, France

Commentary on: *O Leontieva and M Blagosklonny. DNA damaging agents and p53 do not cause senescence in quiescent cells, while consecutive re-activation of mTOR is associated with conversion to senescence. Aging. 2010; 12:924-935.*

Received: *1/9/11; Accepted: 1/12/11; Published: 1/11/12* doi:10.18632/aging.100257

Corresponding to: *vjekoslav.dulic@igmm.cnrs.fr*

Cancer is a multi-step process that involves abrogation of several barriers to uncontrolled proliferation [1]. These barriers include checkpoints that, by activating inhibitory pathways, block cell division either reversibly (quiescence) or irreversibly (senescence, apoptosis). Typically, confluence and the absence of mitogens or nutrients induce quiescence, while cell ageing, inappropriate signaling or irreparable DNA damage lead to senescence, which is characterized by a large and flat cell morphology and expression of specific biomarkers. Cell cycle arrest requires inhibition of cyclin-dependent kinases (CDK), that drive division by both activating diverse regulators involved in replication and mitosis and by inactivating pRb pocket protein family members. While pocket proteins are essential for both quiescence and senescence [2], p53, another tumor suppressor, has been thought to play a key role in senescence, mainly by inducing the CDK inhibitor $p21^{Waf1,Cip1,Sdi1}$ (p21), which permanently blocks cell cycle progression [3]. On the other hand, although clearly involved [4], the role of p53 in quiescence is probably not essential, as this cell cycle arrest is mostly mediated by $p27^{Kip1}$ (p27), a CDK inhibitor whose levels are not controlled by p53 [5]. Consistent with this, both serum deprivation and confluence could efficiently induce quiescence in human fibroblasts expressing the HPV16-E6 viral oncogene, which degrades p53 [6].

The straightforward role p53 in senescence has recently been challenged by Blagosklonny and colleagues, who propose that p53 is primarily a suppressor of the senescent phenotype rather than its "inducer" [7]. In agreement with growing evidence that p53 is involved in cell metabolism [4], they suggest that its another function would be to inhibit mTOR-dependent cell growth in size, thus inducing quiescence by precluding the onset of senescence. Consequently, senescence would occur in situations when the conditions for quiescence are not met and when p53 fails to suppress the mTOR pathway. This exciting but rather heretic hypothesis was based on initial observations showing that senescent phenotype requires cell growth [8, 9] and that, unlike ectopic p21 expression or DNA damage by doxorubicin, p53 induction caused quiescence instead of senescence in some cells [10]. By ingeniously using a cell line in which p21 is expressed from an inducible promoter and Nutlin-3A, an Mdm2 inhibitor and potent p53 stabilizer, they showed that over-expression or stabilization of p53, prevented p21-induced senescence and instead caused quiescence. Moreover, p53 induction could "convert" p21- or oxidative stress-induced senescence into quiescence. The principal target of p53 in this case is the mTOR pathway, which plays a central role in cell size growth, as its inhibition both by nutlin 3A and rapamycin (a classical mTOR inhibitor) favours quiescence over senescence [7, 11-13].

These results led to a testable hypothesis predicting that quiescence (i.e., inactive mTOR) would also prevent senescence caused by genotoxic agents. Indeed, Leontieva and Blagosklonny now show [14] that after serum-deprived or rapamycin-treated normal fibroblasts or epithelial cells have been exposed to etoposide, its removal, concomitant with serum addition, enables proliferation, indicating that quiescence compromised

the onset of the senescence program. In contrast, in the continuous presence of etoposide, serum addition induced senescence, presumably by activating mTOR. Importantly, the authors showed that neither serum deprivation nor rapamycin prevented p21 induction, while the presence of DNA damage was documented by the comet assay. Lastly, they showed that, serum-deprivation prevented Nutlin 3A-induced a large, flat senescent morphology in some cancer cell lines.

Taken at face value, these results are intriguing and support the initial hypothesis. However, many questions remained unanswered. In particular, why were checkpoints not activated once cells entered the cell cycle upon serum addition (one imagines that the DNA damage caused by etoposide had not been repaired)? A possible explanation would be that truly quiescent cells were not (strongly) damaged while those that were not entirely arrested were. It is also not clear how the cells got rid of high p21 levels as they resumed cycling. Another question concerns the role of p27 in p53-induced reversible arrest. This is a highly relevant point, as mTOR inhibition blocks Akt/GSK-3-mediated p27 phosphorylation and cytoplasmic localization and leads to nuclear accumulation of p27 [15]. p27-dependent CDK inactivation together with cyclin D1 down-regulation could drive reversible cell cycle arrest together with p21 induction. Re-activation of mTOR (by serum addition) would revert this process enabling cell cycle entry, probably by degrading p27 (and p21).

The most important contribution of this and previous work is that p53 can no longer be regarded as a *bona fide* "senescence inducer" and that its role is mainly to block cell division (by stimulating p21), thus permitting the onset of senescence program under appropriate conditions [7]. In agreement with this, we showed earlier that, while in ageing human fibroblasts HPV16-E6-dependent p53 degradation failed to block DNA replication and formation of SAHFs (senescence-associated heterochromatin foci, [16]), low p53 levels did not prevent cell growth and led to a flat cell phenotype, which is also observed in senescing p21 KO MEFs [6]. Thus, senescence morphology could be uncoupled from the cell cycle arrest, which fits with the model proposed by Blagosklonny and his co-workers.

REFERENCES

1. Hanahan D and Weinberg RA. The hallmarks of cancer. Cell. 2000; 100:57-70.

2. Sage J et al. Targeted disruption of the three Rb-related genes leads to loss of G(1) control and immortalization. Genes Dev. 2000; 14:3037-3050.

3. Herbig U et al. Telomere shortening triggers senescence of human cells through a pathway involving ATM, p53, and p21(CIP1), but not p16(INK4a). Mol Cell. 2004; 14:501-513.

4. Vousden KH and Ryan KM. p53 and metabolism. Nat Rev Cancer. 2009; 9:691-700.

5. Sherr CJ and Roberts JM CDK inhibitors: positive and negative regulators of G1-phase progression. Genes Dev. 1999; 13:1501-1512.

6. Dulic V et al. Uncoupling between phenotypic senescence and cell cycle arrest in aging p21-deficient fibroblasts. Mol Cell Biol. 2000; 20:6741-6754.

7. Demidenko ZN et al. Paradoxical suppression of cellular senescence by p53. Proc Natl Acad Sci U S A. 2010.;107:9660-9664.

8. Blagosklonny MV. Cell senescence and hypermitogenic arrest. EMBO Rep, 2003; 4:358-362.

9. Demidenko ZN and Blagosklonny MV Growth stimulation leads to cellular senescence when the cell cycle is blocked. Cell Cycle. 2008; 7:3355-33561.

10. Korotchkina LG et al. Cellular quiescence caused by the Mdm2 inhibitor nutlin-3A. Cell Cycle. 2009; 8:3777-3781.

11. Demidenko ZN and Blagosklonny MV. At concentrations that inhibit mTOR, resveratrol suppresses cellular senescence. Cell Cycle. 2009; 8:1901-1904.

12. Korotchkina LG et al. The choice between p53-induced senescence and quiescence is determined in part by the mTOR pathway. Aging. 2010; 2:344-352.

13. Maki CG. Decision-making by p53 and mTOR. Aging. 2010; 2:324-326.

14. Leontieva OV and Blagosklonny MV. DNA damaging agents and p53 do not cause senescence in quiescent cells, while consecutive re-activation of mTOR is associated with conversion to senescence. Aging, 2010; 2:924-935.

15. Toker A. mTOR and Akt signaling in cancer: SGK cycles in. Mol Cell. 2008; 31:6-8.

16. Narita M et al. Rb-mediated heterochromatin formation and silencing of E2F target genes during cellular senescence. Cell. 2003; 113:703-716.

www.aging-us.com AGING 2010, Vol. 2, No. 12

Research Paper

DNA damaging agents and p53 do not cause senescence in quiescent cells, while consecutive re-activation of mTOR is associated with conversion to senescence

Olga V. Leontieva and Mikhail V. Blagosklonny

Department of Cell Stress Biology, Roswell Park Cancer Institute, BLSC, L3-312, Elm and Carlton Streets, Buffalo, NY, 14263, USA

Received: *11/18/10; Accepted: 12/31/10; Published: 12/31/10* doi:10.18632/aging.100265
Keywords: *p53, DNA damage, senescence, quiescence, rapamycin, mTOR*
Correspondence *Mikhail V. Blagosklonny MD, PhD to blagosklonny@oncotarget.com*

Abstract: When the cell cycle is arrested, growth-promoting pathways such as mTOR (Target of Rapamycin) drive cellular senescence, characterized by cellular hyper-activation, hypertrophy and permanent loss of the proliferative potential. While arresting cell cycle, p53 (under certain conditions) can inhibit the mTOR pathway. Senescence occurs when p53 fails to inhibit mTOR. Low concentrations of DNA-damaging drugs induce p53 at levels that do not inhibit mTOR, thus causing senescence. In quiescence caused by serum starvation, mTOR is deactivated. This predicts that induction of p53 will not cause senescence in such quiescent cells. Here we tested this prediction. In proliferating normal cells, etoposide caused senescence (cells could not resume proliferation after removal of etoposide). Serum starvation prevented induction of senescence, but not of p53, by etoposide. When etoposide was removed, such cells resumed proliferation upon addition of serum. Also, doxorubicin did not cause senescent morphology in the absence of serum. Re-addition of serum caused mTOR-dependent senescence in the presence of etoposide or doxorubicin. Also, serum-starvation prevented senescent morphology caused by nutlin-3a in MCF-7 and Mel-10 cells. We conclude that induction of p53 does not activate the senescence program in quiescent cells. In cells with induced p53, re-activation of mTOR by serum stimulation causes senescence, as an equivalent of cellular growth.

INTRODUCTION

Serum growth factors (GF) activate the GF-sensing network, which turns on both cell cycle progression and the mTOR pathway, which in turn stimulates cellular growth in size [1-5]. While growing in size, cells progress through the cell cycle and divide. Thus, in proliferating cells, cellular growth is balanced with cell division.

In normal cells, serum withdrawal both arrests the cell cycle early in G1, also known as G0 and deactivates mTOR. Cells become quiescent: they neither grow in size nor progress through the cell cycle. In contrast, cellular senescence is characterized by cellular hypertrophy (large and flat cell morphology), hypersecretory phenotype, beta-Gal-staining and permanent loss of proliferative potential [6-8]. Cellular senescence is not caused by serum GF withdrawal, but by stresses and oncogenic/mitogenic hyper-stimulation [9-15]. While not inhibiting mTOR, these stimuli incite responses blocking cell cycle.

In theory, if the cell cycle is blocked, while serum continues to activate GF-sensing pathways, cells will senesce [16, 17]. For example, p21 causes cell cycle arrest without inhibiting mTOR, and thus causes senescence. Deactivation of mTOR by rapamycin prevented p21-induced senescence, converting p21-induced arrest into quiescence [18-20].

The tumor suppressor p53 inhibits the mTOR pathway upstream [21-24] and downstream [25, 26] of mTOR. While inhibiting mTOR, p53 suppressed p21-induced

senescence, causing quiescence instead [27]. p53 affects autophagy and metabolic pathways not only via inhibition of mTOR but also probably independently from mTOR [22,28-35]. We use the term mTOR-centric network to encompass not only upstream and downstream but also parallel and TOR-like pathways [36].

p53 can both induce and suppress cellular senescence [37]. First, p53 causes cell cycle arrest, a prerequisite of senescence. Second, p53 inhibits mTOR-centric network and this can prevent senescence, causing quiescence instead. In cell lines with overactivated mTOR, p53 causes senescence [37]. Similarly, "weak" p53 that is not able to inhibit mTOR causes senescence simply by arresting the cell cycle [38]. In other words, p53 causes senescence passively by failing to suppress the senescence program (which in part depends on mTOR), while still causing cell cycle arrest. This model suggests that cell cycle arrest is the only mechanism of how p53 causes senescence. This predicts that induction of p53 will not cause senescence in quiescent cells, since in quiescent cells mTOR is already inhibited. Here we tested this hypothesis.

RESULTS

Induction of p53 by etoposide in quiescent cells has little consequence

As we recently demonstrated, unlike nutlin-3a (an Mdm-2 antagonist), low concentrations of doxorubicin (DOX), a DNA damaging drug (DDD), caused senescent morphology in WI-38t cells [38]. Nutlin-3a causes cell cycle arrest solely by inducing p53, which in turn can inhibit the mTOR pathway. DOX causes cell cycle arrest at concentrations that induce p53 not high enough to inhibit mTOR. Therefore, DOX caused senescence as was determined by senescent morphology [38]. However, DOX is not washable and we could not check whether the condition was irreversible. Here we used etoposide, a DDD that could be washed out. We treated WI-38t cells with either etoposide or nutlin-3a. After 4 days, cells were washed and re-plated without drugs (Figure 1A). After 6 days, the number of nutlin-treated cells increased ~26 fold, whereas etoposide-treated cells could not proliferate (Figure 1A). In parallel, cells were treated with nutlin-3a and etoposide in the presence of rapamycin (Figure 1B). Rapamycin

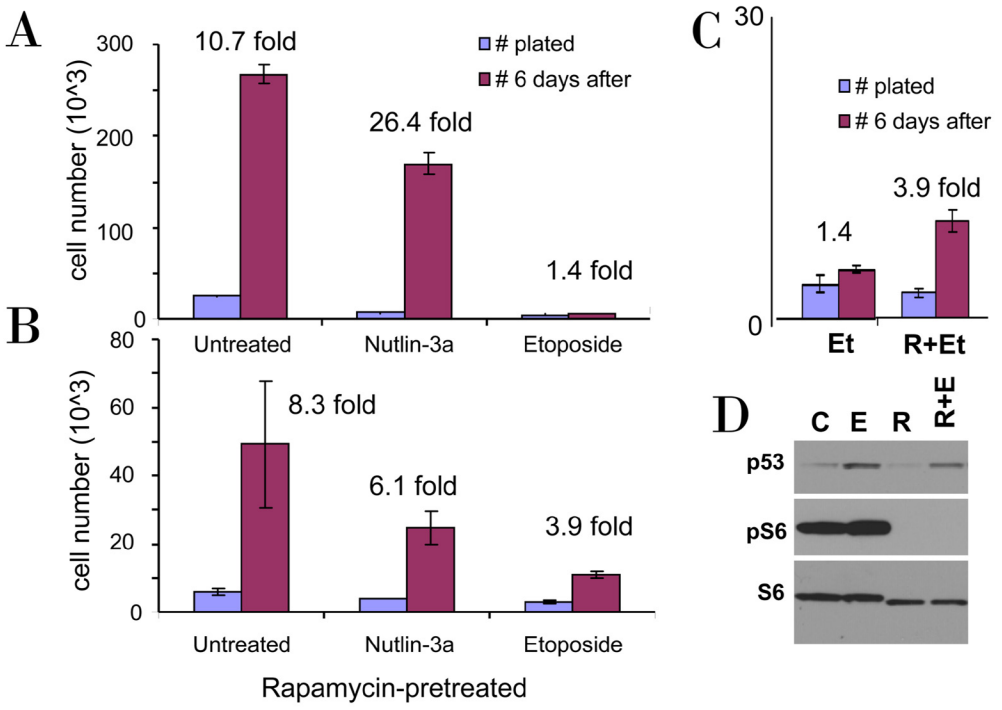

Figure 1. Rapamycin pretreatment prevents loss of proliferative potential during etoposide treatment. A-C. WI-38t cells were plated at 10000 cells/well in 24-well plates, and the next day were either left untreated (**A**) or pretreated with 10 nM Rapamycin (**B**). The next day, cells were treated with either 2.5 μM nutlin-3a or 1 μg/ml etoposide or left untreated. After 4 days, cells were trypsinized and 10% of cells were plated in fresh drug-free medium (blue bars). 6 days later cells were counted (red bars). In **C** the results for etoposide treatment (Et) with or without rapamycin (R) pretreatment are shown in the same scale. (**D**) Cells were lysed after 24 hr treatment with etoposide (E), rapamycin (R), or both (R+E) and immunoblot was performed.

partially sustained the proliferative potential (PP) in etoposide-treated cells. Direct comparison of the proliferative potential of WI-38t cells treated with etoposide in the absence or presence of rapamycin is shown in Figure 1C. Etoposide did not inhibit mTOR and inhibition of mTOR by rapamycin-pretreatment (Figure 1D) favored quiescence over senescence (Figure 1C).

We further investigated effects of etoposide in cells treated by either rapamycin or serum starvation as depicted in Figure 2. Exposure of WI-38t cells to either rapamycin or serum starvation resulted in a lean cellular morphology, a characteristic of quiescence (Figure 3A, left column). Treatment of proliferating WI-38t cells with etoposide caused senescent morphology (Figure 3A, top right panel). Senescent morphology was partially preventable by rapamycin and serum-starvation: most cells were lean and thin (Figure 3A, right column). Rapamycin did not inhibit proliferation completely but rather slowed it down (Figure 3B). In

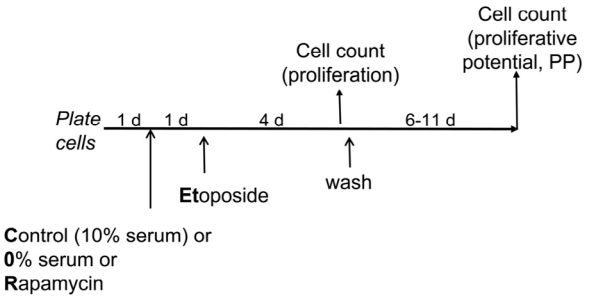

Figure 2. Experimental schema: transient induction of p53 in proliferating versus quiescent cells. Cells are treated (or left untreated) under different condi-tions [control (10% serum), 0% serum or rapamycin] with etoposide for 4 days. Cells are counted twice: 1) at the time of etoposide removal to measure inhibition of proliferation and 2) 6-11 days after wash to measure proliferative potential (PP). PP should not be confused with proliferation. Thus, rapamycin and 0% serum inhibit proliferation but preserve (increase) proliferative potential in etoposide-treated cells.

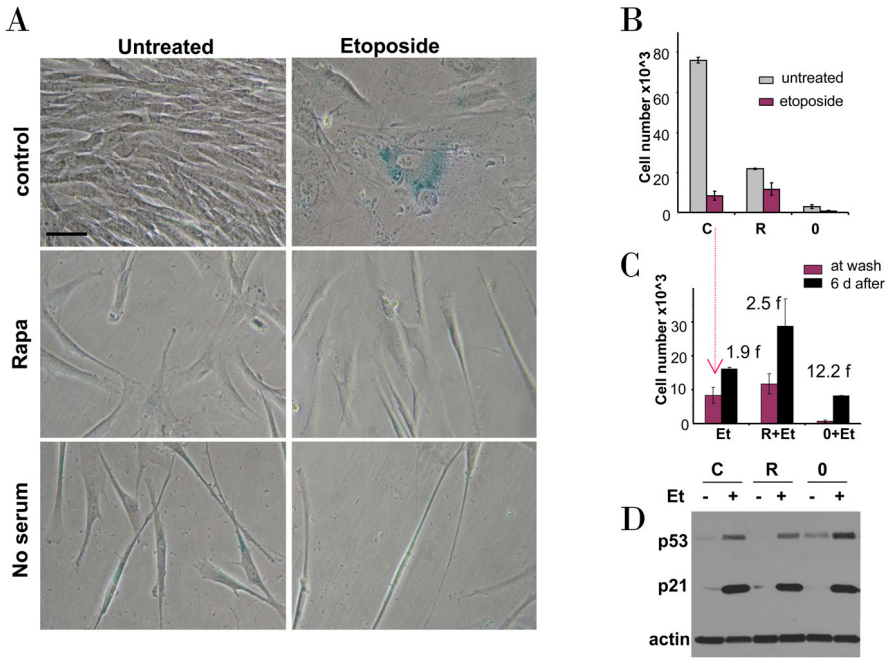

Figure 3. Effects of rapamycin and serum starvation on etoposide-induced senescence in WI-38t cells. A-C. WI-38t cells were plated at 5000/well in 12 well plates, and the next day either treated with 10 nM rapamycin in complete medium (R), or placed in serum-free medium (no serum or 0), or left in complete medium (control)**.** The next day, 1 μg/ml etoposide (Et) was added, as indicated.

A. After 4 days, cells were stained for beta-Gal and microphotographed (bar - 50 micron)

B. After 4 days, cells were counted: control (C), rapamycin (R), no serum(0).

C. Proliferative potential. In replicate plates, cells were washed and incubated in complete, drug-free medium for 6 days and then counted **(**black bars). Note: red bars correspond to red bars in panel B. Fold (f) increase in a cell number after drug removal.

D. Immunoblot. Cells were plated in 6 well plates. The next day, cells were treated with 1 μg/ml etoposide (Et) for 24 hrs: control –C, rapamycin – R, no serum -0.

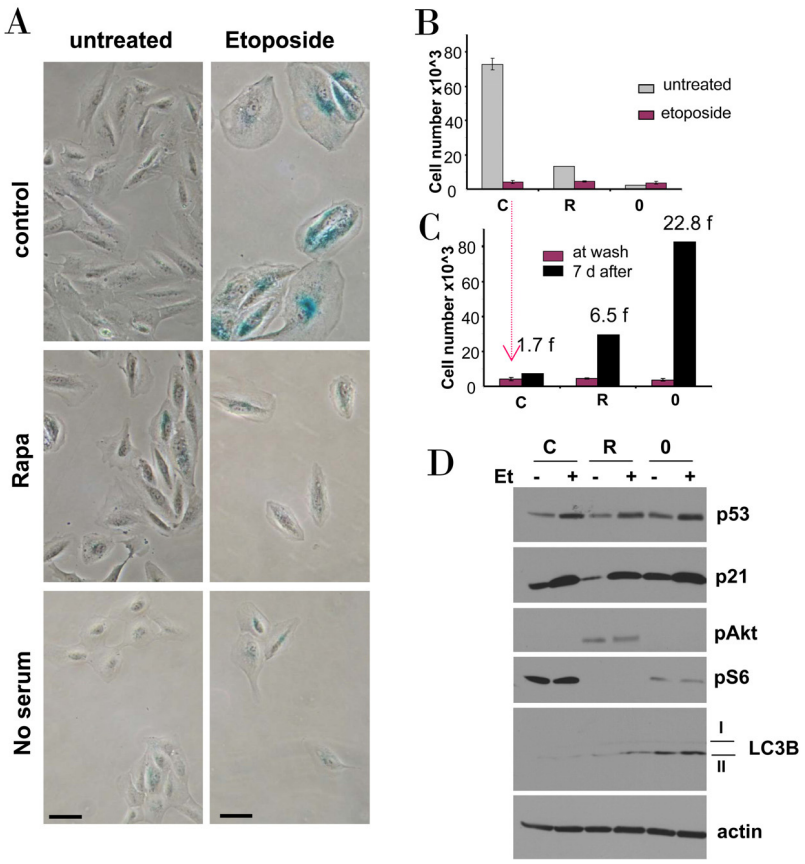

Figure 4. Effects of rapamycin and serum starvation on etoposide-induced senescence in RPE cells.

A-C. RPE cells were plated at 5000/well in 12 well plates, and the next day either treated with 10 nM rapamycin in complete medium (R), or placed in serum-free medium (no serum or 0), or left in complete medium (control)**.** The next day, 0.5 μg/ml etoposide (Et) was added, as indicated.

A. After 4 days, cells were stained for beta-Gal and micro-photographed (bar - 50 micron)

B. After 4 days, cells were counted: control (C), rapamycin (R),no serum (0).

C. Proliferative potential. In replicate plates, cells were washed and incubated in complete, drug-free medium for 6 days and then counted **(**black bars). Note: red bars corre-spond to red bars in panel B. Fold (f) increase in a cell number after drug removal.

D. Immunoblot. Cells were plated in 6 well plates. The next day, cells were treated with 0.5 μg/ml etoposide (Et) for 24 hrs: control –C, rapamycin – R, no serum -0.

agreement with similar experiment (Figure 1C), rapamycin partially prevented loss of proliferative potential caused by etoposide (Figure 3C). Serum starvation preserved proliferative potential (PP) in etoposide-treated cells (Figure 3C). Etoposide induced p53 in serum-starved cells even stronger than in control (proliferating) cells (Figure 3D). So the failure to initiate senescence could not be explained by lack of p53 induction.

We next investigated etoposide-induced senescence in normal retinal pigment epithelial (RPE) cells. Etoposide caused senescent morphology in RPE cells (Figure 4A). Pretreatment with rapamycin and serum-starvation partially prevented senescent morphology caused by etoposide. The senescent morphology was associated with permanent loss of proliferative potential: cells could not resume proliferation, when etoposide was removed (Figure 4B, C). In rapamycin-pretreated cells and, especially, in serum-starved cells, etoposide-induced arrest was partially reversible. Both rapamycin and serum starvation inactivated the mTOR pathway, as measured by a decrease of S6 phosphorylation (Figure 4D), but did not prevent p53 and p21 induction by etoposide (Figure 4D). Noteworthy, rapamycin activated Akt (Figure 4D). Serum-starvation was more effective than rapamycin in preventing etoposide-induced senescence. This suggests that mTOR pathway is not the only pro-senescent pathway and that is why rapamycin was less effective than serum-starvation in preventing senescence. As an example, compared with rapamycin, serum starvation was a more potent inducer of autophagy as judged by accumulation of LC3B-II (Figure 4D).

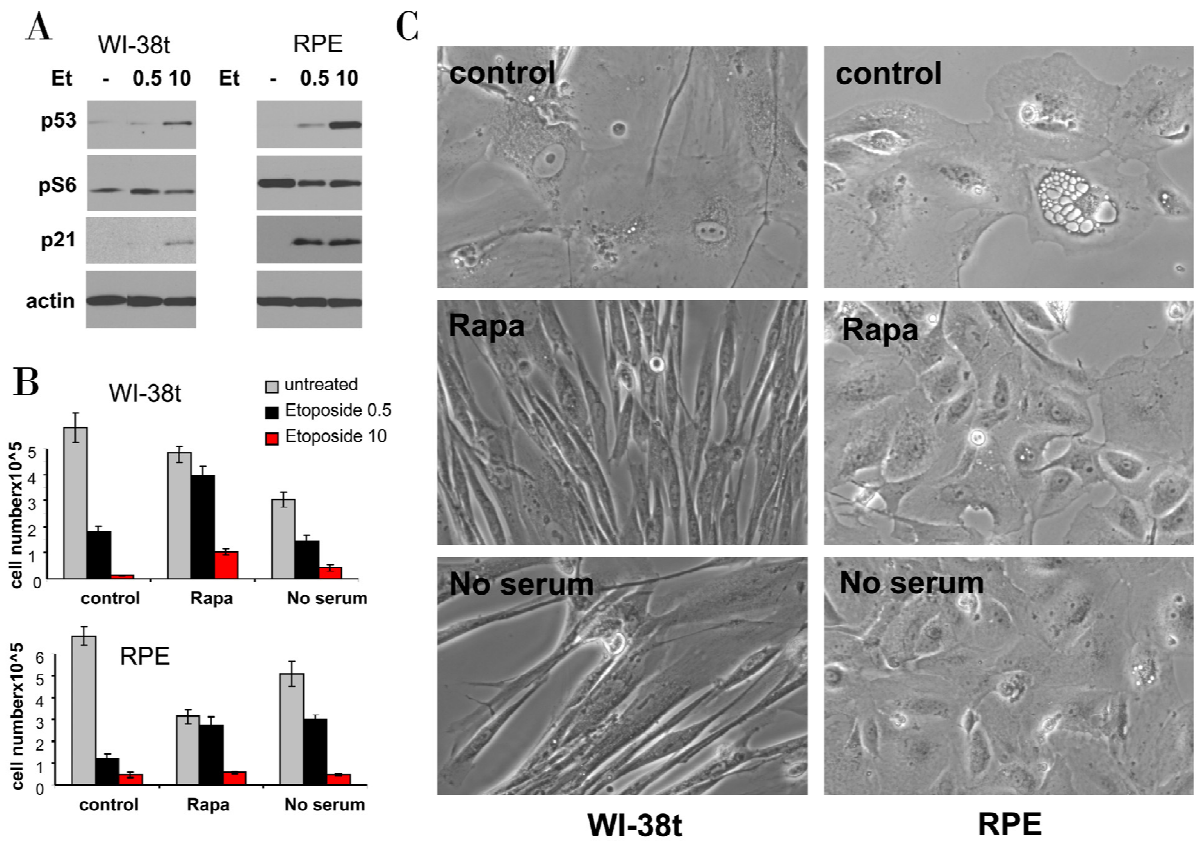

Figure 5. Effects of rapamycin and serum starvation on senescence caused by a higher concentration of etoposide.
A. Immunoblot: WI-38t and RPE cells were treated with 0.5 μg/ml and 10 μg/ml etoposide (Et) or left untreated (-). The next day, cells were lysed and immunoblot was performed.
B-C: WI-38t and RPE cells were plated at 25000/well in 12 well plates, the next day cells were either pretreated with 10 nM rapamycin (Rapa), placed in serum free medium (no serum) or left in complete medium with 10% serum (control). The next day, 0.5 μg/ml and 10 μg/ml etoposide (Et) was added: in complete medium (control) or with 10 nM Rapamycin (Rapa) or in serum free medium (no serum). After 5 days, cells were washed and cultured in fresh, drug free medium for 11 days and then trypsinized and counted. (in panel C): Before trypsinization, cells treated with 10 μg/ml etoposide (under three conditions: control, Rapa and no serum) were microphotographed.

Effects of higher concentrations of etoposide

We next investigated whether higher etoposide concentrations and durations of treatment convert quiescence into senescence. Like 0.5 μg/ml, 10 μg/ml etoposide did not inhibit mTOR (Figure 5A) and thus caused senescent morphology and loss of proliferative potential (Figure 5B, C). In WI-38t cells, rapamycin pretreatment partially preserved proliferative potential in both concentrations of etoposide (Figure 5B). Serum-starvation was insignificantly effective probably due to its toxicity during a 6-day treatment. At the time of cell count (Figure 5B), WI-38t cells treated with etoposide alone retained senescent morphology, whereas co-treatment with rapamycin and serum starvation (no serum) abrogated senescent morphology (Figure 5C). In RPE cells, which are more sensitive to etoposide, rapamycin and serum-starvation significantly preserved proliferative potential of cells treated with 0.5 μg/ml but not 10 μg/ml etoposide (Figure 5B). Still these co-treatments abolished senescent morphology otherwise caused by 10 μg/ml etoposide (Figure 5C).

Conversion from quiescence to senescence

Using the schema depicted in Figure 6, we next investigated the effect of re-addition of serum to cells treated with DDD in serum-free medium without removal of the drug. In WI-38t cells, addition of serum caused phosphorylation of Akt, Erk and S6 and also induced cyclins D1 and E (Figure 7A). When stimulated with serum, these etoposide-arrested cells acquired senescent

morphology (Figure 7B). Thus senescence was characterized by activated mTOR-centric pathways and elevated cyclins D1 and E. Rapamycin prevented S6 phosphorylation (downstream of mTOR), but not phosphorylation of Akt and Erk, which are upstream of mTOR. Simultaneously it diminished senescent morphology, so that most cells remained lean (Figure 7B). Similar results were obtained when cells were blocked with doxorubicin (Figure 8). Re-addition of serum caused senescence instead of proliferation (Figure 8). Similarly, in etoposide- or doxorubicin- blocked RPE cells, serum stimulation caused activation of mTOR (Figure 9A) and senescent morphology (Figure 9 and 10).

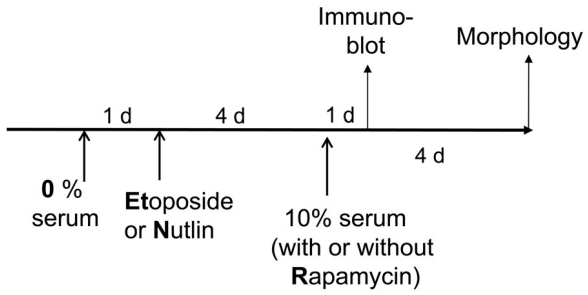

Figure 6. Schema. Serum stimulation of quiescent cells locked by p53.

Conversion between nutlin-induced quiescence and senescence in cancer cells

Whereas nutlin-3a causes quiescence in WI-38t and RPE cells, it causes senescence in some cancer cell lines with high mTOR activity. For example, nutlin-3a did not block phosphorylation of S6 and caused senescence in Mel-10 cells. As we have shown, senescence was preventable by rapamycin [37]. The advantage of the nutlin-based model is that nutlin-3a does not cause DNA damage. Although serum-starvation did not cause genuine quiescence in cancer cells, serum starvation still prevented typical senescent morphology during treatment with nutlin-3a. Mel-10 cells remained slim, when were treated with nutlin-3a in serum-free medium. The cells were beta-gal positive (Figure 11A), because serum starvation alone may cause beta-gal staining. Serum-starvation by itself did not decrease p-S6 by day 1 (Figure 11B), there was a noticeable decrease in phosphorylation of S6 in nutlin-treated cells maintained in a serum-free medium (Figure 11B). Re-addition of serum converted lean morphology into typical senescent phenotype (Figure 11C). In MCF-7 cells, nutlin-3a also induced senescent morphology (Figure 12A) and in agreement did not inhibit S6 phosphorylation (Figure 12C). However, non-proliferating senescent cells co-existed with still proliferating cells, which formed colonies with non-senescent morphology. (Notably, higher concentration of nutlin-3a caused cell death, data not shown). Serum starvation slowed down proliferation of MCF-7 cells (Figure. 12B). Induction of p53 in serum-starved cells by nulin-3a caused rapid and massive cell death (Figure 12A, lower panel). Nutlin-3a induced especially high levels of p53 in serum-starved cells (Fig 12C). This can explain both inhibition of p-S6 and cell death, according to the recent model [38].

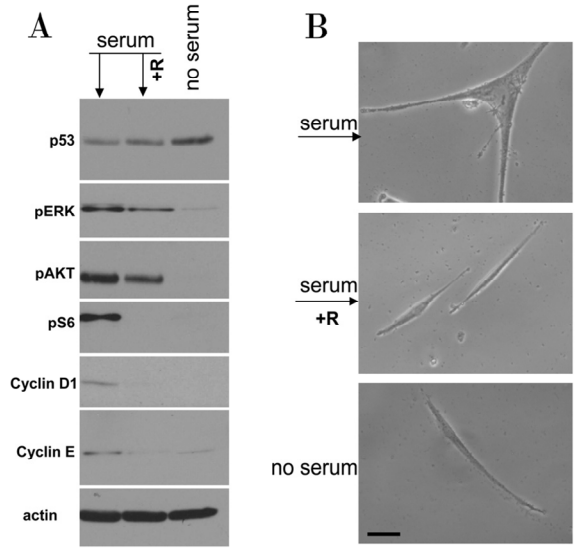

Figure 7. Serum stimulation of etoposide-locked WI-38t cells results in mTOR-dependent sensecence.
A-B. WI38t cells were treated with 1μg/ml etoposide in the absence of serum as shown in Figure 6. Then, 10% serum was added either with 10 nM rapamycin (+R) or alone. No serum indicates that cells were continuously incubated with etoposide in serum free medium. 24 h after serum stimulation, cells were lysed and subjected to immuno-blotting as indicated (**A**). 4 days after serum stimulation cells were microphotographed (**B**).

We also utilized rapamycin, which abrogated S6 phosphorylation, while did not prevent p53 induction by nutlin-3a (Figure 12C). In rapamycin-pretreated MCF-7 cells, nutlin-3a did not cause morphological senescence (Figure 12A). In other words, senescence was converted into quiescence. Unlike senescent cells, quiescent cells were not morphologically distinct from proliferating cells. So after treatment with nutlin-3a plus rapamycin, there could be a mixture of

proliferating and quiescent cells. Therefore, in order to link the morphology to the proliferative potential of arrested cells, we needed to selectively eliminate proliferating cells first. This task unexpectedly merged with our investigation of drug combinations that could protect cells with wt p53 from the toxicity of chemotherapy. Using this approach, we demonstrated that rapamycin converted nutlin-induced senescence into quiescence in MCF-7 cells (MS in preparation).

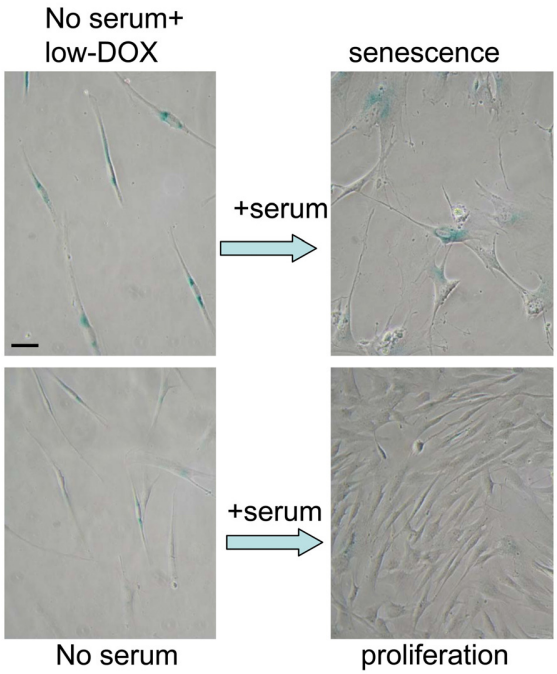

Figure 8. Serum stimulation converts Dox-locked quiescence into senescence in WI-38t cells. WI38t cells were treated with 100 ng/ml doxorubicin (low- Dox) or left untreated in serum-free medium (no serum) for 3 days, and then 10% serum was added. After 3 days of serum stimulation cells were stained for beta-gal and microphotographed. Bar – 50 micron.

DISCUSSION

In this study we tested the idea that while causing senescence in proliferating cells, DNA damaging drugs and induced p53 will not cause senescence in quiescent cells. To this point we 1) induced quiescence prior to p53 induction and 2) used p53-inducing agents that could be washed out to observe whether treated cells would retain proliferative potential. Etoposide, which causes DNA damage, was used for normal cells and nutlin-3a, which induces p53 without DNA damage, was used for cancer cells. Both agents could be washed out to check the reversibility of arrest. We used these

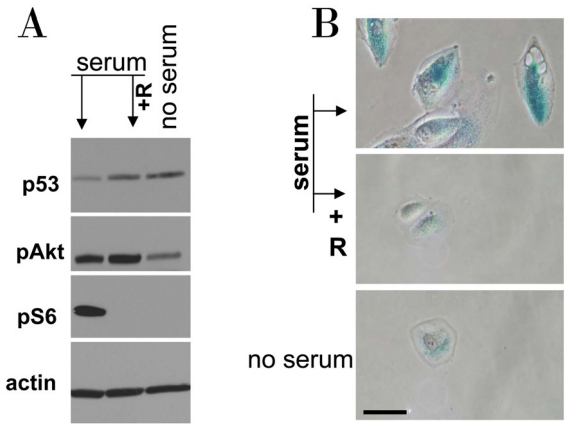

Figure 9. Serum stimulation of etoposide-locked RPE cells results in mTOR-dependent senescence. **A-B**. RPE cells were treated with 0.5 μg/ml etoposide in the absence of serum as shown in Figure 6. Then, 10% serum was added either with 10 nM rapamycin (+R) or alone. No serum indicates that cells were continuously incubated with etoposide in serum free medium. 24 h after serum stimulation, cells were lysed and subjected to immunoblotting as indicated (**A**). 4 days after serum stimulation cells were microphotographed (**B**).

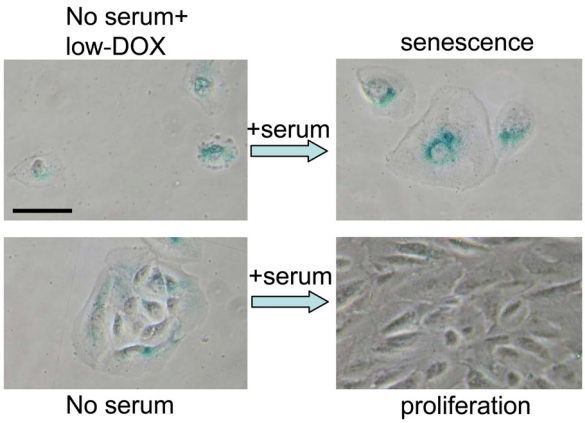

Figure 10. Serum stimulation converts Dox-locked quiescence into senescence in RPE cells. RPE cells were treated with 50 ng/ml doxorubicin (low-Dox) or left untreated in serum-free medium (no serum) for 3 days, then 10% serum was added. After 3 days of serum stimulation cells were stained for beta-Gal and microphotographed. Bar – 50 micron.

drugs at concentrations that caused senescence in proliferating cells. When applied to serum-starved and rapamycin-treated cells, p53-inducing drugs did not

completely convert quiescence into senescence. Cells retained mostly quiescent morphology and some degree of proliferative potential, resuming proliferation in fresh (drug-free, serum-containing) medium.

Although not causing senescence, induction of p53 in quiescent cells 'locked' the cell cycle. In quiescence caused by serum starvation, the cell cycle is inactive (due to low levels of cyclins) but not blocked. In quiescent cells, induction of p53 blocks the cell cycle (in addition to its deactivation). Re-addition of serum to such blocked (locked) quiescent cells did not cause proliferation. Instead it caused senescence. This is in agreement with the notion that senescence is a form of growth, a continuation of growth, when proliferation is impossible [18,39].

Thus, induction of p53 by different agents (including DNA damaging drugs) did not cause senescence in serum-starved and rapamycin-treated cells. It is less clear whether DNA damaging agents induced identical DNA damage in all conditions. One potential problem is that DNA damaging drugs may induce a lesser DNA damage in quiescent cells. However, first, we utilized etoposide, which was reported to induce damage in all phases of the cell cycle [40-45]. Second, etoposide induced the same levels of p53 in proliferating, serum-starved and rapamycin-treated cells. (Note: Although p53 could be induced independently from DNA damage, this has not been described for etoposide. DNA

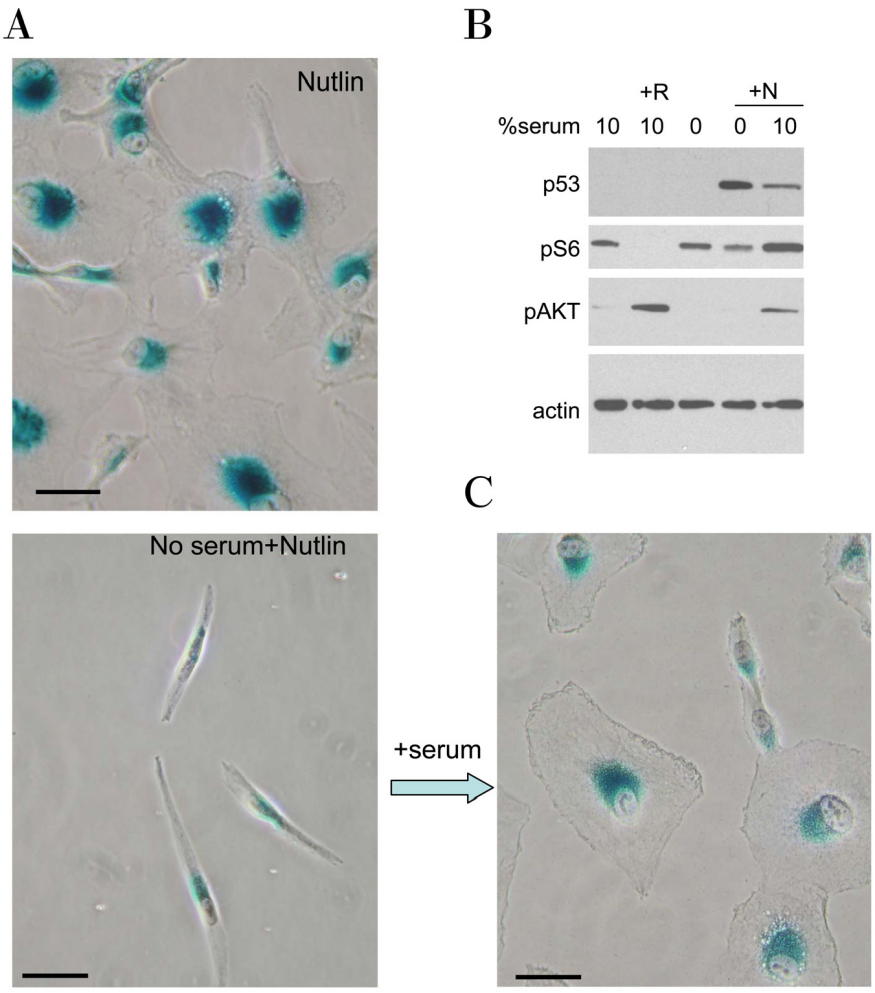

Figure 11. Serum stimulation is required for senescent morphology in nutlin-treated MEL-10 cells. MEL-10 cells treated with 2.5 μM nutlin-3a in the presence (Nutlin) or absence (No serum+Nutlin) of serum for 3 days were stained for beta-Gal and microphotographed (left panels). In parallel, 10% serum was added to a replicate well. After 3 days of serum stimulation cells were stained for beta-Gal and microphotographed (right lower panel). Bars – 50 micron.

A. MEL-10 cells treated with 2.5 μM Nutlin-3a (N) in the absence or presence of 10% serum for 24 hr were lysed and subjected to immunoblotting, as indicated. Treatment with 10 nM rapamycin (R) is used as a control for mTOR inhibition.

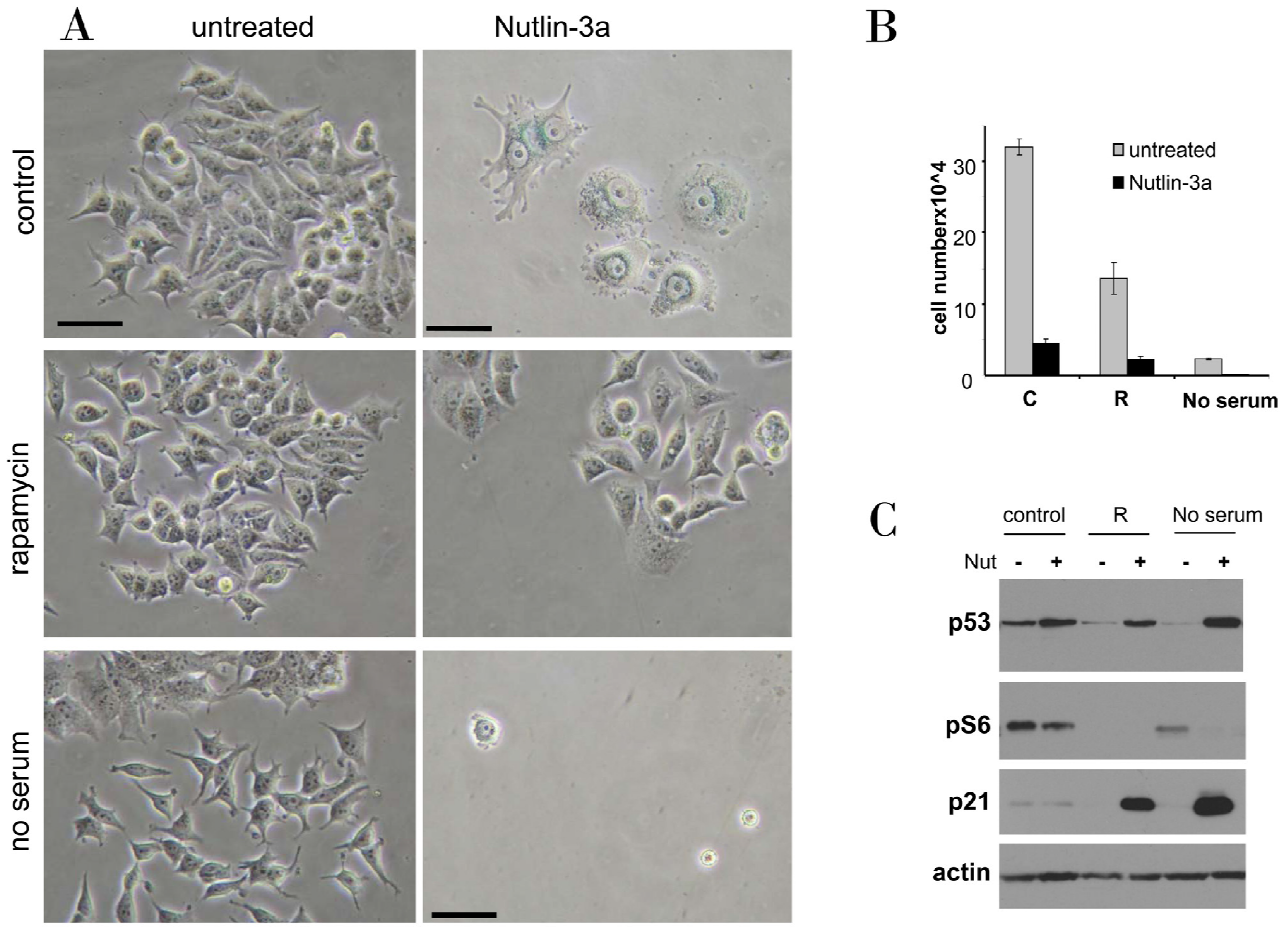

Figure 12. Rapamycin and serum starvation prevents nutlin-induced senescence in MCF-7 cells.
A-B. MCF7 cells were plated at 5000 or 10000/well in 12 well plates, allowed to attach and then were either pretreated with 500 nM rapamycin (R), placed in serum free medium or left untreated in complete medium (control)**.** The next day, 5μM nutlin-3a was added. After 5 days, cells were stained for beta-Gal and microphotographed (bars -50 micron) (**A**)**.** (**B**) In replicate plate, cells were counted.
B. MCF7 cells were treated as indicated for 24 hr, and immunoblot was performed.

damage response such as gamma-H2AX is also not absolutely reliable marker because it may occur in the absence of DNA damage in senescent cells [46,47]). Therefore, direct measurement of DNA damage by comet assay is warranted. 0.5 μg/ml etoposide did not induce obvious comets both in control and serum-free conditions. 10 μg/ml etoposide induced comets in serum-starved cells (Supplemental Figure 1). We conclude that, in agreement with literature data, etoposide induces DNA damage in serum-starved cells (some of which may still cycling at the moment of etoposide treatment) but more detailed measurements are needed for quantitative results. Third, simultaneous serum-withdrawal and addition of doxorubicin also suppressed senescence and this effect cannot be explained by cell cycle arrest caused by serum withdrawal. Fourth, DNA damaging drugs were even more cytotoxic in serum free-medium, indicating damage. Thus, it is not that etoposide is less cytotoxic in serum-free medium but rather that cells retain lean morphology and prolifertative potential (the ability to proliferate in fresh medium). At high concentrations, damaging agents and p53 can induce cell death rather than senescence in serum-starved cells. Yet, according to our preliminary data, if drugs are removed before death occurs, serum-restimulated survived cells can become senescent. TOR-independent latent senescence caused by high levels of DNA damage is an intriguing topic for further investigations.

In conclusion, quiescence is characterized by inactive mTOR both in cell culture [18,19] and in the organism

[48,49]. The inability of p53 to cause senescence in quiescent cells has important physiological applications. Most cells of an adult organism are resting and therefore induction of p53 and DNA damage cannot cause senescence. In contrast, stimulation of GF-sensing mTOR-centric pathways can. 'Locked' quiescent cells represent post-mitotic cells in the organism, including muscle cells, adipocytes and neurons. While not triggering proliferation of such 'locked' cells, stimulation with growth factors, hormones and nutrients may cause their senescence. Conversion of quiescence to senescence is a model of physiological senescence. Locked (non-senescent) cells undergo chronic over-stimulation and eventually senesce. At least in some in vitro cellular models, conversion of quiescence to senescence (physiological senescence) can be suppressed by rapamycin.

MATERIALS AND METHODS

Cell lines and reagents. WI-38-Tert, WI-38 fibroblasts immortalized, and RPE, retinal pigment epithelial cells were described previously [18]. RPE cells were cultured in MEM with 10% FBS, WI-38-tert cells were cultured in low glucose DMEM with 10%FBS. MEL-10, melanoma cell line, and MCF-7, breast cancer cell line, were cultured in DMEM (plus pyruvate) with 10% FBS. Rapamycin was obtained from LC Laboratories, MA, USA. Nutlin-3a, etoposide and doxorubicin were from Sigma-Aldrich.

Immunoblot analysis. Whole cell lysates were prepared using boiling lysis buffer (1%SDS, 10 mM Tris.HCl, pH 74.). Equal amounts of proteins were separated on 10% or gradient polyacrylamide gels and transferred to nitrocellulose membranes. The following antibodies were used: mouse anti-p53 (Ab-6) from Oncogene, mouse anti-p21 from BD Biosciences; rabbit anti-actin from Sigma-Aldrich; rabbit anti-phospho-S6 (Ser235/236), mouse anti-S6, rabbit anti-phospho AKT, rabbit anti-LC3B, anti-phospho ERK from Cell Signaling; anti-cyclins D1 and E from Santa Cruz Biotechnology. Secondary goat anti-rabbit and goat anti-mouse HRP conjugated antibodies were from Chemicon and Bio-Rad, respectively. Signals were visualized using ECL chemilumenescence kit from Pierce.

SA-β-Gal staining. Beta-Gal staining was performed using Senescence-galactosidase staining kit (Cell Signaling Technology) according to manufacturer's protocol. Cells were incubated at 37^{o}C until beta-gal staining becomes visible. Development of color was detected under light microscope.

Neutral comet assay was performed according to manufacturer's protocol.

Proliferative potential was determined as described in detail in Figure legends.

ACKNOWLEDGEMENTS

We thank Dr. Zoya N Demidenko for help with comet assay and suggestions on the manuscript.

REFERENCES

1. Schmelzle T, Hall MN. TOR, a central controller of cell growth. Cell. 2000; 103:253-262.

2. Sarbassov DD, Ali SM, Sabatini DM. Growing roles for the mTOR pathway. Curr Opin Cell Biol. 2005; 17:596-603.

3. Wullschleger S, Loewith R, Hall MN. TOR signaling in growth and metabolism. Cell. 2006; 124:471-484.

4. Hands SL, Proud CG, Wyttenbach A. mTOR's role in ageing: protein synthesis or autophagy? Aging. 2009:586-597.

5. Edinger AL, Thompson CB. Akt maintains cell size and survival by increasing mTOR-dependent nutrient uptake. Mol Biol Cell. 2002; 13:2276-2288.

6. Itahana K, Campisi J, Dimri GP. Methods to detect biomarkers of cellular senescence: the senescence-associated beta-galactosidase assay. Methods Mol Biol. 2007; 371:21-31.

7. CoppŽ JP, Patil CK, Rodier F, Sun Y, Mu–oz DP, Goldstein J, Nelson PS, Desprez PY, Campisi J. Senescence-associated secretory phenotypes reveal cell-nonautonomous functions of oncogenic RAS and the p53 tumor suppressor. PLoS Biol. 2008; 6:2853-2868.

8. Freund A, Orjalo AV, Desprez PY, Campisi J. Inflammatory networks during cellular senescence: causes and consequences. Trends Mol Med. 2010:238-246.

9. Serrano M, Lim AW, McCurrach ME, Beach D, Lowe SW. Oncogenic ras provokes premature cell senescence associated with accumulation of p53 and p16INK1A. Cell. 1997; 88:593-602.

10. Lin AW, Barradas M, Stone JC, van Aelst L, Serrano M, Lowe SW. Premature senescence involving p53 and p16 is activated in response to constitutive MEK/MAPK mitogenic signaling. Genes Dev. 1998; 12:3008-3019.

11. Zhu JY, Woods D, McMahon M, Bishop JM. Senescence of human fibroblasts induced by oncogenic Raf. Genes Dev. 1998; 12:2997-3007.

12. Sherr CJ, DePinho RA. Cellular senescence: mitotic clock or culture shock ? Cell. 2000; 102:407-410.

13. Itahana K, Dimri G, Campisi J. Regulation of cellular senescence by p53. Eur J Biochem. 2001; 268:2784-2791.

14. Serrano M, Blasco MA. Putting the stress on senescence. Curr Opin Cell Biol. 2001; 13:748-753.

15. Baus F, Gire V, Fisher D, Piette J, Dulic V. Permanent cell cycle exit in G2 phase after DNA damage in normal human fibroblasts. Embo J. 2003; 22:3992-4002.

16. Blagosklonny MV. Cell senescence and hypermitogenic arrest. EMBO Rep. 2003; 4:358-362.

17. Blagosklonny MV. Cell senescence: hypertrophic arrest beyond restriction point. J Cell Physiol. 2006; 209:592-7

18. Demidenko ZN, Blagosklonny MV. Growth stimulation leads to cellular senescence when the cell cycle is blocked. Cell Cycle. 2008; 7:3355-3361.

19. Demidenko ZN, Zubova SG, Bukreeva EI, Pospelov VA,

Pospelova TV, Blagosklonny MV. Rapamycin decelerates cellular senescence. Cell Cycle. 2009; 8:1888-95

20. Demidenko ZN, Blagosklonny MV. Quantifying pharmacologic suppression of cellular senescence: prevention of cellular hypertrophy versus preservation of proliferative potential. Aging. 2009; 1:1008-1016.

21. Stambolic V, MacPherson D, Sas D, Lin Y, Snow B, Jang Y, Benchimol S, Mak TW. Regulation of PTEN transcription by p53. Mol Cell. 2001; 8:317-325.

22. Feng Z, Zhang H, Levine AJ, Jin S. The coordinate regulation of the p53 and mTOR pathways in cells. Proc Natl Acad Sci U S A. 2005; 102:8204-8209.

23. Budanov AV, Karin M. p53 target genes sestrin1 and sestrin2 connect genotoxic stress and mTOR signaling. Cell. 2008; 134:451-460.

24. Matthew EM, Hart LS, Astrinidis A, Navaraj A, Dolloff NG, Dicker DT, Henske EP, El-Deiry WS. The p53 target Plk2 interacts with TSC proteins impacting mTOR signaling, tumor growth and chemosensitivity under hypoxic conditions. Cell Cycle. 2009; 8:4168-75

25. Constantinou C, Clemens MJ. Regulation of the phosphorylation and integrity of protein synthesis initiation factor eIF4GI and the translational repressor 4E-BP1 by p53. Oncogene. 2005; 24:4839-4850.

26. Constantinou C, Elia A, Clemens MJ. Activation of p53 stimulates proteasome-dependent truncation of eIF4E-binding protein 1 (4E-BP1). Biol Cell. 2008; 100:279-289.

27. Demidenko ZN, Korotchkina LG, Gudkov AV, Blagosklonny MV. Paradoxical suppression of cellular senescence by p53. Proc Natl Acad Sci U S A. 2010; 107:9660-9664.

28. Maiuri MC, Malik SA, Morselli E, Kepp O, Criollo A, Mouchel PL, Carnuccio R, Kroemer G. Stimulation of autophagy by the p53 target gene Sestrin2. Cell Cycle. 2009; 8:1571-1576.

29. O'Prey J, Skommer J, Wilkinson S, Ryan KM. Analysis of DRAM-related proteins reveals evolutionarily conserved and divergent roles in the control of autophagy. Cell Cycle. 2009; 8:2260-2265.

30. Vousden KH, Ryan KM. p53 and metabolism. Nat Rev Cancer. 2009; 9:691-700.

31. Feng Z, Levine AJ. The regulation of energy metabolism and the IGF-1/mTOR pathways by the p53 protein. Trends Cell Biol. in press

32. Hu W, Zhang C, Wu R, Sun Y, Levine A, Feng Z. Glutaminase 2, a novel p53 target gene regulating energy metabolism and antioxidant function. Proc Natl Acad Sci U S A. 107:7455-7460.

33. Suzuki S, Tanaka T, Poyurovsky MV, Nagano H, Mayama T, Ohkubo S, Lokshin M, Hosokawa H, Nakayama T, Suzuki Y, Sugano S, Sato E, Nagao T, Yokote K, Tatsuno I, Prives C. Phosphate-activated glutaminase (GLS2), a p53-inducible regulator of glutamine metabolism and reactive oxygen species. Proc Natl Acad Sci U S A. 107:7461-7466.

34. Ashur-Fabian O, Har-Zahav A, Shaish A, Amram HW, Margalit O, Weizer-Stern O, Dominissini D, Harats D, Amariglio N, Rechavi G. apoB and apobec1, two genes key to lipid metabolism, are transcriptionally regulated by p53. Cell Cycle. 9:3761-3770.

35. Ide T, Chu K, Aaronson SA, Lee SW. GAMT joins the p53 network: branching into metabolism. Cell Cycle. 9:1706-1710.

36. Blagosklonny MV. Increasing healthy lifespan by suppressing aging in our lifetime: Preliminary proposal. Cell Cycle. 2010; 9:4788-4794.

37. Korotchkina LG, Leontieva OV, Bukreeva EI, Demidenko ZN, Gudkov AV, Blagosklonny MV. The choice between p53-induced senescence and quiescence is determined in part by the mTOR pathway. Aging. 2010; 2:344-352.

38. Leontieva O, Gudkov A, Blagosklonny M. Weak p53 permits senescence during cell cycle arrest. Cell Cycle. 2010; 9:4323-4327.

39. Blagosklonny MV, Hall MN. Growth and Aging: a common molecular mechanism. Aging. 2009; 1:357-362.

40. Sato Y, Kurose A, Ogawa A, Ogasawara K, Traganos F, Darzynkiewicz Z, Sawai T. Diversity of DNA damage response of astrocytes and glioblastoma cell lines with various p53 status to treatment with etoposide and temozolomide. Cancer Biol Ther. 2009; 8:452-457.

41. de Campos-Nebel M, Larripa I, Gonzalez-Cid M. Topoisomerase II-mediated DNA damage is differently repaired during the cell cycle by non-homologous end joining and homologous recombination. PLoS One. 2010; 5(9). pii: e12541.

42. Rojas E, Mussali P, Tovar E, Valverde M. DNA-AP sites generation by etoposide in whole blood cells. BMC Cancer. 2009; 9:398.

43. Robison JG, Dixon K, Bissler JJ. Cell cycle-and proteasome-dependent formation of etoposide-induced replication protein A (RPA) or Mre11/Rad50/Nbs1 (MRN) complex repair foci. Cell Cycle. 2007; 6:2399-2407.

44. Tanaka T, Halicka HD, Traganos F, Seiter K, Darzynkiewicz Z. Induction of ATM activation, histone H2AX phosphorylation and apoptosis by etoposide: relation to cell cycle phase. Cell Cycle. 2007; 6:371-376.

45. Smart DJ, Halicka HD, Schmuck G, Traganos F, Darzynkiewicz Z, Williams GM. Assessment of DNA double-strand breaks and gammaH2AX induced by the topoisomerase II poisons etoposide and mitoxantrone. Mutat Res. 2008; 641:43-47.

46. Pospelova TV, Demidenko ZN, Bukreeva EI, Pospelov VA, Gudkov AV, Blagosklonny MV. Pseudo-DNA damage response in senescent cells. Cell Cycle. 2009; 8:4112-4118.

47. Romanov VS, Abramova MV, Svetlikova SB, Bykova TV, Zubova SG, Aksenov ND, Fornace AJ, Jr., Pospelova TV, Pospelov VA. p21(Waf1) is required for cellular senescence but not for cell cycle arrest induced by the HDAC inhibitor sodium butyrate. Cell Cycle. 9:3945-3955.

48. Gan B, DePinho RA. mTORC1 signaling governs hematopoietic stem cell quiescence. Cell Cycle. 2009; 8:1003-1006.

49. Chen C, Liu Y, Zheng P. mTOR regulation and therapeutic rejuvenation of aging hematopoietic stem cells. Sci Signal. 2009; 2:ra75.Am J Physiol Lung Cell Mol Physiol. 2006; 290: L661-L73.

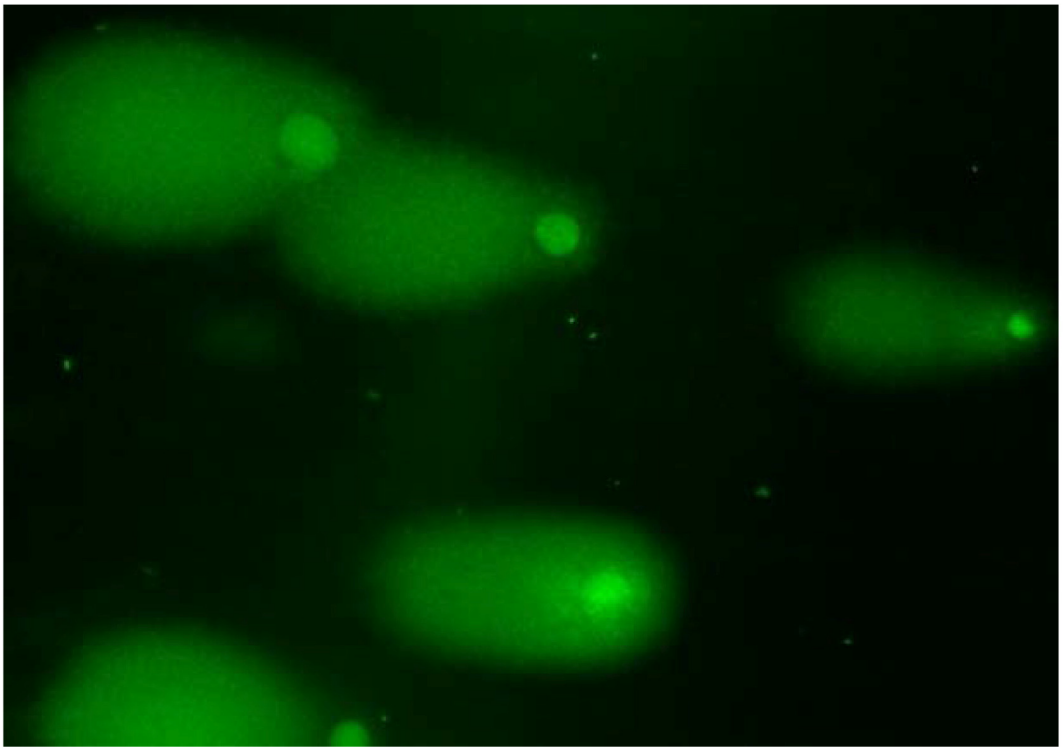

Supplementary Figure 1. Comet assay. RPE cells were seeded at 25,000 per well in 12-well plates. The next day, the medium was changed to 0% serum for 24 hours and then the cells were treated with 10 μg/ml etoposide for 1 hour and neutral comet assay was performed.

Research Paper

Adult-onset, short-term dietary restriction reduces cell senescence in mice

Chunfang Wang[1], Mandy Maddick[1], Satomi Miwa[1], Diana Jurk[1], Rafal Czapiewski[2], Gabriele Saretzki[2], Sabine A.S. Langie[3], Roger W.L. Godschalk[4], Kerry Cameron[1], Thomas von Zglinicki[1]

[1] Centre for Integrated Systems Biology of Ageing and Nutrition, Institute for Ageing and Health, Newcastle University, Newcastle Upon Tyne, UK
[2] Crucible Laboratory, Institute for Ageing and Health, Newcastle University, Newcastle Upon Tyne, UK
[3] Human Nutrition Research Centre and Centre for Brain Ageing and Vitality, Institute for Ageing and Health, Newcastle University, Newcastle Upon Tyne, UK
[4] Nutrition and Toxicology Research Institute Maastricht (NUTRIM), Department of Health Risk Analysis and Toxicology, Maastricht University, Netherlands

Key words: *Dietary restriction, caloric restriction, mice, senescence, telomeres, ageing*
Received: *08/18/10; accepted: 09/09/10; published on line: 09/11/10* doi:10.18632/aging.100196
Corresponding author*: Thomas von Zglinicki, PhD;* ***E-mail:*** *t.vonzglinicki@ncl.ac.uk*

Abstract: Dietary restriction (DR) extends the lifespan of a wide variety of species and reduces the incidence of major age-related diseases. Cell senescence has been proposed as one causal mechanism for tissue and organism ageing. We show for the first time that adult-onset, short-term DR reduced frequencies of senescent cells in the small intestinal epithelium and liver of mice, which are tissues known to accumulate increased numbers of senescent cells with advancing age. This reduction was associated with improved telomere maintenance without increased telomerase activity. We also found a decrease in cumulative oxidative stress markers in the same compartments despite absence of significant changes in steady-state oxidative stress markers at the whole tissue level. The data suggest the possibility that reduction of cell senescence may be a primary consequence of DR which in turn may explain known effects of DR such as improved mitochondrial function and reduced production of reactive oxygen species.

INTRODUCTION

Dietary restriction (DR), whereby total caloric intake is reduced but adequate nutrition is maintained, results in an extension of lifespan. Additionally, DR has been shown to delay the onset and severity of cancer and other diseases associated with ageing [1]. The DR response has been remarkably robust in a wide range of animal species, although both evolutionary models and genetic experiments question its universality in different inbred strains of mice and, importantly, in humans [2,3]. The molecular and cellular mechanisms underlying the response to DR have been intensely examined. It has been proposed that DR prolonged lifespan for example by attenuating oxidative damage, reducing production of reactive oxygen species (ROS), increasing DNA repair capacity, altering the growth hormone/IGF-1 axis, decreasing signaling through the mTOR substrate S6K1 or improving hormesis [4-8]. However, we are still far from a mechanistic and integrative understanding of the DR response [1,9].

This is even more true for the response to adult-onset, short-term DR. While the effect on lifespan becomes less robust if DR is implemented in older animals [10,11], there are still strong beneficial effects on cancer incidence [11-15], immune response [14,16] and cognitive function [17]. Preliminary data from non-human primates [18] and clinical trials [19] have suggested that late onset DR could have at least some beneficial effects in humans.

Recently, evidence is mounting that cellular senescence, which was originally described as the permanent loss of replicative capacity in human fibroblasts *in vitro* [20], is a complex phenotype, possibly causally contributing to aging *in vivo* [21-23]. Senescent cells are found with increasing frequency in many tissues of aging rodents, primates and humans [24-28]. High frequencies of senescent cells have been associated with age-related diseases like osteoarthritis and atherosclerosis [29,30] and were also found in mouse models of accelerated aging [31-34]. Senescent cells are not simply incompetent of proliferating; they display major alterations to their gene expression profiles [35] and secrete bioactive molecules including matrix-degrading enzymes [36], inflammatory cytokines [21,22,37] and ROS [23]. Thus, cell senescence may well be an important driver for the aging process *in vivo* [38,39].

If this concept were correct, one would hypothesize that a reduction of cell senescence might be part, and potentially a causal part, of the beneficial action of DR. This would be interesting because less senescent cells could explain the anti-inflammatory and anti-oxidative action of DR. However, there are few data to support such a hypothesis. There is good evidence that both life-long and adult-onset DR limit T cell senescence in mice and primates [14,40-42], at least partially by maintaining sensitivity to stress-induced apoptosis [43]. However, T cell senescence might be very different from senescence of cells in solid tissues. For instance, while a DNA damage response is the major driver for growth arrest [44] and phenotypic changes [23] in fibroblast senescence, its role in T cell senescence is less well established. Moreover, sensitivity to apoptotic stimuli is generally high in senescent T cells, but decreases during senescence in fibroblasts and other solid tissue cells.

There is very little data available on the impact of DR on cell senescence in solid mammalian tissues. Early data [45,46] showed reduced proliferative activity in various tissues of young mice under DR but improved maintenance of replicative activity and capacity in old mice under life-long DR, which might be due to a decreased accumulation of senescent cells. Krishnamurthy et al. [26] showed that DR reduced staining for senescence-associated β-Galactosidase (sen-β-Gal) and the expression of $p16^{INK4a}$ and $p19^{Arf}$ in the kidney. However, the specificity and sensitivity of sen-β-Gal as a marker for senescent cells *in vivo* has been repeatedly questioned [47,48]. Moreover, $p16^{INK4a}$ and $p19^{Arf}$ expression was similarly changed in postmitotic tissues like brain cortex and heart, suggesting that expression from the INK4A locus might be a better indicator for aging than for cell senescence. Further indirect evidence for decreased cell senescence under DR came from a study showing reduced levels of IGFBP3, a major secretion product of senescent epithelial and mesenchymal cells, following long-term DR [49]. However, while frequencies of senescent cells increased during aging in skin of rhesus monkeys [50] and baboons [25], no decrease of sen-β-Gal-positive epithelial cells and no increase in proliferation-competent skin fibroblasts was found after 9-12 years of DR in rhesus monkeys [50]. To our knowledge, there is no data reporting an effect of shorter term DR on cell senescence in solid tissues.

We tested the impact of short-term (3 months), adult-onset DR on cellular senescence in mice. We concentrated on the small intestine, a highly proliferative organ, and on liver with a slow cell turnover under non-pathological conditions. We had shown before that senescent cell frequencies in these organs increase significantly during normal aging in mice [28]. Using sensitive and specific markers for senescent cells [51,52], we found that short-term, adult-onset DR significantly reduced the frequencies of senescent liver hepatocytes, especially in the centrilobular area, and of senescent intestinal enterocytes in the transient amplifying zone. DR also improved telomere maintenance in liver and intestine and reduced cumulative oxidative stress markers in the same tissue compartments. We propose that reduction of cell senescence might be a primary effect of DR which may explain improved mitochondrial function and reduced ROS production.

RESULTS

Adult-onset, short-term DR reduced the frequencies of senescent cells in small intestine and liver

Male C57/BL mice were subjected to three months of DR by average 26% of food restriction starting at 14 months of age. The study cohort is characterized in supplementary Table S1. We focused on intestinal crypt enterocytes and liver hepatocytes because frequencies of senescent cells in these tissue compartments increased with age or as result of telomere dysfunction in Terc-/- mice [23,28].

We first measured the frequency of intestinal enterocytes showing an active DNA damage response as characterized by nuclear positivity for the DNA damage marker, γ-H2A.X. As we have shown before, there were few γ-H2A.X-positive enterocytes within villi, instead, positive cells centered around the transient amplifying zone in crypts [28]. DR significantly reduced the frequencies of γ-H2A.X-positive intestinal crypt enterocytes (Figure 1A). We compared frequencies of γ-H2A.X-positive and sen-β-Gal-positive

crypt enterocytes, measured on adjacent frozen sections from five AL and five DR mice (Figure 1B). The significant reduction of positive cells by DR was confirmed for both markers, and they were significantly correlated (r^2=0.7080). γ-H2A.X staining on its own may overestimate frequencies of senescent cells, especially in tissue compartments with high proliferative activity such as gut because an active DNA damage response can also be initiated by replication stress in dividing cells. Accordingly, we showed recently that a combination of strong positivity for γ-H2A.X with absence of a proliferation marker results in quantitatively correct estimates of senescent cell frequencies *in vitro* and *in vivo* [52]. Double staining for γ-H2A.X and PCNA in the small intestine (Figure 1C) showed that DR reduced also the frequencies of PCNA positive crypt enterocytes as reported previously [45]. Frequencies of γ-H2A.X positive/PCNA negative intestinal crypt enterocytes in 17 month old mice were 20.0±0.9% under AL conditions and 14.0±1.9% after 3 months DR (Figure 1C). This difference was significant (p=0.02).

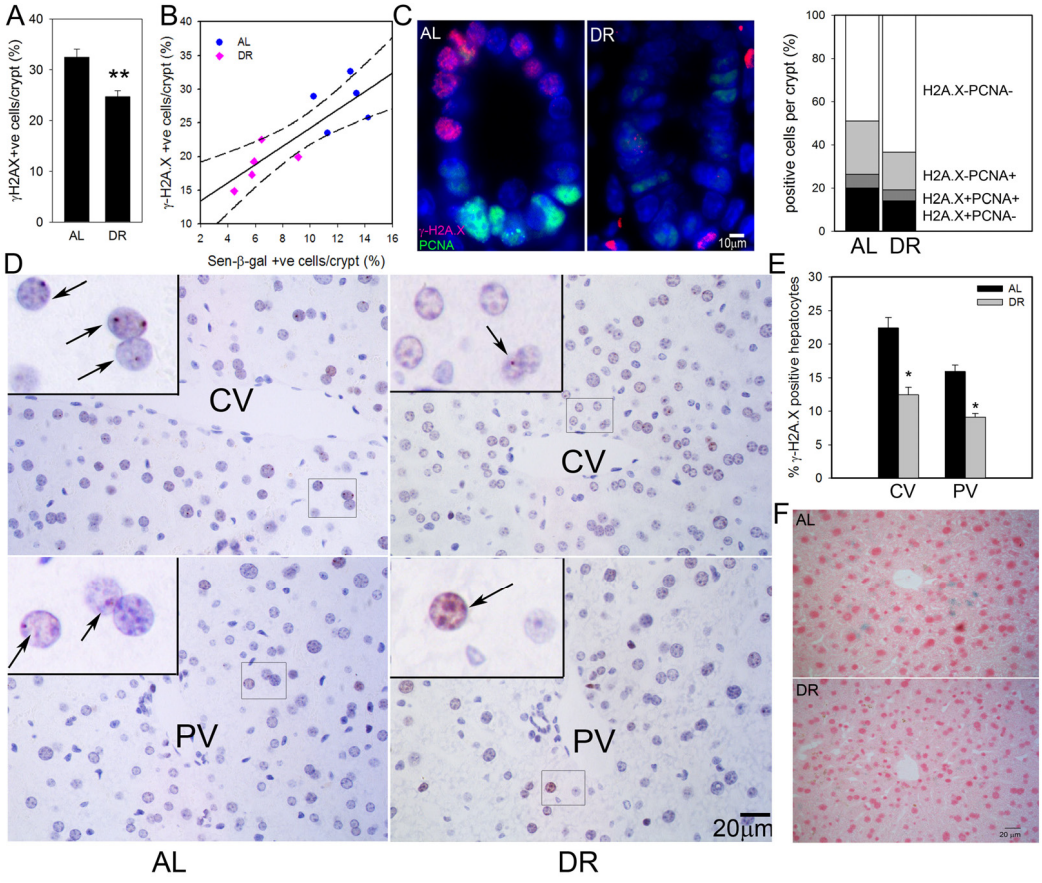

Figure 1. DR reduced frequencies of senescent hepatocytes and intestinal crypt enterocytes. (**A**) Frequencies of γ-H2A.X positive enterocytes per crypt, immunohistochemistry on paraffin sections. ** p<0.005. (**B**) Correlation between sen-β-Gal and γ-H2A.X positive enterocytes (p=0.002). Data points are means per animal (DR: pink; Al: blue). Linear regression (solid line) and 95% confidence intervals (dashed lines) are given. (**C**) Representative images (left) and quantitative evaluation (right) of PCNA and γ-H2A.X double immunofluorescence of intestinal crypts from AL and DR mice. Blue: DAPI; red: γ-H2A.X; green: PCNA. (**D**) Representative images of γ-H2A.X immunohistochemistry in livers from AL (left) and DR (right) mice. Examples of centrilobular (top) and periportal (bottom) areas are shown. CV: central vein; PV: portal vein. Boxed areas are shown at higher magnification. Arrows indicate nuclei containing γ-H2A.X foci (red). (**E**) Quantification of γ-H2A.X positive hepatocytes. * p<0.05. (F) Representative images for sen-β-Gal activity. Pink: nuclei; blue: cytoplasmic sen-β-Gal staining. All data are from 5 animals/group, mean±S.E.M.

In liver, frequencies of γ-H2A.X positive hepatocytes were higher in centrilobular than periportal areas (Figure1D) as shown previously [28]. Importantly, the frequencies of γ-H2A.X positive hepatocytes were significantly reduced following 3 months DR by 6.5 ± 1.8% in the centrilobular area and by 3.3 ± 1.2% in the periportal area (Figure 1E). Results were qualitatively confirmed by sen-β-Gal staining on cryosections (Figure 1F). The frequency of PCNA- or Ki67-positive cells in hepatocytes was less than 1% (data not shown). Therefore, γ-H2A.X positivity on its own is regarded as a good estimate of senescent hepatocytes in liver.

Adult-onset, short-term DR improved telomere maintenance in small intestine and liver

Despite the presence of active telomerase, telomeres shorten with age in various tissues of laboratory mice [28,53]. However, even in very old mice, telomeres are much longer than in humans and aging in mice did not measurably increase the degree of co-localisation of DNA damage foci with telomeres [28]. This suggests that telomere shortening may only be a minor contributor to cell senescence in aging wild-type mice. Here, we measured telomere length by quantitative FISH (Q-FISH) in intestinal enterocytes and liver hepatocytes (Figure 2A, B). Following 3 months of DR, the average telomere length per crypt enterocyte nucleus was significantly higher than in AL fed mice (Figure 2A). The effect of DR on hepatocyte telomere length was smaller than in the intestine (Figure 2B), possibly because of the lower rate of proliferation. However, the difference between DR and AL was still significant in the centrilobular areas. Telomerase activity as measured by TRAP in whole liver and intestinal mucosa homogenates was not significantly changed by DR (Figure 2C). If anything, it tended to decrease under DR, possibly due to the anti-proliferative effect of DR, suggesting that other factors than telomerase must be responsible for the improved telomere maintenance under DR. The most probable of these is reduction of oxidative damage to telomeres [54].

Adult-onset, short-term DR reduced some oxidative damage markers in small intestine and liver

Senescent cells are a major source of ROS because mitochondrial dysfunction and, possibly, other ROS-producing mechanisms are part of the senescent phenotype [23,55-57]. Long-term DR is well known to reduce oxidative stress and mitochondrial ROS production [8,58]. We measured several markers of oxidative damage in small intestine and liver to test whether adult-onset, short-term DR impacts on oxidative stress in the same tissues as it reduced cell senescence.

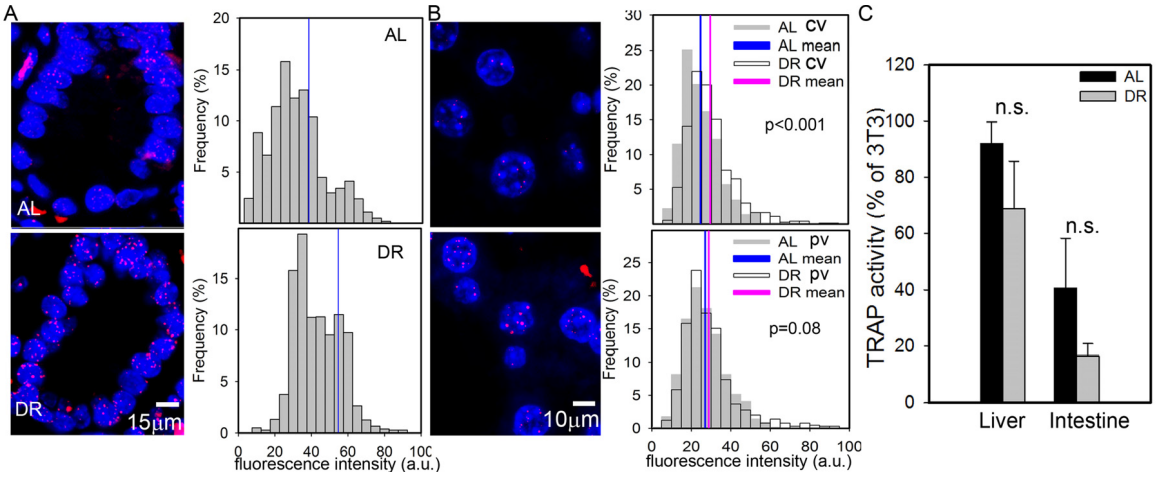

Figure 2. DR improves telomere maintenance. (**A**) Representative Q-FISH images (left panels, red: telomeres, blue: nuclei) and distribution of enterocyte telomere fluorescence intensity per nucleus (right panels, n≥2230 nuclei, 5 animals) in intestinal crypts. Mean nuclear telomere fluorescence intensity is indicated by blue vertical lines. p<0.001, Mann-Whitney rank sum test. (**B**) Representative Q-FISH images (left panels, red: telomeres, blue: nuclei) and distribution of hepatocyte telomere fluorescence intensity in centrilobular (CV, top, n≥560 nuclei) and periportal (PV, bottom, n≥650 nuclei) in liver areas. Mean fluorescence intensities are indicated for AL (blue) and DR (pink). P-values for AL vs DR were calculated by Mann-Whitney rank sum test. (**C**) Telomerase catalytic activity (% of TRAP activity in 3T3 cells) in whole liver (left, n=4) and intestinal mucosa (right, n=5) homogenates. Data are mean±S.E.M. n.s.: not significant (T-test).

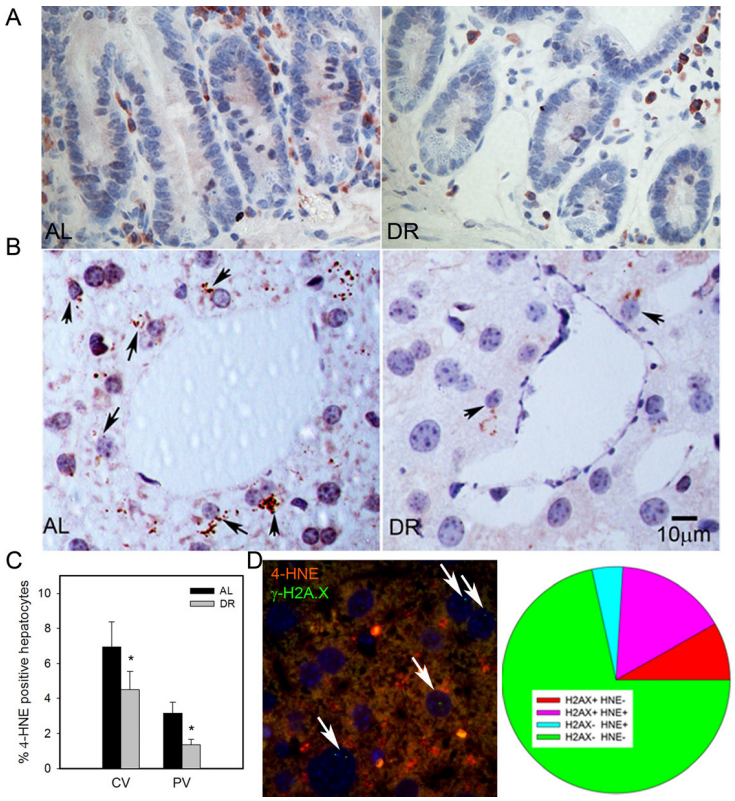

Figure 3. DR decreased lipid peroxidation in liver. (**A**) Representative 4-HNE immunohistochemistry in small intestine from AL (left) and DR(right) mice. Brown: 4-HNE staining; blue: nuclei. (**B**) Representative 4-HNE images from centrilobular areas in liver. Brown: 4-HNE, Blue: nuclei. Arrows indicate examples of positive cells. (**C**) Frequencies of 4-HNE-positive hepatocytes in periportal and centrilobular areas of liver. Data are mean±S.E.M. * $p<0.05$, n=5 animals/group. (**D**) Co-localisation of γ-H2A.X (green) and 4-HNE (red) in AL liver. Representative image, double immunofluorescence, cryosection. Cells with nuclei (DAPI, blue) positive for γ-H2A.X are marked by arrows. Cells were scored as either single positive (H2AX+ HNE – or H2A.X- HNE +), double positive (H2A.X+ HNE+) or double negative (H2A.X- HNE -). Data are from four animals from the AL group.

4-HNE is a major end product of lipid peroxidation and has been shown to accumulate in tissues with age [59]. We found few 4-HNE positive cells in intestinal crypts, and almost all were located in the lamina propria (Figure 3A). Confirming earlier results [28], HNE-positive hepatocytes were more frequent in centrilobular than in periportal areas. Importantly, frequencies of HNE-positive hepatocytes decreased under DR in both areas (Figure 3B, C $p<0.05$). To directly see whether there was an association between cell senescence and oxidative stress in liver hepatocytes, we performed a double staining for γ-H2A.X and 4-HNE (Figure 3D). Quantitative evaluation showed that the majority of senescent hepatocytes (as measured by γ-H2A.X) were also positive for 4-HNE and, vice versa, about three quarters of 4-HNE-positive hepatocytes were probably senescent (Figure 3D), thus confirming a cell-specific association between senescence and a marker of oxidative damage.

Broad-band autofluorescence originates mainly from oxidised and cross-linked cell components, like advanced glycation end products (AGEs) and lipofuscin and is thus regarded as a good cumulative marker for oxidative damage [23,60-62]. Short-term DR significantly reduced the intensity of broad-band autofluorescence from intestinal crypt enterocytes (Figure 4A) and in centrilobular areas of the liver (Figure 4B). The reduction of autofluorescence in the periportal areas of the liver by DR was not significant (Figure 4B), in accordance with this compartment showing the least reduction of senescent cells.

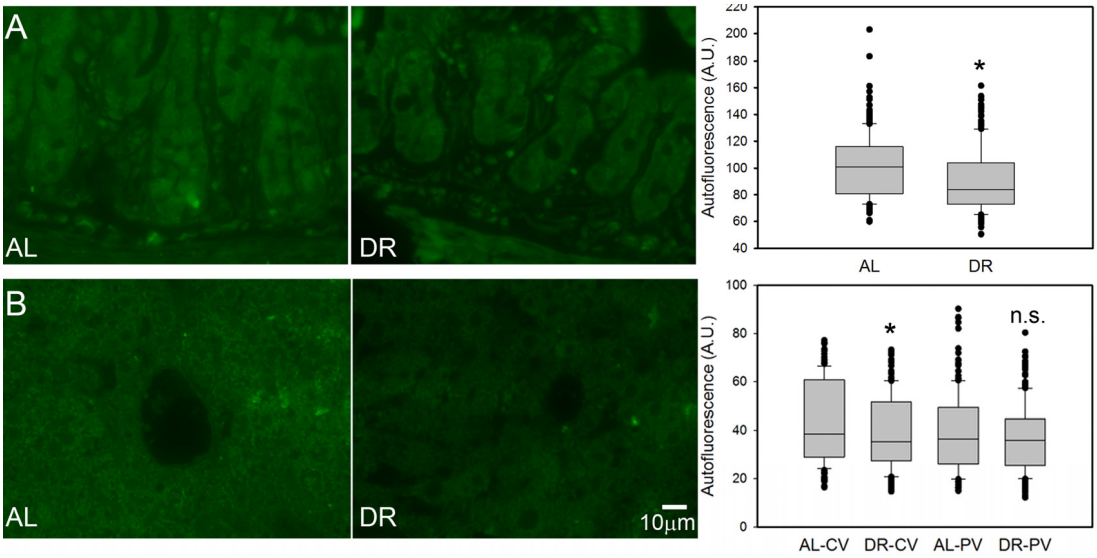

Figure 4. DR decreased the intensity of broad-band autofluorescence. (**A**) Representative autofluorescence images (left) and quantitative data (right) in small intestinal crypts under AL (left) and DR (right). (**B**) Representative autofluorescence images from centrilobular areas in liver (AL left, DR right) and quantitative data in periportal and centrilobular areas. All data are mean±S.E.M from 5 animals/group. *p<0.05; n.s. not significant (T-test).

8-oxodG (a marker for oxidative DNA damage), nitrotyrosine content (a marker for oxidative protein damage) and H_2O_2 release rate from tissue homogenate are indicative of steady-state levels of oxidative stress/ oxidative damage. These markers were measured in whole liver homogenates. None of them were significantly different between AL and DR mice (Figure 5). Similarly, DR did not change 8-oxodG levels in homogenates of the intestinal mucosa (data not shown).

DISCUSSION

This is the first study to show that short-term DR reduced frequencies of senescent cells in solid tissues. It is important to note that the magnitude of the reductions, amounting to between 3.3 and 6.5% depending on the tissue compartment, is very substantial given the short duration of the treatment. Frequencies of senescent cells increase with age in intestinal crypts and liver at rates below 0.5% per month [28], indicating that 3 months DR probably reduced levels of senescent cells beyond that at the start of the treatment. Available data indicate that senescent hepatocytes are turned over slowly in liver [63,64]. Turnover rates of senescent enterocytes in intestinal crypts are unknown. DR could block the induction of senescent cells, increase the rate of their turnover, or both.

Cell senescence *in vitro* is associated with a 3- to 5-fold increase in cellular ROS levels [23,55-57]. Various signaling pathways and feedback loops connect DNA damage response and checkpoint proteins that are activated early and permanently in senescence, notably p21, p16 and Rb, with ROS generation via mitochondrial dysfunction and, potentially, NADPHoxidase activation [23,56,65]. As senescent cells were less in DR, we therefore expected to see lower levels of oxidative stress markers under DR especially in those tissue compartments which showed large reductions of senescent cells. This was indeed the case: autofluorescence was significantly reduced in the intestinal crypts and the centrilobular areas of the liver, but not around the portal vein. While 4-HNE could not be measured in enterocytes, it was more strongly reduced around the central vein than in the periportal areas of the liver. Without increases in telomerase activity, telomere length was better maintained under DR in the crypt enterocytes and in the centrilobular, but not periportal, areas of the liver. Autofluorescence, 4-HNE and telomere maintenance in the absence of changes in telomerase activity are all regarded as cumulative markers of oxidative damage [54,59,62]. In contrast, we did not find any significant effect of DR on the markers of oxidative damage measured in whole tissue homogenates. This was not surprising because 8-oxodG and H_2O_2 release as acute parameters are less sensitive

than the cumulative markers mentioned above. Moreover, an average decrease in the number of senescent cells by about 5% in liver would result in less than 10% decrease in total ROS, which is within the experimental error for these measurements. As there are very few senescent cells in villi, the expected impact of the observed decreases in senescent cell frequencies in the crypts on ROS in the whole intestinal mucosa would be even lower.

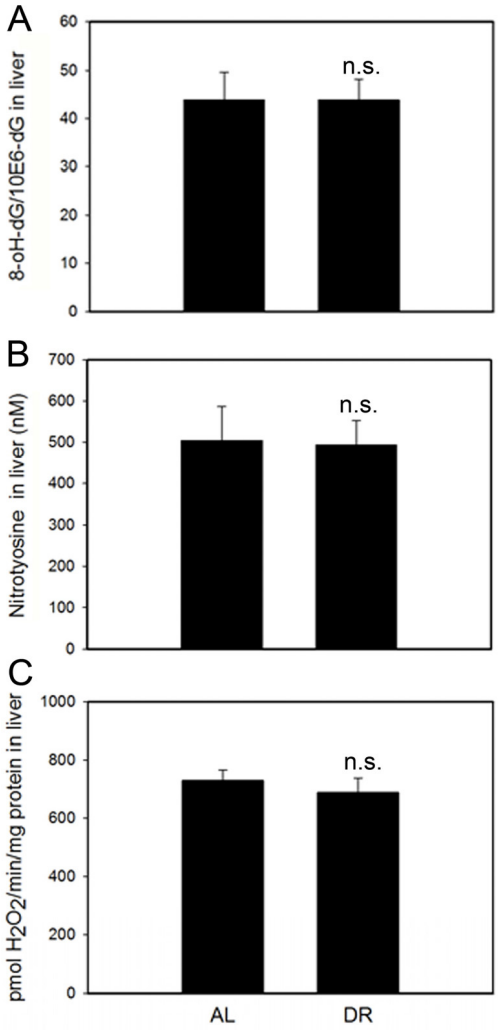

Figure 5. DR does not change oxidative damage markers measured in whole liver homogenates. (**A**) 8-oxodG levels in liver homogenates from AL and DR mice measured by HPLC with electrochemical detection. n=9 animals/group. (**B**) Nitrotyrosine levels in liver homogenates from AL and DR mice measured by ELISA; n=6 animals/ group. (**C**) Steady state hydrogen peroxide release from liver homogenates from AL and DR mice measured by Amplex Red fluorimetry; n=12 animals/ group. All data are mean ±S.E.M.; n.s.: not significant (T-test).

Taken together, our data suggest that at least some of the beneficial effects of DR that have been repeatedly described in the literature, such as improved mitochondrial coupling and reduced ROS release [8,58], could be quantitatively explained as an indirect effect, mediated via reduction of senescent cells. Mitochondria are dysfunctional (i.e. produce more superoxide despite lower membrane potential and induce a retrograde response) not only in senescent human fibroblasts *in vitro* [57]. The same changes were triggered by telomere dysfunction in mouse cells and tissues including the intestinal crypt epithelium. In this system, as in human fibroblasts, mitochondrial dysfunction was dependent on signaling through p21, the central mediator of cell senescence [23,32].

Our results lead to the question of how DR could impact directly on cell senescence. One interesting candidate may be signaling through the mTOR-S6K1 pathway. DR reduced phosphorylation and activity of Akt1, mTOR and its downstream targets S6K1 and 4E-BP1 [66]. Knockout of S6K1 mimics the effects of DR [67]. Importantly, S6K1 is intimately involved in the regulation of cell senescence. S6K1 phosphorylation and activity is altered in replicative senescence [68]. mTOR activation induced senescence in human fibroblasts [69] and the activation state of the mTOR pathway has been shown to be relevant for the decision between reversible arrest and cell senescence in models of DNA damage-independent senescence [70]. Wnt1-driven activation of the mTOR pathway caused epithelial stem cell senescence and loss after a short hyperproliferative period [71]. A mechanistic clue comes from a recent paper showing that activated S6K1 binds more tightly to Mdm2, inhibiting Mdm2-mediated p53 ubiquitination and thus stabilizing p53-dependent DNA damage signaling [72]. Accordingly, suppression of mTOR-S6K1 signaling as occurring under DR would lead to Mdm2 nuclear transduction, activate p53 degradation and reduce thus signaling towards apoptosis and/or senescence.

In conclusion, the data are compatible with the idea that reduction of cellular senescence is a primary effect of DR, possibly mediated via suppression of signaling through mTOR-S6K1, and that this reduction in turn might be sufficient to account for the improvement of mitochondrial function and reduction of ROS production that are known to occur under DR.

METHODS

Animals. From a group of 90 male C57/BL mice aged 14.2 ± 1.2 months, 45 animals were subjected to DR, while the other 45 animals, matched for body mass, food intake and age, served as ad libitum-fed (AL)

controls. The experiment lasted for 3 months with an average food restriction of 26%. All mice were sacrificed at the end of the experiment. Five mice per group were perfused by whole animal fixation with 4% paraformaldeyde followed by dissection. Tissues were paraffin-embedded and 5μm sections were prepared from small intestine and liver. Tissues from five additional mice per group were frozen in OTC for cryosectioning. Tissues from further animals were frozen in liquid N_2. The intestinal mucosa was stripped from the muscle layer before freezing. Further details of the experimental protocol can be found as supplementary material, Tab. S1. The project was approved by the Faculty of Medical Sciences Ethical Review Committee, Newcastle University.

Histochemistry, Immunofluorescence, Telomere Q-FISH and telomerase activity. Sen-β-Gal histo-chemistry, immunohistochemistry and telomere Q-FISH were performed as described [28]. The antibodies used and the dilution factors were: anti-γ-H2A.X (#9718, Cell Signalling, Herts, UK, 1:250), anti-PCNA (#ab27Abcam, Cambridge, UK, 1:1,000) and anti-4-HNE (#MHH-030n, Japan Institute for the Control of Aging, Japan, 1:500). Incubation with all primary antibodies was overnight at 4^{o}C.

For double immunofluorescence, blocked sections were incubated with anti-PCNA and anti- γ-H2A.X anti-bodies together in PBS at 4^{0}C overnight and incubated with Alexa-555-conjugated goat anti-rabbit antibody and biotinylated anti-mouse antibody for 45 min in PBS. Subsequently, tissue sections were washed 3 times and incubated with 0.2% Fluorescein Avidin-DCS in PBS for 30min. Images were taken in a Leica DM5500B microscope with 40x objective. 30-40 crypts were scored for each animal.

Telomerase activity was measured using the TeloTAGGG Telomerase PCR ELISA kit (Roche) according to the manufacturer's recommendations.

Autofluorescence. Autofluorescence was measured on unstained, non-deparaffinized tissue sections using a Leica DM5500B microscope. The sample was excited at 458nm and fluorescence emission captured above 475nm.

8-oxodG. The base oxidation product 8-oxo-7,8-dihydro-2'-deoxyguanosine (8-oxodG) was detected by HPLC with electrochemical detection (ECD). Ground frozen tissues (30-100 mg, n=4-9 per group) were thawed and genomic DNA was obtained using standard phenol extraction [73]. The DNA extraction procedure was optimized to minimize artificial induction of 8-oxodG, by using radical-free phenol, minimizing exposure to oxygen and by addition of 1 mM deferoxamine mesylate and 20 mM TEMPO (2,2,6,6-tetramethylpiperidine-N-oxyl), according to the European Standards Committee on Oxidative DNA Damage [74]. HPLC-ECD was based on a method described earlier [75]. Briefly, 30 μg DNA was digested to deoxyribonucleosides by treatment with nuclease P1 [0.02 U/μl] for 90min at 37 ^{o}C and subsequently with alkaline phosphatase [0.014 U/μl]. for 45min at 37 ^{o}C. The digest was then injected into a Gynkotek 480 isocratic pump (Gynkotek, Bremen, Germany) coupled with a Midas injector (Spark Holland, Hendrik Ido Ambacht, the Netherlands) and connected to an Supelcosil^{TM} LC-18S column (250 X 4.6 mm) (Supelco Park, Bellefonte, PA) and an electrochemical detector (Antec, Leiden, the Netherlands). The mobile phase consisted of 10% aqueous methanol containing 94 mM KH_2PO_4, 13 mMK_2HPO_4, 26 mM NaCl and 0.5 mM EDTA. Elution was performed at a flow rate of 1.0 ml/min with a lower absolute detection limit of 40 fmol for 8-oxo-dG, or 1.5 residues/10^6 2'-deoxyguanosine (dG). dG was simultaneously monitored at 260 nm.

Nitrotyrosine measurement. Ground frozen tissues (8-32mg, n=5 per group) were thawed and total protein was extracted using Microplate BCA^{TM} protein assay kit (Thermo Scientific, UK). Nitrotyrosine was detected by oxiSelect^{TM} Nitrotyrosine ELISA kit (Cell Biolabs, INC, UK) according to the protocol provided by the manufacturer.

H_2O_2 release. Ground frozen tissue was homogenized in PBS and used immediately for the assay. The rate of hydrogen peroxide release was monitored fluoro-metrically as resorufin formation due to oxidation of Amplex Red (10-acetyl-3,7-dihydroxyphenoxazine, purchased from Invitrogen, 50μM) in the presence of horseradish peroxidase (2U/ml), at an excitation 544 nm and an emission 590 nm using a FLUOstar Omega (BMG Labtech). Superoxide dismutase (75U/ml) was included in the assay buffer. The slope was converted into the rate of hydrogen peroxide release with a standard curve. Protein concentration was measured using Bio-Rad DC protein assay kit.

ACKNOWLEDGMENTS

We thank Adele Kitching and Julie Wallace for technical support with the mice; Dr Glyn Nelson for his technical support in the nitrotyrosine measurement and Lou M. Maas for his technical support in the 8-oxodG analysis. This work was funded by BBSRC and EPSRC (CISBAN). Part of the work was subsidized by the Centre for Brain Ageing and Vitality, which is funded

through the Lifelong Health and Wellbeing cross council initiative by the MRC, BBSRC, EPSRC and ESRC.

CONFLICT OF INTERESTS STATEMENT

The authors of this manuscript have no conflict of interests to declare.

REFERENCE

1. Masoro EJ. Dietary restriction: current status. Aging (Milano) 2001; 13: 261-262

2. Liao CY, Rikke BA, Johnson TE, Diaz V, Nelson JF. Genetic variation in the murine lifespan response to dietary restriction: from life extension to life shortening. Aging Cell 2010; 9: 92-95

3. Shanley DP, Kirkwood TB. Caloric restriction does not enhance longevity in all species and is unlikely to do so in humans. Biogerontology 2006; 7: 165-168

4. Yu BP. Aging and oxidative stress: modulation by dietary restriction. Free Radic Biol Med 1996; 21: 651-668

5. Sohal RS, Weindruch R. Oxidative stress, caloric restriction, and aging. Science 1996; 273: 59-63

6. Zainal TA, Oberley TD, Allison DB, Szweda LI, Weindruch R. Caloric restriction of rhesus monkeys lowers oxidative damage in skeletal muscle. FASEB J 2000; 14: 1825-1836

7. Guo ZM, Yang H, Hamilton ML, Van Remmen H, Richardson A. Effects of age and food restriction on oxidative DNA damage and antioxidant enzyme activities in the mouse aorta. Mech Ageing Dev 2001; 122: 1771-1786

8. Gredilla R, Barja G. Minireview: the role of oxidative stress in relation to caloric restriction and longevity. Endocrinology 2005; 146: 3713-3717

9. Anderson RM, Weindruch R. Metabolic reprogramming in dietary restriction. Interdiscip Top Gerontol 2007; 35: 18-38

10. Lipman RD, Smith DE, Bronson RT, Blumberg J. Is late-life caloric restriction beneficial? Aging (Milano) 1995; 7: 136-139

11. Spindler SR. Rapid and reversible induction of the longevity, anticancer and genomic effects of caloric restriction. Mech Ageing Dev 2005; 126: 960-966

12. Pugh TD, Oberley TD, Weindruch R. Dietary intervention at middle age: caloric restriction but not dehydroepiandrosterone sulfate increases lifespan and lifetime cancer incidence in mice. Cancer Res 1999; 59: 1642-1648

13. Volk MJ, Pugh TD, Kim M, Frith CH, Daynes RA, Ershler WB, Weindruch R. Dietary restriction from middle age attenuates age-associated lymphoma development and interleukin 6 dysregulation in C57BL/6 mice. Cancer Res 1994; 54: 3054-3061

14. Weindruch R, Walford RL. Dietary restriction in mice beginning at 1 year of age: effect on life-span and spontaneous cancer incidence. Science 1982; 215: 1415-1418

15. Dhahbi JM, Kim HJ, Mote PL, Beaver RJ, Spindler SR. Temporal linkage between the phenotypic and genomic responses to caloric restriction. Proc Natl Acad Sci U S A 2004; 101: 5524-5529

16. Kubo C, Johnson BC, Day NK, Good RA. Calorie source, calorie restriction, immunity and aging of (NZB/NZW)F1 mice. J Nutr 1984; 114: 1884-1899

17. Means LW, Higgins JL, Fernandez TJ. Mid-life onset of dietary restriction extends life and prolongs cognitive functioning. Physiol Behav 1993; 54: 503-508

18. Anderson RM, Shanmuganayagam D, Weindruch R. Caloric restriction and aging: studies in mice and monkeys. Toxicol Pathol 2009; 37: 47-51

19. Racette SB, Weiss EP, Villareal DT, Arif H, Steger-May K, Schechtman KB, Fontana L, Klein S, Holloszy JO. One year of caloric restriction in humans: feasibility and effects on body composition and abdominal adipose tissue. J Gerontol A Biol Sci Med Sci 2006; 61: 943-950

20. Hayflick L, Moorhead PS. The serial cultivation of human diploid cell strains. Exp Cell Res 1961; 25: 585-621

21. Rodier F, Coppe JP, Patil CK, Hoeijmakers WA, Munoz DP, Raza SR, Freund A, Campeau E, Davalos AR, Campisi J. Persistent DNA damage signalling triggers senescence-associated inflammatory cytokine secretion. Nat Cell Biol 2009; 11: 973-979

22. Kuilman T, Peeper DS. Senescence-messaging secretome: SMS-ing cellular stress. Nat Rev Cancer 2009; 9: 81-94

23. Passos JF, Nelson G, Wang C, Richter T, Simillion C, Proctor CJ, Miwa S, Olijslagers S, Hallinan J, Wipat A, Saretzki G, Rudolph KL, Kirkwood TB, et al. Feedback between p21 and reactive oxygen production is necessary for cell senescence. Mol Syst Biol 2010; 6: 347

24. Dimri GP, Lee X, Basile G, Acosta M, Scott G, Roskelley C, Medrano EE, Linskens M, Rubelj I, Pereira-Smith O, et al. A biomarker that identifies senescent human cells in culture and in aging skin in vivo. Proc Natl Acad Sci U S A 1995; 92: 9363-9367

25. Herbig U, Ferreira M, Condel L, Carey D, Sedivy JM. Cellular senescence in aging primates. Science 2006; 311: 1257

26. Krishnamurthy J, Torrice C, Ramsey MR, Kovalev GI, Al-Regaiey K, Su L, Sharpless NE. Ink4a/Arf expression is a biomarker of aging. J Clin Invest 2004; 114: 1299-1307

27. Jeyapalan JC, Ferreira M, Sedivy JM, Herbig U. Accumulation of senescent cells in mitotic tissue of aging primates. Mech Ageing Dev 2007; 128: 36-44

28. Wang C, Jurk D, Maddick M, Nelson G, Martin-Ruiz C, von Zglinicki T. DNA damage response and cellular senescence in tissues of aging mice. Aging Cell 2009; 8: 311-323

29. Chang E, Harley CB. Telomere length and replicative aging in human vascular tissues. Proc Natl Acad Sci U S A 1995; 92: 11190-11194

30. Price JS, Waters JG, Darrah C, Pennington C, Edwards DR, Donell ST, Clark IM. The role of chondrocyte senescence in osteoarthritis. Aging Cell 2002; 1: 57-65

31. Baker DJ, Perez-Terzic C, Jin F, Pitel K, Niederlander NJ, Jeganathan K, Yamada S, Reyes S, Rowe L, Hiddinga HJ, Eberhardt NL, Terzic A, van Deursen JM. Opposing roles for p16Ink4a and p19Arf in senescence and ageing caused by BubR1 insufficiency. Nat Cell Biol 2008; 10: 825-836

32. Choudhury AR, Ju Z, Djojosubroto MW, Schienke A, Lechel A, Schaetzlein S, Jiang H, Stepczynska A, Wang C, Buer J, Lee HW, von Zglinicki T, Ganser A, et al. Cdkn1a deletion improves stem cell function and lifespan of mice with dysfunctional telomeres without accelerating cancer formation. Nat Genet 2007; 39: 99-105

33. Rudolph KL, Chang S, Lee HW, Blasco M, Gottlieb GJ, Greider C, DePinho RA. Longevity, stress response, and cancer in aging telomerase-deficient mice. Cell 1999; 96: 701-712

34. Tyner SD, Venkatachalam S, Choi J, Jones S, Ghebranious N, Igelmann H, Lu X, Soron G, Cooper B, Brayton C, Hee Park S, Thompson T, Karsenty G, et al. p53 mutant mice that display early ageing-associated phenotypes. Nature 2002; 415: 45-53

35. Shelton DN, Chang E, Whittier PS, Choi D, Funk WD. Microarray analysis of replicative senescence. Curr Biol 1999; 9: 939-945

36. Krtolica A, Parrinello S, Lockett S, Desprez PY, Campisi J. Senescent fibroblasts promote epithelial cell growth and tumorigenesis: a link between cancer and aging. Proc Natl Acad Sci U S A 2001; 98: 12072-12077

37. Coppe JP, Patil CK, Rodier F, Sun Y, Munoz DP, Goldstein J, Nelson PS, Desprez PY, Campisi J. Senescence-associated secretory phenotypes reveal cell-nonautonomous functions of oncogenic RAS and the p53 tumor suppressor. PLoS Biol 2008; 6: 2853-2868

38. Campisi J, Sedivy J. How does proliferative homeostasis change with age? What causes it and how does it contribute to aging? J Gerontol A Biol Sci Med Sci 2009; 64: 164-166

39. Tchkonia T, Morbeck D, von Zglinicki T, van Deursen J, Lustgarten J, Scrable H, Koshla S, Jensen MD, Kirkland JL. Fat tissue, aging and cellular senescence. Aging Cell 2010: epub ahead of print.

40. Miller RA. Age-related changes in T cell surface markers: a longitudinal analysis in genetically heterogeneous mice. Mech Ageing Dev 1997; 96: 181-196

41. Messaoudi I, Warner J, Fischer M, Park B, Hill B, Mattison J, Lane MA, Roth GS, Ingram DK, Picker LJ, Douek DC, Mori M, Nikolich-Zugich J. Delay of T cell senescence by caloric restriction in aged long-lived nonhuman primates. Proc Natl Acad Sci U S A 2006; 103: 19448-19453

42. Messaoudi I, Fischer M, Warner J, Park B, Mattison J, Ingram DK, Totonchy T, Mori M, Nikolich-Zugich J. Optimal window of caloric restriction onset limits its beneficial impact on T-cell senescence in primates. Aging Cell 2008; 7: 908-919

43. Spaulding CC, Walford RL, Effros RB. The accumulation of non-replicative, non-functional, senescent T cells with age is avoided in calorically restricted mice by an enhancement of T cell apoptosis. Mech Ageing Dev 1997; 93: 25-33

44. d'Adda di Fagagna F, Reaper PM, Clay-Farrace L, Fiegler H, Carr P, Von Zglinicki T, Saretzki G, Carter NP, Jackson SP. A DNA damage checkpoint response in telomere-initiated senescence. Nature 2003; 426: 194-198

45. Wolf NS, Penn PE, Jiang D, Fei RG, Pendergrass WR. Caloric restriction: conservation of in vivo cellular replicative capacity accompanies life-span extension in mice. Exp Cell Res 1995; 217: 317-323

46. Pendergrass WR, Li Y, Jiang D, Fei RG, Wolf NS. Caloric restriction: conservation of cellular replicative capacity in vitro accompanies life-span extension in mice. Exp Cell Res 1995; 217: 309-316

47. Severino J, Allen RG, Balin S, Balin A, Cristofalo VJ. Is beta-galactosidase staining a marker of senescence in vitro and in vivo? Exp Cell Res 2000; 257: 162-171

48. Kurz DJ, Decary S, Hong Y, Erusalimsky JD. Senescence-associated (beta)-galactosidase reflects an increase in lysosomal mass during replicative ageing of human endothelial cells. J Cell Sci 2000; 113: 3613-3622

49. Kim KS, Kim MS, Seu YB, Chung HY, Kim JH, Kim JR. Regulation of replicative senescence by insulin-like growth factor-binding protein 3 in human umbilical vein endothelial cells. Aging Cell 2007; 6: 535-545

50. Pendergrass WR, Lane MA, Bodkin NL, Hansen BC, Ingram DK, Roth GS, Yi L, Bin H, Wolf NS. Cellular proliferation potential during aging and caloric restriction in rhesus monkeys (Macaca mulatta). J Cell Physiol 1999; 180: 123-130

51. von Zglinicki T, Saretzki G, Ladhoff J, d'Adda di Fagagna F, Jackson SP. Human cell senescence as a DNA damage response. Mech Ageing Dev 2005; 126: 111-117

52. Lawless C, Wang C, Jurk D, Merz A, Zglinicki TV, Passos JF. Quantitative assessment of markers for cell senescence. Exp Gerontol 2010: epub ahead of print

53. Flores I, Canela A, Vera E, Tejera A, Cotsarelis G, Blasco MA. The longest telomeres: a general signature of adult stem cell compartments. Genes Dev 2008; 22: 654-667

54. von Zglinicki T. Oxidative stress shortens telomeres. Trends Biochem Sci 2002; 27: 339-344

55. Macip S, Igarashi M, Fang L, Chen A, Pan ZQ, Lee SW, Aaronson SA. Inhibition of p21-mediated ROS accumulation can rescue p21-induced senescence. EMBO J 2002; 21: 2180-2188

56. Takahashi A, Ohtani N, Yamakoshi K, Iida S, Tahara H, Nakayama K, Nakayama KI, Ide T, Saya H, Hara E. Mitogenic signalling and the p16INK4a-Rb pathway cooperate to enforce irreversible cellular senescence. Nat Cell Biol 2006; 8: 1291-1297

57. Passos JF, Saretzki G, Ahmed S, Nelson G, Richter T, Peters H, Wappler I, Birket MJ, Harold G, Schaeuble K, Birch-Machin MA, Kirkwood TB, von Zglinicki T. Mitochondrial dysfunction accounts for the stochastic heterogeneity in telomere-dependent senescence. PLoS Biol 2007; 5: e110

58. Merry BJ. Oxidative stress and mitochondrial function with aging--the effects of calorie restriction. Aging Cell 2004; 3: 7-12

59. Chen JJ, Yu BP. Alterations in mitochondrial membrane fluidity by lipid peroxidation products. Free Radic Biol Med 1994; 17: 411-418

60. Sitte N, Merker K, Grune T, von Zglinicki T. Lipofuscin accumulation in proliferating fibroblasts in vitro: an indicator of oxidative stress. Exp Gerontol 2001; 36: 475-486

61. Gerstbrein B, Stamatas G, Kollias N, Driscoll M. In vivo spectrofluorimetry reveals endogenous biomarkers that report healthspan and dietary restriction in Caenorhabditis elegans. Aging Cell 2005; 4: 127-137

62. Sohal RS, Marzabadi MR, Galaris D, Brunk UT. Effect of ambient oxygen concentration on lipofuscin accumulation in cultured rat heart myocytes--a novel in vitro model of lipofuscinogenesis. Free Radic Biol Med 1989; 6: 23-30

63. Panda S, Isbatan A, Adami GR. Modification of the ATM/ATR directed DNA damage response state with aging and long after hepatocyte senescence induction in vivo. Mech Ageing Dev 2008; 129: 332-340

64. Krizhanovsky V, Yon M, Dickins RA, Hearn S, Simon J, Miething C, Yee H, Zender L, Lowe SW. Senescence of activated stellate cells limits liver fibrosis. Cell 2008; 134: 657-667

65. Schilder YD, Heiss EH, Schachner D, Ziegler J, Reznicek G, Sorescu D, Dirsch VM. NADPH oxidases 1 and 4 mediate cellular senescence induced by resveratrol in human endothelial cells. Free Radic Biol Med 2009; 46: 1598-1606

66. Jiang W, Zhu Z, Thompson HJ. Dietary energy restriction modulates the activity of AMP-activated protein kinase, Akt, and mammalian target of rapamycin in mammary carcinomas, mammary gland, and liver. Cancer Res 2008; 68: 5492-5499

67. Selman C, Tullet JM, Wieser D, Irvine E, Lingard SJ, Choudhury AI, Claret M, Al-Qassab H, Carmignac D, Ramadani F, Woods A, Robinson IC, Schuster E, et al. Ribosomal protein S6 kinase 1 signaling regulates mammalian life span. Science 2009; 326: 140-144

68. Zhang H, Hoff H, Marinucci T, Cristofalo VJ, Sell C. Mitogen-independent phosphorylation of S6K1 and decreased ribosomal S6 phosphorylation in senescent human fibroblasts. Exp Cell Res 2000; 259: 284-292

69. Zhuo L, Cai G, Liu F, Fu B, Liu W, Hong Q, Ma Q, Peng Y, Wang J, Chen X. Expression and mechanism of mammalian target of rapamycin in age-related renal cell senescence and organ aging. Mech Ageing Dev 2009; 130: 700-708

70. Korotchkina LG, Leontieva OV, Bukreeva EI, Demidenko ZN, Gudkov AV, Blagosklonny MV. The choice between p53-induced senescence and quiescence is determined in part by the mTOR pathway. Aging (Albany NY) 2010; 2: 344-352

71. Castilho RM, Squarize CH, Chodosh LA, Williams BO, Gutkind JS. mTOR mediates Wnt-induced epidermal stem cell exhaustion and aging. Cell Stem Cell 2009; 5: 279-289

72. Lai KP, Leong WF, Chau JF, Jia D, Zeng L, Liu H, He L, Hao A, Zhang H, Meek D, Velagapudi C, Habib SL, Li B. S6K1 is a multifaceted regulator of Mdm2 that connects nutrient status and DNA damage response. EMBO J 2010; 29:2994-3006

73. Godschalk RW, Maas LM, Van Zandwijk N, van 't Veer LJ, Breedijk A, Borm PJ, Verhaert J, Kleinjans JC, van Schooten FJ. Differences in aromatic-DNA adduct levels between alveolar macrophages and subpopulations of white blood cells from smokers. Carcinogenesis 1998; 19: 819-825

74. ESCODD. Comparison of different methods of measuring 8-oxoguanine as a marker of oxidative DNA damage. Free Radic Res 2000; 32: 333-341

75. de Kok TM, ten Vaarwerk F, Zwingman I, van Maanen JM, Kleinjans JC. Peroxidation of linoleic, arachidonic and oleic acid in relation to the induction of oxidative DNA damage and cytogenetic effects. Carcinogenesis 1994; 15: 1399-1404

SUPPLEMENTAL MATERIAL

Table S1. Characterisation of the experimental cohort

Parameter	Ad libitum (AL)	Dietary restriction (DR)	*P* - value
Mean age at death (months)	17.24±1.20	17.33±1.19	0.822
Animal deaths during experiment other than tumours	3	2	0.738
Macroscopic tumour incidence	6	2	0.150
Mean body mass (g)	39.38±0.37	34.26±2.24	<0.001
Mean food intake (g)	3.59±0.41	2.67±0.00	<0.001
Mean daily body temperature (^{o}C)	35.98±0.11	35.72±0.09	0.002
Mean daily physical activity (arbitrary units)	13.64±2.33	19.63±13.44	0.252

Ninety male mice were taken from a long-established colony of the C57/BL (ICRFa) strain which had been selected for use in studies of intrinsic ageing because it is free from specific age-associated pathologies and thus provides a good general model of ageing (Rowlatt et al 1976).

Mice were housed in cages of groups of 4-6 which did not change from weaning. Mice were provided with sawdust and paper bedding and had *ad libitum* access to water. Mice were divided into 2 groups (N=45/group), matched for age, body mass and food intake. There were eight cages in each group. One group was dedicated to ad libitum (AL) feeding and the other group to dietary restriction (DR). The experiment lasted 3 months.

AL fed mice had access to standard rodent pelleted chow in a hopper at all times (CRM(P), Special Diets Services, Witham, UK). The body mass of each mouse was measured twice a week (±0.01g; Sartorius top-pan balance, Epsom, UK). Body mass of the DR group was always recorded before food was given.
DR mice were offered an average of 26% food restriction relative to the AL group. Mean body mass and food intake were calculated across the whole experiment.

7 mice were culled or found dead in the cage during the experiment (4 AL and 3 DR). AL animals that were culled during the experiment for reasons other than tumors were due to paralysis and bladder stones and one was found dead in the cage with the cause unknown. DR animals were culled due to peritonitis in both cases. One AL mouse was culled due to a tail tumor and 1 DR mouse was culled due to a kidney tumor during the experiment. The other macroscopic tumors were noted when dissecting. Tumors in AL mice were found in the liver, kidney, pancreas, small intestine and colon. One tumor was located in the pancreas of DR mouse when dissecting.

Prior to the experiment, one mouse in each cage (N=8AL and N=8DR) was implanted intraperitoneally with a wireless E-mitter (Model PDT-4000 E-Mitter, Mini-Mitter, OR, USA) to monitor body temperature and activity continuously *in vivo*. Mean values were calculated over the whole duration of the experiment.

At the end of the experiment all mice were dissected. Tissues from five mice per group were frozen for cryosectioning (mean age of AL: 17.80±1.10mo and DR: 17.60±1.34mo, $P = 0.803$) and five mice per group were fixed in 4% paraformaldeyde by whole animal perfusion followed by dissection (all aged exactly 17 mo).

REFERENCE

Rowlatt C, Chesterman FC, Sheriff U. Lifespan, age changes and tumour incidence in an ageing C57BL mouse colony. Laboratory Animals. 1976; 10: 419-442.

Editorial

TP53 and MTOR crosstalk to regulate cellular senescence

Lorenzo Galluzzi[1-3], Oliver Kepp[1-3] and Guido Kroemer[1,4-7]

[1]INSERM, U848, F-94805 Villejuif, France
[2]Institut Gustave Roussy, F-94805 Villejuif, France
[3]Université Paris-Sud, Paris 11, F-94805 Villejuif, France
[4]Metabolomics Platform, Institut Gustave Roussy, F-94805 Villejuif, France
[5]Centre de Recherche des Cordoliers, F-75005 Paris, France
[6]Pôle de Biologie, Hôpital Européen Georges Pompidou, AP-HP, F-75908 Paris, France
[7]Université Paris Descartes, Paris 5, F-75270 Paris, France

Key words: *Aging; cancer; DNA damage response; nutlin; p21; rapamycin*
Received: *09/16/10; accepted: 09/18/10; published on line: 09/18/10* doi:10.18632/aging.100202
Corresponding author: *Guido Kroemer, PhD;* ***E-mail:*** *kroemer@orange.fr*

Abstract: The full spectrum of activities of the tumor suppressor p53 (TP53) has not been completely elucidated yet. Recently, it was demonstrated that TP53 communicates with the metabolic regulator mechanistic target of rapamycin (MTOR) to determine whether stressed cells undergo cell death, reversible quiescence or irreversible senescence, thereby adding yet another level of complexity to the signaling network that emanate from TP53.

The oncosuppressor *TP53*, which is mutated or inactivated in more than 50% of all human neoplasms, is widely known for its ability to orchestrate a transcriptional stress response that can have multiple outcomes including senescence and cell death [1]. Thus, in reaction to a wide array of adverse conditions (*e.g.*, DNA damage, oncogene deregulation), the TP53 protein gets stabilized by post-translational modifications and can transactivate cell cycle-arresting and/or lethal genes like *CDKN1A* (better known as $p21^{CIP1}$) and/or genes that code for pro-apoptotic members of the BCL2 protein family (*e.g.*, *BAX*, *BBC3*), respectively [1]. TP53 has also been shown to exert a number of extranuclear activities [2], including the induction of mitochondrial membrane permeabilization [3], the inhibition of autophagy [4] and the degradation of double-stranded RNA [5].

Recently, Demidenko and colleagues demonstrated that TP53 can convert CDKN1A-induced irreversible senescence into reversible quiescence through a mechanism that involves the central regulator of autophagy mechanistic target of rapamycin (MTOR) [6]. Similar to rapamycin (which is well known for its anti-aging effects) [7], the accumulation of post-translationally unmodified, transactivation-proficient (but not transactivation-deficient) TP53 resulted in MTOR inhibition and senescence suppression [6]. These results suggest that TP53 can exert cell cycle-arresting and senescence-suppressing functions that can be uncoupled, at least in selected experimental settings.

Intrigued by these observations, Leontieva *et al.* have studied the response of immortalized WI-38 human lung fibroblasts to nutlin-3a (an inhibitor of the interaction between TP53 and its major negative regulator HDM2) and doxorubicin (a DNA damaging agent) [8]. In line with previous results [9], low concentrations of doxorubicin induced a prolonged cell cycle arrest and were highly efficient in driving WI-38 cells into senescence, which by definition is irreversible. On the contrary, both high doses of doxorubicin and nutlin-3a promoted quiescence, a reversible cell cycle arrest that can be overcome upon the removal of the triggering stimulus.

At the biochemical level, low doses of doxorubicin induced a modest accumulation of TP53 and CDKN1A transactivation, but did not inhibit the signaling cascade that emanate from MTOR. In this setting, the cell cycle

arresting activity of TP53 prevailed and cells were driven into senescence [8]. On the other hand, both high doxorubicin concentrations and nutlin-3a provoked TP53 superinduction while inhibiting MTOR-mediated phosphorylation, a condition that resulted in reversible quiescence in spite of normal CDKN1A transactivation [8]. Notably, the co-administration of high doxorubicin and nutlin-3a led to TP53 hyperaccumulation, complete suppression of MTOR activity, poor transactivation of CDKN1A and cell death. These results indicate that the levels of TP53 and the activation status of the MTOR pathway are critical to determine whether, in non-apoptotic settings, CDKN1A will orchestrate an irreversible or a reversible cell cycle arrest [8].

Both TP53 and MTOR are known for their autophagy-modulatory functions. While nuclear TP53 stimulates autophagy by transactivating several pro-autophagic genes, both cytoplasmic TP53 and MTOR tonically inhibit the autophagic flow [4]. Nutlin-3a-mediated senescence suppression (which proceeds through TP53 superinduction and MTOR inhibition) requires the transcriptional functions of TP53, implying that at least one, thus far elusive, TP53 target protein is responsible for TP53 senescence-suppressing functions [6]. One such TP53-responsive protein is sestrin 2, which can inhibit MTOR [10] and hence induce autophagy [11, 12]. However, the exact nature of the relevant p53 target(s) that regulate the switch between senescence and quiescence remains elusive.

Based on the fascinating results obtained by Leontieva *et al.* [8], it can be speculated that nuclear TP53 might simultaneously transactivate the cell cycle-arresting factor CDKN1A and one or more hitherto unidentified anti-senescence (and perhaps pro-autophagic?) protein(s) that would operate similar to rapamycin, through the inhibition of MTOR. How would then the senescence-inducing activity of TP53 prevail over TP53-mediated senescence suppression (and *vice versa*)? As a possibility, the promoter of *CDKN1A* might display a high affinity for TP53, while the promoter of the TP53 target that suppresses MTOR activity might require high TP53 concentrations for efficient transactivation. This hypothesis takes into consideration the fact that CDKN1A is induced at similar levels by both low and high doses of doxorubicin, as well as by low and high concentrations of nutlin-3a [8]. In this scenario, the accumulation of TP53 beyond a low threshold would activate CDKN1A-mediated senescence (Figure 1A), whereas high levels of TP53 would be required for the ignition of a senescence-suppressing program that (once started) would always prevail over the effects of CDKN1A (Figure 1B).

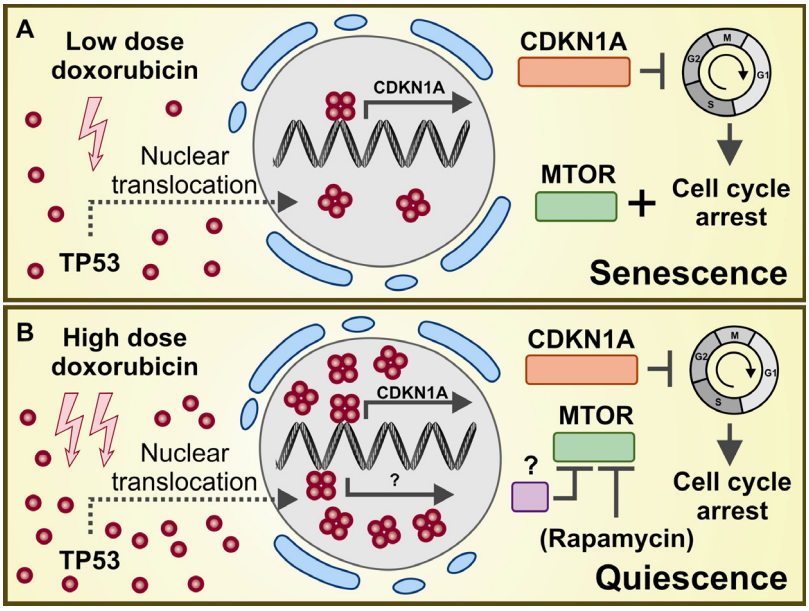

Figure 1. TP53 levels determine whether CDKN1A will orchestrate irreversible senescence or quiescence. (**A**) Low doses of doxorubicin are sufficient to trigger TP53-mediated transactivation of the cell cycle-arresting protein CDKN1A. Under conditions in which the MTOR pathway is active, prolonged cell cycle arrest results in irreversible senescence. (**B**) High doxorubicin concentrations (or nutlin-3a alone or in combination with low doses of doxorubicin) not only drive TP53-mediated CDKN1A transactivation but might also result in the induction of one (or more) senescence-suppressing factors. In this scenario, MTOR activity is suppressed and CDKN1A-mediated cell cycle arrest is reversible (quiescence). By pharmacologically inhibiting MTOR, rapamycin also exerts senescence-suppressing functions.

Further experimental work is urgently required to confirm or invalidate this hypothesis. Beyond these unresolved details, the work by Leontieva *et al.* added yet another important piece to the ever-growing TP53 puzzle.

ACKNOWLEDGEMENTS

GK is supported by the Ligue Nationale contre le Cancer (Equipe labellisé), Agence Nationale pour la Recherche (ANR), European Commission (Active p53, Apo-Sys, ChemoRes, ApopTrain), Fondation pour la Recherche Médicale (FRM), Institut National du Cancer (INCa), Cancéropôle Ile-de-France and AXA Research Fund. LG and OK are supported by the Apo-Sys consortium of the European Union and Association pour la Recherche sur le Cancer (ARC), respectively.

REFERENCES

1. Levine AJ, Oren M. The first 30 years of p53: growing ever more complex. Nat Rev Cancer. 2009; 9: 749-758.

2. Green DR, Kroemer G. Cytoplasmic functions of the tumour suppressor p53. Nature. 2009; 458: 1127-1130.

3. Morselli E, Galluzzi L, Kroemer G. Mechanisms of p53-mediated mitochondrial membrane permeabilization. Cell Res. 2008; 18: 708-710.

4. Maiuri MC, Galluzzi L, Morselli E, Kepp O, Malik SA, Kroemer G. Autophagy regulation by p53. Curr Opin Cell Biol. 2010; 22: 181-185.

5. Galluzzi L, Kepp O, Kroemer G. A new role for cytoplasmic p53: Binding and destroying double-stranded RNA. Cell Cycle. 2010; 9: 13: 2491-2492.

6. Demidenko ZN, Korotchkina LG, Gudkov AV, Blagosklonny MV. Paradoxical suppression of cellular senescence by p53. Proc Natl Acad Sci U S A. 2010; 107: 9660-9664.

7. Madeo F, Tavernarakis N, Kroemer G. Can autophagy promote longevity? Nat Cell Biol. 2010; 12: 842-846.

8. Leontieva OV, Gudkov AV, Blagosklonny MV. Weak p53 permits senescence during cell cycle arrest. Cell Cycle. 2010: 9: in press.

9. Chang BD, Broude EV, Dokmanovic M, Zhu H, Ruth A, Xuan Y, et al. A senescence-like phenotype distinguishes tumor cells that undergo terminal proliferation arrest after exposure to anticancer agents. Cancer Res. 1999; 59: 3761-3767.

10. Budanov AV, Karin M. p53 target genes sestrin 1 and sestrin 2 connect genotoxic stress and mTOR signaling. Cell. 2008; 134: 451-460.

11. Criollo A, Dessen P, Kroemer G. DRAM: a phylogenetically ancient regulator of autophagy. Cell Cycle. 2009; 8: 2319-2320.

12. Maiuri MC, Malik SA, Morselli E, Kepp O, Criollo A, Mouchel PL, et al. Stimulation of autophagy by the p53 target gene Sestrin 2. Cell Cycle. 2009; 8: 1571-1576.

Research Paper

The choice between p53-induced senescence and quiescence is determined in part by the mTOR pathway

Lioubov G. Korotchkina, Olga V. Leontieva, Elena I. Bukreeva, Zoya N. Demidenko, Andrei V. Gudkov and Mikhail V. Blagosklonny

Department of Cell Stress Biology, Roswell Park Cancer Institute, BLSC, L3-312, Buffalo, NY 14263, USA

Key words: *p53, senescence, rapamycin, mTOR, cancer, cell cycle*
Received: *06/05/10; accepted: 06/23/10; published on line: 06/25/10* doi:10.18632/aging.100160
Corresponding author: *blagosklonny@oncotarget.com*

Abstract: Transient induction of p53 can cause reversible quiescence and irreversible senescence. Using nutlin-3a (a small molecule that activates p53 without causing DNA damage), we have previously identified cell lines in which nutlin-3a caused quiescence. Importantly, nutlin-3a caused quiescence by actively suppressing the senescence program (while still causing cell cycle arrest). Noteworthy, in these cells nutlin-3a inhibited the mTOR (mammalian Target of Rapamycin) pathway, which is known to be involved in the senescence program. Here we showed that shRNA-mediated knockdown of TSC2, a negative regulator of mTOR, partially converted quiescence into senescence in these nutlin-arrested cells. In accord, in melanoma cell lines and mouse embryo fibroblasts, which easily undergo senescence in response to p53 activation, nutlin-3a failed to inhibit mTOR. In these senescence-prone cells, the mTOR inhibitor rapamycin converted nutlin-3a-induced senescence into quiescence. We conclude that status of the mTOR pathway can determine, at least in part, the choice between senescence and quiescence in p53-arrested cells.

INTRODUCTION

Depending on the cell type and other factors p53 activation can result in apoptosis, reversible (quiescence) and irreversible (senescence) cell cycle arrest [1-8]. While the choice between apoptosis and cell cycle arrest has been intensively scrutinized, the choice between quiescence and senescence was not systematically addressed and remains elusive. In order to observe whether p53 activation causes either senescence or quiescence, others and we employed nutlin-3a. Nutlin-3a, a small molecular therapeutic, inhibits Mdm2/p53 interaction and induces p53 at physiological levels without causing DNA damage [9-11]. It was reported that nutlin-3a caused senescent morphology and permanent loss of proliferative potential [12, 13]. However, in other cell lines nutlin-3a caused quiescence so that cells resumed proliferation, when nutlin-3a was removed [14-16]. Moreover, we recently reported that in human fibroblasts (WI-38tert) and fibrosarcoma cells (HT-1080-p21-9), in which nutlin-3a caused quiescence [16], p53 acted as a suppressor of senescence [17]. Thus, ectopic expression of p21 in these cells caused senescence, while simultaneous induction of p53 converted senescence into quiescence [17]. In agreement with previous reports [18-20], we found that p53 inhibited the mTOR pathway [17]. Importantly, the mTOR pathway is involved in cellular senescence [21-26]. We suggested that p53-mediated arrest remains reversible as long as p53 inhibits mTOR. If this model is correct, then senescence would occur in those cells, in which p53 is incapable of suppressing mTOR. Here we provide experimental evidence supporting this prediction and demonstrate that irreversibility of p53-mediated arrest may result from its failure to suppress the mTOR pathway.

RESULTS

Depletion of TSC2 favors senescence by p53

We have shown that nutlin-3a caused quiescence in HT-p21-9 cells and WI-38tert cells [16]. In these cells, nutlin-3a actively suppressed senescence and this suppression was associated with inhibition of the mTOR pathway by p53 [17]. Next, we investigated whether nutlin-3a can cause senescence in cells lacking tuberous sclerosis 2 (TSC2) (Figure 1A), given that regulation of mTOR by p53 requires TSC2 [18]. The transduced cells were transiently treated with nutlin-3a as shown (Figure 1B). The Tsc2-depleted cells acquired a large/flat morphology and could not resume proliferation, whereas cells treated with vector and nutlin-3a did not become senescent and resumed proliferation, forming colonies after removal of nutlin-3a (Figure 1C-D). The potency of shTSC2 with different sequences varied and two other shTSC2 were less potent but still depleted TSC2 at some time points (Supplemental Figure 1) and partially decreased the proliferative potential in nutlin-3a-arrested cells (Supplemental Figure 1).

We next extended this observation to WI-38tert cells transduced with shTSC2 (Figure 2A). In control, nutlin-3a caused a lean morphology, a characteristic of quiescence [16]. Depletion of TSC2 by shTSC2 converted quiescent morphology to senescent morphology (Figure 2B). Furthermore, this was associated with permanent loss of proliferative potential (Figure 2C). In control, cells resumed proliferation after removal of nutlin-3a, whereas nutlin-3a caused permanent loss of proliferative potential in shTSC2-treated cells (Figure 2C). In agreement with our results, it was previously observed that knockout of Tsc2 cooperates with p53 in induction of cellular senescence in MEFs [27].

Nutlin-3 causes senescence in Mel-10 and -9 cells

We next wished to identify senescence-prone cells, which undergo senescence in response to nutlin-3a. In MEL-10 and Mel-9, two melanoma-derived cell lines, nutlin-3a induced p53 and p21 (Figure 3A) and caused senescent morphology (Figure 3B) and cells did not resume proliferation, when nutlin-3a was removed (Supplemental Figure 2). In contrast, rapamycin did not cause senescent morphology and cells resumed proliferation, when rapamycin was removed (Figure 3B and Supplemental Figure 2). Unlike rapamycin, nutlin-3a did not inhibit S6 phosphorylation (Figure 3A), a marker of rapamycin-sensitive mTOR activity.

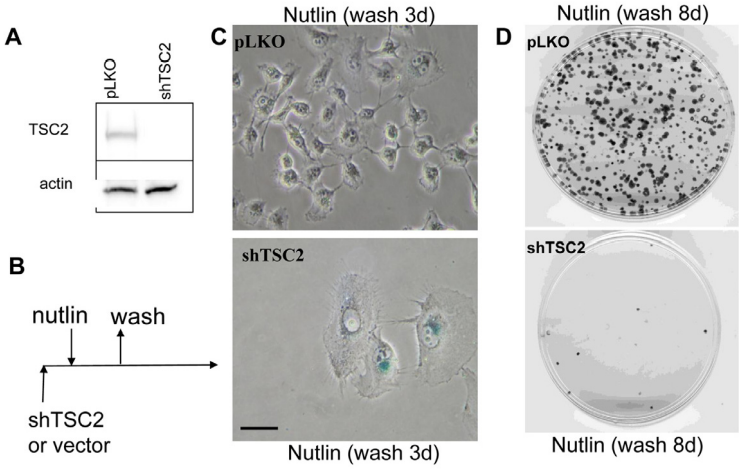

Figure 1. Depletion of TSC2 converts quiescence into senescence in HT-p21-9 cells. (**A**) HT-p21-9 cells were transduced with control lentivirus (pLKO) or lentivirus expressing shTSC2 (sequence # 10) and selected with puromycin for 5 days and then immunoblot was performed. (**B**) Schema: Testing the reversibility of nutlin-3a effects. (**C**) HT-p21-9 cells were transduced with control pLKO or shTSC2 and 5000 cells were plated in 24-well plates and, the next day, were treated with 10 uM nutlin-3a for 3 days. Then nutlin-3a was washed out and the cells were cultivated in fresh medium for 3 days and then stained for beta-Gal and microphotographed. Bars 50 um. (**D**) HT-p21-9 cells were transduced with control pLKO or shTSC2 (and selected for 4 days with puromycin). Then 1000 cells were plated per 60-mm dishes and, the next day, were treated with nutlin-3a for 3 days. Then nutlin-3a was washed out and cells were cultivated in fresh medium for 8 days. Colonies were stained with crystal violet.

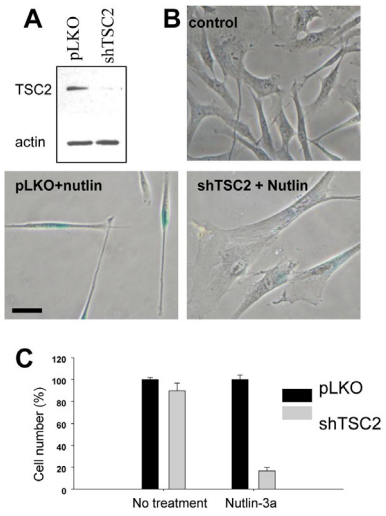

Figure 2. Depletion of TSC2 converts quiescence into senescence in WI-38tert cells. (**A**) Immunoblot. WI-38tert cells were transduced with shTSC or control pLKO and cultured for 5 days. (**B**) WI-38tert cells were transduced with lentiviruses. Next day, medium was replaced and Nutlin (10 uM) with our without rapamycin was added. After 4 days cells were washed and stained for beta-Gal. Bars 50 um. (**C**) WI-38tert cells were transduced with lentiviruses. Next day, medium was replaced and Nutlin (10 uM) was added. After 4 days cells were washed and counted after 6 days.

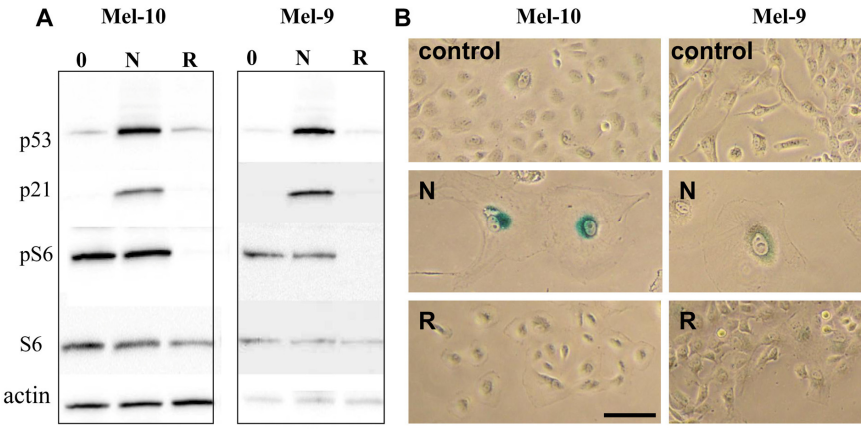

Figure 3. Effects of nutlin-3a and rapamycin on melanoma cells. (A) Mel-10 and Mel-9 cells were incubated with 10 uM nutlin (N) and 500 nM rapamycin (R) for 1 day and immunoblot was performed. (**B)** Mel-10 and Mel-9 cells were incubated with 10 uM nutlin and 500 nM rapamycin for 4 days, then drugs were washed out and cells were incubated for additional 4 days and stained for beta-Gal. Bars 50 um**.**

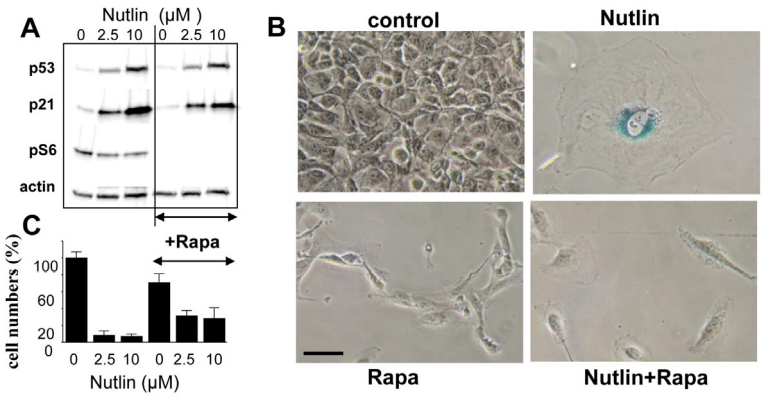

Figure 4. Effect of rapamycin on nutlin-induced senescence in melanoma cells. (A) Mel-10 cells were incubated with 2.5 and 10 uM nutlin with or without 500 nM rapamycin for 1 day and then immunoblot was performed. (**B**) Beta-Gal staining. Mel-10 cells were incubated with 10 M nutlin alone and 500 nM rapamycin for 4 days, then drugs were washed out and cells were incubated for additional 3 days and stained for beta-Gal. Bars 50 um**.**

Rapamycin suppresses nutlin-3a-induced senescence

To establish a causal link between mTOR and senescence, we next investigated whether inhibition of the mTOR pathway by rapamycin could convert nutlin-3a-induced senescence into quiescence. Rapamycin did not affect p53 and p21 induction caused by nutlin-3a but abrogated S6 phosphorylation (Figure 4A), associated with conversion from senescent morphology to quiescent morphology (Figure 4B). Importantly, cells were capable to resume proliferation following removal of nutlin-3a and rapamycin, indicating that the condition was reversible (Figure 4C). Similar results were obtained with Mel-9 cells (data not shown).

Next, we extended this observation to cells of different tissue and species origin. As shown previously, nutlin-3a caused senescence in mouse embryonic fibroblasts (MEFs) [13]. Here we showed that nulin-3a failed to inhibit mTOR pathway in MEF (Figure 5A), and caused senescence (Figure 5 B). Rapamycin inhibited the mTOR pathway and converted senescent morphology to quiescent morphology (Figure 5). This suggests that failure to suppress a rapamycin-sensitive pathway determines nutlin-3a-induced senescence instead of quiescence.

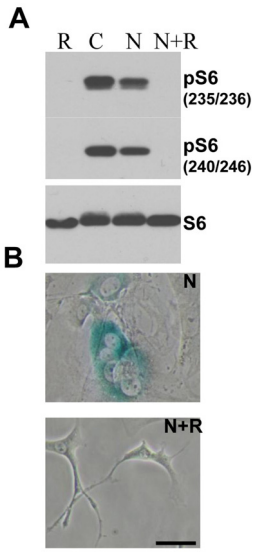

Figure 5. Effect of rapamycin on nutlin-induced senescence in melanoma cells. (**A**) Immunoblot. MEF cells were incubated with 10 nutlin-3a with or without 10 nM rapamycin for 1 day and immunoblot using rabbit anti-phospho-S6 (Ser240/244) and (Ser235/236) and mouse anti-S6 was performed. (**B**) Beta-Gal staining. MEF cells were incubated with 10 uM nutlin alone or with 500 nM rapamycin for 4 days, then drugs were washed out and cells were incubated for additional 4 days and stained for beta-Gal. Bars 50 um**.**

DISCUSSION

The role of p53 in organismal aging and longevity is complex [28-32], indicating that p53 may act as anti-aging factor in some conditions. We have recently de-

monstrated that p53 can suppress cellular senescence, converting it into quiescence [17]. In these quiescence-prone cells, p53 inhibited the mTOR pathway, which is involved in senescence program (Figure 6A). Still p53 induces senescence in numerous cell types. Here we showed that in those cell types, in which nutlin-3a caused senescence, it failed to inhibit the mTOR pathway (Figure 6B). The role of active mTOR as a senescence-inducing factor in these cells was demonstrated by using rapamycin, which partially converted nutlin-3a-induced senescence into quiescence (Figure 6B, lower panel). This indicates that rapamycin-sensitive mTOR activity is necessary for senescence during nutlin-3a-induced cell cycle arrest. And vice versa, in quiescence-prone cells, depletion of TSC2 converted quiescence into senescence (Figure 6A, lower panel). Taken together, data suggest that activation of the mTOR pathway favors senescence (Figure 7). In agreement, Ras accelerated senescence in nutlin-arrested cells [13]. Similarly, activation of Ras and MEK in murine fibroblasts converted p53-induced quiescence into senescence [33]. Interestingly, p53 levels did not correlate with the senescence phenotype, suggesting that factors other than p53 may determine senescence [33]. These important observations are in agreement with our model that senescence requires two factors: cell cycle arrest caused by p53 and simultaneous activation of the growth-promoting mTOR pathway (Note: Ras is an activator of the mTOR pathway). And vice versa it was observed that induction of p53 maintains quiescence upon serum starvation, without causing senescence [34]. In agreement, our model predicts that, by deactivating mTOR, serum starvation prevents senescence.

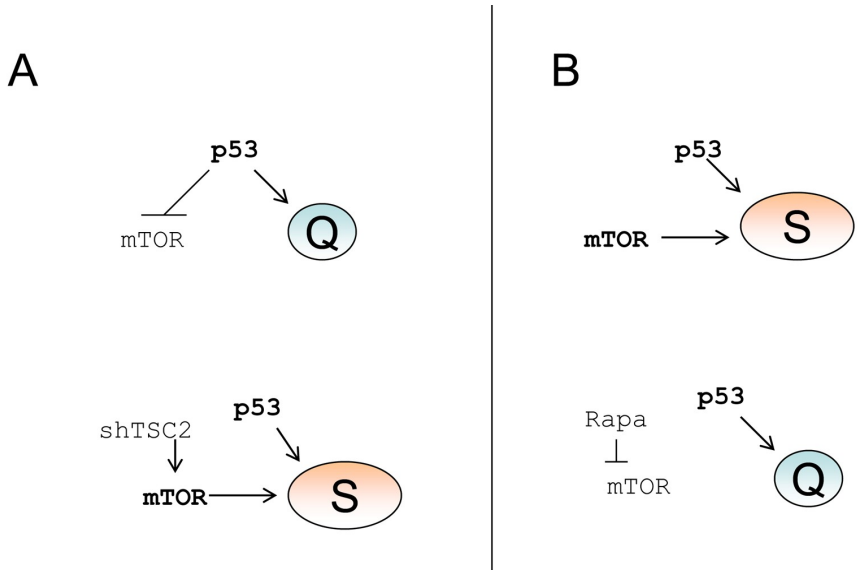

Figure 6. p53 causes senescence by failing to suppress senescence. (**A**) Quiescence-prone cells. Upper panel. P53 causes cell cycle arrest and inhibits the mTOR pathway, thus ensuring quiescence. Lower panel. Transduction of cells with shTSC2 activates mTOR thus converting quiescence into senescence. (**B**) Senescence-prone cells. Upper panel. P53 causes cell cycle arrest without inhibiting the mTOR pathway, thus ensuring senescence. Lower panel. Rapamycin inhibits mTOR thus converting senescence into quiescence

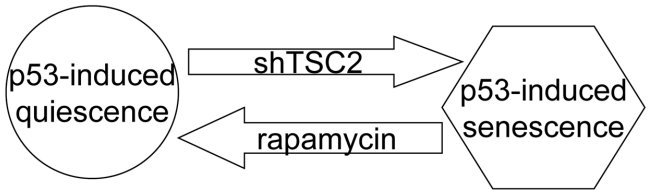

Figure 7. Activation of the mTOR pathway favors senescence in nutlin-3a-arrested cells

Another factor that favors senescence is the duration of cell cycle arrest [13, 35]. Importantly, the duration of the arrest may exceed the duration of treatment with nutlin-3a because of persistent induction of p21 even after removal of nutlin-3a in some cancer cell lines [35]. Additional pathways may be involved in the senescence program. For example, nutlin-3a induces cytoskeletal rearrangement [36]. We speculate that p53 affects not only rapamycin-sensitive mTORC1 but also the mTORC2 complex, given that mTORC2 controls the actin cytoskeleton [37]. Also, p53 inhibits downstream branches of the mTOR pathway [38, 39]. P53 stimulates autophagy [18, 40], which in turn is essential for life-extension by pharmacological manipulations (see [41-44]). Finally, p53 affects cellular metabolism [45-48] and this effect may contribute to suppression of cellular senescence and synergistically potentate metabolic changes caused by mTOR inhibition. The relative contribution of all these mutually dependent factors needs further investigations. The key role of mTOR in cellular senescence links cellular and organismal aging and age-related diseases.

MATERIAL AND METHODS

Cell lines and reagents. HT-p21-9 cells are derivatives of HT1080 human fibrosarcoma cells, where p21 expression can be turned on or off using a physiologically neutral agent isopropyl--thio-galactosidase (IPTG) [16, 49-51]. HT-p21-9 cells express GFP. WI-38-Tert, WI-38 fibroblasts immortalized by telomerase were described previously [16, 17]. Melanoma cell lines, MEL-9 (SK-Mel-103) and MEL-10 (SK-Mel-147), were described previously [52, 53]. RPE cells were described previously [21, 22]. MEF, mouse fibroblasts isolated from 13-day embryos, were provided by Marina Antoch (RPCI) and maintained in DMEM supplemented with 10% FCS. Rapamycin (LC Laboratories, MA, USA), IPTG (Sigma-Aldrich, St. Louis, MO), nutlin-3a (Sigma-Aldrich) were used as previously described [17].

Lentiviral shRNA construction. Bacterial glycerol stocks [clone NM_000548.2-1437s1c1 (#10), NM_000548.x-4581s1c1 (#7) and NM_000548.2-4551s1c1 (#9)] containing lentivirus plasmid vector pLKO.1-puro with shRNA specific for TSC2 was purchased from Sigma. The targeting sequences are: CCGGGCTCATCAACAGGCAGTTCTACTCGAGTA GAACTGCCTGTTGATGAGCTTTTTG(#10),CCGG CAATGAGTCACAGTCCTTTGACTCGAGTCAAAG GACTGTGACTCATTGTTTTTG (#7) and CCGGCG ACGAGTCAAACAAGCCAATCTCGAGATTGGCTT GTTTGACTCGTCGTTTTTG (#9).

pLKO.1-puro lentiviral vector without shRNA was used as a control. Lentiviruses were produced in HEK293T cells after co-transfection of lentivirus plasmid vector with shRNA or control vector with packaging plasmids using Lipofectamine2000 (Invitrogen). After 48h and 72h medium containing lentivirus was collected, centrifuged at 2000g and filtered through 0.22 uM filter. Filtered virus containing medium was used for cell infection or stored at -80 C. Cells were transduced with lentivirus in the presence of 8 mg/ml polybrene and selected with puromycin (1-2 mg/ml) for 4-6 days. Cells were treated with drugs either 24h after transduction or after puromycin selection for infected cells.

Colony formation assay. Plates were fixed and stained with 1.0 % crystal violet (Sigma-Aldrich).

Immunoblot analysis. The following antibodies were used: anti-p53 and anti-p21 antibodies from Cell signaling and anti-actin antibodies from Santa Cruz Biotechnology, rabbit anti-phospho-S6 (Ser240/244) and (Ser235/236), mouse anti-S6, mouse anti-phospho-

p70 S6 kinase (Thr389), mouse anti-p21, rabbit anti-phospho-4E-BP1 (Thr37/46) from Cell Signaling; mouse anti-4E-BP1 from Invitrogen; mouse anti-p53 (Ab-6) from Calbiochem.

Beta-galactosidase staining. beta-Gal staining was performed using Senescence -galactosidase staining kit (Cell Signaling Technology) according to manufacturer's protocol.

CONFLICT OF INTERESTS STATEMENT

The authors of this manuscript have no conflict of interests to declare.

REFERENCES

1. Vogelstein B, Lane DP, Levine AJ. Surfing the p53 network. Nature 2000; 408: 307-310.

2. Itahana K, Dimri G, Campisi J. Regulation of cellular senescence by p53. Eur J Biochem 2001; 268: 2784-2791.

3. Vousden KH. Outcomes of p53 activation--spoilt for choice. J Cell Sci 2006; 119: 5015-5020.

4. Vousden KH, Prives C. Blinded by the Light: The Growing Complexity of p53. Cell 2009; 137: 413-431.

5. Levine AJ, Oren M. The first 30 years of p53: growing ever more complex. Nat Rev Cancer 2009; 9: 749-758.

6. Brown CJ, Lain S, Verma CS, Fersht AR, Lane DP. Awakening guardian angels: drugging the p53 pathway. Nat Rev Cancer 2009; 9: 862-873.

7. Liebermann DA, Hoffman B, Vesely D. p53 induced growth arrest versus apoptosis and its modulation by survival cytokines. Cell Cycle 2007; 6: 166-170.

8. Paris R, Henry RE, Stephens SJ, McBryde M, Espinosa JM. Multiple p53-independent gene silencing mechanisms define the cellular response to p53 activation. Cell Cycle 2008; 7: 2427-2433.

9. Vassilev LT. Small-molecule antagonists of p53-MDM2 binding: research tools and potential therapeutics. Cell Cycle 2004; 3: 419-421.

10. Vassilev LT, Vu BT, Graves B, Carvajal D, Podlaski F, Filipovic Z, Kong N, Kammlott U, Lukacs C, Klein C, Fotouhi N, Liu EA. In vivo activation of the p53 pathway by small-molecule antagonists of MDM2. Science 2004; 303: 844-848.

11. Huang B, Vassilev LT. Reduced transcriptional activity in the p53 pathway of senescent cells revealed by the MDM2 antagonist nutlin-3. Aging 2009; 1: 845-854.

12. Van Maerken T, Speleman F, Vermeulen J, Lambertz I, De Clercq S, De Smet E, Yigit N, Coppens V, Philippé J, De Paepe A, Marine JC, Vandesompele J. Small-molecule MDM2 antagonists as a new therapy concept for neuroblastoma. Cancer Res. 2006; 66: 9646-9655.

13. Efeyan A, Ortega-Molina A, Velasco-Miguel S, Herranz D, Vassilev LT, Serrano M. Induction of p53-dependent senescence by the MDM2 antagonist nutlin-3a in mouse cells of fibroblast origin. Cancer Res. 2007; 67: 7350-7357.

14. Huang B, Deo D, Xia M, Vassilev LT. Pharmacologic p53 Activation Blocks Cell Cycle Progression but Fails to Induce Senescence in Epithelial Cancer Cells. Mol Cancer Res. 2009; 7: 1497-1509.

15. Cheok CF, Kua N, Kaldis P, Lane DP. Combination of nutlin-3 and VX-680 selectively targets p53 mutant cells with reversible effects on cells expressing wild-type p53. Cell Death Differ. 2010; in press.

16. Korotchkina LG, Demidenko ZN, Gudkov AV, Blagosklonny MV. Cellular quiescence caused by the Mdm2 inhibitor nutlin-3a. Cell Cycle 2009; 8: 3777-3781.

17. Demidenko ZN, Korotchkina LG, Gudkov AV, Blagosklonny MV. Paradoxical suppression of cellular senescence by p53. Proc Natl Acad Sci U S A 2010; 9660-4: 9660-9664.

18. Feng Z, Zhang H, Levine AJ, Jin S. The coordinate regulation of the p53 and mTOR pathways in cells. Proc Natl Acad Sci U S A 2005; 102: 8204-8209.

19. Budanov AV, Karin M. p53 target genes sestrin1 and sestrin2 connect genotoxic stress and mTOR signaling. Cell 2008; 134: 451-460.

20. Matthew EM, Hart LS, Astrinidis A, Navaraj A, Dolloff NG, Dicker DT, Henske EP, El-Deiry WS. The p53 target Plk2 interacts with TSC proteins impacting mTOR signaling, tumor growth and chemosensitivity under hypoxic conditions. Cell Cycle 2009; 8: 4168-4175.

21. Demidenko ZN, Blagosklonny MV. Growth stimulation leads to cellular senescence when the cell cycle is blocked. Cell Cycle 2008; 7: 3355-3361.

22. Demidenko ZN, Zubova SG, Bukreeva EI, Pospelov VA, Pospelova TV, Blagosklonny MV. Rapamycin decelerates cellular senescence. Cell Cycle 2009; 8: 1888-1895.

23. Demidenko ZN, Shtutman M, Blagosklonny MV. Pharmacologic inhibition of MEK and PI-3K converges on the mTOR/S6 pathway to decelerate cellular senescence. Cell Cycle 2009; 8: 1896-1900.

24. Demidenko ZN, Blagosklonny MV. At concentrations that inhibit mTOR, resveratrol suppresses cellular senescence. Cell Cycle 2009; 8: 1901-1904.

25. Demidenko ZN, Blagosklonny MV. Quantifying pharmacologic suppression of cellular senescence: prevention of cellular hypertrophy versus preservation of proliferative potential. Aging 2009; 1: 1008-1016.

26. Pospelova TV, Demidenko ZN, Bukreeva EI, Pospelov VA, Gudkov AV, Blagosklonny MV. Pseudo-DNA damage response in senescent cells. Cell Cycle 2009; 8: 4112-4118.

27. Zhang H, Cicchetti G, Onda H, Koon HB, Asrican K, Bajraszewski N, Vazquez F, Carpenter CL, Kwiatkowski DJ. Loss of Tsc1/Tsc2 activates mTOR and disrupts PI3K-Akt signaling through downregulation of PDGFR. J Clin Invest. 2003; 112: 1223-1233.

28. Matheu A, Maraver A, Klatt P, Flores I, Garcia-Cao I, Borras C, Flores JM, Vina J, Blasco MA, Serrano M. Delayed ageing through damage protection by the Arf/p53 pathway. Nature 2007; 448: 375-379.

29. Waskar M, Landis GN, Shen J, Curtis C, Tozer K, Abdueva D, Skvortsov D, Tavare S, Tower J. Drosophila melanogaster p53 has developmental stage-specific and sex-specific effects on adult life span indicative of sexual antagonistic pleiotropy. Aging 2009; 1: 903-936.

30. Biteau B, Jasper H. It's all about balance: p53 and aging. Aging 2009; 1: 884-886.

31. Hur JH, Walker DW. p53, sex, and aging: lessons from the fruit fly. Aging 2009; 1: 881-883.
32. Donehower LA. Longevity regulation in flies: a role for p53. Aging 2009; 1: 6-8.
33. Ferbeyre G, de Stanchina E, Lin AW, Querido E, McCurrach ME, Hannon GJ, Lowe SW. Oncogenic ras and p53 cooperate to induce cellular senescence. Mol Cell Biol. 2002; 22: 3497-3508.
34. Itahana K, Dimri GP, Hara E, Itahana Y, Zou Y, Desprez PY, Campisi J. A role for p53 in maintaining and establishing the quiescence growth arrest in human cells. J Biol Chem 2002; 277: 18206-18214.
35. Shen H, Maki CG. Persistent p21 expression after Nutlin-3a removal is associated with senescence-like arrest in 4N cells. J Biol Chem 2010.
36. Moran DM, Maki CG. Nutlin-3a induces cytoskeletal rearrangement and inhibits the migration and invasion capacity of p53 wild-type cancer cells. Mol Cancer Ther 2010; 9: 895-905.
37. Jacinto E, Loewith R, Schmidt A, Lin S, Ruegg MA, Hall A, Hall MN. Mammalian TOR complex 2 controls the actin cytoskeleton and is rapamycin insensitive. Nat Cell Biol 2004; 6: 1122-1128.
38. Constantinou C, Clemens MJ. Regulation of the phosphorylation and integrity of protein synthesis initiation factor eIF4GI and the translational repressor 4E-BP1 by p53. Oncogene 2005; 24: 4839-4850.
39. Constantinou C, Elia A, Clemens MJ. Activation of p53 stimulates proteasome-dependent truncation of eIF4E-binding protein 1 (4E-BP1). Biol Cell 2008; 100: 279-289.
40. Maiuri MC, Malik SA, Morselli E, Kepp O, Criollo A, Mouchel PL, Carnuccio R, Kroemer G. Stimulation of autophagy by the p53 target gene Sestrin2. Cell Cycle 2009; 8: 1571-1576.
41. Morselli E, Galluzzi L, Kepp O, Criollo A, Maiuri MC, Tavernarakis N, Madeo F, Kroemer G. Autophagy mediates pharmacological lifespan extension by spermidine and resveratrol. Aging 2009; 1: 961-970.
42. Alvers AL, Wood MS, Hu D, Kaywell AC, Dunn WA, Jr., Aris JP. Autophagy is required for extension of yeast chronological life span by rapamycin. Autophagy 2009; 5: 847-849.
43. Bjedov I, Toivonen JM, Kerr F, Slack C, Jacobson J, Foley A, Partridge L. Mechanisms of life span extension by rapamycin in the fruit fly Drosophila melanogaster. Cell Metab 2010; 11: 35-46.
44. Hands SL, Proud CG, Wyttenbach A. mTOR's role in ageing: protein synthesis or autophagy? Aging 2009; 586-597.
45. Vousden KH, Ryan KM. p53 and metabolism. Nat Rev Cancer 2009; 9: 691-700.
46. Feng Z, Levine AJ. The regulation of energy metabolism and the IGF-1/mTOR pathways by the p53 protein. Trends Cell Biol 2010;
47. Hu W, Zhang C, Wu R, Sun Y, Levine A, Feng Z. Glutaminase 2, a novel p53 target gene regulating energy metabolism and antioxidant function. Proc Natl Acad Sci U S A 107: 7455-7460.
48. Suzuki S, Tanaka T, Poyurovsky MV, Nagano H, Mayama T, Ohkubo S, Lokshin M, Hosokawa H, Nakayama T, Suzuki Y, Sugano S, Sato E, Nagao T, Yokote K, Tatsuno I, Prives C. Phosphate-activated glutaminase (GLS2), a p53-inducible regulator of glutamine metabolism and reactive oxygen species. Proc Natl Acad Sci U S A 107: 7461-7466.
49. Chang BD, Broude EV, Dokmanovic M, Zhu H, Ruth A, Xuan Y, Kandel ES, Lausch E, Christov K, Roninson IB. A senescence-like phenotype distinguishes tumor cells that undergo terminal proliferation arrest after exposure to anticancer agents. Cancer Res. 1999; 59: 3761-3767.
50. Chang BD, Broude EV, Fang J, Kalinichenko TV, Abdryashitov R, Poole JC, Roninson IB. p21Waf1/Cip1/Sdi1-induced growth arrest is associated with depletion of mitosis-control proteins and leads to abnormal mitosis and endoreduplication in recovering cells. Oncogene 2000; 19: 2165-2170.
51. Broude EV, Swift ME, Vivo C, Chang BD, Davis BM, Kalurupalle S, Blagosklonny MV, Roninson IB. p21(Waf1/Cip1/Sdi1) mediates retinoblastoma protein degradation. Oncogene 2007; 26: 6954-6958.
52. Mannava S, Grachtchouk V, Wheeler LJ, Im M, Zhuang D, Slavina EG, Mathews CK, Shewach DS, Nikiforov MA. Direct role of nucleotide metabolism in C-MYC-dependent proliferation of melanoma cells. Cell Cycle 2008; 7: 2392-2400.
53. Zhuang D, Mannava S, Grachtchouk V, Tang WH, Patil S, Wawrzyniak JA, Berman AE, Giordano TJ, Prochownik EV, Soengas MS, Nikiforov MA. C-MYC overexpression is required for continuous suppression of oncogene-induced senescence in melanoma cells. Oncogene 2008; 27: 6623-6634.

SUPPLEMENTAL FIGURES

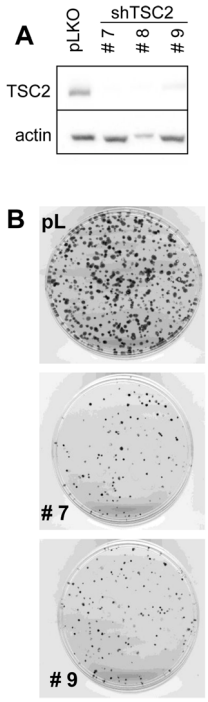

Supplemental Figure 1. Depletion of TSC2 converts quiescence into senescence in HT-p21-9 cells. (**A**) HT-p21-9 cells were transduced with control lentivirus (pLKO) or lentivirus expressing shTSC2 (sequence # 7, 8, 9) and selected with puromycin for 10 days and then immunoblot was performed. (**B**) HT-p21-9 cells were transduced with control pLKO or shTSC2 (and selected for 4 days with puromycin). Then 1000 cells were plated per 60-mm dishes and, the next day, were treated with nutlin-3a for 3 days. Then nutlin-3a was washed out and cells were cultivated in fresh medium for 8 days. Colonies were stained with crystal violet.

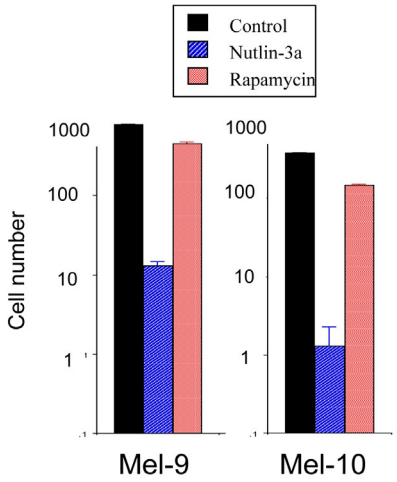

Supplemental Figure 2. Irreversible and reversible effects of nutlin-3a and rapamycin: Mel-10 and Mel-9 cells were incubated with 10 uM nutlin (N) and 500 nM rapamycin (R) for 4 day and then nutlin-3a was washed. After a week, cells were counted.

Commentary

Another "Janus paradox" of p53: induction of cell senescence versus quiescence

Zbigniew Darzynkiewicz

New York Medical College, Valhalla, NY 10595, USA

***Commentary on**: Korotchkina et al. Aging 2010; this issue*
***Received:** 06/23/10; accepted: 06/25/10; published on line: 06/27/10* doi:10.18632/aging.100165
***E-mail:** z_darzynkiewicz@nymc.edu*

No other protein shows such multiplicity and diversity of functions as the tumor suppressor p53 [1,2]. Initially, the role of p53 as "the guardian of the cellular genome" was considered to be providing protection from progression to malignancy. This was mediated by its function as a transcription factor of the genes controlling cell cycle and apoptosis [3]. Subsequent studies have identified a large variety of diverse genes regulated by p53. Among them are the genes modulating cellular senescence, DNA repair, oxidative stress, longevity, angiogenesis, differentiation, glycolysis, tumor motility and invasion, and even bone remodeling [1,2]. Independently of its transcription-regulatory mechanism p53 can also directly interact with proteins of Bcl2 family controlling the execution of apoptotic response [4].

It was recently reported that induction of cell senescence by ectopic expression of p21 and doxorubicin when combined with upregulation of p53 by inhibition of Mdm2, mediated by nutlin-3a, led to cell quiescence. The quiescence was reversible: upon removal of nutlin-3a the cells reentered the cell cycle [5]. This observation prompted the authors to postulate the use of Mdm2 antagonists in conjunction with chemotherapy to reversibly arrest normal cells, thereby protecting them from the drugs targeting cell cycle progression (cyclotherapy) [5]. Consistent with this observation were findings that p53 plays an important role in regulating stem cell quiescence, self-renewal and aging [6].

What is the mechanism by which p53 converts the cell response to the ectopic expression of p21 (cell cycle arrest) from senescence to quiescence? In recent studies Demidenko et al., addressed this question and in elegant experiments the authors demonstrated the "paradoxical" capabilities of p53, one to suppress cell senescence by inducing quiescence and another, already known, to induce senescence [7]. Suppression of senescence paralleled by induction of quiescence by p53 required its transactivation function, and in analogy to rapamycin, was mediated, at least in part, by inhibition of mTOR pathway [8]. Further evidence on the involvement of mTOR pathway in the direction the cell undertakes to become either senescent or quiescent is provided in the article in the current issue of Aging [9] consistent with their prior findings, the authors in this article report that induction of cell cycle arrest in the WI-38-tert or HT-1080-p21 cells, in which nutlin-3a inhibited mTOR, led to quiescence rather than senescence. In contrast, augmentation of mTOR pathway led to induction of senescence [9]. The data collectively suggest that in the process of induction of cells senescence or quiescence the primary role of p53 is in arresting cells in the cell cycle. However, the ongoing cell growth (rRNA synthesis) in the arrested cells mediated by mTOR pathway is the deciding factor as to whether they undergo senescence (mTOR activation) or quiescence (mTOR inhibition). The factor responsible for the apparent "paradoxical" properties of p53 was the dual and separate function of this protein, one arresting cells in cell cycle and another, inhibiting mTOR [7].

Senescent cells are characterized by large cell/nuclear size and "flattened" morphology, a characteristic feature of growth imbalance. It was shown before that cellular content of RNA (of which 95% is rRNA) in cycling cells is > 10-fold higher than in quiescent cells [10]. In

contrast, the induction cell cycle arrest associated with the senescent phenotype is paralleled by several-fold rise in rRNA abundance [11]. It is also known that mTOR pathway regulates the synthesis of ribosomal components including the transcription and processing of pre-rRNA, expression of ribosomal proteins and the synthesis of 5SRNA [12]. The critical role of mTOR is thus in adjusting the ribosome biogenesis and overall protein biosynthetic capacity (cell growth) to the signaling through the growth factors pathway and coordinating it with the rate of cell cycle progression. Within this context cell senescence can be characterized as the uncoupling of the rate of cell cycle progression and cell growth mediated by mTOR. Of interest is the observation that mTOR activity is accelerated in hematopoietic stem cells from old mice compared to young mice prompting the authors to suggest that mTOR inhibitors can be used to rejuvenate aging hematopoietic cells [13].

Not disregarded should be a possibility of regulation of cell senescence by p53 via induction of autophagy. Here again the diverse "paradoxical" properties of p53 have been observed, namely the induction of autophagy upon activation and expression of this protein above the basal level and inhibition of autophagy after its induction to the basal level [14]. This "paradoxical" effect of p53, which on the surface appears to be contradictory, was metaphorically compared with the two-faced Roman mythology God and named The "Janus of Autophagy" [15]. Considering how extensively intertwined are the pathways of autophagy, senescence, apoptosis and aging the elucidation of the mechanisms involved in the induction of senescence versus quiescence by p53 is additionally complicated. Inhibition of mTOR while it enhances autophagy and thus is expected to delay senescence may also be lethal to cancer cells [16]. Further studies are needed to resolve how the "Janus of Autophagy relates to the "Janus of Cell Senescence" or to the "Janus of Cell Quiescence".

REFERENCES

1. Vousden KH, Prives C. Cell 2009; 137:413-431.
2. Pietsch EC, Sykes SM, McMahon SB, Murphy ME. Oncogene 2008; 27:6507-6521.
3. Vogelstein B, Lane D, Levine AJ. Nature 2000, 408:307-310.
4. Moll UM, Wolff S, Speidel D, Deppert W. Curr Opin Cell Biol 2005; 17:631-636.
5. Korotchkina LG, Demidenko ZN, Gudkov AV, Blagosklonny MV. Cell Cycle 2009; 8:3777-81.
6. Liu Y, Elf SE, Asai T et al., Cell Cycle 2009; 8:3120-4
7. Demidenko ZN, Korotchkina LG, Gudkov AV, Blagosklonny MV. Proc Natl Acad Sci USA, 2010; 107: 9660-9664.
8. Demidenko ZN et al. Cell Cycle 2009; 8:1888-1895.
9. Korotchkina LG Leontieva OV, Bukreeva EI, Demidenko ZN, Gudkov AV, and Blagosklonny MV. Aging. 2010: this issue
10. Darzynkiewicz Z, Sharpless T, Staiano-Coico L, Melamed MR. Proc Natl Acad Sci USA 1980; 77:6696-6700.
11. Crissman HA, Darzynkiewicz Z, Tobey RA, Steinkamp JA. J Cell Biol 1985; 101:141-147.
12. Mayer C, Grummt I. Oncogene 2006; 25:6384-6391.
13. Chen C, Liu Y, Liu Y, Zheng P. Sci Signal 2009; Nov 2; 2 (98):ra75
14. Tasdemir E, Maiuri MC, Orhon I *et al.,* Cell Cycle 2008; 7: 3006-3011.
15. Levine B, Abrams J. Nat Cell Biol 2008; 10:637-639.
16. Sini P, Jamed D, Chresta C, Guichard S. Autophagy 2010 May 2;6(4) Epub.

Commentary

mTOR favors senescence over quiescence in p53-arrested cells

Thaddeus T. Schug

Laboratory of Signal Transduction, National Institute of Environmental Health Sciences, National Institutes of Health, Research Triangle Park, NC 27709, USA

***Commentary on**: Korotchkina et al. Aging 2010; this issue*
***Received:** 06/22/10; accepted: 06/25/10; published on line: 06/26/10* doi:10.18632/aging.100164
***E-mail:** Schugt@niehs.nih.gov*

The p53 tumor suppressor protein controls cell fate by inducing apoptosis or cell cycle arrest in response to cell stress [1]. Cell cycle arrest can be temporary (quiescent) or permanent (senescent) depending on p53 regulation [2,3]. Under normal conditions, p53 binds to MDM2, which transports the protein to the cytoplasm where it undergoes rapid proteosomal degradation. A class of chemotherapeutic molecules called Nutlins inhibit p53-MDM2 interaction, and can therefore be used to control p53 activity in cancer cells [4]. In this issue of Aging, Korotchkina et al make use of nutlin-3a to dissect the mechanism by which p53 induces cellular senescence and quiescence [5]. The group demonstrates that p53-mediated senescence is irreversible in cells that maintain mTOR (mammalian target of rapamycn) signaling. However, when mTOR signaling is inhibited, activation of p53 leads to quiescence (Figure 1). These findings may have broad implications because the mTOR pathway is dysregulated in many forms of cancer [6].

Establishing the mechanisms involved in cell cycle arrest and cell dormancy is critical for understanding cancer cell proliferation. Demidenko et al. have previously demonstrated that despite its ability to induce cell cycle arrest, in some cell types p53 is a suppressor, not an inducer of cellular senescence [7]. They have also shown that cells (HT-p21-9) induced into senescence using an ITPG-inducible p21 expression construct, were converted to quiescence in the presence of p53. In the same cells, nutlin-3a-induction of p53 caused reversible cell cycle arrest, and cells resumed proliferation after removal of nutlin-3a.

The same group has also demonstrated that when the cell cycle is blocked, activation of mTOR is required for induction of senescence. Addition of the TOR inhibitor rapamycin converted p21-induced senescent cells back to quiescence [7]. These findings suggest that activation of p53 sets in motion cell cycle arrest, after which its ability to exercise senescence is dependent on its interaction with the mTOR pathway. Senescence is achieved if p53 is incapable of disabling mTOR. Therefore, activating both mTOR and p53 in order to achieve a permanent state of cell dormancy, may prove to be a promising therapeutic strategy for treating cancer. In their current study, Korotchkina et al further explore the role of mTOR as a senescence-inducing factor. They show that nutlin-3a-induced senescent cells converted to a quiescent state when mTOR was inactivated with rapamycin (Figure 1). Furthermore, the authors show that in p53-mediated quiescent cells, depletion of TSC2, a negative regulator of mTOR, results in conversion to senescence. This body of work may also offer explanations as to the role that p53 plays in aging. Others have shown that p53 function declines with age [8,9], and mild activation of p53 may increase the lifespan of mice [10]. It will be interesting to further determine the interactions between p53 and mTOR in both models of cancer and aging.

REFERENCES

1. Junttila MR, Evan GI. Nat Rev Cancer 2009; 9:821-829.
2. Vogelstein B, Lane D, Levine AJ. Nature 2000; 408:307-310.
3. Vousden, Prives C. Cell 2009; 137:413-431.
4. Vassilev LT. Cell Cycle 2004; 3:419-421.
5. Korotchkina LG, Leontieva OV, Bukreeva LI et al. Aging 2010; 2: this issue
6. Beevers CS, Li F, Liu L, Huang S. Int J Cancer 2006; 119:757-64.
7. Demidenko ZN, Korotchkina LG, Gudkov AV, Blagosklonny MV. Proc Natl Acad Sci USA 2009; 107:9660-9664.
8. Feng Z, Hu W, Rajagopal G, Levine AJ. 2008. Cell Cycle 2008; 7:842-847.

9. Feng Z, Hu W, Teresky AK et al. Proc Natl Acad Sci U S A 2007; 104:16633-8.
10. Matheu A, Maraver A, Klatt P et al. Nature 2007; 448:375-9.

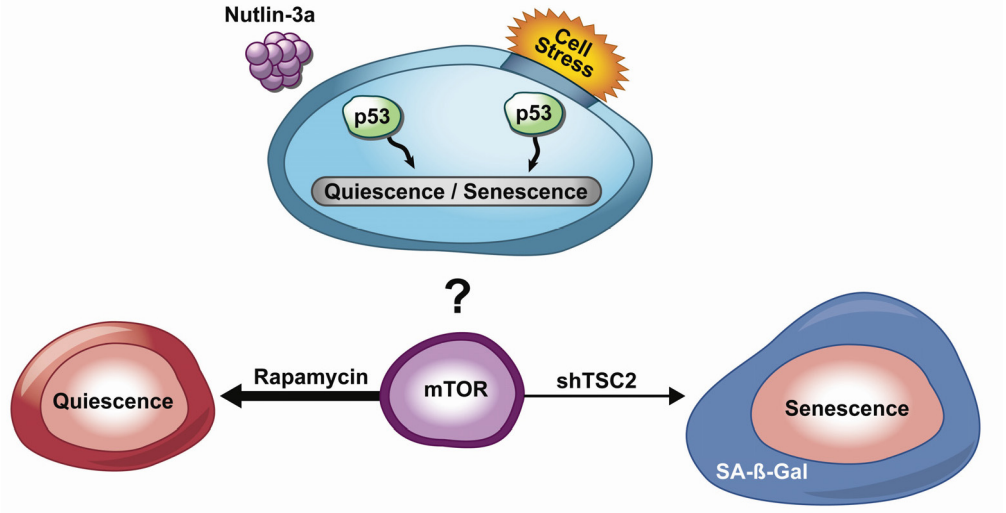

Figure 1. p53-induced senescence or quiescence. Cell stress factors or nutlin-3a activates p53. Rapamycin treatment inhibits mTOR signaling and cells enter a reversible quiescent state. ShTSC2-mediated activation of mTOR sends cells into senescence.

Research paper

Quantifying pharmacologic suppression of cellular senescence: prevention of cellular hypertrophy versus preservation of proliferative potential

Zoya N. Demidenko and Mikhail V. Blagosklonny

Oncotarget, Buffalo, NY 14263, USA
Department of Cell Stress Biology, Roswell Park Cancer Institute, Buffalo, NY 14263

Running title: *Measure of aging suppression*
Key words: *cellular senescence, cellular hypertrophy, aging-suppression, rapamycin, mTOR*
Correspondence: *Mikhail V. Blagosklonny, MD, PhD, Professor, Department of Cell Stress Biology, Roswell Park Cancer Institute, BLSC, L3-312, Elm and Carlton Streets, Buffalo, NY 14263, USA*
Received: *05/25/09; accepted: 12/ 30/ 09; published on line:12/31/09* doi:10.18632/aging.100115
E-mail: *Blagosklonny@oncotarget.com*

Abstract: Development of agents that suppress aging (aging suppressants) requires quantification of cellular senescence. Cellular senescence *in vitro* is characterized by a large cell morphology and permanent loss of proliferative potential. When HT-1080 cells were arrested by p21, they continued to grow exponentially in size and became hypertrophic with a 15-fold increase in the protein content per cell. These changes were mirrored by accumulation of GFP (driven by CMV promoter) per cell, which also served as a marker of cellular hypertrophy. Preservation of proliferative potential (competence) was measured by an increase in live cell number, when p21 was switched off. While modestly decreasing hypertrophy in p21-arresrted cells, rapamycin considerably preserved competence, converting senescence into quiescence. Preservation of proliferative potential (competence) correlated with inhibition of S6 phosphorylation by rapamycin. When p21 was switched off, competent cells, by resuming proliferation, became progressively less hypertrophic. Preservation of proliferative potential is a sensitive and quantitative measure of suppression of mTOR-driven senescence.

INTRODUCTION

In cell culture, cellular senescence is usually defined as a state of irreversible cell cycle arrest [1, 2]. Hence, cellular senescence is sometimes confused with growth inhibition. Here we will use the term 'growth' as an increase in cellular mass, regardless of whether cells proliferate or not. Intriguingly, Ras, MEK and serum, which stimulate growth-promoting pathways, contribute to and facilitate cellular senescence [3-6]. In theory, cellular senescence is caused by inappropriate activation of growth-promoting pathways, when actual growth is impossible [7, 8]. In proliferating cells, growth-promoting mTOR (Target of Rapamycin) and MAPK (Mitogen-activated Protein Kinase) pathways drive both cellular mass growth and cell cycle progression. When the cell cycle is blocked by either p21 or p16, growth-stimulation via mTOR leads to cellular senescence [9]. Serum withdrawal, PI-3K, mTOR and MEK inhibitors, all decreased mTOR activity and prevented permanent loss of proliferative potential [10, 11]. The term "permanent loss of proliferative potential" means that, even when p21 and p16 were shut off, cells cannot resume proliferation [12]. Inhibitors of mTOR such as rapamycin preserved proliferative potential [9-11]. To avoid confusions, we stress that rapamycin does not stimulate proliferation, does not abrogate cell cycle arrest caused by p21 and does not force cells to by-pass cell cycle arrest. Rapamycin converts senescence (an

irreversible condition) into quiescence (a reversible condition). It is still unknown whether rapamycin suppresses senescence in a dose-dependent manner and whether this suppression correlates with the degree of mTOR inhibition.

Another common marker of cell senescence is a large cell morphology (hypertrophy). Cellular hypertrophy is usually measured as a cell diameter. Given that volume (or cell mass) is proportional to the cube of diameter, then the amount of protein per cell (cell mass) may be a more sensitive parameter than cell diameter. For example if diameter is increased 2-fold, cell mass is increased 8-fold. In theory, cell mass could be estimated as an amount of any fluorescent protein such as green fluorescent protein (GFP), expressed by a constitutive viral promoter such as CMV promoter. If the cell cycle is blocked but cells continue to grow in size, then GFP should accumulate. Here we tested this prediction. Independently from our study, a clone of HT-p21 cells, known as p21-9, had been stably transfected with CMV-EGFP [13, 14, 15] and thus expresses enhanced GFP. We predict that induction of p21 by IPTG should increase GFP per cell, as a marker of cellular hypertrophy. Given cell-doubling time of 20 hours, there should be a 10-14 fold increase in GFP/cell in 3 days. Here, we confirmed this prediction. We further investigated the link between mTOR activity, cellular hypertrophy and loss of proliferative potential. We found that preservation of proliferative (competence) was the most sensitive marker of mTOR inhibition, easily detectable even at concentrations of rapamycin when inhibition of mTOR was marginal.

RESULTS

Exponential mass-growth precedes senescence

A number of proliferating cells increased exponentially (with a doubling time 20-24 h). As previously described, induction of p21 by IPTG caused G1 and G2 arrest [1, 4, 5], completely blocking cell proliferation (Figure 1). p21-arrested cells continued to grow in size, becoming hypertrophic. Since the cells contained CMV-driven EGFP, we measured both protein and GFP. Per well, amounts of GFP and protein were increased almost exponentially with or without IPTG (Figure 2). Per cell, amounts of GFP and protein were increased only for IPTG-treated (non-dividing) cells (Figure 3). For proliferating cells (no IPTG), GFP per cell and protein per cell remained constant (Figure 3), because mass growth was balanced by cell division. In contrast, in IPTG-treated cells, protein/cell and GFP/cell increased almost exponentially for 3 days (Figure 3). During induction of senescence by IPTG, cellular mass continued to increase but was not balanced by cell division. In all cases, protein and GFP correlated (Figure 3), making GFP per cell a convenient marker of cellular hypertrophy.

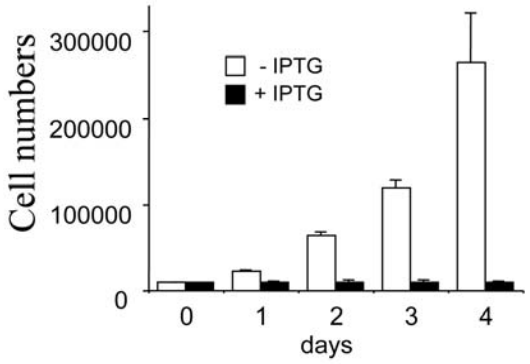

Figure 1. Inhibition of cell proliferation by IPTG. Closed bars: HT-p21 cells were treated with IPTG (+IPTG). Cells do not proliferate. Open bars: Untreated HT-p21 cells. Exponentially proliferating cells. Cells were counted daily.

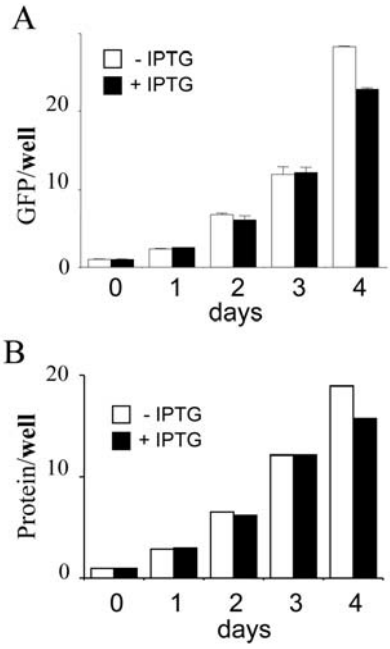

Figure 2. Total cellular mass growth during senescence induction. HT-p21 cells were grown in 60 mm wells and soluble protein and GFP were measured daily. Closed bars: HT-p21 cells were treated with IPTG (+IPTG). Open bars: Untreated HT-p21 cells (-IPTG). In both proliferating (-IPTG) and non-proliferating (+IPTG) conditions, protein per well and GFP per well_were increasing. In panel B, protein was measured in duplicate and shown without standard deviations, therefore statistical difference between –IPTG and + IPTG should not be considered. The panel simply illustrates exponential growth in both conditions.

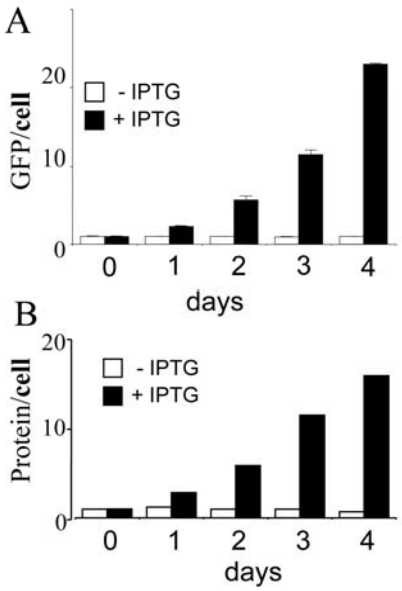

Figure 3. Cellular hypertrophy during senescence induction. HT-p21 cells were grown in 60 mm wells and cell numbers, soluble protein and GFP were measured daily. Closed bars: HT-p21 cells were treated with IPTG (+IPTG). Open bars: Untreated HT-p21 cells (-IPTG). Protein per cell and GFP per cell were constant in proliferating (-IPTG) cells. Protein per cell and GFP per cell increased exponentially in non-proliferating (+IPTG) cells.

Although that was not the goal of our study, our data can explain how induction of p21 can induce GFP without trans-activating CMV promoter: by inhibiting cell cycle without inhibiting cell growth. Furthermore, the notion that GFP per cell is a marker of hypertrophy yields 2 predictions. First, mutant p21 that cannot bind CDKs and thus cannot arrest cell cycle will not induce GFP. Second, anti-hypertrophic agents such as rapamycin will reduce GFP per cell without abrogating cell cycle arrest.

Dose dependent suppression of cellular hypertrophy

We next investigated the effects of rapamycin on hypertrophy of senescent cells. Cells were induced to senesce by IPTG in the presence (+R) or the absence of rapamycin. On days 3 and 5 effects of rapamycin on cellular hypertrophy were evaluated. By microscopy, the anti-hypertrophic effect of rapamycin was the most evident at low cell densities (such as 1000 cells per 60-mm dish) because there was a sufficient space for IPTG-treated cells to grow in size in the absence of rapamycin (Figure 4). However, we could not reliably measure protein levels at such low cell densities. At regular cell densities, rapamycin (500 nM) reduced cellular hypertrophy by 30% -40% (Figure 5A and data not shown). Two markers of hypertrophy (protein/cell and GFP/cell) correlated (Figure 5A). The anti-hypertrophic effect of rapamycin was not statistically significant at concentrations of rapamycin below 20 nM. At first, this was puzzling given that rapamycin inhibits the mTOR pathway at low concentrations in many cell types. Therefore, we investigated a dose response of mTOR inhibition by measuring S6 phosphorylation, a marker of mTOR activity. In agreement with anti-hypertrophic effects, rapamycin inhibited S6 phosphorylation at concentrations 20 nM or higher, achieving maximal effects at 100 nM-500 nM (Figure 5 B). Thus, inhibition of S6 phosphorylation and inhibition of hypertrophy correlated, explaining the requirements of high concentration (100-500 nM) of rapamycin for anti-hypertrophic effects in this particular cell line.

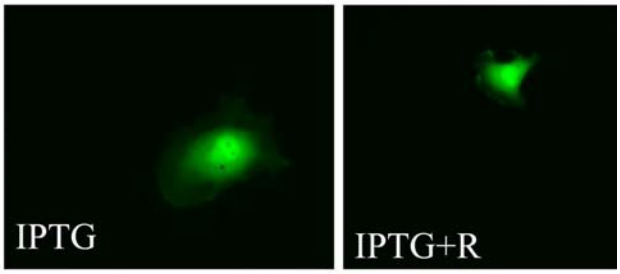

Figure 4. Visualization of cellular hypertrophy. HT-p21 cells express enhanced green fluorescent protein (GFP) under the constitutive viral CMV promoter. Expression of GFP per cell is a marker of cellular hypertrophy. Low cell density – 2 thousand cells were plated in 100 mm dish and treated with either IPTG or IPTG + Rapamacin.

Dose-dependent preservation of cellular competence

Rapamycin preserves proliferative potential in arrested cell, meaning that cells can successfully divide when the arrest is lifted. But rapamycin does not induce proliferation and in contrast can cause quiescence (in some cell types). To clearly distinguish the potential to proliferate (competence) and actual proliferation, we introduce terms competence and incompetence (permanent loss of proliferative potential associated with cellular senescence). In HT-1080 cells, rapamycin preserves competence during cell cycle arrest caused by [10]. Unlike senescent cells, quiescent cells are competent.

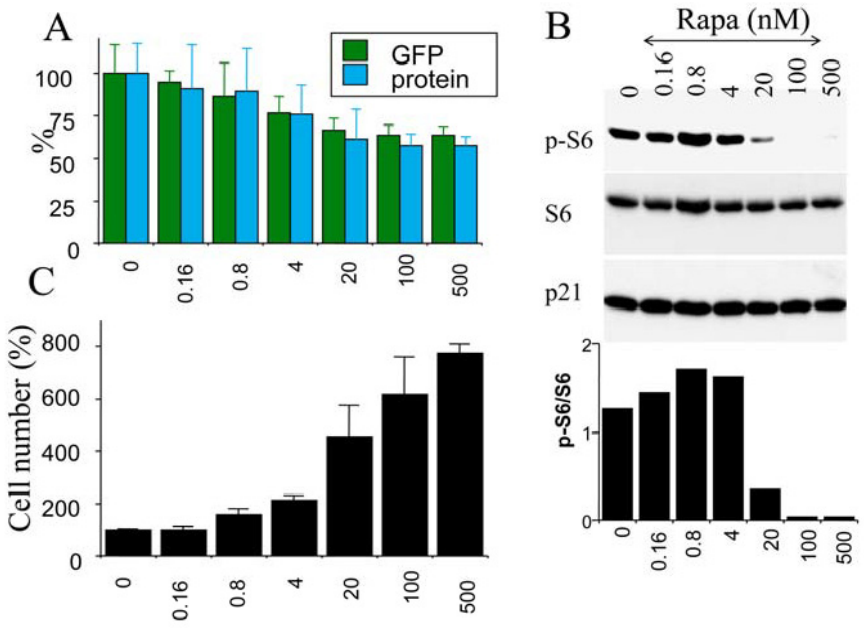

Figure 5. Correlation between S6 phosphorylation, hypertrophy and loss of proliferative potential in senescent cells. HT-p21 cells were plated in 6 well plates and treated with IPTG plus the increasing concentrations of rapamycin (from 0.16 to 500 nM). At concentration 0, cells were treated with IPTG alone. (**A**) Cellular hypertrophy: protein and GFP. After 3 days, soluble protein and GFP were measured per well. [Note: in non-proliferating cells, protein/well is a measure of protein/cells]. Results are shown as percent of IPTG alone (0) without rapamycin. (**B**) After 3 days, cells were lysed and immunobloted for p-S6, S6 and p21. (**C**) PC: preservation of proliferative competence. After 3 days, cells were washed to remove IPTG and RAPA. Cells were incubated for additional 5 days in the fresh medium and then were counted. Results are shown as percent of IPTG alone (0) without rapamycin.

We have demonstrated previously that rapamycin preserved cellular competence (the ability to proliferate after p21 is switched off) in IPTG-arrested HT-p21 cells [10]. We performed these experiments using rapamycin at concentration 500 nM [10], which completely inhibited S6 phosphorylation. Here we determined whether preservation of competence (PC) correlated with inhibition of S6 phosphorylation and the anti-hypertrophic effect of rapamycin. Cells were treated with IPTG and increasing concentrations of rapamycin ranging from 0 to 500 nM (Figure 5 C). After 3 days, IPTG was washed out, thus allowing the cells to proliferate, and after another 5 days cells were counted. As expected, the IPTG-treated cells became incompetent, whereas rapamycin suppressed incompetence (Figure 5 C). Remarkably, preservation of competence was detectable at lower concentrations of rapamycin than those that inhibited either S6 phosphorylation or cellular hypertrophy. In part, such a higher sensitivity of a PC-test compared with inhibition of hypertrophy may be due to the relative magnitudes of the effects (30% inhibition of hypertrophy versus 800% PC). Perhaps even a transient inhibition of mTOR (missed by immunoblot) detectably increased competence. Consistent with this explanation, even when rapamycin was added with delay, preservation of competence was detectable [10].

Exponential proliferation of competent cells

In the presence of IPTG (with or without rapamycin), the cells did not proliferate and did not form colonies. When IPTG was washed out, 3-5% cells remained competent even without rapamycin [10] and Figure 6. Colonies grew in size, while the number of colonies was almost unchanged (Figure 6). Rapamycin increased a number of colonies (a number of competent cells) almost 10- fold. We further compared the proliferative

quality of competent cells remained after treatment with IPTG either without or with rapamycin (I/w and I+R/w, respectively). In I/w and I+R/w conditions, the number of cells started to increase exponentially after 1 day and 3 days, respectively (Figure 7). After 6 days, both curves (I/w and I+R/w) became parallel. The curve "I+R/w" was just shifted to the right on approximately 3 days (Figure 7). This corresponded to a 10-fold difference in an initial number of competent cells, if their doubling time was around one day. Noteworthy, this also corresponds to the initial difference in the number of competent cells as determined by colony formation (Figure 6). Also, both in I/w and I+R/w conditions, doubling time of the competent cells was around 20-24 hours, similar to the proliferative rate of the untreated cells.

Reversal of hypertrophy during proliferation of competent cells

Rapamycin decreased cellular hypertrophy approximately 30% in IPTG treated cells (Figure 5A). When IPTG and rapamycin were washed out, there was a lag period about 24-30 hrs for competent cells to undergo first division (supplementary movie will be available at). During the lag period, cells grew in size, because rapamycin was washed out. Consequently, as measured by GFP per cell (Figure 8A), rapamycin-treated cells reached the size of the cells treated with IPTG alone (Figure 8A: I/w and I+R/w at day one). Similarly, as measured by protein per cell, the cells treated with IPTG plus rapamycin become fully hypertrophic at day one after wash (data not shown). Despite regaining hypertrophy, IPTG+rapamycin-treated cells remained competent (Figures 6, 7). This indicates that hypertrophy was not a cause of proliferative incompetence in IPTG-treated cells. When competent cells divided, GFP per cell decreased (Figure 8 B). In agreement, there was a marked difference in cell morphology of typical cells in both conditions (Figure 9). Under I/w conditions, most of the cells were still large and flat, expressing beta-Gal staining. Under I+R/w conditions, predominant cells were with a small-cell morphology and beta-Gal-negative. These cells formed colonies, indicating that they acquired non-senescent morphology due to proliferation (Figure 10 C, example 1). In contrast, senescent cells that did not resume proliferation remained large (Figure 10 C, example 2). Competent cells, while proliferating and forming colonies, became smaller in size (Figure 10 C, example 1). Eventually, the average cell size dropped to normal levels under I+R/w conditions, coincident with a decrease in both the amount of protein/cell and GFP/cell coincided (Supplemental Figure 2), indicating that both are markers of cellular hypertrophy. Despite reversal of hypertrophy and a drop in GFP/cell, the amount of total GFP and protein per well increased due to cell proliferation (Figure 8 B and data not shown).

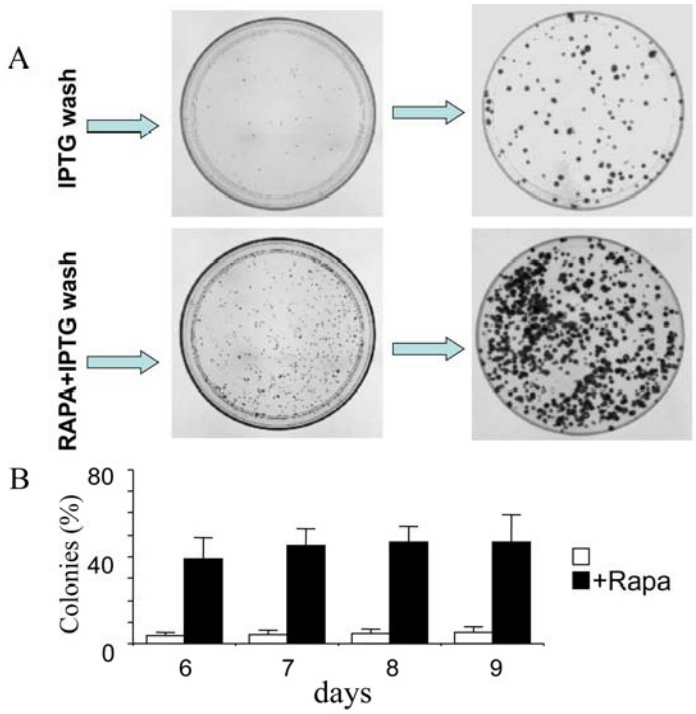

Figure 6. Clonal proliferation of competent cells. HT-p16 cells were plated in 100-mm plates. The next day, 50 μM IPTG with or without rapamycin, if indicated (RAPA), was added. After 3 days, the plates were washed to remove IPTG and RAPA. (**A**) Photographs. Upper panel: On days 5 and 8 (after IPTG removal), plates were fixed, stained and photographed. Lower panel: On days 5 and 8 (after IPTG removal), plates were fixed, stained and photographed. (**B**) Number of colonies. On days 6, 7, 8 and 9 (after IPTG removal), plates were fixed, stained and photographed. The number of colonies was counted and results are shown as percent of plated cells in log-scale.

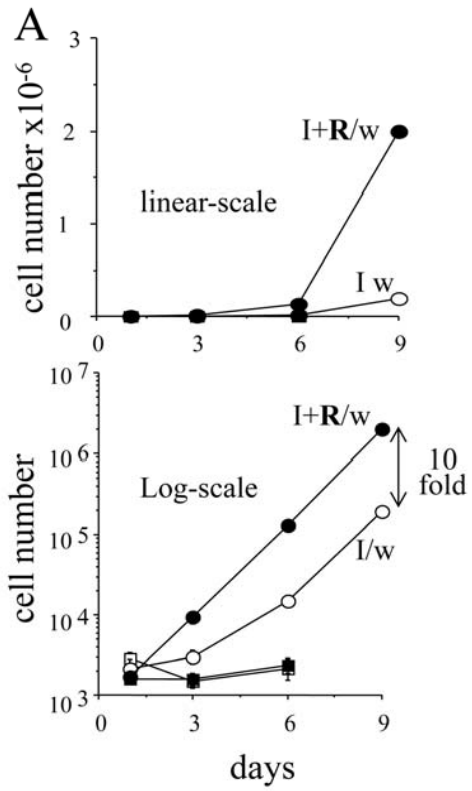

Figure 7. The dynamics of cell numbers. 500 HT-p21 cells were plated in 12 well plates. On the next day, either IPTG alone (I) or IPTG plus rapamycin (I+R) were added. After 3 days, plates were washed (I/w and I+R/w) or left unwashed. Cells were counted at days 1, 3, 6 and 9. Upper panel: linear-scale. Lower panel: log-scale. Open and closed squares: IPTG and IPTG plus Rapa, respectively. Open and closed circles: IPTG washed (I/w) and IPTG plus Rapa washed (I+R/w), respectively. In the presence of IPTG (open squares) and IPTG plus rapamycin (closed squares), the cells did not proliferate.

DISCUSSION

Acting in concert, three conditions can contribute to cellular hypertrophy: cell cycle arrest, continuous protein synthesis and insufficient autophagy. When the cell cycle was blocked by p21, HT-p21 cells grew in size almost exponentially for 3 days, eventually becoming senescent. In parallel with protein content, the amount of GFP (driven by the CMV promoter) per cell was increased up to 15-20-fold in senescent cells, an increase that may be a marker of cellular hypertrophy.

Why cells did not grow in size indefinitely while turning into senescent cells? First, cellular growth may become counter-balanced by autophagy. This is likely, given the increase in beta-Gal staining and vacuolarization in senescent cells and the recent finding that autophagy is activated several days after senescence induction, coincident with spontaneous deactivation of the PI-3K/mTOR pathway [16]. We also observed dephosphorylation of S6, when IPTG-treated cells became terminally-senescent (MS in preparation). Also, senescent cells may become compensatory insensitive to growth factors.

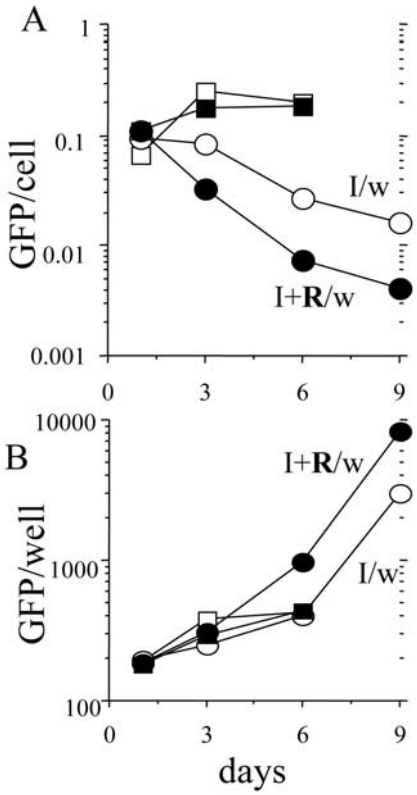

Figure 8. Loss of hypertrophy during proliferation of competent cells. 500 HT-p21 cells were plated in 12 well plates. The next day, either IPTG alone or IPTG plus rapamycin were added. After 3 days, plates were washed (I/w and I+R/w) or left unwashed. GFP per well was measured and cells were counted at days 1, 3, 6 and 9. GFP per cell was calculated (upper panel). Results are shown in arbitrary units (M±m). Open and closed squares: IPTG and IPTG plus Rapa, respectively. Open and closed circles: IPTG washed (I/w) and IPTG plus Rapa washed (I+R/w), respectively. When cells resumed exponential proliferation, GFP per cell dropped to normal levels. Due to robust proliferation, there was an increase of GFP per well.

Rapamycin modestly (30-40%) suppressed cellular hypertrophy and dramatically (10-fold) increased the number of competent (for proliferation) cells. When competent cells were released from p21-induced block, they first grow in size for one day (before division) and

then divided. This indicates that hypertrophy per se does not preclude normal mitosis. While dividing and proliferating, such cells became progressively smaller. This recovery phase is a mirror image of the senescence-induction phase, in which cells grow without division.

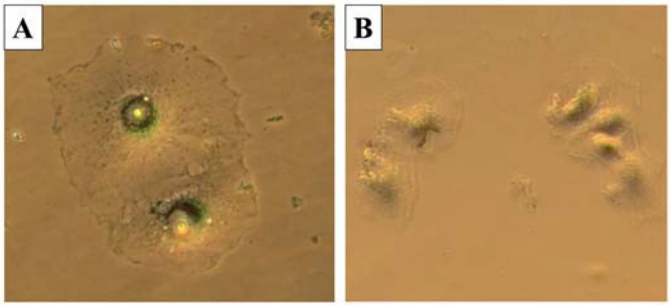

Figure 9. The morphology of cells during recovery. 500 HT-p21 cells were plated in 12 well plates. The next day, IPTG (**A**) or IPTG plus rapamycin (**B**) was added. After 3 days, plates were washed and microphotographs were taken after additional 3 days. Cells were stained for beta-Gal. A: I/w; B: I+R/w.

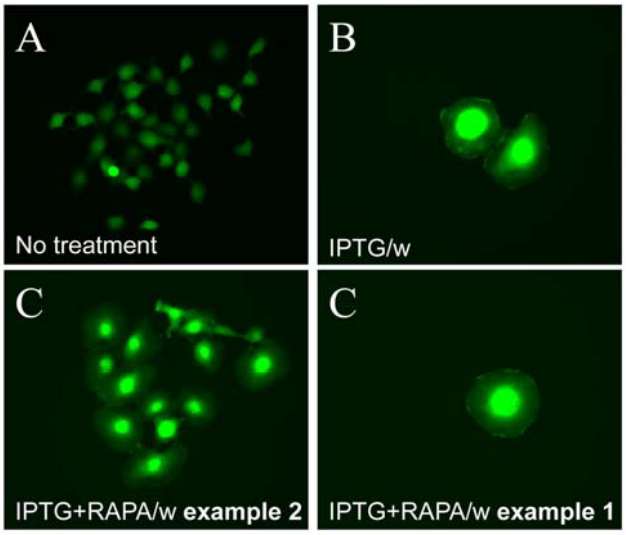

Figure 10. Visualization of loss of hypertrophy during proliferation of competent cells. 500 HT-p21 cells (**A**) were treated with IPTG (**B**) or IPTG plus rapamycin (**C**), as indicated, or left untreated. After 3 days, plates were washed and incubated without drugs to allow proliferation. (**A**) Normal size of proliferating cells. (**B**) Cellular hypertrophy of senescent cells. (**C**) Example 1. Clonal proliferation of competent cells results in loss of hypertrophy. (**C**) Example 2. Cells that remained arrested remained hypertrophic.

How can we explain preservation of mitotic competence by rapamycin? This unlikely results from the anti-hypertrophic effect of rapamycin, given that after rapamycin removal competent cells 'catch up' in size with other cells. We suggest that mitotic incompetence is not caused by hypertrophy but rather hypertrophy and incompetence are independent hallmarks of cellular aging. We hypothesize that mitotic incompetence may result from cellular hyper-activation during cell cycle arrest. Activated mTOR and MAPK pathways may force cell cycle progression despite p21-induced arrest, causing abortive S-phase entry. In fact, cyclin D1 is highly elevated in senescent cells [9] and Rb is depleted [17]. In principle elevation of cyclins and depletion of Rb may allow p21-arrested cells to enter S-phase, thus damaging the cell. Perhaps, premature cell cycle progression and mitotic incompetence are two sides of the same coin: overactivation of growth promoting and mitogen-activated pathways during cell cycle arrest. Then unscheduled S phase re-entry might be preventable by rapamycin. This hypothesis is under investigation. Noteworthy, rapamycin blocks pseudo-DNA damage response, associated with cellular overactivation [18]. Another hallmark of cellular over-activation in senescent cells is hyper-secretory and pro-inflammatory phenotype, characterized by production of cytokins, mitogens and proteases [19-26]. Needles to say, rapamycin is an anti-inflammatory drug and is labeled for use (at high doses) as immunosuppressant in the clinic. It was suggested that rapamycin as an anti-aging drug will extend healthy and maximal lifespan in humans [27-31].

MATERIAL AND METHODS

Cell lines and reagents. In HT-p21 cells, p21 expression can be turned on or off using isopropyl--thio-galactosidase (IPTG) [14, 15]. HT-p21 cells were cultured in DMEM medium supplemented with FC2 serum. Rapamycin was obtained from LC Laboratories and dissolved in DMSO as 2 mM solution and was used at final concentration of 500 nM, unless otherwise indicated. IPTG and FC2 were obtained from Sigma-Aldrich (St. Louis, MO). IPTG was dissolved in water as 50 mg/ml stock solution and used in cell culture at final concentration of 50 µg/ml.

Immunoblot analysis. Cells were lysed and soluble proteins were harvested as previously described [9]. Immunoblot analysis was performed using mouse monoclonal anti-p21, mouse monoclonal anti-phospho-S6 Ser240/244 (Cell Signaling, MA, USA), rabbit polyclonal anti-S6 (Cell Signaling, MA, USA) and mouse monoclonal anti-tubulin Ab as previously described [9].

Cell counting. Cells were counted on a Coulter Z1 cell counter (Hialeah, FL).

Colony formation assay. Two thousand HT-p21 cells were plated per 100 mm dishes. On the next day, cells were treated with 50 μg/ml IPTG and/or 500 nM rapamycin, as indicated. After 3 days, the medium was removed; cells were washed and cultivated in the fresh medium. When colonies become visible, plates were fixed and stained with 0.1% crystal violet (Sigma). Plates were photographed and the number of colonies were determined as previously described [9].

SA--Gal staining. Cells were fixed for 5 min in beta-galactosidase fixative (2 % formaldehyde; 0.2% glutaraldehyde in PBS), and washed in PBS and stained in -galactosidase solution (1 mg/ml 5-bromo-4-chloro-3-indolyl-beta-gal (X-gal) in 5 mM potassium ferricyamide, 5 mM potassium ferrocyamide, 2 mM $MgCl_2$ in PBS) at 37 ºC until beta-Gal staining become visible in either experiment or control plates. Thereafter, cells were washed in PBS, and the number of -galactosidase activity-positive cells (blue staining) were counted under bright field illumination.

ACKNOWLEDGEMENTS

We thank Lioubov Korotchkina (RPCI) for help with microphotographs shown in figure 10, members of Department of Cell Stress Biology (RPCI, Buffalo, NY) for helpful discussion and assistance, Dr. David Sinclair (Harvard Univ., Boston, MA) for editing of the first version of the manuscript.

CONFLICT OF INTERESTS STATEMENT

MVB is a founder of Oncotarget.

REFERENCES

1. Serrano M and Blasco MA. Putting the stress on senescence. Curr Opin Cell Biol. 2001, 13:748-53.

2. Shay JW and Roninson IB. Hallmarks of senescence in carcinogenesis and cancer therapy. Oncogene 2004, 23: 2919-2933.

3. Ferbeyre G, de Stanchina E, Lin AW, Querido E, McCurrach ME, Hannon GJ, and Lowe SW. Oncogenic ras and p53 cooperate to induce cellular senescence. Mol Cell Biol. 2002, 22: 3497-3508.

4. Ruggero D, Montanaro L, Ma L, Xu W, Londei P, Cordon-Cardo C and Pandolfi PP. The translation factor eIF-4E promotes tumor formation and cooperates with c-Myc in lymphomagenesis. Nat Med. 2004, 10: 484-486.

5. Efeyan A, Ortega-Molina A, Velasco-Miguel S, Herranz D, Vassilev LT and Serrano M. Induction of p53-dependent senescence by the MDM2 antagonist nutlin-3a in mouse cells of fibroblast origin. Cancer Res. 2007, 67: 7350-7357.

6. Satyanarayana A, Greenberg RA, Schaetzlein S, Buer J, Masutomi K, Hahn WC, Zimmermann S, Martens U, Manns MP and Rudolph KL. Mitogen stimulation cooperates with telomere shortening to activate DNA damage responses and senescence signaling. Mol Cell Biol 2004, 24: 5459-5474.

7. Blagosklonny MV. Cell senescence and hypermitogenic arrest. EMBO Rep. 2003, 4: 358-362 .

8. Blagosklonny MV. Cell senescence: hypertrophic arrest beyond restriction point. J Cell Physiol. 2006, 209: 592-7.

9. Demidenko ZN and Blagosklonny MV. Growth stimulation leads to cellular senescence when the cell cycle is blocked. Cell Cycle 2008, 7: 3355-3361.

10. Demidenko ZN, Zubova SG, Bukreeva EI, Pospelov VA, Pospelova TV and Blagosklonny MV. Rapamycin decelerates cellular senescence. Cell Cycle 2009, 8: 1888-1895.

11. Demidenko ZN, Shtutman M and Blagosklonny MV. Pharmacologic inhibition of MEK and PI-3K converges on the mTOR/S6 pathway to decelerate cellular senescence. Cell Cycle 2009, 8: 1896-1900.

12. Blagosklonny MV. Aging-suppressants: cellular senescence (hyperactivation) and its pharmacologic deceleration. Cell Cycle 2009, 8: 1883-1887.

13. Kandel ES, Chang BD, Schott B, Shtil AA, Gudkov AV and Roninson IB. Applications of green fluorescent protein as a marker of retroviral vectors. Somat Cell Mol Genet. 1997, 23: 325-340.

14. Chang BD, Broude EV, Dokmanovic M, Zhu H, Ruth A, Xuan Y, Kandel ES, Lausch E, Christov K and Roninson IB. A senescence-like phenotype distinguishes tumor cells that undergo terminal proliferation arrest after exposure to anticancer agents. Cancer Res. 1999, 59: 3761-3767.

15. Chang BD, Broude EV, FangJ, Kalinichenko TV, Abdryashitov R, Poole JC and Roninson IB. p21Waf1/Cip1/Sdi1-induced growth arrest is associated with depletion of mitosis-control proteins and leads to abnormal mitosis and endoreduplication in recovering cells. Oncogene 2000, 19: 2165-2170.

16. Young AR, Narita M, Ferreira M, Kirschner K, Sadaie M, Darot JF, Tavaré S, Arakawa S, Shimizu S, Watt FM and Narita M. Autophagy mediates the mitotic senescence transition. Genes Dev. 2009, 23: 798-803.

17. Broude EV, Swift ME, Vivo C, Chang BD, Davis BM, Kalurupalle S, Blagosklonny MV and Roninson IB. p21(Waf1/Cip1/Sdi1) mediates retinoblastoma protein degradation. Oncogene 2007, 26: 6954-6958.

18. Pospelova TV, Demidenko ZN, Bukreeva EI, Pospelov VA, Gudkov AV and Blagosklonny MV. Pseudo-DNA

damage response in senescent cells. Cell Cycle 2009, 8: 4112-4118.

19. Coppé JP, Kauser K, Campisi J and Beauséjour CM. Secretion of vascular endothelial growth factor by primary human fibroblasts at senescence. J Biol Chem. 2006, 281: 29568-29574.

20. Coppé JP, Patil CK, Rodier F, Sun Y, Muñoz DP, Goldstein J, Nelson PS, Desprez PY and Campisi J. Senescence-associated secretory phenotypes reveal cell-nonautonomous functions of oncogenic RAS and the p53 tumor suppressor. PLoS Biol. 2008, 6: 2853-2868.

21. Rodier F, Coppé JP, Patil CK, Hoeijmakers WA, Muñoz DP, Raza SR, Freund A, Campeau E, Davalos AR and Campisi J. Persistent DNA damage signalling triggers senescence-associated inflammatory cytokine secretion. Nat Cell Biol. 2009, 11: 973-979.

22. Bhaumik D, Scott GK, Schokrpur S, Patil CK, Orjalo AV, Rodier F, Lithgow GJ and Campisi J. MicroRNAs miR-146a/b negatively modulate the senescence-associated inflammatory mediators IL-6 and IL-8. Aging 2009, 1: 402-411.

23. Acosta JC, O'Loghlen A, Banito A, Raguz S and Gil J. Control of senescence by CXCR2 and its ligands. Cell Cycle 2008, 7: 2956-2959.

24. Kuilman T, Michaloglou C, Vredeveld LC, Douma S, van Doorn R, Desmet CJ, Aarden LA, Mooi WJ and Peeper DS. Oncogene-induced senescence relayed by an interleukin-dependent inflammatory network. Cell 2008, 133: 1019-1031.

25. Patil CK, Mian IS and Campisi, J. The thorny path linking cellular senescence to organismal aging. Mech Ageing Dev. 2005, 126: 1040-1045.

26. Campisi J. Senescent cells, tumor suppression, and organismal aging: good citizens, bad neighbors. Cell 2005, 120: 513-522.

27. Blagosklonny MV. Aging and immortality: quasi-programmed senescence and its pharmacologic inhibition. Cell Cycle 2006, 5: 2087-2102.

28. Blagosklonny MV. An anti-aging drug today: from senescence-promoting genes to anti-aging pill. Drug Disc Today 2007, 12: 218-224.

29. Blagosklonny MV. Aging, stem cells, and mammalian target of rapamycin: a prospect of pharmacologic rejuvenation of aging stem cells. Rejuvenation Res. 2008, 11: 801-808.

30. Blagosklonny MV. Prevention of cancer by inhibiting aging. Cancer Biol Ther. 2008, 7: 1520-1524.

31. Blagosklonny MV. Validation of anti-aging drugs by treating age-related diseases. Aging 2009, 1: 281-288.

SUPPLEMETAL FIGURES

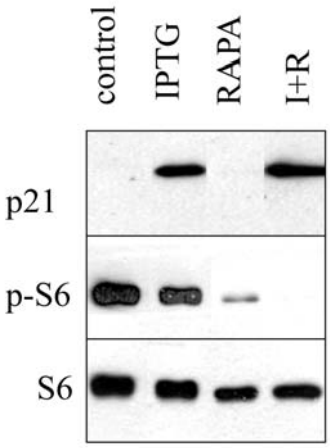

Figure S1. Induction of p21 by IPTG. HT-p21 cells were plated in 6 well plates and treated with IPTG with or without rapamycin as indicated. The next day, cells were lysed and immunoblot for p-S6, S6 and p21 was performed as described in Methods. IPTG dramatically induced p21, without affecting S6 phosphorylation, whereas rapamycin inhibited S6 phosphorylation, without affecting p21 induction.

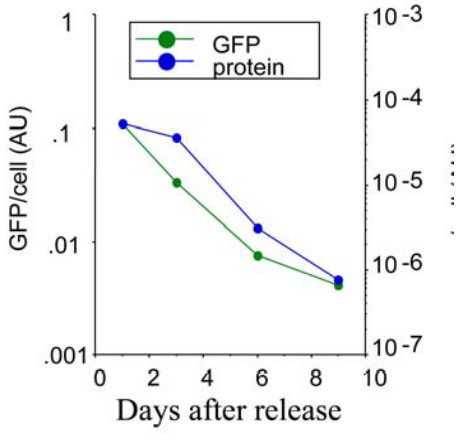

Figure S2. Loss of hypertrophy following release. HT-p21 cells were treated with IPTG plus 500 nM rapamycin for 3 days. Then the cells were washed and the cells were incubated in the fresh medium without drugs. At indicated days, soluble protein, GFP and cell numbers were measured per well. Protein (pr) per cell and GFP per cell were calculated and plotted in arbitrary units.